Trace Inorganics In Water

Published on June 1, 1968 on http://pubs.acs.org | doi: 10.1021/ba-1968-0073.fw001

Trace Inorganics In Water

A symposium sponsored by the Division of Water, Air, and Waste Chemistry at the 153rd Meeting of the American Chemical Society, Miami Beach, Fla., April 10-13, 1967.

Robert A. Baker

Symposium Chairman

ADVANCES IN CHEMISTRY SERIES 73

AMERICAN CHEMICAL SOCIETY

WASHINGTON, D.C. 1968

Library of Congress Catalog Card 68-25996

PRINTED IN THE UNITED STATES OF AMERICA

Advances in Chemistry Series

Robert F. Gould, *Editor*

AMERICAN CHEMICAL SOCIETY PUBLICATIONS

FOREWORD

ADVANCES IN CHEMISTRY SERIES was founded in 1949 by the American Chemical Society as an outlet for symposia and collections of data in special areas of topical interest that could not be accommodated in the Society's journals. It provides a medium for symposia that would otherwise be fragmented, their papers distributed among several journals or not published at all. Papers are refereed critically according to ACS editorial standards and receive the careful attention and processing characteristic of ACS publications. Papers published in ADVANCES IN CHEMISTRY SERIES are original contributions not published elsewhere in whole or major part and include reports of research as well as reviews since symposia may embrace both types of presentation.

PREFACE

Isolation, quantification, and understanding of the role of increasingly smaller quantities of matter is important in all scientific regimes and in no case is this truism of greater applicability than in water chemistry. Research trends, like fashions, vary in point of time. Recently, emphasis on synthetic detergent biodegradability, pesticides, and other organics has dominated the field. This attention has been prompted by actual or potential physiological, sensory and esthetic effects. Development of improved analytical devices such as ionization-detection gas-liquid chromatography made it possible in many cases to conduct investigations involving nanogram or smaller units of certain materials. Thus, the need and the means to study trace organics developed simultaneously.

Trace inorganics, with the possible exception of radionuclides, have not been the objective of as much attention as the organics. Nevertheless, advances have been occurring and current development of improved analytical devices and techniques promises to accelerate trace inorganic research. Dissolved and colloidal inorganic materials are involved solely and in complex mixtures with organic substances in corrosion, eutrophication, microbiological, and other processes of economic and general concern.

The symposium which resulted in this publication was organized as a result of discussions at the Gordon Research Conference on Microcontaminants in Water held in June, 1964. That conference was dominated by organic-related findings. A need to summarize developments concerning trace inorganics in water was deemed appropriate. Technical programs with such broad objectives rarely satisfy all needs. This is no exception. However, these papers constitute a representative progress report.

The symposium and this publication divide naturally into three parts: critical assessments of broad subjects; applied and fundamental research reports; and analytical developments. Many of these papers are contributed by investigators from chemical disciplines other than those normally identified with water chemistry. This is as it should be for maximum information exchange and research concept stimulation. The

cooperation of the authors, Division officers, and ACS staff during the course of the symposium and publication preparation is gratefully acknowledged.

ROBERT A. BAKER

Pittsburgh, Pennsylvania
July 1967

The Effect of Water Structure on the Transport Properties of Electrolytes

ROBERT L. KAY

Carnegie-Mellon University, Mellon Institute, Pittsburgh, Pa.

The abnormal transport properties (conductances and viscosities) of electrolytes in aqueous solution are explained in terms of the effect ions can have on water structure. Various theories that treat the solvent as a continuum are shown to be incapable of explaining these abnormalities. The Frank-Wen model is used to classify ions as electrostrictive structure-makers, Li^+, F^-, Ca^{2+}; hydrophobic structure-makers, Bu_4N^+, Ph_4B^-; and structure-breakers, Cs^+, I^-, Me_4N^+. These effects can be detected by comparing data for aqueous solutions with nonaqueous solutions, by investigating the temperature coefficient of ionic mobilities and viscosity B coefficients, by comparing ionic mobilities in H_2O and D_2O, and by comparing the particular hydrophilic properties of the $(EtOH)_4N^+$ ion with its alkyl analog, the Pr_4N^+ ion.

In the past few years considerable interest has developed in the structure of water in electrolytic solutions (25). This renewed interest is the result of a number of extensive experimental investigations and the realization that many otherwise unexplainable observations can be accounted for if water is considered as a structured medium rather than as a continuum. This paper will consist of a review of some of the more recent advances that have been made in elucidating the factors determining the properties of electrolytes in aqueous solution. Transport properties will be dealt with almost exclusively since the author's main interests lie in that direction. Owing to the unique mechanism of proton conduction in aqueous solution, acids and bases will not be considered and the discussion will be limited exclusively to salt solutions.

The problem of explaining the magnitude of ionic mobilities in aqueous solutions has baffled the electrolyte chemist for a considerable time. Two major factors have contributed to the slow progress in this field.

First, water has been considered for so long as the typical solvent whereas we now know this to be a poor assumption. It is one of the few solvents in which three-dimensional structure can exist. These three dimensional structures are formed by water's ability to form hydrogen bonds in a tetrahedral configuration. As a result of this high degree of hydrogen bonding, water has a number of unique properties among which are its exceedingly high heat capacity, viscosity, and dielectric constant and its maximum density of 4°C. It is the only known liquid whose viscosity decreases with increasing pressure (*22*). Possibly better progress would have been made in this field if a non-hydrogen bonded solvent like acetonitrile had first received our undivided attention instead of water. The lack of good data for ionic properties in any solvent other than water has been a big handicap. For instance, for a considerable time we did not know the temperature coefficient of ionic conductances in any solvent other than water. This deficiency has been rectified only recently by the measurements of transferance numbers and conductances in methanol at 10°C. (*36*).

The second reason for slow progress in the field is the lack of a good theory in which water is treated as a structured medium rather than as a continuum. Considering the solvent in an electrolytic solution as a uniform medium with the same physical properties as the pure solvent has certain mathematical advantages, and this approach has enjoyed considerable success. However, this success has been limited generally to the prediction of the concentration dependence of various transport and thermodynamic properties, and then only in extremely dilute solutions. The continuum theory is not as successful in explaining the change in magnitude of these properties as the solvent or temperature are changed, as I shall point out later. The success of the continuum theory in predicting the concentration dependence is not difficult to understand. Interionic effects are longer ranged than ion-solvent effects and, therefore, are sizeable effects in very dilute solutions. On the other hand, one must go well above what is considered the dilute range (ionic strength 0.01) before any one ion has an appreciable effect on the interaction of a second ion with the solvent. One would expect that any effect of water structure on the property of an electrolyte would be fairly concentration independent in this dilute range and, consequently, would not interfere with a continuum calculation. However, there are exceptions in the case of very large ions. The continuum theory is not as successful in explaining the temperature dependence of various properties of aqueous solutions. It is interesting to note that the structure existing in water is extremely temperature dependent, owing to the fact that thermal energies approach the strength of the hydrogen bonds involved. Thus, an appeal to structural effects to account for the unexplained temperature coefficients of transport properties of electrolytes is certainly reasonable.

Experimental and Results

In considering the dependence of limiting ionic mobilities on solvent and temperature it is most useful to apply Stokes' law (*30*). For univalent ions (*34*) it is given by

$$\lambda_o\eta_o = 15.4/6\pi r_S \tag{1}$$

and states that the limiting ionic conductance-solvent viscosity product is inversely proportional to the radius, r_S, of the moving ion. It should be remembered at this point that the limiting ionic conductance is proportional to the limiting ionic mobility, the proportionality factor being the Faraday constant. Stokes' law is based on the assumption that an ion moves in the direction of the field by pushing solvent molecules out of its path. This involves doing work in overcoming the viscous drag of the solvent molecules and this viscous drag is assumed to be identical to that of the bulk solvent.

An application of Equation 1 to experimental results for aqueous and acetonitrile (*4, 27*) solutions at 25°C. is shown in Figure 1. Here $\lambda_0\ \eta_0$ or the Walden product (*37, 38*) as it is sometimes known, is plotted against the reciprocal crystallographic (*33*) or estimated (*34*) radii of the alkali and tetraalkylammonium cations and the halide anions. Equation 1 or Stoke's law is shown as the broken line and at first glance appears to be an exceedingly poor representation of the data. Stoke's law is not as poor as it first appears if certain deviations, attributable to deficiencies in the model on which it is based, are taken into account. Since smaller ions must be solvated to some extent, they must carry a solvent sheath through the solution. Consequently, the ordinate in Figure 1 should represent the solvated rather than crystallographic radius. This could possibly account for the ions lying below the Stokes' line but it will not account for those lying above the line. If complete "slippage" of the solvent past the ion is assumed to take place, the numerical constant in Equation 1 is reduced from 6 to 4. This helps but it is not sufficient and a considerable number of ions still lie above the Stokes' line indicating a higher mobility than the theory predicts.

Another interaction between ions and solvent molecules besides solvation has been identified by Born (*1*) and latter by Fuoss (*13*). A moving ion can orient the solvent dipoles as they move through the solution. Owing to the finite time required for the relaxation of such orientations, a retarding force is exerted on the moving ion. Zwanzig (*42*) has quantitatively evaluated this effect and showed that Equation 1 becomes

$$\lambda_o\eta_o = 15.4/6\pi[r_S + A/r_S^3] \tag{2}$$

Here, the constant A depends on various dielectric properties of the solvent. Frank (*10*) has discussed this result in considerable detail and

showed that this theory predicts a maximum λ_0 of about 30 for aqueous solutions at 25°C., whereas values as high as 75 have been observed. Kay (*27*) has made a similar calculation for methanol solutions and obtained a comparable result. There is little doubt that this Born-Fuoss effect exerts some influence on ionic mobilities, but it certainly will not explain the very high mobilities exhibited by some ions in aqueous solution.

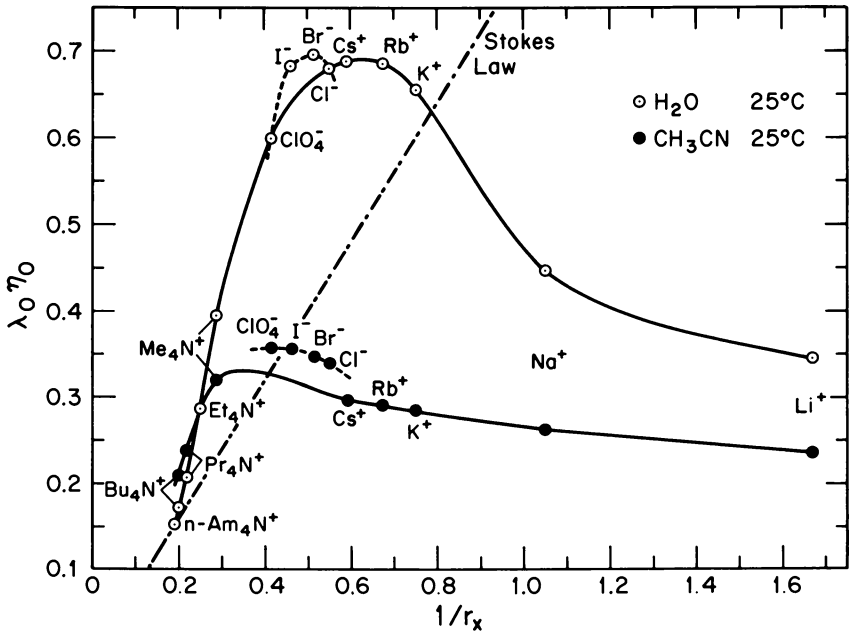

Figure 1. The limiting ionic conductance-solvent viscosity product plotted as a function of the reciprocal ionic radii for several ions in aqueous and acetonitrile solutions at 25°C.

A further attempt to rectify the situation was introduced by Robinson and Stokes (*34*) and extended by Nightingale (*31*). Noting that Stokes' law appears to fit better for large ions in aqueous solutions (*see* Figure 2), and since Stokes' law holds only if the ions are large compared with the solvent molecules, Stokes and Robinson assume that only the *n*-Am_4N^+ ion is large enough to fulfill this requirement. They then assumed that the other tetraalkylammonium ions were not hydrated but deviated from Stokes' law owing to a size deficiency. In essence, they forced the Stokes' line through the tetraalkylammonium ions, thereby producing negative deviations for all the other ions in aqueous solutions. In this way they were able to use solvation to explain the resulting negative deviations and, in fact, calculated hydration numbers for each ion.

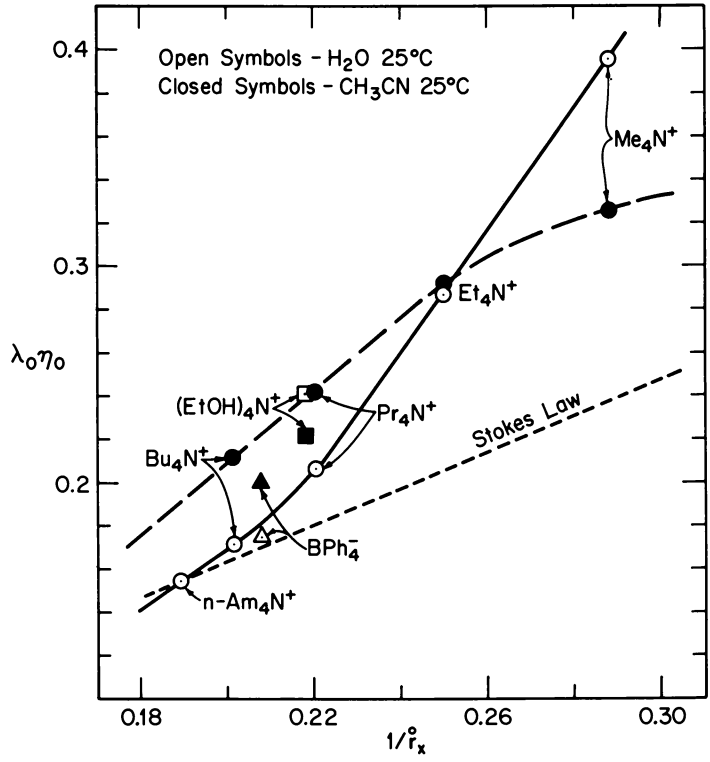

Figure 2. An enlargement of the left-hand side of Figure 1

This approach suffers from one serious flaw. The basic assumption on which this approach rests is that the $\lambda_0\ \eta_0$ product is invariant with temperature, whereas Kay and Evans have shown this assumption to be incorrect (*9, 27*). This can be seen in Figure 3 where the ratio C_{10}^{25} given by

$$C_{10}^{25} = (\lambda_0\eta_0)_{25°C.}/(\lambda_0\eta_0)_{10C°}. \quad (3)$$

is plotted *vs.* the ionic conductance at 25°C. As a matter of fact, the deviation of this ratio from unity increases with increasing size, suggesting that interaction of these large ions with the solvent increases with increasing size. This experimental result indicates that the calibration curves and the resulting hydration numbers (*31*) obtained from this type of correction to Stokes' law are meaningless.

Two facts stand out in the conductance data shown in the first three figures. All except the smaller halide and alkali metal ions appear to have a large excess mobility (Figure 1) whereas the larger ions with hydrocarbon surfaces exhibit a mobility deficiency (Figure 2) in aqueous

solution compared with nonaqueous solution. At the same time, ions showing a mobility excess in aqueous solution also have negative temperature coefficients of $\lambda_0\eta_0$ in aqueous solution, whereas ions with mobility deficiencies in aqueous solution have positive coefficients of $\lambda_0\eta_0$ (Figure 3). Although the comparison in Figures 1 and 2 is only to acetonitrile solutions, it has been shown (*27*) that the $\lambda_0\eta_0$ for methanol, ethanol, and nitromethane (the only solvents for which precise transference numbers are available) lie very close to the acetonitrile line and actually are identical as the ion size becomes large. Furthermore, the deviation of C_{10}^{25} from unity for methanol solutions have been shown to be small compared with those in Figure 3 for aqueous solution (*36*).

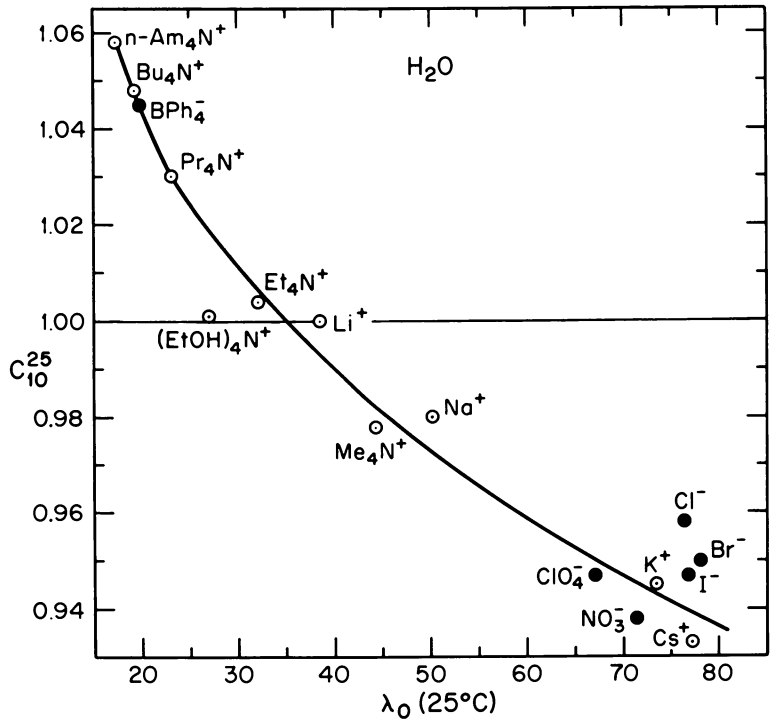

Figure 3. A plot of Equation 3 for aqueous solution against the ionic conductance in water at 25°C.

Another transport property sensitive to solvent structural effects is the viscosity *B* coefficient obtained from the Jones-Dole equation (*23*),

$$\eta = \eta_0(1 + A'C^{1/2} + BC) \quad (4)$$

where η is the solution viscosity. The coefficient A' is small and is the

result of interionic forces that tend to interfere with the flow of one layer of solution past another. It can be determined experimentally or calculated from the Falkenhagen equation (*18*). Considering the solvent as a continuum, B can be obtained from the Einstein equation (*6, 7*)

$$B = 2.5v/c \tag{5}$$

which predicts B to be proportional to the ionic volume since v is the volume of the ions per cc. of solution and c is the concentration in moles per cc. of solution.

Equation 5 predicts that the viscosity B coefficient should increase with increasing ion size and should be independent of temperature and solvent inasmuch as the ionic size is temperature and solvent independent. The data for the alkali metal and halide ions (*24*) in Table I and for the tetraalkylammonium bromides (*28*) in Figure 4 show that neither of the predictions is verified by experiment.

Table I. Aqueous Viscosity B Coefficients and Dependence on Temperature

$t°C.$	Li^+	Na^+	K^+	Cs^+	Cl^-	Br^-	I^-
15	0.162	0.086	−0.020		−0.020	−0.06[a]	
25	0.150	0.086	−0.007	−0.045	−0.007	−0.04[a]	−0.069
35	0.139	0.085	+0.005		+0.005	−0.03[a]	−0.054

[a] Interpolated from date in Ref. 28.

Nearly all the ions show some temperature dependence in aqueous solution, but at least for the tetraalkylammonium ions, very little in methanol solutions (Figure 4). Instead of increasing, B decreases with increasing size for the alkali metal and halide ions. The negative values of B indicate that most of these ions actually decrease the viscosity upon their addition to water. The B coefficients for the tetraalkylammonium ions increase with increasing size; but for the larger ions, B is much larger in aqueous than in methanol solutions and extremely temperature dependent in aqueous solution.

These experimental facts can be explained in a consistent manner by considering water as a structured medium and investigating the possible effect of ions on that structure. Numerous early workers, including Lewis and Randall (*29*) in their famous treatise on thermodynamics, considered the possibility that electrolytic properties for aqueous solutions were influenced to a considerable extent by the presence of hydrogen-bonded aggregates of water molecules. Frank and Evans (*11*) were among the first systematically to consider this problem by investigating both entropies of solution and viscosity increments of ions in aqueous solution. Gurney (*16*) collected much of the early data and

clarified some of the principles involved, particularly in regard to conductance and viscosity data. Here, the model of Frank and Wen (*12*) for ionic solutions will be used. It is somewhat more specific than that of Gurney and has been expanded to include the tetraalkylammonium ions.

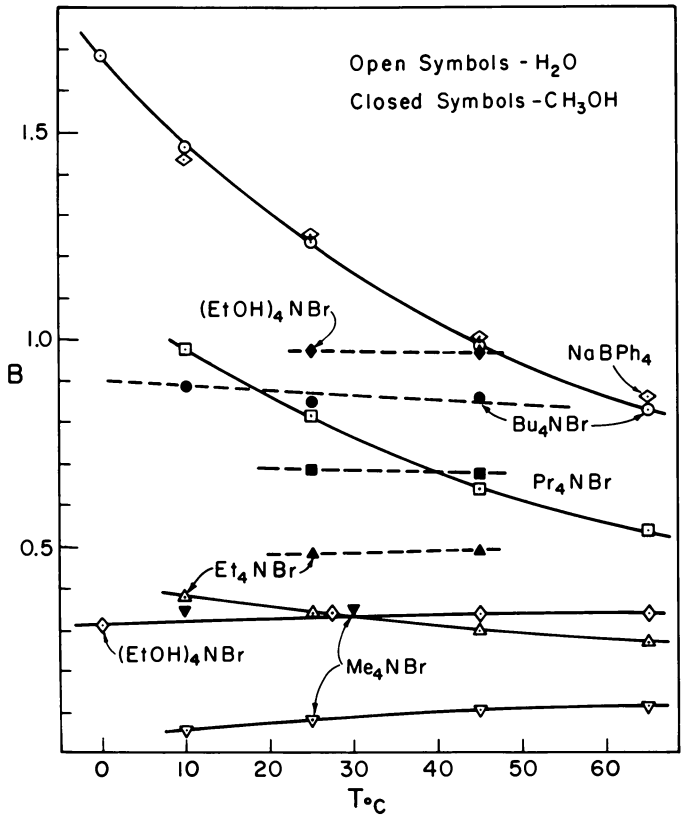

Figure 4. Viscosity B *coefficients for the tetraalkylammonium and tetraethanolammonium bromides in aqueous and methanol solutions at several temperatures*

In the Frank-Wen model, water in the vicinity of an ion is divided into three regions as shown in Figure 5. In region A, the ionic charge predominates and the water dipoles are completely oriented towards the central ion. Although water in this region is exchanging rapidly (*35*), it is immobilized to a considerable extent compared with bulk water; and the ion is said to be electrostrictively solvated. Since water in this region is more ordered than in pure water, the ion can be said to be an electrostrictive structure-maker. Water in the second and third solvation sheath

will be less immobilized until region B is reached. In this intermediate region, the effect of the ionic charge has diminished to such an extent that it can only partially orient the water dipoles; but such orientations are still of sufficient magnitude to interfere with the formation of the normal three-dimensional structures present in pure water. Water in this region, therefore, has a lower degree of hydrogen bonding and structure, and consequently, if the size of region B is very extensive, the ion can be said to be a net structure-breaker. At much larger distances, region C is reached where the effect of the ionic charge is insignificant and the water dipoles are oriented solely by neighboring water molecules, and this region will have the properties of pure water.

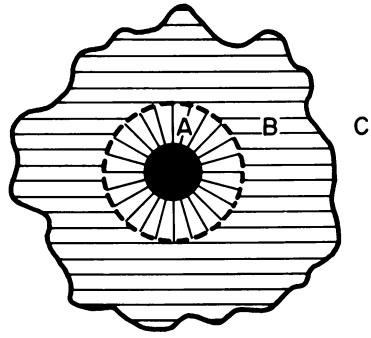

Figure 5. A model for aqueous electrolyte solutions

It has been necessary to postulate another effect to account for the behavior of the quaternary ammonium ions that possess large hydrophobic surfaces. Water molecules at the surface of these large ions are influenced very little by either the ionic charge or the inert hydrocarbon on their one side. Consequently, the water molecules on their other side can orient these surface water molecules to a greater extent than normal and can, in effect, result in a greater degree of hydrogen bonding or structure to form along the hydrocarbon side chains. This type of ion can be considered to be a hydrophobic structure-maker; and this type of structure-making plays an important role in the formation of clathrate hydrates.

Using this model, the conductance and viscosity behavior in Table II can be accounted for. Note that in this table both $\partial\lambda_o\eta_o/\partial T$ and $\partial B/\partial T$ refer to aqueous solutions. Electrostrictive structure-makers are those ions of large charge, Z, or extremely small crystallographic radius. The relative properties in aqueous and nonaqueous solvents cannot be predicted since the relative size, dipole moments, basicity, etc., of the solvent molecules will be the determining factors. The large solvation energy of

small ions like the Li^+ or the highly charged La^{3+} ion should be much greater than thermal energies in the temperature region considered here, and consequently, the degree of solvation should decrease only very slowly with increased temperature.

Table II.

	Z/r_x	$\frac{(\lambda_o\eta_o)_{aq.}}{(\lambda_o\eta_o)_{nonaq.}}$	$\frac{B_{aq.}}{B_{nonaq.}}$	$\frac{\partial(\lambda_o\eta_o)}{\partial T}$	$\frac{\partial B}{\partial T}$	*Examples*
Electrostrictive Structure-Makers	large	—	—	small positive	small negative	Li^+F^- La^{3+}
Structure-Breakers	small	>1	<1	negative	positive	Cs^+, Me_4N^+ I^-, ClO_4^-
Hydrophobic Structure-Makers	very small	<1	>1	positive	negative	Bu_4N^+ Ph_4B^-

Those ions with small charge-to-size ratios should be good structure-breakers. They should have an excess mobility in aqueous solutions since they are moving into the cosphere (region B of Figure 5) where the degree of hydrogen bonding and, consequently, the viscosity are less than the viscosity of pure water. This excess mobility should decrease with increasing temperature since at higher temperatures there is less structure to break. The viscosity B coefficient for structure-breakers should be smaller in aqueous than in nonaqueous solutions or smaller than that predicted from Equation 5 because these ions have depolymerized the water and therefore reduced its viscosity. As a matter of fact, many structure-breaking ions like K^+ and I^- have negative B coefficients. However, a negative B is not a necessary condition for a structure-breaker. Some ions like Me_4N^+ are moderately good structure-breakers but have positive B coefficients. Their structure-breaking properties are best seen in the temperature dependence because these structural effects are sensitive to temperature changes. As the temperature increases and the amount of structure in the water decreases, the B for these ions increases to a higher value more consistent with Equation 5.

Only extremely large ions with alkyl or aryl side chains have been found to be good hydrophobic structure-makers. The tetraalkylammonium and the tetraphenylboride ions are good examples. Owing to the high degree of hydrogen bonding about the side chains, they appear to have a mobility deficiency in aqueous compared with nonaqueous solvents (Figure 2). This structured water on their surface is extremely temperature sensitive, and as the temperature increases rapidly "melts," producing a positive temperature coefficient for the $\lambda_o\eta_o$ product (Figure 3), and a large absorption of heat that appears in the extremely large apparent molar heat capacity (*12*). The increased degree of hydrogen

bonding about the surfaces of these ions results in a higher B in aqueous than in nonaqueous solutions, and the temperature coefficient is negative because this excess structural viscosity disappears as the temperature increases (Figure 4).

It can be noted in Table II that the conductance behavior is just opposite the viscosity behavior, which is as it should be. This is seen more readily in Figure 6 where the temperature coefficient of the B coefficients is plotted against the temperature coefficient of the limiting conductance-viscosity product. Structure-breakers are now found in the top left-hand quadrant, and hydrophobic structure-makers in the bottom right-hand quadrant. Electrostrictive structure-makers, on the other hand, should now lie quite close to the origin.

Most of the more familiar ions can now be placed in these three groups. The strong structure-breakers include the K^+, Rb^+, Cs^+, Cl^-, Br^-, I^-,

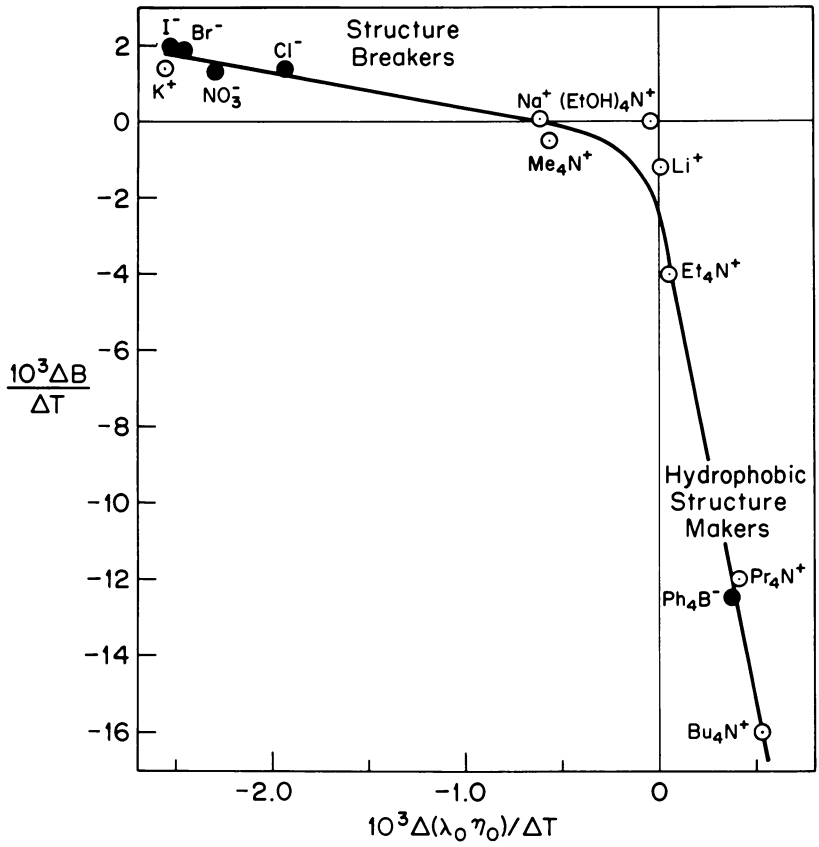

Figure 6. A comparison of the temperature coefficients of viscosity B *coefficients and limiting ionic conductance-viscosity products*

and ClO_4^- ions, while the Pr_4N^+, Bu_4N^+, and Ph_4B^- ions are good hydrophobic structure-makers. The Li^+ and F^- ions are strong electrostrictive structure-makers, as are the divalent and higher charged ions that are not included here (*27*). The Na^+, Me_4N^+, and Et_4N^+ are borderline cases that have properties of two or more of these groups. These ions will be expected to act differently depending on the property being investigated, since different properties are affected to different degrees by water structure.

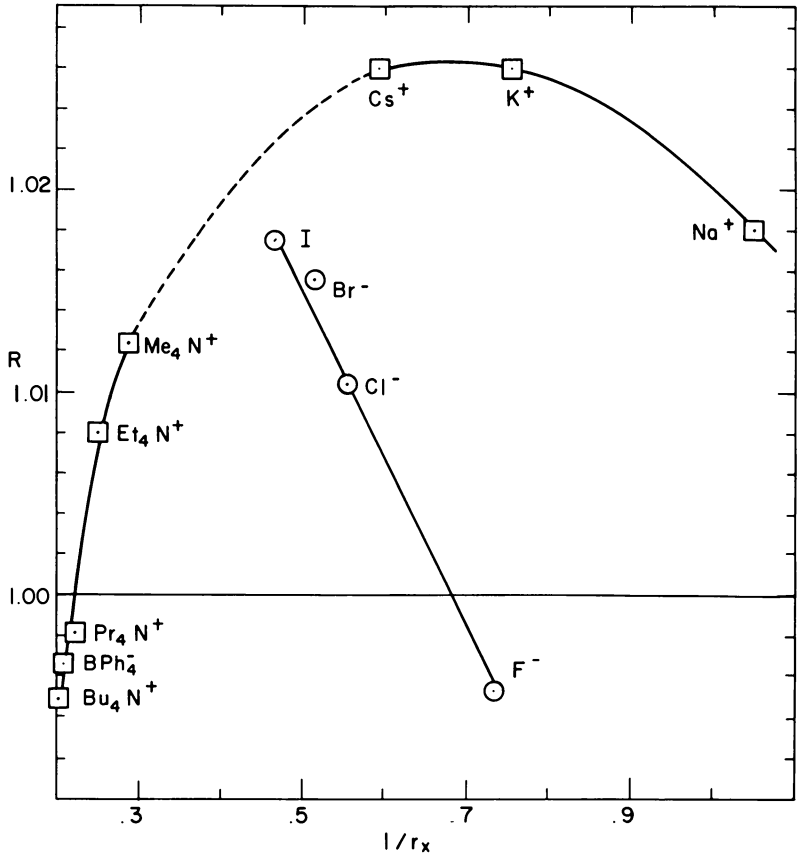

Figure 7. A plot of Equation 6 as a function of reciprocal ionic radii

The structural properties of these ions can be seen further by comparing their conductances in D_2O compared with H_2O (*26*). The results are seen in Figure 7, where R, given by

$$R = (\lambda_o\eta_o)_{D_2O}/(\lambda_o\eta_o)_{H_2O} \qquad (6)$$

is plotted against the reciprocal crystallographic radii. The higher degree of structural order in D_2O over that in H_2O is evident from its higher entropy of vaporization, melting point, and viscosity (*25*). Owing to this increased degree of hydrogen bonding, structure-breaking ions should have an enhancement of mobility in D_2O over that in H_2O and R should be greater than unity. Structure-making ions of both kinds show R values less than unity as would be expected. It should be noted that the Et_4N^+ ion shows up here as a structure-breaker although in most other properties it shows up as a very weak structure-maker (Figures 3 and 4). The conclusions reached from conductance measurements are in good agreement with those arrived at by Greyson (*14, 15*) from entropy data for transfer of these ions from D_2O to H_2O.

Verification of the conclusion that the transport properties of the tetraalkylammonium ions are affected by water structural effects has been obtained by studying a most interesting ion, the tetraethanolammonium ion, $(EtOH)_4N^+$ (*3, 8*). It will be remembered that the enforcement of water structure on the hydrocarbon side chains of the larger tetraalkylammonium ions was the result of no interaction between the ions and water molecules on their surfaces. If the terminal methyl groups in the Pr_4N^+ ion are exchanged for hydroxyl groups to form the $(EtOH)_4N^+$ ion, an interacting functional group is introduced into the otherwise inert hydrocarbon chains. This functional group should interfere with the enforcement of water structure, and $(EtOH)_4N^+$ should show none of the structure-making properties of its alkyl analog, the Pr_4N^+ ion. That this is essentially the case can be seen in Figure 6, where the $(EtOH)_4N^+$ ion is shown to have zero temperature coefficients of both the $\lambda_o\eta_o$ product and the viscosity B coefficient in aqueous solutions in contrast to the large temperature coefficients of the Pr_4N^+ ion. Here again the results of transport measurements are confirmed by heat capacity and also by heat of transport data (*40*). If anything, the $(EtOH)_4N^+$ ion could be considered a slight structure-breaker as seen from a comparison of its properties in aqueous and nonaqueous solvents (Figures 2 and 4).

Confirmation of the ideas expressed here has come from NMR relaxation studies (*20, 21*), dielectric dispersion (*17*), near infrared spectra (*2*), and various thermodynamic measurements a few of which have been mentioned. Another thermodynamic property, the apparent molar volume, is particularly interesting since it is very sensitive to structural effects in the very dilute concentration range. For instance as shown in Figure 8, the data for Bu_4NBr in water (*39*) approaches infinite dilution with a negative slope although the Debye-Hückel limiting slope is positive. As a matter of fact, the large tetraalkylammonium salts actually show a minimum at higher concentrations. It is interesting to note that φ_v for the nonhydrophobic $(EtOH)_4N^+$ ion approaches infinite dilution

with close to the correct Debye-Hückel limiting slope and has a much lower infinite dilution value of φ_v than its alkyl analog, the Pr_4N^+ ion (*40*). The same behavior is exhibited by Bu_4NBr in methanol (*32*) as shown in Figure 8, where no three-dimensional structural effects are to be expected. The difference in φ_v^0 of about 16 ml./mole must be attributed to the volume increase in aqueous solution owing to water structure enforcement after correction for the difference in the electrostrictive volume of the bromide ion.

One item of evidence seemingly in contradiction to the above ideas comes from a consideration of the chemical shift measurements of Hertz and Spalthoff (*19*) for Bu_4NBr in concentrated solutions and verified by Davis and Kay (*5*) for the dilute range as shown in Figure 9. Their results showed that the difference in the chemical shift between the water protons in the solution and the methyl protons of the butyl groups in Bu_4NBr in aqueous solution decreased with increasing concentration. This is equivalent to an upfield shift of the water protons; the same effect on water as an increase in temperature and almost identical to the effect of KBr on water. Thus, by this criterion, the Bu_4N^+ ion appears to be a structure-breaker. However, the problem of accounting for the absolute magnitude of chemical shifts is quite formidable, and no good theory is available. A consideration of the temperature dependence of chemical shifts should be much more sensitive to strictly structural effects. In that respect, Bunzl (*2*) showed that structural effects cannot be detected in the excess near infrared absorption of salts in aqueous solution but that

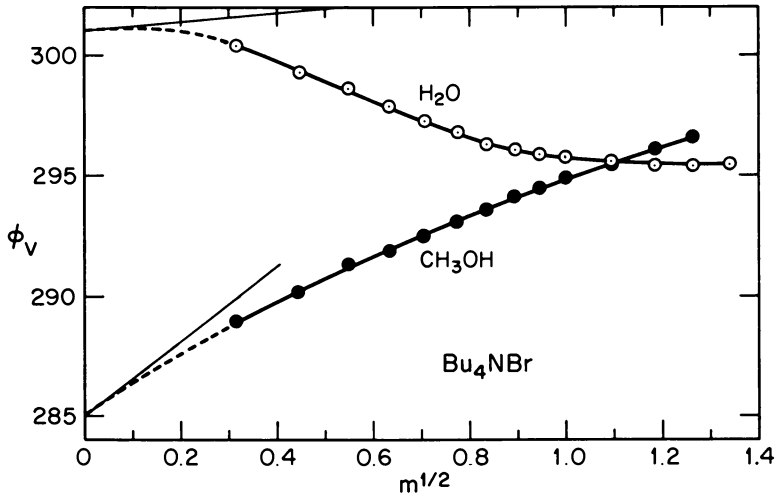

Figure 8. The concentration dependence of the apparent molar volumes of Bu_4NBr in aqueous and methanol solutions at 25°C.

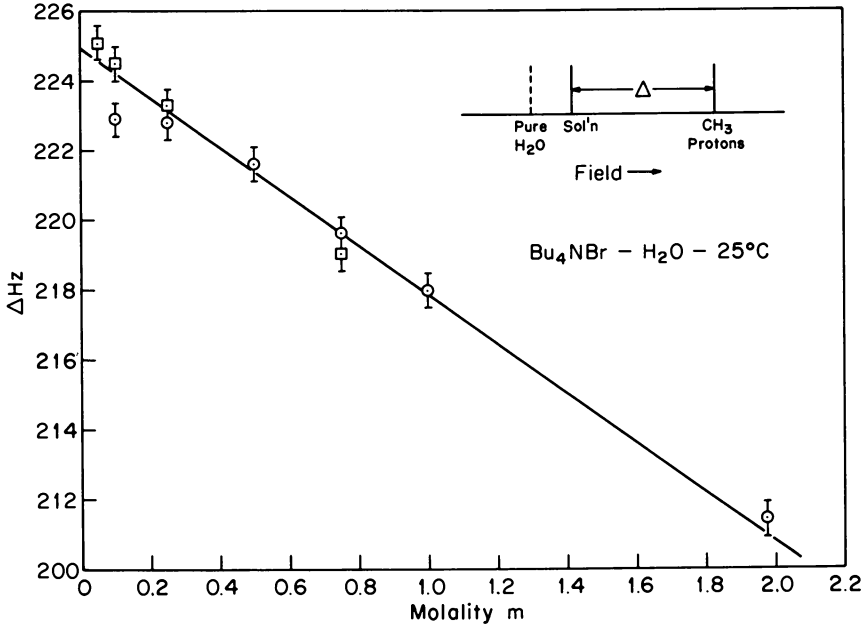

Figure 9. The effect of concentration of Bu_4NBr on the proton chemical shift in water

such effects are quite distinct in the temperature dependence of such absorption measurements.

Up to this point, only symmetrical ions have been considered, although structural effects can also be identified in the case of unsymmetrical ions. For instance, all the atoms in the NO_3^- ion are planar and consequently this ion can be a structure-breaker in the planar direction but an electrostrictive structure-maker at 90° to the plane. Thus, this ion could be said to be polyfunctional. As it turns out, the NO^-_3 ion is a net structure-breaker as shown in Figure 6. The cationic $CH_3–(CH_2)_n–N^+–(CH_3)_3$ and anionic $CH_3–(CH_2)_n–SO_4^-$ surfactants can also be polyfunctional, but as n becomes large, they should be net hydrophobic structure-makers (*8*). Another class of polyfunctional ionic species are the dipolar ions such as the amino acids,

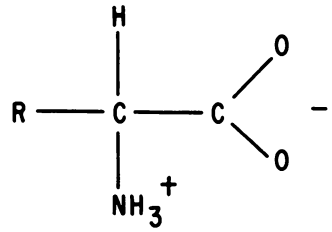

Such ions have been shown to be structure-breaker if R = H (glycine), but as R becomes butyl or larger, these dipolar ions have been shown to be net structure-makers (*27*).

Concluding Remarks

The advantages of studying structural effects by conductance measurements should be pointed out. They can be carried out rapidly with such a high degree of precision that even small effects can be detected with some confidence. Conductance data can be easily extrapolated to infinite dilution thereby eliminating ion-ion interactions as a complicating process. Perhaps the greatest advantage is the fact that with transference measurements, it is possible to determine the ionic rather than salt conductances. This permits cations and anions to be compared at any temperature without any kind of arbitrary split. Recently, a second unambiguous method of splitting has been introduced that enables ionic partial molar volumes to be obtained from ultrasonic vibration potential (*41*) without any arbitrary assumptions.

Acknowledgement

I wish to thank my associates, D. F. Evans, G. P. Cunningham, G. A. Vidulich, and D. G. Davis, who were responsible for carrying out most of the work described here. I am grateful to the Office of Saline Water, U. S. Department of the Interior, for their continued support.

Literature Cited

(1) Born, M., *Z. Physik* **1**, 45 (1920).
(2) Bunzl, K. W., *J. Phys. Chem.* **71**, 1358 (1967).
(3) Cunningham, G. P., Evans, D. F., Kay, R. L., *J. Phys. Chem.* **70**, 3998 (1966).
(4) Cunningham, G. P., Hales, B. J., Kay, R. L., *J. Phys. Chem.* **71**, 3925 (1967).
(5) Davis, D. G., Kay, R. L. (unpublished data).
(6) Einstein, A., *Ann. Physik* **19**, 289 (1906).
(7) *Ibid.*, **34**, 591 (1911).
(8) Evans, D. F., Cunningham, G. P., Kay, R. L., *J. Phys. Chem.* **70**, 2974 (1966).
(9) Evans, D. F., Kay, R. L., *J. Phys. Chem.* **70**, 366 (1966).
(10) Frank, H. S., "Chemical Physics of Ionic Solutions," p. 60, B. E. Conway, R. G. Barrados, eds., John Wiley and Sons, Inc., New York, 1966.
(11) Frank, H. S., Evans, M. W., *J. Chem. Phys.* **13**, 507 (1945).
(12) Frank, H. S., Wen, W. Y., *Discussions Faraday Soc.* **24**, 133 (1957).
(13) Fuoss, R. M., *Proc. Natl. Acad. Sci.* **45**, 807 (1959).
(14) Greyson, J., *J. Phys. Chem.* **66**, 2218 (1962).
(15) *Ibid.*, **71**, 2210 (1967).
(16) Gurney, R. W., "Ionic Processes in Solution," Chapters 4 and 9, McGraw-Hill Book Co., Inc., 1953.

(17) Haggis, G. H., Hasted, J. B., Buchanan, T. J., *J. Chem. Phys.* **20,** 1452 (1952).
(18) Harned, H. S., Owen, B. B., "The Physical Chemistry of Electrolytic Solutions," 3rd Ed., p. 240, Reinhold Publishing Corp., New York, 1958.
(19) Hertz, H. G., Spalthoff, W., *Z. Elektrochem.* **63,** 1096 (1959).
(20) Hertz, H. G., Zeidler, M. D., *Ber. Bunsenges. Physik. Chem.* **67,** 774 (1963).
(21) *Ibid.,* **68,** 821 (1964).
(22) Horne, R. A., Johnson, D. S., *J. Phys. Chem.* **70,** 2182 (1966).
(23) Jones, G., Dole, M., *J. Am. Chem. Soc.* **51,** 2950 (1929).
(24) Kaminsky, M., *Discussions Faraday Soc.* **24,** 171 (1957).
(25) Kavanau, J. L., "Water and Solute-Water Interactions," Holden-Day, Inc., San Francisco, 1964.
(26) Kay, R. L., Evans, D. F., *J. Phys. Chem.* **69,** 2416 (1965).
(27) *Ibid.,* **70,** 2325 (1966).
(28) Kay, R. L., Vituccio, T., Zawoyski, C., Evans, D. F., *J. Phys. Chem.* **70,** 2336 (1966).
(29) Lewis, G. N., Randall, M., "Thermodynamics," 2nd ed., p. 378, K. S. Pitzer, L. Brewer, eds., McGraw-Hill Book Co., Inc., New York, 1961.
(30) Lorenz, R., *Z. Physik Chem.* **37,** 252 (1910).
(31) Nightingale, E. R., Jr., *J. Phys. Chem.* **63,** 1381 (1959).
(32) Padova, J., Abrahamer, I., *J. Phys. Chem.* **71,** 2112 (1967).
(33) Pauling, L., "The Nature of the Chemical Bond," Chap. 10, Cornell University Press, 1940.
(34) Robinson, R. A., Stokes, R. H., "Electrolyte Solutions," 2nd Ed. Revised, p. 125, Butterworths, London, 1959.
(35) Schuster, R. E., Fratiello, A., *J. Chem. Phys.* (in press).
(36) Vidulich, G. A., Cunningham, G., Kay, R. L. (unpublished data).
(37) Walden, P., *Z. Physik Chem.* **55,** 207 (1906).
(38) *Ibid.,* **55,** 246 (1906).
(39) Wen, W. Y., Saito, S., *J. Phys. Chem.* **68,** 2639 (1964).
(40) *Ibid.,* **69,** 3569 (1965).
(41) Zana, R., Yeager, E., *J. Phys. Chem.* **71,** 521 (1967).
(42) Zwanzig, R., *J. Chem. Phys.* **38,** 1603 (1963).

RECEIVED July 25, 1967.

2

Anions in Aqueous Solution

JACK L. LAMBERT

Kansas State University, Manhattan, Kan.

Recent innovations and improvements in methods for the determination of trace concentrations of common anions in water are reviewed and speculations are made regarding future research in this area. Most noteworthy are potentiometric methods utilizing ion-selective electrodes, which may replace many chemical methods in situations where repetitive analyses must be made. The most interesting developments among the more conventional types of analyses are spectrophotometric methods involving ion association compounds in ion exchange, solvent extraction, and reverse solvent extraction procedures. The possibility of increasing the sensitivity of spectrophotometric methods by chemical amplification of the absorbing species has received some attention recently. Fluorimetric methods for anions are few but the area is an attractive one for study because of the extreme sensitivities attainable.

We are interested in anions because of their possible biological or corrosive effects. Even if they are present in such small concentrations that they are essentially harmless, they may indicate sources of pollution where they may be in sufficient concentration to concern us. Since it would be impossible and probably pointless to attempt to discuss all anions or even all types of anions here, this paper will be restricted to those which are stable in the presence of dissolved oxygen and which are found in natural waters, and domestic and industrial water supplies. Specifically, the anions to be included will mainly be those covered in the "Standard Methods for the Examination of Water and Waste Water." The literature reviewed is that from 1960 to the present, with some discussion of earlier work where necessary.

The current literature on anions in aqueous solution continues to be concerned largely with methods for their determination, with much effort directed to the development of more sensitive, more convenient, or more selective methods of analysis. The physiological effects of a few anions in trace concentrations, such as fluoride, phenolate and its numerous derivatives, and the phosphates of biological interest, continue to attract the attention of biochemists. Since very little new information has come to light regarding the corrosive or anti-corrosive effects of trace concentrations of the anions with which this paper is concerned, the main concern of this review will be the current status of trace analytical methods and possible new approaches. The treatment will be selective rather than comprehensive.

From the view point of analytical chemistry, the literature is well covered in various reference texts and reviews. A comprehensive review of the literature up to 1957 is contained in "Methods of Quantitative Inorganic Analysis," by Kazunobu Kodama (*18*). Another more detailed and selective book dealing only with anions is "Colorimetric Determination of Nonmetals," edited by D. F. Boltz (*6*). The *Analytical Chemistry* Annual Reviews Issue in April of each year is invaluable for complete surveys of the recent literature. For tested and reliable methods, the usual source is "Standard Methods for the Examination of Water and Waste Water," (*28*).

The desirable characteristics of any trace analytical method are appropriate sensitivity, convenience, speed, and selectively or specificity. The suitability of a method depends upon the purpose for which it is intended, and the competence of the analyst or operator. The continuous monitoring of an on-stream chemical process will call for electrical methods and meter readers or automated feed-back controls. On the other hand, intermittent and diversified checks may call for chemical methods and skilled chemists.

As any method of anion analysis may be applied if isolation techniques such as evaporation, precipitation, ion exchange, or solvent extraction are employed, we shall limit the discussion to direct methods and admit isolation techniques only if they are simple and rapid. The methods apparently best suited to the direct analysis of trace amounts of anions therefore are limited to selective membrane potentiometric, atomic absorption, fluorescence, and spectrophotometric methods following oxidation-reduction or complexometric reactions, or solvent extraction. Most of the traditional analytical methods—gravimetric, titrimetric, emission spectrometric, and electrical methods involving oxidation and reduction are less suitable, as are most radioactive procedures including neutron activation analysis, except in special cases.

Recent Developments

Of the electrical methods which have received attention recently, the development of selective electrodes appears to hold the most promise. Rechnitz (*23*) has recently written a comprehensive review on this subject. Anion selective electrodes consisting of sparingly soluble salts imbedded in a silicone rubber matrix were first prepared and studied by Pungor and co-workers in Hungary (*20, 21*). Rechnitz described two electrodes of this type as indicator electrodes for the direct potentiometric measurement of sulfate ion, using barium sulfate as the salt in the silicone rubber matrix, and of iodide ion, using silver iodide (*7, 24, 25*). Frant and Ross (*11*) have reported an electrode which is specific for fluoride ion. Single crystals of some rare earth fluorides, such LaF_3, NdF_3, and PrF_3, are unique among crystalline materials in having a high electrical conductance. The electrode membrane described is a disk-shaped section of LaF_3 doped with Eu^{2+}. As LaF_3 has a K_{sp} of 10^{-29} (and a solubility of between 10^{-7} and $10^{-8}M$), no correction has to be made for the fluoride ion it introduces into solution. The electrode response is usable from 10^{-1} to $10^{-6}M$ (down to 0.01 p.p.m.) between pH 5 and 8. Hydroxide ion, being similar to fluoride in charge and ionic radius, is the only serious interference and can be eliminated by control of pH. The electrode also can be used as an endpoint indicator in the titration of fluoride ion by $La(NO_3)_3$ solution. In an advertisement in *Science* (*27*), Orion Research offered a new meter having specific electrodes for F^-, Ca^{2+}, Cu^{2+}, Cl^-, Br^-, I^-, and ClO_4^-, as well as total hardness and pH.

While flame photometry could be used for the determination of complex anions containing metals (although for the most part anions are nuisances at best in this technique), the companion technique of atomic absorption has been applied to selenium by Rann and Hambly (*22*). They have determined selenium in the 10 to 100 p.p.m. range, using the 2040 A. $3S \rightarrow 3P^1$ transition and a propane-air flame.

A specific and highly sensitive fluorescence method for cyanide ion has been reported by Guilbault and Kramer (*12*). It differs from many fluorescence methods, which involve the quenching of fluorescence by the anion being determined, by producing an as yet uncharacterized fluorescent compound through the reaction of quinone monoxime benzene sulfonate ester with cyanide ion. Thirty common and uncommon ions produce no interference with the reaction. The solution is excited at 440 mμ and the green fluorescence measured at 500 mμ. Cyanide ion can be determined down to 0.5 micrograms CN^- per ml., or 0.5 p.p.m.

The use of solid phase ion (or ligand) exchange reagents is a particularly promising area of research for spectrophotometric methods.

Typical of work in this area is the use of salts of chloranilic acid as selective ion exchange reagents. Chloranilic acid, 2,5-dichloro-3,6-dihydroxy-*p*-benzoquinone, was first reported as a reagent for the gravimetric determination of cations such as Ca^{2+} by Barreto (*2*):

$$Ca^{2+} + H_2Ch \rightarrow CaCh + 2H^+$$

Coutinho and Almeida (*9*) later used the insoluble silver salt as a reagent for Cl^-

$$Ag_2Ch + 2Cl^- \rightarrow 2AgCl + Ch^{2-} \text{ (absorbs at 332 and 530 m}\mu\text{.)}$$

Bertolacini, Barney, and Hensley, following the same line of reasoning in a series of papers, developed a method for sulfate ion using barium chloranilate (*5*), for chloride ion using mercuric chloranilate (*1*), and for fluoride ion using thorium chloranilate (*15*).

$$BaCh + SO_4^{2-} \rightarrow BaSO_4 + Ch^{2-}$$

$$HgCh + 2Cl^- \rightarrow HgCl_2 + Ch^{2-}$$

$$ThCh_2 + 6F^- \rightarrow ThF_6^{2-} + 2Ch^{2-}$$

Hayashi, Danzuka, and Ueno (*13*) described the use of the lanthanum salt for phosphate determination

$$La_2Ch_3 + 2PO_4^{3-} \rightarrow 2LaPO_4 + 3Ch^{2-}$$

These ion (or ligand) exchange reactions are subject to interferences which may have to be removed, and mixed water-alcohol solvents must be used to suppress the color of the blanks.

The solvent extraction of ion association compounds, in contrast to the use of solvent extraction for isolation and concentration of inorganic ions, is highly selective in nature. In general, cations of large size and low charge tend to form salts which have low solubility in water but sometimes greater solubility in organic solvents. The solubility characteristics of such compounds in aqueous solution has been discussed by Rich in a recent book (*26*), but an extension of this study to those compounds soluble in organic solvents is needed. It would appear that those which form ion association rather than crystal lattice compounds are insoluble in polar solvents and soluble in nonpolar environment. Examples of solvent extraction with spectrophotometric measurement for inorganic anions are the compounds formed by perchlorate ion with *tris*-(1, 10-phenanthroline)iron(II) cation (*31*), which is soluble in nitrobenzene

$$2ClO_4^-{}_{(aq)} + Fe(phen)_3{}^{2+}{}_{(aq)} \rightarrow \underset{\text{(sl. sol. } H_2O\text{)}}{Fe(phen)_3(ClO_4)_2 \text{ (red)}}$$

$$Fe(phen)_3(ClO_4)_2 \xrightarrow{\phi NO_2} \underset{\text{(sol. } \phi NO_2\text{)}}{[Fe(phen)_3(ClO_4)_2]^\circ \text{ (red)}}$$

and the compound formed between perchlorate and periodate ions and crystal violet (*14*), which are soluble in benzene. The characteristic color of the colored cation is carried over into the nonaqueous phase, perhaps with some shift in absorption caused by either ionic interaction or the influence of the extracting solvent.

A step further in the utilization of these solvent-extracted compounds is their use as reagents. Irving and co-workers (*8, 16*) have reported what they call a colored liquid anion exchanger based on this concept. They use a xylene-hexone solution of tetrahexylammonium erdmannate. Erdmannate ion is the yellow $[Co(NH_3)_2(NO_2)_4]^-$anion, which absorbs strongly at 353 mμ in aqueous solution. The exchange reaction is

$$NR_4^+E^-_{(org)} + ClO_4^-{}_{(aq)} \rightarrow NR_4^+ClO_4^-{}_{(org)} + E^-_{(aq)}$$

Perchlorate ion down to approximately 5 x $10^{-5}M$, or 5 p.p.m., displaces erdmannate ion at pH 6 to 10. Interferences from chlorate, chlorite, hypochlorite, nitrate, and nitrite can be eliminated by fuming the sample with concentrated hydrochloric acid after which the pH is adjusted to within the permissible bounds. A rather large blank correction must be made, but no significant effects were noted from variation in ionic strength over a considerable range.

Two similar methods for phosphate ion which involve an amplification reaction, solvent extraction, and reverse solvent extraction were described at about the same time by Umland and Wünsch (*29*) and Djurkin, Kirkbright and West (*10, 30*). An acidic solution containing the phosphate ion is treated with an excess of molybdate ion to form the phosphomolybdic acid, which is extracted into a water-immiscible solvent to free it of excess molybdate ion. The phosphomolybdic acid is then broken down and re-extracted by an aqueous basic solution and the molybdate ion determined colorimetrically through the use of 2-amino-4-chlorobenzenethiol or thiocyanate ion. The effective molar absorptivities of the reagents are 359,000 at 710 mμ. for 2-amino-4-chlorobenzenethiol and 150,600 at 470 mμ. for thiocyanate, which represent multiplication factors of 10 and 12, respectively, caused by phosphate: molybdate ratio in the extracted phosphomolybdic acid.

Research on soluble reagents for trace analysis of inorganic anions has been centered largely on the exchange of a ligand (usually colored) in a metal complex or chelate for a more strongly complexing anion from the sample solution. Many of the extremely sensitive and reliable methods for fluoride ion have been based on this idea. The widespread use of artificial fluoridation over the last two decades has prompted a large amount of research on methods for the determination of this anion. The Scott-Sanchis method, the Megregian-Maier method, and the SPADNS method all rely upon the displacement of a chelating dye anion from a

zirconium complex. The color of the displaced dye anion differs sufficiently from the color of the zirconium chelate to permit the determination of the fluoride ion concentration as a function of the decrease or change in hue of the solution. The study of reaction involving the formation of a colored double complex of Alizarin Complexan (3-aminomethylalizarin-*N*,*N*-diacetate or 1,2-dihydroxyanthraquinone-3-ylmethyl-*N*,*N*-diacetate), Ce(III) or La(III), and F^- resulted in a series of articles by West, Leonard and co-workers (*3*, *4*, *17*, *19*), and Yamura, Wade, and Sikes (*32*). Alizarin Complexan forms two usable chelates of composition 1:1 and 2.5:1 with Ce(III), which are red and which react to add F^- to form a blue double complex. The authors describe this as the first reaction reported in which fluoride ion forms a colored compound of which it is a part. The method is sensitive down to 0.1 p.p.m. F^- and is tolerant of most common interfering ions.

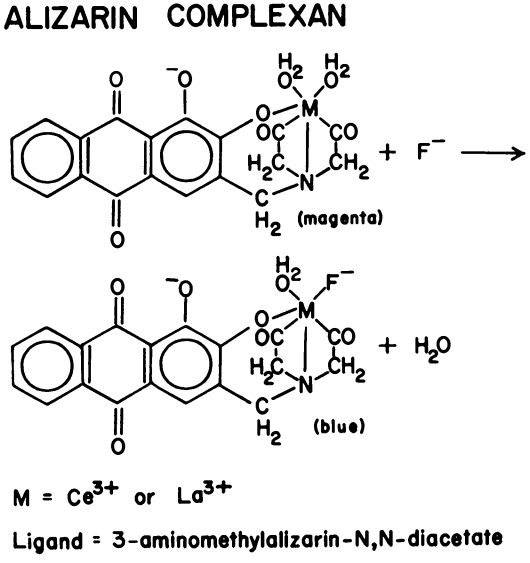

Promising Areas for Future Research

It is safe to predict that most of the emphasis on analytical research on methods for trace concentrations of anions in water during the next several years will continue to be on spectrophotometric chemical methods, and that interest in ion-selective electrodes for potentiometric analysis probably will continue to grow. It remains to be seen whether the scope of the latter method is limited. If these electrodes prove to be as simple and effective as reported, they may revolutionize the monitoring of water supplies and replace many chemical methods in situations where large numbers of repetitive analyses must be made.

Spectrophotometric procedures, including absorptimetric and fluorimetric, will continue to be popular and important because they can be sensitive and accurate, and because the necessary instruments are now familiar laboratory tools. Intrinsically, fluorimetric methods can be several orders of magnitude more sensitive than absorptimetric. To date, most direct fluorimetric methods are for the determination of metals, while anions are determined by their quenching action on fluorescent compounds. Hopefully, other new direct fluorimetric reagents for anions similar to the one described above for cyanide ion using quinone monoxime benzene sulfonate ester will be developed either as the result of chance observations or the application of increased fundamental knowledge of the fluorescence process. There probably will be few if any major advances in the quality of the instruments used in these methods; improved methods mainly will be the result of more sensitive and more selective analytical reagents.

An ideal analytical reagent for colorimetric analysis is one that reacts rapidly and specifically (or selectively) to produce a colored substance in direct proportion to the concentration of the ion being determined, with no interference from other substances likely to be present. A minimum of manipulative steps is desirable, both from the standpoint of economical use of the analyst's time and the decreased likelihood for error. The most convenient reagent would be one that is soluble in the sample solution and produces a colored substance that can be measured in solution or extracted into a water-immiscible solvent. Almost as convenient would be a water-insoluble compound used as a reagent by itself or dissolved in a water-immiscible solvent. In any case, a minimal blank is desirable. Examples of all these various types of reagents have been reported in the methods described above, and it is reasonable to suppose that more will be forthcoming.

Much of the research on analytical methods in recent years appears to have been influenced by concurrent trends in research in other fields of chemistry. For example, much of the work on colorimetric methods for anions has involved ligand exchange with metal complexes, which paralleled at a distance in time the research being done in inorganic chemistry. Most of the colorimetric methods for fluoride ion, the close control of which is important in the fluoridation of public water supplies, have been of this type. Selective solvent extraction of colored ion association compounds in analytical chemistry is an outgrowth of the research on solvent extraction for the isolation and purification of inorganic compounds. An increased interest in fluorimetric methods is becoming apparent as a consequence of photochemical studies in physical organic chemistry and theoretical work on molecular structure in physical chemistry and physics.

Much more study of ion association compounds involving inorganic complexes and organic dyes for absorptimetric and fluorimetric methods can be expected. Their selective solubility in organic solvents is another fertile field to be investigated. Dyes by themselves constitute a broad field for study. Much of the previous work on dyes has been on their uses in the textile and photographic areas and as biological stains, and the only commercially available dyes were those that had been found suitable for those purposes. For example, dyes for textiles generally have been designed for fastness to light, which is not a major consideration for their use in spectrophotometric methods. Only recently have analytical chemists begun in earnest to synthesize dyes tailored specifically to their needs. As an example of dyes useful primarily to analytical chemists are those to which an *N*-methyleneiminodiacetate group has been added for purposes of complexation. Research on ion association compounds truly should be interdisciplinary between all fields of chemistry.

It is never safe to make predictions regarding the future course of research—certainly not about the research of others, and seldom about one's own. As trace constituents in water become a greater concern of more people, and especially as support for studies in this area becomes more available, research is almost certain to take new and unexpected paths. What we can predict now is merely the probable course of events.

Literature Cited

(1) Barney, J. E., II, Bertolacini, R. J., *Anal. Chem.* **29**, 1187 (1957).
(2) Barreto, A., *Bol. Soc. Brasil. Agron.* **8**, 351 (1945).
(3) Belcher, R., Leonard, M. A., West, T. S., *Talanta* **2**, 92 (1959).
(4) Belcher, R., Leonard, M. A., West, T. S., *J. Chem. Soc.* **1959**, 3577.
(5) Bertolacini, R. J., Barney, J. E., II, *Anal. Chem.* **29**, 281 (1957).
(6) Boltz, D. F., ed., "Chemical Analysis," Vol. 8, Interscience Publishers, Inc., New York, 1958.
(7) *Chem. and Eng. News* **44**, No. 5, 24 (1966).
(8) Clifford, W. E., Irving, H., *Anal. Chim. Acta* **31**, 1 (1964).
(9) Coutinho, A., Almeida, M., *Anais Assoc. Quim. Brasil* **10**, 83 (1951).
(10) Djurkin, V., Kirkbright, G. F., West, T. S., *Analyst* **91**, 89 (1966).
(11) Frant, M. S., Ross, J. W., Jr., *Science* **154**, 1553 (1966).
(12) Guilbault, G. G., Kramer, D. N., *Anal. Chem.* **37**, 918 (1965).
(13) Hayashi, K., Danzuka, T., Ueno, K., *Talanta* **4**, 244 (1960).
(14) Hedrick, C. E., Berger, B. A., *Anal. Chem.* **38**, 791 (1966).
(15) Hensley, A. L., Barney, J. E., II, *Anal. Chem.* **32**, 828 (1960).
(16) Irving, H. M. H., Damodaran, A. D., *Analyst* **90**, 1073 (1965).
(17) Johnson, C. A., Leonard, M. A., *Analyst* **86**, 101 (1961).
(18) Kodama, Kazunobu, "Methods of Quantitative Inorganic Analysis," Interscience Publishers (John Wiley and Sons), New York, 1963.
(19) Leonard, M. A., West, T. S., *J. Chem. Soc.* **1960**, 4477.
(20) Pungor, E., Havas, J., Toth, K., *Acta Chim. Acad. Sci. Hung.* **41**, 239 (1964).
(21) Pungor, E., Havas, J., Toth, K., *Z. Chem.* **5**, 9 (1965).
(22) Rann, C. S., Hambly, A. N., *Anal. Chem. Acta* **32**, 346 (1965).
(23) Rechnitz, G. A., *Chem. & Eng. News* **45**, No. 25, 146 (1967).

(24) Rechnitz, G. A., "Abstracts of Papers" ACS Winter Meeting, 1966, **B 023.**
(25) Rechnitz, G. A., Kresz, M. R., Zamochnick, S. B., *Anal. Chem.* **38,** 973 (1966).
(26) Rich, R., "Periodic Correlations," W. A. Benjamin, Inc., New York, 1965.
(27) *Science* **155,** 34 (1967).
(28) "Standard Methods for the Examination of Water and Waste Water," American Public Health Association, Inc., New York.
(29) Umland, F., Wünsch, G., *Z. Anal. Chem.* **213,** 186 (1965).
(30) West, T. S., *Analyst* **91,** 69 (1966).
(31) Yamamoto, Y., Kotsuji, K., *Bull. Chem. Soc. Japan* **37,** 785 (1964).
(32) Yamura, S. S., Wade, M. A., Sikes, J. H., *Anal. Chem.* **34,** 1308 (1962).

RECEIVED April 24, 1967.

Some Effects of Trace Inorganics on the Ice/Water System

GERARDO WOLFGANG GROSS

New Mexico Institute of Mining and Technology, Socorro, N. M.

Trace inorganic impurities cause specific changes in the conductivity, dielectric constant and dielectric relaxation, thermoelectric power, mechanical relaxation, and the microstructure of ice. Most of these effects are explained by changes in the populations of ion defects and valence defects. The freezing potential (Workman-Reynolds effect) occurs when trace amounts (10^{-6}M to 10^{-3}M) of many inorganic and some organic salts are present in a freezing solution. Selective ion incorporation induces a charge layer at the advancing phase boundary. Its effect on the overall distribution of impurities between the phases is probably small. The distribution coefficient increases with freezing rate. For a given ion species and freezing rate it is a function of all impurity species present in solution, their concentrations, and the shape and surface structure of the phase boundary. Typical values of distribution coefficients for ionic solutes in ice range from 10^{-5} to 10^{-3}.

Trace inorganics are the cause of specific electrochemical phenomena at the phase boundary of growing ice; these are the freezing potential and the preferential incorporation into the solid phase of certain ions over others. The physical and chemical properties of the phases are more or less deeply affected by such interface processes. These processes raise fundamental questions concerning the mechanisms by which solute ions are incorporated into the ice structure and what their positions and effects are once they get there. This paper proposes to review these phenomena, the experimental evidence available, and the theories that have been formulated to account for them. A major difficulty in the critical evaluation of the data is their great sensitivity to the experimental conditions, which are difficult to define completely in most instances.

Excluded from consideration is the voluminous body of literature concerning heterogeneous reactions in three-phase and four-phase systems (vapor, liquid, solid, condensation nuclei), which particularly interest the atmospheric physicist. Also excluded are surface phenomena other than those referring specifically to an advancing ice surface.

The Ice/Solution Interface

Electrical currents and potentials specifically related to a phase change (heterogeneous reaction) were first described by Costa Ribeiro (*30, 31, 32*) and by B. Gross (*62, 64*). Costa Ribeiro investigated the phase-boundary potentials and currents that arise during the solidification of certain dielectrics, such as carnauba wax, and of water. He reported that the charge transfer was difficult to measure (by a Wulff single-string electrometer) if the dielectric contained conducting impurities. Costa Ribeiro called the phenomenon he discovered the *thermodielectric effect.* He observed that the rate of charge transfer was proportional to the rate of phase change.

Simultaneously and independently, Workman and Reynolds (*158, 159*) discovered and investigated the charge separation that takes place during the phase change at the ice/water phase boundary as a result of preferential ion incorporation. The samples grown by these investigators consisted of columnar aggregates of crystals oriented with the c-axis parallel to the direction of growth. In their classical paper (*158*), Workman and Reynolds described in detail the specific effects of ionic impurities on the sign and magnitude of the freezing potentials and currents. They showed that these depend not only on the type of ions but also on the concentration and pointed out the role of discharge currents but denied a dependence on freezing rate. Workman and Reynolds were particularly interested in these phenomena as a possible source of thunderstorm electricity. Their findings and conclusions were received with skepticism. Schaefer (*134*), however, confirmed their experimental results and coined the term *Workman-Reynolds effect.*

Subsequently, other investigators (*22, 56, 57, 109*) made experimental investigations of the Workman-Reynolds effect. B. Gross (*63*) made a theoretical analysis of the thermodielectric effect for a perfect insulator. Krause and Renninger (*96*) observed negative potentials of the order of hundreds of volts with respect to the solution on pentaerythritol crystals growing from a supersaturated solution. The potential appeared to be proportional to the crystal volume; thus, discharge currents appeared to be absent, or minimal, as in the model of B. Gross. Hence, the charging mechanism in this instance probably differed from that observed for ice. A melting potential of opposite sign was observed.

Mascarenhas (*115*) and Mascarenhas and Freitas (*116*) investigated the thermodielectric effect at the liquid-solid phase boundary of polycrystalline and oriented single crystals of naphthalene. They found that the charge transfer depended strongly on the impurity content (in contrast to Costa Ribeiro's findings, purification reduced it by a factor of 40). Single crystals showed up to 100 times higher charge transfer than polycrystalline aggregates. If the crystal were grown in the c-axis direction, the charge transfer was about 10 times higher than if growth took place in a direction of the basal plane. The charge transferred per unit mass was independent of solidification rate. For the ice/water system, Cobb (*26*) found that in lake ice impurity content depended on crystallographic orientation. However, no systematic laboratory studies have been made. The charge-mass ratio is definitely dependent on freezing rate (*66*).

Heinmets (*72*) investigated the freezing of solutions of HCl and KOH. Cobb (*27*) systematically studied the electrical freezing effects of a large number of ionic solutes as a function of concentration, of pH, and of electrode material. G. W. Gross (*65, 66, 67, 68*) investigated the effects of the freezing rate on freezing potentials and charge separation, the effect of the interface processes during ice growth on the d.c. conductivity characteristics of the solid phase, and the distribution coefficient. V. LeFebre (*104*) analyzed the potentials arising during ice growth and related them to the electrochemical reactions taking place at the phase boundaries. His model takes into account both the freezing rate and the finite ice conductivity.

The preceding discussion suggests that the Workman-Reynolds effect is one of a broad class of electrochemical phenomena connected with heterogeneous reactions. This does not imply that the charge transfer mechanism is the same in all cases. Electrons and holes may be involved in certain cases (*116, 127, 129*). Impurities create or modify electronic energy levels. By contrast, in the ice/water system, ions are the charge carriers. Thus, the conceptual distinction between the thermodielectric effect (in the freezing of nominally pure substances) and the Workman-Reynolds effect (in the freezing of defined aqueous solutions) should be maintained at least until such time as the mechanisms are better understood. In comparing the experiments made with water and with other dielectrics, such as waxes or naphthalene, it must further be borne in mind that water and ice have a comparatively high conductivity, even in the pure state, and this has important effects on the phenomena observed.

Phenomenological Description. Figure 1 shows a typical experimental setup for measuring freezing potentials and currents. The ice is grown on a platinum (or palladium) base or substratum that serves the double purpose of heat sink and electrical ground. A platinum electrode

dips into the solution. It is connected to an electrometer of high input impedance; *e.g.*, 10^{14} ohms. A low shunt resistance (10 K. in Figure 1) affords the means of creating a closed circuit for the flow and measurement of freezing currents. The current or potential are recorded on a strip chart.

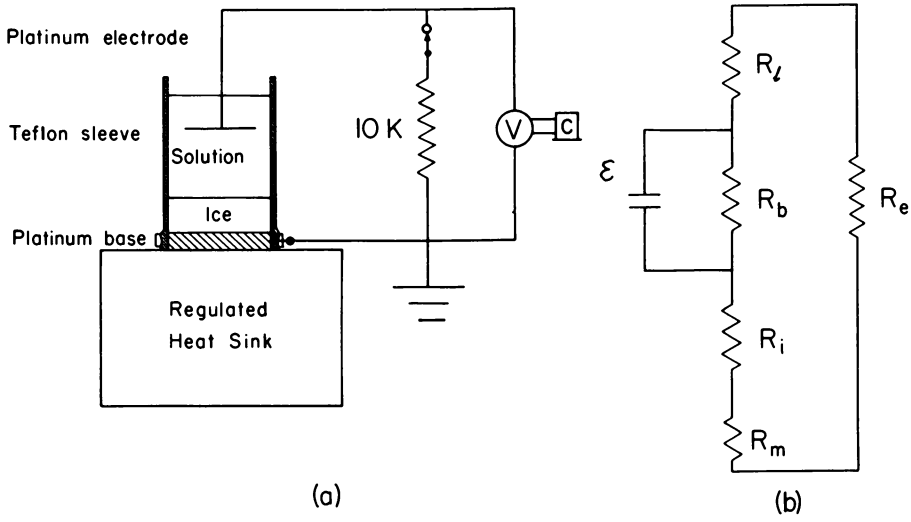

Figure 1. (a) Experimental arrangement for the measurement of freezing potentials (10 K. resistor not in circuit) and currents (10 K. resistor shunting the phases). V = electrometer; C = recorder. (b) Electric analog of the system in the shunt case. R_b *= interface barrier resistance;* R_e *= external shunt resistance;* R_l *= ice resistance;* R_l *= solution resistance;* R_m *= ice metal interface resistance;* ϵ *= interface charge separation*

If heat flow occurs through the base only, the freezing rate diminishes according to the relation

$$dx/dt = At^{-1/2}, \quad (1)$$

in which A is a constant that may be computed from heat-flow theory (23); x is the distance from freezing base to ice surface; t is time elapsed since freezing began.

For the experimental arrangement used by Workman and his coworkers, the interface generally is slightly convex.

G. W. Gross (68) has used an apparatus achieving constant freezing rates. For the purpose of this discussion, constant and declining freezing rates yield equivalent results.

After freezing begins, the potential (or current) rises to a maximum, then decays slowly. For a given solute, the shape and maximum value of the potential curve depend on the concentration at the interface and on the freezing rate. The instantaneous potential value at any moment is the algebraic sum of the potential drops of a charging current, caused by ion separation, and a neutralizing or discharge current through the phase boundary.

Figure 2 shows maximum freezing potentials as a function of ionic species and concentration. Figure 3 illustrates the freezing-rate and concentration dependence of the maximum potential.

On the basis of charge transfer characteristics, three groups of solutes may be distinguished.

In Group I, typified by the alkali halides and ammonium fluoride, the anion is preferentially incorporated into the ice. The solution electrode shows a positive potential with respect to the base. Highest potentials are typically observed for concentrations of the order of $10^{-5}M$ and range from 20 to 40 volts. For ammonium fluoride, however, the highest potential (*27, 67*) of nine volts occurs at a concentration of about $10^{-3}M$. Shunting of the interface by a 10 K-ohm resistor (external shunt) results in a freezing current that generally rises and decays faster than the open-circuit potential. Electrolytic production of hydrogen and oxygen gas occurs at the electrode and base, respectively (*27*). The maximum charge flow takes place at a concentration of about $10^{-4}M$, or 10 times as concentrated as for the highest potential. Thus, for example, Cobb measured 4.9×10^{16} electron charges per cubic centimeter of ice for a $3 \times 10^{-4}M$ KF-solution.

A similar shunting effect is obtained by placing platinum or palladium wires in the freezing container itself so as to cross the phase boundary (internal shunt).

For ammonium fluoride, Cobb measured a maximum of 0.25×10^{16} e/cm^3 for a concentration of $4.5 \times 10^{-4}M$ (a concentration more dilute than for the highest potential).

Group II comprises ammonium salts (except the fluoride) and lead salts. Ammonium carbonate, chloride, iodide, formate, acetate, and lead formate and nitrate were investigated by Workman and Reynolds (*158*) or by Cobb (*27*). The solution electrode gives a high negative potential (>200 volts for ammonium carbonate at $1.5 \times 10^{-5}M$) that decays more slowly than in Group I. Ion incorporation and charge transfer into the ice are extremely small, often below detectability limits. The concentration dependence of the freezing potential is much smaller than in Group I. Shunting the interface with a low resistance does not increase the charge transfer.

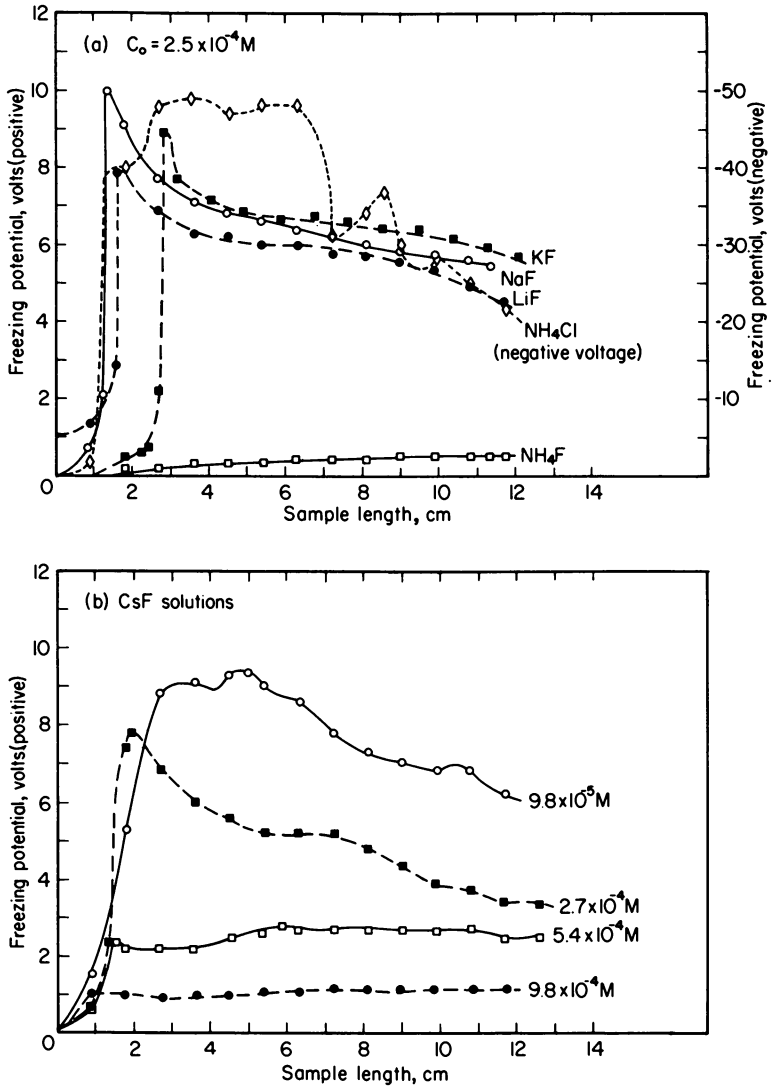

Figure 2. Freezing potential curves for different ionic species (a) and concentrations (b). Freezing rate was 5 microns a second. Ionic distributions for the 2.5 × 10^{-4}M solutions (except NH_4Cl) are shown in Figure 10. Potential of NH_4Cl solution is negative with respect to the ice, all others are positive

Group III consists of the halogen acids and of carbonate-free bases of the alkali metals, carbonate-free ammonium hydroxide, and pure water. This writer has investigated HF and HCl at constant freezing rates and observed a small potential, of a few tenths of a volt, with the

solution electrode negative. This potential builds up rather slowly, then remains constant (in contrast with the true freezing potential, which declines). It is interpreted as a diffusional potential, determined by the thermal gradient in the sample and by the greater diffusion coefficient of the hydrogen ion (*13*). More dissociation takes place at the warm end and more hydrogen ions diffuse from the warmer to the colder end of the sample than in the reverse direction. Latham and Mason (*102*) theoretically and experimentally investigated these potentials, and Cobb (*27*) investigated carbonate-free ammonium hydroxide. He reported a potential of only 0.1 volt. Pure water does not show potentials other than those related to thermal gradients. The slightest amount of impurity may, of course, induce freezing potentials. Especially, such spurious potentials may be caused by traces of ammonia plus carbon dioxide that either remained in the distilled water or were absorbed from the atmosphere; tobacco smoke is a source of ammonia.

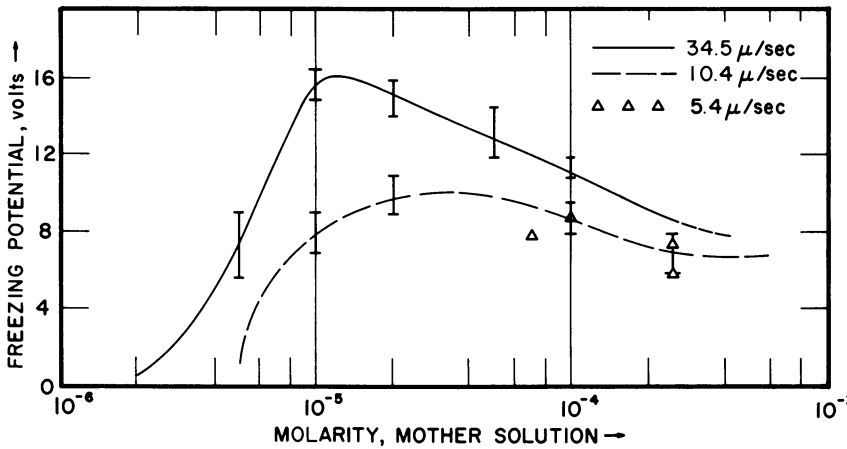

Figure 3. Dependence of the maximum potential on the freezing rate and concentration. Potassium fluoride solutions (68)

Chemical and Charge Balance. The terms ion, and ion incorporation, used in this paper, refer primarily to analysis results obtained from the melted ice phase and from the supernatant liquid. It does not necessarily follow that these impurities actually exist as ions in the solid phase.

GROUP I SOLUTES. The anion is preferentially incorporated into the solid. Charge balance is restored by hydrogen ions. Cations rejected into the solution are neutralized by hydroxide ions. The number of hydrogen ions transferred into the ice equals, within experimental error, the number of charges transferred according to the current record. The difference between solute anions and solute cations in the ice increases

with decreasing freezing rate (Figure 4). The anion concentration in the ice, and therefore the over-all impurity content, is affected little or not at all by a low-resistance shunt (Figure 5) but the solute cation concentration decreases appreciably in favor of the hydrogen ion (Figure 6). This difference between samples grown with shunt and those without shunt decreases as the sample length (resistance) increases. It also decreases with increasing freezing rate (Figure 7). This suggests that the degree to which solute cations can be rejected by the solid phase depends on the rate at which hydrogen ions can be made available to restore electrical and chemical neutrality. For this neutralization current, the shunt provides an alternate path which under certain conditions has a lower resistance than the path through the interface (Figure 1). These conditions are low ice resistance and low ice/metal contact resistance. In Group I solutes, when these obtain, the electrolytic production of hydrogen ions at the ice/metal interface and of OH^- ions at the solution electrode is favored over the transfer of neutralizing hydrogen ions through the interface.

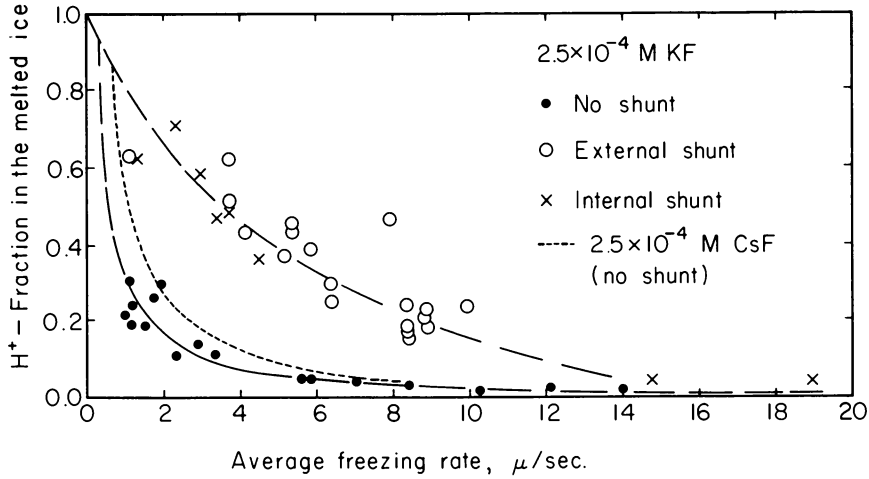

Figure 4. Hydrogen-ion fraction in the melted ice (ratio of hydrogen-ion concentration to all cations) as a function of average freezing rate for samples grown with or without a shunt at continuously decreasing freezing rates (66). *The solute cations are increasingly replaced by hydrogen ions as the freezing rate decreases*

When a shunt is used, two factors are important for the interpretation of results: (a) The external shunt resistance carries only a fraction of the total neutralizing current, depending on freezing rate and ice length. (b) For an ice of a given composition, the ice/metal contact resistance depends on the material of the base, the nature of the surface,

and the treatment of the surface. Carlin (*22*) and Cobb (*27*) found that electrolytic deposition of hydrogen on the base prior to freezing increases the charge transfer through the shunt. The ice/metal contact resistance is, in general, rather low for Group I solutes grown on platinum, palladium, or gold.

The effect of the shunt in Group I solutions may be interpreted in terms of an interface resistance which is virtually in parallel with the shunt resistance under the conditions specified above. Typically, the interface resistance is of the order of 10^6 to 10^8 ohms per cm^2 of interface (*66, 67*).

Cobb (*27*) showed that the freezing potential is very sensitive to pH changes of the solution. He found that, in general, the maximum potential was obtained between pH values of 7 and 8. This is also true for the Group II solutes.

GROUP II SOLUTES. With these, the cation is preferentially incorporated and neutralized by OH^- ions supplied from the solution. The solute anion, rejected in part into the solution, is neutralized by hydrogen ions. The high potentials in the Group II systems indicate a large interface resistance. Ion incorporation is much smaller than with most Group I solutes; frequently it is below the sensitivity of available analysis methods. Atmospheric CO_2 interferes with the process by reducing the number of available OH^- ions. In contrast to Group I solutes, a low-resistance shunt does not increase the neutralization current. LeFebre (*104*) showed the reason to be a high potential barrier at the ice/metal interface, comparable in size with the potential at the ice/water phase boundary (but opposite in sign). The presence of this high ice/metal contact potential makes it impossible to measure the true resistance of Group II ice.

GROUP III SOLUTES. No ion separation takes place with HF and HCl. The only difference between these two acids appears to be that, for a given mother solution concentration and freezing rate, the concentration in the ice is smaller for HCl. Basic solutions have not been systematically investigated under conditions ensuring absence of carbonates.

Discordant Results. Heinmets (*72*) observed potential transients from a few volts to close to 1000 volts when freezing HCl solutions on a mercury base. The maximum potentials were observed for solutions of $10^{-6}M$. The solution electrode was platinum. The potential transients lasted from a few minutes to 15 minutes. He concluded that the hydrogen ion is incorporated preferentially into the ice but he did not suggest a mechanism by which charge balance would be maintained. Reproducibility, according to Heinmets, was poor.

Parreira and Eydt (*122*), working with solutions of NaCl (a Group I impurity), found that at concentrations below $10^{-5}M$ the potential sign changed, the ice becoming positive. The numerical values of potential

in this dilute region were much higher (70 volts at $10^{-7}M$) than in the region above $10^{-5}M$ (a maximum of about 10 volts for $2 \times 10^{-4}M$). Reproducibility was good. Bi-distilled water (conductivity of 1.2×10^{-6} mhos. per cm.) gave potentials of 75 volts (ice positive). Workman and Reynolds (*158*) reported a similar change in potential with concentration and attributed it to residual ammonia in the water.

Levi and Milman (*107*) measured freezing potentials of $7 \times 10^{-7}M$ to $7 \times 10^{-5}M$ NH_4OH solutions and $4 \times 10^{-4}M$ NaCl solutions at several approximately constant freezing rates (2.8 to 26.7 microns a second). They found a concentration and freezing-rate dependence of the potential similar to those discussed here. Their potentials did not diminish with time. For NH_4OH, this may be explained by the very high ice resistance. For NaCl ice, perhaps, the runs were not long enough. Concentration dependence implies a time dependence because of the concentration buildup at the interface. Differential ion segregation was not observed for NaCl ice because measurement errors were $\leq 10\%$, a circumstance also pointed out by De Micheli and Iribarne (*36*). Differential ion segregation frequently is smaller; it is the difference between two relatively large numbers and therefore is best determined by careful pH measurements.

Discussion of Interface Models. THE WORKMAN-REYNOLDS MODEL. These authors did not publish a detailed theory to account for the electrical effects described. Their ideas are disseminated through papers and private research reports (*157, 158, 159*) and have been summarized by Loeb (*110*). Drost-Hansen (*41, 42*) recently gave a detailed discussion. Water being one of the most polar molecules known, Workman and Reynolds suggested that the incorporation of foreign ions into its structure reduces the energy of its crystal form and leads to the formation of a nonpolar crystal. It is well known that minute traces of foreign substances help in the condensation and freezing of water. Workman and Reynolds postulated, furthermore, that the electrical polarity of ice during growth is determined in some measure by conditions of the substratum prior to freezing. The solid substratum exerts an orienting effect on the adjacent liquid layer. This influence is propagated for at least a millimeter into the crystal grown on the substratum. The dipole field of oriented water molecules in the initial ice layer, according to this concept, accounts for the selective incorporation of ions of one sign into the growing ice. Under the influence of this dipole field, liquid molecules adjacent to the phase boundary are also oriented; selective incorporation of ions thus continues while ice growth continues. The authors conceived the interface structure as a double layer formed by ions selectively adsorbed at the ice surface, layers of oriented water dipoles, and a diffuse

ionic layer in the liquid. The thickness of this double layer would be of the order of hundreds of Angstrom units.

Two difficulties remain to be explained: the change of polarity of Group II electrolytes compared with those of Group I and the energy requirements for ions to cross the potential barrier at the interface.

POLARITY OF THE PHASE BOUNDARY. Workman and Reynolds explained the change of polarity by assuming that the dipole orientation depends on the ions present in the solution. Thus, the ions best suited to the ice structure will always be accommodated regardless of sign. In the beginning of freezing, a polarity reversal is sometimes observed. This was interpreted to mean that the initial dipole orientation, perhaps determined by the substratum as pointed out above, changes to accommodate the solution composition. Such reversals can, under certain conditions, be induced at will by growing ice of one sign (say, of a Group I solution), then pouring off the solution and replacing it by one of the opposite sign (Group II). It is observed that, when the growth resumes, the polarity remains at first that of the substratum ice (*126*). (However, an instantaneous polarity reversal occurs when a cold Group I solution is poured onto a Group II ice. This sheds doubt on the validity of the above argument concerning the influence of the substratum.)

Camp (*19*) investigated the morphology of ice growth on different substrates (glass, aluminum, Lucite, gold) and concluded that the two dominant factors determining interfacial ice structure are the temperature of the interface and the material of the substratum, but not its thermal properties. It is not known if the different ice morphologies described by Camp correspond also to differences in the electrochemical interface phenomena.

Fletcher (*50, 51; see 42* also) concluded on the basis of thermodynamic arguments, that an ice surface can not have a surface orientation because of the large loss of configurational entropy that this entails. The surface energy may, however, be lowered if the surface is covered by a thin water layer or quasiliquid film in which a transition from molecular dipole orientation to the "normal random ice surface" can take place. Fletcher showed that the dipole charge on this layer should be negative. These investigations apply to the static ice surface.

It is conceivable that the presence of ionic impurities in the solution during ice growth provides an alternate or concurrent means of surface relaxation of fast growing ice crystals, as proposed by Workman and Reynolds; or perhaps Fletcher's oriented quasiliquid interface transition layer alone is the seat of the freezing potential.

DEPTH OF THE CHARGE LAYER. Workman and Reynolds pointed out that in their model the energy required for a single ion to cross the measured potential difference at the interface is equivalent to the latent

heat of 3000 water molecules or 200 to 300 times the total energy of attraction per molecule in ice. They spoke of a "large-scale collective action" at the advancing interface. To circumvent this difficulty, Gill and Alfrey (*57*) suggested that a small contact potential, of a fraction of a volt, at the ice/water interface causes the fixation of charges of one sign from the water. As the interface advances, this charge is frozen in, a new charged layer forms, and so on. Thus a volume distribution of charge is created. The total interface potential is the sum of a large potential drop across this volume distribution plus a small drop owing to the contact potential at the phase boundary proper. Thus, the energy requirements for differential ion incorporation would be much smaller than with the Workman-Reynolds model. LeFebre (*104*) showed experimentally that the concept of a volume distribution of charge adjacent to the interface is correct. He allowed the interface to move past a very fine wire electrode. From the potential decay curve and the freezing rate he was able to compute a rough order of magnitude for the depth of the charged layer, 0.1 cm. under the particular experimental conditions. From this he went on to show that, for a total potential drop across the interface of 200 volts and for an actual phase boundary of the order of 10^{-7} cm. deep, the potential barrier at the phase boundary is of the order of 10^{-4} volts. From this, and making use of rate theory, he concluded that the effect of the interface potential on the distribution coefficient of the preferentially incorporated ion (*see* Impurity Distribution in the Ice) is small (the calculated difference was of the order of 2%), a fact that had been found experimentally by G. W. Gross (Figure 5, and (*66*)).

INTERFACE MODELS OF B. GROSS AND V. LEFEBRE. B. Gross (*63*) gave a theoretical treatment in which he showed that preferential ion incorporation because of different potential barriers and energy levels for positive and negative ions gives rise to a frozen-in space charge on the solid side and a surface charge on the liquid side of the phase boundary; this accounts for the large potentials and the interface currents. This treatment is valid only for nonconductors.

Lefebre's model (*104*) takes into account the finite ice conductivity by representing the interface as a capacitance shunted by a resistance and a charge generator. He expresses the rate of charge addition to the ice phase as a function of unequal distribution and diffusion coefficients for cations and anions, of the ion distribution in the solution, and of freezing rate. Assuming a charge distribution function for the volume charge, one can then find an expression for the potential as a function of charge density at the phase boundary and approximate the charge distribution by a parallel-plate capacitance. Its magnitude and plate separation can be expressed in terms of the interface potential, the thickness of the charged layer (measured quantity) and the charge distribution function

(assumed). Next, the discharge currents can be expressed as a function of charge density and interface resistance. Similar expressions can be formulated for the ice/metal interface and the potential drop through the internal ice resistance. It is now possible to compute freezing potential curves and to relate the difference between the cationic and anionic distribution and diffusion coefficients, the freezing rate, and the interface resistance to the time and magnitude of the potential maximum. Independent measurements of some of these parameters (such as, for instance, the distribution coefficients) would be required to verify and refine the theory.

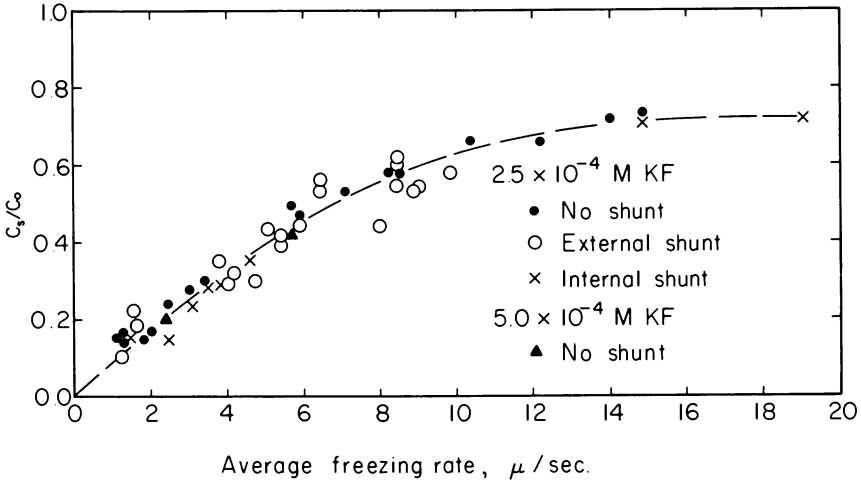

Figure 5. Anion distribution curve for KF solutions grown at continuously decreasing speeds with or without a shunt (66). *C_s = concentration in melted ice (room temperature); C_0 = mother solution concentration. This curve suggests that the large interface potential (of the order of 5 to 20 volts, depending on freezing rate) has but a small effect on over-all solute partition*

THE MODEL OF R. G. SEIDENSTICKER. This model (*138*) treats ice as a protonic semi-conductor. Fluorine and nitrogen, substituting for oxygen in ice, act as proton donors and acceptors, respectively. Specific energy levels are associated with the characteristic proton configurations (valence defects and ion defects, to be discussed later) created by thermal motion or associated with these impurities. Seidensticker's model qualitatively explains the freezing potential and the sign reversal depending on the type of impurity. The polarization of the interface (positive or negative) depends on the ratio of interface states to interface oxygen sites. Normally bonded interface water dipoles present a negative charge to the interface. An interface state is characterized by an oxygen atom with

two associated protons, only one of which forms a hydrogen bond to neighboring oxygen atoms and therefore presents a positive charge to the interface. Their number is small if HF is the impurity; surface polarization is negative. Their number is large with ammonia, and the interface is positively polarized. If the number of surface states is exactly one-half of the available surface sites, the polarization is zero. This generalized qualitative model does not in its present state account for the fact that only salts but neither their acids nor their bases give a freezing potential. Seidensticker points out that for a quantitative evaluation of the interface dipole potential two further steps are necessary: (1) a detailed system of proton interface levels must be constructed; (2) the effects of interface electron configurations must be analyzed.

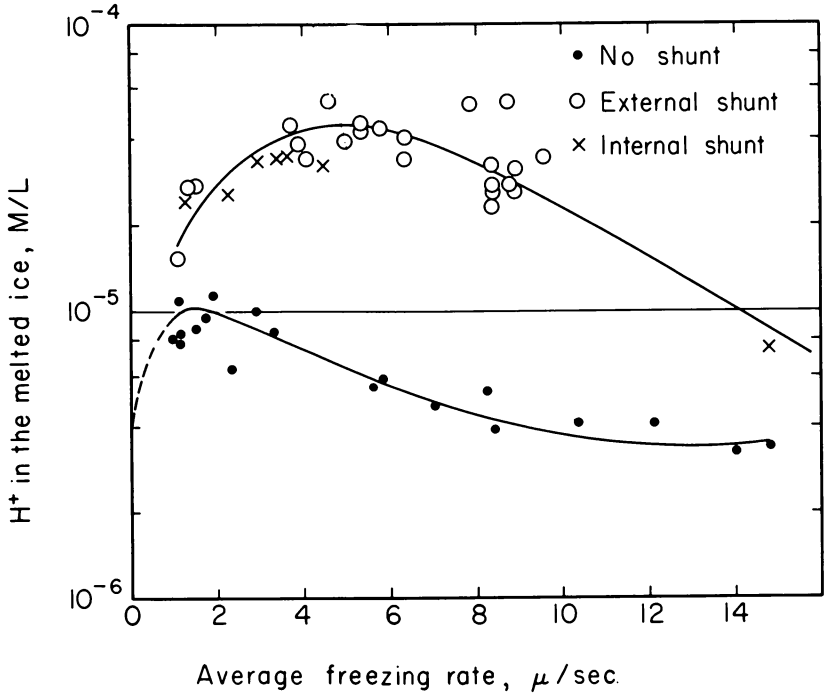

Figure 6. Hydrogen-ion concentration in the melted ice as a function of average freezing rate for ice grown from 2.5 × 10^{-4}M KF solution at continuously decreasing speeds with and without a shunt (66)

Even if cationic and anionic distribution coefficients are identical, charge separation processes can still occur at the advancing surface because of the difference in diffusion coefficients. Actually, both distribution and diffusion coefficients differ for anions and cations, and are a

function of concentration. This makes the analysis and interpretation very complicated.

Summing up, Workman and Reynolds conceived the presence at the ice/water interface of a dipole field (microscopic field) that attracts ions of one sign thus generating the freezing potential (macroscopic field). The dipole field is continually regenerated as the phase boundary advances. The same result is achieved by Gill and Alfrey's contact potential. The magnitude of the macroscopic field can be estimated from freezing-potential experiments; that of the microscopic field is unknown. The models of B. Gross and LeFebre consider in detail the freezing potential and relate it to the transfer of ions across the phase boundary. They leave largely unexplained the cause for selective ion incorporation. Seidensticker's proton semiconductor model accounts for the freezing potential in terms of "interface states." Finally, differential diffusion is theoretically capable of producing the freezing-potential effect.

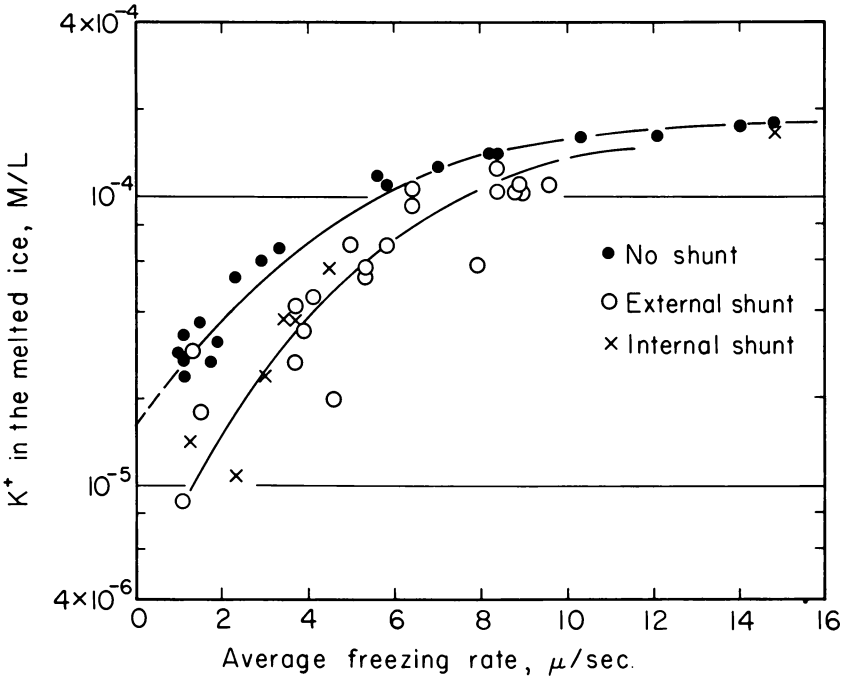

Figure 7. Potassium-ion concentration in the ice grown at continuously decreasing freezing speeds from 2.5 × 10⁻⁴M KF with or without a shunt (66)

NATURE OF INTERFACE PROCESSES. At least three processes must be considered in the analysis of the freezing potential phenomenon. They

are differential adsorption at the phase boundary, differential incorporation into the ice structure, and differential diffusion into the liquid away from the phase boundary. Theoretically each of these alone may perhaps account for the measurements, but the evidence suggests that they act in combination. Their relative importance cannot be fully assessed at this time; only the most general and qualitative discussion is possible.

DIFFERENTIAL ADSORPTION AT THE PHASE BOUNDARY. It is conceivable that the structurally complex region of charge separation that straddles the advancing phase boundary may start out as an ordinary ionic double layer (*32*). Thus, if one could produce such a double layer under equilibrium conditions and measure its potential as a function of ionic species and concentration, one might be able to determine the nature of the surface forces, the charge density, and the double-layer conductivity. Unfortunately, the best one can hope to produce experimentally is an ice/water interface in dynamic equilibrium, with melting and freezing going on simultaneously. An interpretation of such measurements would be difficult. Under actual experimental conditions, the nonequilibrium stems from two sources: first, the displacement of the interface due to ice growth and the consequent modification of the ion distribution in the solution and of the charge distribution in the ice adjacent to the phase boundary. A quasisteady state may be reached after a short time. Second, the neutralizing current passing through the interface. A fundamental issue is whether the charge separation is caused by "chemical" adsorption of ions at an originally uncharged phase boundary or whether it is determined by polar orientation of water molecules according to the Workman-Reynolds concept (*71*). This question could perhaps be answered if one could measure the equilibrium phase-boundary potential in a pure water/ice system. The charge density may be expected to depend on the mechanism of charge adsorption because the surface density of sites would presumably differ. The interface conductivity may be responsible for the decline of the potential maximum as the concentration increases beyond a certain value.

DIFFERENTIAL INCORPORATION INTO THE ICE STRUCTURE. Anions and cations are incorporated into the ice structure at different rates; *i.e.*, they have different distribution coefficients (*see* Impurity Distribution in the Ice). Differential incorporation may be contingent on differential adsorption as the initial step, but lattice as well as surface energy changes must be taken into account. Costa Ribeiro (*32*) suggested differential carrier transfer rates across the phase boundary as a source of the thermodielectric effect.

DIFFERENTIAL DIFFUSION. Distribution coefficients for ice are very small, of the order of 10^{-4} to 10^{-3}. Hence, a liquid boundary layer of high

concentration quickly builds up at the interface. Its shape (width and concentration amplitude) depend on the presence and intensity of convection. Assume that convection is absent or negligible. Solute transport away from the interface is then exclusively controlled by diffusion. If diffusion coefficients for anions and cations differ, the ion with the lower coefficient will be enriched relative to its counterion. Thus, a differential incorporation and the consequent charge imbalance (leading to the freezing potential) may occur even if the distribution coefficients for both ions are identical and/or if no preferential adsorption takes place at the equilibrium phase boundary. Deryagin and coworkers (*40*) showed that differential diffusion of ions in the vicinity and toward the surface of a moving particle may give rise to a diffuse or secondary double layer (*43*) and to an electrical potential independent of and perhaps superposed on the zeta potential (diffusional Dorn effect). The nonequilibrium feature is the most interesting aspect of this mechanism in connection with the freezing potential studies. An analytical relation has been shown to exist between electrokinetic nonequilibrium processes and the secondary double layer (*43, 44*). The freezing potential could perhaps be likened to a diffusional Dorn effect in reverse, since diffusion is away from rather than toward the phase boundary. However, the evidence discussed in the next section does not point to differential cation-anion diffusion as the principal factor in the process of selective ion incorporation. The available evidence suggests that of the three processes discussed, differential adsorption, differential incorporation, and differential diffusion, the dominant role is played by differential incorporation.

CONCENTRATION DEPENDENCE OF FREEZING POTENTIAL AND SHUNT CURRENT. As has been pointed out, in Group I solutes the freezing potential curve in any experimental run builds up to a maximum, after which it declines as the concentration on the liquid side of the phase boundary increases. The height of this maximum is itself a function of the initial solution concentration and shows a maximum value at an optimum concentration that depends on the particular solute.

If the surface charge density is a function of the surface alone, that is, if it is independent of solution concentration, the zeta potential also decreases with concentration (*139*). At the low concentration end, the potential must also decrease, perhaps when the concentration becomes so low that the surface sites exceed the number of ions available to fill them and the charge density therefore decreases.

It appears plausible that the freezing potential maximum corresponds to an optimum combination of adsorbed charge density and interface resistance. The charge transfer through an external shunt shows a similar maximum size at an optimal mother solution concentration, which averages 10 times the concentration giving the optimum freezing potential.

This maximum represents perhaps a maximum of the ratio of interface resistance to ice resistance.

Still another explanation of the decrease of maximum freezing potential with concentration is possible. As discussed later in this paper, interface morphology depends on the solute concentration and on the temperature gradient in the liquid at the interface. A cellular structure (and, eventually, formation of dendrites) is most likely to occur as the concentration is raised, other conditions (freezing rate and temperature gradient) remaining equal. Such a cellular or dendritic structure increases the transport of solute (Tiller's three-dimensional segregation, *see 149*). If concomitantly the rate of ionic neutralization were also increased (perhaps because of the larger interface area and, therefore, greater availability of neutralizing ions) the potential could be expected to decrease.

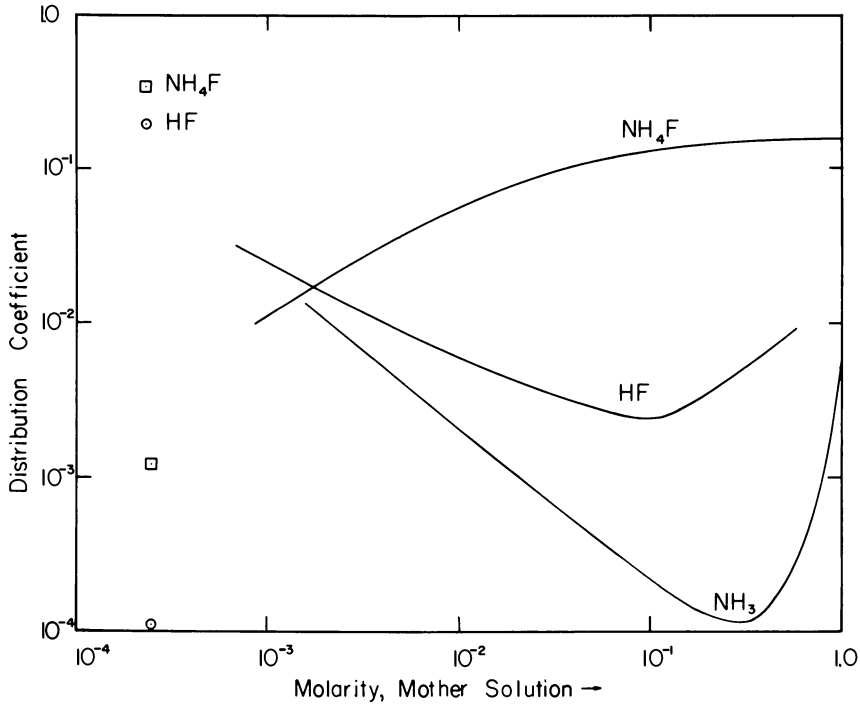

Figure 8. Concentration dependence of the distribution coefficient for NH_3, HF, and NH_4F after Jaccard and Levi (84). Two values, for 2.5 × 10^{-4}M HF and NH_4F, respectively, measured by G. W. Gross, are shown for comparison. The one for NH_4F lies tolerably close to the extension of Jaccard and Levi's curve; the HF point is about three orders of magnitude lower. See text for discussion

Contact Electrification. Reynolds, Brook, and Gourley (*126*) showed that if two pieces of pure ice of different temperature are brought into frictional contact, charge separation occurs, with the warmer ice acquiring a negative charge. If one of the two pieces of ice was made of $10^{-4}M$ NaCl, however, it would become negative even if it were several degrees colder than the piece of pure ice. The writers explained this phenomenon in terms of melting and refreezing of a liquid layer at the contact and the attendant charge separation according to the Workman-Reynolds effect. They calculated from their measurements that this mechanism could quantitatively account for charge separation in thunderstorms. Magono and Takahashi (*113*) made similar experiments with somewhat different results. Brook (*13*) described experiments suggesting that proton transfer from one ice piece to the other could also account for the observations without need for melting and refreezing. The determining factors are temperature gradient and proton concentration. Latham and Stow (*103*), working with pure ice, showed that the shape of the ice pieces, impact velocity, and contact time, are also factors of importance.

Takahashi (*143*) obtained less clear-cut charge separation effects when an ice rod was broken. This effect occurred even if no temperature gradient was present, and its magnitude depended on crystallinity (mono- or polycrystalline ice), bubble content, and temperature gradient.

(*See* further the discussion of thermoelectric effects in Miscellaneous Investigations.)

Impurity Distribution in the Ice

In the preceding section it was shown that differential ion transfer takes place at the phase boundary. This process can be modified by using a shunt resistance or by changing the solution pH or by altering the freezing rate. Differential ion transfer is a second-order phenomenon superimposed on the rejection, from the solid, of the major portion of all the impurities, anions and cations alike. Thus, the solute becomes distributed unequally between the phases. The parameter governing the distribution is the solute partition coefficient, interface distribution coefficient, or simply distribution coefficient, defined as

$$k = \frac{C_s(i)}{C_l(i)}, \tag{2}$$

where $C_s(i)$ is the solute concentration directly adjacent to the interface on the solid side and $C_l(i)$ is the concentration directly adjacent to the interface on the liquid side at any position of the phase boundary.

The coefficient, k, to be discussed in this section, is different from the thermodynamic equilibrium coefficient, k_o, obtainable only at rates slow

enough that no concentration gradients develop in the liquid phase (strictly satisfied only with a zero freezing rate, or, perhaps, intense stirring). For ice, $k > k_o$. Values of k_o can be extrapolated from actual measurements. The interface distribution coefficient increases with the freezing rate (*25, 111*). As a consequence of the process of rejection, as soon as freezing starts, the solute begins to build up in front of the advancing interface. A steady state will eventually be reached when the solute diffuses away from the interface as fast as it is rejected from the advancing phase boundary. Thus, the shape and width of this boundary layer of increased concentration (assuming no convection takes place) is a function of freezing rate, distribution coefficient, and diffusion coefficient of the solute. If the liquid column is "infinite," the solute concentration in the ice increases until the steady state is reached, at which point the concentration in the ice must equal the mother solution concentration before freezing started (*123*).

The effective distribution coefficient is defined as

$$k_{eff} = \frac{C_s}{C_o}, \tag{2a}$$

where C_o is the concentration of the bulk solution at a distance far away from the interface. In a column of infinite length, this is the concentration of the liquid before the start of freezing. The effective distribution coefficient is computed from experimental data. In the nonsteady state, it is a function of sample length. In the steady state it is equal to one provided there is no convection. From the preceding discussion it follows that in ice grown from a solution free of convection

$$k_o < k < k_{eff}$$

The interface distribution coefficient is a measure of the distortion the solute imposes on the lattice of the solid (*148*). The distortion is zero if $k = 1$. For ionic solutes in water, it is always very much smaller than one. This means that the solute weakens the binding between atoms, increasing their interatomic distances. Consequently, the melting point of the solvent is lowered.

In ionic crystals, trace element partition coefficients are inversely proportional to the ionic radius of the impurity ion. Nagasawa (*118*) obtained good agreement between experimentally determined coefficients and values calculated from the energy required for introducing the impurity ion into the host lattice, if the substituting ion was larger than the host ion. No such calculations have been made for ice.

Ionic distribution curves (Figures 9 to 17) are plots of the effective distribution coefficient (or of solute concentration in the solid) against sample length. They are used for evaluating the interface distribution coefficient (Equation 2).

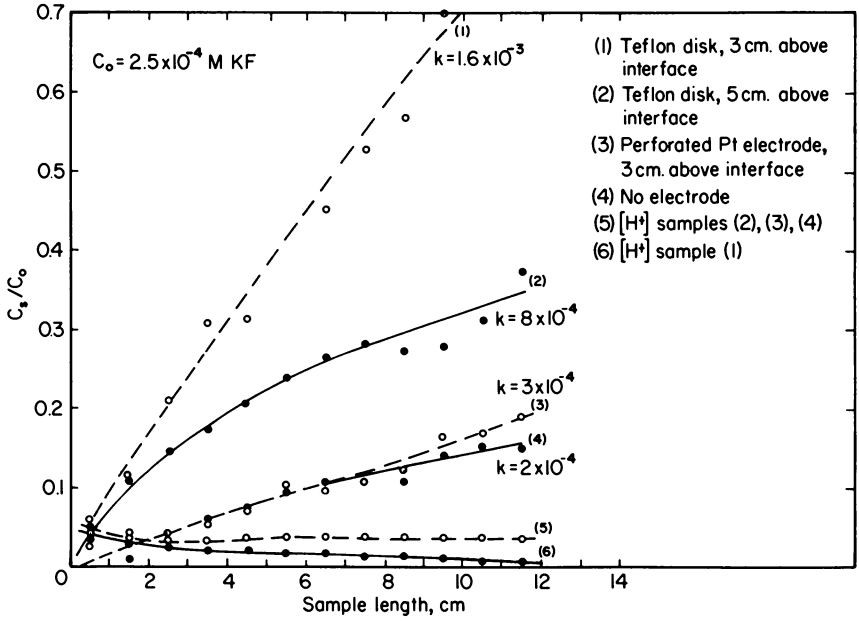

Figure 9. Effect of hindered diffusion on the solute distribution curves and the apparent distribution coefficient

Much experimental and theoretical work has been done on distribution coefficients of metals and semiconductors. Little information is available on distribution coefficients in the ice/water system.

Brill (*10*) and Zaromb and Brill (*162*) investigated aqueous solutions of NH_4F. Jaccard and Levi (*84*) studied NH_3, HF, and NH_4F and compared the experimental curves, most of them obtained with stirred solutions, with a theoretical analysis. G. W. Gross (*68*) made an experimental determination of the diffusion-controlled distribution coefficients for solutions of several fluorides and of HF. Blicks, Egger, and Riehl (*8*) investigated radial concentration gradients. Jaccard (*83*) made a theoretical analysis for radial concentration gradients as a function of interface curvature. The effect of thermal gradients in the liquid on the interface morphology and on the distribution of impurities in the ice phase have been studied, experimentally and theoretically, by Tiller (*144, 145, 146*), and by Harrison and Tiller (*69, 70*), who also determined distribution coefficients in ice at constant freezing rates.

Distribution Coefficient for a Diffusion-Controlled Process. Consider an interface advancing into a solution. If transport of the rejected solute occurs by diffusion only (no convection), the change of solution

concentration, c, with time and with distance, x', from the interface is given by

$$D\frac{d^2c}{dx'^2} + R\frac{dc}{dx'} = \frac{dc}{dt}, \tag{3}$$

where D = diffusion coefficient, R = rate of advance of the interface (rate of phase change). The distribution is assumed to be independent of the sample radius and the radial angle, which is strictly true only if the interface is horizontal (*see* discussion below). This equation has been solved for the four additional conditions: diffusion in the solid is negligible; k is constant; D is constant; the liquid column is infinite. Solutions have been published by Tiller, Jackson, Rutter, and Chalmers (*147*), by Pohl (*125*), and by Jaccard and Levi (*84*). Depending on the approximations and boundary conditions chosen, the three solutions differ slightly, but for the very small distribution coefficients encountered in ice (of the order of 10^{-4} to 10^{-3}), the resultant discrepancies are smaller than the experimental uncertainties.

For k small and D small (true in the ice/water system), Pohl obtained, for the concentration in the liquid at distance x' from the interface,

$$C_l(x',t) \simeq C_o\left\{1 + \frac{1-k}{k}\left[\exp\left(-\frac{R}{D}x'\right) - exp\left(-\frac{(1-k)R}{D}x'\right)\cdot exp\left(-\frac{(1-k)kR}{D}Rt\right)\right]\right\}. \tag{4}$$

Setting $x' = 0$ and $Rt = x$, distance from the starting point of crystallization, the composition of the solid becomes.

$$C_s(x) = kC_l\left(0, \frac{x}{R}\right) \simeq kC_o\left\{1 + \frac{1-k}{k}\left[1 - exp\left(-\frac{(1-k)kR}{D}x\right)\right]\right\}. \tag{5}$$

Curves computed from this relation may be compared with experimental curves obtained by plotting the solute concentration in the ice against sample length (*68, 84*).

Applicability to the Ice/Water System. This discussion concerns the restrictions imposed on the mathematical solution of Equation 3 as they apply specifically to the ice/water system.

Convection Negligible. Because of the temperature-density relationship of water, it is difficult, if not impossible, completely to exclude convection. The experimental evidence suggests, however, that if the temperature difference in the solution does not exceed 2°-3°C., the ion transport will be essentially diffusion-governed in the vicinity of the interface even with a freezing rate as low as 5 microns a second. Convection can theoretically be eliminated by letting the crystal grow downward into

or pulling it out from the melt (*92*). Because the heat flow is through the solid in this case, it is difficult to maintain a constant freezing rate, particularly in view of the low heat conductivity coupled with a high heat of fusion, characteristic of ice. For the same reason, a large range of freezing rates cannot be achieved with such a technique. This is in contrast to metals and semiconductors for which a practical technique has been described by Tiller and Rutter (*148*).

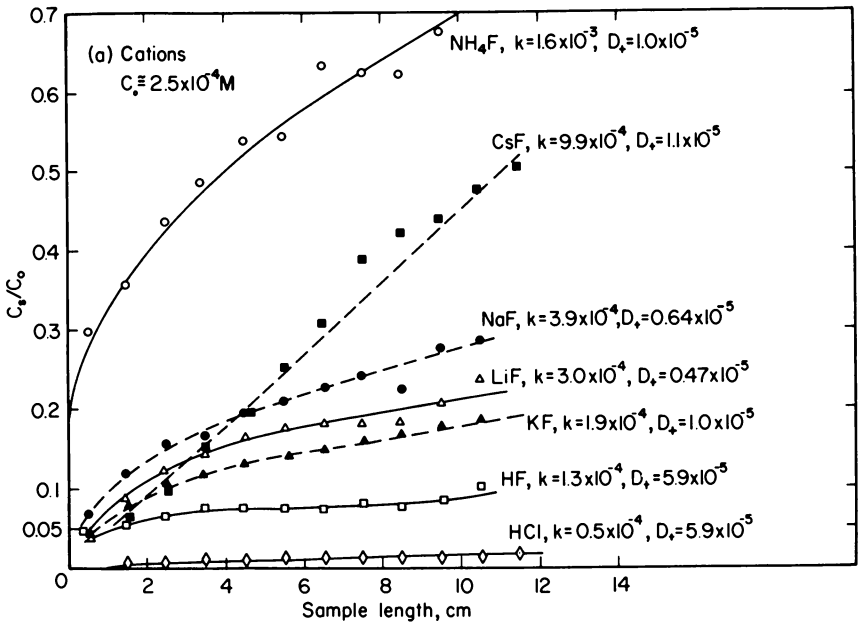

Figure 10. (a) Distribution curves for a 2.5 × 10^{-4}M solution of several fluorides and of HCl. Growth rate 5 microns a second. No stirring. No relation exists between the apparent distribution coefficients (k; *computed from the slope of the cation curve) and the diffusion coefficients of the cations* D_+

DIFFUSION NEGLIGIBLE IN THE SOLID. It is clear from diffusion studies (*11, 94, 140*) that for the present purpose diffusion in the solid may be neglected.

DISTRIBUTION COEFFICIENT CONSTANT. Investigations by Jaccard & Levi (*84*) and by G. W. Gross (*68*) indicate that k is more or less strongly concentration-dependent (Figure 8). Since D is also dependent on the concentration, the effects cannot be separated. At sufficiently high freezing rates, however, a quasisteady interface concentration is established quickly so that k and D may be considered as changing slowly.

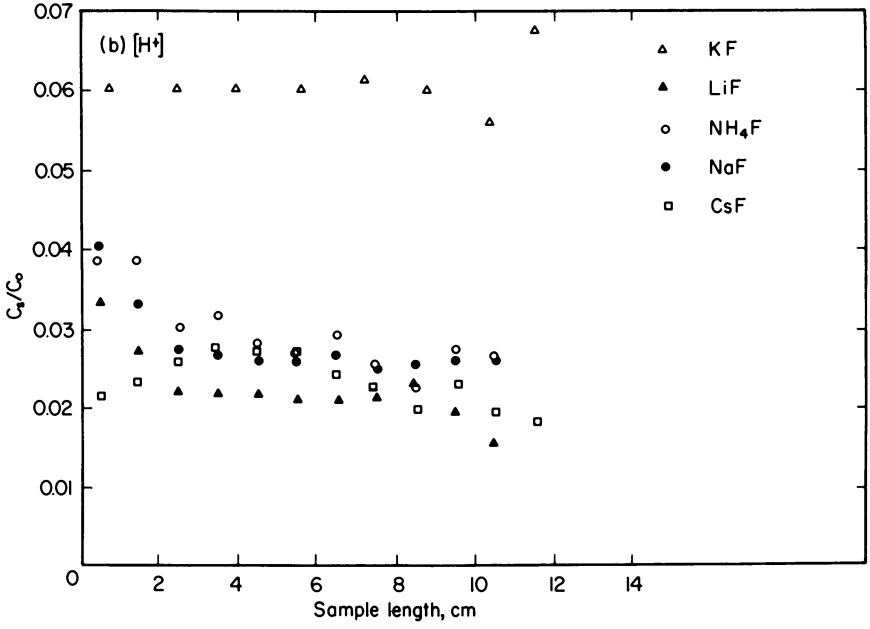

Figure 10. (b) Corresponding hydrogen-ion distribution curves. Freezing potential curves for some of these solutions are shown in Figure 2.

DIFFUSION COEFFICIENT CONSTANT. The diffusion coefficient is computed from the equivalent ionic conductance, λ,

$$D_{\pm} = \frac{300kT\lambda_{\pm}}{4.8 \times 10^{-10}|z_{\pm}|F}; \quad (6)$$

z = numerical value of valence (regardless of sign); F = Faraday; $\pm$ = pertaining to cation or anion, respectively. Typically, for the electrolytes under consideration, at 0°C., the diffusion coefficient decreases by about 30%, because of the change in mobility, as the concentration increases from infinite dilution to 1*M*, the interface concentration range that appears to encompass most, if not all, of the cases here under study. A further reduction, owing to nonideality of the solution in the vicinity of the interface (*87*), is probably present but cannot be assessed.

The average diffusion coefficient for an electrolyte is given by (*152*)

$$\overline{D} = \frac{|z_+| + |z_-|}{|z_+|D_+ + |z_-|D_-} D_+D_-. \quad (7)$$

This expression is used when dealing with an electrolyte on a macroscopic scale. When dealing with dimensions on the scale of the double layer, however, the difference between cation and anion mobilities may become important. Because of electrostatic interaction, their effective

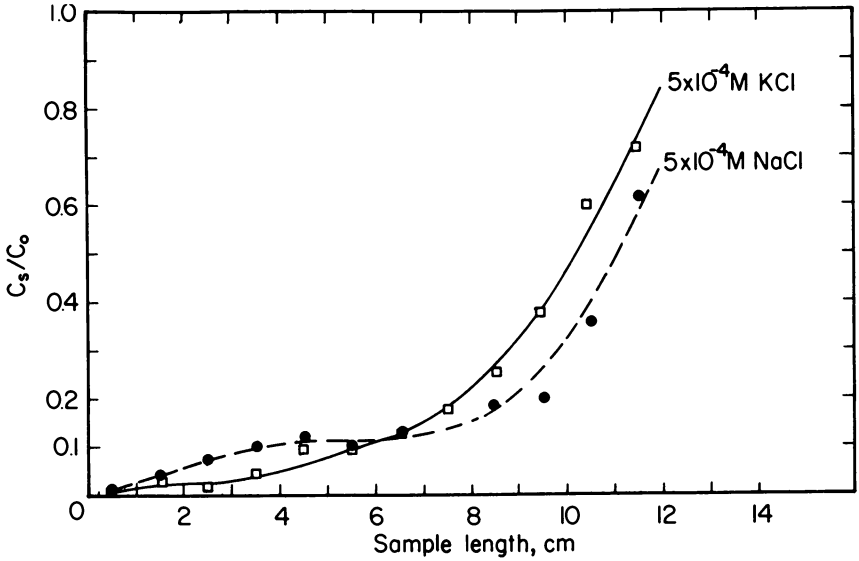

Figure 11. Typical distribution curves for two chlorides. Growth rate 5 microns a second. No stirring. The strong concavity upward suggests a small distribution coefficient (and/or large diffusion coefficient) and, therefore, rapid arrival of the diffusion front at the extremity of the sample holder

difference is probably smaller than the differences between single ions shown in Table I. The resultant uncertainty in the distribution coefficient could be avoided by using the ratio k/D as a distribution parameter. At any rate, the error introduced by the assumption of a constant diffusion coefficient appears smaller than the experimental uncertainty in the solute distribution curves. The "limiting" diffusion coefficients used in this paper (Tables I and II) were computed for 0°C. and infinite dilution.

THE LIQUID COLUMN IS INFINITE. Practically, this condition holds until the diffusion of ions rejected from the phase boundary reaches the end of the liquid column.

DIFFERENTIAL ION INCORPORATION. Differential ion incorporation may be due to different distribution coefficients of anions and cations or different diffusion coefficients or both. Furthermore, both coefficients are concentration-dependent. The presence of more than one solute species, electrically charged and which are incorporated at different rates, plus the concentration dependence of these distribution rates, is not taken into account by the analytical expressions discussed. As explained earlier in this paper, the macroscopic (or freezing-potential) electric

field exerts a rather small effect on the number of impurity atoms incorporated. It does affect the cation *species* in Group I solutes (Figures 6 and 7).

The work by Baker (*2, 3*) and Malo and Baker (*114*) indicates that nonionized solutes are rejected more efficiently from the solid than ions. The presence of both ionized and non-ionized solutes in the freezing solution reduces the separation efficiency of the latter.

Table I. Radius, Mobility, and Diffusion Coefficient of Monovalent Ions at 0°C. and Infinite Dilution.

Ion	*Ionic Radius* A	λ_0 *cm.²/ volt-sec.*	*D cm.²/sec.* $\times 10^5$	*Ion*	*Ionic Radius* A	λ_0 *cm.²/ volt-sec.*	*D cm.²/sec.* $\times 10^5$
Cs^+	1.65–1.69	44.0	1.075	I^-	2.16–2.20	41.4	1.012
Rb^+	1.48	43.9	1.072	Br^-	1.95	42.6	1.04
K^+	1.33	40.4–40.7	0.995	Cl^-	1.81	41.0–41.1	1.00
NH_4^+	—	40.2	0.985	F^-	1.33–1.36	27.5	0.671
Na^+	0.95	26.0–26.5	0.635	OH^-	—	105.0	2.57
Li^+	0.6–0.78	19.0–19.4	0.465	O^{2-}	1.76[a]	—	—
H^+	—	225–240	5.86				

[a] Univalent radius.

Table II. Average Diffusion Coefficient (0°C. and Infinite Dilution) of Some Mono-Monovalent Electrolytes.

	D cm²/sec. $\times 10^5$		*D cm²/sec.* $\times 10^5$
CsCl	1.035	KF	0.80
KCl	1.00	NH_4F	0.80
NH_4Cl	0.99	NaF	0.65
NaCl	0.78	LiF	0.55
LiCl	0.63	HF	1.21
HCl	1.71	KOH	1.43
CsF	0.83		

Tiller and Sekerka (*149*) investigated mathematically the effect of an *external* field on the distribution coefficient of ionized solutes in the absence of convection. The distribution coefficient may be larger or smaller than k_o, or it may even be negative, depending on the field's strength and direction. This may become a valuable means of investigating distribution coefficients in the ice/water system. Techniques adaptable to this end have been proposed by Pfann and Wagner (*124*).

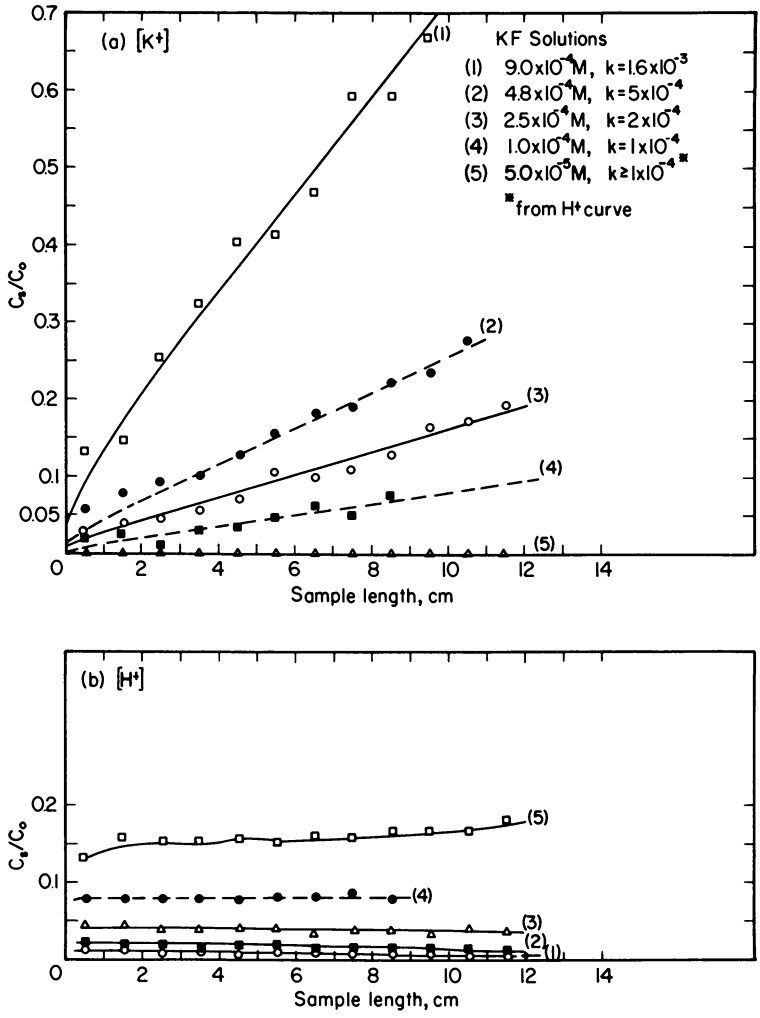

Figure 12. Distribution curves for KF solutions of different initial concentrations. (a) Potassium ions. (b) Hydrogen ions. Growth rate 5 microns a second. No stirring. The relative proportion of hydrogen ions decreases as the solution concentration increases. Further, the hydrogen-ion fraction increases with sample length for the most dilute solution; it decreases for the most concentrated solution

Application of the Tiller-Sekerka model to the internal field of the freezing potential leads to results both self-contradictory and in conflict with experimental evidence. The major difficulty occurs when both selective incorporation of negative ions (Group I solutes) and of positive ions (Group II solutes) is considered, all other conditions being equal.

At relatively high and at very low freezing rates, a quasisteady state of interface concentration is rapidly established, in which diffusion and distribution coefficients may be considered constant or changing only very slowly.

It is concluded that, in many instances, existing theory for the diffusion-governed solute partition gives reasonable approximations to the distribution coefficient, particularly in view of the relatively low accuracy of experimental curves.

In the presentation of this writer's experimental results (below) the term *apparent distribution coefficient* is taken to mean the interface distribution coefficient computed according to Equation 5 and the five assumptions listed with Equation 3. The adjective *apparent* acknowledges the fact that these assumptions may not be satisfied. The k-values shown in Figures 9 to 17 are *apparent* distribution coefficients according to this definition.

Nonuniform Freezing Rates. No Convection. An important case, approximated by freezing-cup studies, is that of the freezing rate diminishing with time according to Equation 1. For this, Wagner (*154*) showed that the interface concentration is constant and is given by

$$C_i = C_o \frac{1}{1 - \sqrt{\pi}(1 - k_o)(A/\sqrt{D}) exp\left(\frac{A^2}{D}\right) erfc\left(\frac{A}{\sqrt{D}}\right)}. \quad (8)$$

(Compare further *69, 144, 145*). k and D can be treated as constants.

For ice, while the experimental method under discussion ideally yields a constant ion concentration in terms of total number of ions per unit volume, the cation fraction consisting of hydrogen ions increases with decreasing freezing rate (*66*) when Group I solutes are used, so that the actual sample composition and conductivity vary continuously along the length of the sample.

Convection-Governed Impurity Distribution with Uniform Freezing Rate. The diffusion-controlled solute build-up at the interface can be minimized by stirring the solution. Burton, Prim, and Slichter (*17*) showed that, in this case, a steady state will be reached in which

$$k = \frac{k_o}{k_o + (1 - k_o) exp\left(-\frac{Rd}{D}\right)}; \quad (9)$$

d = thickness of the diffusion layer.

Pfann (*123*) described an empirical procedure by which Equation 9 may be used to determine k_o by using identical stirring conditions but different freezing rates. It was applied to ice by Jaccard and Levi (*84*).

Experimental Results. Jaccard and Levi (*84*) determined distribution coefficients for solutions of HF, NH_4F, and NH_3 (Figure 8) in a range of rather high concentrations. They used uniform freezing rates obtained by lowering a vertical tube with the solution (initially at room temperature) into a freezing mixture at a constant velocity. Most of the solutions were stirred below a snugly fitting polyethylene plug which was maintained at a constant distance (a few millimeters) from the interface to prevent or reduce heat convection (*84*). Such a plug (and stirring) also eliminates concentration control by diffusion, however, and invalidates the assumption of an effectively infinite column for all but a very short crystal length. As a result, distribution coefficients are high, perhaps by orders of magnitude, compared with those for which the assumption is valid (Figure 9). This is especially evident for HF (Figure 8). In this case, however, the concentration dependence of the distribution coefficient may explain a major part of the discrepancy for another reason: Since stirring decreases the interface concentration, a higher coefficient may be expected in this case. Unpublished experimental results by G. W. Gross confirm this view. Jaccard and Levi observed a very strong concentration dependence of their distribution coefficients. The coefficients for NH_4F increase with concentration. Those for HF and NH_3 show a minimum above $10^{-1}M$. This minimum may possibly correspond to the solubility limit in the solid phase (Figure 8).

De Micheli and Iribarne (*36*) investigated the effective distribution coefficients of a number of salts, acids, and bases at different freezing rates and stirring very close to the interface. No attempt was made to compute interface coefficients. No freezing-rate dependence was observed; however, experimental conditions are not well defined in their paper. Salts showed higher coefficients than their acids and bases. The concentration dependence was higher in acids and bases than in the corresponding salts. The coefficients varied greatly, depending on the substratum on which the freezing was initiated, being ice or not ice. This is perhaps related to the fact that the initial freezing rate is difficult to control if a sample is grown from a substratum that is not ice. The coefficients of De Micheli and Iribarne are expressed as the reciprocal of Equation 2a.

Levi and Milman (*107*) determined "apparent segregation factors" (concentration of the supernatant to the concentration in the ice) for NH_3 and NaCl solutions grown at constant freezing rates without stirring. The results are inconclusive.

G. W. Gross (*68*) uses an arrangement somewhat similar to that of Jaccard and Levi. Convection is minimized by maintaining a much lower temperature gradient in the liquid (about 3°C. per 25 cm. column length). A disk electrode of perforated platinum suspended at a constant distance from the interface (2-3 cm.) measures the freezing potential. It hinders diffusion only slightly (Figure 9) but is believed to reduce convection. In some experiments, the interface shape can be controlled by a supplemental heater riding on the freezing tube at the interface level.

The results discussed below were obtained at a freezing rate of 5 microns a second, without stirring, and with a concave interface. The mother solutions ranged from $10^{-3}M$ to $10^{-5}M$. The concentrations in the melted ice fell between $10^{-6}M$ and $10^{-4}M$. The ice consisted of large

grains (greatest dimension up to 2 cm.) with the c-axes oriented conically in the direction of heat flow. The solute concentrations in the melted ice were measured, and apparent distribution coefficients were computed according to Equations 3 to 5 and the assumptions discussed thereunder. The detailed procedure has been described elsewhere (*68*).

Figure 10 shows distribution curves for one solution of each of the alkali fluorides, except RbF, and for ammonium fluoride. The contrast in apparent distribution coefficients exceeds an order of magnitude. No obvious relation exists between apparent distribution and limiting diffusion coefficients of the cations. The very low distribution coefficient of HF comes as a surprise, since HF is supposed to enter the lattice substitutionally with a minimum of distortion. NH_4F shows the highest distribution coefficient, as expected (*67*, *162*), and HCl is lower than HF, also as expected (*65*). Two typical chloride curves are shown in Figure 11 for comparison.

Figures 12 to 14 show distribution curves for KF, HF, and HCl, respectively, as a function of concentration. Within the concentration range covered (*see* Figures) for KF as well as for CsF, the coefficient increases with concentration; for HF it decreases; for HCl it remains approximately constant. The curves for NH_4F (Figure 15) indicate a strong change of the coefficient with distance from the starting point of freezing (strongly curved semilog plots; *see* Ref. *68*), but the dependence on the mother solution concentration (C_o) is weak in the range investigated.

The hydrogen-ion distribution curves are nearly horizontal. This means that at a given freezing rate the difference between solute anions and solute cations in the ice remains approximately constant. For the same reason, the hydrogen ion concentration does not appreciably affect the distribution coefficients computed from the slopes of semilogarithmic plots (*68*), except for some very dilute solutions, such as $5 \times 10^{-5}M$ KF (Figure 12), in which k could not be computed from the potassium distribution curve.

Figure 16 shows the effect of different stirring rates on the ionic distribution curves for $4.8 \times 10^{-4}M$ KF. An increased stirring rate causes a marked decrease in the potassium concentration in the ice but a marked increase in the hydrogen concentration. Stirring appears to increase the availability of hydrogen ions at the interface. (If the effect were primarily caused by the decreased availability of solute cations, stirring should cause an increase in freezing potential.) This may explain why stirring reduces the freezing potential, even though it also reduces the interface concentration, which tends to increase the potential. For $2.4 \times 10^{-4}M$ HF (Figure 17), a maximum flattening of the ionic distribution curve was obtained at about 160 r.p.m. This is taken to mean that under the particular experimental conditions the diffusion layer thickness was reduced to its practical minimum at this speed. At a concentration of $1 \times 10^{-3}M$, a stirring rate of more than 320 r.p.m. was required. For a given stirring rate and solution, the results depend on the shape of the stirrer, and its distance from the interface (about 1 to 2 cm. in these experiments).

Figure 9 shows the effects of different experimental arrangements on the distribution curves of 2.5 × $10^{-4}M$ KF. In one instance, the perforated platinum electrode was replaced by a snugly fitting Teflon disk, located about 3 cm. from the interface, provided with only two small holes (⅛ inch in diameter) to allow fluid transfer. The apparent distribution coefficient is about four times that found for unhindered diffusion. Hydrogen ion transfer is appreciably less. Constitutional supercooling (*see* below and Ref. *146*) in the interface region may perhaps have contributed to this rise of the distribution coefficient. Qualitatively similar results were found for HF.

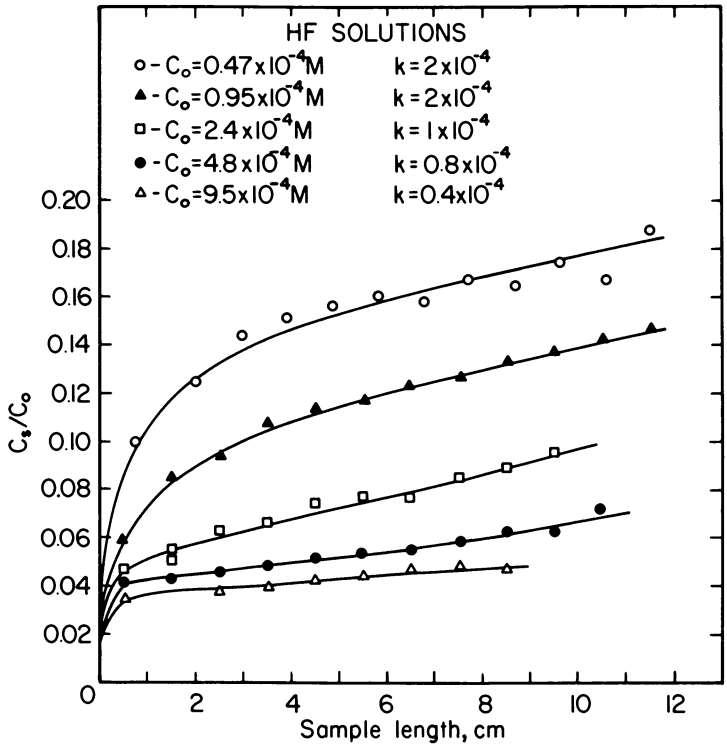

Figure 13. Distribution curves for HF solutions of different initial concentrations. Growth rate 5 microns a second. No stirring

Discussion of Experimental Results. ROLE OF DIFFUSION. Small differences between cation and anion diffusion coefficients (differential diffusion) theoretically can account for the differential ion distribution even if the distribution coefficients themselves are assumed to be identical for cations and anions. If ionic distribution curves are determined mainly by differential diffusion, then little information can be obtained from them about the acceptability of different ions in the ice structure.

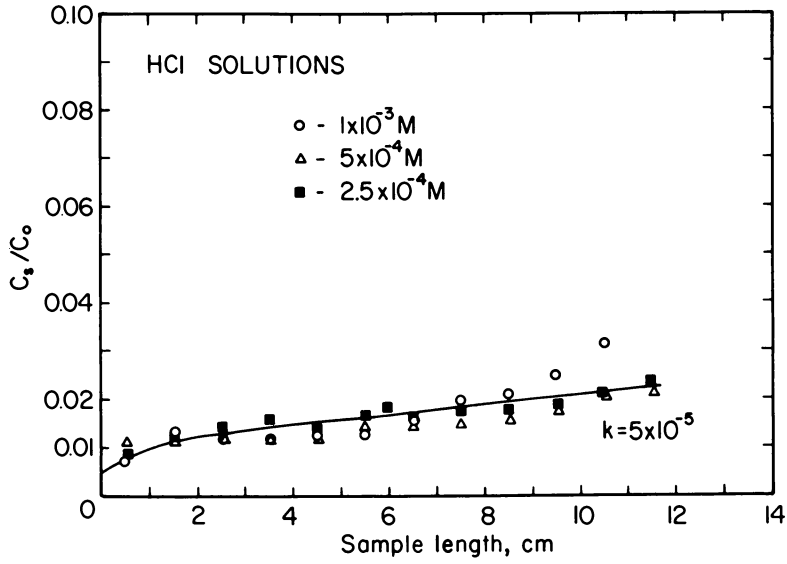

Figure 14. Distribution curves for HCl solutions of different initial concentrations. Growth rate 5 microns a second. Upward concavity of 1×10^{-3}M solution suggests that column is no longer infinite at this point

Quite aside from a differential diffusion effect, differences in the limiting average diffusion coefficients (as defined by Equation 7) may account for different incorporation rates of a given pair of solutes; *e.g.*, HF and HCl. The experimental evidence, though fragmentary at this writing, supports the view that diffusion, provided it is undisturbed is less important in shaping the distribution curve than other, perhaps structural, factors. (Inasmuch as diffusion is one controlling factor of the interface concentration, any process that disturbs diffusion, such as heat convection or stirring, will also affect the solute distribution curve as well as the interface coefficient.)

If differential diffusion is the determining mechanism, the slower ions should be preferentially incorporated into the ice structure and should determine the sign of the freezing potential. A glance at Figure 10 shows that there is no correlation between the distribution coefficients of different cations and their limiting diffusion coefficients. The ions potassium and ammonium have the same limiting diffusion coefficient (Table I), which is about 48% higher than the diffusion coefficient of F^-. Yet the distribution coefficient for K^+, in KF solutions, is about one tenth of that for NH_4^+ in NH_4F of the same concentration.

On the other hand, the diffusion coefficients of NH_4^+ and K^+ are very nearly the same as that of Cl^- (Table I). NH_4Cl solutions show a high

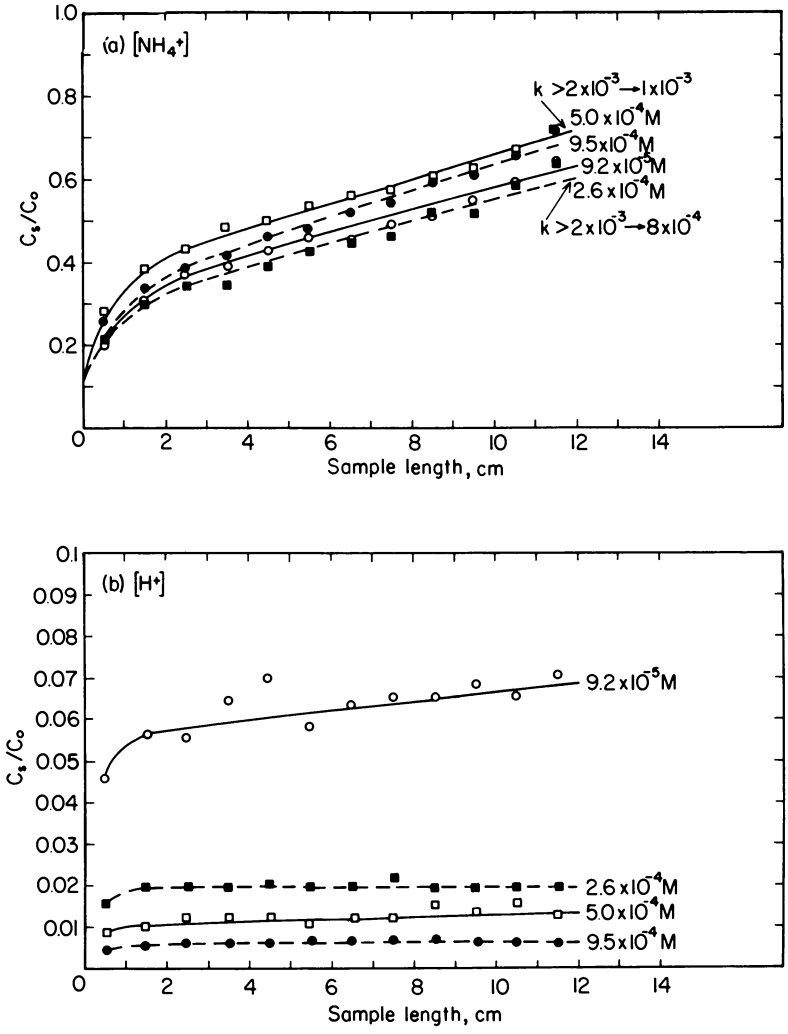

Figure 15. Distribution curves for NH_4F solutions of different initial concentrations. Growth rate 5 microns a second. (a) Ammonium ions. (b) Hydrogen ions. The semilog plots of these distribution curves (68) *are curved and suggest a strong concentration dependence of the apparent distribution coefficient. The hydrogen-ion fraction increases with decreasing mother solution concentration*

potential with the ice positive and therefore incorporation, which is very small, of ammonium ions. KCl solutions of the same concentration show a smaller potential of the opposite sign and a perhaps somewhat higher incorporation of Cl^- ions. Taken by itself, this could be interpreted quite plausibly in terms of very small differences in diffusion coefficients only.

Relatively small differences in diffusion coefficients may be paired with high freezing potentials, as in the examples just given. For HF solutions we have a large contrast between anionic and cationic diffusion coefficients (the ratio exceeds 1:8), yet the freezing potential is negligible within experimental accuracy. Thus the potential reversal in potassium and ammonium chlorides is probably best explained in terms of differences in distribution coefficients rather than of diffusion coefficients.

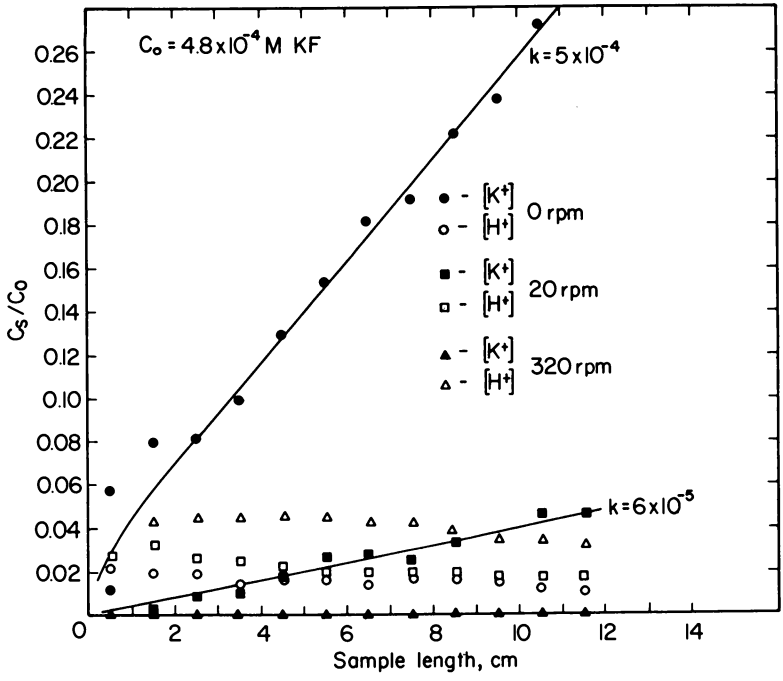

Figure 16. Ionic distribution curves for 4.8 × 10^{-4}M KF solution frozen at a rate of 5 microns a second with different stirring speeds. The potassium-ion fraction decreases and the hydrogen-ion fraction increases as the stirring rate is increased. This may explain the reduction of the freezing potential by stirring (if the liquid phase is close to 0°C.)

The remarkable steepening with increasing concentration of ion distribution curves in solutions of KF and CsF may be explained by assuming that distribution and diffusion coefficients both decrease with concentration but that the diffusion coefficient decreases more rapidly. This, however, is contradicted by the experimental evidence which shows that the concentration dependence of the distribution coefficient is much stronger than that of the diffusion coefficient. This writer feels that this

increase may be attributed to the formation of localized regions of high concentration because of the limited solubility of these compounds in ice and as a result of constitutional supercooling (*see* below).

The difference between incorporation of HCl and HF (Figure 10) qualitatively agrees with the large difference in the *average* diffusion coefficients of these two compounds. Yet, in this instance, the computed difference in distribution coefficients is of the same order. Thus, the evidence here is inconclusive.

If diffusion coefficients were of decisive importance, then a large increase in freezing rate should cause a decrease in potential, just as it decreases ion separation (Figure 6). The converse is true. (A possible reason: Some cations are trapped in interstitial positions rather than incorporated into the ice structure. Therefore the decrease of ion separation with rising freezing rate is only apparent.) Furthermore, stirring should reduce or eliminate differential ion incorporation if it were diffusion-controlled. Instead, in Group I solutes, stirring improves differential ion segregation by continually bringing to the interface a fresh supply of hydrogen ions. (Group II solutes have not been studied and Group III solutes do not show differential incorporation under any conditions.)

Structural Significance of ion Distribution Curves. The effect of solutes, ionic and not ionic, on the structure of water has been the object of much research, especially since the fundamental investigations of H. S. Frank and co-workers (*52, 53, 54, 88, 132, 133, 135*). By contrast, relatively little is known about the way solutes fit into the ice structure. Subsequent sections of this paper review some pertinent evidence.

On the basis of thermodynamic arguments, Frank and coworkers distinguished between structure-making and structure-breaking ions. In trying to apply such concepts to ice, one must remember that ions that are structure-making in water, that is, which surround themselves with a domain of ordered and relatively immobile water molecules, may actually distort the ice structure to a greater degree than those that are structure-breaking in water and whose effective radius actually is smaller.

The smallness of the apparent distribution coefficients of ionic solutes in water suggests that all of them impose a considerable distortion on the ice lattice. Ionic distribution curves such as those discussed above show that there are differences in degree. Furthermore, the distortion imposed by a given ion depends also on its counterion. Thus, the ammonium ion in combination with the chloride ion is largely rejected, but in combination with the fluoride ion it is absorbed more readily than any other ion combination investigated. The freezing potential indicates that, even in NH_4F, F^- is somewhat more readily taken into the ice structure than NH_4^+.

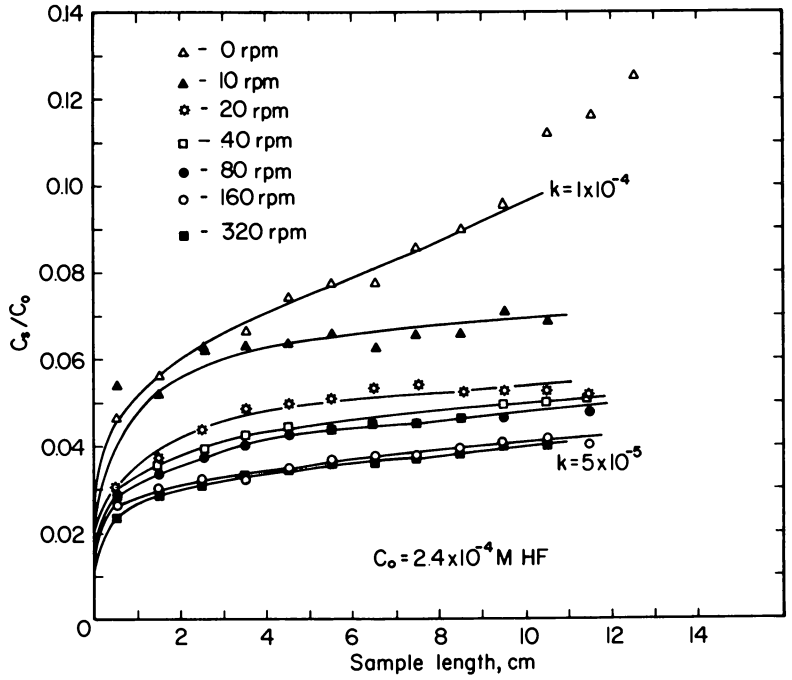

Figure 17. Ionic distribution curves for 2.4 × 10⁻⁴M HF. Growth rate 5 microns a second. Different stirring speeds

According to Frank and Wen (*54*), F^- alone of the halogen anions is structure-making in water. It is also the anion that appears to impose the least distortion on the ice lattice.

In the fluoride salts of alkali metals, those cations considered structure-breaking by Frank and Wen, such as cesium, show the highest apparent distribution coefficients (Figure 10). Conversely, lithium, a structure-maker in water, is taken into the ice lattice with greater difficulty. From a consideration of Figure 10 we arrive at the following tentative series, in order of decreasing acceptability:

$$NH_4^+ > Cs^+ > Na^+ > Li^+ > K^+ > H^+.$$

This order is valid only for the fluorides. It is contingent on the assumption that the observed distribution curves reflect a homogeneous distribution of the impurity ions in the ice lattice without formation of channel networks or interstitial zones of high solute content.

Much more research remains to be done on this topic before any valid conclusions may be drawn.

Effect of Crystallographic Orientation. The investigations of Mascarenhas and Freitas (*116*) on naphthalene, and by Cobb (*26*) on ice,

mentioned earlier, suggest that distribution coefficients in the ice/water system may depend on the crystallographic orientation of the solid phase. Future investigations should clarify this important point. This orientation dependence of the distribution coefficient (if it is confirmed) might be explained by an electric field effect on solute redistribution if the interface contact potential were a function of orientation.

Relation Between Temperature Gradient, Interface Morphology, and Impurity Distribution. The shape of the phase boundary is related to the distribution of lines of heat flow. Heat flow characteristics not only determine the rate of phase change but also the rate of transfer of solute atoms as well as their spatial distribution within the phases.

CONSTITUTIONAL SUPERCOOLING. This condition occurs if the temperature of the highly concentrated solution near the interface is below the equilibrium liquidus temperature (*147*). A consequence of this condition is the formation of cells, spikes, and finally of dendrites (*146*). Between these, zones of very high concentration develop which may become trapped in the advancing interface. The measured distribution coefficient for such a system will, of course, be too high. Constitutional supercooling occurs if (*146, 147, 148*).

$$\frac{G}{R} \leq \frac{mC_o}{D} \frac{1-k}{k} \tag{10}$$

where G is the actual temperature gradient in the liquid near the interface and m is the slope of the liquidus line at the interface. (In this formula, both phases are assumed to have the same density.)

For the experiments already discussed, the calculation according to Equation 10 indicates the absence of constitutional supercooling. However, the uncertainties in G and D are large. The increase in apparent distribution coefficients with concentration for solutions of CsF and KF suggests that constitutional supercooling did take place in some instances.

INTERFACE MORPHOLOGY. Harrison and Tiller (*69, 70*) studied the effect of ionic solutes on the interface morphology of ice by direct observation. The solute build-up ahead of the solid/liquid interface leads to constitutional supercooling and the formation, first, of a cellular interface and, later, of dendrites as the degree of constitutional supercooling increases. Working with freezing rates of 0.1 to 10 microns a second, the authors found interface distribution coefficients $\lesssim 10^{-4}$ for NaCl. The increase of the distribution coefficient as cells and dendrites develop, is presented for several equilibrium coefficients in a graph as a function of freezing rate, diffusion coefficient of the solute, and radius of curvature of cells and dendrites.

Jaccard (*83*) has derived expressions relating the curvature of the interface to the radial distribution of impurities in the steady state. For

a cylindrical sample with a concave interface, the concentration will be higher at the cylinder axis. For a convex interface, the converse is true. Since G. W. Gross's samples were mostly grown with concave interfaces, the coefficients may be expected to be too high (because some of the outer mantle is melted away while the sample is processed for analysis). Preliminary results obtained with an improved technique yielding perfectly plane interfaces appear to confirm this conclusion.

In addition to the radial concentration gradients caused by the heat flow conditions, Blicks *et. al.* (*8*) found that impurities tend to accumulate in a thin peripheral layer at the boundary between the ice and its container.

Effect of Impurities on the Ice Structure

Lattice Constants. Truby (*150*) measured the lattice constants of HF ice with x-rays; Brill and Camp (*11*) used a similar technique for NH_4F ice. In both instances, a shortening of the c/a ratio gives support to the concept of substitutional (as opposed to interstitial) emplacement of the impurities.

Electron Microscopy. An electron microscopic investigation by Truby (*151*) of the advancing ice/solution interface established the existence of a hexagonal honeycomb microstructure, the cells of which are typically 1/2 micron to 20 microns in diameter. The center of each cell consists of a depressed concentric step dislocation, perhaps an expression of surface strain. When solutions of increasing CsF content are frozen, these depressions flatten out and finally disappear for $10^{-3}M$. (Thus they cannot be the result of interface breakdown due to constitutional supercooling.) This observation seems to support the suggestion by Workman and Reynolds that impurity ions are required by an advancing ice surface to relieve strain energy. These structures appear to have the same characteristics for polycrystalline ice grown at large freezing rates, for single crystals grown slowly in the laboratory, and for single crystals from an Alaskan glacier presumably grown extremely slowly (recrystallized over a time span of perhaps hundreds of years).

Gentile and Drost-Hansen (*55*) observed that the microstructure progressively develops with time and concluded that it depends on the amount of cooling and aging of the ice after freezing has been completed. Stresses owing to cooling were believed to cause condensation of vacancies into dislocation rings and formation of additional dislocations by a Frank-Read mechanism.

Shifts in infrared interference and absorption spectra observed by Vanderberg and Ellis (*153*) were attributed to changes in hydrogen

bridging between water molecules, either as a result of aging or of varying growth conditions. These authors excluded strain as a possible explanation. Vanderberg later found (personal communication to M. Kopp) that these shifts had been caused by rather involved faults in the equipment used. Introduction of a germanium filter eliminated the effects which had been interpreted as a change in the absorption spectrum of ice.

Effects of Trace Inorganics on the Electrical Properties of Ice

Experimental evidence indicates that charge transport in ice occurs by proton transfer exclusively (*34, 97, 160*). Intrinsic electron conduction appears to be excluded because of the width of the forbidden gap (7.42 e.v.) but extrinsic electron conduction is at least a possibility (*61*).

Effects of inorganic impurities on the electrical properties of ice are of interest to such widely diverse branches of science as solid-state physics, atmospheric physics, organic chemistry, biology, and psychology. In atmospheric physics, the processes of condensation and charge separation are influenced by and related to the electrical properties of the solid phase. Ice has been called a proton semiconductor. A detailed discussion of this interesting concept is beyond the scope of the present paper (*46, 127, 128*). From this point of view, ice is the simplest of the proton semiconductors, a class that, for instance, includes the proteins (*129*). Gosar and Pintar (*58*) proposed a theory of H_3O^+ ion energy bands in ice crystals that can account for the measured mobility value. A detailed quantitative model of ice as a protonic semiconductor has recently been developed by Seidensticker (*138*). The transfer of energy via hydrogen bonds (*130, 131*) may be of fundamental importance for an understanding of the transmission of nerve impulses and of information storage in the brain; a mechanism for binary storage may be available in the two alternate positions the proton can occupy on the hydrogen bond.

Electrical measurements on pure and doped ice give valuable information concerning its structure. Gränicher (*59, 60*) gave comprehensive reviews.

Theory. LATTICE DEFECTS. A convenient starting point for a discussion of the effect of trace inorganic impurities on the structure and electrical properties of ice is the model of the ideal ice structure given by Bernal and Fowler (*5*). Water molecules preserve their identity in the lattice, that is, each oxygen atom has associated with it two hydrogen atoms. The protons lie on the straight bonds connecting neighboring oxygen atoms, with only one proton on each bond. If this structure were strictly preserved under all circumstances, ice would be a perfect insulator, since protons cannot move without violating these rules. Bjerrum

(*6*) explained the appreciable electrical conductivity and the dielectric dispersion of ice by the interaction of two kinds of structural defects that violate the Bernal-Fowler rules.

(1) By rotation of a whole molecule about one of the four bonds linking it to its nearest neighbors, a pair of *valence defects* is created: The *L defect* is a bond between adjacent oxygen atoms not containing any proton; the *D defect* is a bond with two protons. The rotating molecule remains electrically neutral, except that a displacement of electron clouds takes place during the rotation.

(2) By displacement of a proton along an oxygen-oxygen bond, a pair of ionic defects is created, an OH^- ion and an H_3O^+ ion, with a net charge transfer.

Once created, the valence defects or ions of each pair may migrate independently, that is, the defects are completely dissociated from the sites at which they originated.

The introduction of impurity ions alters the concentrations of these four types of defects, thus giving rise to characteristic changes in the dielectric dispersion and in the conductivity.

Gränicher and his coworkers first formulated a detailed theory, based on careful experimental measurements (*60, 61, 77, 80, 140, 141*). According to this theory, valence defects and ion defects are completely independent from and can not recombine with each other.

Onsager and Dupuis (*119, 120*), on the other hand, proposed that the ionic charge is partly compensated by one or two associated valence defects and is surrounded by a cloud of valence defects in a manner reminiscent of the Debye-Hückel ion atmospheres in aqueous solutions. Conclusions from Onsager's theory are qualitatively similar to those of Gränicher *et al.*

Dougherty (*J. Chem. Phys.* 43 (9), 3247, 1965) extended the theory to include interactions between Bjerrum faults and their effect on relaxation in pure ice. He concluded that this effect is small. It may, however, be considerable in HF ice. The interaction between ions and their atmosphere of Bjerrum faults is more important in an analytic treatment of ice conductivity.

Zaromb (*161*) suggested that the formation or motion of ions by proton displacements may be coupled to rotations of neighboring molecules leading to the formation of valence defects.

Several investigators (*28, 29, 45, 94*) criticized as energetically unfavorable the Bjerrum concept of a valence defect pair formed by rotation of a rigid molecule in an otherwise undisturbed lattice. Alternative mechanisms were proposed.

Based on the experimental observation that self-diffusion of water molecules in ice has an activation energy similar to that of the dielectric and mechanical relaxations (~13.5 kcal./mole), some investigators (*121*) see a connection between the formation and migration of valence defects

and the diffusion of interstitial water molecules or vacancies in the ice lattice. Kopp (*94*) has discussed in detail how the formation and migration of vacancies (sites at which whole water molecules are missing) in the ice lattice may facilitate the formation of valence defects at an energetically more favorable level ("invested vacancies") and how impurities, such as HF or NH_4F, may affect such processes. He supports his conclusions with nuclear magnetic relaxation measurements and the known data on diffusion, dielectric relaxation and elastic relaxation.

For diffusion of HF in ice, Kopp, Barnaal, and Lowe (*95*) propose a mechanism of "intermittent interstitials," that is, dissociation of HF, ejection of F^-, interstitial migration, and entrapment at vacant O^- sites giving rise to one *L* defect per F^- ion. Alternatively, an HF molecule may be ejected in toto from its lattice position and migrate interstitially or it may become associated with a vacancy and migrate together with the latter.

Ramseier [*J. Appl. Phys.* **38**, 2553 (1967)] found an anisotropy of 12% for the self-diffusion coefficients of tritium in ice, but the same activation energy, in the directions parallel and perpendicular to the c-axis. His numerical results are in substantial agreement with those given in Table VII. He favors a vacancy mechanism with entire H_2O molecules diffusing.

While the theories discussed above are based on reactions between defects, somewhat similar to reactions between chemical species, Seidensticker's proton semiconductor model (*138*) considers proton populations as a whole. Each proton arrangement or "proton configuration state" (*e.g.*, an *L* defect, *D* defect, positive or negative ion) has a characteristic energy level. From these energy levels the defect populations are computed. Impurities introduce new energy levels and change the defect populations. These changes are predicted by the model, and the results are compared with those obtained from the earlier theories and the experimental data available. The model accounts for the experimental data and, furthermore, has the advantages of both greater simplicity and of being able to predict the effects of complex impurities, such as NH_4F, as well as of surface and interface effects, from the energy levels associated with each species or interface state.

DIELECTRIC DISPERSION. This discusses the effects of impurities on four characteristic properties, the dielectric constant, the a.c. and d.c. conductivities, and the relaxation time. Brill (*10*) gave an excellent discussion of dielectric dispersion as it pertains to ice.

Ice is a (leaky) dielectric and may therefore contain polarization charges from three sources making characteristic contributions to the dielectric constant. At optical frequencies, the high-frequency dielectric constant is caused by the displacement of electron clouds and of atomic nuclei from their equilibrium positions. It is temperature-independent,

having a value of about 3.2. In the kilocycle range, molecular rotation gives rise to a Debye dispersion; the reciprocal of its characteristic angular frequency is the relaxation time. The translation of ion states is thought to make only a relatively small contribution to this dispersion (*130, 131, 141*). The static dielectric constant is extrapolated from the Debye dispersion curve. The "Debye relaxation time" (Table III) depends on impurity concentration and on temperature. At very low frequencies or in a static field, "space charges" make a third contribution to the dielectric constant. It gives rise to a low-frequency dispersion (Maxwell relaxation) that appears to be related to impurities. In this frequency range, the dielectric constant is proportional to the sample thickness and to the square root of the impurity concentration (at least for low concentrations of HF). Although this dispersion is predicted by theory that refers only to nonconducting solids (*141*), it is possible that at least part of this contribution to the dielectric constant stems from space charges accumulated at partly blocking electrodes; their contribution can not be separated from bulk polarization.

When referring to a Debye dispersion, it should be kept in mind that Debye's theory applies exclusively to rotational polarization of molecules with permanent dipoles, without net charge transfer (*33, 90*). The occurrence of an appreciable ionic transfer complicates the picture, as in ice doped with ionic impurities. A further complicating factor is aging. Steinemann observed that thin crystals (0.1 to 0.2 cm.) showed a decrease of both the low-frequency dielectric constant and the low-frequency conductivity, suggesting diffusion of impurity (HF) out of the sample into the electrodes. Thicker samples (of the order of 1 cm.) were not affected.

Charge Transport. Transport of charges through the ice requires the cooperation of both ions and valence defects, since the passage of a defect of one kind and sign leaves the bond polarized against the passage of a defect of the same kind and sign. Thus, transit of the next ion over a particular bond must await passage of a *D* defect in the same direction, or of an *L* defect in the opposite direction (*see 80*). For this reason, if valence defects and ions are present in unequal numbers, the conductivity will show a characteristic behavior, depending on the frequency of the applied electric field.

At very high frequencies, the displacement of individual defects between direction changes of the field is small; hence, there is no or little interaction between them, and the displacement is in phase with the applied field. The total conductivity is simply the sum of the contributions from each type of defect, the defect with the largest contribution (the majority defect) determining the over-all conductivity. (The majority or minority character of a given type of defect is determined by the product of concentration times mobility.) The dielectric constant is low.

At lower frequencies (Debye dispersion region), charge transport is limited by the minority carriers which form a "bottleneck." Applied field and current are no longer in phase; this results in a polarization and rise of the dielectric constant from its high-frequency value. The conductances of the different defect types act as though in series. The minority carrier determines the over-all conductivity.

The relative as well as the absolute number of majority and minority carriers changes as a function of impurity concentration and of temperature.

RELATION BETWEEN CONDUCTIVITY AND DIELECTRIC CONSTANT. Even pure ice is a leaky dielectric and in the following considerations is represented as a capacitance shunted by a resistance (*77, 140, 141*).

In the presence of relaxation effects, the dielectric constant is conveniently written in complex form (*33, 90*):

$$\epsilon^*(\omega) = \epsilon_1(\omega) - i\epsilon_2(\omega) = \frac{\epsilon_s - \epsilon_\infty}{1 + i\omega\tau} + \epsilon_\infty. \tag{11}$$

ϵ_s = static dielectric constant $\simeq$ 100 about 0°C.; ϵ_∞ = high-frequency dielectric constant $\simeq$ 3.2 (not dependent on temperature); τ = relaxation time = $\frac{1}{2\pi f'}$, where f' is the Debye relaxation frequency (of the order of kilocycles in "pure" ice); ω = angular frequency. From Equation 11, the real and imaginary parts of the dielectric constant follow as

$$\epsilon_1(\omega) = \frac{\epsilon_s - \epsilon_\infty}{1 + \omega^2\tau^2} + \epsilon_\infty \qquad \text{and} \tag{12a}$$

$$\epsilon_2(\omega) = \frac{\epsilon_s - \epsilon_\infty}{1 + \omega^2\tau^2}\,\omega\tau. \tag{12b}$$

The current through the sample is given by

$$j = \sigma_0 E + \frac{\delta D}{\delta t} = [\sigma_0 + i\omega\epsilon_0\epsilon^*(\omega)]E; \tag{13}$$

j = current density; $E = E_0 e^{i\omega t}$ is the electric field; $D = \epsilon_0\epsilon^*(\omega)\,E$ = electric displacement; σ_0 = d.c. conductivity; ϵ_0 = permittivity of free space = 8.854×10^{-12} mks. The expression in brackets represents a complex conductivity. Its real part is

$$\sigma_1 = \sigma_0 + \epsilon_0\epsilon_2(\omega)\omega \tag{14}$$

and is thus related to the imaginary part of the dielectric constant; ϵ_1 and σ_1 are the magnitudes measured experimentally. The loss angle, δ, is given by

$$\tan\delta = \frac{\epsilon_2(\omega)}{\epsilon_1(\omega)}. \tag{15}$$

The relaxation time, the d.c. and a.c. conductivities, the equilibrium constants of ions and valence defects, and the mobility of valence defects show a temperature dependence with characteristic activation energies (Table III). The mobility of ions is held to be temperature independent (tunnel effect). Magnan and Kahane (*112*), however, determined mobilities at very low temperatures (−80°C. to −120°C.) which show a pronounced temperature dependence (1.4×10^{-3} to 1.2×10^{-5} cm.^{2}volts^{-1} sec.$^{-1}$).

The activation energy, by definition, expresses the temperature dependence of a rate constant and is obtained from the slope of an Arrhenius plot. As used in the study of physical processes of ice, however, the "activation energy" obtained from the slope of Arrhenius plots may have contributions from enthalpies or heats of reaction other than an activation energy *sensu stricto*. Thus, for instance, the "activation energy" of d.c. conduction is assumed to be the sum of one half the energy of ionization plus, perhaps, the activation energy of the mobility (*see* other examples in Table III). The energy of ionization, however, expresses the temperature dependence of an equilibrium constant rather than of a rate constant. It is thus the difference between two reaction enthalpies. For this reason the term "apparent activation energy" (*117*) would be more appropriate.

The measurements of conductivities and dielectric constants furnish data for the computation of concentrations of the different types of defects as a function of solute concentration and of temperature, as well as interpretations in terms of lattice position, thermodynamics, and kinetics of these defects (*77, 79*). The quantitative evaluation of these measurements depends critically on the determination of the proton mobility, ion concentration, and dissociation constant in pure ice (Table IV) made by Eigen and coworkers (*46, 47*).

Experimental Results. Figures 18 to 24 show some effects of impurity ions on the electrical properties of ice.

HALOGEN ACIDS AND ALKALI HALIDES. The most extensive work has been done with HF, CsF, and KF (*65, 67, 77, 140, 141*). Samples grown from dilute fluoride solutions ($10^{-3}M$ or less) at low freezing rates (5 microns a second or less) behave like samples from dilute acid solutions because of differential ion incorporation that replaces part of the cations by protons in the ice structure.

HF molecules are held to occupy oxygen sites in the ice lattice. Since only one proton is associated with the fluoride ion, each acid molecule introduces into the lattice one *L* type valence defect. In addition, HF is held to ionize according to the mass-action law, so that at a given temperature the number of ions increases with the square root of the concentration. Thus, in ice doped with HF there are hydronium ions from the dissociation of both the water molecules and the HF impurities. The negative ions, OH^- and F^-, are believed to have a very much lower mobility and are therefore neglected. Table III gives the relations obtained

by Gränicher *et al.* for the defect concentrations and conductivity of HF ice. From these relations, the conductivity contributions of both valence defects and ions can be computed as a function of impurity concentration and temperature. Figure 19 shows the results for −3°C. The ions are the minority carriers over the whole range of concentration and determine the over-all conductivity which varies approximately as the square root of concentration.

D.c. conductivity measurements at −15°C. for polycrystalline ice doped with HF (Figure 20 and Ref. *67*) show substantially the same square root of concentration dependence, and so do Steinemann's (*140*) low-frequency results.

Figure 21 shows the static dielectric constant extrapolated from the Debye dispersion (at −3°C.) as a function of HF concentration (*140*). According to Gränicher (*60*) and Jaccard (*77, 80*), the two minima correspond to impurity concentrations such that the conductivity contributions of valence defects and ions are equal. Therefore, dipole polarization is absent or minimal and the dielectric constant approaches its high-frequency value. The minima, according to this interpretation, represent the points where the majority character of conductivity shifts: In Regions I and III, valence defects are held to be majority carriers; in Region II, the ions predominate. This follows from the inference that at very high HF concentrations (Region III), valence L defects should predominate over ions since the former increase with the first power of concentration. Therefore, curves for valence defect conductivity and ion conductivity (Figure 19) should intersect twice, thus delimiting region II. Instead, they only approach each other between $10^{-3}M$ and $10^{-4}M$ but not enough to alter the net minority character of ions over the whole range. Jaccard (*77*) compared a.c. and d.c. conductivities in the critical concentration range and concluded that the ion majority character in Region II is weak.

(Jaccard (*77*) based his ion conductivity calculations on experimental data taken from Steinemann (*140*) but did not convert from units of $ohm^{-1}cm^{-1}$ to $ohm^{-1}m^{-1}$. As a result, his computed dissociation constant is two orders of magnitude too high. *See* his equation 2.4.11.)

An intersection of the computed curves probably does occur well below −30°C. but at concentrations under $10^{-5}M$.

Corresponding to Region II, the experimental low-frequency (*140*) and d.c. conductivity curves (Figure 20) at −10°C. and −15°C., respectively, should show a change of slope corresponding to Region II, but they do not. Neither did Kopp observe clear slope changes corresponding to the majority carrier transitions in high-frequency conductivity curves (*92*).

Summing up, experimental plots of ice conductivity *vs.* HF concentration do not show slope changes indicative of a shift in the majority carrier. Curves of ion conductivity against concentration (derived from d.c. conductivity measurements) and of valence defect conductivity against concentration (derived from high-frequency conductivity measurements) do not intersect as they should according to the theory. The experimental curves are not very accurate, so they are not conclusive. Computed curves depend on empirical parameters whose accuracy is no better.

In conclusion: The arguments used in explaining the dielectric minima (Figure 21) are plausible. Not so plausible is perhaps the concept of extrinsic—(*i.e.*, impurity-related), ionization according to the mass-action law (since it implies a complete independence of ions from the sites at which they formed) and, correspondingly, the concept of complete independence of extrinsic valence defects. Further, the concept of complete independence of ions and valence defects from each other has been criticized on energetical grounds. If these three concepts can be modified, sharply defined slope values and slope changes may no longer be required to accompany changes in majority character of the different carriers. A careful investigation of the apparent disagreement between dielectric and conductivity data is therefore warranted.

The effect of HF on the *dielectric relaxation time* in ice will be discussed later, together with mechanical relaxation studies.

The following d.c. conductivity results by G. W. Gross are mostly unpublished. Samples were prepared after techniques described in (*67*)

Table III. Formulas and Experimental Parameters Used in the Calculations on Electrical Conductivities of Pure and HF-Doped Ice [a]

Pure Ice

Valence defects

Concentration $[L] \cdot [D] = K_v = 2.5 \times 10^{-3}$ exp. $(-0.68$ e.v./$kT)$ moles^{2}cm.$^{-6}$

Mobility (rotation) $u_L \simeq u_D = u_v = 5.8$ exp. $(-0.235$ e.v./$kT)$ cm.^{2}v^{-1}sec.$^{-1}$

Effective charge $q_v = |q_L| = |q_D| = (0.43)(1.6 \times 10^{-19})$ coul.

[Revised value: $q_v = 0.55$ e. (Ref. 79)]

Conductivity $\sigma_v = \sqrt{K_v} N_A u_v q_v$

Debye relaxation $\frac{1}{\tau} = 2A\sqrt{K_v} u_L = 2 \times 10^{15}$ exp. $(-0.575$ e.v./$kT)$

(This assumes $[L] = [D]$.)

Ions

Concentration $[H_3O^+][OH^-] = K_w = 4 \times 10^{-4}$ exp. $(-1.2$ e.v./$kT)$ moles^2 cm.$^{-6}$

Mobility (displacement along bond) $u_+ = 2 \times 10^{-1}$ cm.^{2} v^{-1} sec.$^{-1}$ (all temperatures) (see also Table IV for other possible values)

$u_- << u_+$

Effective charge $q_i = |q_+| = |q_-| = (0.57)\ (1.6 \times 10^{-19})$ coul.

[Revised value: $q_i = 0.45$ e. (Ref. 79)]

Conductivity $\sigma_i = \sqrt{K_w} N_A u_+ q_i$

Over-all conductivity

High frequency: $\sigma_\infty = \sigma_v + \sigma_i \simeq \sigma_v$

D.c.: $\sigma_0 \cong \frac{4\sigma_v\sigma_i}{\sigma_v + \sigma_i} \simeq 4\sigma_i$

$\sigma_v >> \sigma_i$ (Ref. *80*)

HF Ice

Table III. Continued

Valence defects

Concentration: $n_v = [L] + [D] = N_A\,[\mathrm{HF}]\left(1 + \frac{4K_v}{[\mathrm{HF}]^2}\right)^{1/2}$ moles cm.$^{-3}$

Mobility and effective charge as in pure ice

Conductivity: $\sigma_v = n_v u_v q_v$

Debye relaxation (Ref. *140* and Ref. *77*):

(a) Low concentrations and/or low temperatures (Region I of Figure 21) $1/\tau$ shows little variation with concentration.

(b) Intermediate concentrations and/or higher temperatures (Region II of Figure 21)
$1/\tau = \mathrm{C}[\mathrm{HF}]^{1/2}u_+$
(ion concentration $= [\mathrm{HF}]^{1/2}$)

(c) High concentrations or very low temperatures (−55°C.) (Region III of Figure 21)
$1/\tau = \mathrm{B}[\mathrm{HF}]u_L = 1/\tau_0 \exp.\ (-0.235\ \mathrm{e.v.}/kT)$
(L defect concentration $= [\mathrm{HF}]$.)

Ions

Ionization (of HF in ice): $\frac{[\mathrm{H_3O^+}]\,[\mathrm{F^-}]}{[\mathrm{HF}]} = K_F = 2.42 \times 10^{-3} \exp.\ (-0.65\ \mathrm{e.v.}/kT)$ moles cm.$^{-3}$

Concentration: $[\mathrm{H_3O^+}] = N_A(K_w + K_F[\mathrm{HF}])^{1/2}$

Conductivity: $\sigma_i = [\mathrm{H_3O^+}]u_+q_i$

Over-all conductivity

High frequency: $\sigma_\infty = \sigma_v + \sigma_i$

D-c: $\sigma_0 \simeq 4\,\frac{\sigma_v\sigma_i}{\sigma_v + \sigma_i}$

[a] Based on the work of Gränicher, Steinemann, and Jaccard (see Refs. *77*, *140*, *141*), except where otherwise noted. All concentrations are in moles cm.$^{-3}$. The *letters* and *subscripts* used in this table are defined as follows:

Letters

A, B, C = constants
D = D defect
e = electron charge
K = dissociation constant
L = L defect
N_A = Avogadro's number
q = effective charge
u = mobility
σ = conductivity
τ = relaxation time

Subscripts

D = D defects
F = ions from HF molecules
i = ions in general (without regard to source and sign)
L = L defects
v = valence defects in general
w = ions from H_2O molecules
$\pm$ = positive or negative ions

and measurement methods were discussed in (*65*). Figure 22 and Table V show activation energy measurements for HF ice. A peculiar flattening-out of the curves frequently occurs at the high temperature end. It was not observed in KF ice. Ice with an HF content as low as $10^{-8}M$ was reported to show the same activation energy (*67*). The validity of this

result may, however, be questionable because of the use of sandwich electrodes (*see* below). The conductivity of KF ice (Figures 23 and 24) is determined by its content of HF (because of differential ion incorporation), but a sufficiently wide concentration range, so as to allow comparison with the HF curve (Figure 20), could not be achieved. The conductivity of KF samples grown with a shunt (Figure 23) is about half that of HF ice with the same hydrogen-ion concentration (as measured in the melted ice at room temperature). Thus, perhaps, the potassium ion reduces the mobility of the carriers. Aging effects (Figure 24) were observed in KF ice grown without shunt (high potassium content), but those grown with shunt were remarkably stable (Figure 23). In the KF

Table IV. Dissociation and Charge Transport in Pure Ice at —10°C.[a]

	Measured values		
	d.-c. conductivity	*Activation energy*	
Author and reference	$\Omega^{-1}cm.^{-1}$	*kcal./mole*	*e.v.*
Johnstone (*86*)	1.1×10^{-9}	19.6	0.85
Bradley (*9*)	1.4×10^{-9}	12.3	0.53
Jaccard (*77*)	$\sim 10^{-9}$	13.8	0.6
Riehl (*108*)	4×10^{-10}	—	—
Heinmets and Blum (*73*)	1.6×10^{-9}	24.2	1.05
Eigen *et al.* (*47*)	$1.0 \times 10^{-9} \pm 15\%$	11 ± 1.5	0.48
Bullemer and Riehl (*15*)			
bulk	$\sim 10^{-9}$	8.5	0.37
surface	$\sim 10^{-9}$ ohms^{-1}	14 to > 30	0.61 to > 1.3
Camp *et al.* (*20*)	$< 2 \times 10^{-11}$	~ 0	~ 0
Kopp (*93*)			
surface (snow)	$(.01 \text{ to } 2) \times 10^{-9}$	16.2 to 25.4	0.7 to 1.1
Dissociation rate constant (k_D)	3×10^{-9} sec.$^{-1}$	22.5 kcal./mole	0.98 e.v.
Mobility ratio $\frac{u_+}{u_-}$	10 to 100		
"Effective" dielectric constant	3.2 to 15		

Derived values

Equilibrium concentration of H^+ or OH^- ions	$3 \times 10^{-11}M$ to $1.5 \times 10^{-10}M$
Dissociation constant (K_{H_2O})	$2 \times 10^{-23}M$ to $4 \times 10^{-22}M$
Mobilities: u_+	0.1 to 0.5 cm.^{2} volt^{-1} sec.$^{-1}$
u_-	$\leq 5 \times 10^{-2}$ cm.^{2} volt^{-1} sec.$^{-1}$
u_+ (Ref. *47*)	8×10^{-2} cm.^{2} volt^{-1} sec.$^{-1}$
Rate constant of recombination $\left(\frac{k_D}{K_{H_2O}}\right)$	10^{13} to 10^{14} l mole^{-1} sec.$^{-1}$

[a] Ref. *46* unless otherwise indicated.

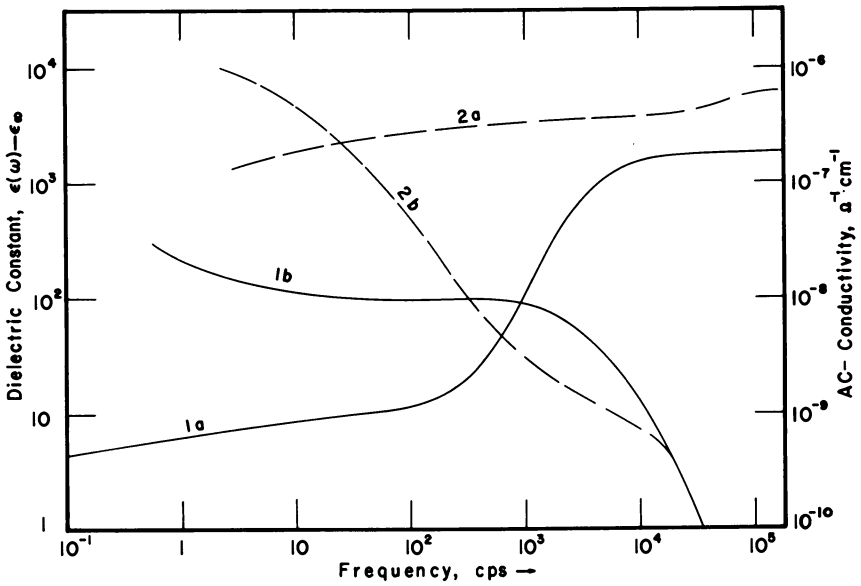

Figure 18. Frequency dependence of the a-c conductivity and of the dielectric constant after Steinemann (140). *(1) Pure ice. (2) Slightly impure ice. (a) Conductivity. (b) Dielectric constant. Curves for pure ice closely follow Equations 12a and 14, except for an incipient low-frequency dispersion that may result from very slight impurity content or from electrode polarization. Debye dispersion between 10^3 and 10^4 cps. As the impurity content increases (curves 2), the low-frequency dispersion (Steinemann's F dispersion) becomes more prominent and tends to coalesce with the Debye dispersion. Interpretation then becomes difficult. At still higher concentrations, the two dispersions separate again* (see *Ref.* 140). *A slight anisotropy of the dielectric constant, observed by Decroly* et al. (34) *for measurements parallel and perpendicular to the c axis of single crystals, has not been considered*

ice samples without shunt (samples > 1 cm. thick), conductivity increased with age, while Steinemann (*140*) observed a decrease of the a.c. conductivity in his thin crystals.

HCl ice (Figure 25 and Ref. *65*) shows d.c. characteristics identical, within experimental accuracy, to those of HF ice.

Levi and Arias (*105*) measured the d.c. conductivity of frozen solutions of HF, HCl, HBr, HI, and HNO_3. They found a similar concentration dependence (in both slope and magnitude) for all of these acids. At the high concentration end ($> 10^{-3}M$), however, a departure occurs from the square-root law similar to that shown in Figure 20 of this paper. The authors attribute this behavior to the presence of an appreciable fraction of trapped ions at these high concentrations. Results for sulfuric acid were inconclusive. Boric acid did not affect the conductivity at all.

AMMONIUM FLUORIDE. Theories discussed earlier were primarily formulated to take account of electrical measurements made on pure

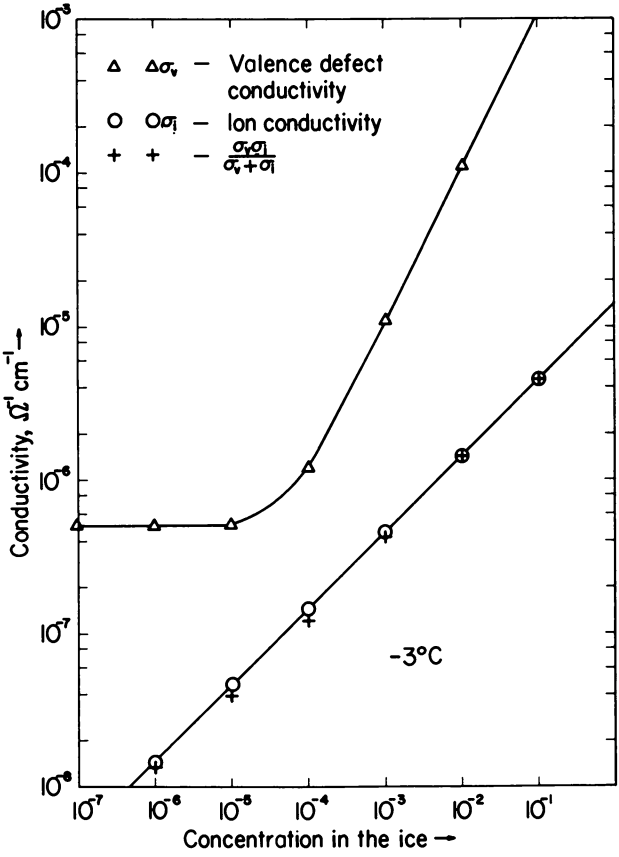

Figure 19. Valence defect, ion, and total conductivity at −3°C. as a function of HF concentration (computed from formulae and data in Table III of this paper)

ice and on ice doped with HF. No satisfactory account has yet been given of the observations on ammonium fluoride ice. Ammonium fluoride is very soluble in ice (*99, 162*), close to 10% by weight ($\sim 2.7M$). Brill (*10*) attributes this to the similarities in shape and polar groups of the two molecules. Two oxygen atoms have the same number of outer shell electrons as N + F combined. It is therefore believed that one NH_4F molecule occupies the sites of two water molecules in the ice lattice. Complex changes take place in the defect equilibria (*60, 119*) of NH_4F-doped ice compared with pure or HF ice.

A.c. Measurements. Zaromb and Brill (*162*) found that the activation energy for dipole rotation (that is, for the relaxation time) is about 4 kcal./mole. On the basis of Cole plots, they deduced the existence of a spectrum of relaxation times. The "average relaxation time" decreased with increasing concentration, as is true for HF ice.

Later work on more carefully prepared samples indicated, however, that both the activation energy of dipole rotation and the relaxation time are independent of concentration (*11, 12, 39*).

To explain these results, Brill *et al.* postulated that, in the ice, each NH_4F molecule creates about itself a domain of strongly oriented water molecules. Molecules at the domain boundaries rotate more easily, accounting for a low activation energy (Table VI). Two factors are responsible for the concentration independence of the relaxation time: (1) Even the lowest concentration investigated contains more than the necessary number of dipoles at the domain boundaries required to account for the high dielectric constant; (2) the "normal" dipoles (those not related to the domains) do not appreciably affect the relaxation time because of their much higher activation energy of rotation. Hence, even a large change in concentration has no effect on the relaxation time as long as the domains do not overlap.

Camp (*18*) discussed further work with single crystals grown from dilute solutions ($6.7 \times 10^{-4}M$ to $1.1 \times 10^{-3}M$). He found evidence that at temperatures above about −30°C., thermally produced (intrinsic) valence defects provide the major contribution to the dielectric polarization (activation energy 13.2 kcal./mole) while at lower temperatures,

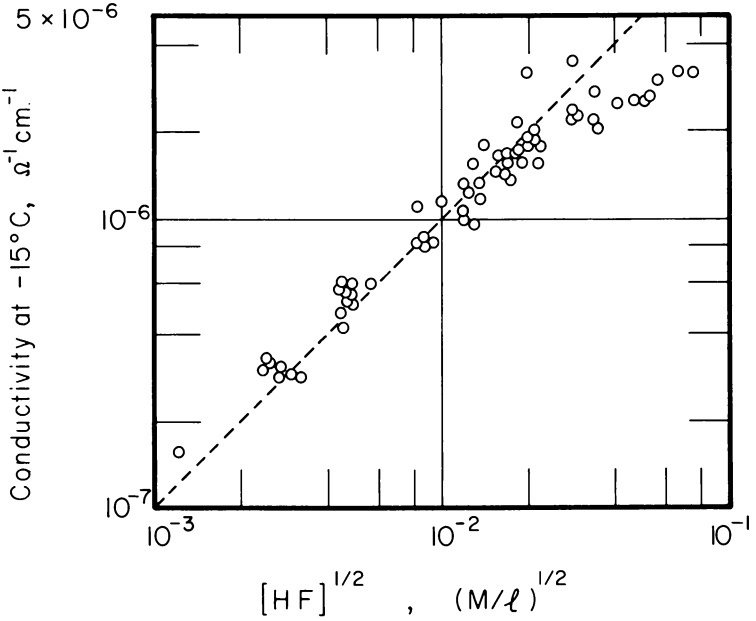

Figure 20. Conductivity of HF ice at −15°C. as a function of concentration (in the melted ice at room temperature) (67). The deviation of the experimental points from the straight line near the high concentration end possibly marks the solubility limit

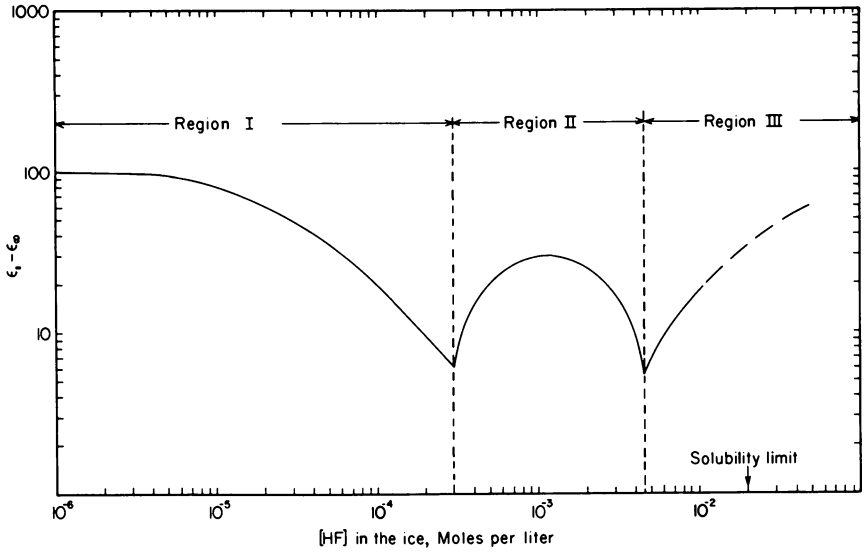

Figure 21. Static dielectric constant as a function of HF concentration at −3°C. after Steinemann (140). According to Jaccard (77), in Regions I and III valence defects (L defects in Region III) are the majority carriers; in Region II, ions predominate

impurity-produced (extrinsic) defects (0.6 kcal./mole) prevail (Table VI). According to Camp, this new evidence indicates that local disturbance about the impurity ions (Brill's domains) is not an important factor, but, rather, that NH_4F introduces valence defects with an excess of one type over the other.

A.c. conductivity measurements (39) did not show a clear concentration dependence.

None of the workers with NH_4F ice has attempted to relate its characteristics in detail to those of HF ice.

D.c. Measurements. Workman (57), Brill (*10*), Iribarne *et al.* (75), and G. W. Gross (67) reported that the resistivity of ice doped with NH_4F increases with concentration (Figure 26). Gross also reported that the activation energy increases systematically (from 6.4 to 9.1 kcal./mole) with concentration (from $8 \times 10^{-6}M$ to $7 \times 10^{-3}M$). Levi, Milman, and Suraski (*108*) measured the d.c. conductivity of ice from solutions containing different proportions of NH_4F, NH_4F + HF, and NH_4F + NH_4OH. They found that the conductivity shows a minimum slightly below the point where the concentration of ammonium ion equals that of fluoride ion in the ice (Figure 27). This minimum is a function of the ratio only, not of the absolute concentrations, of the two components. G. W. Gross has observed a systematic change in hydrogen-ion ratio of NH_4F ice (Figure 15). Levi *et al.* suggest that the concentration dependence of the conductivity may be attributed to a difference in cationic and anionic distribution coefficients. (Their numerical values for these coefficients are higher by orders of magnitude than those mentioned

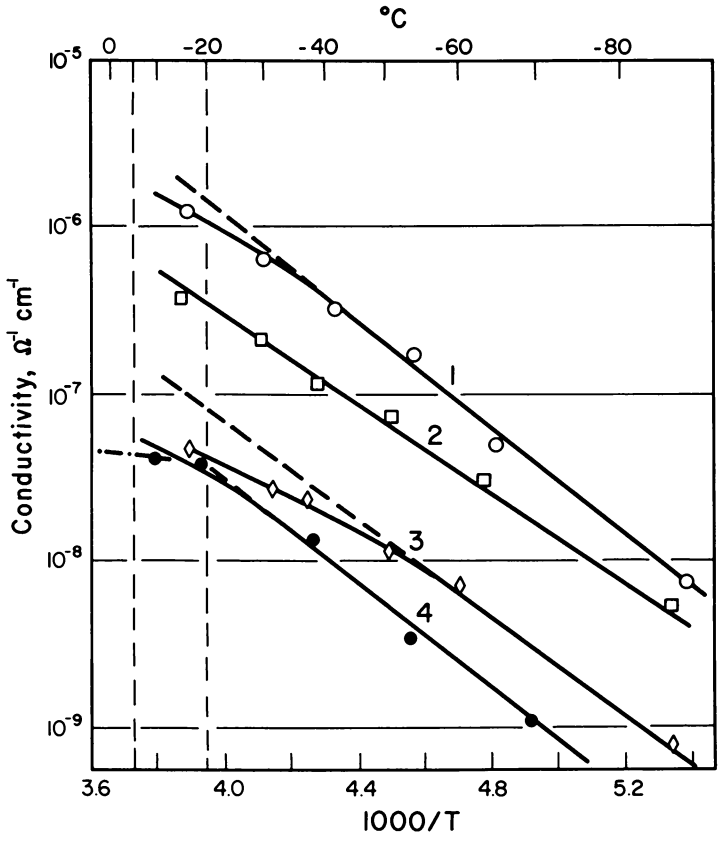

Figure 22. D.-c. conductivity vs. *1000/T for four samples of (polycrystalline) HF ice (strongly oriented parallel to the* c *axis) at different concentrations (in the melted ice at room temperature)*

Numbers (1-4) relate these curves to data given in Table V. Essentially similar results were obtained with single crystals (85). *The dashed vertical lines show the temperature range of Chai and Vogelhut's work* (24). *Flattening in the high temperature region is similar to results of Camp* et al. (20) *for very pure ice, not annealed, in the absence of surface conduction and was attributed by these authors to the existence of two conduction processes in series. Interpretation of the apparent activation energies according to Gränicher, Steinemann, and Jaccard is given in Table III. Samples were prepared with one or two HF sandwich electrodes* (65). *Their number, concentrations, and time (days) elapsed between sample preparation and first conductivity measurement were as follows. Curve 1: one; 1* × 10^{-1}M; *3.—Curve 2: one; 1* × 10^{-2}M; *2.—Curve 3: two; 5* × 10^{-4}M; *one.—Curve 4: one; 5* × 10^{-4}M; *7.*

earlier in this paper, because they are effective rather than interface coefficients.) In their results, Levi *et al.* see evidence that the conductivity of pure ice is one-half or one-third of that previously assumed (a view shared by Camp *et al., 20*) and that the proton mobility is from one-fourth

to one-ninth of Eigen and De Maeyer's value, so that it becomes comparable in magnitude to the OH^- mobility.

In conclusion, reliable experimental data, or perhaps a completely different approach, are needed to clarify the contradictory hypotheses that have been formulated for NH_4F ice. Above all, a quantitative theory is needed that will explain both a.c. and d.c. measurements consistent with the facts, as the theory by Gränicher *et al.* has done for HF ice. Such an approach may be available in Seidensticker's model (*138*). By assuming that NH_4F exists in ice as isolated HF and NH_3 molecules, it

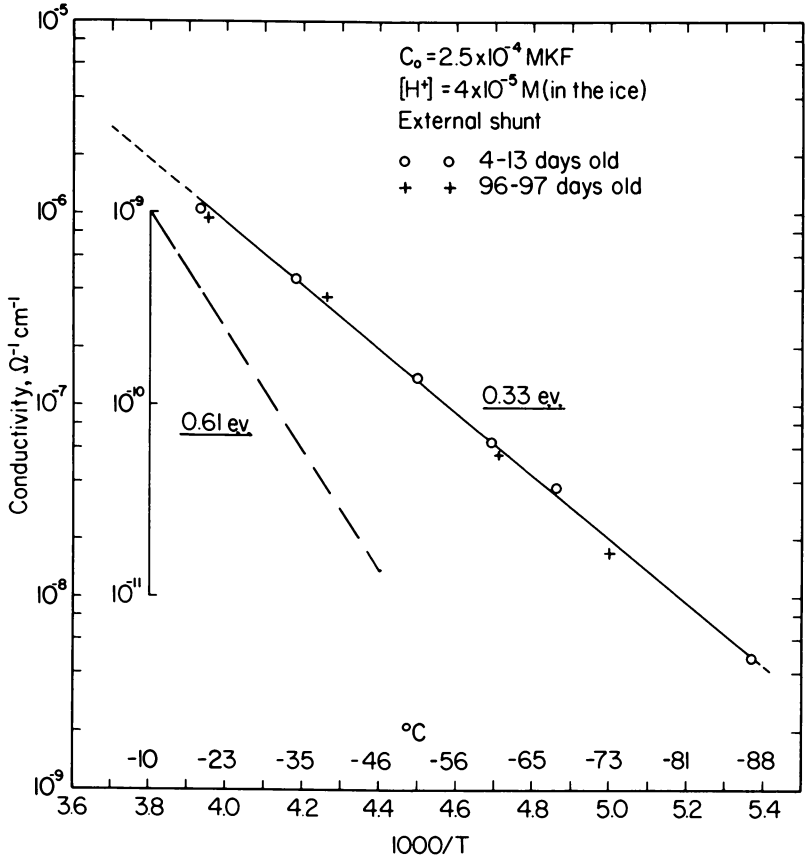

Figure 23. Full line: temperature dependence of the conductivity of KF ice grown with a shunt. (One sandwich electrode, prepared with 1 × 10^{-1}M HF. Sample stored four days at −20°C. before measurements.) No appreciable aging effect after storage at −20°C. for more than 80 days between measurements

Dashed line: data for pure ice, after Jaccard (77). If Camp et al. *(20) are right, this represents mainly surface conductivity, since the bulk conductivity of pure ice, according to these authors, is nearly independent of temperature within the range shown*

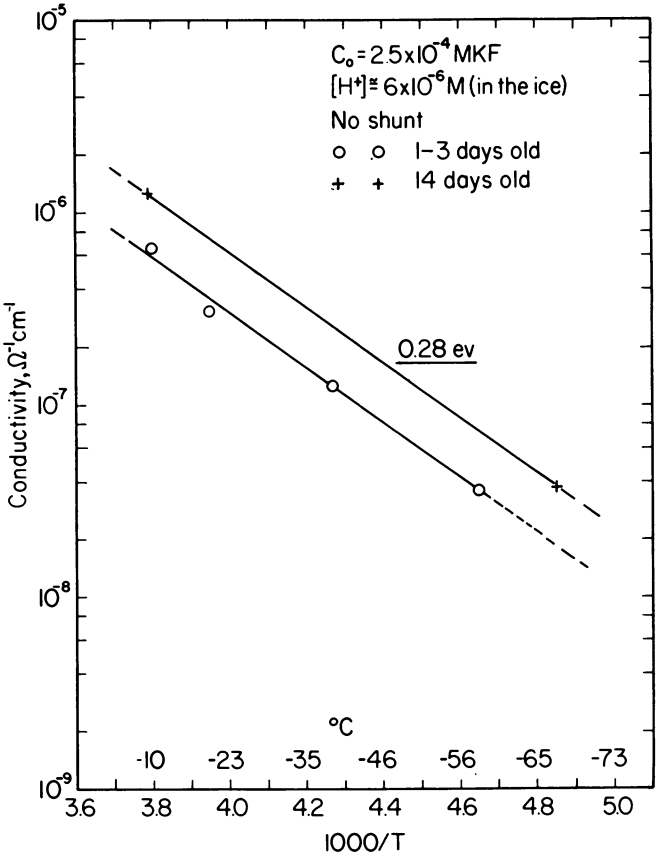

Figure 24. Temperature dependence and aging effects in KF ice grown without shunt. Notice invariance of slope (apparent activation energy). (One sandwich electrode, prepared with 1 × 10^{-1}M HF. Sample stored one day at −20°C. before measurements)

arrives at the result that proton donors and acceptors are (nearly) compensated. This would qualitatively account for the low conductivity. The high solid solubility stems from the fact that in the case of compensation there is no additional contribution from defect formation to the free energy.

MISCELLANEOUS IMPURITIES. Iribarne *et al.* (*75*) and Levi and Lubart (*106*) measured d.c. conductivities of ice doped with LiOH, NaOH, NH_4OH, LiF, NaF, LiCl, NaCl, KCl, RbCl, CsCl, and NH_4Cl as a function of concentration at −10°C. For the salts, they did not obtain a clear concentration dependence of the conductivity. In any event, the interpretation of such measurements is complicated by differential ion incorporation, not taken into account by the authors. They did, however,

assume different dissociation constants for the several ionic species, and computed equilibrium concentrations. For NH_4OH, they found a dependence of conductivity on the square root of concentration, below $2 \times 10^{-3}M$. NaOH ice showed the conductivity of pure ice below $1 \times 10^{-3}M$. In ice containing low NH_4OH concentrations, measurement of the dielectric constant and of the conductivity as a function of frequency yielded curves very similiar to those for pure ice; curves similar to those for HF were obtained in highly doped NH_4OH crystals. Interpretation of these measurements is complicated by the presence of traces of carbonates (unless the samples are grown and analyzed in a CO_2-free atmosphere) and by a high electrode contact resistance, as discussed in the section on the ice/solution interface.

Table V. Impurity Concentrations and Activation Energies of the Samples Shown in Figure 22.

Curve No.	Average freez. rate (mm./min.)	Concentrations (moles per liter)		Activation energies (e.v.)	
		Mother Soln.	Melted Ice	Str.-line section	Flat section
1[a]	1.3	5×10^{-4}	1 to 2×10^{-4}	0.32	0.24
2	1.5	1×10^{-5}	5×10^{-6}	0.26	0.26
3[a]	0.9	1×10^{-5}	2×10^{-6}	0.29	0.15
4	0.2	1×10^{-7}	5×10^{-8}	0.31	0.06 or 0.21
Average energy:				0.29 ± 0.03	0.16 ± 0.10 or 0.21 ± 0.05

[a] Stirred during freezing to prevent cloudiness and to ensure greater uniformity of concentration.

Dielectric and conductivity measurements of NH_3-doped ice were discussed by Arias, Levi, and Lubart (*1*). They observed a dielectric dispersion which, for all concentrations ($2 \times 10^{-5}M$ to $10^{-1}M$), and temperatures (−10°C. to −40°C.) was qualitatively similar to that for pure ice or ice of slight impurity content (Figure 18). The a.c. conductivity curves also look like those of Figure 18. Above $10^{-3}M$ the conductivity was independent of concentration and about equal to the d.c. conductivity. No specific expressions were given for the temperature and concentration dependence. These results point to a role for NH_3 in ice quite different from HF. Ionization appears to be much smaller in ice doped with the former; or the difference is caused by the smaller mobility of hydroxide ions as compared to hydrogen ions.

Seidensticker's model (*138*) accounts for the d.c. and a.c. conductivity measurements on NH_3-doped ice in terms of hybrid levels, that is, levels where both Bjerrum (D) and ionic defects are present at the same nitrogen site. If, further, the D defects associated with ammonia are only slightly dissociated, the model predicts that both a.c. and d.c. conduc-

tivities should exhibit a dependence on the square root of nitrogen concentration. This dependence is indeed suggested by the results of Arias *et al.* (*1*) and Levi and Lubart (*106*), respectively.

Discordant Results. Chai and Vogelhut (*24*) observed an apparently concentration-dependent change in the activation energy of d.c. conduction in HF- and NH_3-doped ice. They related this to the majority carrier shift discussed above. They covered a very narrow temperature range, thus introducing an element of considerable uncertainty (Figure 22). Their higher concentrations approach the solubility limit for HF in ice. It is not clear if Chai and Vogelhut plotted conductivity *vs.* ice concentration or *vs.* mother solution concentration. Neither do they discuss the concentration gradients in their samples. Their conductivity *vs.* concentration curves differ greatly from those of Steinemann (*140*) and of G. W. Gross (Figure 20) for HF, and from those of Levi and Lubart (*106*) for NH_4OH. Chai and Vogelhut do not discuss these discrepancies.

Sources of Error in Electrical Measurements. This discussion mainly concerns electrode effects, diffusion effects, and surface conductivity.

Nonpolarizing and low-resistance electrodes are extremely important. The electrolytic discharge of hydrogen and oxygen at the electrodes gives rise to troublesome polarization effects unless special precautions are taken. Ingenious techniques have been proposed by different investigators (*9, 15, 46, 48, 49, 65, 67, 73, 77, 112*). Krishnan, Young, and Salomon (*97*) even constructed and investigated a reversible hydrogen electrode in ice with fine platinum powder.

Sandwich electrodes minimize polarization effects and reduce the electrode contact resistance by increasing the contact surface. Typically, they may consist of a porous conductor saturated with a dilute HF solution or with the solution from which the sample was grown, frozen unto the latter (*65, 67, 77*). They are particularly beneficial as anodes, which suggests their role as proton sources. Gränicher *et al.* (*61*) explain the depolarizing mechanism of these electrodes by a cancellation of two space charges opposite in sign. At the same time, they state that the "bulk of sandwich crystals is homogeneously crowded by defects which were generated by the HF content of the electrode layers." They conclude that this may explain the much higher conductivity and low activation energy of pure ice crystals prepared with such sandwich electrodes. Kopp (*92*) found that the d.c. conductivity of such crystals increased with time and (after 50 to 100 hours at −23°C.) reached a plateau. The height of the plateau and time it took to reach depended on the concentration of the HF-ice layer and the temperature. He measured the HF content of slices of his samples. From these and nuclear magnetic relaxation studies, Kopp (*92*) and Kopp, Barnaal, and Lowe (*95*) found that the diffusion coefficient of HF in ice may be higher by as much as

five orders of magnitude than the self-diffusion coefficient of H_2O in ice, measured for diffusion of O^{18}, deuterium, and tritium in pure ice or in ice doped with HF or NH_4F (*see* Table VII). The results of Kopp *et al.* may be affected by surface (as opposed to bulk) diffusion, but they raise the definite possibility that the fluoride ion is much more mobile in the ice lattice than had previously been assumed. If true, this would seriously put in question many results based on measurements with HF sandwich electrodes. G. W. Gross used HF sandwich electrodes with doped samples over a wide concentration range (freezing solutions: $10^{-6}M$ to $10^{-3}M$; electrodes: 10 to 100 times mother solution concentration). Effects clearly attributable to diffusion were not observed. Obviously, the role of fluoride-ion diffusion merits a most careful experimental re-examination.

(Klinger (*91*) in his work on diffusion of HF in ice took precautions to prevent surface effects. His numerical value for the diffusion constant (Table VII) is only about one order of magnitude lower than Kopp's.)

Proton donor electrodes consisting of platinized platinum in contact with a thin layer of sulfuric acid or glycerol were used by Magnan and Kahane (*112*) for d.c. measurements of pure ice at temperatures from −80°C. to −120°C. and potential differences from 10 to 50 k.v. The current through the samples was non-ohmic (space-charge limited proton current). The effectiveness of these electrodes in preventing blocking effects was not discussed.

Surface conductive effects in snow were investigated by Kopp (*93*) who found that conductivity and activation energy were larger than expected from its ice content. Blicks, Egger, and Riehl (*8*) investigated surface conductive effects in ice single crystals. They found a higher concentration of impurities at the ice surface. Bullemer and Riehl (*15*) found the same temperature dependence (8.5 kcal./mole) for the bulk conductivity of pure and HF-doped ice.

Jaccard (*81, 82*) measured the surface conductivity of thin samples of pure ice. He concluded from his measurements that in a surface layer of at most 0.1 mm. thickness the d.c. conductivity is at least an order of magnitude larger than in the bulk. This indicates perhaps that the mobility, the charge carrier concentration, or both, are larger in this surface layer than in the bulk.

Camp, Kiszenick, and Arnold (*20*) measured a.c. and d.c. conductivities of pure ice and concluded that the bulk conductivity may be completely masked by the increased conductivity of a surface layer whose thickness is also a function of temperature. This results in a fictitious activation energy that is too high, in qualitative agreement with the findings of Bullemer and Riehl. As a consequence, the conductivity of pure ice may actually be orders of magnitude lower than the best values

hitherto obtained (Table IV). G. W. Gross (unpublished results) has observed that continuous application of constant d.c. voltages may result in a progressive current increase that cannot be explained by Joule heating of the bulk but which becomes plausible if an appreciable fraction of the current flows in a thin surface layer. (D.c. conductivity measurements by G. W. Gross were generally made with rather high currents (10^{-6} to 10^{-3} amps.)

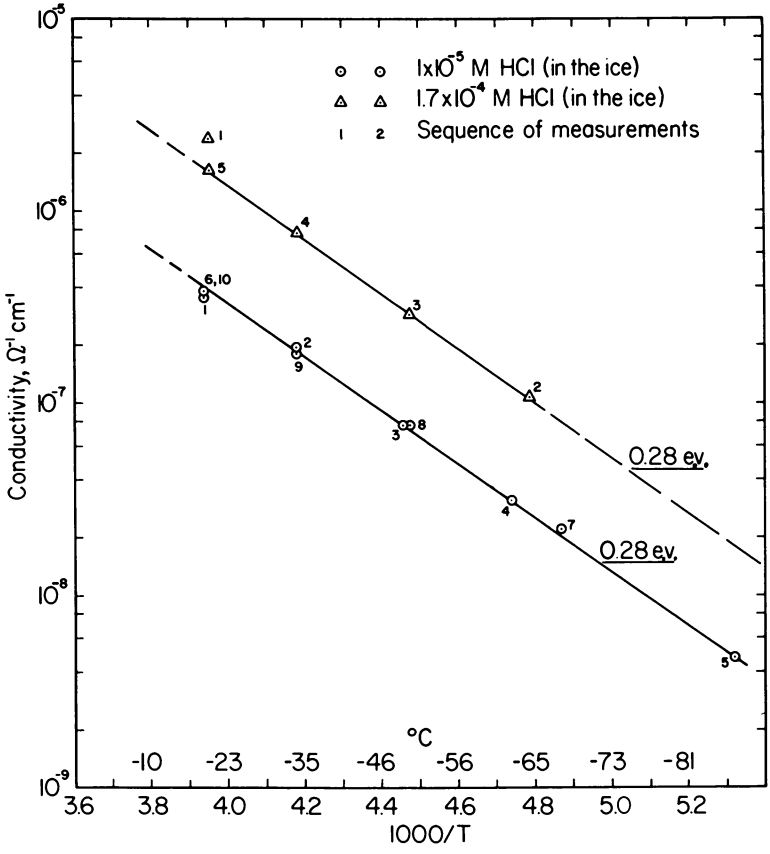

Figure 25. Temperature dependence and reproducibility of conductivity of HCl ice. Upper curve: One sandwich electrode (1 × 10^{-4}M HF); sample stored one day at −20°C. before measurements. Measurements extended over three days. Lower curve: One sandwich electrode (5 × 10^{-3}M HF); sample stored three days at −20°C. before measurements. Measurements extended over nine days

According to Bullemer (personal communication), water electrodes (*47*) make an almost ideal electrical connection to the ice surface but are poor proton injectors into the bulk. Surface currents obtained with

such electrodes are about 10 times those obtained with metal electrodes (and these, in turn, are about 10 times the bulk currents). This explains perhaps the high activation energies measured by Heinmets and Blum (73) for pure ice.

Miscellaneous Investigations

Pruppacher [*Z. Naturforsch.* **22a**, 895 (1967); *J. Glaciology* **6**, 651 (1967); *J. Chem. Phys.* **47** (**5**), 1807 (1967)] investigated the effect of acids, bases, and salts on the growth rate and morphology of ice in supercooled solutions as a function of degree of supercooling and of concentration ($10^{-6}M$ to $10^{-1}M$). Special precautions were taken to limit the number and size of solid particles introduced into the solutions with the reagents. Drops varying from 0.5 to 2.0 c.c. in volume were used, or the samples were contained in capillary tubes of 1.2 mm. internal diameter. Pruppacher found that most impurities in concentrations higher than $10^{-3}M$ caused a decrease in the growth rate relative to that in pure water. The fluorides, however, caused an increase in the freezing rate for a given degree of supercooling. Growth rates were of the order of centimeters per second. The growth morphology (dendrites) was primarily determined (a) by the degree of supercooling, (b) by the impurity concentration. The dendritic splitting angle was the most important morphologic element measured. The reduction of the freezing rate in solutions stronger than $10^{-3}M$ was explained by the initial reduction of the amount of supercooling induced at the interface by the rejected impurities—*i.e.*, by a reduced rate of dissipation of latent heat because of a lowering of the freezing point). The reduction of the freezing rate is, therefore, in part, a function of the diffusion coefficients of the impurity ions in the liquid phase. Furthermore, a correlation was found to exist between the amount a given ion pair depresses the equilibrium freezing point and the freezing-rate reduction caused by the same ion pair in supercooled solutions. This specific effect was interpreted in terms of the structure-breaking and hydrating properties of the ions. The increased freezing rate in fluoride solutions remains unexplained.

Both twinning and a stepped-growth mechanism have been proposed to explain the effect of degree of supercooling and of soluble impurities on the dendrite morphology. In the latter mechanism, the ratio between step height and distance between steps is affected—*i.e.*, the ratio of growth velocities parallel and perpendicular to the c-axis direction. Pruppacher points out that neither of the two explanations is satisfactory. He concludes that in aqueous solutions the rate of advance in the c-axis direction is reduced more strongly than that in the basal plane.

Table VI. A.c. Measurements on NH_4F Ice

(1) Brill and Camp (*11*): $\frac{1}{\tau} = 10^{15} \exp.\left(\frac{E\text{-}E'}{a}\right) \exp.\left(-\frac{E}{kT}\right)$

E: activation energy of dipole rotation in NH_4F ice (1.7–5.7 kcal./mole)
E': activation energy of dipole rotation in pure ice (13.2 kcal./mole)
a: 550 cal.
Temperature range: ~ −5°C. to ~ −45°C.

(2) Camp (*18*): $\frac{1}{\tau} = 3.3 \times 10^{15} \exp.\ (-E'/kT) + 1.9 \times 10^{4} \exp.\ (-E/kT)$

$E = 0.6$ kcal./mole (0.026 e.v.)
$E' = 13.5$ kcal./mole (0.59 e.v.)
Temperature range: ~ −5°C. to ~ −45°C.

(3) Dengel *et al.* (*39*): $\frac{1}{\tau} = 1.89 \times 10^{15} \exp.\ (-E'/kT)$

$E' = 13.2$ kcal./mole (0.57 e.v.)
Temperature range: −10°C. to −14°C.

Mechanical Relaxation. Mechanical relaxation in pure and doped ice was investigated experimentally (*136*) and theoretically (*4*). Relaxation occurs in the frequency range of the dielectric Debye dispersion, but the variation in the measured quantity (logarithmic decrement) is only about 1/100 of that for dielectric measurements, The relaxation time, τ, is given by

$$\frac{1}{\tau} = 3 \times 10^{15}\left[exp.\left(-\frac{0.58 \text{ e.v.}}{kT}\right)\right],$$

identical, within experimental uncertainty, with the dielectric Debye relaxation time (Table III). This led to the conclusion that both dielectric and mechanical relaxation result from the same process, that is, a reorientation of water molecules (*142*). Diffusion of lattice defects is rate-determining. The introduction of suitable impurities into the lattice should facilitate the relaxation process and reduce the activation energy of the mechanical relaxation time. Walz and Magun (*155*) found that this is indeed true for ammonium-fluoride ice. In analogy with the dielectric studies by Camp (*18*), they found that at low temperatures, the activation energy is low (2.3 kcal./mole or 0.1 e.v.; process controlled by impurities), changing to 13.4 kcal./mole (0.58 e.v.) at high temperatures (intrinsic range). The reciprocal relaxation time

$$\frac{1}{\tau} \propto [NH_4F]^{1/2}.$$

For ice doped with HF, Schulz (*137*) found

$$\frac{1}{\tau} \propto [HF]^{1/3}.$$

The activation energy of 6.8 kcal./mole (0.3 e.v.) is again similar to the dielectric case. A transition to intrinsic defect control at higher temperatures was not observed.

In HF doped ice, Kopp (personal communication) found exponents of 0.4 and 0.6 for the concentration dependence of the dielectric relaxation and of the nuclear magnetic relaxation, respectively. He suggests that the mass-action law does not hold for the relaxations.

Steinemann (*140*) found that, at a given temperature, the dielectric relaxation time was inversely proportional to the HF concentration if the concentration was high, and inversely proportional to the square root of the concentration if it was lower. (The relations are listed in Table III.) Thus, the concentration dependence of the dielectric relaxation time does not follow a simple law. The formulation depends on the assumptions one makes about the nature of the relaxation process or processes (ion translation or molecular rotation), carrier concentration and dissociation, and the energies involved.

Optical Production of Defects. Theoretically, this is a means to change defect concentrations without introducing impurities or changing

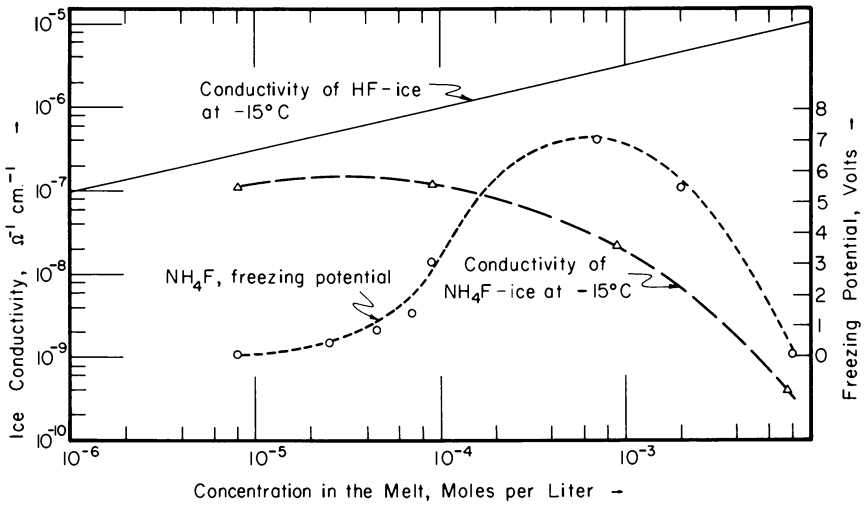

Figure 26. Conductivity at −15°C. and highest value of the freezing potential as a function of concentration (melted ice, room temperature) for ice grown from dilute ammonium-fluoride solutions. Curve of HF ice for comparison (67). The ammonium-fluoride samples were prepared in pairs, with one sandwich electrode made from 5 × 10⁻³M HF, and stored from two to 27 days at −20°C. before measurements. No effects of diffusion from sandwich electrodes into the samples were observed

the temperature. Thus, it would allow independent checks on some of the parameters derived from electrical measurements. Camp (*18*) observed that irradiation of ice with certain wave lengths increased the a.c. and d.c. conductivities. Camp and Spears (*21*) made further experiments to ascertain whether the effect was caused by production of defects by photon interaction with water molecules or to thermal absorption and dissociation. Both processes appeared to occur in the same region of the spectrum (0.8 to 2.7 μ). The authors concluded that heating is limited to a thin surface layer of the sample and masks genuine optical responses that may exist.

Hall-Effect Measurements. Bullemer and Riehl (*16*) made these measurements. The experimental difficulties are great because of high electrode resistance, polarization effects, surface conductivity, and a low signal-to-noise ratio. Special palladium-black electrodes were used. The majority carriers were found to have a positive sign, as they should if they are protons. At −2°C. and −8°C., respectively, their concentration was 1.0 and 0.4 $\times$ 10^{10} $cm.^{-3}$, and the Hall mobility was 0.8 and 1.4 $cm.^2$/volt-sec. These values are 10 to 20 times lower and higher, respectively, than the results found by Eigen and De Maeyer from the saturation current and dissociation field effect (Table IV).

Rectifying Ice "p,n" Junctions. These were constructed by Eigen and De Maeyer (*46*). They placed in contact an HF ice, acting as a proton donor, and an acceptor made of LiOH or NH_4OH ice. Special protonic electrodes consisting of semipermeable membranes, acid and alkaline solutions respectively, and reversible electrodes were used. No details have been published.

Thermoelectric Effects in Ice. This type of effect was mentioned earlier in connection with Group III solutes and with contact electrification. Latham and Mason (*102*) proposed a theory in which the roles of Bjerrum defects and of electrode contact potentials were neglected. In pure ice, they found the thermoelectric potential given by: $V = 2\Delta T$ mv. They found that adding HCl increased and NaCl decreased the charge separation with respect to that for pure water. Jaccard (*78*) derived an expression for the thermoelectric potential difference per degree of temperature difference (thermoelectric power) as a function of mobility ratios of the defects (ion and valence defects, respectively), their concentrations, their energies of formation and diffusion, and their effective charge. Latham (*101*) reported that the thermoelectric potential in pure ice was greater than predicted by the theory if the specimen was at temperatures above −7°C. He ascribed this to increased charge transfer in a surface layer having a larger variation of conductivity with temperature than the bulk ice. Non-uniformity of temperature gradients also increased the charge transfer (*100*). Bryant and Fletcher (*14*)

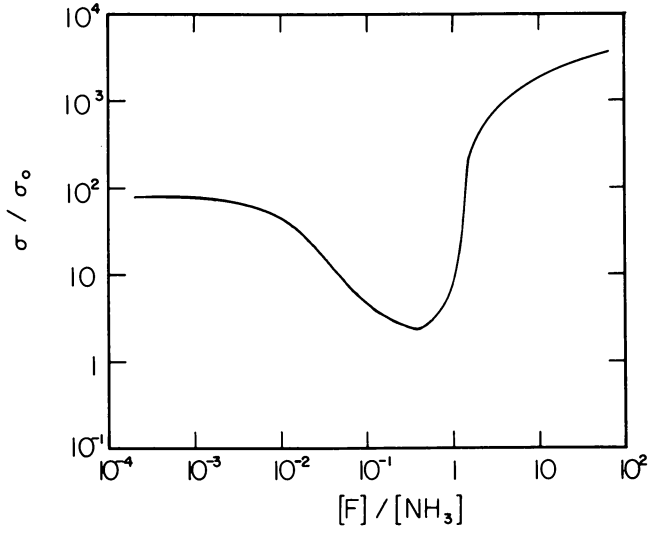

Figure 27. Ratio of the conductivities of doped ice (σ) to pure ice (σ_0) as a function of the concentration ratio of fluoride ion to ammonium ion (in the ice). The conductivity ratio is a minimum when the concentration ratio is close to one. After Levi, Milman, and Suraski (108)

experimentally determined the thermoelectric power of ice doped with HF and NH_3, respectively. Their work qualitatively confirmed Jaccard's theory. The thermoelectric power is concentration-dependent. The potential sign is opposite for NH_3 as compared with HF ice. This appears to confirm the concept that NH_3 and HF act as acceptors and donors, respectively, of hydrogen ions. The authors qualitatively corrected for the electrode contact potentials by comparing results obtained with brass and palladium electrodes.

Brownscombe and Mason [*Phil. Mag.* **14**, 1037 (1966)] used an electrodeless induction method to determine the thermoelectric power of pure ice. The data are strongly scattered but, in the mean, lead to results comparable with those of Latham and Mason (*102*). Measurements on ice doped with HF and NH_3 showed fair agreement with values computed from Jaccard's theory (*78*).

The thermoelectric effect, in theory, is still another method for investigating the effects of impurities on the ice structure, and of determining experimental parameters, such as effective charge and mobility ratios. Since the potentials generated are of similar magnitude to electrode contact potentials, the interpretation is difficult.

Table VII. Diffusion in Ice

Diffusing Species	*Diffusion Constant (cm.²/sec.)*	*Temp. (°C.)*	*Activation Energy kcal./mole*	*e.v.*	*Ref.*
HF	$\sim 10^{-11}$	−10	—	—	(*140*)
HF	$\sim 10^{-11}$ or $\sim 10^{-6}$ [a]	−10	—	—	(*92*)
HF	$\sim 10^{-6}$ / $\sim 10^{-7}$	−8 / −30	13.8	0.6	(*94*)
HF	8×10^{-8}	−13	—	—	(*91*)
NH_4F	$\sim 5 \times 10^{-9}$ and $\sim 5 \times 10^{-8}$	between −6 and −20	—	—	(*11*)
O^{18}, H^2	$\sim 10^{-10}$	−1.8	—	—	(*98*)
O^{18}	5×10^{-11}	−20	—	—	(*89*)
O^{18}	1.6×10^{-11}	−14.4	15.7	0.68	(*35*)
H^3	2×10^{-11} / 1×10^{-12}	−7 / −33	13.5	0.59	(*38*)
H^3	2.8×10^{-11}	−10	15.4	0.67	(*76*)
H^3 [b]	$\sim 2 \times 10^{-11}$	−10	14.5	0.63	(*7*)
H^3 [c]	$\sim 2 \times 10^{-11}$	−10	14.5	0.63	(*37*)

[a] Depending on method of evaluation, Kopp *et al.* (*95*) found that diffusion into a piece of pure ice from one containing a high HF concentration, in intimate contact with the former (diffusion couple), is limited by a "filter effect." This means that, regardless of actual concentration, only a limiting concentration of $1.4 \times 10^{-3} M$ can be admitted to the pure ice. If this filter effect is not taken into account, the computed diffusion coefficients will be too low by orders of magnitude.

[b] In pure and HF ice.

[c] In NH_4F ice.

Summary and Conclusions

Charge separation processes at the ice/water phase boundary are primarily attributed to the incorporation into the ice lattice of certain impurity ions in preference to others. An electrical double layer at the interface consists of a deep zone of frozen-in charge on the solid side and a diffuse layer of counterions on the liquid side. Hydrogen and hydroxide ions provide the neutralization current, their availability determining the interface resistance. According to the characteristics of the ion and charge transfer reactions, inorganic ionic solutes may be divided into three groups: (I) Alkali halides plus ammonium fluoride; negative ions are preferentially incorporated into the ice; freezing potentials are strongly dependent on concentration and freezing rate; an external shunt intensifies the charge transfer. (II) Certain ammonium and lead salts;

positive ions are preferentially incorporated into the ice, but their number is always small; freezing potentials are high; charge transfer is always small. (III) Halogen acids, alkali hydroxides, and ammonium hydroxide; no charge separation takes place; incorporation for the acids decreases from the hydrofluoric to the iodic.

Differential ion transfer across the phase boundary is manifest in small differences of distribution coefficients for the species of an ion pair. The distribution coefficient for a given ion depends also on the other ionic species present in solution and their concentrations. The apparent distribution coefficients, determined from experiment, depend on both freezing rate and concentration. Differential diffusion appears to play only a secondary role. The apparent distribution coefficients for potassium and cesium fluoride are higher than those for HF solutions of the same concentration. They appear to increase with concentration while those for HF decrease. The increase is perhaps explained by the formation of regions of higher concentration at cell or grain boundaries, or it may be related to the possibility that most cations enter the ice lattice interstitially rather than substitutionally. The interpretation of solute distribution curves in ice is difficult.

Impurities tend to concentrate at the boundary between ice and container. Within the solid, their distribution depends on the shape of the ice/water interface and on its surface structure (cells, dendrites, constitutional super-cooling).

The crystallographic c/a ratio of ice doped with HF and NH_4F is slightly shortened. This confirms the concept of substitutional emplacement of these impurity molecules. A hexagonal microstructure, which develops as a consequence either of crystallization stress or of aging, is relieved in highly doped crystals.

Electrical measurements of ice are difficult to interpret because of polarization effects, surface conductivity, injection of defects and/or impurity atoms from sandwich electrodes, diffusion effects, differential ion incorporation, and concentration gradients due to nonsteady state impurity distribution. Theories formulated for pure ice and for ice doped with HF (KF and CsF) in terms of ion states and valence defects, qualitatively account for experimental data, although the problem of the majority and minority carriers in doped ice, as a function of concentration and temperature, requires further examination. The measurements on ice prepared from ionic solutes other than HF, KF, and CsF are largely unexplained. An alternative approach that treats ice as a protonic semiconductor accounts for results obtained for both the before-named impurities as well as ammonia and ammonium fluoride.

Acknowledgement

This paper was written at the suggestion of R. A. Baker, Senior Fellow, The Mellon Institute, Pittsburgh, Pennsylvania. Mr. Chen-ho Wu did most of the experimental work for the second part of this paper. P. R. Camp kindly gave permission to quote his measurements on surface conductivity before publication. Marcel Kopp critically reviewed the manuscript and supplied numerous unpublished data and observations. This work was supported by the Office of Naval Research under Contract Nonr 815(05).

Literature Cited

(1) Arias, D., Levi, L., Lubart, L., *Trans. Faraday Soc.* **62,** 1955 (1966).
(2) Baker, R. A., *Water Research* **1,** 61 (1967).
(3) Baker, R. A., *Water Research* 1, 97 (1967).
(4) Bass, R., *Z. Physik* **153,** 16 (1958).
(5) Bernal, J. D., Fowler, R. H., *J. Chem. Phys.* **1,** 515 (1933).
(6) Bjerrum, N., *Dan. Mat. Fys. Medd.* **27** (1), 1 (1951).
(7) Blicks, H., Dengel, O., Riehl, N., *Physik Kondensierten Materie* **4,** 375 (1965/66).
(8) Blicks, H., Egger, H., Riehl, N., *Physik Kondensierten Materie* **2,** 419 (1964).
(9) Bradley, R. S., *Trans. Faraday Soc.* **53,** 687 (1957).
(10) Brill, R., *U. S. Army Snow, Ice and Permafrost Research Establishment* (now CRREL, which stands for *Cold Regions Research and Engineering Laboratory,* located at U.S. Army Material Command Command, Hanover, N. H. 03755) **Report 33** (1957).
(11) Brill, R., Camp, P. R., *CRREL* **Research Rept. 68** (1961).
(12) Brill, R., Ender, H., Feuersänger, A., *Z. Elektrochem.* **61,** 1071 (1957).
(13) Brook, M. "Recent Advances in Atmospheric Electricity," pp. 383-389, Pergamon Press, New York, 1959.
(14) Bryant, G. W., Fletcher, N. H., *Phil. Mag. 12 (Eighth Series)* **165** (1965).
(15) Bullemer, B., Riehl, N., *Solid State Communications* **4,** 447 (1966).
(16) Bullemer, B., Riehl, N., *Physics Letters* **22,** 411 (1966).
(17) Burton, J. A., Prim, R. C., Slichter, W. P., *J. Chem. Phys.* **21,** 1987 (1953).
(18) Camp, P. R., *CRREL,* **Research Report 114** (1963).
(19) Camp, P. R., *Ann. N. Y. Acad. Sci.* **125,** 317 (1965).
(20) Camp, P. R., Kiszenick, W., Arnold, D. A., *CRREL,* **Research Report 198** (in press).
(21) Camp, P. R., Spears, D. L., *CRREL,* **Research Report 175** (1966).
(22) Carlin, J. T., M.S. Thesis. New Mexico Institute of Mining and Technology, Socorro (1956).
(23) Carslaw, H. S., Jaeger, J. C., "Conduction of Heat in Solids." Clarendon Press, Oxford, 1959.
(24) Chai, S. Y., Vogelhut, P. O., *Science* **148,** 1595 (1965).
(25) Chernov, A. A., *Soviet Phys. "Doklady" (English Transl.)* **5** (3), 470 (1960).
(26) Cobb, A. W., *Science* **141,** 733 (1963).
(27) Cobb, A. W., "Interfacial Electrical Effects Observed During the Freezing of Water." Unpublished research report, on file at New Mexico Institute of Mining and Technology, Socorro, 1964.

(28) Cohan, N. V., Cotti, M., Iribarne, J. V., Weissmann, M., *Trans. Faraday Soc.* **58**, 490 (1962).
(29) Cohan, N. V., Weissmann, J., *Nature* **201**, 490 (1964).
(30) Costa Ribeiro, Jr., Ph.D. Thesis. Univ. of Brazil, Rio de Janeiro (1945).
(31) Costa Ribeiro, J., *Anais Acad. Brasil. Cienc.* **19** (4), Resumos, p. 6. (1947).
(32) Costa Ribeiro, J., *Anais Acad. Brasil. Cienc.* **22** (3), 325 (1950).
(33) Debye, P., "Polar Molecules." Dover Publications, 1929.
(34) Decroly, J. C., Gränicher, H., Jaccard, C., *Helv. Phys. Acta* **30**, 465 (1957).
(35) Delibaltas, P., Dengel, O., Helmreich, D., Riehl, N., Simon, H., *Physik Kondensierten Materie* **5**, 166 (1966).
(36) De Micheli, S. M. de, Iribarne, J. V., *J. Chim. phys. (France)* **60**, 767 (1963).
(37) Dengel, O., Jacobs, E., Riehl, N., *Physik Kondensierten Materie* **5**, 58 (1966).
(38) Dengel, O., Riehl, N., *Physik Kondensierten Materie* **1**, 191 (1963).
(39) Dengel, O., Riehl, N., Schleippmann, A., *Physik Kondensierten Materie* **5**, 83 (1966).
(40) Deryagin, B. V., ed., "Research in Surface Forces" (2 vols.). Consultants Bureau, N. Y., 1966.
(41) Drost-Hansen, W., "Anomalies in the Properties of Water." Intern. Symp. on Water Desalination, 1st, Dept. of Int., Wash., D. C., Oct. 3-9, 1965.
(42) Drost-Hansen, W., *J. Coll. and Interface Sci.* **25** (2), 131 (1967).
(43) Dukhin, S. S., "Research in Surface Forces," vol. 1, pp. 27-34. Consultants Bureau, N. Y., 1966.
(44) Dukhin, S. S., "Research in Surface Forces," vol. 2, pp. 54-74. Consultants Bureau, N. Y., 1966.
(45) Dunitz, J. D., *Nature* **197**, 860 (1963).
(46) Eigen, M., De Maeyer, L., *Proc. Roy. Soc. (London), Ser. A* **247**, 505 (1958).
(47) Eigen, M., De Maeyer, L., Spatz, H.-Ch., *Ber. Bunsenges. Physik. Chem.* **68**, 19 (1964).
(48) Engelhardt, H., Riehl, N., *Physics Letters* **14** (1), 20 (1965).
(49) Engelhardt, H., Riehl, N., *Physik Kondensierten Materie* **5**, 73 (1966).
(50) Fletcher, N. H., *Phil. Mag. (Eighth Series)* **7**, 255 (1962).
(51) *Ibid.*, **8**, 1425 (1963).
(52) Frank, H. S., Evans, M. W., *J. Chem. Phys.* **13**, 507 (1945).
(53) Frank, H. S., Robinson, A. L., *J. Chem. Phys.* **8**, 933 (1940).
(54) Frank, H. S., Wen, Wen-Yang, *Discussions Faraday Soc.* **24**, 133 (1957).
(55) Gentile, A. L., Drost-Hansen, W., *Naturwissenschaften* **43**, 274 (1956).
(56) Gill, E. W. B., *Brit. J. Appl. Phys., Suppl.* **2**, 16 (1953).
(57) Gill, E. W. B., Alfrey, G. F., *Nature* **169**, 203 (1952).
(58) Gosar, P., Pintar, M., *Physica Status Solidi* **4**, 675 (1964).
(59) Gränicher, H., *Z. Krist.* **110**, 432 (1958).
(60) Gränicher, H., *Physik Kondensierten Materie* **1**, 1 (1963).
(61) Gränicher, H., Jaccard, C., Scherrer, P., Steinemann, A., *Discussions Faraday Soc.* **23**, 50 (1957).
(62) Gross, B., *Anais Acad. Brasil. Cienc.* **18** (2), 127 (1946).
(63) Gross, B., *Phys. Rev.* **94**, 1545 (1954).
(64) Gross, B., "Charge Storage in Solid Dielectrics. A Bibliographical Review on the Electret and Related Effects." Elsevier, New York, 1964.
(65) Gross, G. W., *Science* **138**, 520 (1962).
(66) Gross, G. W., *J. Geophys. Res.* **70**, 2291 (1965).
(67) Gross, G. W., *Ann. N. Y. Acad. Sci.* **125**, 380 (1965).

(68) Gross, G. W., *J. Coll. and Interface Sci.* **25** (2), 270 (1967).
(69) Harrison, J. D., Tiller, W. A., "Ice and Snow. Properties, Processes and Applications," W. D. Kingery, ed., Chap. 16, MIT Press, Cambridge, Mass., 1963.
(70) Harrison, J. D., Tiller, W. A., *J. Appl. Phys.* **34**, 3349 (1963).
(71) Haydon, D. A., "Recent Progress in Surface Science," J. F. Danielli, K. G. A. Pankhurst, A. C. Riddiford, eds. Vol. 1, pp. 94-158. Academic Press, New York, 1964.
(72) Heinmets, F., *Trans. Faraday Soc.* **58** (Part 4), 788 (1962).
(73) Heinmets, F., Blum, R., *Trans. Faraday Soc.* **59** (Part 5), 1141 (1963).
(74) Humbel, F., Jona, F., Scherrer, P., *Helv. Phys. Acta* **26**, 17 (1953).
(75) Iribarne, J. V., Levi, L., de Pena, R. G., Norscini, R., *J. Chim. phys. (France)* **58**, 208 (1961).
(76) Itagaki, K., *J. Phys. Soc. Japan* **19**, 1081 (1964).
(77) Jaccard, C. *Helv. Phys. Acta* **32**, 89 (1959); and Cloud Physics Lab., Univ. of Chicago, *Technical Note 33* (Engl. transl).
(78) Jaccard, C., *Physik Kondensierten Materie* **2**, 143 (1963).
(79) Jaccard, C., *Physik Kondensierten Materie* **3**, 99 (1964).
(80) Jaccard, C., *Ann. N. Y. Acad. Sci.* **125**, 390 (1965).
(81) Jaccard, C., *Proc. Intern. Conf. on Cloud Physics*, May 24 to June 1, 1965, Tokyo and Sapporo.
(82) Jaccard, C., *Z. Angew. Math. Phys.* **17**, 657 (1966).
(83) Jaccard, C., *Physik Kondensierten Materie* **4**, 349 (1966).
(84) Jaccard, C., Levi, L., *Z. Angew. Math. Phys.* **12**, 70 (1961).
(85) Jarvela, G. N., M.S. Thesis. New Mexico Institute of Mining and Tech., Socorro (1965).
(86) Johnstone, J. H. L., *Proc. Trans. Nova Scotian Inst. Science* **13**, 126 (1911-12).
(87) Jost, W., "Diffusion in Solids, Liquids, Gases." Academic Press, N. Y., 1952.
(88) Kavanau, J. L., "Water and Solute-Water Interactions." Holden-Day Inc., San Francisco, 1964.
(89) Kingery, W. D., Adams, Jr., C. M., *Air Force Cambridge Res. Lab.*, **Rept. 1080**, 7 (1962).
(90) Kittel, Ch., "Introduction to Solid State Physics." 2nd ed., John Wiley, New York, 1959.
(91) Klinger, J., Diploma Thesis, Technische Hochschule München, Munich, 1966.
(92) Kopp, M., Diploma Thesis, Eidgenössische Technische Hochschule, Zurich, 1959.
(93) Kopp, M., *Z. Angew. Math. Phys.* **13**, 431 (1962).
(94) Kopp, M., M.S. Thesis, University of Pittsburgh, 1965.
(95) Kopp, M., Barnaal, D. E., Lowe, I. J., *J. Chem. Phys.* **43**, 2965 (1965).
(96) Krause, B., Renninger, M., *Acta Cryst.* **9**, 74, 1956.
(97) Krishnan, P. N., Young, I., Salomon, R. E., *J. Phys. Chem.* **70**, 1595 (1966).
(98) Kuhn, W., Thürkauf, M., *Helv. Chim. Acta* **41**, 938 (1958).
(99) Labowitz, L. C., Westrum, Jr., E. F., *J. Phys. Chem.* **65**, 408 (1961).
(100) Latham, J., *Brit. J. Appl. Phys.* **14**, 488 (1963).
(101) Latham, J., *Nature* **200**, 1087 (1963).
(102) Latham, J., Mason, B. J., *Proc. Roy. Soc. (London), Ser. A* **260**, 523 (1961).
(103) Latham, J., Stow, C. D., *Quart. J. Roy. Meteorol. Soc.* **91**, 462 (1965).
(104) LeFebre, V., *J. Coll. and Interface Sci.* **25** (2), 263 (1967).
(105) Levi, L., Arias, D., *J. Chim. Phys. (France)* **61**, 688 (1964).
(106) Levi, L., Lubart, L., *J. Chim. Phys. (France)* **58**, 863 (1961).

(107) Levi, L., Milman, O., *J. Atmospheric Sciences* **23**, 182 (1966).
(108) Levi, L., Milman, O., Suraski, E., *Trans. Faraday Soc.* **59**, 2064 (1963).
(109) Lodge, J. P., Baker, M. L., Pierrard, J. M., *J. Chem. Phys.* **24**, 716 (1956).
(110) Loeb, L. B., "Static Electrification." Springer, Berlin, 1958.
(111) McFee, R. H., *J. Chem. Phys.* **15**, 856 (1947).
(112) Magnan, D., André Kahane, M., *Comptes Rendus de l'Académie des Sciences, Paris* **256**, 5539 (1963).
(113) Magono, C., Takahashi, T., *J. Meteorol. Soc. Japan* **41**, 71 (1963).
(114) Malo, B. A., Baker, R. A. (1967), ADVAN. CHEM. SER. **73**, 149 (1968).
(115) Mascarenhas, S., Thesis. Escola de Engenharia de Sao Carlos, Universidade de Sao Paulo, 1958.
(116) Mascarenhas, S., Freitas, L. G., *J. Appl. Phys.* **31**, 1684 (1960).
(117) Moore, W. J., "Physical Chemistry," 2nd ed., Prentice-Hall, Englewood Cliffs, N. J., 1955.
(118) Nagasawa, H., *Science* **152**, 767 (1966).
(119) Onsager, L., Dupuis, M., *Rend. Scuola Intern. Fis. "Enrico Fermi"* **10**, 294 (1960).
(120) Onsager, L., Dupuis, M., "Electrolytes," pp. 27-46, Pergamon Press, New York, 1962.
(121) Onsager, L., Runnels, L. K., *Proc. Nat. Acad. Sci. U.S.* **50**, 208 (1963).
(122) Parreira, H. C., Eydt, A. J., *Nature* **208**, 33 (1965).
(123) Pfann, W. G., "Zone Melting," John Wiley, New York, 1958.
(124) Pfann, W. G., Wagner, R. S., *Trans. AIME* **224**, 1139 (1962).
(125) Pohl, R. G., *J. Appl. Phys.* **25**, 1170 (1954).
(126) Reynolds, S. E., Brook, M., Gourley, M. F., *J. Meteorol.* **14**, 426 (1957).
(127) Riehl, N., *Naturwissenschaften* **43**, 145 (1956).
(128) Riehl, N., *Kolloid-Z.* **151**, 66 (1957).
(129) Riehl, N., "Festkörperprobleme," vol. 4, pp. 45-56. Friedrich Vieweg & Sohn, Braunschweig, 1965.
(130) Riehl, N., *Trans. N. Y. Acad. Sci., Ser. II*, **27**, 772 (1965).
(131) Riehl, N., "Energy Transfer in Radiation Processes," G. O. Phillips, ed., pp. 95-104. Elsevier, Amsterdam, 1966.
(132) Samoilov, O. Ya., *Discussions Faraday Soc.* **24**, 141 (1957).
(133) Samoilov, O. Ya., "Structure of Aqueous Electrolyte Solutions and the Hydration of Ions." Consultants Bureau, New York, 1965.
(134) Schaefer, V. J., *Phys. Rev.* **77**, 721 (1950).
(135) Scheraga, H. A., *Ann. N. Y. Acad. Sci.* **125**, 253 (1965).
(136) Schiller, P., *Z. Physik* **153**, 1 (1958).
(137) Schulz, H. *Naturwissenschaften* **48**, 691 (1961).
(138) Seidensticker, R. G., Ph.D. Thesis. Carnegie Institute of Technology, Pittsburgh, Pa., 1967.
(139) Sennett, P., Olivier, J. P., "Chemistry and Physics of Interfaces," pp. 75-92. American Chemical Society Publications, Washington, D. C., 1965.
(140) Steinemann, A., *Helv. Phys. Acta* **30**, 581 (1957).
(141) Steinemann, A., Gränicher, H., *Helv. Phys. Acta* **30**, 553 (1957).
(142) Stephens, R. W. B., *Advan. in Physics* **7**, 266 (1958).
(143) Takahashi, T., *J. Meteorol. Soc. of Japan* **40**, 277 (1962).
(144) Tiller, W. A., *Trans. AIME* **224**, 448 (1962).
(145) Tiller, W. A., "The Art and Science of Growing Crystals," J. J. Gilman, ed., Chap. 15. John Wiley, N. Y., 1963.
(146) Tiller, W. A., *Science* **146**, 871 (1964).
(147) Tiller, W. A., Jackson, K. A., Rutter, J. W., Chalmers, B., *Acta Met.* **1**, 428 (1953).
(148) Tiller, W. A., Rutter, J. W., *Can. J. Phys.* **34**, 96 (1956).

(149) Tiller, W. A., Sekerka, R. F., *J. Appl. Physics* **35**, 2726 (1964).
(150) Truby, F. K., *Science* **121**, 404 (1955).
(151) Truby, F. K., *J. Appl. Phys.* **26**, 1416 (1955).
(152) Tyrrell, H. J. V., "Diffusion and Heat Flow in Liquids," Butterworths, London, 1961.
(153) Vanderberg, R. M., Ellis, J. W., *J. Chem. Phys.* **22**, 2088 (1954).
(154) Wagner, C., *Trans. AIME* **200**, 154 (1954).
(155) Walz, E., Magun, S., *Z. Physik* **157**, 266 (1959).
(156) Workman, E. J., *Phys. Rev.* **74**, 709 (1948).
(157) Workman, E. J., Dept. of the Army Project 399-07-022, Signal Corps Project 24-172B-1. Final Report, New Mexico Inst. Mining and Technology, Socorro, 1951.
(158) Workman, E. J., Reynolds, S. E., *Phys. Rev.* **78**, 254 (1950).
(159) Workman, E. J., Reynolds, S. E., *Nature* **169**, 1108 (1952).
(160) Workman, E. J., Truby, F. K., Drost-Hansen, W., *Phys. Rev.* **94**, 1073 (1954).
(161) Zaromb, S., *J. Chem. Phys.* **25**, 350 (1956).
(162) Zaromb, S., Brill, R., *J. Chem. Phys.* **24**, 895 (1956).

RECEIVED April 24, 1967.

4

Aluminum Species in Water

JOHN D. HEM

U. S. Geological Survey, Menlo Park, Calif.

Polymeric species of aluminum and hydroxide formed in 0.01M $NaClO_4$ solutions $10^{-3.34}$M in aluminum after adding sufficient OH to reach pH 4.75 - 6.50 were identified by electron microscopy as gibbsite. The particles had diameters near 0.10μ after 10 days of aging, when the molar ratio of bound OH/total Al (r) was between 2.0 and 3.0. The amount of OH in bridging positions in the polymer structure was determined by the kinetics of dissolution of the polymer in acid. When r exceeded 3 the precipitate formed was bayerite. Standard free energy values determined, in kcal. per mole, include: $AlOH^{2+}$, −165.2; $Al(OH)_4^-$, −311.7; $Al(OH)_3$ (microcrystalline gibbsite), −272.3; $Al(OH)_3$ (bayerite), −274.0. Many natural waters contain enough fluoride that predominant aluminum solutes are fluoride complexes.

Although it is the most abundant of the metallic elements in the outer crust of the earth, aluminum usually occurs in natural waters in concentrations below 100 micrograms per liter. High concentrations occur rarely and usually are associated with water having a low pH. The chemical properties of aluminum which control its behavior in water have been studied extensively. This paper is based on current research by the U.S. Geological Survey and on published literature. The principal topics considered here are the processes by which aluminum combines with hydroxide ions to form complexes and polymers, the influence of these processes on solubility of aluminum and the forms of dissolved species to be expected in natural water, and the relative importance of fluoride and sulfate complexes of aluminum. The experimental work is briefly summarized here. Details are published elsewhere (*6*).

Structure of Aluminum Solute Complexes

The structural patterns described here for aluminum species in water are based on evidence obtained in our experiments as well as on data

reported by others. The discussion of structure precedes the presentation of experimental results, however, in order to provide a logical framework for interpretation of these results.

The O^{-2} ion, the OH^- ion and the water molecule have similar radii and are of the correct size so that one may expect the dissolved aluminum to be six-coordinated with water molecules. The form $Al(H_2O)_6^{3+}$ is generally agreed to predominate in acidic solutions. Figure 1 is a schematic representation of the $Al(H_2O)_6^{3+}$ ion. The ionic dimensions are not drawn to scale.

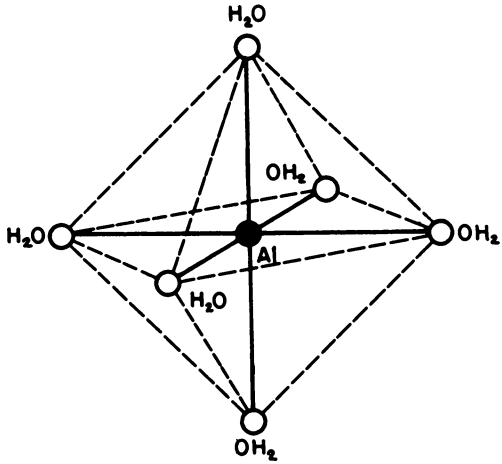

Figure 1. Schematic representation of aquoaluminum ion $Al(H_2O)_6^{6+}$

When the pH of the solution is raised, the first step is the loss of one H^+ to give the unit $AlOH(H_2O)_5^{2+}$. This ion has the same octahedral structure as that in Figure 1, but the distance between the aluminum and the hydroxide ion is slightly less than the Al–H_2O distance. This monomeric complex ion has been reported by many workers. In our experiments, and in the work of others, however, these monomeric ions showed a strong tendency to polymerize into larger units. The basis of the polymerization process is the formation of a double OH bridge between adjacent aluminum ions (*8, 16*).

Figure 2 shows a dimeric $Al_2(OH)_2(H_2O)_8^{4+}$ ion which is the simplest species that contains the double OH bridge. The dimer was described by Johansson (*10*). Larger structural units may evolve owing

to the formation of more double OH bridges (8). The polymerization tendency, or the tendency for these double OH bridges to be formed, is increased by increased availability of hydroxide ions and increased concentration of aluminum, but polymerization into large units is a relatively slow process at 25°C. Our results show that it may require ten days or more for the particles to reach a diameter of 0.10μ, and Hsu (9) has reported aging times of six months to a year were required before some of his solutions became turbid. The diameters of aluminum hydroxide particles in the turbid solutions were not reported, but must have been substantially more than 0.10μ.

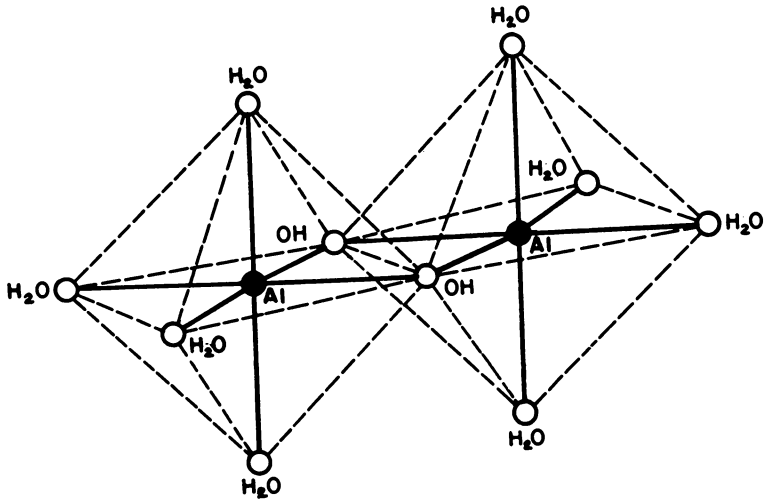

Figure 2. Schematic representation of dimeric ion $Al_2(OH)_2(H_2O)_8^{4+}$

In a solution containing only the monomeric and dimeric ions the molar ratio of bound OH to aluminum cannot exceed 1.0. As the molar ratio (r) increases above 1.0 further deprotonation of the aluminum species must occur, causing OH ions to appear at vertices of the octahedra. These constitute sites for polymerization to give larger units. Figure 3 shows how three dimers can join to form a branched chain structure by sharing edges B–D with A′–C′; and B′–D′ with A″–C″. The pattern in which the polymerization can occur appears from our work to be restricted by the requirement that an aluminum ion can participate in only one double OH bridge in the same plane. Although no calculations of orbital configurations were made in this study, the

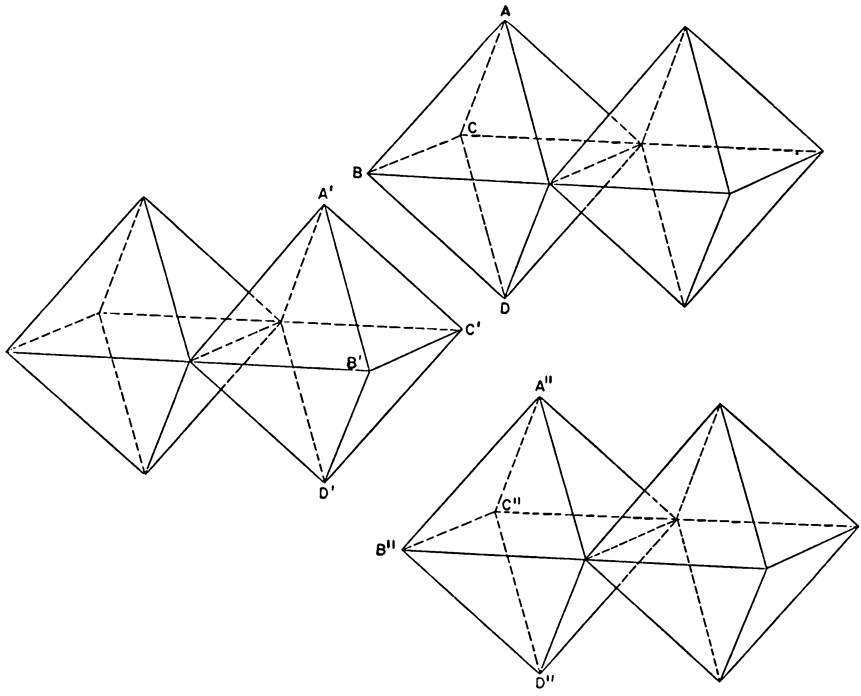

Figure 3. Three dimeric ions which may unite to form branched chain $Al_6(OH)_{10}(H_2O)_6^{8+}$

polymer was shown to evolve into gibbsite. In the gibbsite crystal lattice the aluminum ions each participate in three double OH bridges, and three planes are defined by the central aluminum ion and the two OH ions of each bridge. Because of the geometric requirement, as polymerization proceeds, a network of branched chains of octahedra is formed and the structure ultimately becomes a sheet of coalesced six-membered rings. Figure 4 depicts a single ring structure with the formula $Al_6(OH)_{12}(H_2O)_{12}^{6+}$. A solution containing no structures larger than this would have an r of 2.0 or less. Larger structures such as that in Figure 5 are required if r exceeds 2.0. In Figure 5 there are three complete rings and two additional octahedra, giving the formula $Al_{16}(OH)_{36}(H_2O)_{24}^{12+}$. The value of r in this unit is 2.25. The sheet structures can increase in size by adding more octahedra around the edges. In the structure of gibbsite, the sheets are stacked one above the other, in an open packing arrangement (*10*).

The aluminum-hydroxide structures shown in Figures 2–5 utilize only the minimum amount of hydroxide required to hold the units together. This is equivalent to assuming that the polymerization tendency

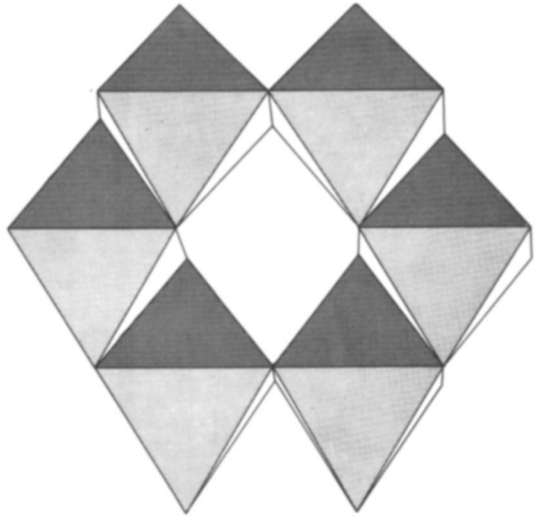

Figure 4. Six-membered ring $Al_6(OH)_{12}(H_2O)_{12}^{6+}$

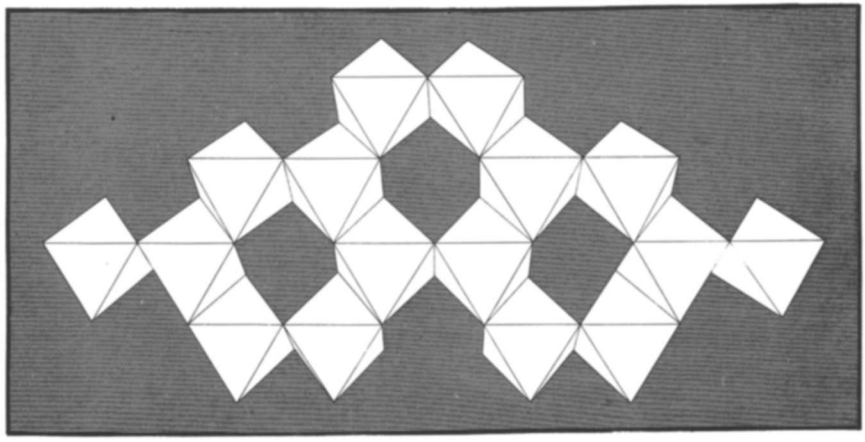

Figure 5. Sheet structural pattern. Composition of unit shown $Al_{16}(OH)_{36}(H_2O)_{24}^{12+}$

is so strong that coordinated hydroxide only occurs in bridging, or structural, positions, except in the monomer $AlOH(H_2O)_5^{2+}$. Figure 6 shows the molar ratio of structural OH to aluminum required in various sizes of chain, double chain, and sheet structures. If the bound OH occupies only structural positions, the higher values of r require large units. Smaller structural units than those specified by Figure 6 could exist at

values of r above 2, if some of the bound OH were assigned to nonstructural positions.

In several of the studies of aqueous chemistry of aluminum that have been made since about 1950, polynuclear complexing mechanisms have been proposed to identify and describe the dissolved aluminum hydroxide complex species (*3, 10, 11*). The formulae proposed have generally been based on stoichiometric considerations and pH measurements assuming the polynuclear species were ionic, and that equilibrium was attained. The complex ions reported by Hsu and Bates (*8*) were single six-membered rings $Al_6(OH)_{12}^{6+}$ or multiples of this unit. Johansson (*10*) identified a structural unit containing 13 aluminum and 40 oxygen atoms with various numbers of protons in crystalline basic aluminum sulfate. Because this solid formed readily, the same structural unit of aluminum was proposed as a solute species. Most of the proposed formulae for polynuclear complexes, however, have not been derived from structural considerations.

It is of interest to apply to some of the proposed polynuclear complex formulae the structural pattern outlined here. For example, Kenttamaa (*11*) reported the species $Al_4(OH)_{10}^{2+}$. This would have to be a chain structure, either straight or branched in which no more than six

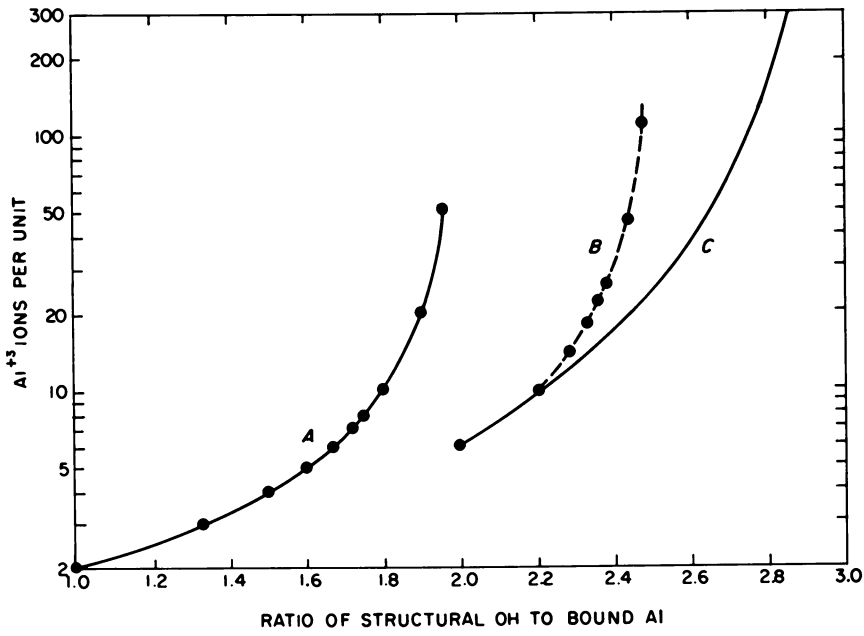

Figure 6. Calculated mole ratio of structural hydroxide to aluminum for three structural patterns: A—chain, B—double chain, C—sheet polymer

of the OH groups could be utilized in bridging positions. The remaining four OH groups would have to be present in external positions, each one tied to one aluminum ion rather than to two. Such a structure cannot be ruled out as impossible, although in view of the polymerization tendency of the aluminum hydroxide units, rather special conditions would probably be necessary to hold the chain length down to four aluminum ions.

The value of r in a solution containing only $Al_4(OH)_{10}^{2+}$ ions would be 2.5. Of the total bound OH, 60% would be held in the double OH bridges and 40% would be nonbridging. The bridging OH is obviously more firmly held in the structure of the aluminum hydroxide species than is the nonbridging OH held at the edges of the units. For this reason one would expect bridging OH to react differently from the nonbridging OH when such structures are attacked chemically. A major part of the laboratory studies described here has been concerned with means for differentiating between bridging and nonbridging hydroxide in the various complexes and polymers of aluminum and hydroxide.

Experimental Studies

The laboratory studies were designed to examine in detail the composition of aluminum species in dilute solutions having values of r between 0.5 and 4.0, after various periods of aging. The behavior of OH bound to aluminum was examined by kinetic methods, precipitated solids were identified by the electron microscope and x-ray diffractometer, and equilibrium solubilities were calculated for stable and metastable aluminum hydroxides.

The initial solutions contained aluminum perchlorate at concentrations of $10^{-4.34}$ or $10^{-3.34}M$. They were maintained at constant total aluminum concentration and at an ionic strength of 0.01, and dilute sodium hydroxide was added slowly to each to attain the desired value of bound OH. The solutions were then aged in a CO_2-free atmosphere at 25°C. in polyethylene bottles.

Solutions $10^{-3.34}M$ in aluminum in which r was between 0.5 and 1.0 reached a pH near 4.5 and maintained this pH with practically no change for as long as 12 months. Where r was between 1.0 and 2.0, the initial pH was generally between 4.5 and 4.75 but decreased slowly on aging and did not stabilize until several months had passed. Where r was between 2.0 and 3.0, the initial pH ranged up to about 6.5, but decreased rather rapidly for the first few days and then more slowly. Most of the pH change, however, usually took place within the first ten to 14 days. The downward shift in pH was probably caused by release of protons during the polymerization process. The downward drift of pH was much less noticeable in solutions containing $10^{-4.34}$ moles per liter of aluminum.

Determinations of aluminum were made by a complexing procedure using ferron (*14*). After $10^{-3.34}M$ aluminum solutions had been aged for ten days, however, the aluminum in some of them became difficult to determine by this procedure. A similar effect was reported by Hsu (7). The solutions showing the effect most strongly were those where r was

between 2.0 and 3.0. The solutions had no visible opalescence, but when they were filtered through plastic membrane (Millipore) filters with 0.10 micron pores, a considerable part of the aluminum was removed (Figure 7). The material on the filters was identified by x-ray diffraction as gibbsite. Electron micrographs of this material (Figure 8) showed hexagonal crystals mostly with diameters near 0.10 micron, although some smaller particles also were present. Crystalline material in this size range does not seem to have been looked for by other investigators of aluminum chemistry.

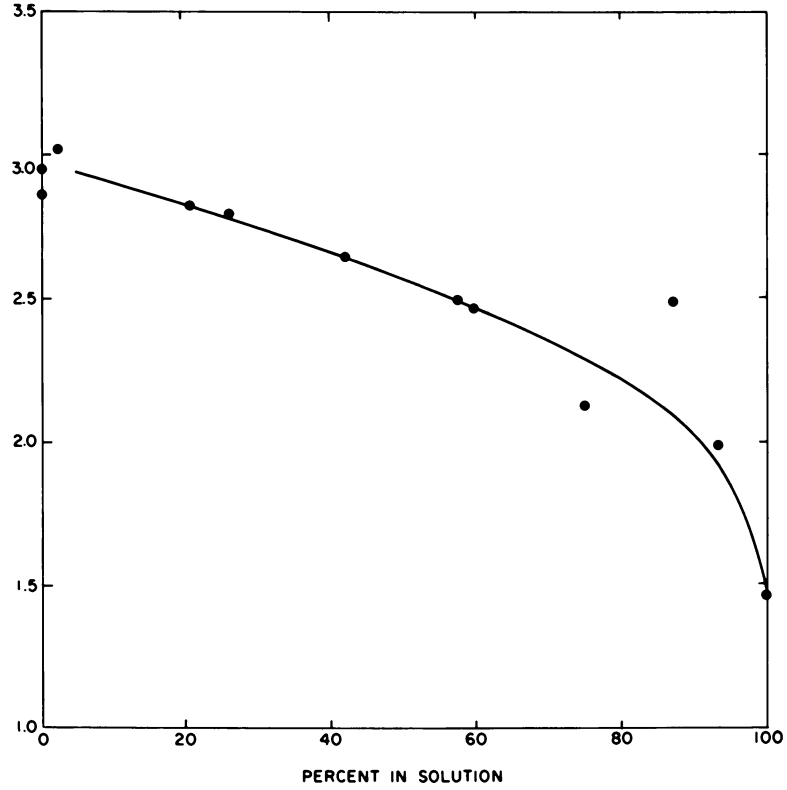

Figure 7. Percentage of aluminum ion aged solutions passing filter with 0.10μ pores as a function of mole ratio of OH_{Bound} to total aluminum

The rate at which the polymerized material was attacked by acid was systematically observed. Aliquots of unfiltered aged solutions with *r* values ranging from 1.0 to 3.0 were acidified by addition of perchloric acid and maintained at a constant pH for periods of two to eight hours by continued addition of acid using a Radiometer automatic titrator. The rate at which acid was consumed in these aliquots was a measure of the rate at which the polymeric structure was destroyed by reaction of the bound OH with H^+.

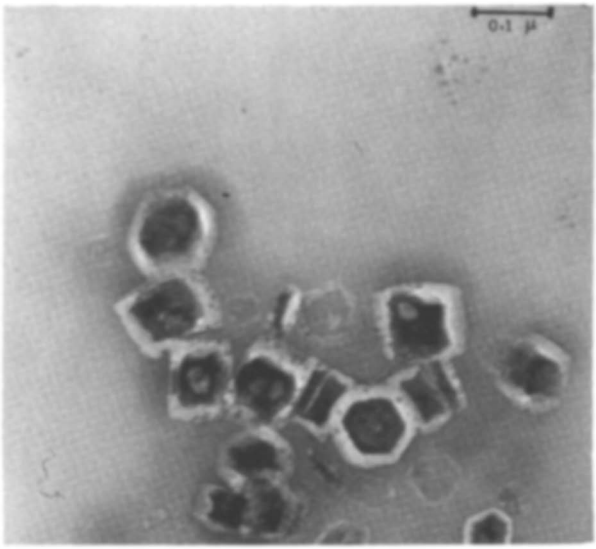

Figure 8. Electron micrograph of polymerized aluminum hydroxide particles (microcrystalline gibbsite)

The results of two titrations are given in Figure 9, which is a plot of the log of the concentration of unreacted bound OH against time. The upper set of points were observed in titrating at pH 2.88 and 25.0°C. a solution with $r = 2.99$, after 24 hours of aging. The bound OH in this solution does not all have the same kinetic behavior but consists of a fast-reacting portion, used up in the first 40 minutes, and a more slowly reacting fraction which persisted after that time.

The second set of points represented by X's are for a second aliquot of the same solution, titrated at the same pH after four days of aging. The points which define the straight lines A and B represent the behavior of the slowly reacting fraction of the bound OH. When these rates are extrapolated to zero time, the intercept gives the initial concentration of this part of the bound OH. The remainder of the total bound OH is the fast reacting fraction. The first order rate constant for the four-day aged material was 1.3×10^{-5} sec.$^{-1}$. A rate about twice as fast is indicated for the one-day aged material, but the data are not fully conclusive because some of the faster reacting material could still have been present in the latter part of the titration. In any event, however, the kinetic approach provides a means of distinguishing between the bridging or structural OH and the nonbridging OH ions which are bound to aluminum.

More than 30 of these rate studies were made, using the same temperature but different pH's, and using solutions with longer aging times and having different r values. Some of these solutions were known to contain only the microcrystalline gibbsite shown in Figure 8, and these contained almost no fast reacting bound OH. The slowly reacting bound OH in these solutions must have been present in bridging positions. In eight of nine experiments where more than a few days of aging had

occurred and where some microcrystalline gibbsite was known to be present, the rate constant for the structural fraction of the bound OH at pH 2.88 was between 1.2×10^{-5} and 2.0×10^{-5} sec.$^{-1}$. In the ninth experiment, material aged 11 days ($r = 3.00$) gave a rate constant of 0.8×10^{-5} sec.$^{-1}$. In all the nine solutions, 89% or more of the bound OH was structural.

In aged solutions where r was near or below 1.0, no structural OH was found.

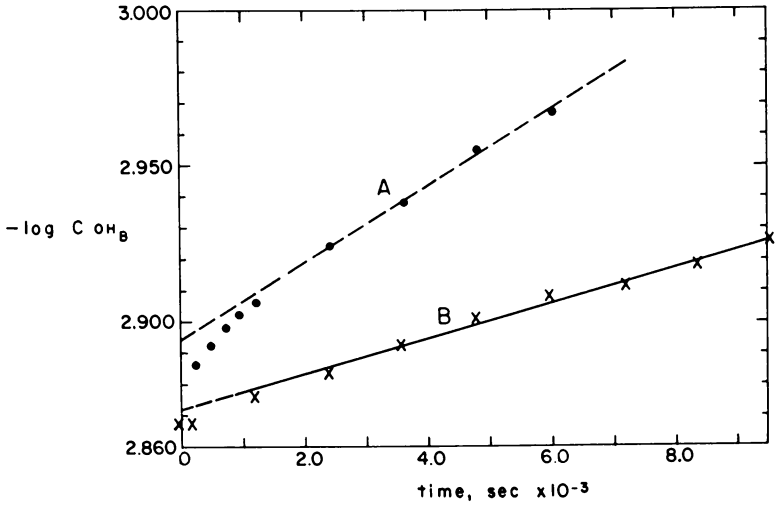

Figure 9. Rate of reaction of bound OH with acid, pH − 2.88, temperature 25.0°C. A—after one day aging; B—after four days aging. ^cOH_B = concentration of unreacted bound OH

These results and others for other titration pH's gave a set of values for concentration of nonstructural OH, and bridging OH. The total aluminum and total bound OH in these solutions were known from their original composition when they were made up. The pH was measured and the ionic strength was 0.01. From these data it is possible to calculate the solubility of microcrystalline gibbsite, and the stability of the monomer $AlOH(H_2O)_5^{2+}$ and the standard free energies of formation derived from these results are given in Table I. The calculations were based on two assumptions:

1. All nonstructural OH is present as the monomer $AlOH(H_2O)_5^{2+}$,
2. All structural OH is present as a polymer whose formula is $Al(OH)_3$.

It must be admitted that neither of these assumptions will hold exactly. Some of the nonstructural OH is probably held along the edges of larger units, hence assumption 1, above, tends to give too high a value for the concentration of the monomer. Assumption 2 may assign too much of the aluminum to the uncomplexed form.

Table I. Standard Free Energy of Formation ΔG° for Various Aluminum Species

Species	ΔG°, *kcal. per mole*	*Source of data*
$Al^{3+}aq$	−115.0	Latimer (*13*)
$AlF^{2+}aq$	−190.64	Calc. from data of King and Gallagher (*12*)
AlF_2^+aq	−264.55	do.
$AlF_3^\circ aq$	−336.46	do.
AlF_4^-aq	−406.22	do.
$AlF_5^{2-}aq$	−473.92	do.
$AlF_6^{3-}aq$	−539.93	do.
$AlSO_4^+aq$	−296.7	Calc. from data of Behr & Wendt (*1*)
$Al(SO_4)_2^-aq$	−476.6	do.
$AlOH^{2+}aq$	−165.2	Hem & Roberson (*6*)
$Al(OH)_4^-aq$	−311.7	do.
$Al(OH)_3c$ (microcrystalline gibbsite)	−272.3	do.
$Al(OH)_3c$(gibbsite)	−273.9	Latimer (*13*)
$Al(OH)_3c$(bayerite)	−274.0	Hem & Roberson (*6*)

The accuracy of the assumptions was checked by determining dissolved aluminum in aged solutions by a modified procedure of aluminum determination with ferron designed to be sensitive only to unpolymerized species (*6*) and by comparing the computed values for the standard free energies for the monomeric ion and for microcrystalline gibbsite that were obtained using the assumptions with data in the literature. The value −165.2 kcal. per mole for free energy of $AlOH^{2+}$ is 0.3 kcal. more negative than the value of Schofield and Taylor (*15*). Several other investigators have reported values agreeing with that of Schofield and Taylor. The difference of 1.4 kcal. between the free energy of gibbsite reported by Latimer (*13*) and the one determined here is about the amount to be expected as a particle-size effect. The modified aluminum procedure gave values for determined aluminum within 10% of the sum of calculated $AlOH(H_2O)_5^{2+}$ and uncomplexed Al. It would seem that the two assumptions are reasonable.

The points on the left-hand regression line, Figure 10, represent the calculated activity of uncomplexed aluminum present at various pH's based on observed reaction rates of bound OH in the experimental solutions that contained microcrystalline gibbsite. Aging times for these solutions ranged up to about four months. Circles are for solutions initially $10^{-3.34}M$ in aluminum and X's for solutions initially $10^{-4.34}M$ in aluminum.

The experiments with solutions where r was below 3.0 indicate that from pH 4.5 to 6.5, with the aluminum concentrations and ionic strengths used here, show polymerization of solute species containing aluminum and hydroxide can be expected. The polymer evolves into gibbsite crystals whose diameters remain near 0.10μ long enough that the material

can be assigned a definite free energy. The reactions in this pH range, however, are slow and the rates and intermediate products are likely to be affected by experimental conditions. Metastable forms are no doubt possible. Some of these might persist for considerable periods, depending on conditions in the solution. However, the polynuclear complex species reported in the literature did not seem to occur in our solutions in significant amounts where aging had proceeded far enough to produce gibbsite that could be identified with the electron microscope.

The conclusion that polynuclear hydroxide complex ions do not constitute a significant part of the solute species of aluminum at equilibrium in the solutions studied here is in accord with the conclusions of Frink and Sawhney (*4*). The microcrystalline gibbsite itself is metastable in the sense that as crystals grow in size with longer aging time their solubility decreases. Although at equilibrium metastable species can be ignored, it can be so difficult to attain an equilibrium condition that the concept has little practical usefulness.

In those solutions where r exceeded 3.0 a precipitate rapidly formed, consisting of $Al(OH)_3$, in relatively large aggregates. The material obtained after one day of aging was amorphous to x-rays. After ten days of aging, however, the precipitates were identified by x-ray as bayerite. A considerable decrease in solubility occurred during the aging period.

By assigning all dissolved aluminum to the form $Al(OH)_4^-$, the practice followed by other investigators who have worked in this pH range (*3*), the two solubility lines on the right side of Figure 10 were obtained. The calculated standard free energy for bayerite obtained from these data is −274.0 kcal. per mole (Table I). The points which were used to locate the lines for fresh $Al(OH)_3$ precipitate and for bayerite do not appear on Figure 10. For the freshly precipitated material, 22 different solutions were examined, with pH ranging from 6.50 to 9.26. The thermodynamic equilibrium constants for the reaction

$$Al(OH)_3c + H_2O = Al(OH)_4^- + H^+$$

ranged from 0.99×10^{-13} to 2.83×10^{-13}. The solutions containing bayerite had a pH range from 7.50 to 9.70 and the range for the calculated equilibrium constant was from 0.66×10^{-14} to 2.4×10^{-14}. The free energy of formation for the fresh precipitate at alkaline pH was assumed to be the same as that of the first solid appearing in the acid solutions (microcrystalline gibbsite).

The activities of dissolved uncomplexed aluminum in the presence of microcrystalline gibbsite can be predicted from the pH using the left-hand line in Figure 10, and the activity of $Al(OH)_4^-$, the predominant form in alkaline solution, is indicated by the two lines on the right. The graph assumes, however, no other solutes that might complex aluminum are present. In most natural water there are other species present which may affect aluminum behavior. The most important such ion is probably fluoride, and perhaps in some waters complexes of sulfate with aluminum might be important. Other complexing ions could be significant also, but probably more rarely.

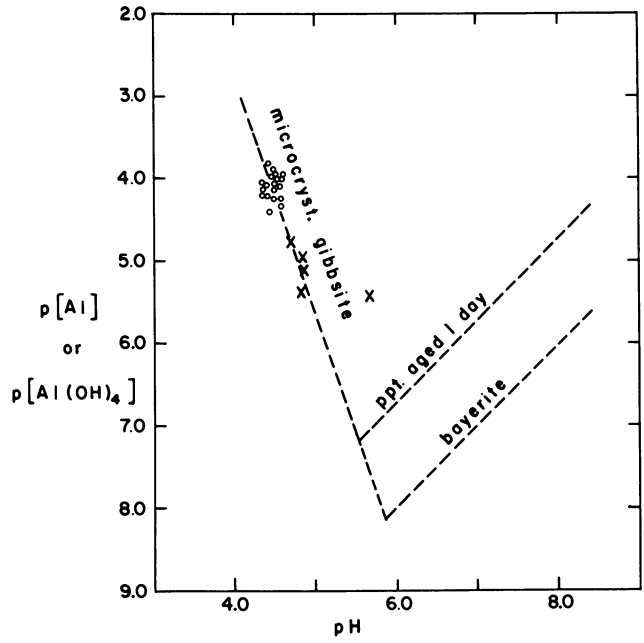

Figure 10. Activity of two dissolved aluminum species as a function of pH and form of solid. Experimental points based on kinetic determinations of structural OH

Complexes of Aluminum with Fluoride

The thermodynamic data for fluoride complexes of aluminum, from published literature (*12*), were recalculated to zero ionic strength by means of the Debye-Hückel equation. These, with stability data from our experiments with aluminum hydroxide species, provide a basis for deciding which complexes will be predominant when pH and dissolved fluoride concentrations are known. Conclusions drawn concerning the hydroxide species show that the polymeric aggregates of $Al(OH)_3$ should be considered colloidal and they are not included in this calculation as equilibrium solute species. Hydroxide complexes of significance are the monomer $AlOH^{2+}$ and the anion $Al(OH)_4^-$. Fluoride complex species constitute the series AlF_n^{3+-n} where n ranges from one to six.

Where both fluoride and hydroxide ions are present, equilibria of the type

$$AlF^{2+} + OH^- = AlOH^{2+} + F^-$$

will hold. The equilibrium constant for this reaction can be calculated from thermodynamic data in Table I. Over the range of conditions where

these two complexes are the predominant ones, the stipulation that activity of fluoride complexes = activity of hydroxide complexes permits writing

$$\frac{[AlOH]}{[AlF]} = K\,\frac{[OH]}{[F]} = 1.0.$$

This relationship defines a segment of a line on a graph where abscissa and ordinate are [OH] and [F] (Figure 11). As activities of both anions are increased the nature of the complexes changes and other complexing equilibria or combinations of several equilibria must be used. The dashed line on Figure 11 was located in this way.

The solid lines within the areas of dominance of the two forms of complexes represent values of the ratio [Al]/Σ Conc. of Al. This is a measure of the proportion of free to complexed aluminum, and is calculated by simultaneous solution of equations that describe the system.

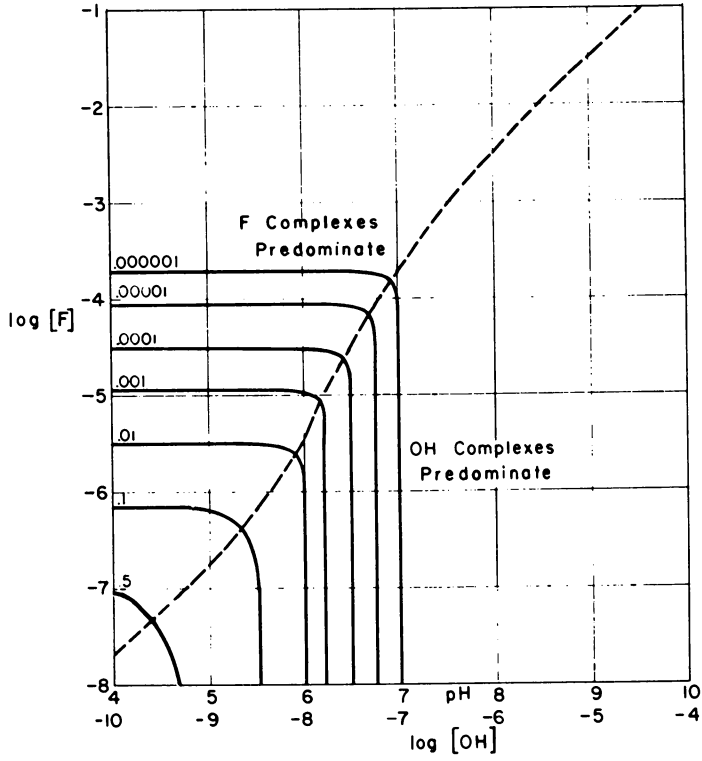

Figure 11. Predominant form of complex and ratio of free aluminum activity to total dissolved aluminum as a function of pH and fluoride activity

In the domain of fluoride complexing these include equilibria of the series

$$Al^{3+} + nF^- = AlF_n^{3+-n},$$

and summations of the species present in significant quantity,

$$\Sigma Al = [Al^{3+}] + [AlF^{2+}] + [AlF_2^-] \text{ etc., and}$$

$$\Sigma F = [F^-] + [AlF^{2+}] + 2[AlF_2^+] \text{ etc.}$$

The value of the ratio $[Al^{3+}]/\Sigma Al$ is assigned. To have enough equations to give specific values to all the variables, it is necessary to specify that the total aluminum concentration is always small enough so that fluoride is present in excess. Under these conditions, the total fluoride can be considered approximately equal to the free fluoride.

The straight portions of the lines in the fluoride complex domain were drawn from calculations of the type outlined above. The straight portions of the lines in the hydroxide complex domain were drawn from a similar set of equations. The hydroxide equilibria, however, include a solubility expression so the aluminium concentration in the hydroxide domain is related to the pH. The dashed line on Figure 11 may be considered as defining the fluoride activity above which the solubility of microcrystalline gibbsite will be significantly greater than would be calculated from consideration of hydroxides alone. Ionic strength was assumed to be zero for these calculations but a diagram can be prepared for any desired ionic strength.

The lines showing proportion of free to total aluminum should meet in a smooth curve rather than at a 90° angle in the region where both fluoride and hydroxide species are important. A simple procedure for calculating the positions of such a curve has been described by the writer (*5*) for systems where only two complex species need to be considered at a time.

As Figure 11 demonstrates, fluoride complexed species of aluminum will predominate in many natural waters even if only a few tenths p.p.m. ($\sim 10^{-5}$ molal) of fluoride are present, below a pH of 6.6. At a pH of 7.0, the fluoride activity would have to exceed 3 p.p.m. to have a stronger effect on complexing than the hydroxide activity.

Complexes of Aluminum with Sulfate

Two sulfate complexes of aluminum $AlSO_4^+$ and $Al(SO_4)_2^-$ also are reported (*1*). The same type of computation as that described for fluoride-hydroxide systems was used to prepare Figure 12, showing the predominant species to be expected at various pH's and sulfate activities.

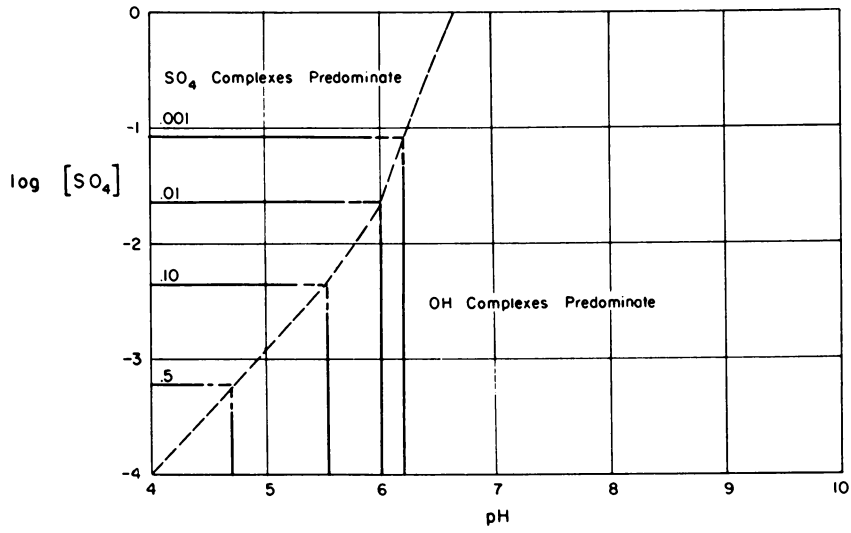

Figure 12. Predominant form of complex and ratio of free aluminum activity to total dissolved aluminum as a function of pH and sulfate activity

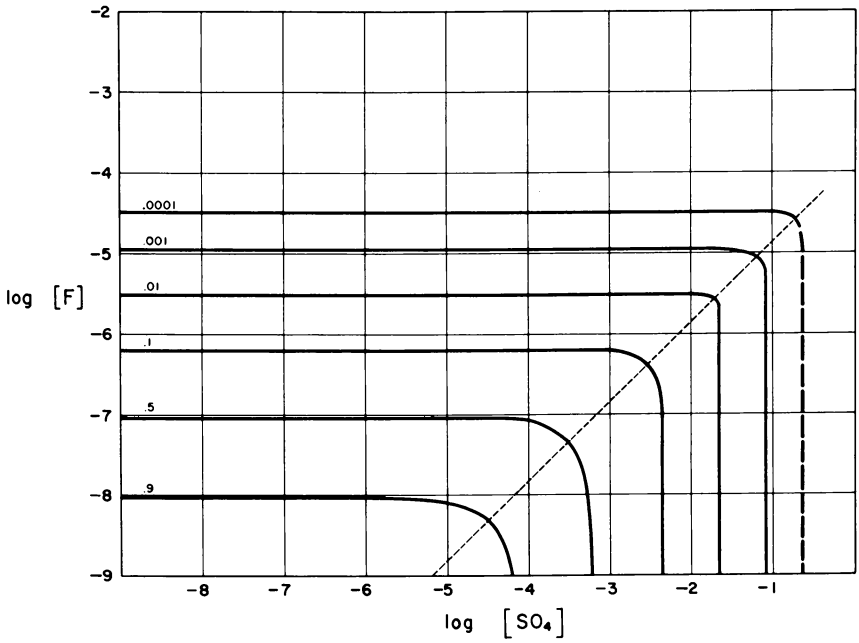

Figure 13. Predominant form of complex and ratio of free aluminum activity to total dissolved aluminum as a function of sulfate and fluoride activities (at low pH)

This diagram shows that aluminum sulfate complex species will probably not predominate except in waters high in SO_4^- and low in pH.

Figure 13 represents the effects to be expected in the presence of both sulfate and fluoride when pH is low enough to be an insignificant factor (below about 6.0).

Probable Aluminum Species in Natural Water

The aluminum present in ionic form in natural water can normally be expected to occur for the most part as complexes of fluoride or hydroxide, or of sulfate in some waters of low pH. These are possibly overshadowed in waters whose pH is below neutrality by polymerized hydroxide aggregates of colloidal or subcolloidal size. The occurrence of polymerized hydroxide will depend on the past history of the water and on kinetic rather than equilibrium considerations. Some standard procedures for determination of aluminum are insensitive to the hydroxide polymer and many existing analyses probably reflect this fact. The behavior of aluminum in natural water is probably also related to concentrations of dissolved silica. This aspect of aluminum chemistry is being studied in our laboratory.

Literature Cited

(1) Behr, Barbara, Wendt, H., *Z. Elektrochem.* **66,** 223 (1963).
(2) Brosset, Cyrill, Orring, Jonas, *Svensk. Kem. Tidskr.* **55,** 101 (1943).
(3) Brosset, Cyrill, Biedermann, G., Sillen, L. G., *Acta Chem. Scand.* **8,** 1917 (1954).
(4) Frink, C. R., Sawhney, B. L., *Soil Sci.* **103,** 144 (1967).
(5) Hem, J. D., *J. Chem. Eng. Data* **8,** 99 (1963).
(6) Hem, J. D., Roberson, C. E., *U. S. Geol. Surv. Water Supply Papers* **1827-A** (1967).
(7) Hsu, Pa Ho, *Soil Sci.* **96,** 230 (1963).
(8) Hsu, Pa Ho, Bates, T. F., *Mineral. Mag.* **33,** 749 (1964).
(9) Hsu, Pa Ho, *Soil Sci. Soc. Am. Proc.* **30,** 173 (1966).
(10) Johansson, Georg, *Svensk. Kem. Tidskr.* **2,** 6 (1963).
(11) Kenttämaa, J., *Ann. Acad. Sci. Fennicae, Ser. A, II* **no. 67** (1955).
(12) King, E. L., Gallagher, P. K., *J. Phys. Chem.* **63,** 1073 (1959).
(13) Latimer, W. M., "Oxidation Potentials," 2nd ed., Prentice-Hall, Inc., Englewood Cliff, New Jersey, 1952.
(14) Rainwater, F. H., Thatcher, L. L., *U. S. Geol. Surv. Water Supply Papers* **1454** (1960).
(15) Schofield, R. K., Taylor, A. W., *J. Chem. Soc.* **1954,** 4445.
(16) Thomas, A. W., Tai, A. P., *J. Am. Chem. Soc.* **54,** 841 (1932).

RECEIVED April 24, 1967. Publication authorized by the Director, U. S. Geological Survey.

Interaction Between Aluminum and Phosphate in Aqueous Solution

PA HO HSU

Rutgers—The State University, New Brunswick, N. J.

Hydroxy aluminum solutions of basicity (NaOH/Al molar ratio) ranging from 0 to 2.7 were prepared and mixed with a NaH_2PO_4 solution to give a H_2PO_4/Al molar ratio varying from 0 to 15. It was found that hydroxy-aluminum polymers and Al^{3+} yielded different reaction products with phosphate. Hydroxy-aluminum polymers were completely and immediately precipitated by phosphate at their isoelectric points. This precipitation is interpreted to be a simple "neutralization" of the net positive charge of polymer by the phosphate anion. Al^{3+} formed soluble complexes with phosphate, no precipitate being observed up to a H_2PO_4/Al molar ratio of eight. In solutions which contain both polymers and Al^{3+}, each reacted with phosphate separately, because a rapid equilibrium between Al^{3+} and polymers does not exist.

Interaction of aluminum and phosphate has long been a problem of interest to soil scientists and water chemists. Many different precipitates have been prepared by mixing solutions of aluminum salts and phosphate (*4, 5, 6, 17*). Some of these precipitates are crystalline, but many others are amorphous. Some have definite stoichiometric compositions, but many others do not. Some are dissolved in 1*N* HCl almost instantaneously, but others can be dissolved only after prolonged heating. On the other hand, the formation of soluble complexes of aluminum and phosphate has been suggested (*3, 8, 14*).

Despite considerable information in published reports, it has not yet been possible to define exactly the conditions under which the various products are formed, nor to interpret satisfactorily the diverse nature of the products. Obviously, the reaction mechanism must be complicated and the nature of the products may be affected by a number of factors,

such as the concentration of aluminum and phosphate in the preparation, the Al/P ratio, the nature and concentration of other components, the solution pH, temperature, the order of mixing, and possibly many others (*4, 11, 13, 15, 16*). Therefore, further study of this problem seems desirable.

This report illustrates that Al^{3+} and hydroxy-aluminum polymers react with phosphate differently. Al^{3+} tends to form soluble complexes with phosphate, whereas the polymers can be precipitated by phosphate easily. Because a rapid equilibrium between Al^{3+} and polymers does not exist, the reaction products will be dependent on the nature of aluminum species originally present in the solution.

Experimental Methods

Preparation of Sample. Hydroxy-aluminum solutions were prepared by the dropwise addition of 0.1*N* NaOH to 200 ml. of 0.2*M* $AlCl_3$ solution, after which the solution was diluted to 2000 ml. (*10*). To avoid any possible complication caused by aging, these solutions were used at least two days, but not more than two months after the preparation. The amount of NaOH was adjusted to give a basicity (defined here as the molar ratio of NaOH to aluminum) varying from 0 to 2.7. The addition of NaOH was maintained at a rate of approximately 50 ml. per 15 minutes. Varying amounts of NaH_2PO_4 were added to 250 ml. portions of each hydroxy-aluminum solution to give a H_2PO_4/Al molar ratio = 0 to 15. The solution was then diluted to 500 ml. The final concentration of aluminum in all samples was 270 p.p.m.

Analysis of Sample. Fifty ml. of the sample aliquot was centrifuged with an International Centrifuge Size 2 at 2000 r.p.m. (approximately 1000 G) for 20 minutes. The centrifugates were analyzed for their pH, concentrations of aluminum and phosphate, and the rate of aluminum-aluminon color development. The precipitates were washed with 30 ml. of water four times, dissolved in 10 ml. of *N* HCl, and analyzed for their concentrations of aluminum, phosphate, and sodium.

General Chemical Determinations. The solution pH was determined with a Beckman Research or a Heath recording pH meter. The concentrations of aluminum and phosphate were determined colorimetrically with, respectively, aluminon (*9*) and molybdenum blue (*12*). Sodium was determined with a Perkin-Elmer Atomic Absorption Spectrophotometer Model 290.

Rate of Aluminum-Aluminon Color Development. The preparation of color solution for rate measurement was similar to the procedure for aluminum determination (*9*), but the following remarks are important:

1. The sample aliquots were not preheated with HCl. Instead, the HCl required was mixed with aluminon-acetate reagent and H_2O prior to adding the sample aliquot.

2. The concentration of aluminum was maintained at 0.4 ± 0.02 p.p.m. in the final solution for all samples for the sake of comparison. The

rate of color development is related to the concentration of aluminum present.

3. Because both rate of color development and total color intensity are extremely sensitive to temperature, a control was maintained with each rate measurement. This control was prepared by heating an identical aliquot of the sample solution with the required amount of HCl for 30 minutes and then mixed with other reagents; color intensity was read along with that of the sample.

X-ray Diffraction. Appropriate aliquot of sample suspension containing 50 to 100 milligrams of precipitate was centrifuged and washed once with 100 ml. of H_2O, then dispersed in 2 ml. of H_2O, poured onto a glass slide, and dried at room temperature. The dried specimen was x-rayed with a GE XRD 5 diffractometer with $Cu_{k\alpha}$ radiation.

Results and Discussion

Reaction with Aluminum Solutions of High Basicity. RESULTS. Three hydroxy-aluminum solutions whose basicities were 2.7, 2.55, and 2.4 were used. Aluminum is known to be present entirely as high hydroxy-polymers, with little free Al^{3+}, in these solutions (*10*). Both aluminum and phosphate were found to precipitate immediately and completely at the isoelectric point, which was defined as the point where the sum of $H_2PO_4^-$ and OH^- equals Al^{3+} on an equivalent basis. As an example, the results for the solution of basicity of 2.55 are shown in Table I.

Prior to the isoelectric point, stable turbid suspensions of positively charged colloidal particles were obtained, but in all instances only a very small portion of aluminum and of phosphates was found in the precipitate (Table I). These suspensions were stable for at least six months, during which time there was no noticeable increase in the amount of aluminum or phosphate precipitated.

With phosphate concentrations higher than the isoelectric point, aluminum was also completely and immediately precipitated after preparation, but a large amount of phosphate remained in solution. A small amount of sodium was also found in the precipitate. Both the P/Al molar ratio and the sodium content in the precipitate increased with increases in the H_2PO_4/Al ratio in the preparation (Table I).

Variation in the solution pH values was only slight (Table I); the values did not appear to be affected significantly by the precipitation reaction. The precipitates were amorphous and dissolved in 1*N* HCl almost instantaneously; no gibbsite or any crystalline phase of aluminum phosphate was observed with x-ray diffraction or electron microscope. No change in composition, crystallinity, and morphology was noticed during aging up to at least six months.

MECHANISM OF PRECIPITATION. It has been proposed (*10*) that hydroxy-aluminum polymers are composed of two closely packed planes

Table I. Data Illustrating the Precipitation of the Composition of Precipitates at

H_2PO_4/Al Molar Ratio in Prep.	Centrifugates			
	pH	Appearance	Al	P
			p.p.m.	
0.0	5.37	clear	265.8	0.0
0.1	4.67	turbid	270.8	31.5
0.2	4.61	turbid	266.5	62.0
0.3	4.57	turbid	257.9	90.0
0.45	4.92	clear	0.0	4.92
0.6	5.89	clear	0.1	45.8
1.0	5.94	clear	0.2	139.4
2.0	5.66	clear	0.25	421.9
5.0	5.40	clear	0.20	1031.3
10.0	4.98	clear	0.60	—

[a] Al present = 270 p.p.m. Basicity of original Al solution = 2.55. Analysis made one

of hydroxyl ions, with Al^{3+} residing in the octahedral holes. Like the fragments of gibbsite, Al^{3+} ions are distributed as multiples of six-member rings, except that the Al^{3+} ions at the edge are not fully satisfied by OH^- ions. The size of the polymers may be dependent on the conditions of preparation, but they always exist as stable inner cores surrounded by anions attracted by the residual positive charge of Al^{3+} at the edge. The schematic diagram of several polymers of different sizes are shown in Figure 1.

The net positive charge per aluminum atom decreases with increase in polymer size. The stability of these polymers is dependent on the thickness of the diffuse double layer, which in turn is dependent on the net positive charge per aluminum atom and also on the nature of the counter anions. In the case of NO_3^- or ClO_4^-, the counter anions may be distributed in the diffuse layer and the polymers can be flocculated only in media of high electrolyte concentration. However, because of its strong affinity for aluminum, phosphate ion tends to be held tightly by the edge aluminum in its first coordination sphere; or, a Stern layer is formed in terms of the double-layer concept. The aluminum ion at the edge is coordinated with four OH^- ions and two H_2O molecules (*7*, *10*). The OH^- ions form stable bridges linking together Al^{3+} ions, but the H_2O molecules outside the core are labile. Consequently, before the isoelectric point is reached, the phosphate added will always be taken by polymers by replacing the H_2O outside the core but will not replace the structural OH^- in the polymer. The net positive charge per aluminum atom gradually decreases with addition of phosphate. At the isoelectric point, the polymers are completely neutralized by the phosphate anion.

Hydroxy-Aluminum Polymers by Phosphate and Various $NaH_2PO_4/AlCl_3$ ratios[a]

P Added p.p.m.	*Precipitates*			
	Na	*Al*	*P*	*P/Al*
	mg./Liter Sample			*Molar Ratio*
0.0	—	—	—	—
31.0	—	—	—	—
62.0	—	—	—	—
93.0	—	—	—	—
139.5	1.26	267.6	133.2	0.433
188.0	2.60	275.4	145.0	0.459
310.0	5.04	261.0	147.6	0.492
620.0	6.90	264.8	161.6	0.532
1240.0	—	266.4	176.4	0.578
3100.0	15.76	268.4	200.2	0.658

[a] week after preparation.

All particles then cluster together and are immediately precipitated from the solution.

Stumm and Morgan (*15*) have also emphasized the chemical aspect of precipitation, although they did not take into consideration the structure of hydroxy aluminum polymers.

Composition of Precipitate. Following the reasoning described, the precipitation of phosphate becomes the following simple neutralization of the net positive charge of aluminum polymers by phosphate:

$$[Al(OH)_{2.7}]^{0.3+} + 0.3\ H_2PO_4^- = Al(OH)_{2.7}(H_2PO_4)_{0.3} \downarrow$$

$$[Al(OH)_{2.55}]^{0.45+} + 0.45\ H_2PO_4^- = Al(OH)_{2.55}(H_2PO_4)_{0.45} \downarrow$$

$$[Al(OH)_{2.4}]^{0.6+} + 0.6\ H_2PO_4^- = Al(OH)_{2.40}(H_2PO_4)_{0.6} \downarrow$$

With phosphate concentrations higher than that at the isoelectric point, the excess phosphate in the solution competes with the structural OH^- for aluminum and may break the polymers into smaller units. The P/Al ratio of the precipitate, therefore, gradually increased with increased H_2PO_4/Al ratio in the preparation. The composition of the precipitate from the smallest possible polymer unit, a single six-member ring, will be $Al_6(OH)_{12}(H_2PO_4)_6$. The presence of sodium in the precipitates suggests that the hydroxy-aluminum phosphates obtained at high H_2PO_4/Al ratios probably are negatively charged, and thus are capable of adsorbing cations.

Growth in Particle Size. The solution appeared turbid with additions of phosphate, but little aluminum or phosphate was precipitated from the solution prior to the isoelectric point. To interpret this, the fol-

lowing two assumptions should be considered: (1) the relative attractive force of hydroxy-aluminum polymers for phosphate is proportional to their charge density, or the net positive charge per aluminum atom; and (2) the phosphate ion tetrahedron tends to link two aluminum polymers together rather than to stay with any one polymer. In an ideal system containing polymers of identical size, all polymers will have the same attractive force for phosphate. The first phosphate ion added may be adsorbed by any two polymers it first encounters. The polymers which receive this phosphate ion then become less positively charged than their neighbors. Consequently, the second phosphate ion added will not go to the first pair of polymers but rather to its neighbors. Based on this reasoning, statistically all polymers tend to increase uniformly in size with the addition of phosphate. As long as the amount of phosphate added is not sufficient completely to neutralize all the polymers present, all polymers remain positively charged and thus tend to stay in suspension.

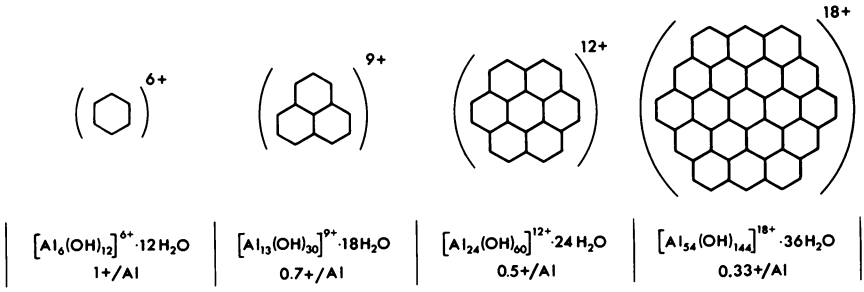

Figure 1. Schematic diagram of four hydroxy-aluminum polymers. Each hexagonal ring is composed of 6 Al and 12 OH ions (10)

A similar reasoning has been proposed to interpret the formation of amorphous and crystalline $Al(OH)_3$ (*10*). A distinction, however, must be made between the two systems. Hydroxyl ion is a part of the polymer structure. By continuing addition of OH^- to the isoelectric point, crystalline $Al(OH)_3$ is obtained in a matter of hours. Nevertheless, because of steric reasons, all the phosphate ion tetrahedra can only stay between polymers and twist them to different orientations. Therefore, hydroxy-aluminum phosphates obtained at the isoelectric points at room temperature have always been amorphous. The crystallization of such precipitates involves a drastic rearrangement of the structure, and a high activation energy may be required.

Reaction with $AlCl_3$. When solutions of NaH_2PO_4 and $AlCl_3$ were mixed together, clear solutions were obtained up to a phosphate/aluminum molar ratio of eight, but a small portion of aluminum was precipitated at the ratio of nine and above (Table II; Curve 1 in Figure 2). The

Table II. Data Illustrating the Precipitation of Aluminum by Phosphate and the Composition of Precipitate from the Reaction Between $AlCl_3$ and NaH_2PO_4.[a]

NaH_2PO_4/Al Molar Ratio in Prep.	Centrifugates			Precipitates			
	pH	Appearance	Al p.p.m.	mg./Liter Sample Na	Al	P	P/Al Molar Ratio
9	2.87	clear	242.7	0.80	39.5	54.5	1.20
10	2.90	clear	218.8	1.30	49.5	66.2	1.17
11	2.93	clear	212.3	1.64	61.8	85.0	1.20
12	2.94	clear	209.3	2.02	70.8	97.6	1.20
13	2.98	clear	200.0	2.34	77.4	111.4	1.25
14	3.00	clear	195.3	3.10	83.8	118.8	1.23
15	3.01	clear	184.3	3.70	88.0	127.6	1.26

[a] Al present = 270 p.p.m. Analysis made one week after preparation.

amount of aluminum precipitated increased slightly with increases in the NaH_2PO_4/Al ratio. All precipitates have a nearly constant P/Al molar ratio of about 1.2, and also contain small amounts of sodium. They were easily separated from the solution by centrifugation, and the centrifugates were clear. The precipitates were relatively compact and resistant to acid. It took an hour or longer to dissolve the precipitates obtained in this experiment in 1*N* HCl, whereas the precipitate obtained from phosphate and hydroxy-aluminum polymers was dissolved in 1*N* HCl almost instantaneously. The x-ray diffraction showed some broad bands, which indicated some degree of crystallization but was too poor for identification. In summing up, the precipitates obtained in this experiment are distinctly different from those obtained with high hydroxy-aluminum polymers presented in the previous section, but a more quantitative description has not been possible.

The rate of aluminum-aluminon color development is shown in Figure 3. In this experiment, aluminon was added to aluminum solutions and the color intensity measured at various intervals. It was found that free Al^{3+} reacted with aluminon very rapidly, the color intensity reaching 75% of its maximum intensity in two minutes, and 95% in about 20 minutes. The rate of color development was considerably lowered when phosphate was present in the original solutions (Figure 3), whereas the final color intensity was not affected. The absorption spectra in the

visible range were practically identical during the entire period of color development, the only difference being in the absorption intensity (9). When the phosphated aluminum solutions were heated in 1*N* HCl prior to color development, the rate curve as well as those of the absorption spectra coincided with the corresponding Al^{3+}—aluminon curves. These phenomena indicate that some soluble aluminum phosphate complexes are formed in these systems. The aluminum complexed by phosphate can only partially react with aluminon. Such complexes are, nevertheless, not stable under the experimental conditions for color development; thus, the rate of color development can be considered to be the measure of the stability and amount of aluminum phosphate present in the solution.

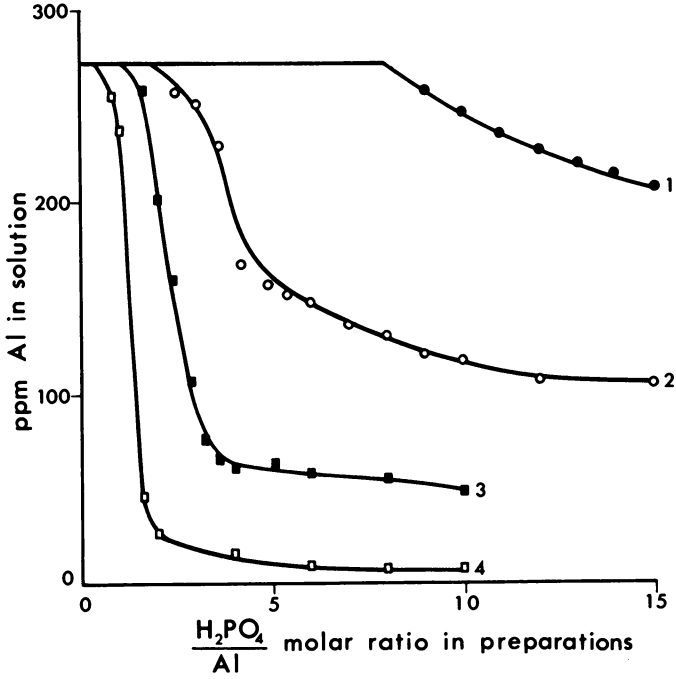

Figure 2. Precipitation curves for four Al solutions of different NaOH/Al molar ratio in the preparation. Initial Al concentration = 270 p.p.m. Analysis made one week after preparation

1. *$AlCl_3$ only*
2. *$NaOH/AlCl_3 = 0.6$*
3. *$NaOH/AlCl_3 = 1.2$*
4. *$NaOH/AlCl_3 = 1.8$*

The reaction mechanism between aluminum and aluminon probably is complicated and is extremely sensitive to temperature. To derive reproducible information, it was found necessary to maintain definite

concentrations of aluminum and aluminon in the final solution and to maintain constant temperature throughout the whole period of experimentation.

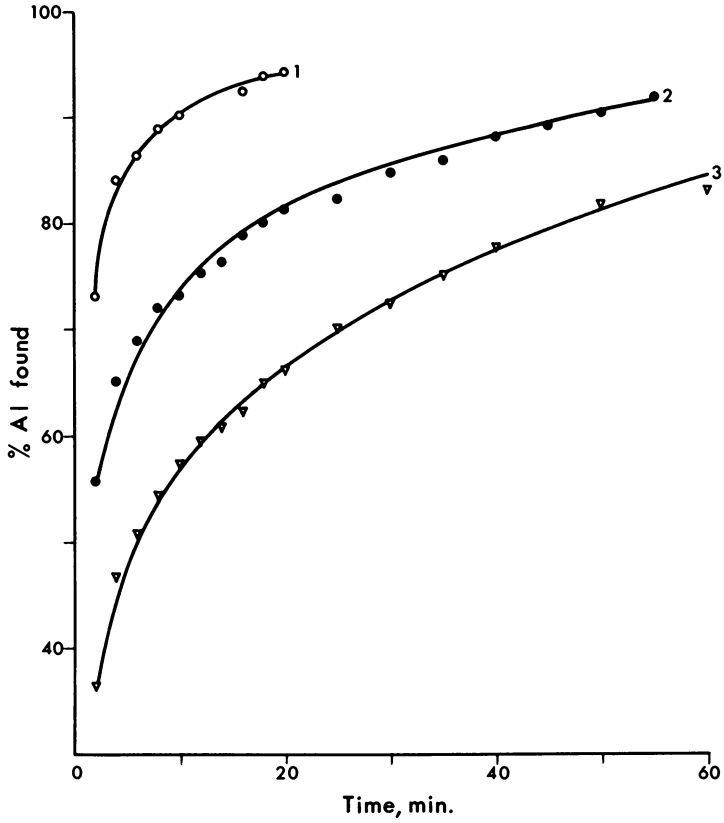

*Figure 3. Rate of aluminum-aluminon color development. The color intensity is converted to % Al found for plotting. All solutions are 0.01*M *in Al*

1. *$AlCl_3$ only*
2. *$AlCl_3$ + NaH_2PO_4 (2:1 molar ratio)*
3. *$AlCl_3$ + NaH_2PO_4 (4:1 molar ratio)*

With increased NaH_2PO_4/Al molar ratio, the pH values of the resultant solution first decreased and then, after passing through a point of minimum at the NaH_2PO_4/Al ratio of 1 to 2 (Curve 1, Figure 4), increased. The pH values of all resultant solutions in the entire range of NaH_2PO_4/Al ratios were lower than those of their parent solutions, indicating that proton was released in association with the formation of aluminum phosphate complex.

Although the nature of the complex and the mechanism for their formation is not clearly known, two possible mechanisms may be considered: (a) That Al^{3+} hydrolyzes in its aqueous solution is known to result in a decrease in pH; if phosphate forms a complex with the hydrolyzed species, more Al^{3+} must be hydrolyzed and the solution becomes more acidic. (b) If Al^{3+} form complexes with HPO_4^{2-}, excess H^+ will be released to the solution from $H_2PO_4^-$ and cause a decrease in pH. This hypothesis was previously proposed by Salmon and Wall (*14*) and Stumm and Morgan (*15*).

Experiments designed to study the detailed mechanism are under way.

Reaction with Solutions of Intermediate Basicity. In this experiment, the basicities of the three solutions used were 0.6, 1.2, and 1.8. In all three solutions three stages of precipitation were observed (curves 2-4, Figure 2). In the first stage, the products were either clear solutions or stable turbid suspension, with little aluminum precipitated. In the second stage, the amount of aluminum precipitated increased with the increase in the H_2PO_4/Al ratio, and the centrifugates were still turbid after being centrifuged at 2000 r.p.m. for 20 minutes. The slopes of the precipitation curves were much sharper in this stage than in the third stage, but not as sharp as those obtained with hydroxy-aluminum solutions of high basicities. The completion of this stage was far beyond the corresponding isoelectric points. In the third stage, the aluminum precipitation increased slightly with increases in the H_2PO_4/Al ratio; in all instances the centrifugates were clear, although considerable aluminum was present in the solution. With increases in the H_2PO_4/Al ratio, the solution pH values first decreased and then, after passing through a point of minimum (Curves 2-4, Figure 4), increased.

An attempt to interpret these results with the prevailing concept of the hydrolysis of Al^{3+} has not been successful. Because of indisputable evidence that polymers are present in hydroxy-aluminum solutions, many chemists suggested the following expression for the hydrolysis of Al^{3+} (*1*, *2*).

$$pAl^{3+} + qH_2O = \underset{\text{polymer}}{[Al_p(OH)_q]^{(3p-q)+}} + qH^+ \qquad (1)$$

In the three solutions studied, both Al^{3+} and polymers were present (*10*). If a rapid equilibrium between Al^{3+} and polymers does exist, the rest of the Al^{3+} must be further hydrolyzed and polymerized when the polymers originally present in the solution were removed by phosphate. In the excess of phosphate, aluminum should be completely precipitated unless the solution pH value becomes too low for further hydrolysis. This

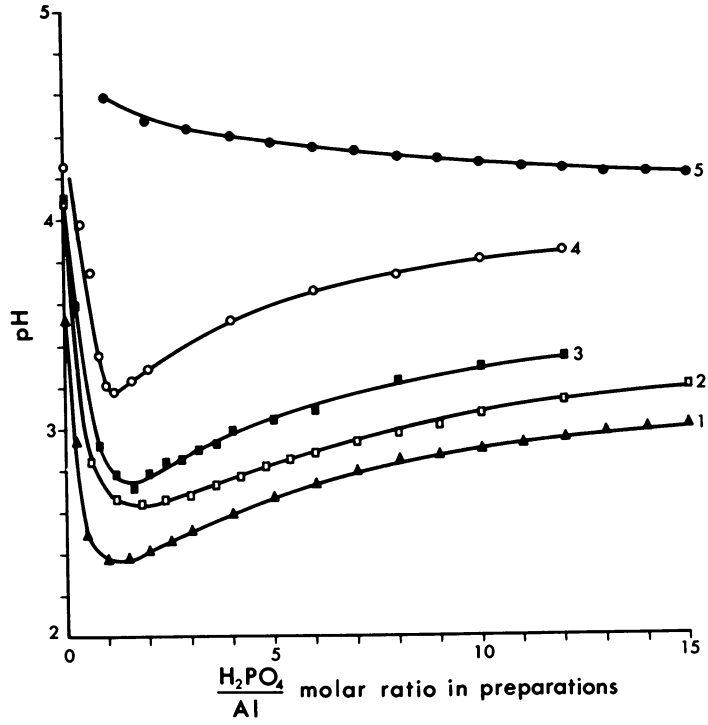

Figure 4. pH curves for four Al solutions of different NaOH/Al molar ratio in the preparation. All samples except control are 0.01M in Al. Analysis made one week after preparation

1. *$AlCl_3$ only*
2. *$NaOH/AlCl_3 = 0.6$*
3. *$NaOH/AlCl_3 = 1.2$*
4. *$NaOH/AlCl_3 = 1.8$*
5. *Control (NaH_2PO_4 only)*

solubility product principle has been frequently employed by soil scientists to interpret the fixation of phosphate in soils by aluminum or iron. The precipitation curves shown in Figure 2 do not follow the predicted trend. That pH is not the determining factor is clearly indicated by the following two phenomena: (a) After the second inflection point, the solution pH value increased slightly with an increase in the H_2PO_4/Al ratio whereas considerable aluminum was present in the solution. (b) Precipitation of samples of identical pH value, but prepared from aluminum solutions of different basicity, differ considerably (Table III).

This writer recently found that the spontaneous hydrolysis of Al^{3+} yields only monomeric species, such as $Al(OH)^{2+}$, but adding NaOH

produces polymers (manuscript in preparation), as shown in Equations 2 and 3, respectively:

$$Al^{3+} + H_2O = Al(OH)^{2+} + H^+ \quad (2)$$

$$pAl^{3+} + qOH^- = \underset{\text{polymer}}{[Al_p(OH)_q]^{(3p-q)+}} \quad (3)$$

Because Al^{3+} and polymer react with phosphate differently, the reaction product with phosphate will depend greatly on the nature of the aluminum originally present in the solution. In the first stage of precipitation, phosphate reacts with both Al^{3+} and polymer. Its reaction with Al^{3+} accounts for the decrease in pH, and its reaction with polymer accounts for the turbid appearance. In the second stage, the decrease in aluminum in solution is caused by the precipitation of polymer by phosphate. This precipitation was completed at a point far beyond the isoelectric point because part of the phosphate was consumed by Al^{3+}. After the polymers were completely removed from the solution, the further addition of phosphate reacted with Al^{3+} only.

Table III. Comparison of Aluminum Precipitation from iso-pH Solutions

NaOH/Al Molar Ratio in Prep.	*H_2PO_4/Al Molar Ratio in Prep.*	*p.p.m. Al in Solution*
	pH = 2.85	
0.0	8.0	270
0.6	5.4	143
1.2	2.8	102
	pH = 2.94	
0.0	11.0	235
0.6	7.0	132
1.2	3.6	60

Many workers have tended to restrict their interpretations to thermodynamic approaches. The application of thermodynamics to aqueous aluminum chemistry, however, may be restricted as follows: (a) In many cases, a true equilibrium state may not have been reached, yet the rate of equilibration is too slow to be detected under ordinary laboratory conditions. (b) The position of equilibrium and/or the rate of equilibration may vary with the nature and concentration of the counter anions present, yet in most studies of aluminum hydrolysis the role of counter anions has not been considered. Therefore, the conclusion derived under one condition is not necessarily valid under another condition in which different counter anions are present. A failure to recognize these possible

restrictions may account for much of the confusing and conflicting information in published reports.

Acknowledgments

This study was initiated by the author at the Pennsylvania State University and is now carried on at Rutgers-The State University, supported by a grant from the office of Water Resources Research, Department of the Interior. The author wishes to express his sincere thanks to H. L. Motto, Rutgers University, for his critical review and comments in the preparation of this report.

Literature Cited

(1) Aveston, J., *J. Chem. Soc.* **1965**, 4438 (1965).
(2) Biedermann, G., *Svensk. Kem. Tidskr.* **76**, 1 (1964).
(3) Bjerrum, J., Dahm, C. R., *Chem. Abstrs.* **26**, 666 (1931).
(4) Cole, C. V., Jackson, M. L., *J. Phys. Colloid Chem.* **54**, 128 (1950).
(5) Haseman, J. F., Brown, E. H., Whitt, C. D., *Soil Sci.* **70**, 257 (1950).
(6) Haseman, J. F., Lehr, J. R., Smith, J. P., *Proc. Soil Sci. Soc. Am.* **15**, 76 (1951).
(7) Hem, J. D., ADVAN. CHEM. SER. **73**, 98 (1968).
(8) Holroyd, A., Salmon, J. E., *J. Chem. Soc.* **1956**, 269 (1956).
(9) Hsu, Pa Ho., *Soil Sci.* **96**, 230 (1963).
(10) Hsu, Pa Ho., Bates, T. F., *Mineral Mag.* **33**, 749 (1964).
(11) Hsu, Pa Ho., *Soil Sci.* **99**, 398 (1965).
(12) Jackson, M. L., "Soil Chemical Analysis," p. 141, Prentice-Hall, Inc., Englewood Cliffs, N. J., 1958.
(13) Matijevic, E., Milic, I., *Kolloid-Z.* **118**, 129 (1963).
(14) Salmon, J. E., Wall, J. G. L., *J. Chem. Soc.* **1958**, 1128 (1958).
(15) Stumm, W., Morgan, J. J., *J. Am. Water Works Assoc.* **54**, 971 (1962).
(16) Swenson, R. M., Cole, C. V., Sieling, D. H., *Soil Sci.* **67**, 3 (1949).
(17) Taylor, A. W., Gurney, E. L., Lindsay, W. L., *Soil Sci.* **90**, 25 (1960).

RECEIVED May 25, 1967.

6

Mineral-Water Interaction During the Chemical Weathering of Silicates

OWEN P. BRICKER[1] and ANDREW E. GODFREY[2]

The Johns Hopkins University, Baltimore, Md.

EMERY T. CLEAVES

Maryland Geological Survey, Baltimore, Md.

The geochemical balance of a 103 acre watershed underlain by silicate bedrock was investigated. Base flow composition of the stream water was essentially constant, but flood flows showed a decrease in concentration of silica, bicarbonate, and sodium and an increase in sulfate, magnesium, calcium, and potassium. Laboratory experiments indicate that fresh rock or soil reacts rapidly with distilled water and achieves a composition similar to the stream water, suggesting control of water composition by reaction with the silicate minerals. The alumino-silicate minerals react with CO_2 charged water to form kaolinite, releasing cations and silica to solution. The products of weathering are removed as particulate matter (0.28 metric tons per year) and dissolved material (1.5 metric tons per year).

Silicate minerals constitute approximately 95% of the earth's crust. Most natural waters, at some time during the hydrologic cycle, contact and react with these minerals, altering them, forming new minerals, and reflecting the interaction by changes in their own composition. One of the most obvious and widespread examples of this process is the weathering of silicate rocks at the surface of the earth. Water is a primary agent of rock weathering and conversely the chemical behavior of silicate minerals in the earth's surface environment plays an important role in governing the composition of natural waters (*1*).

[1] Geology Department
[2] Isaiah Bowman Department of Geography

To assess the behavior of some common silicate minerals in the weathering environment and the effect of water-silicate reactions on both the minerals and the resulting solution composition, we investigated the geochemical balance of a small wooded watershed underlain by silicate bedrock.

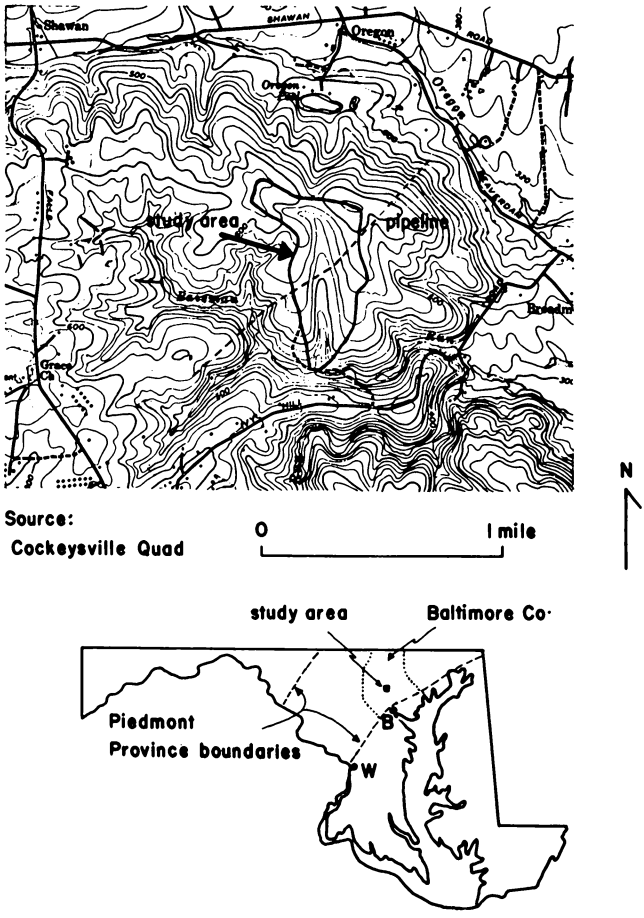

Figure 1. Location of Baisman Run and Pond Branch

Location and Description of the Watershed

Pond Branch of Baisman Run is located in the Piedmont Province of Maryland about eight miles north of Baltimore City (Figure 1). This area was chosen for study because: (1) Pond Branch is a perennial stream that drains a small (103 acre) watershed, (2) all waters draining

from the basin originate as precipitation on the watershed, (3) the watershed is entirely underlain by one rock type, the Lower Pelitic Schist of the Wissahickon Formation (*11*), (4) the watershed is entirely forested except for a narrow transverse band of grasses, and (5) there is a pond at the mouth of the stream that was surveyed for sediment accumulation.

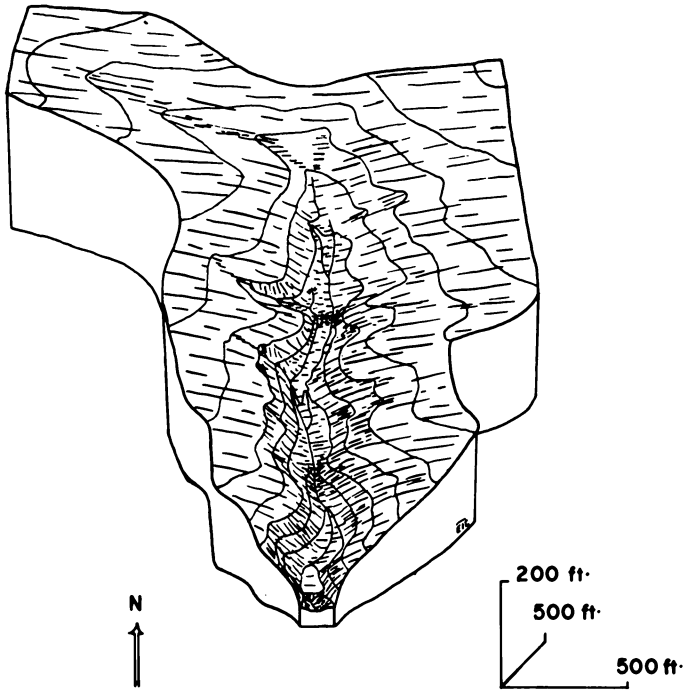

Figure 2. Block diagram showing topography of the watershed

The upper portion of the watershed is a broad, open swale that changes into a narrow "V" shaped gorge toward the lower end (Figure 2). Total relief in the upper part of the valley is about 40 feet; in the gorge the valley has a relief of over 100 feet. The long profile of the stream bed and two cross-sections of the watershed are shown in Figure 3.

The maximum and minimum average annual temperatures of the area are 65° and 45°F. respectively. Water temperature of the stream varied between 34° and 50°F. during period of study. Average annual precipitation is 40 inches. Precipitation for the year 1966 was below average and amounted to 33.7 inches (Maryland State Climatologist, per. comm.).

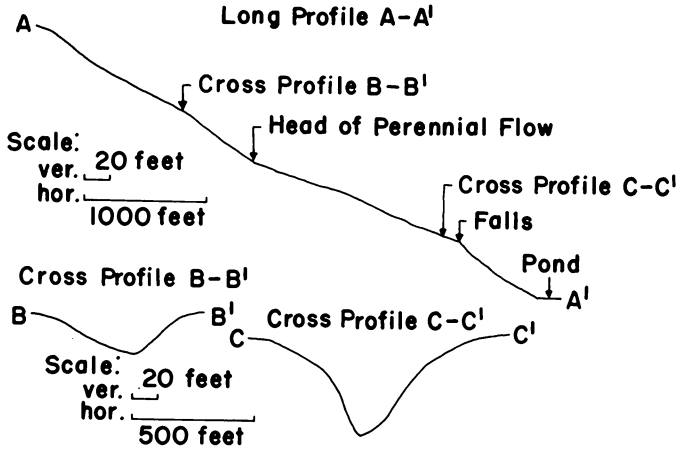

Figure 3. Long profile of Pond Branch and two cross profiles of watershed

Stream run-off of Pond Branch has been measured on a continuously recording stream gage since March 1, 1966. Despite the severe drought in the northeastern United States during the summer of 1966, the base flow remained constant at two liters per second (0.07 cu. ft./sec.). The maximum flow observed, 17 liters per second (0.6 cu. ft./sec.) occurred on March 7, 1967. Six floods were recorded during the one year record of stream level. From the data at hand we estimate that these floods amounted to less than 1% of the total annual discharge. No overland flow of any kind was observed even during the heaviest storms. Calculations based on yearly input from rain and snow indicate that stream run-off removes about 20% of the average annual precipitation. The remaining 80% must leave as evapo-transpiration, percolation through the floodplain of the stream, or through deep circulation.

Bedrock and Soil Mineralogy

The watershed is underlain by the Lower Pelitic Schist of the Wissahickon Formation. The minerals constituting the rock, in order of abundance, consist of quartz, muscovite, oligoclase ($An_{24}Ab_{76}$), biotite, and staurolite with minor amounts of garnet, tourmaline, zircon, apatite, chlorite, and pyrite. The bulk chemical composition of the unweathered rock calculated from the modes is shown in Table I. The mantle of weathered rock and soil consists primarily of quartz and muscovite in the sand sized fraction and kaolinite and illite in the clay sized fraction. Gibbsite was observed in samples from the tops of the drainage divides.

Minor amounts of vermiculite and mixed layer illite-vermiculite were found in several samples and appear to be intermediate products in the weathering sequence of muscovite and biotite to kaolinite.

Table I. Chemical Analysis of Fresh Rock[a]

Oxide	*Wt. %*
SiO_2	64.3
Al_2O_3	19.8
Fe_2O_3	2.8
FeO	3.9
MgO	2.6
CaO	0.4
Na_2O	0.9
K_2O	3.6
P_2O_5	0.1
ZrO_2	0.1
H_2O	1.5
	100.0

[a] Calculated from modal analysis.

The weathering sequence for oligoclase and biotite has been established as follows:

oligoclase → kaolinite → gibbsite (on drainage divides)
oligoclase → kaolinite (side slopes, valley bottom)
biotite → vermiculite → kaolinite

The minerals in the unweathered rock were identified with a petrographic microscope, and their weathering products by x-ray diffraction. Material to establish these sequences was obtained from exposures of bedrock, from pits dug on the side slope in the gorge area, and from hand auger holes along the ridge and in the swale. Pseudomorphs after oligoclase and biotite were picked from the soil samples.

Although garnet, staurolite, and muscovite alter to new mineral phases under the influence of this environment, they are much less susceptible to weathering than are oligoclase and biotite. Quartz appears to be relatively inert to weathering reactions.

The overall weathering relations in this system may be summarized by the general equation:

Primary alumino-silicates + H_2O + CO_2 → Aluminum rich solids + alkali cations + alkaline earth cations + HCO_3^- (aq) + H_4SiO_4 (aq)

Water Composition

The compositions of rain and stream waters were monitored for a one year period and a limited number of samples of soil water were obtained. The stream was sampled on the average of twice a month with the exception of the summer months (*see* Figure 4). To minimize contamination the samples were collected in polyethylene bottles. Stream samples were collected by immersing the bottles in the stream just above the gage. Rain samples were collected at the site of the stream gage by inserting a polyethylene funnel into a polyethylene bottle and mounting this apparatus about one foot above ground level. Rain sampling was limited to the fall, winter, and spring seasons, because of the unusually dry summer. A total of seven samples were collected. On the basis of this and other rainfall data (*2*), we believe that the average composition of these samples approximates the yearly average rainfall composition.

Table II. Analytical Methods

Constituent	*Method*	*Reference*
silica	colorimetric as reduced silicomolybdate complex	(*7*)
aluminum	colorimetric as colored "lake" of aurine tricarboxylate	(*8*)
potassium	flame spectrophotometric	(*9*)
sodium	flame spectrophotometric	(*9*)
calcium	EDTA compleximetric with spectrophotometric end point	(*10*)
magnesium	EDTA compleximetric with spectrophotometric end point	(*10*)
iron	colorimetric as bipyridine complex	(*10*)
sulfate	thorin method	(*10*)
chloride	indirect colorimetric	(*5*)
bicarbonate	acidimetric titration pH end point	(*10*)
pH	potentiometric	(*10*)

Soil water samples were collected by inserting a poly(vinyl chloride) pipe into an auger hole. One end of the pipe was covered by cementing a Millipore filter (0.45μ) sandwiched between two supporting screens of nylon. The other end was fitted with a rubber stopper and hose arrangement that allowed a vacuum to be drawn on the tube. Three samples were collected in April, May, and June of 1966.

The waters were analyzed for SiO_2 (aq), aluminum, iron, magnesium, calcium, sodium, potassium, bicarbonate, chloride, and sulfate (Table II). The pH was measured in the field using a glass electrode. The average compositions of these waters are shown in Table III. The stream composition represents the average of 18 samples taken at base

Table III. Average Chemical Analyses of Rain, Stream, and Soil Water at Pond Branch[a]

	Rain	*Stream*	*Soil*
SiO_2	0	15.46	16.3
Al	0	T	T
Fe	0	T	T
Mg	1.52	4.08	3.29
Ca	2.07	3.89	4.15
Na	1.30	7.80	5.45
K	1.27	2.26	4.86
HCO_3	0	10.88	[b]
SO_4	4.58	5.08	[b]
Cl	2.91	6.48	[b]
pH	4.63	6.56	5.45

[a] Molal concentrations $\times 10^5$.
[b] Not determined.

flow; two flood samples were not included. The rain composition represents the average of the seven rain samples. The soil water composition represents the average of three samples.

Except during periods of flood, the composition of the stream water remained surprisingly constant throughout the year. Flood waters did not simply reflect dilution but were characterized by a decrease in the concentration of silica, bicarbonate, and sodium, a depression of pH, and an increase in sulfate, magnesium, calcium, and potassium (Figure 4). Almost all of the sulfate and a large portion of chloride are derived from rain.

No aluminum was found in rain and the concentration of aluminum in the stream never exceeded 0.05 p.p.m. The maximum Al/SiO_2 (aq) ratio in the stream water is less than 5×10^{-3}, thus aluminum appears to be relatively immobile in this system. As an approximation we will assume that aluminum is conserved in the solid phases. With this stipulation, stability diagrams for some of the common silicate minerals can be constructed. Figure 5 is a stability diagram showing relations among some minerals in the system Na_2O–H_2O–Al_2O_3–SiO_2. A similar diagram for the system K_2O–H_2O–Al_2O_2–SiO_2 is shown in Figure 6.

The average compositions of soil and stream waters from Pond Branch watershed are plotted on the diagrams. The points indicate that the stable silicate phase in contact with these waters is kaolinite. Field data suggest that kaolinite is the stable product of weathering throughout the watershed except at the crests of drainage divides where a kaolinite-gibbsite assemblage is present. No soil water samples are available from the drainage divides but we would predict that their composition would

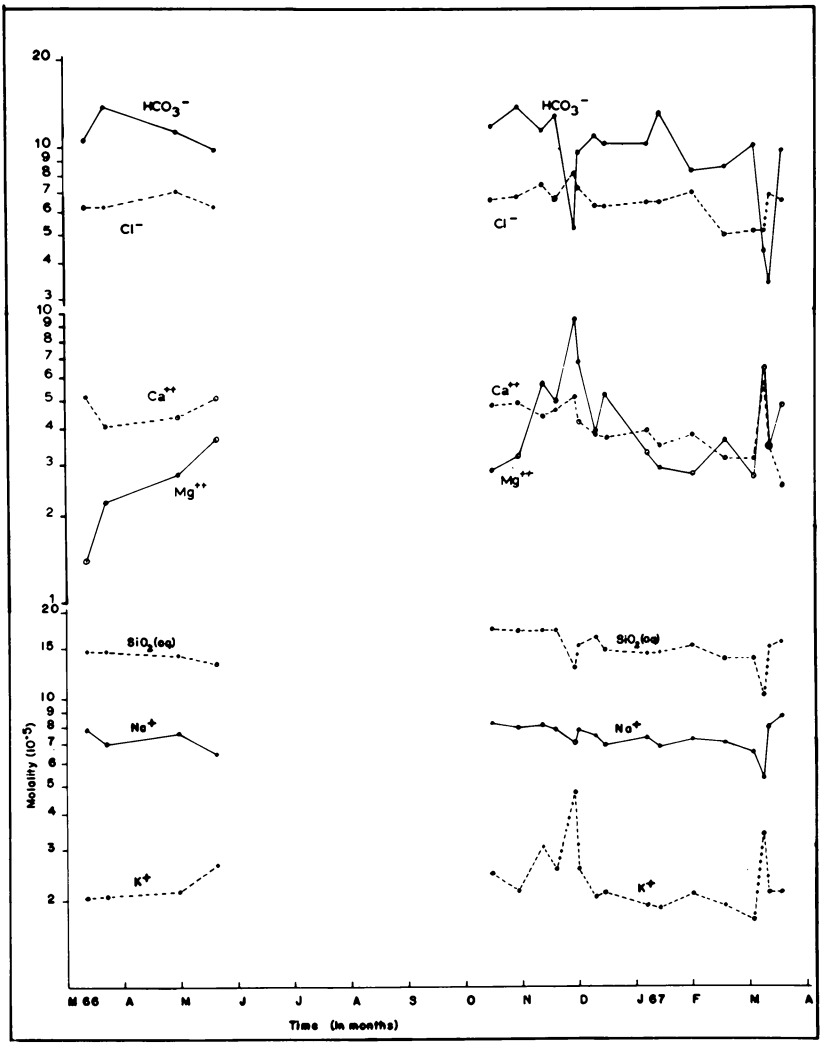

Figure 4. Temporal variation of seven ions in Pond Branch
Two floods are represented, one on 12/66 and the other on 3/67

fall somewhere along the gibbsite-kaolinite boundary with respect to silica concentration. The soil water samples collected from the side slopes have essentially the same composition as the stream water and appear to be in equilibrium with kaolinite.

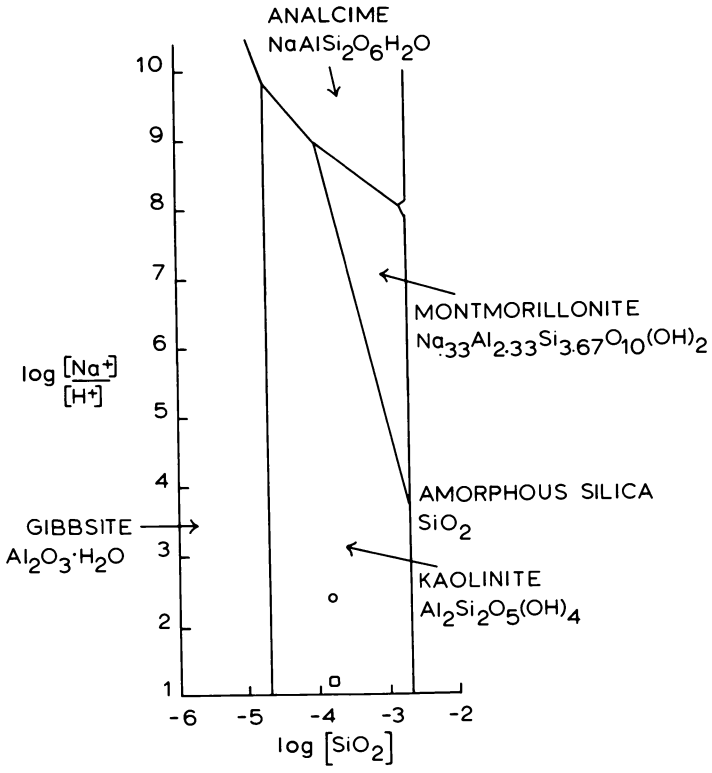

Figure 5. Stability relations of some phases in the system Na_2O-Al_2O_3-SiO_2-H_2O at 25°C. and one atmosphere, as functions of $[Na^+]/[H^+]$ and $[SiO_{2(aq)}]$ (3)

Circle represents analysis of Pond Branch water, square represents analysis of soil water

Reactivity of Silicate Minerals

The small magnitude and short duration of the compositional variation of the stream in flood stage and the constancy of base flow composition suggest that the water-silicate reactions are rapid. The rapidity with which water equilibrates with the fresh and weathered bedrock was tested in the laboratory (term project of Thomas Dunne and Terrance Smith). Two columns of soil were collected from the side slopes of the watershed. Plexiglass tubes 6 inches inside diameter by 3½ feet long were forced into the soil, then dug up.

Distilled water was continuously added to the first tube and allowed to percolate through it. The effluent was sampled and then discarded. Distilled water was initially allowed to percolate through the second

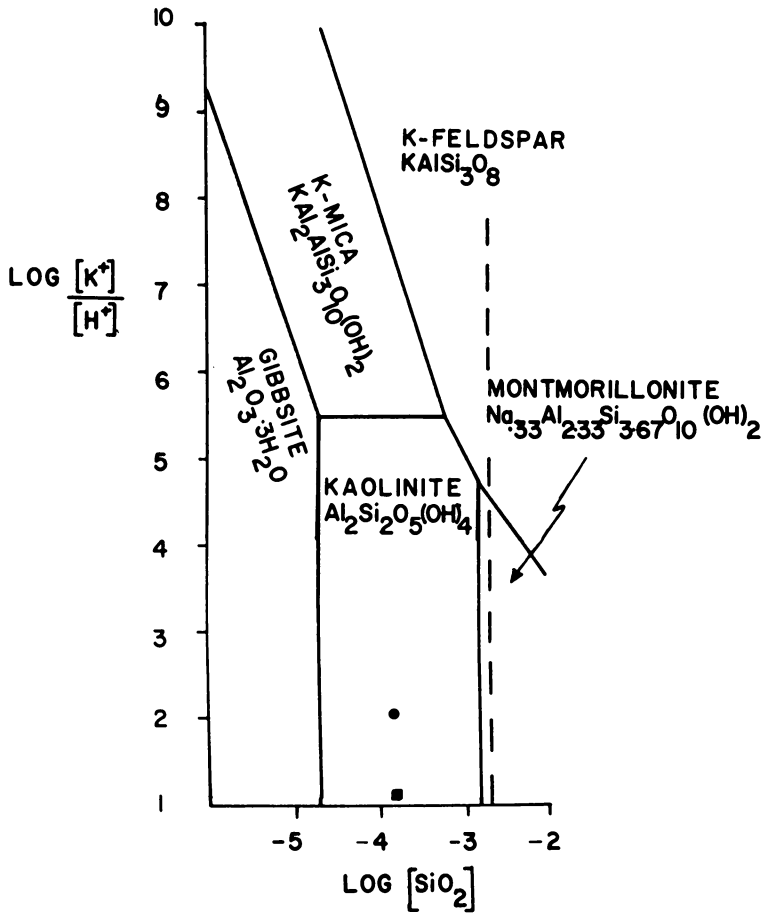

Figure 6. Stability relations of some phases in the system K_2O-Al_2O_3-SiO-H_2O at 25°C. and one atmosphere, as a function of $[K^+]/[H^+]$ and $[SiO_{2(aq)}]$ (3)

Circle represents analysis of Pond Branch water, square represents analysis of soil water

tube, the effluent was sampled and then continuously recirculated through the tube, no more distilled water being added during the course of the experiment. In a matter of days the effluent from both tubes achieved a composition similar to that of the stream water (Table IV). The effluent from the tubes maintained this composition for a period of 19 weeks during which time a volume of water estimated to be equivalent to six years of rainfall was passed through the tubes. This phase of the study was then terminated and the soil columns were dried. A solution containing 50 p.p.m. SiO_2 (aq) was prepared and circulated through

tube two. Concentration of silica in the effluent stabilized in a matter of hours at the same value observed in the leaching experiments ($\sim$ 9 p.p.m.). Distilled water was passed through tube one and the effluent again achieved a stable silica concentration of 9 p.p.m. in a matter of hours. Other dissolved species were not determined in this experiment.

Table IV. Composition of Waters from Soil Column Experiments[a]

Ion	*Tube 1*	*Tube 2*
$SiO_{2(aq)}$	15.50	15.58
Na	4.35	5.00
K	5.08	4.60
Ca	5.62	4.68

[a] Molal concentration $\times 10^5$.

In another experiment several grams of crushed unweathered rock from the watershed were placed in distilled water in a polyethylene bottle. In a second bottle, several grams of fresh rock were placed in stream water. The bottles were then placed on a shaker table, and the waters were analyzed periodically. Within a week the distilled water had achieved a composition similar to the stream (less rain water contribution) and the stream water had not changed (Table V). We conclude from the experiments that the water reacts rapidly with the silicate minerals and the final concentrations of the dissolved constituents in the water are controlled by the silicate minerals. (The results of these experiments and data for a group of individual minerals will be presented in detail in a separate publication.)

Table V. Composition of Waters from Crushed Rock Experiments[a]

Ion	*Crushed Rock in Distilled Water*	*Crushed Rock in Stream Water*
$SiO_{2(aq)}$	15.13	15.49
Na	5.60	7.46
K	0.93	2.45
Ca	1.73	3.97

[a] Molal concentration $\times 10^5$.

Calculation of Weathering Reactions

The contribution of minerals in the fresh rock to the dissolved load of the stream can be assessed by calculating the weathering reactions in

reverse; *i.e.*, by reconstituting the original minerals by back reaction of the stream water with the products of weathering (*6*). The results of a balance of this type for the Pond Branch watershed is shown in Figure 7. The contribution of rain to the stream water composition is subtracted and leaves that portion of the dissolved load that is supplied by rock weathering. Goethite, an abundant iron oxide in the weathered mantle, was used to back react all of the sulfate, forming pyrite and liberating some bicarbonate. The sodium and calcium in the stream is supplied by the breakdown of oligoclase. Reaction of all of the sodium and calcium with kaolinite and gibbsite to reconstitute oligoclase accounts for most of the dissolved silica. Note that the composition of the reconstituted oligoclase is almost the same as the composition of the oligoclase in the fresh rock, which suggests that the assumption concerning the source of sodium and calcium is correct.

At this point a small amount of silica and bicarbonate and all of the potassium, magnesium, and chloride remain. Biotite, an alumino-silicate containing magnesium, iron, and potassium, is the most abundant magnesian mineral in the rock. Reconstituting biotite of the composition found in the fresh rock (*4*) by the reaction of the potassium, bicarbonate, silica, and magnesium in the water with kaolinite and goethite leaves a residual of chloride, a slight deficit of bicarbonate and some magnesium. The small imbalance in charge of the residual ions is a reflection of the initial small error of the stream water analysis.

Although this balance is rather crude, it shows that most of the dissolved constituents in the stream water can be accounted for by the breakdown of oligoclase. The weathering of biotite probably contributes the rest of the silica, the potassium and a portion of the magnesium. These two minerals, however, constitute only about 20% by weight of the original rock. This implies that the rate of weathering of the other minerals in the rock is slow with respect to that of oligoclase and biotite.

The excess of chloride (and the balancing cations) is hard to explain in terms of rock weathering as none of the minerals constituting the fresh rock are known to contain chloride. Gambell and Fisher (*2*) observed a chloride excess in a comparison of rain and river compositions in North Carolina and Virginia. They attribute the excess chloride in the streams to rock weathering. Therefore there is either a mineralogic source of chloride that has been overlooked or our rain samples are not representative. It is also possible that there is a contribution to the watershed from fallout of airborne dust. We cannot evaluate the importance of this source at the present time.

	Moles of Material in				
	SiO_2	Ca^{2+}	Mg^{2+}	Na^+	K^+
stream	15.46	3.89	4.08	7.80	2.26
rain	15.46	1.82	2.56	6.50	0.99
geothite → py	15.46	1.82	2.56	6.50	0.99
gibbsite → olig.	12.68	1.60	2.56	5.72	0.99
kaolinite → olig.	1.26	0	2.56	0	0.99
kaolinite → bio	0	0	0.91	0	0
residual	0	0	0.91	0	0

Reactions

(1) Geothite → py: $0.25FeOOH + 0.5SO_4^{2-} + CO_2 = 0.25FeS_2 + 1.0HCO_3 + 0.94O_2 + 0.38H_2O$

(2) Gibbsite → olig: $0.61Al_2O_3 \cdot 3H_2O + 0.78Na^+ + 0.22Ca^{2+} + 2.78SiO_2 = Na_{0.78}Ca_{0.22}Al_{1.22}Si_{2.78}O_8 + 1.22H^+ + 1.22H_2O$

Figure 7. Mass balance calculation for Pond Branch Watershed. The balance weathering to reconstitute the original mineral constituents of the rock (see text

Weathering Model

On the basis of mineral distribution and water compositions a simple model of weathering can be deduced. Rain, low in cations and devoid of silica, falling on the drainage divides contacts a kaolinite-gibbsite assemblage. It reacts with kaolinite to form gibbsite, releasing silica to the solution until the silica concentration of the gibbsite-kaolinite equilibrium is achieved. As the water percolates downward into less weathered material it encounters and reacts with more siliceous minerals than kaolinite. The silica concentration of the solution increases. Gibbsite is no longer stable, and kaolinite alone becomes the stable phase. It is this water that emerges as the base flow of the stream.

Transport of Material

The products of weathering are removed from the watershed as dissolved and particulate material. Baseflow of the stream for the year of record removed 1.5 metric tons of dissolved material, or 0.015 metric tons per acre. This figure is a minimum value, and would be increased by material leaving the basin by deeper circulation and by flood flow.

Mechanical transport of solids by the stream, as suspended or bed load, removes additional material. Direct measurement of suspended load yields a figure of 0.28 metric tons, or 0.0027 metric tons per acre for the

10^5 Liters of Water

H^+	SO_4^{2-}	HCO_3^-	Cl^-	Amount of material produced by the back reaction of 10^5 l. stream water with weathered rock
0.02	5.08	10.88	6.48	
−2.33	0.50	10.88	3.57	
−2.33	0	11.88	3.57	0.25 mole FeS_2
−1.11	0	11.88	3.57	1 mole olig.
0	0	4.07	3.57	7.32 mole olig.
0	0	−0.22	3.57	1.18 mole biotite
0	0	−0.22	3.57	

(3) Kaolinite → olig: $4.47Al_2Si_2O_5(OH)_4 + 5.72Na^+ + 1.60Ca^{2+} + 11.42SiO_2 + 7.81HCO_3^- = 7.32Na_{0.78}Ca_{0.22}Al_{1.22}Si_{2.78}O_8 + 12.29H_2O + 1.11H^+ + 7.81CO_2$

(4) Kaolinite → bio: $0.96Al_2Si_2O_5(OH)_4 + 1.25SiO_2 + 4.29HCO_3^- + 0.99K^+ + 1.65Mg^{2+} + 1.59FeOOH = 1.18K_{0.84}Mg_{1.40}Fe_{1.35}Al_{1.63}Si_{2.69}O_{10}(OH)_2 + 7.97H_2O + 4.29CO_2 + 0.71O_2$

is based on the reaction of 10^5 liters of Pond Branch water with products of for discussion)

year of record. Flood flows carried about the same concentration of suspended load as baseflow.

The sediment trapped in the pond at the lower end of Pond Branch provides a nine year record of suspended and bedload. The pond was surveyed in 1957 and again in 1966. Comparison of the two surveys shows a slight deficit in accumulation. Thus, if there was any accumulation it was less than the errors in measurements.

The ratio of material removed as dissolved load to that transported as clastic load is 5.5 on the basis of figures cited above. This ratio may be somewhat high because of the limited number of very high flows. Calculations suggest that it would take a stream similar to Pond Branch 3.5 million years to remove the amount of material necessary to form the gorge and swale areas of the present watershed.

Conclusions

This work, although a modest beginning in our effort to understand the geochemical balance of a small watershed, permits us to draw some tentative conclusions:

(1) The major portion of the dissolved load of Pond Branch is derived from rock weathering.

(2) CO_2 charged rain reacts rapidly with the silicate minerals in the fresh rock and soil producing solid phases higher in aluminum than

the original silicates; the solution is enriched in dissolved silica, cations, and bicarbonate ion.

(3) Aluminum and iron are conserved in the solid phases.

(4) The reactions of water with silicates are so rapid that the waters remain in near-equilibrium with one or more solid phases at all times.

(5) The major portion of the dissolved silica in the stream is derived from the breakdown of oligoclase feldspar even though quartz is the major silica mineral in the rock.

(6) The rate of removal of material as dissolved load is about five times greater than the rate of mechanical removal for this small wooded watershed.

Acknowledgements

We would like to thank M. A. Wolman and B. F. Jones and C. B. Hunt for reading the manuscript and for offering many useful suggestions. Terrance Smith and Thomas Dunne were most helpful in various aspects of both the field and laboratory work.

This work was supported by grants from the Petroleum Research Fund of the American Chemical Society (665-G2) and National Science Foundation (GP 2660).

Literature Cited

(1) Bricker, O. P., Garrels, R. M., "Principles and Applications of Water Chemistry," p. 449, S. D. Faust and J. V. Hunter, eds., John Wiley & Sons, New York, New York, 1967.
(2) Gambell, W. A., Fisher, D. W., *U. S. Geol. Surv. Water Supply Papers* **1535-K** (1966).
(3) Hess, P. C., *Am. J. Sci.* **264**, 289 (1966).
(4) Hopson, C. A., "The Geology of Howard and Montgomery Counties," Maryland Geol. Surv., 1964.
(5) Iwasaki, Iwaji, Utsumi, S., Ozawa, T., *Bull. Chem. Soc. Japan* **25**, 226 (1952).
(6) Mackenzie, F. T., Garrels, R. M., *Am. J. Sci.* **264**, 507 (1966).
(7) Mullin, J. B., Riley, J. P., *Anal. Chim. Acta* **12**, 162 (1955).
(8) Packham, R. F., *Proc. Soc. Water Treat. Exam.* **7**, 102 (1958).
(9) Pinta, M., "Recherche et Dosage des Elements Traces," Dunod, Paris, 1962.
(10) Rainwater, F. H., Thatcher, L. L., *U. S. Geol. Surv. Water Supply Papers* **1454** (1960).
(11) Southwick, D. L., Fisher, G. W., "Revision of Stratigraphic Nomenclature in the Glenarm Series, Appalachian Piedmont," Maryland Geol. Surv., (report in preparation).

RECEIVED May 11, 1967.

Biological Studies of Manganese Solution from Its Dioxide

ROBERT S. INGOLS and MINE E. ENGINUN

Georgia Institute of Technology, Engineering Experiment Station, Atlanta, Ga.

Studies of the solution of manganese from manganese dioxide by reaction with sterile and inoculated bacterial media indicate that the inoculation is unnecessary for the solution. Actually, the growing organisms compete for the reactive capacity of the food in the medium; the more rapidly that the organisms develop the greater is the competitive interference. Under natural conditions, the organisms contribute to the manganese solution by developing an oxygen free environment for the maintenance of a manganous solution at the neutral pH values typical of natural lakes.

For many years it has been realized that manganese disperses or dissolves in the hypolimnion of a lake only after the dissolved oxygen has disappeared from the hypolimnion. It is generally conceded that the disappearance of the dissolved oxygen is brought about through the activity of microorganisms or in other words that this is a result of biological activity. There has been some question for a long time as to the source of the manganese that disperses and the mechanism by which it is reduced and dissolved. The senior author advanced the hypothesis (*3*, *4*) that the oxidized manganese dissolved as a carbon dioxide complex which was reduced by bacteria and that this occurred inside of the microorganism. In a more recent publication (*1*), it was indicated that the reduction was more probably caused by a by-product of bacterial metabolism rather than the actual entry of a particle of oxidized manganese into the bacterial cell. The authors of this paper then set about finding the species of bacteria and the conditions which would most rapidly dissolve the manganese from the particles of manganese dioxide in the soil and to compare these against the time required. In a recent article including a review of the controversy between the biologically and the

abiologically induced reduction of manganese dioxide in lake bottom muds, Gabe, Troshanov, and Sherman (2) conclude from their data that the reduction is biological.

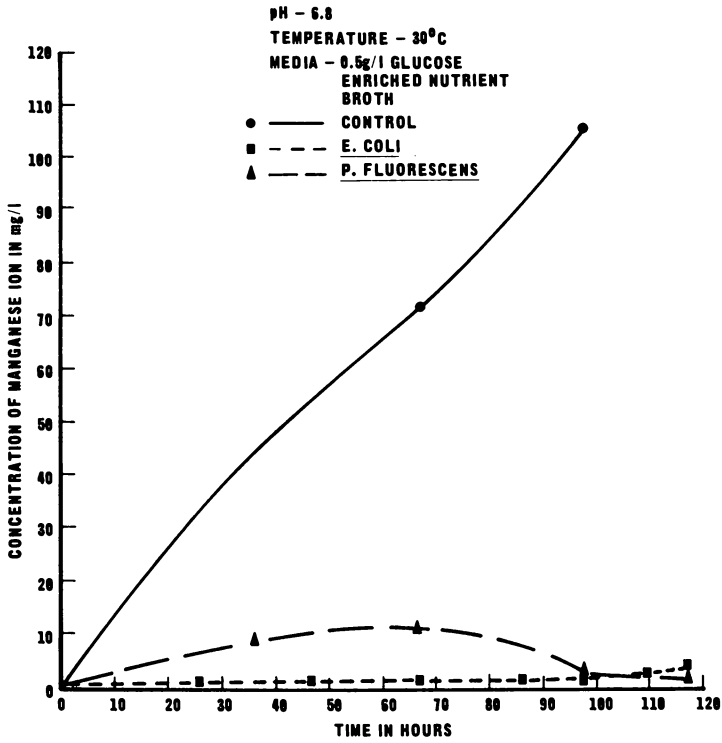

Figure 1. A comparison of the rate of manganese solution in uninoculated and inoculated glucose enriched nutrient broth

With a strong indication of the biological mechanism of manganese solution, it was concluded that the rate of manganese solution should be positively correlated with the rate of bacterial activity. Thus, the identity of both the most effective bacterium as well as the optimum conditions for manganese solution were considered important. Previous work (3) had indicated that *E. coli* was not effective, but further work at room temperature instead of 37°C. indicated otherwise. Therefore, cultures of both *E. coli* and *P. fluorescens* were incubated in parallel experiments at the optimum temperature for each bacterium to observe their rate of manganese solution. Less manganese was dissolved by each organism when it was incubated at its optimum temperature. This indicated that the dissolving or reduction of the manganese was inversely correlated with the growth rate of the organisms. Further, the data from

a long incubation period indicated that manganese was first dissolved and then precipitated as the time of incubation increased. This could only mean that reaeration of the samples occurred.

It was necessary to find a better procedure for obtaining and maintaining the cultures free of dissolved oxygen during the entire period of incubation and then to repeat the experiments to find the most effective bacteria and the optimum conditions.

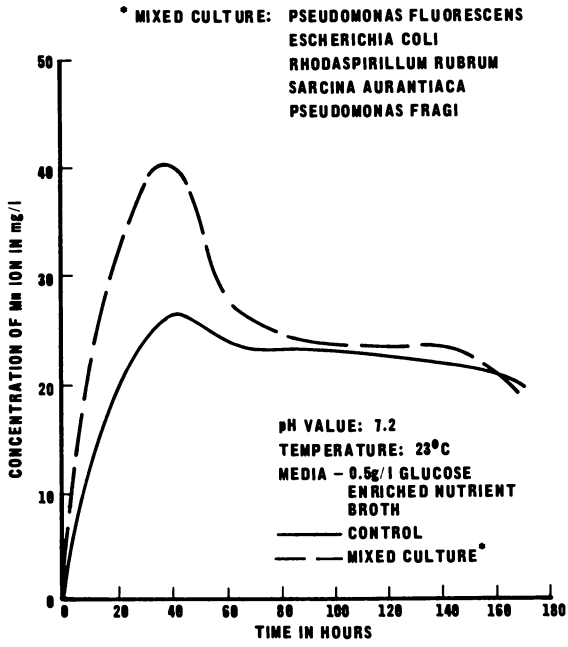

Figure 2. A comparison of the rate of manganese solution in uninoculated glucose enriched nutrient broth and in the same medium with an inoculation of five cultures

Procedures

The manganese has been determined by the formaldoxime procedure recommended by Morgan and Stumm (5). This is more simply performed than the persulfate procedure, though it does have a limited range of concentration for comparison with standards.

All samples for study of the rate of manganese solution were prepared in a glucose enriched nutrient broth medium adjusted to a desired pH and poured into five replicate test tubes for each observation point. The sterilized tubes were taken from the autoclave as hot as possible for safe handling. Crystals of sterilized manganese dioxide were added. A vaspar plug was poured on top of the mixture and a screw cap tightened

immediately. The tubes were then placed in an incubator at 37°C. or left at 23°C.

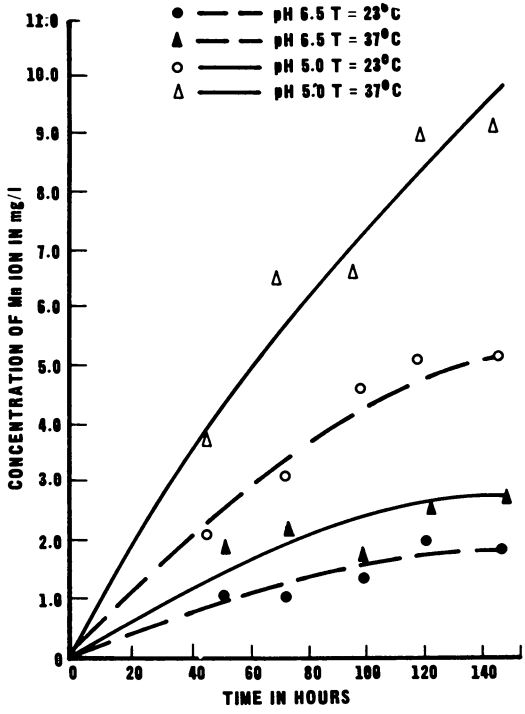

Figure 3. A comparison of the rate of manganese solution in uninoculated glucose enriched nutrient broth adjusted before sterilization to 2 pH values. After adding manganese all replicates were stored at different temperatures

Results

The data of Figure 1 indicates that the controls were much better in dissolving manganese than the inoculated samples of pure cultures of *E. coli* or *P. fluorescens*. This one experiment was so completely different from all previous work that only very little more work was performed with inoculated culture media. The data of Figure 2 indicates that with a mixed culture in a medium of higher pH and lower incubation temperature as much manganese can dissolve in the inoculated tubes as in the control tubes. The marked difference in the amount of manganese dissolved in the controls of experiments reported in Figures 1 and 2 may be understood from the results shown in Figure 3. The more rapid solution occurs at the lower pH and at the higher reaction temperature.

The experiment of Figure 3 has been repeated at pH values of 5.5, 6.5, 6.8, 7.2, and 7.8 with the same general results that the higher temperatures and lower pH values of the media favor a higher rate of manganese solution. The lower pH values again would not favor the action of bacteria in dissolving manganese.

Discussion

The data leads to the conclusion that biological activity is not necessary when the media is obtained without oxygen as the manganese dioxide is added and when it is maintained free of oxygen during the reaction period. This means that any biological activity is an interfering or competitive reaction for the glucose instead of its being available for reducing the manganese dioxide. Because the metabolism of microorganisms under anaerobic conditions changes the net amount of energy only slightly, the by-products would appear less reactive with manganese dioxide than the chemicals of original medium. This again is in direct conflict with earlier conclusions by the senior author.

Since the reaction is purely chemical, the factors favoring the reduction of manganese dioxide will be very important in defining the rate of the solution of the manganese. Thus a drop in pH (as shown by the following equation) will make the manganese a much stronger oxidant:

$$MnO_2 + 4H^+ \rightarrow Mn^{2+} + 2H_2O - 2e^- \quad (E^\circ = 1.28)$$

The rise in temperature of 10°C. will increase the rate of reaction several fold also.

It is obvious that in the hypolimnion of a lake that the biota remove the dissolved oxygen, but the organic debris in the muds cause reduction of the manganese. The soluble manganese can then diffuse through the oxygen-free, water above the muds. It may also be true that organic compounds in the muds form complexes with the manganese and diffuse along with the reduced manganese.

Acknowledgment

This work was supported jointly by the Engineering Experiment Station and the Water Resources Center, Georgia Institute of Technology.

Literature Cited

(1) Enginun, M. E., Ingols, R. S., *Proc. Georgia Acad. Sci.*, April 22, 1966.
(2) Gabe, D. R., Troshanov, E. P., Sherman, E. E., "Applied Capillary Microscopy," Consultants Bureau, New York, 1965.
(3) Ingols, R. S., Esterman, M., Enginun, M., *Southeastern Sect. Am. Water Works Assoc.* 29, (1), 48 (1965)

(4) Ingols, R. S., Wilroy, R. D., *J. Am. Water Works Assoc.* **55**, (3), 283 (1963).
(5) Morgan, J. J., Stumm, Werner, *J. Am. Water Works Assoc.* **57** (1), 107 (1965).

RECEIVED April 24, 1967.

Cationic Concentration by Freezing

B. A. MALO and R. A. BAKER

Carnegie Mellon University, Mellon Institute, Pittsburgh, Pa.

The results of an investigation of cationic separation during the freezing process as it applies to concentration of trace contaminants from water are reported. The cations including Fe, Cu, Zn, Mn, Pb, Ni, Ca, Mg, and K were studied at concentrations of 0.1 to 10 mg./liter. For any given cation, recovery does not vary over the experimental concentration range. However, selective ion incorporation into the ice matrix was observed when demineralized, laboratory prepared solutions and highly mineralized, naturally buffered waters were concentrated. Increasing mixing rate up to some limiting value increases cationic recovery. Whether initial pH increases or decreases, recovery depends on the nature of the cation. Alkali metals (K, Ca, and Mg) concentrate best at acid pH. Heavy metal cations (Pb, Ni, and Cu) concentrate best at alkaline pH. Generally, increasing initial total dissolved solids decreases cationic recovery.

In order to separate, identify, and quantify trace contaminants in water, the analyst must employ concentration procedures preliminary to analyses. Continuing studies in these laboratories have examined the freeze concentration techniques for μg/liter to mg./liter levels of organics from aqueous solution. It was observed that inorganic salts significantly affect organic recovery efficiency. An investigation to determine the nature of this effect afforded an opportunity simultaneously to examine inorganic cationic separation during the freezing process.

The subject of salt effects on the freezing process is not new. Nevertheless, despite many years of study, it is still an inadequately understood process (*12*). Recent applications of the freeze concentration technique to inorganic recovery from water have been reported (*2, 9, 10, 16*). Many of these studies were prompted by a communication (*15*)

which renewed interest in freezing of water as a means of concentration, particularly for recovery of volatile, heat-labile substances.

The objective of this paper is to describe preliminary results obtained from the investigation of the process of cationic separation during the freezing process as it applies to concentration of trace contaminants from water.

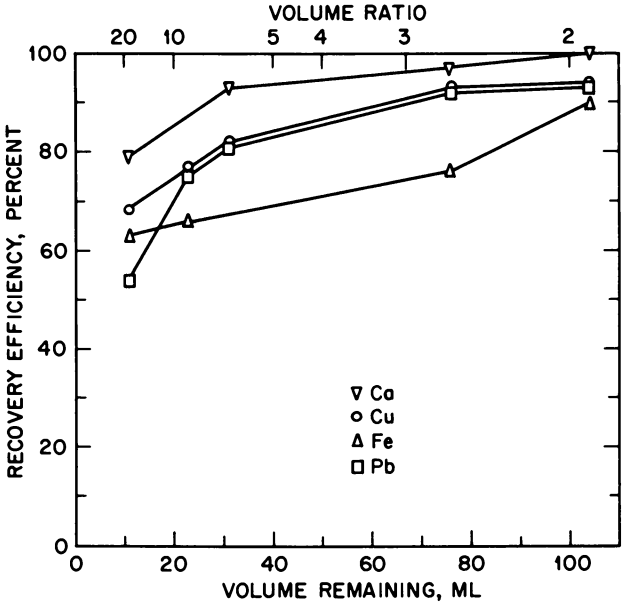

Figure 1. Influence of selective ion incorporation on the freeze concentration efficiency of metal cations

Matrix: U.S. Mean Water. Mixing Rate = 80 r.p.m. Bath Temperature = −12°C. Initial: volume = 200 ml.; pH = 6.6; specific conductance = 225 μmhos/cm.; cation concentration, mg./liter = 7.5 Ca, 96. Cu, 0.2 Fe and 9.7 Pb

Experimental

The experimental procedure for freeze concentration used in this study has been detailed elsewhere (3). In brief, a specific sample volume is chilled to approximately 1°C. and transferred to a round-bottom flask that has been prechilled and seeded with a few ice crystals. The flask capacity is selected to exceed two sample volumes. The flask is immediately attached to a mixing device and lowered into an ice-salt bath maintained at approximately −12°C. The flask is rotated at a predetermined rate until the desired volume, judged by experience and estimated by elapsed time, has been frozen. The cations are concentrated in the

residual liquid. The flask is disconnected and the residual liquid is transferred and its volume measured. The ice is melted and both liquid and ice (when possible) are analyzed for pH, specific conductance and cations by atomic absorption spectrometry. The efficiency of recovery in percent is calculated from:

$$\% \text{ Recovery} = \frac{\text{chemical concentration ratio}}{\text{volume ratio}} \times 100$$

$$= \left[(C_{L(2)}/C_{L(1)}) \Big/ (V_1/V_2) \right] 100$$

$C_{L(1)}$ = initial solute concentration in liquid, mg./l.

$C_{L(2)}$ = final solute concentration in liquid, mg./l.

V_1 = initial sample volume, ml.

V_2 = final volume of liquid, ml.

The experimental aqueous matrices included deionized-distilled water, laboratory-prepared phosphate buffer solutions, U.S. mean water (*1*), and tap waters. U.S. mean water is a solution of specified mineral content which may be prepared and used as a reference standard. These aqueous systems were supplemented with known quantities of Fe, Cu, Zn, Mn, Pb, Ni, Ca, Mg, and K singly and in mixtures. Cations with the exception of Fe and K were added as nitrates. Fe and K were added as chlorides. The freezing rate is controlled by the vessel rotation rate and bath temperature. Specific conductance is used as an indicator of the dissolved solids concentration, although it is recognized that this property is influenced by the hydrogen ion concentration as well as the nature of the dissolved constituents.

Results

The effect of certain factors on the recovery efficiency of various cations from water by freezing was studied. These included the mixing rate, initial pH, specific conductance or total dissolved solids, cation concentration and initial and final volume.

When a mixture of cations in water is concentrated by freezing, individual recovery efficiency usually varies. This is illustrated by the result of a single-stage freeze concentration shown in Figure 1. In this case, a quaternary mixture of cations was recovered in the sequence Ca>Cu>Pb>Fe. These cations were initially dissolved in a U.S. mean water. Initial conditions were: pH, 6.6; specific conductance, 225 μmhos/cm.; and the cations at 7.5 to 9.7 mg./liter. The variation in cationic recovery in the concentrated liquid is caused by selective ion incorporation in the residual ice. Because of this selective incorporation, it is not possible to predict the final abundance of a cation relative to the other components in the liquid phase. The recovery efficiency of the four cations cited is

unique to this test. It applies only for this water and the operating conditions specified.

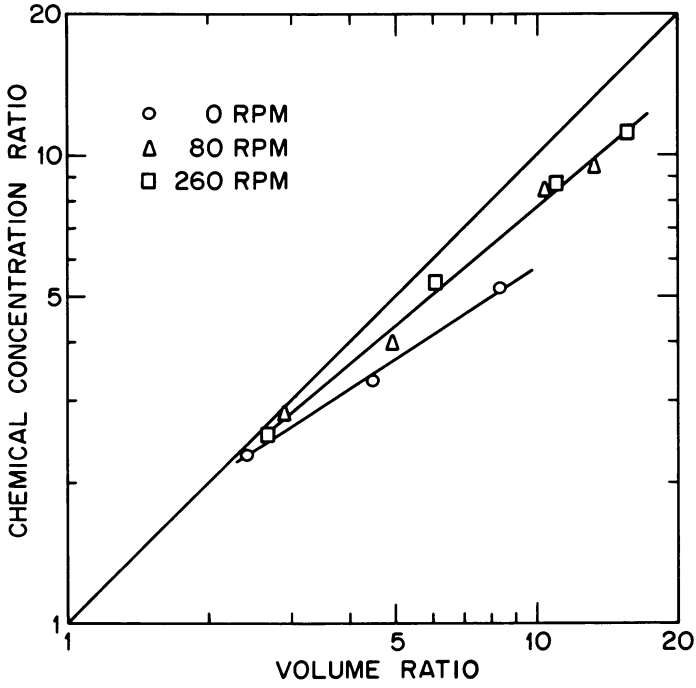

Figure 2. The effect of mixing rate on the recovery of Mn from a deionized-distilled water matrix

Initial: volume = 200 ml.; pH = 3.8; specific conductance = 164 μmhos/cm.; Mn = 1.0 mg./liter

With the procedure practiced in these studies, mixing was varied by changing the rotation rate of the flask containing the sample. No internal stirrers were used. The effect of mixing, or rotation, on cationic recovery efficiency from a deionized-distilled water and a tap water is presented in Figures 2 and 3 respectively. These waters were initially supplemented by mg./l. concentrations of Mn, Fe, Pb, Ni, Cu, and Zn. Only the manganese recovery data are presented since the effect was similar for all cations. In these illustrations, the solid, diagonal line represents ideal or total concentration efficiency—*i.e.*, the volume and chemical concentration ratios are identical. The amount of departure of the experimental data from this line is a measure of loss of efficiency. With both waters, mixing improved cationic recovery over quiescent freezing. However, increasing rotation rate from 80 to 260 r.p.m. did not further improve

separation. This effect was previously observed in the freeze concentration of organics (*4*). These results also demonstrate the interrelationship of initial total dissolved solids content, mixing rate and recovery efficiency. For example, manganese recovery from the 660 μmhos/cm. tap water at 260 r.p.m. is comparable in efficiency to that at 0 r.p.m. from the 164 μmhos/cm. deionized-distilled water. The elapsed time required to freeze a given aqueous volume at −12°C. bath temperature is twice as great at 80 r.p.m. than at 260 r.p.m. (*3*). Since increased mixing tends to improve recovery, field applications of this procedure should be made at the highest practical mixing rate. The influence of dissolved solids content is treated in subsequent paragraphs.

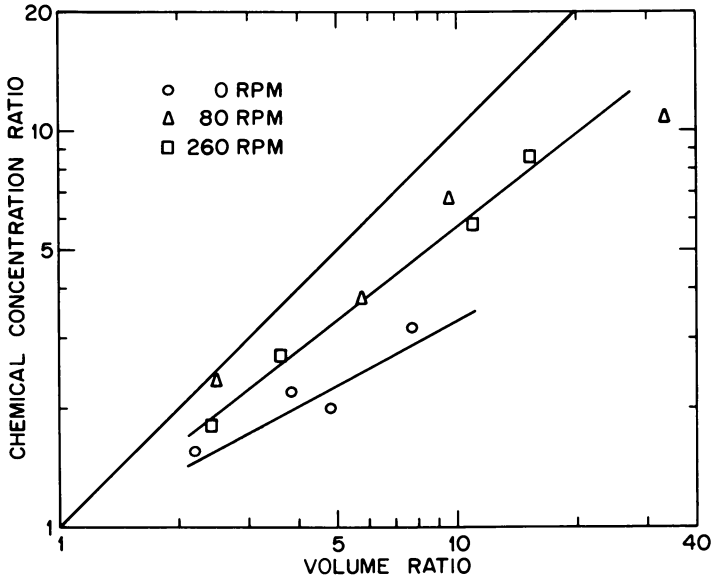

Figure 3. The effect of mixing rate on the recovery of Mn from tap water

Initial: volume = 200 ml.; pH = 6.0; specific conductance = 660 μmhos/cm.; Mn = 1.0 mg./liter

The pH of the ice-liquid system influences cationic separation and recovery. Figure 4 depicts the effect of pH on recovery of manganese from a tap water which was supplemented by 1 mg./liter quantities of Mn, Fe, Cu, Zn, Pb, and Ni. The initial pH of 6.1 was adjusted to 3.6 and 10.2 with HCl and NaOH respectively. The manganese recovery was slightly greater at alkaline pH for comparable volume ratios. The pH effect is also shown in Figure 5 for lead, nickel, and copper and in Figure

6 for calcium, magnesium and potassium. Improved recovery of Pb, Ni, and Cu in the liquid phase is favored by increased alkalinity while increased acidity enhances Ca, Mg, and K separation. These observations are particularly applicable to volume ratios greater than 5:1. Little difference is evident at lower volume ratios. The consistency of selective recovery order for these ternary cationic mixtures over a range of volume ratios confirms the phenomenon of selective incorporation.

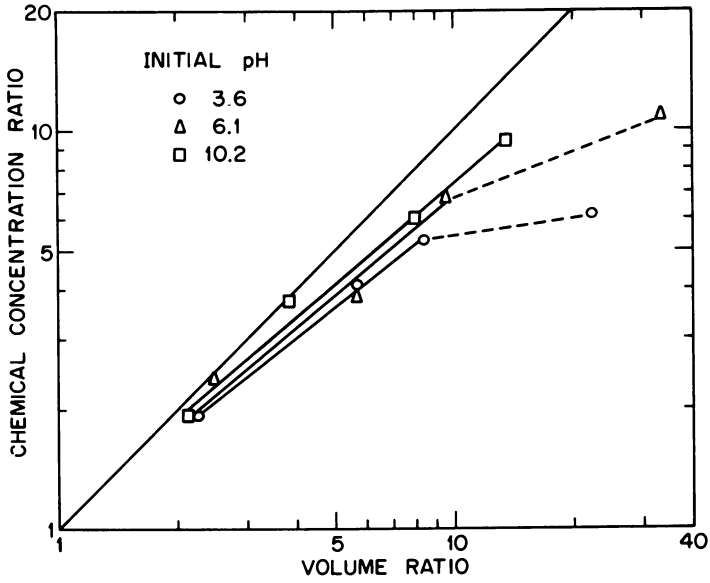

Figure 4. The effect of pH on the recovery of Mn from a tap water

Mixing Rate = 80 r.p.m. Initial: volume = 200 ml.; Mn = 1.0 mg./liter; specific conductance = 955, 655, and 919 μmhos/cm. for pH = 3.6, 6.1 and 10.2 respectively

Organic recovery efficiency from aqueous solution by freeze concentration has been reported (*4*) to decrease as the specific conductance or total dissolved solids increased. A similar effect has been observed for the recovery of heavy metals from a variety of aqueous solutions. Figure 7 illustrates the recovery-suppressing effect of dissolved solids on copper as measured by specific conductance in the range of 40 to 40,000 μmhos/cm. The matrices include deionized-distilled water, 10^{-3} to $10^{-4}M$ phosphate buffers and tap waters originally at pH 4 ± 0.5, and 0.12*N* (approximate) HCl solution at pH 1.4. The recovery of other heavy metal cations follows in a similar manner.

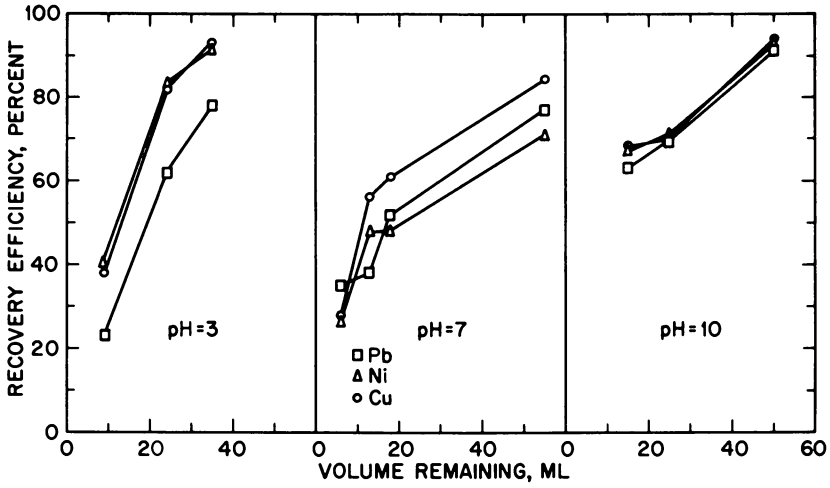

Figure 5. The effect of pH on the recovery of Pb, Ni, and Cu from tap water at low residual volumes

Mixing Rate = 80 r.p.m. Initial: volume = 200 ml.; cation concentration, mg./liter = 2.3 Pb, 1.0 Ni, and 1.0 Cu; specific conductance = 955, 680, and 919 μmhos/cm. for pH ≅ 3, 7 and 10 respectively

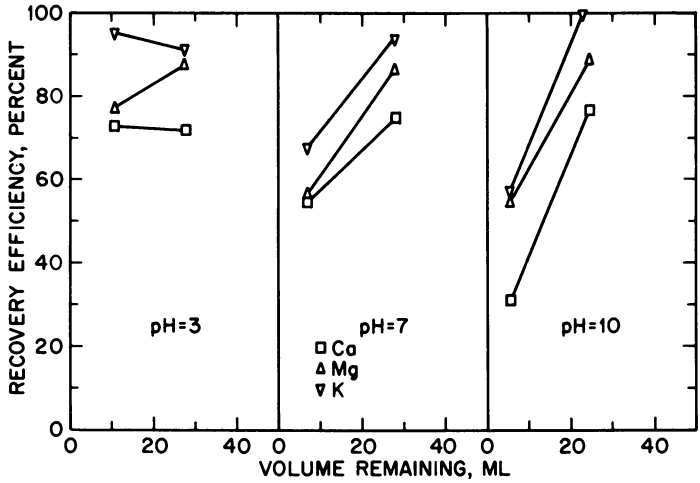

Figure 6. The effect of pH on the recovery of Ca, Mg, and K from tap water at low residual volumes

Mixing Rate = 80 r.p.m. Initial: volume = 200 ml.; cation concentration, mg./liter = 28.0 Ca, 6.3 Mg and 1.8 K; specific conductance = 1080, 360 and 413 μmhos/cm. for pH ≅ 3, 7, and 10 respectively

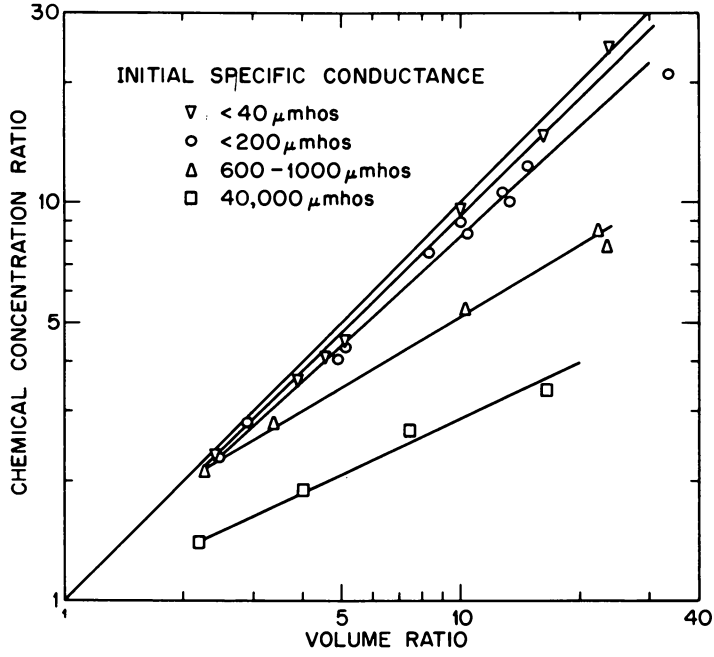

Figure 7. The effect of specific conductance on the recovery of Cu

Mixing Rate = 80 r.p.m. Initial: volume = 200 ml.; pH ≅ 4; Cu = 1.0 mg./liter

Single-stage freeze concentration recovery efficiency was not affected by initial cationic content in the range of 0.1 to 10 mg./liter. Figure 8 shows this for copper recovery from a synthetic aqueous solution prepared by adding equal quantities of copper and lead to U.S. mean water. This water contained Ca, Mg, Fe, Mn, Na, and K. The recovery of other heavy and alkali metal cations followed that of copper.

The initial volume employed for a single-stage freeze concentration is not in itself a controlling factor in contaminant recovery efficiency. It does limit the extent of volume concentration which may be achieved at maximum efficiency. There is a critical final volume of unfrozen liquid below which recovery is impaired. This limiting range varies for the water and operating conditions being used. This is a mechanical-experimental limitation for the procedure being used and involves the residual liquid volume held on the ice, flask, etc. The ice was not washed in these tests. Some concentrated liquid is expected to freeze on the ice surface during the sample transfer operation. A similar observation was reported by Baker (3) who suggested a limiting final volume of 30 ml. per unwashed

single-stage freeze concentration from waters of low dissolved solids content for maximum recovery of trace organics. A representative cationic recovery-volume ratio relationship is shown in Figure 9 for lead. Other heavy metals give similar results. Here efficiency loss begins to occur between 50 and 70 ml. residual volume. The initial volume selected per single-stage freeze is determined by considering the desired volume ratio and the limiting final volume. For high volume ratios larger initial sample volumes are required. The data point indicated by the triangle (△) at 30 ml. residual volume resulted from a single stage freeze of 1000 ml. This represents a volume ratio of 33.3 and it was performed with the same efficiency, 75%, as a 200 ml. freeze at a volume ratio of 8.7. The time required for the 1000 ml. freeze was 55 minutes, while the 200 ml. freeze took 21 minutes. Both were performed at 80 r.p.m. mixing rate and −12°C. bath temperature. A three-liter, round-bottom flask was used for the 1000 ml. initial volume tests. An alternative to the use of greater initial volumes and associated increased mixing load is the cascade freeze concentration technique (3). This procedure requires more time than the high volume single-stage freeze, but it permits almost any desired level of concentration at maximum efficiency. The data point represented by the inverted triangle (▽) at 74 ml. residual volume is a 27.0:1 volume

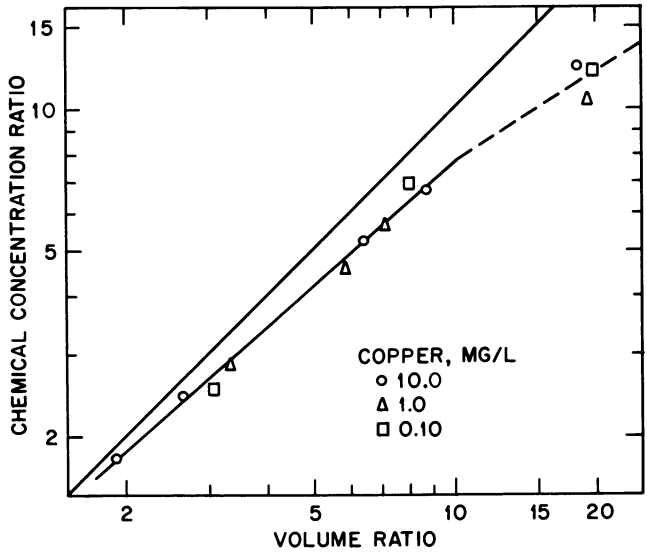

Figure 8. The effect of initial Cu concentration on its recovery from U. S. mean water

Mixing Rate = 80 r.p.m. Initial: volume = 200 ml.; pH = 6.6 to 7.1; specific conductance = 200 to 226 μmhos/cm.

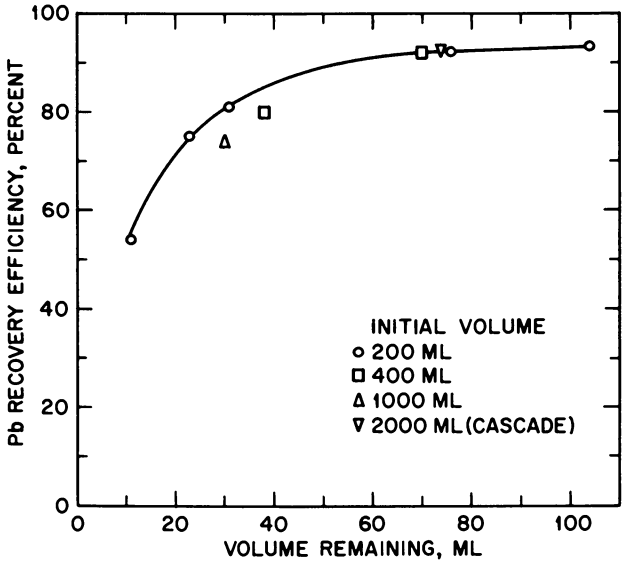

Figure 9. The effect of initial sample volume on the recovery of Pb from U. S. mean water

Mixing Rate = 80 r.p.m. Initial: pH = 6.6 to 7.35; specific conductance = 190 to 226 μmhos/cm.; Pb = 1.8 to 9.7 mg./liter

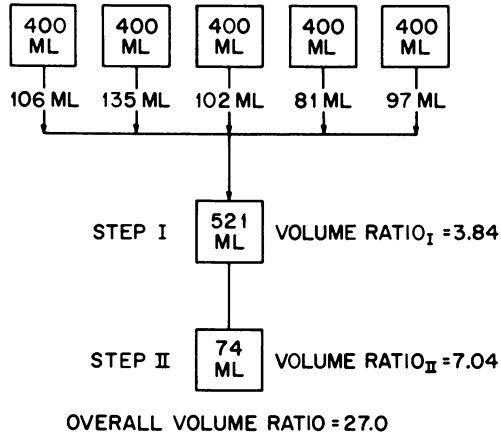

Figure 10. An experimental, two-step cascade scheme for cation recovery from a 2000 ml. initial volume

concentration yielding maximum recovery for Pb (92%). This was an 80 r.p.m., two-stage cascade freeze involving concentration of five 400 ml.

individual volumes to approximately 100 ml. (4:1), compositing the concentrates and freezing this composite to 74 ml. residual volume (Figure 10). The time required for the cascade freeze was 220 minutes. Availability of multiple mixing devices for simultaneous concentration of a number of single-stages and higher mixing capacity would markedly shorten this time. A multi-step cascade freeze concentration such as that in Figure 10 maximizes recovery efficiency and yields sufficient concentrate volume for extensive inorganic and organic analyses.

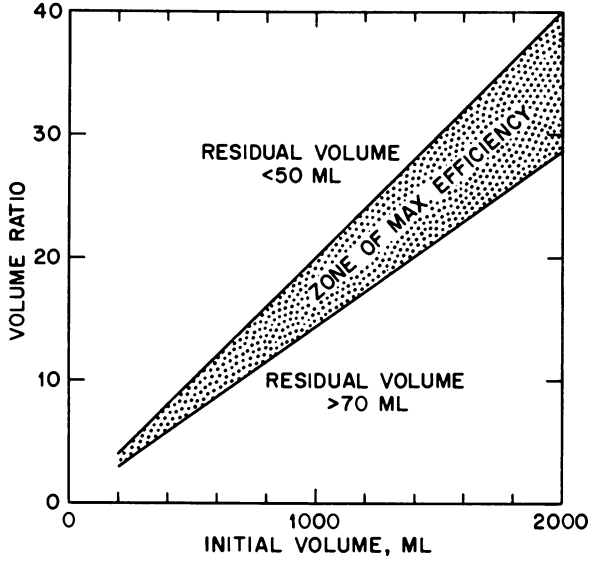

Figure 11. Limiting volume concentration ratio for maximum recovery efficiency as a function of initial sample volume

A graphical representation, Figure 11, shows the limiting volume concentration ratio for maximum recovery efficiency as a function of initial sample volume. For any given sample volume, recovery is maximum over the volume ratio range in the crosshatched area. Further increase in volume ratio yielding residual volumes lower than 50 ml. will appreciably decrease recovery. This limiting volume concept applies to any given single-stage freeze concentration whether it is (a) separate or (b) part of a multi-step cascade sequence.

Discussion

Workman and Reynolds (*18*) originally documented observations of charge separation and associated electrical potential at the growing ice surface. This phenomenon is now called the Workman-Reynolds Effect.

Subsequent investigations by others (*7, 8, 11*) contributed further to understanding of this effect although much remains to be explored. Among the factors examined were ionic radius, electronegativity, nature and concentration of solutes and freezing rate. These experiments were idealized and were conducted with selected systems in apparatus permitting measurements such as interfacial potential, current, and freezing rate when ice growth was unidirectional. The preliminary results reported here were obtained during a study of macrovariables with apparatus in which controls were not as rigorous. Thus, some of the postulates advanced in other studies are not readily applicable. Selective cationic recovery is suggested from the results (Figures 1, 5, and 6) but the order of recovery was not predictable over the range from 0.1 to 10 mg./liter initial concentration. Even if the physical parameters of freezing rate, temperature gradient across the ice-liquid interface and orientation of crystallographic axis of the ice had been controlled, a number of other factors would have to be considered if the results are to be adequately explained. These include: proton conductance; dipole orientation of water molecules at the interface; ionic entrapment in the ice lattice; and ionic diffusion. The processes may function singly or in combination, depending upon the constituents of the solution and their concentration. Parreira and Eydt (*13*), for example, speculated that in the range of 10^{-7} to $10^{-5}M$ NaCl, proton conduction may originate the freezing current whereas dipole orientation is responsible for the buildup of the large freezing potential observed. For this case, ionic entrapment and diffusion processes may have been operating, but their contribution was estimated to be slight.

Nucleation, the first step in crystallization (*12*), is induced by the practice of flask seeding. The second step, ice formation or growth is of greatest importance in the concentration procedure. The manner in which latent heat of fusion is conducted away from the ice-liquid interface determines the nature of the resulting ice surface. Thermal conduction away from the interface through the ice produces ice which is smooth on an atomic scale with propagation at the edge of the crystalline basal plane proceeding laterally. Lateral growth rate is greater than that perpendicular to the basal plane. Thermal conduction may also be into the liquid phase if this phase is supercooled. A very branched, uneven growth then occurs. This dendritic or branched morphology (5) is strongly influenced by the presence of solutes. The solutes may (1) reduce the melting point or degree of supercooling, thereby reducing the freezing rate, or (2) by changing ice growth patterns increase the rate of the advancing ice front. The latter condition is expected to predominate. Irregular ice growth would entrap solute-rich liquid precluding migration of the solute

into the bulk liquid. The concept of the planar growth pattern for ice and the assumption of a distinct boundary layer is idealized. Drost-Hansen (*6*) reports that surface orientation of the advancing ice front may extend 1000 A. or more into the liquid phase and be highly irregular. Mixing or turbulence may also affect dendritic growth.

Mixing induces turbulence and a decrease in the boundary layer thickness at the ice-liquid interface. The thinner the boundary layer, the shorter the time interval necessary for solute diffusion from the interface into the bulk liquid. The extent of incorporation in the ice depends in part on the relative velocity of solute diffusivity and the advancing ice front formation. Therefore, once a critical mixing rate is reached, further turbulence increase has no appreciable effect (Figures 2 and 3).

Dissolved inorganic solids have been shown to inhibit organic recovery efficiency by freeze concentration from aqueous solution (*4*). Similarly, increased salt content reduces cationic recovery (Figure 7). As ionic concentration increases at the interface, there is an increase in tendency toward dendritic growth and associated entrapment, changes in surface tension and induced interfacial potential, and impedance of specific ionic migration.

Movement of suspended and nondissociated materials ahead of the advancing ice front has been reported to be more efficient than for completely dissociated constituents (*4, 14, 17*). The previous statement may be valid for organics and to a degree for heavy metals, Figure 5, but it does not explain the observed separation of the alkali metals. The heavy metal cationic recovery is greater at increased pH but the alkali metal recovery is lower. The results of Figures 5 and 6 pertain only to recoveries measured when residual volumes were less than 50 ml.

The occurrence of selective ion incorporation has precluded the use of an internal standard as an indicator of the overall recovery efficiency, a technique applied successfully to the concentration of organics (*4*). Because of this inability at the present time to quantify the efficiency of concentration, the application of the freeze concentration technique solely for the determination of trace inorganics is impractical. There are more precise methods available for inorganic concentration—*e.g.*, evaporation or solvent extraction. Further refinement of the freeze concentration technique for cations may be achieved by washing the ice after transfer of the residual liquid. This point is being confirmed by current studies.

Summary

The study is a direct outgrowth of a continuing investigation of the freeze concentration of organic microcontaminants in water. The concentration of inorganic constituents is being monitored by atomic absorption

spectroscopy. The results will contribute fundamental information elucidating the parameters observed to affect organic concentration and permit development of a supplementary trace inorganic concentration scheme for water analysts. Waters of varying composition are being investigated. Specific observations include:

(a) Selective ion incorporation in the ice has been observed in freezing from all aqueous matrices. The cations studied were Fe, Mn, Cu, Zn, Pb, Ni, Ca, Mg, and K. Selective incorporation precludes use of a cation as an internal standard for estimating overall recovery efficiency as is the case with complex mixtures of organic compounds.

(b) Increasing mixing rate (or turbulence) increases cationic recovery up to some limiting value for any given initial total dissolved solids content. Further increase in mixing has no effect on recovery efficiency. This is controlled by the cationic migration rate through the interfacial boundary layer ahead of the advancing ice front. The boundary layer thickness and hence, the required distance for diffusion and associated migration time interval depends on mixing rate.

(c) The effect of initial pH on recovery efficiency depends on the nature of the cation. Alkali metals (K, Ca, and Mg) concentrate best at acid pH. Heavy metal cations (Pb, Ni, and Cu) concentrate best at alkaline pH.

(d) As initial total dissolved solids (specific conductance) increase, recovery of specific cations decreases.

(e) No variation in recovery efficiency of individual cations originally present in the concentration range of 0.1 to 10 mg./liter has been observed in single-stage freezes. For example, this was the case even in a complex mineralized water matrix of approximately 100 mg./liter total dissolved solids and 200 μmhos/cm. conductivity.

(f) With the experimental equipment and operating procedure being used, a physical limitation for single-stage volume concentration ratio was observed. The final volume of a single-stage freeze should be greater than 50 to 70 ml. regardless of initial volume to avoid marked decrease in cationic recovery.

(g) A cascade of single-stage freeze concentration such as that used in achieving high organic concentration ratios has been shown to be advantageous in concentrating cations at trace and micro levels.

Acknowledgment

This paper is a contribution by the Environmental Sciences Fellowship, Mellon Institute, Pittsburgh, Pennsylvania. The investigation was supported by DHEW (NIH) General Research Grant FR 558001-5.

Literature Cited

(1) *ASTM Std.* **23**, 306 (1964).
(2) Baker, R. A., *J. Water Poll. Cont. Fed.* **37**, 1164 (1965).
(3) Baker, R. A., *Water Research* **1**, 61 (1967).
(4) *Ibid.* **1**, 97 (1967).

(5) Chalmers, B., Edgar Marburg Lecture, 64th Ann. Meeting Am. Soc. Testing and Mater. (1961).
(6) Drost-Hansen, W., *Ind. Eng. Chem.* **57**, 18 (1965).
(7) Gross, G. W., *J. Geophys. Res.* **70**, 2291 (1965).
(8) Heinmets, F., *Trans. Faraday Soc.* **58**, 788 (1962).
(9) Kobayashi, S., Lee, G. F., *Anal. Chem.* **36**, 2197 (1964).
(10) Lecointe, M., *Rev. Gen. Thermique* **4**, 629 (1965).
(11) Lodge, J. P., Baker, M. L., Pierrard, M. J., *J. Chem. Phys.* **24**, 716 (1956).
(12) Melia, T. P., *J. Appl. Chem.* **15**, 345 (1965).
(13) Parreira, H. C., Eydt, A. J., *Nature* **209**, 33 (1965).
(14) Parungo, F. P., Lodge, J. P., *J. Atm. Sciences* **22**, 309 (1965).
(15) Shapiro, J., *Science* **133**, 2063 (1961).
(16) Smith, G. H., Tasker, M. P., *Anal. Chim. Acta.* **33**, 559 (1965).
(17) Uhlmann, D. R., Chalmers, B., Jackson, K. A., *J. Appl. Phys.* **35**, 2986 (1964).
(18) Workman, E. J., Reynolds, S. E., *Phys. Rev.* **78**, 254 (1950).

RECEIVED May 29, 1967.

9

New Automated Microanalyses for Total Inorganic Fixed Nitrogen and for Sulfate Ion in Water

A. LAZRUS, E. LORANGE, and J. P. LODGE, JR.

National Center for Atmospheric Research, Boulder, Colo.

For the past several years a network of stations throughout the United States has been collecting monthly samples of atmospheric precipitation. These samples are analyzed for trace contaminants using automated methods when possible. In the course of this work, a new colorimetric test for sulfate ion, with a 0.5 p.p.m. limit of detection, has been developed. It is fully automated and capable of testing 30 samples per hour. A new fully automated analysis for total inorganic fixed nitrogen has also been developed. This test determines directly ammonia and total inorganic fixed nitrogen. The detection limit is 10 p.p.b. of inorganic fixed nitrogen in aqueous solution.

The National Center for Atmospheric Research maintains a network of precipitation sampling stations throughout the United States. Cumulative monthly samples are sent to the laboratory for chemical analysis. By examining concentration patterns, levels, and ratios it is possible to make deductions regarding the sources, distribution, and sinks of trace chemicals in the atmosphere. The large number of analyses required and the necessity of maintaining good reproducibility over periods of years make automation of the chemistry desirable.

Total Fixed Inorganic Nitrogen Determination

For the purpose of our investigation a test indicating ammonia and total oxidized forms of inorganic nitrogen is highly useful. To satisfy this need we developed a fully automated method comprised of two steps: first, an efficient reduction of nitrite and nitrate by copper-zinc alloy to

ammonia; and second, a sensitive indo-phenol ammonia test. The latter is an automated adaptation of the method described by Tetlow and Wilson (*22*). Reduction of nitrite and nitrate by Cu–Zn alloy has been used since the 19th century (*1, 12, 20, 23*). However, reaction times varying from several hours to overnight in acidic solution are recommended in these methods. Arnd, who devoted a series of papers extending over a period of twenty years to the determination of total inorganic fixed nitrogen (*2, 3, 4, 5, 6, 7, 8, 9, 10*), found that concentrated electrolytes enhanced the reducing power of Cu–Zn alloy. However, he did not report the effect of pH on the rate of reduction in the presence of concentrated electrolyte. We have observed that Cu–Zn alloy is capable of essentially instantaneous quantitative reduction of nitrite and nitrate in the presence of high concentrations of NaCl at an apparent pH of 1.8.

The instrumentation used is part of the AutoAnalyzer system manufactured by Technicon, Inc. (*19*). The AutoAnalyzer modules required are the sampler, the proportioning pump, the colorimeter with range expander, and the recorder. The AutoAnalyzer sampler alternately delivers sample solution and cleansing water from a small reservoir. The quantity of sample is controlled by the sampling rate, adjusted by means of a cam on a clock mechanism, and by the diameter of the sample tube on the manifold of the pump.

The AutoAnalyzer pump is capable of regulated simultaneous delivery of up to 15 fluids. This is accomplished by the action of steel rollers forcing the fluids through flexible tubes of selected internal diameters.

The effluents of the pump tubes are mixed in the proper reaction sequence, and the final solution enters a tubular flowcell in the colorimeter. A single light source provides twin beams, one passing through the flowcell to a photocell, and the second to an identical reference photocell. A null balance system in the recorder continuously measures the ratio of the sample to reference voltage.

As indicated in Figure 1, the sample stream is joined by an electrolyte solution which is 4.49*N* NaCl and 0.04*N* HCl. The liquid is then segmented by air bubbles to maintain sharp concentration gradients along the stream. The solution passes through a vertical glass column 150 mm. length, 4 mm. i.d.) packed with Zn–Cu alloy produced in the following way:

Ten grams of zinc granules, 20 mesh, are etched for 1 minute with HCl (1/5) and washed thoroughly with H_2O. To the zinc is rapidly added a solution prepared by dissolving 0.25 grams of $CuCl_2 \cdot 2H_2O$ in 20 ml. of H_2O containing three drops of 1*N* HCl. The reaction mixture is shaken vigorously until the blue color just disappears. Immediately, the alloy is swirled onto a filter paper in a Büchner funnel which has been kept under suction, washed once with H_2O, once with methyl alcohol,

and then quickly air-dried. Speed is necessary in these steps for two reasons: (1) lengthy contact with moisture at this stage reduces the potency of the reducing agent, and (2) prolonged contact with volatile solvents such as acetone or alcohol used to accelerate the drying process causes flaking off of copper particles.

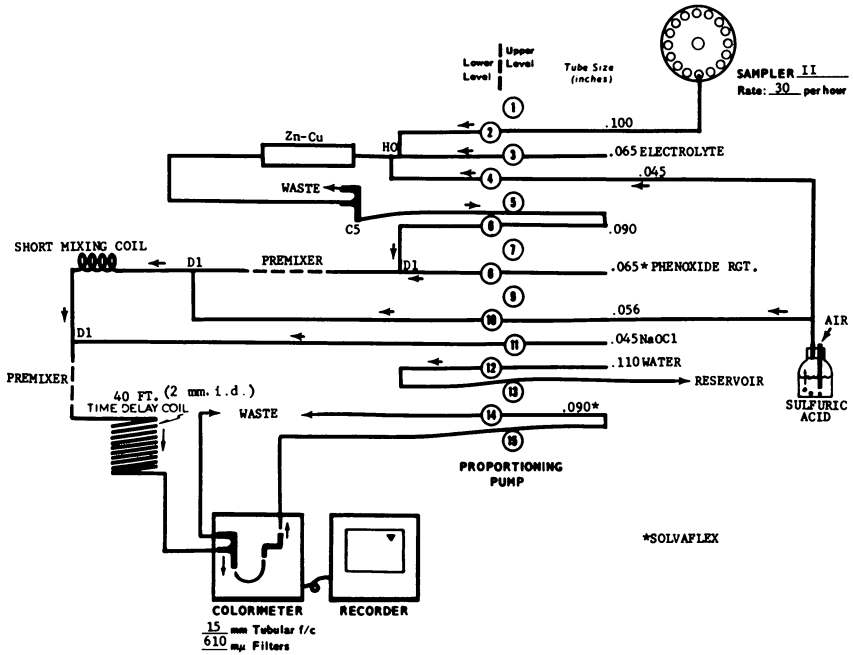

Figure 1. Flow diagram of the total inorganic fixed nitrogen test

The sample stream is debubbled and mixed with sodium phenoxide reagent, prepared by adding 135 ml. of 5*N* sodium hydroxide to 62.5 grams of phenol in a 250 ml. beaker. When the phenol is dissolved, it is transferred to a 500 ml. volumetric flask. Fifty milliliters of 6% ethylenediaminetetraacetic acid (12.0 grams of EDTA dissolved in 65 ml. of 5*N* NaOH and diluted to 200 ml. with H_2O) and 15 ml. of acetone are added. The solution is brought to volume with H_2O. After again segmenting the stream with air and mixing, a sodium hypochlorite solution containing 1% (w/v) available chlorine (*11*) is introduced. A reaction period is allowed before the color intensity is measured, at 610 mμ.

Bypassing the reduction column permits determination of ammonium ion only.

The detection limit of the test is 10 p.p.b. nitrogen with recorder range expansion. The calibration curves deviate from the Beer-Lambert

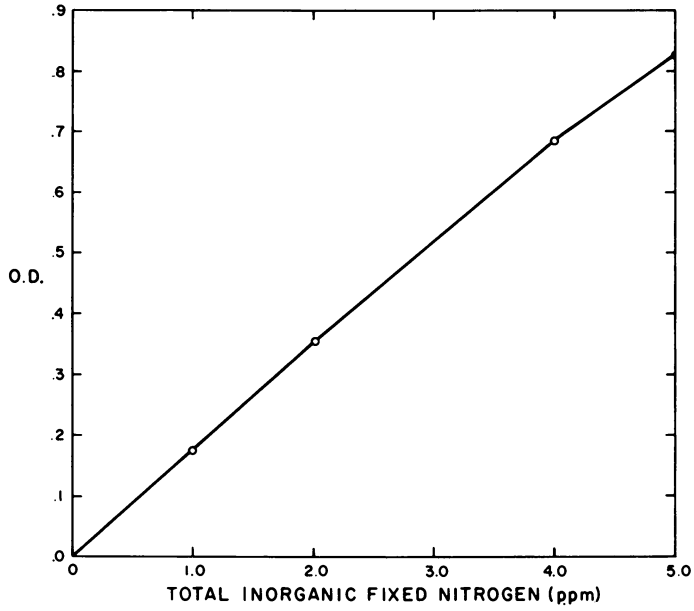

Figure 2. Typical total inorganic fixed nitrogen calibration curve

law, being slightly convex (Figure 2). The precision obtained at various concentrations is indicated in Table I.

Table I. Nitrogen Test Reproducibility and Accuracy

Nitrogen Taken	*Run*						*Mean Nitrogen*
(p.p.m.)	*1*	*2*	*3*	*4*	*5*	*6*	*Found (p.p.m.)*
5.00	4.96	5.00	5.00	5.07	5.03	4.93	5.00[a]
4.00	3.98	4.02	4.03	3.99	4.02	3.97	4.00[a]
2.00	2.02	2.03	1.97	1.98	1.98	1.97	1.99[a]
1.00	0.96	0.98	0.99	1.00	1.01	0.99	0.99[a]
0.500	0.488	0.494	0.508	0.494	0.510	0.507	0.500[b]
0.250	0.247	0.248	0.250	0.240	0.248	0.254	0.248[b]
0.100	0.100	0.102	0.101	0.095	0.099	0.103	0.100[b]
0.050	0.047	0.050	0.053	0.057	0.047	0.055	0.052[b]

[a] With no recorder range expansion.
[b] With recorder range expanded ×4.

The system is calibrated once for each revolution of the sampler turntable, which accommodates 40 sample cups.

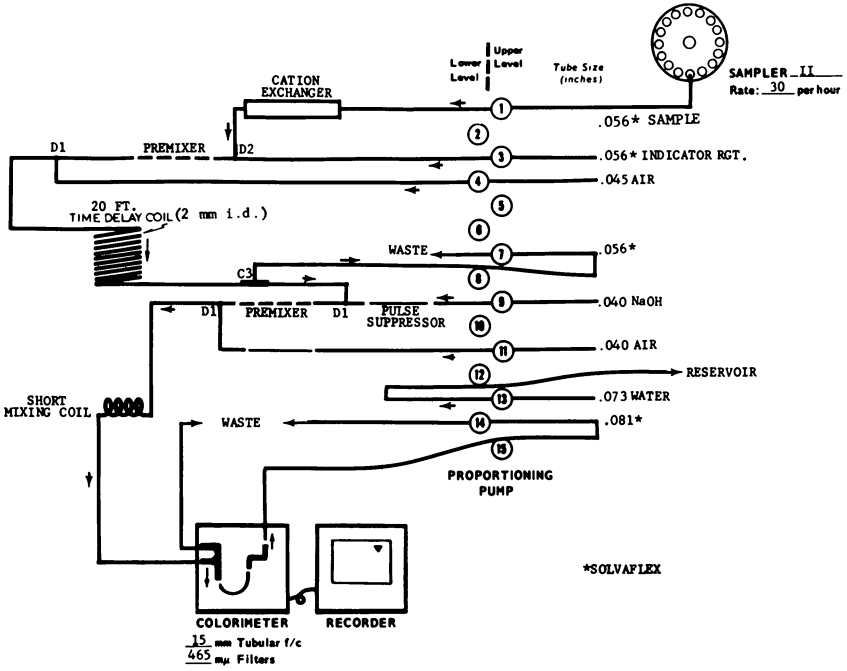

Figure 3. Flow diagram of the colorimetric sulfate ion test

The colorimetric responses to equivalent amounts of nitrogen as ammonia, nitrite ion, nitrate ion, and hydroxylamine are identical within experimental error. Diethylamine, ethylamine, alanine, and acetamide, each present at a concentration of 0.50 p.p.m. nitrogen, yield null response. Phosphate at a concentration of 0.50 p.p.m. phosphorus does not interfere in the determination of 1.0-p.p.m. nitrogen. There is no interference by Cu^{2+}, Zn^{2+}, Cd^{2+}, Ni^{2+}, Fe^{2+}, Pb^{2+}, or Ca^{2+}, each at a concentration of 10 p.p.m, in the determination of 1.0 p.p.m. nitrogen.

Sulfate Ion Determination

This test is based upon formation of barium sulfate in the presence of excess barium, followed by chelation of the remaining barium with methylthymol blue, a metallochrome indicator recently developed for complexometric titrations (*13, 14, 15, 16, 17*). The reagent is a solution containing equimolar amounts of barium chloride and methylthymol blue at a concentration equivalent to the largest amount of sulfate ion anticipated in the test solution (*18*).

The concentration range of the test is 0.5 p.p.m. to 50.0 p.p.m., but the upper limit may be extended by arranging the pump manifold to dilute the sample appropriately. The reagent routinely used in our laboratory has an upper limit of 30.0 p.p.m. sulfate, although other limits may be achieved by adjusting the amount of dye and barium in the solution. The methylthymol blue used was Eastman No. 8068. Twenty-five milliliters of solution of 1.5258 grams of barium chloride dihydrate dissolved in sufficient water to make one liter are added to 0.1182 grams of methylthymol blue in a 500 ml. volumetric flask. To this is added 4 ml. of 1*N* hydrochloric acid, which changes the color to bright orange. After adding 71 ml. of water, the solution is made up to 500 ml. with undenatured 95% ethanol. The apparent pH of the solution toward a glass electrode is 2.6.

The flow diagram for the sulfate determination is depicted in Figure 3. The sample stream is first passed through a glass column (170 mm. long, 2 mm. i.d.) containing an indicating cationic exchange resin to remove interfering cations. A suitable resin is Dowex HCR, Hydrogen Form, Dyed Resin (Nalco Chemical Co.). The indicator reagent now joins the sample stream, and a time-delay coil (20 ft. long, 2 mm. i.d.) is inserted in the system to allow complete formation of barium sulfate.

At this stage the solvent is 40% ethanol, the pH is acidic, and the color is light orange. Complexation of barium by methylthymol blue is not a rapidly reversible process (*21*); indeed sulfate ion will not readily remove barium from its methylthymol blue complex in basic solution. To avoid this problem the reagent is initially acidic, allowing only negligible chelation of the barium until the precipitation of the barium sulfate is completed.

Subsequent addition of 0.1*N* sodium hydroxide to an apparent pH of 12.8 causes methylthymol blue to become either blue in the presence of barium, or grey in its uncomplexed form. The maximum absorption of the uncomplexed form is at 465 mμ, and the reaction stream is conducted through the colorimeter equipped with filters transmitting at this wavelength. Since the indicator reagent is initially equimolar in barium ion and methylthymol blue, the amount of uncomplexed indicator remaining is directly related to the concentration of sulfate ion in the original sample.

The premixers indicated in the flow diagrams were constructed by sleeving the ends of 0.5 inch lengths of No. 22 Teflon spaghetti with No. 19 Teflon spaghetti. The sleeved ends were fitted into 0.5 inch lengths of 0.056 inch i.d. Solvaflex tubing. The end effect is to have 0.25 inch sections of 0.056 inch i.d. alternating with 0.5 inch lengths of 0.028 inch i.d. tubing.

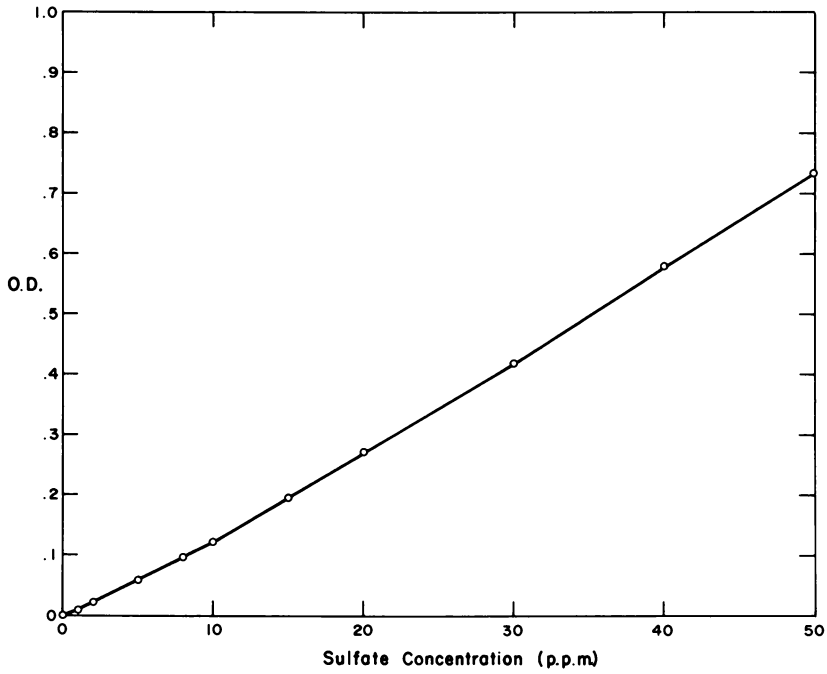

Figure 4. Typical sulfate ion calibration curve

A typical calibration curve is shown in Figure 4. The plot does not follow the Beer-Lambert law, but is slightly concave. Typical data are shown in Table II.

Table II. Accuracy and Reproducibility of Sulfate Test

Sulfate Taken	*Run*						*Mean Sulfate*
(p.p.m.)	*1*	*2*	*3*	*4*	*5*	*6*	*Found (p.p.m.)*
30.0	29.5	29.5	29.5	30.4	30.4	30.8	30.0
20.0	19.3	19.9	19.8	19.7	20.4	20.8	20.0
10.0	10.0	9.80	9.80	9.85	10.1	10.1	9.94
5.00	5.10	4.80	4.80	4.95	4.95	5.10	4.95
1.00	1.00	1.00	1.00	1.10	0.95	1.10	1.02

Concentrations of up to 50 p.p.m. carbonate ion did not interfere with determination of 10 p.p.m of sulfate ion.

The system is calibrated with each revolution of the sampler turntable.

Because the reagent tube is gradually affected by the 80% ethanolic solvent, it is necessary to replace it every one or two days. The method

also requires a rather long warm-up time, two or three hours, with the proportioning pump operating.

The indicator solution, when alkaline, oxidizes on exposure to the air. Efforts to inhibit this process have so far been unsuccessful, so that the method is limited to the automated system.

Literature Cited

(1) Allport, N. L., Brocksopp, J. E., "Colorimetric Analysis," Vol. 2, p. 228, Chapman and Hall, Ltd., London, 1963.
(2) Arnd, T., *Chem. Ztg.* **45**, 537 (1921).
(3) Arnd, T., *Angew Chem.* **30(I)**, 169 (1917).
(4) *Ibid.*, **33(I)**, 296 (1920).
(5) *Ibid.*, **45**, 22 (1932).
(6) *Ibid.*, **45**, 745 (1932).
(7) Arnd, T., *J. Chem. Soc.* **112 (II)**, 504 (1917).
(8) Arnd, T., Segerberg, H., *Angew Chem.* **49**, 166 (1936).
(9) *Ibid.*, **50**, 105 (1937).
(10) Arnd, T., Segerberg, H., *Bodenkunde u. Pflanzenernahrung* **6**, 195 (1937).
(11) Furman, N. H., ed., "Scott's Standard Methods of Chemical Analysis," Vol. 1, 6th ed., p. 340, D. Van Nostrand Co., Inc., Princeton, N. J., 1962.
(12) Gladstone, J., Tribe, A., *J. Chem. Soc.* **33**, 139 (1878).
(13) Körbl, J., Přibil, R., *Chem. Listy* **51**, 302 (1957).
(14) *Ibid.*, **51**, 1061 (1957).
(15) *Ibid.*, **51**, 1304 (1957).
(16) *Ibid.*, **51**, 1680 (1957).
(17) Körbl, J., Přibil, R., *Chem. & Ind.* **1957**, 233.
(18) Lazrus, A., Hill, K., Lodge, J., "Automation in Analytical Chemistry, Technicon Symposia 1965," p. 291, Mediad, Inc., New York, 1965.
(19) Lingemen, R., Musser, A., "Standard Methods of Chemical Analysis," F. J. Welcher, ed., Vol. 3, Part B, 6th ed., p. 975, D. Van Nostrand Co., Inc., Princeton, N. J., 1966.
(20) Navrone, R., *J. Am. Water Works Assoc.* **56**, 781 (1964).
(21) Přibil, R., *Talanta* **3**, 91 (1959).
(22) Tetlow, J., Wilson, A., *Analyst* **89**, 453 (1964).
(23) Williams, M., *J. Chem. Soc.* **39**, 100 (1881).

RECEIVED April 24, 1967. The National Center for Atmospheric Research is operated by the University Corporation for Atmospheric Research with sponsorship of the National Science Foundation.

10

Polarographic Methods in Determination of Trace Inorganics in Water

E. JUNE MAIENTHAL and JOHN K. TAYLOR

Institute for Materials Research, Division of Analytical Chemistry, National Bureau of Standards, Washington, D. C.

Polarography is a particularly suitable method for the determination of trace inorganic material in water. Owing to the selectivity of electrode processes, interferences and hence prior chemical separations are minimized. Often several elements may be determined concurrently in the same supporting electrolyte. Anodic stripping and linear sweep voltammetry give an increased sensitivity which permits determinations in the p.p.b. range to be made. Polarographic methodology is reviewed. A survey of the literature concerned with determination of trace inorganic material in water is given. Procedures used in this laboratory for the determination of such elements as aluminum, arsenic, cadmium, copper, indium, iodine, iron, lead, tellurium, and zinc are discussed. The matrices include laboratory distilled water, river water, and reactor cooling water. In addition a comparative technique is described whereby precisions of better than 1% can be obtained at the 0.1 p.p.m. level.

Polarographic techniques are highly applicable to trace analysis and are particularly useful for the determination of inorganic constituents of water. Not only is the sensitivity of polarography competitive with other techniques, but its selectivity permits the determination of many constituents without prior chemical separations. Moreover, the range of concentrations which can be determined makes possible the analysis of all types of water ranging from highly contaminated industrial effluents and mineral springs to water of the highest purity prepared for laboratory use by distillation or ion exchange.

In principle, any ion which can be oxidized or reduced or which will form a stable complex or slightly soluble salt with mercury can be determined polarographically. A survey of the literature indicates that the polarographic behavior of some 80 elements has been described and analytical determinations of most of these have been accomplished. Accordingly, polarography should be useful for determining most of the cations and indeed a number of anions of interest to water analysts.

The present paper reviews the polarographic techniques which are presently in use including some of the more important applications of water analysis described in the literature. In addition, some work in the authors' laboratory related to water analysis is presented.

Survey of Applications

The general principles of polarography have been described in a number of publications. The technique has been reviewed particularly with respect to its application to trace analysis by the present authors (*52*). Table I presents a summary of some of the important publications concerned with polarographic analysis of water. Some of these will be discussed according to the technique used in the analysis.

Conventional Polarography. Conventional polarography using a dropping mercury electrode achieves sensitivities in the vicinity of $10^{-5}M$ in concentration. Water has the advantage of being an almost ideal matrix, permitting preconcentration by evaporation to an extent that is limited in practice by the amount of sample available. In many cases, the dissolved salts may serve as the sample's own supporting electrolyte. Preconcentration, if necessary, may also be done by solvent extraction or by co-precipitation using a suitable carrier.

Some of the earliest work utilizing polarography for water analysis was done by Heller and co-workers in 1935 (*19*). They determined as little as 0.01 mg./liter of copper, bismuth, lead cadmium, and zinc polarographically after extraction with dithizone and carbon tetrachloride. This work also described conditions of extraction for minimizing interferences in certain cases.

An interesting method, though limited in scope, for improving the sensitivity of conventional polarography makes use of catalytic effect of a desired ion on some component of the solution. Thus the catalytic effect of uranyl ions on nitrate reduction was used by Korkisch and coworkers (*30*); however, this method is subject to many interferences.

Pulse Polarography. The development of pulse polarography by Barker and co-workers (*7, 8*) has extended the sensitivity of determination of many ions to the $10^{-7}M$, and in some cases, to the $10^{-8}M$ level. This

technique uses a dropping mercury electrode and consists in the application of small voltage pulses applied on either a constant or gradually increasing background voltage. The latter case, which gives rise to the greater sensitivity, produces derivative type polarograms. Since the charging current in both cases is permitted to decay before the measurement of the faradaic current, the sensitivity is greater than that of conventional polarography. Several commercial instruments are available.

Table I. Polarographic Methods of Water Analysis

Element or Group	*Matrix*	*Technique*[a]	*Sample Size*	*Range of Sensitivity*	*Ref.*
Ca,Mg, Na + K	Drinking and industrial water	Streaming Hg electrode		10^{-3}-$10^{-4}M$	*45, 46*
Na,Li	Natural waters			10^{-3}-10^{-5} grams	*49*
Al	Sea water				*23*
Al,Zn,Sn	Water		25-50 ml.	50 p.p.m.	*22*
Al,Pb,Fe, Er,Ga,In, Co,Ni,V, Bi,Zn,Zr (total)	Reactor water	CRP	100 ml.	1 p.p.b.	*42, 43*
As	Mineral waters		50 ml.		*41*
Cu	Dead Sea brine	ASP		10^{-6}-$10^{-7}M$	*4*
Cu,Zn,Mn, Cl,Pb,O	Sea water	CRP		0.05 μg./ml.	*56*
Cu,Zn	Industrial effluent waters			5 μg.	*14*
Cu	Hot springs			2-163 mg./liter	*34*
Cu,Pb,Cd	Water	Hanging drop		10^{-7}%	*31*
Cu,Bi,Pb, Cd,Zn	Mineral waters	DME		0.01 mg./liter	*19*
Cu,Ni,Co	Mineral waters	DME	1 liter	3-0.0063 μg./ml.	*10, 11*
Cu,Zn,Co	Mineral waters		0.5-1 liter	5-128 μg./ml.	*54*
Cu,Bi,Pb Cd,Zn	Natural waters			10^{-6}-10^{-8} grams	*48*
Cu,Cd,Zn	Water			review paper	*6*
I,Br,S	Petroleum water			0.1 mg./liter	*20*
Cl,Br,I	Natural waters	CSP		10^{-5}-$10^{-6}M$	*28*
Br,I	Mineral waters			10^{-5} grams/liter	*5*
Br	Mineral waters		50-200 ml.	100 μg.	*25*
F	Natural waters	Amp.		>0.001 mg./ml.	*29*
I	Water			0.5 μg.	*18*
I	Water				*24*

Table I. (Continued)

Pb	Hot springs, sea water, tap water		250 ml. 0.5-1 liter	3.6-62.5 μg./liter	*33*
Pb,Zn	Natural waters			0.01-0.02 mg./liter	*44*
Pb,Cd,Sn Zn	Water from PVC pipes			0.005-0.015 mg./liter	*55*
CN	Water	CRP	5 ml.	0.05 p.p.m.	*21*
NO_3	Well water			0.02-25 p.p.m.	*47*
NO_3	Water			0.2 mg./liter	*16*
NO_3	Water			review	*15*
O	Water	DME	1 ml.	0-15 p.p.m.	*9*
O	Water				*12, 37*
O	Sea water	DME or Pt micro-electrode		0.02 ml./liter	*17*
O	River water			0.1-13 p.p.m.	*50*
O	Water			1-20%	*51*
Se	Water		100-500 ml.	0.5-10 μg./ml.	*13*
SO_4	Water			$10^{-3}M$	*40*
U	Radioactive waste streams	DME		10^{-2}-$10^{-4}M$	*1*
U	Water			10^{-5}-$10^{-8}M$	*2*
U	Sea water	Pulse		3 μg./liter	*38, 57*
Zn	Sea water	ASP		1 μg./liter	*35*
Zn	Dead Sea brine	ASP	50 ml.	$5.7 \times 10^{-7}M$	*3*
Zn	Sea water and hot springs water			136 μg./ml.	*32*

[a] ASP, anodic stripping polarography; CRP, cathode-ray polarography; DME, dropping mercury electrode; CSP, cathodic stripping polarography; Amp., amperometric end point.

This technique has been used by Milner, Wilson, and co-workers (*38, 57*) to determine the uranium content of samples from the Bay of Biscay and from the English Channel. The first reference involves extraction of the uranium with chloroform and 8-hydroxyquinoline while the second included extraction with carbon tetrachloride and di-(2-ethylhexyl) phosphoric acid.

Cathode-ray Polarography. Cathode-ray polarography involves measurement of a current-voltage curve resulting from the application of a rapid potential sweep during a portion of the life of a single mercury drop. The resultant peaked wave displayed on a cathode-ray tube is ordinarily about $4n^{1/2}$, where n is the electron change, greater than the conventional diffusion current. Sensitivities greater than $10^{-7}M$ can often be obtained. Moreover, the peaked wave form allows better resolution of

closely occurring reductions. Peaks differing by 100 m.v. may be resolved by use of the normal mode of operation while the derivative current measurement increases the resolution to 40 m.v.

Cathode-ray polarography has found considerable use in water analysis. Four commercial models are available. Southern Analytical Ltd., manufacturer of one of the commercial instruments, has prepared a series of bulletins describing the determination of some 30 anions or cations in water or related materials.

Hetman (*21*) has used this type of instrument for the determination of cyanide ions in water. By the use of an anodic voltage sweep he was able to determine as little as 0.05 μg./ml. of cyanide in a sodium hydroxide supporting electrolyte. Whitnack (*56*) has used this technique to determine copper, lead, zinc, and manganese at the 0.05 μg./ml. level in sea water. He also used it for continuous monitoring of chloride and dissolved oxygen.

Pohl has used cathode-ray polarography to determine group impurities in the parts-per-billion range in reactor water (*42, 43*). In this interesting application, he adds an excess of EDTA to form complexes with the metal ions in the water. A known excess of cadmium ion is then added which complexes with the remaining EDTA, yet does not disturb the more stable complexes of the metals of interest. The excess cadmium is then determined polarographically from which the total metal content is calculated. He suggests that the total aluminum, lead, iron, erbium, gallium, indium, cobalt, nickel, vanadium, bismuth, zinc, and zirconium may be determined in this manner.

Anodic Stripping Polarography. This technique involves plating with a cathodic electrode at a fixed potential for a given period of time, then applying a potential scan in the anodic direction. The enhanced peak current resulting from oxidation of the metal concentrated at the electrode surface is then measured. Because of the preconcentration feature, sensitivities greater than $10^{-9}M$ can be achieved. Solid and hanging drop electrodes and also mercury-film electrodes have been used. Kemula and Kublik (*26, 27*) and also Nikelly and Cooke (*39*), pioneered in utilizing this technique for trace analysis. Kublik (*31*) has described the determinations of copper, cadmium, and lead at the 10^{-7} % level in water by use of anodic stripping from a hanging mercury drop. Ariel and co-workers (*3, 4*) have determined copper and zinc in Dead Sea water in which their concentrations were in the $10^{-8}M$ range.

Combination Techniques. A combination of two techniques—cathode-ray and anodic stripping voltammetry—would appear to offer excellent sensitivity. The current enhancement resulting from the combination of pre-concentration at the electrode and a subsequent very rapid anodic voltage scan would seem to be greater than that achieved by either

technique alone. However, differential capacity effects from high scan rates cause some peak distortion and reduce the accuracy of measurement with a single cell mode of operation. Tyler (*53*), by use of a single cell instrument, a Kemula-type electrode, and ten min. plating, found a 200-fold increase in the sensitivity for the determination of lead.

Macchi (*35*) used a cathode-ray polarograph with a slow dropping mercury electrode so that it was, in effect, stationary during a 60-second plating time. He was able to determine zinc in sea water directly with a sensitivity of 1 μg./liter.

NBS Experience. Both anodic stripping and cathode-ray polarography have been used in the authors' laboratory for water analyses of interest to several programs and methods used will be described briefly. In general, the sensitivities required for a particular analytical problem have not been at the limit of detection of the technique. Accordingly, suitable modification would extend the range of utility in most instances.

Determinations of copper and zinc in river water were made at intervals to determine its suitability for use, after appropriate treatment, for the proposed National Aquarium. One hundred-, and in a few cases, 500-ml. samples were filtered, evaporated with a small amount of perchloric acid to destroy organic matter, and made up to a volume of 5 or 10 ml. in a supporting electrolyte of ammonium chloride and ammonium hydroxide. Copper and zinc were then determined concurrently with a cathode-ray polarograph using the single cell mode of operation at about −0.4 and −1.2 volts *vs.* a mercury pool anode, respectively. Over a period of about a year, the copper content varied, with time and also at different sampling locations, from about 20 to 90 p.p.b., while the zinc content varied from about 3 to 60 p.p.b. Typical sets of results are shown in Table II.

Table II. Copper and Zinc in Aquarium Water[a]

	Station 2	*Station 4*	*Station 6*
p.p.b. Cu	43 ± 3	48 ± 1	40 ± 2
p.p.b. Zn	12 ± 0.5	9 ± 1	8 ± 2

[a] For comparison, zinc and copper are generally present in sea water in the 5-10 p.p.b. range.

Cathode-ray polarography has been very useful in a number of analyses of water used in reactor circulating systems. To determine the extent of contamination from some aluminum and steel containers, aluminum and iron were determined on 25 ml. samples of water after evaporation and ignition to determine the weight of the residue. The residues, weighing about 3 mg. each, were qualitatively identified as chlorides. The residues were dissolved in 5*M* $HClO_4$ and sodium acetate to obtain a pH of

about 4.5. Solochrome Violet RS was added, the solutions were diluted to 50 ml. and heated to form the metal-dye complexes. Aluminum and iron were then determined concurrently on the cathode-ray polarograph at −0.7 and −0.8 volts respectively. The results are given in Table III.

Table III. Analysis of Reactor Coolant Water

	p.p.m.	
Sample Designation	*Al*	*Fe*
Demineralized H_2O	0.02	<0.1
Helium return from reactor	0.17	<0.1
Helium system suction of circulators	0.15	<0.1

Copper was determined in the cooling water of a linear accelerator (Linac) as part of an attempt to determine the cause of a brown sludge appearing on a plastic sight tower. In this case, organic material was destroyed by fuming with perchloric acid after which copper was measured in a pyridine-pyridinium perchlorate supporting electrolyte at about −0.5 volts. The results are shown in Table IV.

Table IV. Copper in Linac Water

Sample Designation	*p.p.m.*
MS, 16 June '65	0.22
W.G. Station 6	0.03
60° water, 18 Dec. '64	0.18
W.G. Station 5, 1 July '65	0.02
60° water, 1 July '65	0.16

Polarography is highly useful in the determination of the bromide and iodide content of saline water. The anions are oxidized to bromate and iodate, respectively, prior to polarographic determination. Chlorate is not polarographically reducible, hence chlorides do not interfere in the determination. A number of saline waters have been so analyzed.

By utilizing a double-cell comparative mode of operation, cathode-ray polarography can give a higher degree of precision and accuracy than is usually found in trace analysis. This is illustrated by determining trace amounts of iodide in animal-feed water used in a medical research program. Sufficient sample was taken to permit a ten-fold concentration by evaporation in preparing the final solution. The method consisted in adjusting the pH to a value of 3.0 and oxidation of the iodide to iodate by bromine water. The polarographic peak is measured at −1.2

volts in a supporting electrolyte 0.1*M* in sodium carbonate and potassium chloride. Comparison is made with an iodide solution of known concentration which is handled in the same manner. The precision obtainable is illustrated by the results for two independent determinations on two different solutions, supposedly containing the same amount of iodide, shown in Table V.

Table V. Iodide in Animal Feed Water

Solution A, p.p.m.	*Solution B, p.p.m.*
0.1423	0.1444
0.1451	0.1451

Cathode-ray polarography has been used to monitor the quality of the house-supply of distilled water available in the NBS Chemistry Building. In each case, the element that was determined depended on the trace determinations being made in one of the laboratories at that time and would constitute a blank correction. In general, water samples were concentrated 10 to 100-fold and measurements were made in 0.1*N* hydrochloric acid, which permitted simultaneous determination of the elements noted.

Table VI. Analysis of Distilled Water

	p.p.b.			
Sampled	*Cu*	*Pb*	*Zn*	*Cd*
5-9-66	4.0	8.0	5.0	—
5-10-66	3.0	—	5.0	—
6-7-66	—	0.6	—	—
7-14-66	—	1.0	—	—
12-19-66	0.5	0.6	—	<0.02

To check possible contamination in various steps of a food processing procedure under development in another government laboratory, it was necessary to analyze distilled water for lead. Polarographic measurements were made in a supporting electrolyte of 1*N* hydrochloric acid after a 20-fold concentration of the water by evaporation. The original distilled water used was found to contain 10 p.p.b. of lead. Rinsings from a blender used in this process showed the lead concentration increased to a value of 20 p.p.b. which was considered within acceptable limits.

In addition to these actual water samples, many dilute aqueous solutions have been run in this laboratory. The procedures used here would be directly applicable in most cases to water analysis.

The arsenic content of an ammonium dihydrogen phosphate solution was determined after adding sulfuric acid, reducing with hydrazine sulfate, and adjusting the volume to give a solution 1*N* in sulfuric acid. The sensitivity under these conditions was about 0.01 p.p.m. in the final solution.

A method developed in this laboratory for determining tellurium (*36*) in brasses and cast irons has been also applicable to ultratrace determinations in almost any matrix. The sensitivity in the final solution (1.5*M* phosphoric acid) by using the subtractive mode of operation of the cathode-ray polarograph is several p.p.b.

Indium and cadmium were found to have sensitivities in the 0.01 p.p.m. range by the subtractive mode of operation. Determinations in this range and lower, however, may be more readily done by anodic stripping. In this laboratory a fast scan polarograph and a Kemula-type electrode have been used for this purpose. This electrode uses a mercury drop whose size is controlled by a micrometer type syringe. For most of the work done here a drop of 0.5 mm. in diameter or less was used. Copper, cadmium and lead have been determined in 1*N* hydrochloric acid supporting electrolyte. Using a 5-minute pre-electrolysis time, the sensitivity was in the 1 p.p.b. range for lead and cadmium, and slightly higher for copper. This sensitivity could be increased if necessary by increasing the electrode area and the time of electrolysis.

A major limitation in the sensitivity of most analytical techniques is the blank which comes from reagents, atmospheric, and container contamination. It was recently necessary, in connection with the analysis of 99.9999% zinc, to use acid of greater purity than was commercially available. The copper, cadmium and lead content of some hydrochloric acid distilled by the NBS Separation and Purification Section was monitored in this laboratory by using anodic stripping. The results are shown in Table VII.

Table VII. Analysis of Hydrochloric Acid by Anodic Stripping

		p.p.b.		
Element	*Unpurified*	*Fraction 1*	*Fraction 2*	*Fraction 3*
Cd	3	—	—	—
Pb	13	2	7	3
Cu	21	16	11	4

Polarographic techniques have been shown to provide rapid, sensitive, and reliable analyses of water and related materials. Instrumental sensitivity is available for sub-p.p.b. level determinations provided the blank can be kept to a minimum. At present, few reagents of sufficient purity are commercially available. It is then the analyst's burden further to purify the reagents for his particular purpose, or to develop analytical procedures whereby the addition of reagents is kept below the interference level. Improvement is to be expected in both directions so that polarography can provide ultra-trace analyses even beyond its present capacity.

Literature Cited

(1) Alkire, G. J., Koyama, K., Hahn, K. J., Michelson, C. E., *Anal. Chem.* **30**, 1912 (1958).
(2) Antal, P., *Mikrochim. Acta* **2**, 235 (1961).
(3) Ariel, M., Eisner, U., *J. Electroanal. Chem.* **5**, 362 (1963).
(4) Ariel, M., Eisner, U., Gottesfield, S., *J. Electroanal. Chem.* **7**, 307 (1964).
(5) Bakhman, V. I., *Gidrokhim. Materialy* **18**, 59 (1950).
(6) Ballinger, D. C., Hartlage, T. A., *Water Sewage Works* **110**, 31 (1963).
(7) Barker, G. C., Gardner, A. W., *Z. Anal. Chem.* **173**, 79 (1960).
(8) Barker, G. C., Jenkins, I. L., *Analyst* **77**, 685 (1952).
(9) Briggs, R., Dyke, G. V., Knowles, G., *Analyst* **83**, 304 (1958).
(10) Canals, E., Marignan, R., Cordier, S., *Trav. Soc. Pharm. Montpellier* **8**, 57 (1948).
(11) *Ibid.* **9**, 55 (1949).
(12) Carritt, D. E., Kanwisher, J. W., *Anal. Chem.* **31**, 5 (1959).
(13) Cervenka A., Korbova, M., *Chem. Listy* **49**, 1158 (1955).
(14) Chizhevskaya, M. S., *Sb. Nauch. Rabot, Molotov Med. Inst., Molotov* **79** (1955).
(15) de Salas, M., *Rev. Obras Sanit. Nacion (Buenos Aires)* **15**, 23 (1951).
(16) Frazier, R. E., *J. Am. Water Works Assoc.* **55**, 624 (1963).
(17) Giguere, P. A., Lauzier, Louis, *Can. J. Res.* **23B**, 76 (1945).
(18) Godfrey, P. R., Parker, H. E., Quackenbush, F. W., *Anal. Chem.* **23**, 1850 (1951).
(19) Heller, K., Kuhla, G., Machek, F., *Mikrochemie* **18**, 193 (1935).
(20) Hemala, N., Marek, J., Valcikova, Z., *Sb. Pracivyzkumn. Ust. E* 111 (1955).
(21) Hetman, J., *J. Applied Chem.* **10**, 16 (1960).
(22) Hodgson, H. W., Glover, J. R., *Analyst* **76**, 706 (1951).
(23) Ishibashi, M., Fujinaga, T., *Sb. Mezinarod. Polarog. Sjezdu, Praze, 1st Congr.* **Pt. I**, 106 (1951).
(24) Jazemskaja, V. Ya., Stukovskaja, L. A., *Gigenia i Sanit.* **27**, 52 (1962).
(25) Kekedy, L., Manok, F., Albu, I., *Stud. Cercet. Chim., Cluj* **7**, 61 (1956).
(26) Kemula, W., Kublik, Z., *Anal. Chim. Acta* **18**, 104 (1958).
(27) Kemula, W., Kublik, Z., *Chem. Anal., Warsaw* **3**, 483 (1959).
(28) Kemula, W., Kublik, Z., Laraszewski, J., *Chemia Anal. (Warsaw)* **8**, 171 (1963).
(29) Kemula, W., Michalski, M., Zdrodowski, Z., *Prace Glownego Inst. Chem. Przemyslowej* **2**, 5 (1951).
(30) Korkisch, J., Thiard, A., Hecht, F., *Mikrochim. Acta* **9**, 1422 (1956).
(31) Kublik, Z., *Acta Chim. Acad. Sci. Hung.* **27**, 79 (1961).

(32) Kuroda, K., *Bull. Chem. Soc. Japan* **15**, 88 (1940).
(33) *Ibid.* **15**, 153 (1940).
(34) *Ibid.* **16**, 69 (1941).
(35) Macchi, G., *J. Electroanal. Chem.* **9**, 290 (1965).
(36) Maienthal, E. J., Taylor, J. K., *Anal. Chem.* **37**, 1516 (1965).
(37) Meyling, A. H., Frank, G. H., *Analyst* **87**, 684 (1962).
(38) Milner, G. W. C., Wilson, J. D., Barnett, G. A., Smales, A. A., *J. Electroanal. Chem.* **2**, 25 (1961).
(39) Nikelly, J. G., Cooke, W. D., *Anal. Chem.* **29**, 233, (1957).
(40) Ohlweiler, O. A., *Anal. Chim. Acta* **11**, 590 (1954).
(41) Olivier, H. R., *Bull. Soc. Chim. Biol.* **36**, 695 (1954).
(42) Pohl, F. A., *Mikrochim. Ichnoanal. Acta* **5-6**, 855 (1963).
(43) Pohl, F. A., *Z. Anal. Chem.* **197**, 193 (1963).
(44) Popova, T. P., *Sb. Nauch. Tekhn. Inform. Min. Geol. i Okhrany Nedr.* **129** (1955).
(45) Proszt, J., Gyorbiro, K., *Anal. Chim. Acta* **15**, 585 (1956).
(46) Proszt, J., Gyorbiro, K., *Chem. Anal., Warsaw* **1**, 21 (1956).
(47) Rand, M. C., Heukelekian, H., *Anal. Chem.* **25**, 878 (1953).
(48) Reznikov, A. A., *Trudy Vsesoyuz. Konferentsii Anal. Khim.* **2**, 573 (1943).
(49) Reznikov, A. A., Starik-Smagina, A. S., *Trudy Vsesoyuz. Konferentsii Anal. Khim.* **2**, 559 (1943).
(50) Seaman, W., Allen, W., *Sewage Ind. Wastes* **22**, 912 (1950).
(51) Takahashi, T., Sakurai, H., Sakamoto, T., *Japan Analyst* **13**, 627 (1964).
(52) Taylor, J. K., Maienthal, E. J., Marinenko, G., "Electrochemical Methods, Trace Analysis," G. Morrison, ed., Interscience, N. Y., 1965.
(53) Tyler, J. F. C., *Analyst* **89**, 775 (1964).
(54) Virf, L., Makai, V., *Stud. Univ. Babes-Bolyai, Cluj. Chim.* **8**, 221 (1963).
(55) Visintin, B., Monteriolo, S., Giuseppi, S. A., *Ann. Idrol.* **1**, 212 (1963).
(56) Whitnack, G. C., *J. Electroanal. Chem.* **2**, 110 (1961).
(57) Wilson, J. D., Webster, R. K., Milner, G. W. C., Barnett, G. A., Smales, A. A., *Anal. Chim. Acta* **23**, 505 (1960).

RECEIVED April 24, 1967.

11

Principles and Practice of Atomic Absorption

HERBERT L. KAHN

Perkin-Elmer, Norwalk, Conn.

The atomic absorption method for determining the concentration of metallic elements has now gained wide acceptance. Instrumentation is relatively inexpensive and simple to use. Analytical interferences are less prevalent than with most other techniques; means of recognizing and combating the interferences that do exist are described. The article discusses the basic principles of atomic absorption and also describes the fundamental design and modern improvements in the major components of instrumentation: hollow-cathode lamps, burners, photometers, and monochromators. Atomic absorption is compared with some of its rival techniques, principally flame emission and atomic fluorescence. New methods of sampling and the distinction between sensitivity and detection limit are discussed briefly. Detection limits for 65 elements are tabulated.

The atomic absorption method for the determination of metallic element concentrations has made great strides since 1963, when commercial equipment capable of routine operation was first introduced. As of early 1967, it was estimated that 3,000 atomic absorption instruments were in use in North America alone.

This rapid acceptance of a new technique is attributed to a number of favorable circumstances. Equipment is moderate in cost, with installations ranging between $4,000 and $12,000. Detection limits, precision, and accuracy are at useful levels for about 65 elements in a large number of matrices. For solutions or fine suspensions, there is often little or no sample preparation. Finally, most users have relatively little to learn. An atomic absorption spectrophotometer reads out either in concentration or a close analog of it; there is no such thing as "interpretation" of results.

Many laboratories turn out useful data within days of the installation of an instrument.

Shortly after the first publication on atomic absorption in 1955 by the Australian physicist Alan Walsh (*11*), isolated researchers built the simple instrumentation required to test the technique. However, there was little interest outside Australia until commercial equipment became available, and problems involving burners and emission sources were solved. Analytically, the major advantage of atomic absorption is that it has almost no spectral and few chemical interferences with its determinations. Chemical separations are thus rarely necessary and are simple when they are required.

Instrumental Principle

The basic principle of atomic absorption can well be described as the inverse of that of emission methods for determining metallic elements. In all emission techniques (flame, arc and spark, x-ray fluorescence, and neutron activation), the sample is somehow excited to make it give off radiation of interest. At the same time, the sample cannot be prevented from giving off radiation which is not of interest. The appropriate type of filtering system is employed to select the radiation which the analyst wants; the radiation intensity is measured; and by comparison with standards, the concentration of the desired element in the sample is found.

In atomic absorption, the opposite process takes place. The element of interest in the sample is not excited, but is merely dissociated from its chemical bonds, and placed into an unexcited, un-ionized "ground" state. It is then capable of absorbing radiation at discrete lines of narrow bandwidth—*i.e.*, the same lines as would be emitted if the element were excited.

The literature describes a number of proposed ways of dissociating the elements of interest from their chemical bonds, but at present, with very few exceptions, the dissociation is always achieved by burning the sample in a flame. The design of the burner is one of the critical factors of atomic absorption instrumentation, and a great deal of effort has been devoted to it.

The narrow emission lines which are to be absorbed by the sample are generally provided by a hollow cathode lamp—*i.e.*, a source filled with neon or argon at a low pressure, which has a cathode made of the element being sought. Such a lamp emits only the spectrum of the desired element, together with that of the filler gas. The considerations affecting the design and choice of lamps will be treated later in some detail.

Figure 1 is a sketch of the atomic absorption process. In 1A, the emission spectrum of a hollow-cathode lamp is shown, with emission lines whose half-width is typically about 0.02 A. For most practical purposes, the desired element in the sample can be considered as being able to absorb only the "resonance" lines, whose wavelengths correspond to transitions from the minimum energy state to some higher level. In 1B, the sample is shown to absorb an amount "x" which corresponds to the concentration of the element of interest. As seen in Figure 1C, after the flame, the resonance line is reduced while the others are unaffected. In order to screen out the undesired emission, the radiation is now passed through a filter or monochromator (1D) which is tuned to pass the line

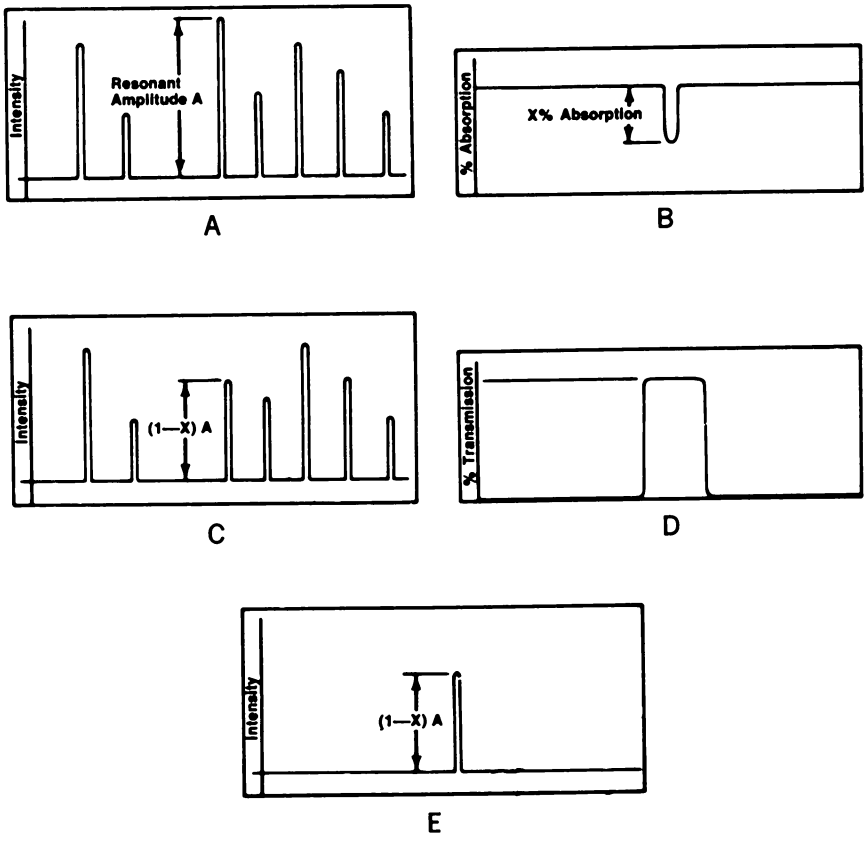

Figure 1. (A) Hollow cathode lamp emits line spectrum of element to be determined. (B) Sample absorbs energy at the resonance line. (C) Resultant spectrum after absorption by sample. (D) Monochromator isolates resonance wavelength, and rejects all others. (E) Photodetector sees only the resonance line, diminished by sample absorption

of interest but screen out the others. The photodetector (1E) then sees only the diminished resonance line.

Advantages

From the sketch of Figure 1, it is possible to deduce some of the advantages of the atomic absorption technique. First, properly designed atomic absorption equipment, correctly used, is subject to very few spectral interferences, and from an analytical viewpoint these rarely present problems.

Spectral interferences occur in emission, when the radiation from the sample is closely surrounded by radiation from other elements or molecules. The desired radiation cannot be separated from the unwanted output, and the resultant reading depends on the concentration of more than one element.

Theoretically, spectral interferences in atomic absorption can occur in three ways.

1. Absorption lines of two elements coincide within 0.05 A. Diligent searches have turned up only a few such coincidences, almost none of them with analytical significance.

2. Molecules formed in the flame can have absorption bands at the analytical wavelengths of particular elements. These molecular bands occur most often when low temperature flames or special burner systems of peculiar design are used. With Perkin-Elmer's air-acetylene burner, one such interference has been noted: when barium is determined in the presence of a large excess of calcium, calcium molecules absorb radiation at the barium wavelength. Even this interference vanishes in the higher temperatures generated by a nitrous-oxide-acetylene flame.

3. An unsought element in the sample absorbs light from the same element present by accident or improper design in the hollow-cathode lamp. This problem limits the number and type of elements that can be combined in one lamp; responsible manufacturers do not generally design lamps which may produce spectral interferences.

Atomic absorption is also relatively free from chemical interferences, largely because the requirements of sampling are much easier than in emission techniques. For atomic absorption, the element of interest need only be dissociated from its chemical bonds, but need not be excited. Many elements can be completely dissociated at readily achievable temperatures. The compounds of zinc, for example, are completely dissociated far below the temperature of an air-acetylene flame (2300°C.) while only one zinc atom in 10^9 is excited. Small differences in flame temperature or chemistry will therefore have negligible influence on zinc determinations.

In emission and other types of spectroscopy, on the other hand, the atom must be excited, and for most elements, at presently achievable energies, there is no such thing as complete excitation. One is always

on a rather steep slope in the energy-excitation curve, so that instrumental and chemical conditions have a strong bearing on the analytical result.

Furthermore, atomic absorption generally works with a larger number of atoms than do other techniques. Sodium, for instance, is one of the elements most favorably determined by flame emission; yet only 1.5% of the atoms are excited at the highest obtainable flame temperatures. Most of the remaining atoms are dissociated from their compounds and unexcited, and thus available for atomic absorption. For calcium under similar circumstances, the ratio in favor of atomic absorption is much greater. For every atom that is excited and available for flame emission, at least 1,000 are dissociated and accessible to atomic absorption.

It cannot be deduced from this ratio that atomic absorption is 1,000 times more sensitive to calcium than is flame emission (indeed, proponents of both techniques claim a better detection limit for that particular element). The reason is that it is easier to work with an excited atom than an unexcited one; the excited atom merely has to be seen, while it is necessary to hit the unexcited atom with a photon.

More important, however, is what happens if the flame conditions should change so dramatically that twice as many atoms are excited as before. Now, two atoms are available for flame emission, and 999 for atomic absorption. An event which has caused a change of 100% in the emission value has only reduced the atomic absorption result by 0.1%. It can therefore be deduced that atomic absorption is a technique from which high precision can be expected. In fact, with optimum equipment, a standard deviation of 0.2% is achievable (*7, 16*).

Analytical Possibilities

The energy required to atomize the sample can theoretically be supplied in a rather large number of ways; plasma jet, electrical discharge, laser, furnace, etc. However, with very few exceptions, present-day instrumentation always employs a flame to effect the dissociation. Mercury, which has an appreciable vapor pressure at room temperature, is often determined by merely heating the sampling cell; in fact the mercury vapor detector is the oldest form of analytical atomic absorption. Articles have been published on the determination of uranium and other elements through the use of a second, demountable hollow-cathode lamp as the sampling device. Nevertheless, nonflame sampling devices, though very promising and interesting, have not yet achieved general analytical importance and will not be discussed further in this article.

The use of a flame implies the presence of flame materials, and these, in turn, limit the usable range of atomic absorption to the region where

they do not absorb. The resonance line for arsenic at 1937A. is presently the lower limit at which atomic absorption can be carried out. The element with its resonance line at the longest wavelength is cesium at 8521A. The wavelength range for atomic absorption is thus similar to that of ultraviolet-visible spectrophotometry. It includes all metals and semi-metals, but excludes such elements as sulfur, phosphorus, the halogens, and other gases whose resonance wavelengths lie in the atmospheric-absorption region. Methods exist for the indirect determination of phosphorus, sulfur, and chlorine, by compounding them with a metal and then analyzing for the metal (*3, 10, 20*).

In the early days of atomic absorption, it was not analytically useful to use flames developing temperatures higher than that of the air-acetylene combination. (This is discussed in more detail in the section on burners.) The temperature of the air-acetylene burner is not sufficient to dissociate the compounds of refractory elements like titanium, aluminum, and vanadium, and for several years these elements were considered to be out of reach of analytical atomic absorption, though some data could be obtained by special and rather cumbersome methods.

In early 1965, the Australian chemist John Willis (*17*) showed that a burner using nitrous oxide and acetylene would develop enough energy to dissociate the compounds of many of the refractory elements. The temperature of the nitrous-oxide flame is thought to be about 2900°C. With it, routine analyses have been established for nearly all the remaining metallic elements; the only ones which have so far resisted determination are cerium and thorium.

Interferences

There is a considerable literature on atomic absorption interferences, which fall generally into three types, and can be controlled to some extent by choosing the proper sampling system. The three forms of interference are classifiable as "chemical," "ionization," and "bulk," or "matrix."

Chemical interferences are usually the result of incomplete dissociation of the compounds of the element being determined. When the dissociation is incomplete, some compounds are dissociated less completely than others, and the analytical result for a metal may depend on the other elements and radicals present in the solution. A flame of higher temperature often removes such interferences completely. For example, early workers in England, using air-coal gas flames, reported a multiplicity of chemical interferences with iron. When acetylene came into use, however, most of these interferences disappeared.

Figure 2 shows the effect of the interference of silicon and aluminum with strontium. A small concentration of either causes a profound depression in the absorbance of the strontium, when an air-acetylene flame is used. The upper line in the figure represents the result of a common measure taken to remove this particular interference—the addition of an excess of lanthanum, which preferentially binds the interferents and thus leaves the strontium unbound. For calcium, a similar figure could be drawn.

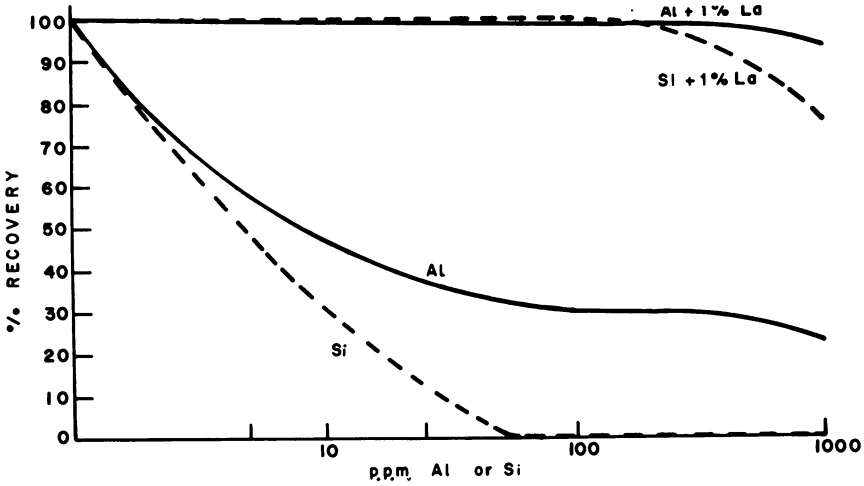

Figure 2. Removal of chemical interferences

Aluminum and silicon both severely depress strontium absorption. Adding lanthanum to the solution removes the interferences by binding the interfering elements

The chemical interferences with calcium disappear when a nitrous-oxide-acetylene flame is used, and the calcium compounds are completely dissociated. However, an interference of the second kind, ionization, is introduced instead.

Ionization interference takes place when a substantial proportion of the atoms in the sample become ionized, causing them to absorb at a different radiation line. Since the different line may be outside the passband of the monochromator, such atoms are in practice lost to the determination. Since the degree of ionization depends on the flame temperature, burning conditions have a real effect on the determination of easily ionized elements.

Ionization interference is usually controlled by adding a large excess of a more easily ionized element—*e.g.*, for the calcium problem, described above, a substantial amount of potassium might be added. More generally, it is not always useful to operate with the hottest possible flame; a

temperature a little above the point of complete dissociation would probably be ideal from the viewpoint of interferences.

Bulk or matrix interferences are changes in the analytical result caused by the viscosity or nature of the sample solution. One common matrix effect is the enhancement caused by organic solutions—*e.g.*, a given concentration of an element in an organic solvent absorbs between two and four times as much as it does in water. There is not complete agreement on the reason for the improvement, but it is clear that the effect of the organic solvent improves the efficiency of the burner.

Another matrix effect is caused by different concentrations of dissolved solids in the sample solution. As the solution becomes more concentrated, it flows more slowly through the burner, and absorption is therefore decreased. Figure 3 shows such an interference, which can be distinguished from chemical interferences in that its slope is much more gradual, and that it does not reach an asymptote.

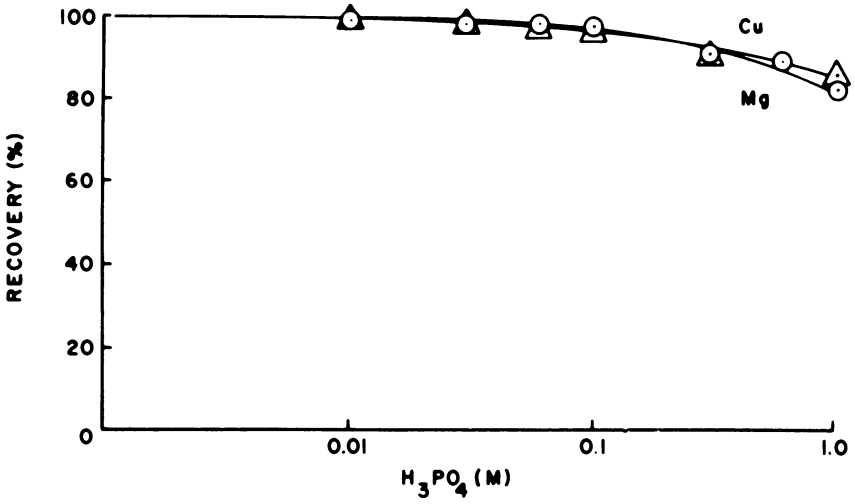

Figure 3. Matrix effect

The curves show the effect of increasing concentrations of phosphoric acid on the absorption from copper and magnesium. Curve shape is typical for matrix effect. The similarity of the curve for the two different elements is a further indication

⊙ *Mg* ($2 \times 10^{-5}M$)
△ *Cu* ($8 \times 10^{-5}M$)

Both the number and intensity of interferences seem to depend greatly on the design of the burner being employed. There is therefore not always general agreement on the presence or absence of interferences in specific analyses. More detail on this problem is given in the section on burners.

Sensitivity and Detection Limit

Before different systems and components are discussed in detail, it is worthwhile to make an effort to understand the difference between the concepts of sensitivity and detection limit. In this area, the atomic absorption field has been subjected to a barrage of claims, counter-claims, distortions, exaggerations, half-truths, and over-simplifications.

Sensitivity, in atomic absorption, is a measure of the amount of absorption produced by a given sample concentration and is generally given as p.p.m./1% absorption. *Detection limit* is defined in various ways to represent the minimum sample concentration which it is possible to distinguish from zero. The most common misconception is the belief that an increase in sensitivity—*i.e.,* higher absorption for the same concentration—automatically produces an improved detection limit. This is by no means true since the detection limit depends also on the stability and freedom from fluctuation of the signal produced.

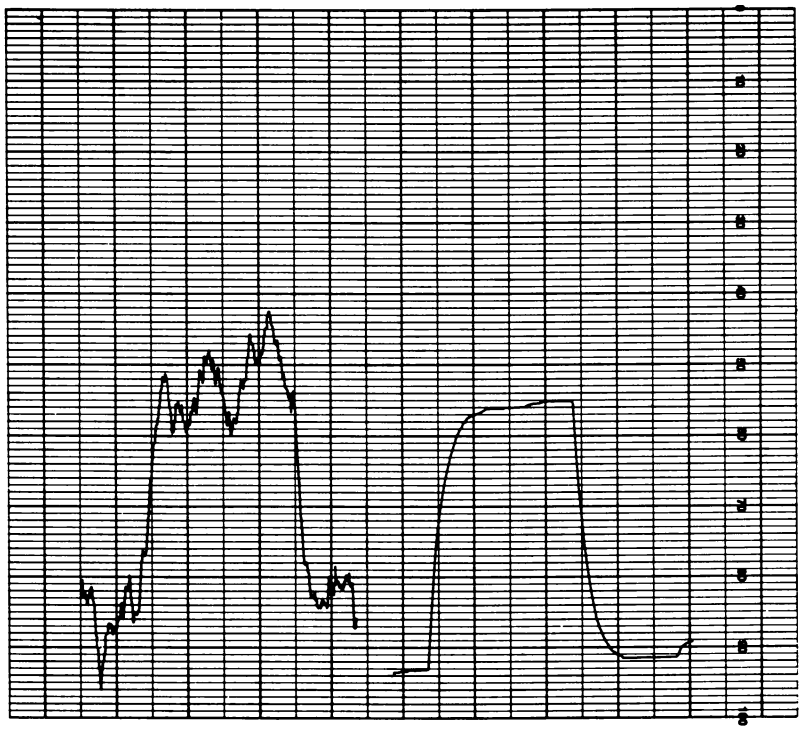

Figure 4. Sensitivity vs. detection limits

Curves show the absorption of 10 p.p.m. silicon under identical conditions, except that poorer quality lamp was used for tracing on the left. Sensitivities are equal, but detection limit for right hand curve is far better

The two traces in Figure 4 prove the point. Each represents the absorption from 10 p.p.m. silicon, run under identical conditions, with only one difference: Trace A used an ordinary silicon hollow-cathode lamp, (vintage 1966), while Trace B was made with a much superior "High-Brightness" lamp. The sensitivity (in p.p.m./1%) is the same for the two traces, but the signal-to-noise ratios, and therefore the detection limits, are clearly very different indeed.

The chief usefulness of the "sensitivity" concept lies in the estimation of optimum concentration for the sample, and as a test of proper performance of an instrument. When it is possible to choose the approximate concentration of the element to be determined, it should lie between 10 times and 100 times the sensitivity. An instrument or analysis yielding a given sensitivity should continue to yield it as time passes, and another instrument of the same design should yield about the same sensitivity.

The detection limit of an analysis is estimated in different ways by different workers. One definition, which is gradually gaining ground, is the concentration of an element in water solution which gives a signal twice the size of the peak-to-peak variability of the background. In statistical terms, the concentration of an element at the detection limit can be determined with a coefficient of variation of 50%. The detection limits given in Table I for one type of instrument were measured according to this formula.

There is a long history of efforts to produce such tight definitions for detection limits that no play is afforded to the human imagination in their establishment. However, up to the present, little success has been achieved. Nevertheless, atomic absorption has shown better repeatability of detection limits than most other techniques. When one laboratory using a given type of instrument achieves a certain limit, it can be expected that another laboratory with the same type of instrument can duplicate the limit within a factor of about three.

One reason why controversies persist is the common practice of calculating detection limits on theoretical grounds, rather than direct measurement. In the author's opinion, detection limits must be measured, rather than abstractly calculated. It is also suggested that the concentration used for the measurement must be no more than five times higher than the detection limit that is finally claimed.

Atomic Absorption Systems

In Figure 1, the principle of atomic absorption is shown. The simplest possible system to carry out this principle appears in Figure 5. Light from the hollow-cathode lamp passes through the flame, after which the resonance wavelength is isolated by a monochromator or filter, and

Table I. Atomic Absorption Detection Limits

	Metal	*Detection Limit*	*Analytical Wavelength*	*Suggested Resolution*
Ag	Silver	0.005	3281	7A.
Al	Aluminum[a]	0.1	3093	2A.
As	Arsenic[b]	0.1	1937	7A.
Au	Gold	0.02	2428	7A.
B	Boron[a]	6.0	2497	7A.
Ba	Barium[a]	0.05	5536	4A.
Be	Beryllium[a]	0.002	2349	20A.
Bi	Bismuth	0.05	2231	2A.
Ca	Calcium	0.002	4227	13A.
Cd	Cadmium[b]	0.001	2288	7A.
Co	Cobalt	0.005	2407	2A.
Cr	Chromium	0.005	3579	2A.
Cs	Cesium	0.05	8521	40A.
Cu	Copper	0.005	3247	7A.
Dy	Dysprosium[a]	0.2	4212	2A.
Er	Erbium[a]	0.1	4008	2A.
Eu	Europium[a]	0.08	4594	4A.
Fe	Iron	0.005	2483	2A.
Ga	Gallium	0.07	2874	7A.
Gd	Gadolinium[a]	4.0	3684	2A.
Ge	Germanium[a]	1.0	2651	2A.
Hf	Hafnium[a]	8.0	3072	2A.
Hg	Mercury	0.5	2537	20A.
Ho	Holmium[a]	0.1	4103	2A.
In	Indium	0.05	3040	7A.
Ir	Iridium	2.0	2640	2A.
K	Potassium	0.005	7665	13A.
La	Lanthanum[a]	2.0	3928	4A.
Li	Lithium	0.005	6708	40A.
Lu	Lutetium[a]	3.0	3312	—
Mg	Magnesium	0.0003	2852	20A.
Mn	Manganese	0.002	2795	7A.
Mo	Molybdenum	0.03	3133	2A.
Na	Sodium	0.002	5890	4A.
Nb	Niobium[a]	3.0	4059	2A.
Nd	Neodymium[a]	2.0	4634	2A.
Ni	Nickel	0.005	2320	2A.
Pb	Lead	0.03	2833	7A.
Pd	Palladium	0.02	2476	2A.
Pr	Praseodymium[a]	10.0	4951	2A.
Pt	Platinum	0.1	2695	7A.
Rb	Rubidium	0.005	7800	40A.
Re	Rhenium[a]	1.0	3460	2A.
Rh	Rhodium	0.03	3435	2A.
Ru	Ruthenium	0.3	3499	2A.
Sb	Antimony	0.1	2175	2A.
Sc	Scandium[a]	0.1	3912	7A.

Table I. Atomic Absorption Detection Limits (Continued)

	Metal	*Detection Limit*	*Analytical Wavelength*	*Suggested Resolution*
Se	Selenium[b]	0.1	1961	20A.
Si	Silicon[a]	0.1	2516	2A.
Sm	Samarium[a]	2.0	4297	2A.
Sn	Tin[b]	0.02	2246	7A.
Sr	Strontium	0.01	4607	13A.
Ta	Tantalum[a]	5.0	2715	2A.
Tb	Terbium[a]	2.0	4326	4A.
Te	Tellurium	0.1	2143	7A.
Ti	Titanium[a]	0.1	3643	2A.
Tl	Thallium	0.025	2768	20A.
Tm	Thulium[a]	0.15	4106	2A.
U	Uranium[a]	30.0	3514	2A.
V	Vanadium[a]	0.02	3184	7A.
W	Tungsten[a]	3.0	4008	2A.
Y	Yttrium[a]	0.3	4077	2A.
Yb	Ytterbium[a]	0.04	3988	2A.
Zn	Zinc	0.002	2138	20A.
Zr	Zirconium[a]	5.0	3601	2A.

[a] Nitrous oxide flame required. [b] Indicates use of argon-hydrogen flame.

Detection limits for the double beam Model 303 Atomic Absorption Spectrophotometer are for elements in water solution. Organic solvents, such as MIBK, improve detection limits by factors of 2 to 4.

then falls onto the photodetector and electronics. Some early commercial atomic absorption instrumentation was indeed built in this way, and functioned well enough to indicate that the method had great inherent usefulness. The system of Figure 5 is called the single-beam d.c. system, because the light from both the flame and the lamp is unchopped and therefore produces a direct current, or d.c., in the detector.

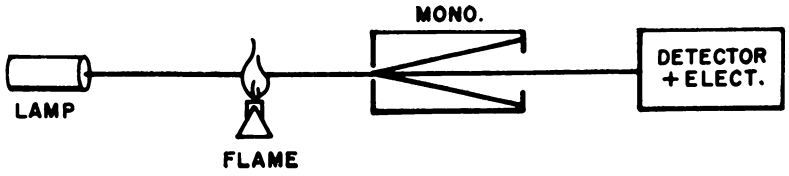

Figure 5. The d.c. system

This is the simplest possible configuration but suffers from problems

Early workers soon found problems in the d.c. system for certain real analyses, owing to emission from the flame. In atomic absorption, the flame is ideally no more than a heated sampling cell, which should

not emit radiation; however, it does. Calcium, for example, has a radiation continuum around the resonance line of sodium. When the d.c. system is used in the analysis for sodium in the presence of much calcium, the detector cannot tell whether a given photon that strikes it is a legitimate sodium photon from the lamp, or an illegitimate calcium photon from the flame. The results from the analysis therefore depend on the sodium concentration as well as on the calcium; therefore, calcium interferes spectrally with sodium in the d.c. system.

Research, therefore, soon turned to the system of Figure 6, in which the source light is chopped and the flame light left unchopped. Since the chopped light produces an alternating current in the detector, this is known as the single-beam a.c. system. The electronics are designed to amplify alternating current only, thereby causing the light from the flame to be ignored. The method of chopping is shown schematically in Figure 6 as a rotating chopper, but in actual instrumentation, the same effect can be achieved by supplying the lamp with a chopped electrical current.

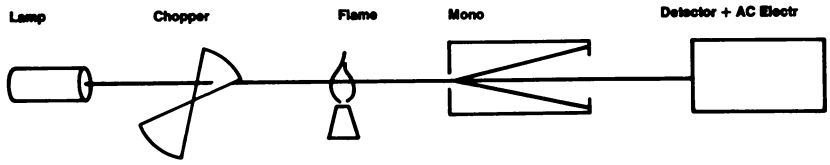

Figure 6. Single beam a.c. system

A chopper distinguishes flame emission from lamp emission. This is the most common system for atomic absorption

Most commercial equipment utilizes the single beam a.c. system. However, one atomic absorption instrument employs a double beam a.c. system, which is shown in Figure 7. Here, the rotating chopper becomes a rotating sector mirror, which passes the beam from the lamp alternately through the flame (sample beam), and past the flame (reference beam). The sample and reference beams are recombined by a half-silvered mirror and then passed together through the rest of the system. The electronics are designed to measure the ratio of the two beams. The readout is the fraction produced by the sample beam as the numerator, and the reference beam as the denominator. Changes in lamp emission, detector sensitivity, and electronic gain appear in numerator and denominator and are canceled out.

The advantages and limitations of this type of double beam system are worth discussing. Clearly, the double beam system cannot overcome instability and noise from the burner since the burner is only in one of

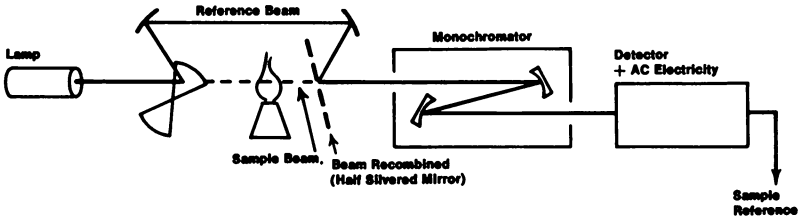

Figure 7. Double beam a.c. system

The effects of variations in lamp emission, detector sensitivity, and electronic gain are canceled out by this system

the two beams. There had, therefore, been no point in using a double beam system until 1962, when a burner was developed which was instrumentally and audibly quiet, with a constant aspiration rate and little tendency to clog. An examination of the single beam atomic absorption system then showed that the burner was no longer the limiting factor but that the stability of the hollow cathode source had become the weakest link. The lamp may take five minutes to a half-hour to come to stable emission (less than 1% drift in five minutes), and even then the lamp emission changes because of a variety of factors, including current, ambient temperatures, and the length of time it has been on.

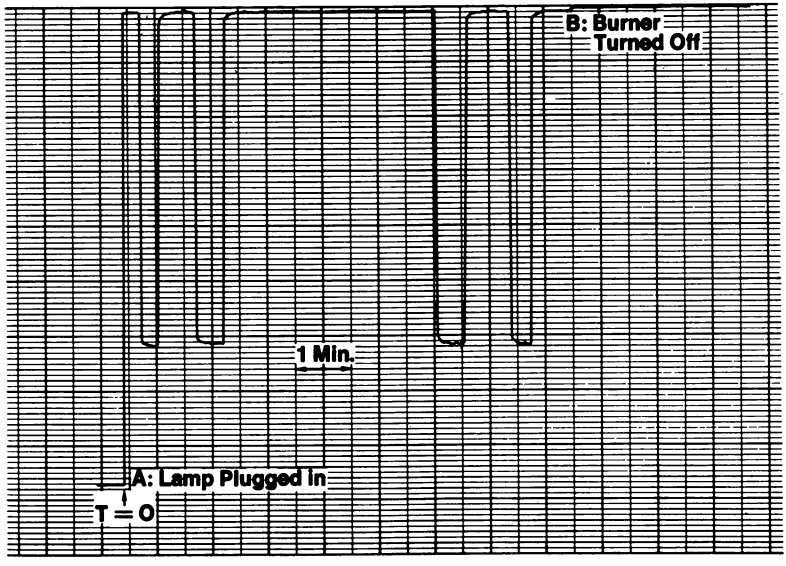

Figure 8. Calcium from a cold start

A cold hollow cathode lamp is plugged into a double beam instrument and operated immediately. Operation begins at point A. Flame is switched off at point B

The ability of the double beam system to overcome the effects of lamp drift and changes in detector sensitivity is shown in Figure 8. Here, a calcium-magnesium hollow cathode lamp is used at the calcium wavelength. The rest of the instrument is warmed up, but the lamp is started cold at point A. A stable baseline is established immediately. The absorption of 5 p.p.m. calcium is measured 23 seconds later. At intervals throughout the rest of the run, which shows absorption *vs.* time, the absorption is remeasured. The baseline continues stable, and the absorption for the 5 p.p.m. calcium does not change during the run.

The double beam system thus gives a stable baseline almost immediately, and has the following advantages: lamps can usually be inserted and operated at once, with little or no wait for warm-up; the stability of the baseline makes it possible to see small departures from it, thereby improving detection limits over the single beam approach; and a stable baseline implies good analytical precision. With double beam, very high values of scale expansion are possible (*see* for example Figure 9).

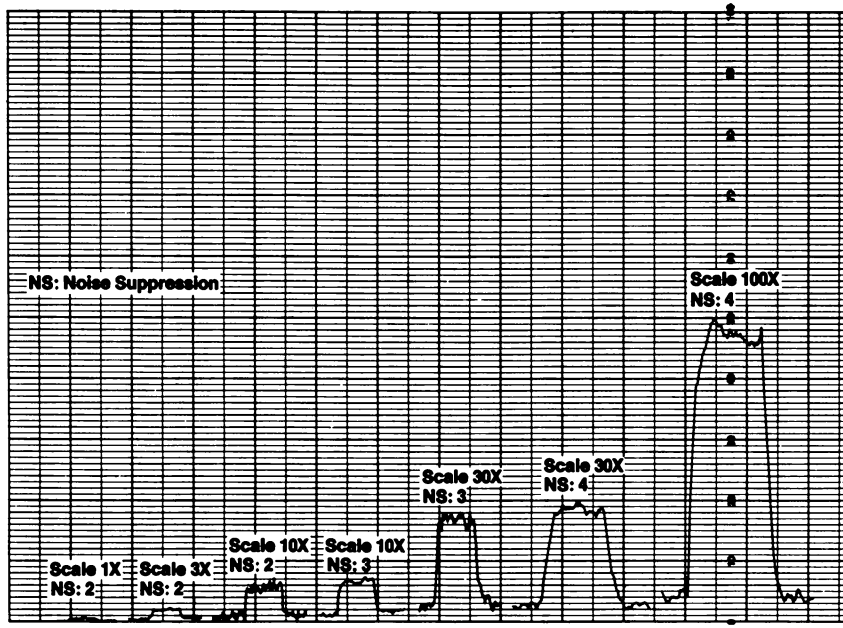

Figure 9. High scale expansions

A double beam instrument is used to determine 0.025 p.p.m. manganese. Scale expansions of 1X, 3X, 10X, 30X, and 100X are used in successive traces

Among the liabilities of the double beam approach are the lengthened optical path which is required, and the increased complexity of the instrumentation. A substantial percentage of the analyses for which

atomic absorption is being used and contemplated can be adequately performed by the simpler single beam equipment.

Burners

The burner system is probably the most important and controversial portion of atomic absorption instrumentation, and active work is taking place on various improvements. Some of the criteria of good burner designs are:

1. Stability. The absorption for a given concentration should remain constant, preferably even from day to day.
2. Sensitivity. Absorption for a given concentration should be high.
3. Quietness. The burner should be audibly and instrumentally quiet, and not induce flicker in the output.
4. Ability to burn concentrated solutions. In real samples, the detection limit is often set by the concentration of solution that can be tolerated.
5. Freedom from memory. The content of one sample should not affect the result from the next.
6. Freedom from background. There should be little or no absorption from the flame itself, or from blank solutions free from the element of interest.
7. Linearity. Working curves of concentration *vs.* absorbance should be straight over as large a range as possible.
8. Versatility. A large number of elements and types of samples should be handled with the same burner.
9. Speed of response. In sample-limited situations, full absorption should be established rapidly after sample introduction.
10. Minimal emission. In an a.c. system, emission from the burner will not produce a photometric error. However, high emission will contribute to the flicker of the output, because the noise current from the photomultiplier detector increases as a function of the total light falling on it. A very bright flame will therefore tend to produce a fluctuating output.

Other obvious requirements are ease of cleaning, freedom from corrosion, and ease of adjustment.

Total Consumption vs. *Premix*

Two basic types of burners have been used for atomic absorption. The one is the "total consumption" or "diffusion" burner, of the type long used by Beckman and others for flame emission work. The other is the "premix" type, in a variety of designs, in which sample, fuel, and oxidant are mixed in a chamber before entering the flame.

The total consumption burner is too well known to need much description. In essence, the fuel, oxidant, and sample are all passed through separate channels to a single opening from which the flame

emerges. The flame is turbulent and relatively small in cross-section, with the hottest portion probably no more than 1 cm. across. This form has been considered advantageous for flame photometry, in which the source of emission should be as small as practicable.

For atomic absorption, many workers recognized the deficiencies of the total consumption burner from the beginning. The Australians almost immediately went over to a premix burner. At the present time, only a rapidly diminishing number of workers are continuing to use the total consumption burner for atomic absorption. (Recently, persuasive evidence has come to light indicating that the premix burner is also superior for flame emission.)

Despite the high efficiency implied by the name of the total consumption burner, both it and most of the premix burners are only about 5% efficient. In the total consumption burner, the entire sample passes into the flame, but in the rapid transit of the droplets through the hot region only the smallest droplets have time to be dried and burned. In the premix burner, shown in Figure 10, the large droplets in the mixing chamber are collected on the walls and pass down the drain, while only the small droplets travel to the flame.

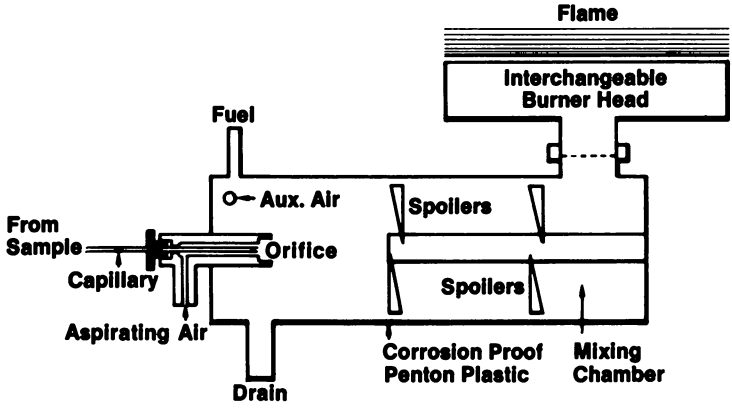

Figure 10. Atomizer and burn system

In this premix burner the sample is aspirated through a thin capillary tube by the air flowing into the atomizer section. The air-sample mixture emerges from the atomizer as a fine spray of droplets, which is then mixed with the fuel, usually acetylene. The mixture is rendered turbulent by the flow spoilers, and is then forced up into the burner head

A more recent innovation is the addition of an auxiliary air supply to the atomizer air and fuel supplies. Auxiliary air makes it possible to operate at higher gas flows than had previously been feasible. The higher

gas flows produce a stiffer flame which is less affected by the ambient atmosphere.

The design of the premix burner shown in Figure 10 also presents a number of other advantages and disadvantages as compared with the total consumption type. The flame is not very luminous, and flicker and turbulence are quite low, so that for many elements the flame contributes no apparent noise to the output (Figure 8). Furthermore, there is rather little dependence of absorption upon sample flow rate. This is of benefit in two ways. First, the length of sample capillary, and its depth of immersion in the solution, are not very critical, so that samples can be aspirated from any vessel. For total consumption burners, by contrast, Petri dishes or very small sample containers are often recommended. Second, viscosity interferences caused by variations in sample concentration are minimized, though not eliminated. In the Perkin-Elmer burner, when the sample flow rate is cut by a factor of 2, absorption is reduced by approximately 4%.

The total consumption burner has the advantage of having, in principle, a faster response time, a lower memory effect, and a greater versa-

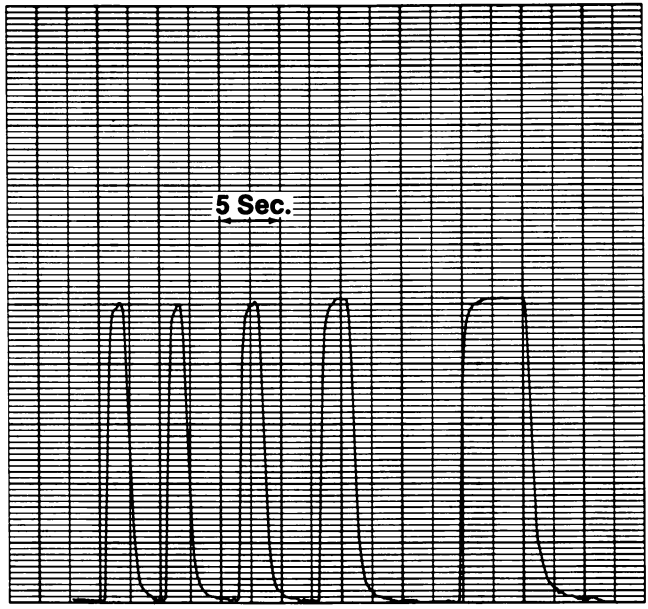

Figure 11. Recorder traces of the absorbance of 1.0 μg./ml. magnesium with aspiration times of 1 sec. each. 5-sec. trace at right represents steady-state value for comparison purposes. Chart speed is 12 inches/minute. Burner typically consumes 3 ml./minute; therefore, sample consumption is approximately 0.05 ml. here

tility regarding the choice of oxidant. The Perkin-Elmer burner, though probably slower to come to equilibrium, nevertheless does so in under one second, as shown in Figure 11.

The chamber of the Perkin-Elmer burner is made of remarkably inert Penton plastic, so that, in very extensive analytical work involving hundreds of instruments, cross-contamination of samples has not been a problem. For the sake of certainty, a blank is usually run for a few seconds after every sample. When very high concentrations of an element are run, there will be some persistence. For example, after several percent sodium are aspirated for some time, traces of sodium will persist in the flame up to a few hours, unless the burner is taken apart and cleaned.

A number of different burner heads are available for different purposes, with all heads fitting the same mixing chamber atomizer system. Two of these heads, which are described in Table II, are capable of burning rather concentrated solutions without clogging. The "high-solids" burner head, which has a wider slot than the standard one, can burn 1:1 dilutions of blood serum, or 10% sugar solutions, indefinitely. Its only disadvantage is that it whistles on warm-up, before becoming as inaudible as the standard head.

Table II. Burner Heads

Name, Description	*Features*
303-0023 Standard burner head, 4 in. × 0.015 in. slot	For air-acetylene or air-hydrogen. Standard on Model 303
Propane burner head, 4 in. × 0.06 in. slot	For propane, coal gas, or natural gas with air
High solids burner head, 4 in. × 0.025 in. slot	Similar to 303-0023, except that it can burn concentrated solutions without clogging. Whistles while warming up
290 Burner head, 2 in. × 0.020 in. slot	For air-acetylene or air-hydrogen. Despite shorter length, provides approximately equal sensitivity to 303-0023. Can burn moderately concentrated solutions. Can be turned 90° in its mount, reducing sensitivity by 10–20 times
Three-slot burner head, three parallel 4 in. × 0.025 in. slots	For air-acetylene or air-hydrogen. Can burn concentrated solutions without clogging. Provides 1.5–2 times better sensitivity for many metals, is less critical to adjust than standard burner head for molybdenum, chromium, and calcium
Nitrous oxide head, 3 in. × 0.02 in. slot	For nitrous oxide with acetylene or hydrogen. Required for refractory elements. Can also be used with air, for non-refractory elements. Somewhat more difficult to clean than other heads

With the premix burner it is possible to obtain better linearity of working curves, fewer interferences, and the ability to determine more metals, than with the total consumption burner. These differences stem from the fact that the premix flame is laminar and contains no large, unburnable sample droplets, while the total consumption flame is turbulent and includes large droplets.

Interferences. One study of relative interferences is shown in Figure 12. Here the effect of fluoride concentration on the absorption of barium is measured, both when a total consumption burner and a Perkin-Elmer premix burner are used. It will be seen that the effects are negligible with the premix burner, and immediate and severe with total consumption (*1*). In another study, it was found that the presence of phosphate interferes seriously with the absorption of magnesium with a total consumption burner (*9*). With a well-designed premix unit, there is no such effect (*2*).

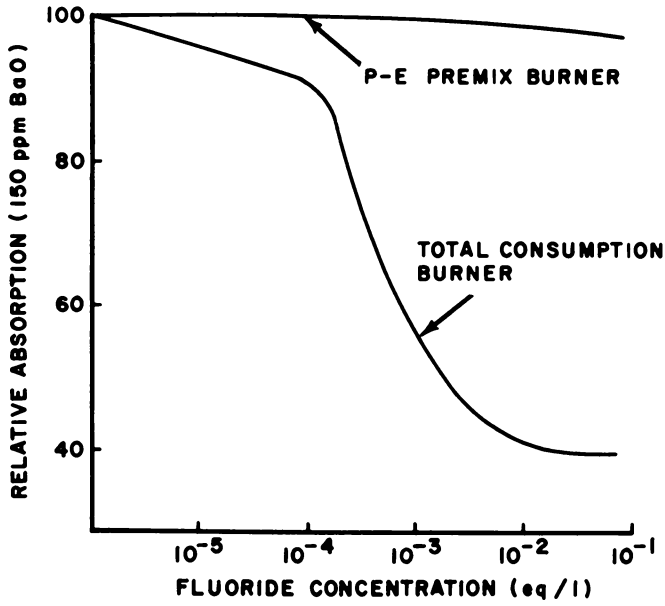

Figure 12. Total consumption and premix burners are compared for interferences of fluoride with the determination of barium (Ref. 1)

Linearity. In Figures 13 and 14, the absorption for calcium in water solution is given for two different instrumental arrangements. In Figure 13, a premix burner is used, and the sample beam is passed once through the flame (*21*). In Figure 14, a total consumption burner is employed,

in an instrument where the sample beam is passed five times through the flame in the interests of better absorption (*15*). It will be seen that the premix burner gives better linearity by a considerable factor. In fact,

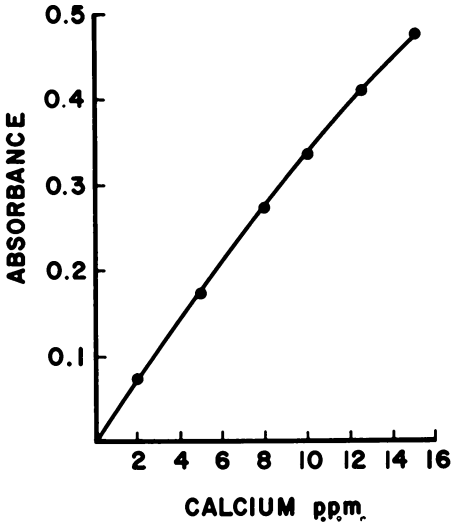

Figure 13. Working curve for calcium, with a premix burner and one pass through the flame (Ref. 21)

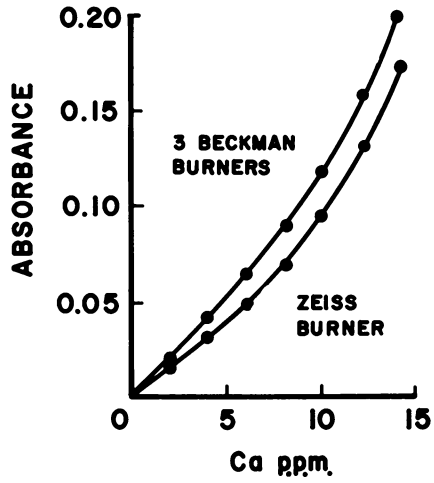

Figure 14. Working curves for calcium, with total consumption burners and five passes through the flame (Ref. 15)

between 0 and 10 p.p.m., it would be possible to obtain accurate results with a single standard. With the total consumption burner, by contrast, the linearity is far poorer, and several standards are required. It is also of interest to note that the absorption for 10 p.p.m. calcium is considerably better for the premix burner, despite the fact that the sample beam is passed through the flame only once.

Element Versatility. A considerable number of elements require temperatures higher than those of the air-acetylene flame to dissociate them from their chemical compounds. In atomic absorption, these elements are known generally, though somewhat inaccurately, as "refractory" elements. These elements, of which silicon, titanium, and vanadium are examples, are difficult and in some cases impossible to determine with the total consumption burner, although they are quite readily determined with a properly designed and used premix system. The reason is believed to be that the turbulence of the total consumption flame causes entrained air to penetrate throughout the cone, thereby lowering the effective flame temperature (*12*).

Variations in Solvents, Fuel, and Oxidant

For premix burners, the most common supply gases are air and acetylene, while the total consumption burners generally use air and hydrogen. All detection limits are usually given in water solution.

When organic solvents are used, such as alcohol or methyl isobutyl ketone, the absorption for a given element concentration is enhanced by factors between 2 and 5. As with nearly everything else having to do with burners, the reasons for the improvement are under debate. One plausible explanation is that the organic solvents, having a lower surface tension, produce smaller droplets and thus promote higher efficiency.

The effects of different fuels for the premix burner have been studied in some detail. At air-acetylene temperatures, the alkalis and alkaline earths ionize to an appreciable extent, and ionized atoms are lost to the determination. Also, for elements whose compounds are dissociated at low temperatures, such as lead and zinc, the absorption is higher when lower temperature fuels are used, such as propane or natural gas. As flame temperature is reduced, pressures in the flame become lower, and more atoms remain in the optical path. Ionization interferences between alkali elements are also reduced.

However, experience indicates that low temperature fuels should be used with great circumspection if at all. The propane flame is not as stable as the acetylene flame so that the improvement in sensitivity cannot generally be translated into an advantage in detection limit. More-

over, a large number of elements show interferences when low-temperature flames are used, which disappear when acetylene is employed.

For the premix burner, the best fuel for all elements seems to be acetylene, with the mysterious exception of tin. For tin, hydrogen improves the absorption several-fold over acetylene. The reason is not understood.

Fuel economy is also on the side of acetylene, since a 300 cu. ft. tank lasts approximately three working weeks. A similar tank of hydrogen, required by the total consumption burner, is consumed in about three hours. Ordinary welding-grade acetylene is adequate for atomic absorption. The air supply must be free from dust and oil.

Refractory Elements: the Nitrous Oxide Burner

The air-acetylene combination is not hot enough to dissociate most compounds of a considerable number of elements, such as aluminum, boron, and silicon, and it incompletely dissociates those of other metals like chromium, molybdenum, and barium. An additional problem is that the "refractory" elements are quick to form stable oxides.

Some years ago it was discovered that the refractory elements could be made to absorb in a fuel-rich oxy-acetylene flame. The oxygen provided a higher temperature, and the excess of acetylene kept the flame sufficiently reducing to delay recombination.

The high burning speed and explosive potential of oxy-acetylene flames made it difficult to produce a usable premix oxy-acetylene burner. The total consumption burner, on the other hand, while capable of burning such a fuel combination, produced such a brilliant and turbulent flame that it was difficult to obtain analytical results with it. Various efforts to modify the total consumption burner met with only moderate success.

So matters stood until John Willis (*17*) in Australia found that a combination of nitrous oxide and acetylene would not only dissociate refractory compounds, but could also be used in premix burners with minor modifications. The burner head was changed in only two ways: the material was thickened to withstand the higher temperature, and the slot was shortened to minimize the potential of flashback.

In Table I, the elements marked with a superscript *a* are determined with nitrous oxide.

For certain elements, determinable with the air-acetylene flame, a better analysis is obtained with nitrous oxide. For example, the hotter flame dissociates calcium, barium, and strontium more completely from their chemical compounds, leading to better detection limits and fewer

interferences than occur in the air-acetylene flame. Chromium and molybdenum should also probably be determined with nitrous oxide. Here, the detection limits are not improved, but the fairly complex interferences that occur in the air-acetylene flame are removed.

It is worthwhile to add a note on the safety of the nitrous oxide acetylene burner. Although not difficult to use, this gas combination is somewhat more likely to flash back than air-acetylene, when not used in accordance with instructions. A flashback is often accompanied by a rather loud explosive sound, and may rupture the burner chamber. However, well-designed burners include guard wires and metal casings, which contain any fragments that might be ejected. Therefore, a nitrous oxide burner flashback may be nerve-wracking to the operator and his neighbors, but is absolutely free from any risk of injury.

Methods to Improve Sensitivity

In common with other techniques, there is a constant search in atomic absorption for means of improving the detection limits. One approach is to improve the stability of the system, thereby making possible the use of higher scale expansions, and thus enabling the measurements of smaller changes in absorption. With one double-beam instrument, it is possible to measure absorption differences of the order of 0.02 to 0.04%. At the present state of the art, it is probably unfruitful to attempt to lower this value. Accordingly, effort is being concentrated on means of actually producing a greater absorption for a given concentration. If such an increase can be achieved without sacrificing stability or freedom from noise, an improvement in detection limit can be obtained. Some approaches to the problem are described below.

Heated Chamber Burner. One approach, which is now being offered commercially, is a burner in which the mixing chamber is heated to a temperature between 300° and 500°C. by infrared radiation. After introduction, the sample is converted into a vapor. It then passes into a cooling chamber, where the steam is condensed and allowed to flow out of a drain tube. In the ideal case, only the solid components of the sample are passed into the burner head. The heated chamber system overcomes the previously noted factor that standard premix burners are only 5% to 10% efficient. By being able to use all of the sample that had been introduced, the heated chamber burner can produce ten to twenty times higher absorption for a given concentration.

However, present heated-chamber designs are by no means free of problems. Because of the complicated path pursued by the sample, serious memory effects can occur, so that the concentration of one sample will affect the results obtained with the next. In addition, this burner

type is very sensitive to clogging; in some samples, concentrations of dissolved solids as low as 0.5% cannot be run. Chemical and matrix interferences occur which do not exist for other burners. Finally, the tracings tend to be noisier than those of standard premix burners, so that most, if not all, of the improvement gained by the sensitivity increase is lost in the quality of the tracings. In general, it is fair to say that the heated chamber burner has not yet led to improvements in detection limits.

The Long Tube. As first reported by Fuwa and Vallee (*5*), the flame from a total consumption burner is so tilted as to pass down a horizontal ceramic tube, which is typically up to 90 cm. long and about 1 cm. in diameter. This tube lies along the optical path of the spectrophotometer. The atoms in the flame therefore spend a considerably longer time in the optical path than they do with a conventional burner. For elements whose compounds are dissociated at relatively low temperatures, such as zinc, very notable increases in absorption are obtained.

The earlier long tubes suffered from problems of coating the sides of the tubes, and from serious non-repeatability. Now, through the expedient of heating the tube walls electrically to a temperature of between 800° and 1,000°C., many of these problems are reported to have been overcome (*8*). When certain elements are to be determined in very small sample amounts, it may be expected that the long tube method will provide a real advantage. However, there are again a number of serious problems with the technique, which keep it from being even close to universal. First, the coolness of the extended flame leads to interferences which do not exist in standard burners. Second, the lengthy path leads to a large background absorption which must be subtracted from the analytical result. Third, only a minority of elements are susceptible to this technique. Fourth, the long tube technique requires much more skill in its use. Finally, the long tube requires a very narrow optical beam, leading to a loss of light in comparison with conventional atomic absorption. This light loss tends to reduce the ratio between signal and noise, and makes the improvement in detection limit not as great as might have been hoped.

The Sampling Boat. The author has had some success with a different approach. Here, the sample is loaded into a narrow boat-shaped vessel, made out of tantalum or a similar material, and dried. The boat is then placed into the middle of a standard air-acetylene flame. For lead, selenium, cadmium, silver, and zinc, encouraging results have been obtained. The detection limit for lead, for example, is about one-fifteenth that of conventional atomic absorption spectroscopy. However, at least at the present stage of development, drawbacks exist here also. Interferences are multiplied, because of the low temperatures at which atomiza-

tion takes place. Also, again only a minority of elements are suitable for this technique.

Further developments on these three techniques, as well as others involving graphite furnaces, plasma jets, and other sampling devices, may be expected in the coming years.

Sources for Atomic Absorption

Many of the virtues of atomic absorption stem from the fact that the desired element absorbs only at very narrow lines, with a half-width of the order of 0.03A. Instrumental design is therefore greatly simplified if the emission sources emit lines no wider than this, and narrower if possible. Discharge lamps and hollow cathodes have been found to fill the requirements, and particularly the latter have been developed to a considerable level of sophistication.

Other sources have been proposed and in some cases developed. It has been suggested that a flame containing a high concentration of the element of interest would produce a simple, versatile, and inexpensive source, but difficulty was encountered in achieving the requisite stability and freedom from background radiation. Fassel *et al.* of Iowa State have used the bright continuum of a xenon arc as a source (*4*), depending on the monochromator to achieve a narrow wavelength range. Working with an instrument of about 0.2A. resolution, they achieved useful detection limits.

With the continuous source, it is possible to produce analyses for a number of elements. However, the complexity of the required instrumentation, and the necessary operator skill, are far higher than are needed when working with sharp-line sources. Also, there are far higher risks of encountering spectral interferences, while sensitivity values are much lower. Largely for these reasons, there has not yet been any commercial development of continuous source atomic absorption equipment.

Single Element Hollow Cathodes

A single-element hollow-cathode lamp is shown in Figure 15. The active components are a cathode made of or lined with the element of interest, generally in the shape of a cylinder closed at one end, about 1 cm. deep and 1 cm. across, and an anode which is merely a straight metal wire. Neon or argon is used at a few millimeters pressure as a filler gas. The front face of the lamp is made of quartz or any of several types of glass, depending on the wavelength range it must transmit and also on the preference of the manufacturer.

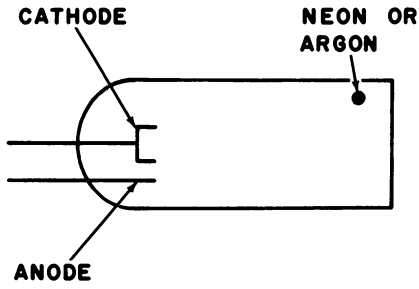

Figure 15. Schematic of hollow cathode lamp
The cup-like cathode is made of or contains the element of interest. The envelope is filled with argon or neon at a low pressure

When the current flows, metal atoms are sputtered from the cathode into the area within and in front of the cup. Collisions with the neon or argon ions cause a proportion of the metal atoms to become excited and emit their characteristic radiation. The choice of filler gas depends on the element: lead, iron, and nickel perform far better with neon than with argon; however, neon is not suitable with some elements, such as lithium and arsenic, because a strong neon emission line is close to the best resonance line. For many elements, there is little to choose between the two gases.

Optimum lamp currents vary between elements and designs, from 5 to 100 ma. at 100–300 volts. Manufacturers' rated maxima represent values above which the cathodes are in danger of destruction. Below the maximum, the lamp emission increases as the current is raised, improving the signal-to-noise ratio and reducing the flicker in the instrument output reading. However, for many elements the absorption for a given concentration of sample is reduced as the current rises over a certain value, since the emission line becomes somewhat self-absorbed. In self-absorption, sputtered ground state atoms in the lamp itself absorb the lamp

Figure 16. Resonance line emission of a hollow cathode lamp
(A) Normal emission. (B) Self-reversed emission, caused by excessive current, or flaws in design

radiation, causing the emission to assume the form of Figure 16. Recommended lamp currents represent a compromise between emission intensity and sensitivity (absorption for a given concentration).

Hollow Cathode Lamp Logistics

Hollow cathode lamps are made by several manufacturers, most of whom guarantee them for a use period of five ampere hours. When this figure is divided by typical operating currents, the average guarantee extends to between 300 and 500 hours of use. In practice, most lamps last a great deal longer.

Lamps produced during the past two years, for all but a few particularly recalcitrant elements, have shown such long life that it has been all but impossible to gather statistical data on failure rates. For example, if one determination per minute is made on a double-beam instrument which does not expend any lamp life in warm-up, a 500-hour performance corresponds to 30,000 determinations.

Until recently, the greatest problem in producing, using, or maintaining lamps was the possible presence of hydrogen within the metal cathodes. Hydrogen produces a strong emission continuum in the ultraviolet region, and also has strong emission in the visible. The effect of its presence is to reduce the intensity of the resonance line and to produce a pronounced flattening and bending of the working curve, as shown in Figure 17.

When a lamp is failing, the most common effects are a reduction in analytical sensitivity and an increase in output fluctuation. If the instrument behaves properly for other elements, it can be deduced that the lamp is at fault. Particularly if the trouble occurs after the lamp has not been used for some time, it can sometimes be cured by operating the lamp at maximum current overnight.

Multi-Element Lamps

The thought of building several elements into one cathode occurred to workers in atomic absorption almost immediately after equipment became available. Initial efforts were defeated mainly by the metallurgical naiveté of the experiments. However, at the present time a considerable variety of multi-elements lamps are available, although they vary in usefulness. Depending on the metals involved, the cathodes are made from alloys, intermetallic compounds, or mixtures of powders sintered together.

The importance and value of multi-element lamps should be appraised realistically and not over-estimated. Many presently available

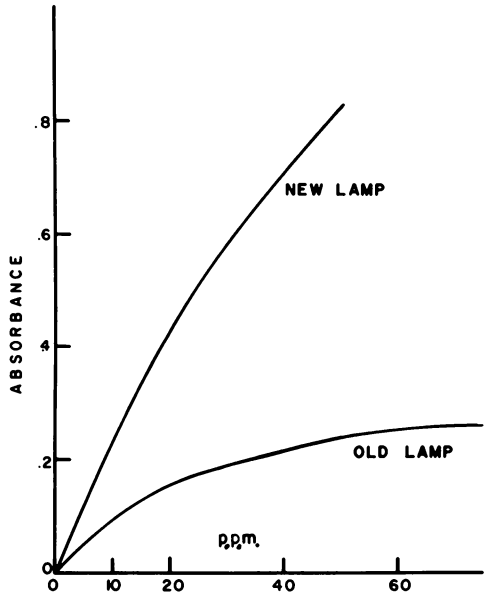

Figure 17. Effect of background hydrogen emission on the working curve

Instead of assuming the shape of the upper line, the working curve shows a lower sensitivity, has early curvature, and reaches an asymptote. Similar effects could be caused by the presence of unabsorbable lines within the passband of the monochromator

combinations can be used without disadvantage as compared with single-element lamps, and can usually be obtained at a financial saving. Other combinations present problems because of line selection and potential spectral interferences, but may nevertheless be worth having if the limitations are understood.

All commercial atomic absorption equipment offers easy interchange of lamps, usually in some sort of pre-focused mount. In single-beam instruments, where warm-up time delays are appreciable, a multi-element lamp is attractive because all its elements are ready when one is. In double-beam equipment, lamp warm-up time is not a factor. Here, the charm of multi-element lamps is confined to their lower cost, and the smaller requirement for storage.

Not all elements can be usefully combined in multi-element lamps. Some combinations are difficult or impossible from a metallurgical viewpoint. More important to the user, some combinations, though feasible to manufacture, yield spectral interferences. Here, the emission lines

from one element lie too close to those of another element, so that spurious absorption signals can result, if the second element is also present in the sample. Occasionally, it is possible to remove the spectral interferences by narrowing the bandpass of the monochromator. However, as will be shown later, such a procedure is not without disadvantages.

When three or more elements are combined in a lamp, it is also frequently true that the emission from the individual elements is not as

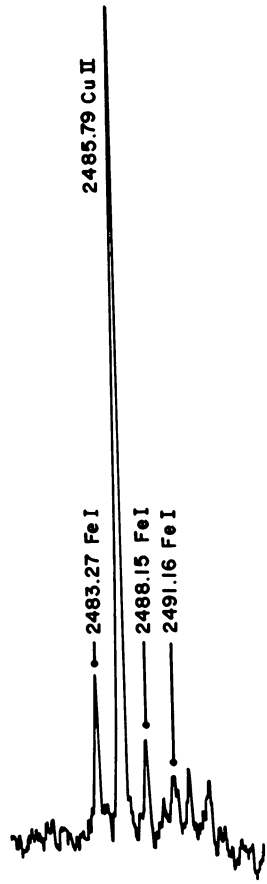

Figure 18. Emission of Perkin-Elmer 6-element lamp around iron resonance line

A very strong Cu II line is shown only 2.5A. away. This causes problems with iron determination when the six-element lamp is used. The scan was made with the Perkin-Elmer Model 303, equipped with emission accessory. As a result of this scan, the iron-copper combination lamp was modified

bright as that from single-element lamps. Again, no universal rule can be made. For example, one manufacturer has found that the brightest emission for zinc comes from a zinc-calcium alloy. Thus, a dual-element lamp for zinc and calcium is actually brighter than a lamp made solely out of zinc. Furthermore, some single-element lamps are so bright that little or nothing is lost by a slight decrease in brightness. In Figure 18, there is shown a scan of a multi-element hollow cathode lamp, including both iron and copper. A strong copper ion line lies close to the primary resonance line for iron. As a result of this scan, the copper-iron combination was modified to contain more iron and less copper. With a more favorable iron/copper ratio, and some of the improvements described below, the iron-copper combination proved useful and feasible.

Recent Improvements in Hollow Cathode Lamps

Recently (about mid-1967), some important improvements were made in the design of hollow cathode lamps, yielding units with longer life, higher emission, and greater spectral purity than had been available previously. The emission stability has also been enhanced, and the warm-up time shortened. Basically, four changes were responsible for these improvements.

1. Shielding. In the open hollow cathode design, shown schematically in Figure 15, there is glow not only inside the cathode but also outside the cathode and along the electrodes. The new lamps have shielding along the electrodes and outside the cathodes, as shown in Figure 19. The glow is thus restricted to the inside of the cathode, leading to longer life and better emission.

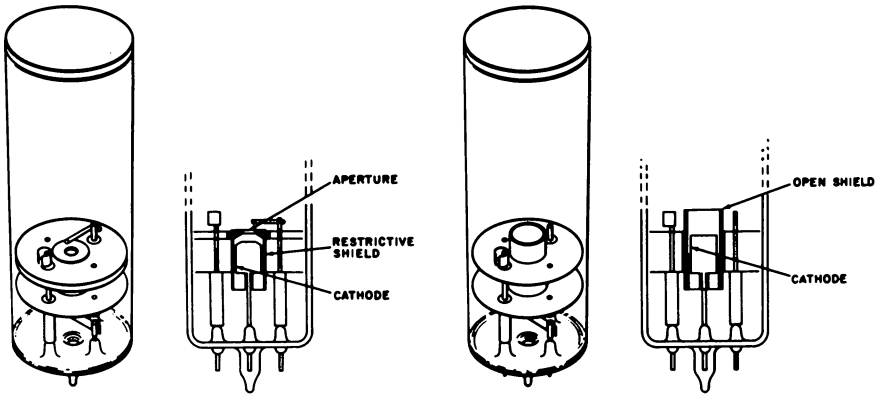

Figure 19. Diagram of a typical shielding structure for a hollow cathode lamp
The washers are mica, while the insulators are ceramic

2. Molten cathodes. Certain elements, such as lead, have the problem that, when a high current is passed through them, the cathodes melt. On the other hand, when a low current is used, there is little emission. In a new design, the lead lamps were made by coating lead on the inside of a cup made of a less easily melted metal, such as titanium. Now, when a high current is passed through the lamp, the lead melts, adheres to the titanium through surface tension, and serves as the source of emission in its molten state. Lamps of this design are more than 20 times brighter than older lead lamps. Similar "molten" designs are available for thallium, gallium, indium, tin, and bismuth.

3. Different cathode sizes. For certain elements, it was shown that the 3/8″ cathode that had been standard was not optimum. Different configurations, usually smaller, proved substantially brighter.

4. For some elements, better alloy combinations have been found which make it possible to use higher lamp currents with no sacrifice of lamp life.

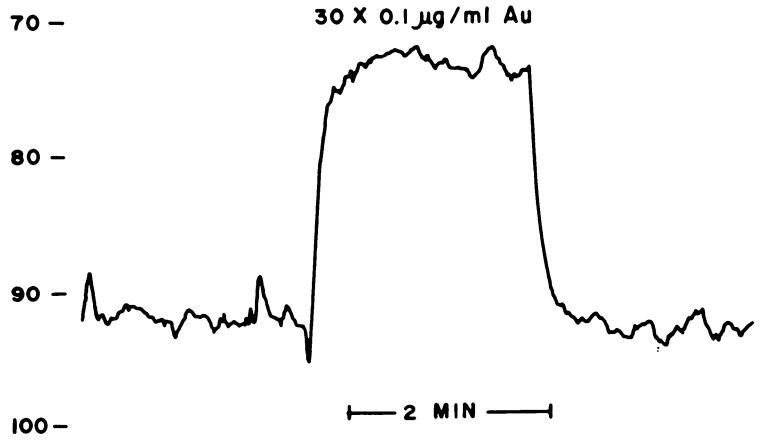

Figure 20. Absorption of 0.1 p.p.m. gold

Scale expansion is 30X, on double beam instrument. Detection limit is deduced to be 0.03 p.p.m.

From a user's viewpoint, the major improvement from more emissive lamps is the ability to produce traces with smaller fluctuations. Thus, higher scale expansions are achievable. For example, Figure 20 shows the absorption of 0.1 p.p.m. gold at 30X scale expansion with a double-beam instrument. The detection limit is better than 0.02 p.p.m., which is about five times superior to previously achievable limits. For some elements, though not the majority, it is also possible to achieve straighter and in some cases more sensitive working curves. A prime example is nickel. Nickel has an unabsorbable ion line at 2319.76A., which is almost

directly superimposed on the best analytical line at 2320.03A., leading to bending and flattening of the working curve. With the shielded design, the intensity of the ion lines is much reduced in comparison with the ground state lines. As a result, an improvement in linearity is apparent. This is demonstrated in Figure 21.

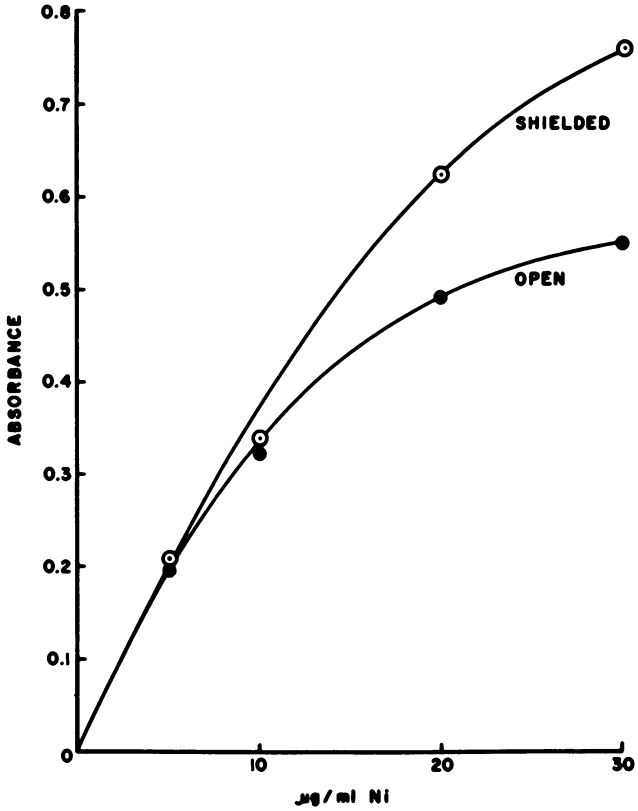

Figure 21. Working curves for nickel

Lower curve was made with an older lamp and shows the effect from unresolved ion line

High-Brightness Lamps

High-brightness lamps, which were developed at CSIRO (Commonwealth Scientific and Industrial Research Organisation, Australia), are based on standard hollow cathodes, but contain a pair of auxiliary electrodes (*13*). In ordinary hollow cathode lamps, not all the atoms which are sputtered off the cathode are excited. Since only the excited

atoms are capable of emitting radiation, the purpose of the auxiliary electrodes is to pass a secondary current which will excite the remaining sputtered atoms. Thus, an increase in emission can be expected.

When these lamps first became available in pilot quantities two years ago, increases of 50 to 100 fold in emission were claimed. However, since that time the standard hollow cathode lamps have been greatly improved. As a result, the advantage in emission enjoyed by the high brightness lamps has markedly decreased. At the present time, it is probably not worthwhile to use the high-brightness lamps (which are more complex and require an auxiliary power supply) for atomic absorption analysis. However, for special purposes, the high brightness lamps may still be of interest. Currently, some high brightness lamps are still several times brighter than their ordinary counterparts, while others give no improvement in emission intensity.

It is worth stating that, after a certain limit has been reached, further increase in lamp brightness is not useful for atomic absorption. Thus, when a lamp is bright enough to permit, say, 100X scale expansion, a further brightness increase will not lead to better results. (However, in the new technique of atomic fluorescence, detection limits are directly proportional to lamp brightness.)

Vapor Discharge Lamps

Vapor discharge lamps produce emission by passing an electric current through a vapor composed at least partly of the element of interest. Such lamps are produced by Osram in Germany and Philips in Holland. Osram lamps exist for the elements mercury, thallium, zinc, cadmium, and the alkalis.

Osram lamps for mercury cannot be used in atomic absorption, because they contain vapor at so high a pressure that the emission line is almost completely self-absorbed, and the sensitivity is very small. It is also generally agreed that hollow-cathode lamps for thallium, zinc, and cadmium are superior to the discharge lamps.

Osram lamps require special mounts, and a special power supply capable of delivering a 1-ampere current at a starting voltage of about 300 volts and a running voltage of about 50 volts. Furthermore, even in double-beam equipment, they require a wait of about ten minutes for warm-up, while the time in single-beam instruments is in excess of a half hour.

Until quite recently, vapor discharge lamps were recommended for the determination of sodium and potassium, despite the fact that they are relatively troublesome to use. However, newly available hollow cathode lamps are as bright as the discharge lamps at both the primary

and secondary wavelengths, and are now to be preferred. The last stronghold of the vapor discharge lamps (at the time of writing) is the fact that they are required for cesium and rubidium, where they are still far brighter than the hollow cathode equivalent.

Monochromators

The wavelength range for atomic absorption is the same as that of flame emission and of ultraviolet spectrophotometry; as a result, it is possible to work successfully with atomic absorption accessories to equipment originally designed for other purposes. However, in many respects, the requirements of atomic absorption are different.

In an atomic absorption monochromator, one is concerned mainly with resolution and with energy. Roughly speaking, resolution is defined as the ability of the monochromator to distinguish between two lines different in wavelength by a certain amount; that is, a monochromator with a resolution of 1A. can distinguish two lines which are 1A. apart. Energy is the amount of light which the monochromator is capable of passing; clearly, higher energy is better.

The ability of atomic absorption to distinguish between elements and avoid spectral interferences does not depend on the monochromator. It depends instead on the emission line width of the hollow cathode lamp (typically 0.02A.), and the absorption line width of the element in the flame (typically 0.04A.). These values are far superior to the resolution capabilities of commonly available monochromators. Therefore, the monochromator does not enter directly into the ability of the atomic absorption instrument to give a specific result. (*See* Figure 1.)

The major function of the monochromator is to separate the resonance line of the element of interest from the nonabsorbable lines which are emitted by the hollow cathode lamp. Experiments performed over a number of years indicate that, for the elements with the most complicated spectra, a resolution of 2A. is needed. (Approximate required resolution settings are shown in Table I.) For ordinary atomic absorption, there is no advantage in having better resolution. For example, a monochromator with a resolution of 0.5A. is no better for atomic absorption than one with a resolution of 2A.

If the resolution of a monochromator is inadequate for the element that is being determined, nonabsorbable lines will pass through the instrument. While there will be no loss of specificity, inadequate resolution will lead to a loss of sensitivity and a bending of the working curve. In Figure 22, nonabsorbable lines pass through the monochromator. A large sample concentration is aspirated, absorbing essentially the entire resonance line. Nevertheless, the nonabsorbable lines cannot be absorbed.

The maximum absorption, and therefore the working curve, will be asymptotic to a certain absorption, in this case 50%. The working curve will therefore be flattened and made nonlinear. The working curve for nickel with an older hollow cathode lamp, shown earlier in Figure 21, is exhibiting this phenomenon. Here, the cause is an ion line in the nickel lamps which is only 0.2A. away from the resonance line.

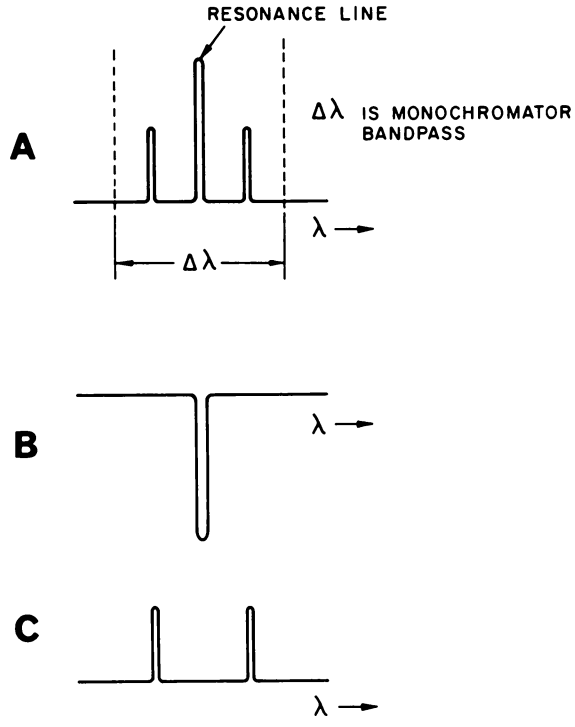

Figure 22. Effect of inadequate resolution

(A) Monochromator does not resolve two non-resonance lines from the resonance line. (B) Concentrated sample absorbs entire resonance line. (C) Detector continues to see unabsorbed radiation

Another requirement of the monochromator is that it should be capable of using wide slits—*i.e.*, wide bandpasses, for elements whose emission spectra are uncomplicated. Zinc, arsenic, selenium, calcium, lead, and the alkalis are examples of such elements. When the bandpass is wider, more energy can be passed through the monochromator and the obtainable precision and detection limits are better.

It is important to note that it is disadvantageous in atomic absorption to operate the monochromator at a resolution setting which is narrower

than that required. Narrower resolution settings will reduce the energy and thereby the obtainable precision and detection limits of the results. The reason is as follows. Resolution settings in monochromators are altered by changing the widths of the entrance and exit slits. (*See* schematic of Figure 23.) Most spectrophotometers are designed in such a way that an image of the source, in this case the hollow cathode lamp, is placed on the entrance slit of the monochromator. The bright area of a hollow cathode lamp is a circle several millimeters in diameter. Therefore, the entrance slit, with the image of the source placed upon it, will look like Figure 24. It will be seen that only a fraction of the source

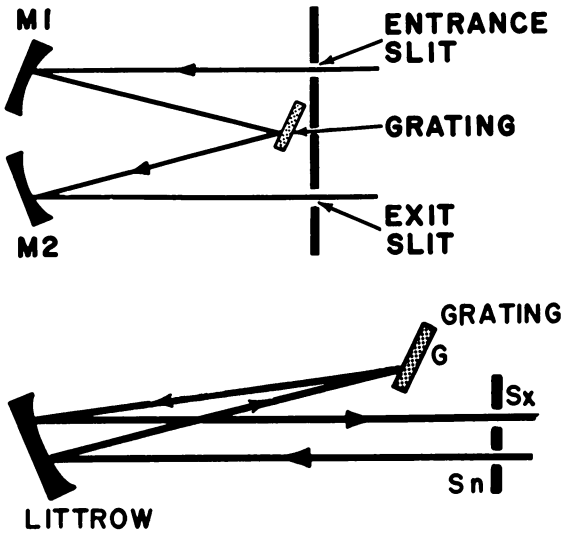

Figure 23. Simplified schematics of monochromator designs

(A) Ebert-Fastie. Minor modification of this is known as Czerny-Turner. (B) Littrow

light passes into the monochromator. As the entrance slit becomes wider, more source light passes through. It would therefore be a mistake, for example, to determine zinc at a resolution setting of 2A., with correspondingly narrow slits, when it is possible without degradation to run zinc at a setting of 20A. or more.

By the same token, an important criterion of monochromator performance is reciprocal linear dispersion, commonly expressed in Angstroms/millimeter. If the reciprocal linear dispersion of a given monochromator is, say, 10A./mm., then at a slit width of 1 mm., the resolution of the unit is 10A. For best energy, the reciprocal linear dispersion

should be low. If two monochromators are being compared for atomic absorption, the one with lower reciprocal dispersion is better in that respect. The light transmission of a monochromator also varies directly with the surface area of a prism or grating, and with focal length of the monochromator.

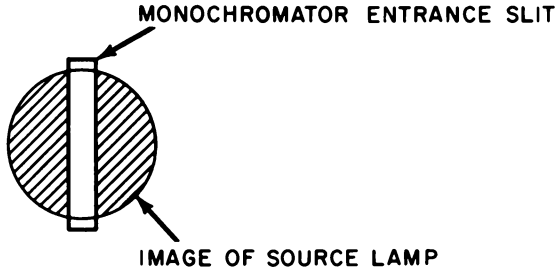

Figure 24. Entrance slit of monochromator with image of hollow cathode source superimposed on it. Shaded area represents unused light

To achieve the above goals with reasonable economy, certain features required of monochromators for different purposes can be sacrificed. A first-rate ultraviolet spectrophotometer, for example, has a wavelength accuracy of about 1A., and a stray light level of 0.0001%. In atomic absorption the wavelength can be "tuned in," so that a 10A. wavelength accuracy is sufficient. Furthermore, stray light levels of perhaps 0.1% can be tolerated.

Some atomic absorption instruments are also designed to be capable of flame emission work. When scanning flame emission is contemplated for qualitative analysis, the monochromator must distinguish between a multiplicity of lines. For this purpose, resolution becomes important. For scanning flame emission, a monochromator of better resolution than 2A. is useful, though by no means always required.

The two most popular monochromator designs are the Littrow and the Ebert-Fastie, shown schematically in Figure 23. The merits of the two systems have been compared for many years; for atomic absorption purposes, there seems to be little to choose between them.

In photomultipliers, the choice is generally between the Bi–O–Ag and Cs–Sb types of cathode. The popular and widely used RCA 1P28 has a Cs–Sb cathode; the more expensive Bi–O–Ag material has advantages in the far ultraviolet (arsenic and selenium), and even greater advantages in the red (potassium, rubidium and cesium). At the potassium wavelength (7665A.) the Bi–O–Ag surface has perhaps ten times

the efficiency of the Cs–Sb. Between 2200 and 5800A., the two surfaces are about equal.

Resonance Detectors

The newest device to be added to the arsenal of the atomic absorption spectroscopist is the resonance detector, a photomultiplier combined with a system which responds only to the resonance line of the element for which it is designed (*14*). A resonance detector can replace the monochromator in an atomic absorption instrument designed to measure only one element.

A typical design based on a resonance detector is shown in Figure 25. The light from a hollow cathode lamp is passed through the flame in a conventional manner. It then falls upon the resonance detector, which includes a device for producing a cloud of atoms of the element of interest. Thus, if magnesium is being determined, the resonance detector sputters a cloud of magnesium atoms into the indicated space.

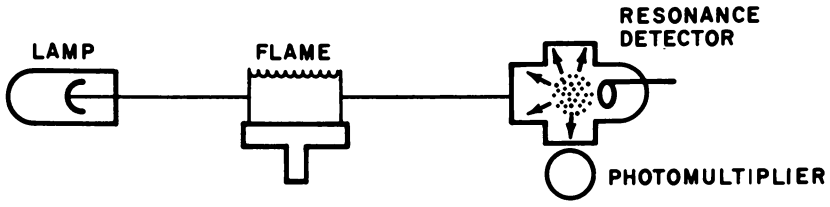

Figure 25. Resonance detector system

The cloud of sputtered atoms in the resonance detector fluoresces proportionately to incoming intensity

If the resonance detector is well-designed, the vast majority of the magnesium atoms are unexcited. The resonance lines from the magnesium hollow cathode lamp will cause the magnesium atoms in the resonance detector to fluoresce. Some of this fluorescence will fall on a photomultiplier detector placed at right angles to the optical path. The intensity of fluorescence is proportional to the intensity of emission. Nonresonant lines from the lamp or from the flame will have no effect on the resonance detector. Therefore, a system of narrow bandwidth is produced without the requirement of a monochromator.

The resonance detector offers a number of attractive possibilities. Instruments designed around it can inherently be made rugged, since there are no monochromator settings to drift. For single-element instruments, the absence of the monochromator may also effect a slight cost reduction. Most important, perhaps, is the potential of a lineup of reso-

nance detectors as part of an eventual multi-element absorption instrument.

In analytical work, a resonance instrument can produce good results, though these will be in no case better and in some cases poorer than the results from a well-designed conventional instrument. Since many elements have a number of resonance lines with different sensitivities, and the resonance detector does not distinguish between them, the sensitivities achieved with resonance detectors are often poorer than those with monochromators. Baseline drift for single beam instrumentation is likely to be comparable. The considerations affecting the signal-to-noise ratio are complex, but the upshot is that the two types of instruments are comparable in this respect also.

The Place of Flame Emission

Atomic absorption and flame emission analysis are in some ways complementary, and in other ways competitive. There is a considerable difference of opinion among researchers, as to the relative importance of the two techniques.

At technical meetings, it is a favorite occupation of some spectroscopists in the universities to present comparative tables of detection limits contrasting atomic absorption and flame emission. At the present state of the art, the honors are divided about 50:50. However, the analytical user should be aware of an important difference. Detection limits are ordinarily measured when the element itself is present alone in a water solution, while real samples are almost never of such a nature. As the solution becomes more concentrated, and as a multiplicity of elements are present, the detection limits for atomic absorption are degraded only slightly if at all, while the detection limits for flame emission tend to change very greatly. Although there is disputation of the point, it is the author's opinion that, with very few exceptions, all elements determinable by atomic absorption are done better by that technique than by flame emission. For example, although the alkali elements have traditionally been determined well by flame emission, atomic absorption still presents advantages. Ionization interferences are reported to be much lower by atomic absorption, and the spectral interference from calcium disappears. Also, many samples themselves give background emission, requiring a separation procedure before flame emission analysis is feasible. Such sample preparation can generally be omitted when atomic absorption is used.

For most elements, flame emission analysis requires the elimination or recognition of spectral interferences and excitation problems, which can usually be ignored in atomic absorption.

Flame emission is, however, useful for a number of purposes. First, if a laboratory wishes to analyze for an element for which they do not have a hollow cathode lamp, flame emission can be thrown into the breach. Second, it is possible in some cases to determine phosphorus and sulfur by flame emission by making use of the oxide bands that appear in the flame. Phosphorus and sulfur are, of course, inaccessible to atomic absorption. Finally, it is possible to make a flame emission scan of a sample and thereby obtain a qualitative knowledge of the elements that are present. It should be stressed, however, that none of these flame emission procedures are completely straightforward. In all cases, the analyst requires considerable spectroscopic skill and sophistication in chemistry. A qualitative scan, for example, is likely to lead to a wilderness of emission lines. Considerable knowhow is required before the analyst can pick his way through that wilderness. Atomic absorption, by contrast, requires a considerably lesser degree of operator skill and involvement.

Flame emission has traditionally been performed with total consumption burners. However, it has recently been shown that the premix burner, with a nitrous oxide head, is an excellent source for flame emission measurements, and is in many cases superior. In Figure 26, a flame emission scan is shown for aluminum in ethanol, with a premix nitrous oxide burner as a source.

Atomic Fluorescence

In the past few years, another analytical method, related to both flame emission and atomic absorption, has made its appearance. This is the technique of atomic fluorescence (*18*).

The schematic for atomic fluorescence instruments is shown in Figure 27. As before, the sample is atomized in the flame. However, unlike atomic absorption, the sample in the flame is illuminated by a line emission source which is at an angle to the path between the flame and the monochromator. As the atoms in the flame absorb radiation from the lamp, they fluoresce at the resonance or a higher wavelength, with an intensity proportional to the concentration of the element of interest.

Atomic fluorescence has certain intrinsic advantages over atomic absorption, particularly for elements which have simple emission spectra, such as cadmium and zinc. For these and several other elements, detection limits far below those of atomic absorption have been reported. In addition, the use of a continuous source is more attractive with atomic fluorescence than it is with atomic absorption. In principle, it should be possible to use scanning atomic fluorescence to produce a qualitative and

at the same time semi-quantitative analysis of a sample for a limited number of elements.

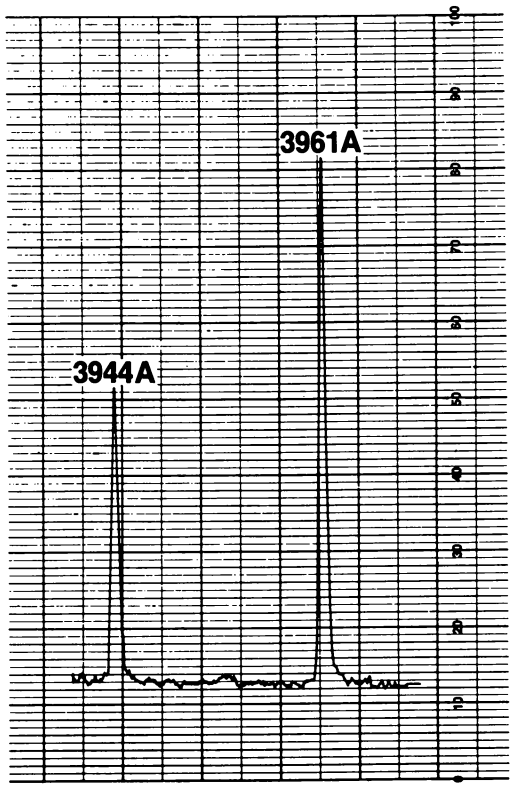

Figure 26. Flame emission of 10 p.p.m. aluminum in ethanol

A nitrous oxide burner is used, and the monochromator of the Model 303 is set to a resolution of 0.3A.

At the time of writing, the majority of elements have not yet been determined by atomic fluorescence, nor has there been a very meaningful study of the usefulness of atomic fluorescence in real samples. Currently, no commercial atomic fluorescence equipment is yet available, although many existing atomic absorption instruments can readily be modified for atomic fluorescence use. The only major requirement is that the burner is sufficiently accessible so that a hollow cathode or other source can be placed at an angle to the optical path.

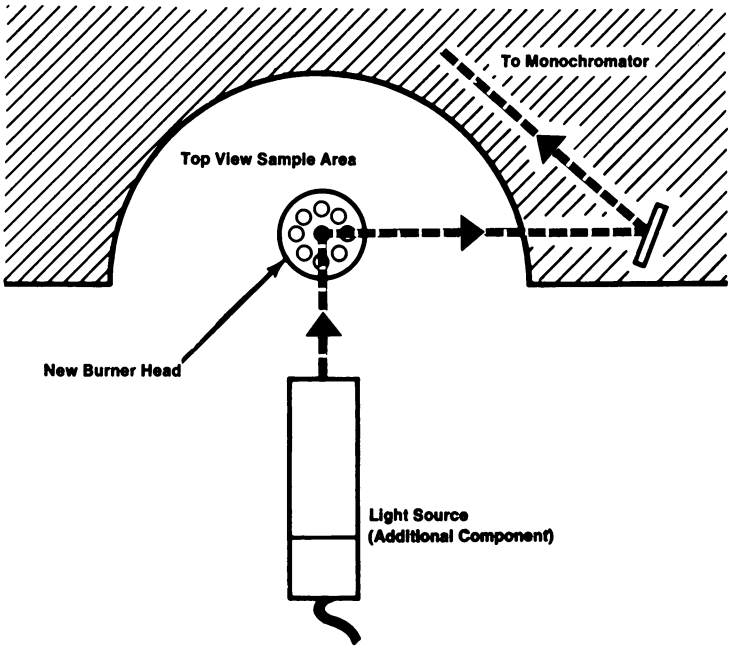

Figure 27. Schematic of atomic fluorescence

Emission from hollow cathode lamp causes sample to fluoresce proportional to concentration of desired element

Readout Devices

Atomic absorption, when properly designed, obeys Beer's Law—*i.e.*, concentration is proportional to the negative logarithm of transmittance, over an appreciable concentration range. The readouts of many atomic absorption instruments are linear in transmittance or absorption, and the appropriate Beer's Law absorbance values are found by referring to a logarithmic chart or table. It is also possible to obtain readouts which are linear in absorbance, or even calibrated directly in concentration.

In most analyses, the precision and detection limit are limited by the readout, unless scale expansion is provided. Different readout devices therefore give scale expansion up to 100X. All commercial atomic absorption instruments can also be connected to recorders, which often produce improvements in performance.

As scale expansion is increased, the fluctuation in the signal level (noise) rises proportionately. Very frequently, it is possible to reduce the effect of these fluctuations, and their size, by using readout damping. Damping, which is also sometimes called increasing the time constant,

makes the entire system slower to respond to changes in signal. The fluctuations that occur at relatively high frequencies are thereby removed. In essence, the operator trades an increase in sampling time for a decrease in fluctuation.

Most commercially available atomic absorption spectrophotometers have damping built in. Single beam instruments can usefully employ damping time constants up to about 20 seconds. Double beam instruments, with their greater freedom from drift, can benefit from damping time constants as high as two minutes.

The obverse side of this coin is not to be neglected. Since every atomic absorption user will at one time or another wish to determine a considerable number of samples in succession, the instrument should be capable of a fast response. At the fastest speed setting (lowest time constant), the meter needle or recorder pen should come to a balance in less than two seconds.

Concentration Readout

It is highly desirable, especially for routine analysis, that the readout of the atomic absorption instrument be capable of being calibrated linearly and directly in concentration. Many commercially available spectrophotometers are capable of being converted to this type of operation, while some of the newer instruments have direct concentration read out built in.

The importance of direct concentration read out can be seen by a study of the time factors involved. Once sample preparation is completed and the samples are lined up ready for analysis, it is possible to analyze each sample in 15 seconds or less. If the readout is direct and linear in concentration, no further work is required. If, however, it is necessary to measure several standards, draw a working curve manually, convert the absorption reading for each sample to absorbance, and then compare it to the working curve, at least 30 extra seconds are consumed for each determination.

Many of the commercially available atomic absorption instruments which read out in percent absorption can be equipped with digital devices to readout in concentration. In general, the concentration read out is then accomplished on four illuminated digits, which are relatively easily calibrated. Some digital readout accessories also include other features. Some have "working curve straighteners" which are capable of straightening a bent working curve in order to minimize the number of standards that must be used. Most can be used directly with digital printers which produce a permanent record. Some are capable of automatically repeating

a determination up to 16 times, and computing the average, thereby improving the precision of the analysis.

As hollow cathode lamps, instruments, and burner designs are improved, more and more elements produce straight working curves over a useful analytical range. Equipment has become available which reads out linearly in concentration, with very much less complexity than was formerly required. In general, a logarithmic conversion is made electronically inside the instrument, and the readout takes place on a meter scale or recorder. Figure 28, for example, shows direct linear measurement of calcium concentration made on a relatively simple atomic absorption instrument.

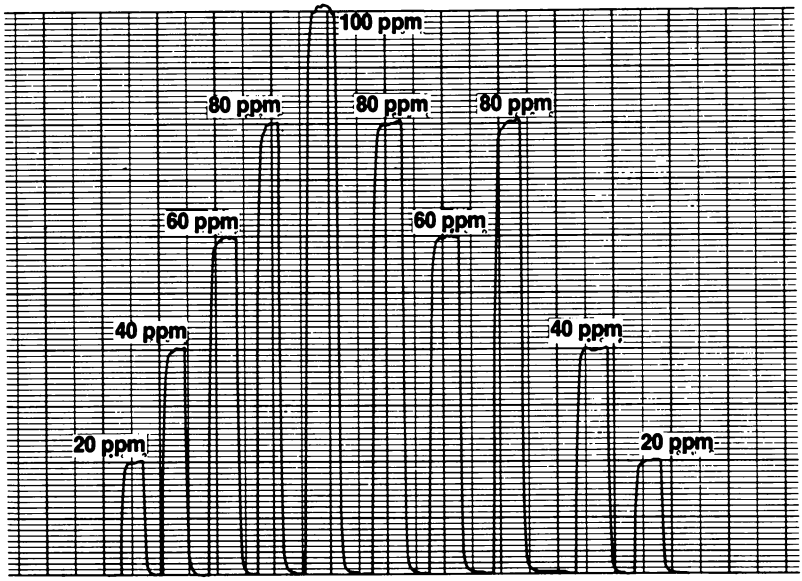

Figure 28. Direct measurement in concentration

With readout linear in absorbance, (− Log T), and variable scale expansion concentration can be recorded directly. In this chart, made with a Perkin-Elmer Model 290B, concentration values are read directly from the recorder

Instrumentation Costs

It would not be reasonable to close this chapter without adding some information on the approximate cost involved in atomic absorption analysis. Depending on the degree of elaboration, basic atomic absorption instruments are currently priced between $3,000 and $8,000 in the U.S. In addition, hollow cathode lamps are required. For estimation purposes, it should be assumed that these will run in the neighborhood

of $100 per element. An exhaust vent required in order to remove the noxious and possibly toxic gases from the flame, will cost a few hundred dollars. A typical laboratory can enter the atomic absorption field for as little as $4,000 but may find it sensible to spend as much as $12,000.

Conclusions and Prognosis

Despite its youth, atomic absorption is at present already a well-developed technique of analysis, which has enormously shortened the time required to make very many different determinations. In many disciplines, it has made possible studies which were formerly out of reach.

In the opinion of the author, the greatest progress is destined to be in the direction of multi-element atomic absorption instrumentation, and automated analysis. Both of these disciplines are already being explored but not yet with the sophistication that the future will bring.

The advent of the resonance detector has greatly simplified the potential problem of multi-element analysis. It is in principle possible to line up a number of resonance detectors, and, combining this with a multi-element hollow cathode lamp and a single burner, analyze a sample for a number of elements simultaneously.

Both ends of the atomic absorption analysis are subject to automation. At one end, there is the automatic dilution and presentation of samples to the instrument. The results are then fed directly to a computer or other storage device, via cards, punched tape, or magnetic tape. Thus, it will eventually be possible to complete an entire series of analyses, possibly including interpretation of the meaning of the data, without intervention of the operator.

The major advances will come in speed and convenience, rather than in improvement of data. Therefore, it can be expected that none of the developments which are now contemplated as being on the horizon will obsolete the equipment that is presently available.

The atomic absorption field has been a very interesting one, for both producers and users, and the prognosis is that it will continue to be so for a long time to come.

Literature Cited

(1) Adams, P. B., Passmore, W. O., *Anal. Chem.* **38**, 630 (1966).
(2) Allan, J. E., *Analyst* **83**, 466 (1958).
(3) Ezell, J. B., Jr., *At. Absorption Newsletter* **6**, 84 (1967).
(4) Fassel, V. A., Mossotti, V. G., Grossman, W. E. L., Kniseley, R. N., *Spectrochim. Acta* **22**, 347 (1966).
(5) Fuwa, K., Pulido, P., McKay, R., Vallee, B. L., *Anal. Chem.* **36**, 2407 (1964).
(6) Goleb, J. A., *Anal. Chim. Acta* **36**, 130 (1966).

(7) Meddings, B., Kaiser, H., *At. Absorption Newsletter* **6,** 28 (1967).
(8) Nelson, K. W. (Private Communication).
(9) Rains, T. C., Menis, O., *17th Pittsburgh Conf. Anal. Chem. Appl. Spectry.*, Pittsburgh, Pa., Paper no. **174,** Feb. 1966.
(10) Roe, D. A., Miller, P. S., Lutwak, L., *Anal. Biochem.* **15,** 313 (1966).
(11) Russell, B. J., Shelton, J. P., Walsh, A., *Spectrochim. Acta* **8,** 317 (1957).
(12) Slavin, W., *At. Absorption Newsletter* **6,** 9 (1967).
(13) Sullivan, J. V., Walsh, A., *Spectrochim. Acta* **21,** 727 (1965).
(14) *Ibid.*, **22,** 1843 (1966).
(15) Sunderman, F. W., Jr., Carroll, J. E., *Am. J. Clin. Path.* **43,** 302 (1965).
(16) Weir, D. R., Kofluk, R. P., *At. Absorption Newsletter* **6,** 24 (1967).
(17) Willis, J. B., *Nature* **207,** 715 (1965).
(18) Winefordner, J. D., Vickers, T. J., *Anal. Chem.* **36,** 161 (1964).
(19) Woodson, T. T., *Rev. Sci. Instr.* **10,** 308 (1939).
(20) Zaugg, W. S., Knox, R. J., *Anal. Chem.* **38,** 1759 (1966).
(21) Zettner, A., Seligson, D., *Clin. Chem.* **10,** 869 (1964).

RECEIVED September 30, 1967.

12

Extraction Techniques for the Determination of Cobalt, Nickel, and Lead in Fresh Water by Atomic Absorption

MARVIN J. FISHMAN and MARYLAND R. MIDGETT

U. S. Geological Survey, Denver, Colo.

The detection limits for cobalt, nickel, and lead in aqueous solution by atomic absorption are about 50 μg. per liter. Normally these elements occur at lower concentrations in fresh waters, and direct measurement by atomic absorption is not possible. A rapid, simple, accurate, and sensitive chelation-extraction method for determining lead, cobalt, and nickel is attained by chelating the metals with ammonium pyrrolidine dithiocarbamate at a pH of 2.8, extracting the metal-chelates with methyl isobutyl ketone, and aspirating the ketone layer. Results obtained by this method agreed well with results obtained by spectrographic methods. As little as 1 μg. of lead, cobalt, and nickel per liter can be detected. This is at least one order of magnitude lower than most other wet chemical procedures.

Atomic absorption is being used routinely for the direct determination of sodium, potassium, calcium, magnesium, and several trace elements: strontium, lithium, manganese, copper, and zinc in natural waters (*4*). There is ordinarily no need to concentrate these trace elements since most waters contain detectable amounts. However, certain other trace elements, such as cobalt, nickel, and lead normally occur in fresh waters at concentrations less than can be detected by atomic absorption directly.

Table I shows the minimum, maximum, and median concentrations for lead, cobalt, and nickel in the water supplies of the 100 largest cities in the United States (*3*). Spectrographic methods were used to obtain these data. Only nine samples contained detectable concentrations of cobalt. The highest concentration was 9.5 μg. per liter, whereas the cobalt found in the other samples were listed as "less-than" values. Ninety-five per cent

of the water supplies contained less than 10 μg. per liter of both nickel and lead. The detection limits for lead, cobalt, and nickel by atomic absorption are approximately 50, 30, and 20 μg. per liter, respectively. These detection limits were determined with a Perkin-Elmer Model 303 atomic absorption spectrophotometer by aspirating aqueous standards. A preconcentration procedure is, therefore, essential if these elements are to be determined by atomic absorption.

Table I. Concentration of Lead, Cobalt, and Nickel in Public Water Supplies of the 100 Largest Cities in the United States[1]

	Minimum	*Maximum*	*Median*
Pb	ND[2]	62.0	3.7
Co	ND[2]	9.5	ND[2]
Ni	ND[2]	34.0	<2.7

[1] All results in μg. per liter.
[2] "ND"—not detected.

Several methods have been reported for concentrating lead, cobalt, and nickel in blood, urine, brines, and water prior to final determination by atomic absorption. Sprague and Slavin (*6*) described a procedure for determining these elements plus copper, cadmium, iron, and manganese in concentrated potassium chloride solutions. The metals were chelated with ammonium pyrrolidine dithiocarbamate (APDC) and extracted with methyl isobutyl ketone (MIBK). It was reported that the optimum pH for the extraction was approximately 2.8. Berman (*1*) described a similar chelation-extraction procedure for determining lead in urine and blood. Burrell (*2*) developed a procedure for determining cobalt and nickel in natural waters by atomic absorption in which both metals are first co-precipitated with ferric chloride from ten liters of water. The separated precipitate is subsequently dissolved and made up to 100 ml. volume with hydrochloric acid and water so that the final pH of the solution is 2.5. The nickel and cobalt are then chelated with APDC and extracted with three 10 ml. volumes of MIBK. Three extractions are necessary to achieve complete recovery of the chelated cations. A detection limit of 0.3 μg. of nickel per liter and 0.15 μg. of cobalt per liter was found.

Experimental

Our laboratory decided to investigate further the extraction system of Sprague and Slavin (*6*) wherein APDC is used as the chelating agent, and MIBK as the extractant. No investigation was made on concentrating trace elements from extremely large volumes of water as Burrell did, since a rapid and simple routine method was needed; however, a detection limit of at least 1 μg. per liter was sought.

The volume of sample used during the investigation varied from 25 to 200 ml., and 5 or 10 ml. of MIBK was used for extraction. It was found that a 1 μg. per liter detection limit could be obtained if the metal-chelates were extracted from a 100 ml. sample with 5 ml. MIBK. However, if there is sufficient water, the sample volume, and all reagents, should be doubled because of the solubility of MIBK in water (approximately 2.2 ml. per 100 ml.). If 5 ml. of MIBK is used, only 2.8 ml. are available for aspiration. This is usually sufficient for determining either cobalt or nickel; however, for the lead determination it is a bare minimum since the lead lamp is noisier and more noise suppression is required, resulting in a slower meter response.

The amount of APDC required for chelation depends on the total quantity of heavy metals present which may be chelated. To chelate the heavy metals from samples containing up to 1,000 mg. of dissolved solids per liter, 2.5 ml. of a 1% solution of APDC is generally sufficient. The ammonium pyrrolidine dithiocarbamate is prepared in the laboratory. The procedure is described by Slavin (5).

The pH for optimum extraction was investigated and all three elements can be extracted at pH 2.8. The 2.8 pH is critical for lead; however, cobalt and nickel can be extracted even at pH 5. Since all three elements are extracted at a pH of 2.8, they may be determined simultaneously. If the sample volume and the reagents are increased proportionally, the extractant volume will be sufficient to determine all three elements. Only the lamp and instrument settings must be changed in the atomic absorption unit.

With a 100 ml. sample and 5 ml. MIBK, or proportionally increased volumes, the detection limits for cobalt and nickel are approximately 0.4 μg. per liter, and approximately 0.8 μg. per liter for lead.

Table II shows the instrument conditions for lead, cobalt, and nickel which were used with the Perkin-Elmer Model 303 atomic absorption spectrophotometer. Nickel and cobalt working curves were prepared up to 20 μg. per liter, and a lead working curve up to 40 μg. per liter. Table III shows scale readings observed.

The determination is especially susceptible to contamination from glassware. Extreme care must be exercised and all glassware must be rinsed with 1:1 nitric acid before use.

Procedure. Pipet 100 ml. of sample containing less than 20 μg. of cobalt or nickel per liter or 40 μg. of lead per liter into a 200 ml. volumetric flask. Prepare a blank of 100 ml. demineralized water and sufficient standards, and adjust the volumes of each to approximately 100 ml. Add 3 drops 0.1% bromophenol blue indicator. Raise the pH of the sample, which should be acidified at time of collection, by dropwise addition of 10% sodium hydroxide until the blue coloration of the indicator appears. Add 2.5% hydrochloric acid dropwise until the blue color just disappears in both the standards and the sample, and then add 2.0 ml. 2.5% hydrochloric acid in excess (pH 2.3). Add 2.5 ml. 1% APDC, mix (pH 2.8), add 5.0 ml. MIBK, and shake the containers for 60 seconds. Allow the layers to separate and then add demineralized water until the ketone layer is completely in the neck of the flask. Aspirate the ketone layer and record the scale reading for each standard and sample. Approximately 2.8 ml. of ketone is recovered from the extraction, a volume sufficient for

Table II. Instrument Conditions for Lead, Cobalt, and Nickel[1]

	Lead	*Cobalt*	*Nickel*
Grating	ultraviolet	ultraviolet	ultraviolet
Wavelength	217.0 (2170A)	240.9 (2409A)	232.2 (2322A)
Scale expansion	5 X	10 X	10 X
Slit	4	3	3
Source	Hollow cathode	Hollow cathode	Hollow cathode
Lamp current	10 ma	35 ma (multi-element)	35 ma (multi-element)
Air pressure	28 p.s.i.g.; 4.0 on flowmeter	28 p.s.i.g.; 4.0 on flowmeter	28 p.s.i.g.; 4.0 on flowmeter
Fuel: acetylene pressure	8 p.s.i.g.; 3.0 on flowmeter	8 p.s.i.g.; 3.0 on flowmeter	8 p.s.i.g.; 3.0 on flowmeter
Sample uptake	approx. 4 ml. per min.	approx. 4 ml. per min.	approx. 4 ml. per min.
Response time control	3	2	2

[1] PE Model 303. The authors have recently found that the same concentration ranges can be covered using 10 ml. MIBK if the following instrument conditions are changed: burner—Boling, lamps—shielded cathode, and scale expansion of 10 X for all three elements.

Table III. Observed Scale Readings for Different Concentrations of Lead, Cobalt, and Nickel[1]

Conc. μg. per Liter	*Scale Reading*		
	Pb	*Co*	*Ni*
2.5	6.8	12.5	13.0
5.0	13.0	24.5	25.8
10.0	26.0	46.4	46.3
20.0	48.8	87.0	78.0
30.0	72.3	—	—
40.0	91.5	—	—

[1] Scale readings can be converted to percent absorption by dividing by the scale expansion.

only one reading. If sufficient sample is available, both sample and reagent volumes may be doubled and duplicate values obtained. If all three elements are to be determined from the same sample, the sample and reagent volumes must be proportionally increased.

Determine the μg. of lead, cobalt, or nickel per liter in the sample from a plot of scale readings of standards. Since scale expansion of 5 X

and 10 X is used, it is not necessary to convert scale reading to absorbance. Exact reproducibility is not obtained and a working curve must be prepared with each set of samples. Report concentrations of lead, cobalt, and nickel to the nearest μg. per liter.

Table IV. Comparison of Results for Determination of Lead, Cobalt, and Nickel by Atomic Absorption (A) and Emission Spectroscopy (B)

Sample No.	*μg. per Liter*					
	Lead		*Cobalt*		*Nickel*	
	A	*B*	*A*	*B*	*A*	*B*
1	6	5	3.4	5	46	46
2	5	3	74	70	28	26
3	19	15	60	56	4	5
4	29	26	47	47	2	2
5	9	8			14	12
6	5	<8			80	87
7	3	<5			42	44
8	5	<4			1	3

Discussion

Table IV shows the results that were found for nickel, cobalt, and lead in several fresh waters. Results obtained by atomic absorption, using the described procedure, are compared with results obtained by spectrographic analysis. The most significant thing about the data is the fact that two different laboratories using two entirely different methods agreed so favorably. The maximum difference for nickel was 7 μg. per liter (sample No. 6, which contained the greatest amount of nickel). The maximum difference for the other samples was 2 μg. per liter. Cobalt was detected in only four samples. The results agree well and there should be no problem determining cobalt by atomic absorption. The results found for lead are in good agreement, but some which were reported by the spectrographic procedure were "less than" values. Known amounts of lead were added to several of these samples and lead re-determined. For all but

Table V. Recovery of Lead by Atomic Absorption

	Present	*Added*	*Total*	*Found*
No.		*μg. of Pb per Liter*		
1	7	5	12	11
2	2	5	7	7
3	5	5	10	10
4	19	10	29	31
5	29	10	39	38
6	9	5	14	13

one sample, the amount recovered was within 1 μg. per liter of the amount of lead added (Table V).

In regard to interferences, none have been found. The alkali and alkaline earth metals are not chelated with the APDC and, therefore, are not extracted. Spectral interferences do not occur. Several minor elements, such as iron, copper, manganese, and zinc at concentrations of 1,000 μg. per liter were added to lead, cobalt, and nickel solutions; however, this was done mainly to check if there was sufficient APDC to chelate the elements and not as a spectral interference effect.

Conclusions

The extraction procedure as described offers a rapid, simple, accurate, and sensitive means for determining lead, cobalt, and nickel in fresh waters. The detection limits are at least one order of magnitude lower than most other wet chemical procedures. There is less chance for contamination since the entire determination is done in one container. The results found are in good agreement with spectrographic analysis and as little as 1 μg. per liter of the element can be determined.

Literature Cited

(1) Berman, E., *At. Absorption Newsletter* 3, 11 (1964).
(2) Burrell, D. C., *At. Absorption Newsletter* 4, 309 (1965).
(3) Durfor, C. N., Becker, E., *U. S. Geol. Surv. Water Supply Papers* 1812 (1964).
(4) Fishman, M. J., Downs, S. C., *U. S. Geol. Surv. Water Supply Papers* 1540-C (1966).
(5) Slavin, W., *At. Absorption Newsletter* 3, 141 (1964).
(6) Sprague, S., Slavin, W., *At. Absorption Newsletter* 20, 11 (1964).

RECEIVED April 24, 1967. Publication authorized by the Director, U. S. Geological Survey.

13

Water Analysis by Atomic Absorption and Flame Emission Spectroscopy

EDWARD A. BOETTNER and FRED I. GRUNDER

Department of Industrial Health, School of Public Health,
University of Michigan, Ann Arbor, Mich.

Several elements (Zn, Pb, Cu, Ni, Ca, Mg, Fe, and Mn) are determined routinely in water samples using atomic absorption spectroscopy. Sodium and potassium are determined by flame emission. The preparation of the samples, the analytical method, the detection limits and the analytical precisions are presented. The analytical precision is calculated on the basis of a sizable amount of statistical data and exemplifies the effect on the analytical determination of such factors as the hollow cathode source, the flame, and the detection system. The changes in precision and limit of detection with recent developments in sources and burners are discussed. A precision of 3 to 5% standard deviation is attainable with the Hetco total consumption and the Perkin-Elmer laminar flow burners.

THIS laboratory is concerned with the analysis of a wide range of materials which include a variety of biological specimens, mineral samples, air particulate matter, and water samples. The information obtained is used to evaluate various individual and environmental problems. Two of the techniques which have been used for water analysis are atomic absorption (*1, 4*) and flame emission (*2*) spectroscopy, and a study of factors affecting these methods is described here. The samples came from a number of sources which included well water and city water. Consequently, the concentration ranges of some of the elements were quite wide. Five determinations were made daily on both the samples and standards for each element over a period of several months to provide sufficient data for an adequate evaluation of precision. At present, ten elements (Na, K, Ca, Mg, Zn, Pb, Mn, Cu, Fe, and Ni) are being determined quantitatively.

To carry out the analysis in the best manner possible, a study was conducted on the various hollow cathode lamps, burners, and optical systems to assess them as to their advantages and disadvantages in the analysis of water. Particular emphasis was given to the comparison of the total consumption and premix burners (*6, 7*). The results are presented here in the form of conservative values attainable of sensitivity and precision, and a discussion of the differences noted.

The first portion of the study was carried out on natural and treated water samples. When the statistical data showed a need to examine several parameters more thoroughly, we shifted to laboratory water standards containing known amounts of five elements which are representative minor and major contaminants in waters.

Experimental Procedure

Water samples were collected in large plastic bottles in the field direct from kitchen spigots. These bottles were acid cleaned and flushed thoroughly with distilled water before use. A 500 ml. sample of this water was placed in an evaporating dish and 15 ml. of concentrated nitric acid added. This was evaporated on a steam bath to approximately 25 ml., transferred to a 50 ml. acid washed volumetric flask, and brought up to volume with double distilled water. This portion was then analyzed for K, Zn, Pb, Mn, Cu, Fe, and Ni, using standards containing the elements of interest.

For the analysis of Ca, Mg, and Na, 10 ml. of the water samples were added to an acid washed 50 ml. volumetric flask. One ml. of a 10% solution of lanthanum, prepared from lanthanum oxide (*3, 8*), was added and brought up to volume with double distilled water. Standards were prepared containing the elements of interest and the lanthanum.

The analyses were performed on a Jarrell-Ash Model No. 32-360 multipass atomic absorption spectrophotometer equipped with a Beckman total consumption three burner set operated on a hydrogen-air mixture, and Westinghouse single element hollow cathode lamps.

Na and K were done by flame emission and the rest of the elements by atomic absorption. The samples and standards were poured into porcelain combustion boats and placed in position for aspiration. Distilled water was aspirated alternately with the solutions to provide a baseline. All data was recorded on a Sargent Model SR recorder with 1 millivolt sensitivity.

Results

Samples were collected, prepared, and analyzed once a month. Every month five determinations for each element were made on both the samples and standards. To obtain precision data eight samples, selected on the basis of their determined concentrations, were prepared and analyzed each month for five months. A large quantity of these eight samples was collected to eliminate natural variations which may occur.

The samples were first run on the Jarrell-Ash instrument, with the three burner set and the same instrument was used as a flame emission spectrophotometer for the determination of sodium and potassium. A statistical summary of analytical precision for eight elements in the eight samples are shown in Table 1. Here the precision is expressed as the % standard deviation (coefficient of variation), which is defined as one hundred times the ratio of standard deviation to the mean concentration (9). It can be seen from this data that the last three elements, which are present in a quantity near the limit of detection, have large deviations. It is clear that these figures could be lowered if the analysis were run using higher concentrations. But our purpose was to evaluate the usefulness of the technique for routine determinations.

Table I. Precision of Analyses Using Original Three-Burner Set

Statistical Summary

Element	*Range (p.p.m.)*	*Mean Conc. (p.p.m.)*	*Std. Dev. (p.p.m.)*	*% Std. Dev.*
Na	0.7 -30.0	8.3	0.9	10.8
K	16.2 -40.2	29.7	3.7	12.4
Mg	4.8 -11.2	8.8	1.0	11.3
Ca	0.4 -29.9	10.3	2.3	22.3
Zn	0.3 - 9.1	1.6	0.3	18.8
Pb	0.10- 0.39	0.25	0.12	48.0
Mn	0.02- 0.36	0.10	0.04	40.0
Cu	0.06- 0.21	0.15	0.08	53.0

To investigate some of the factors affecting precision, lead and magnesium were chosen, as the first represents elements present in concentrations near the limit of detection and the second those elements well above this limit. Figure 1 shows a calibration curve for lead using the Beckman three burner set. The standard deviation of the water standards is indicated at each concentration. The calculations for this curve were based on data taken over a period of four months which would consist of a total of twenty determinations with one set of samples being prepared and analyzed each month. To illustrate the effect of some of the instrumental parameters, Figure 2 shows the % standard deviation plotted versus concentration. The amount of variation caused by instrumental factors, such as the flame, hollow cathode lamps, and detecting system, was expected to be a function of the concentration, and such an effect is shown in Figure 2, where the deviation for the lowest concentration is 50% and for the highest, only 7% Figure 3 shows the calibration curve for magnesium with the standard deviation of the standards indicated. Here, an air flow that aspirated a smaller amount of sample into the flame was used to permit the analysis of the high concentrations of

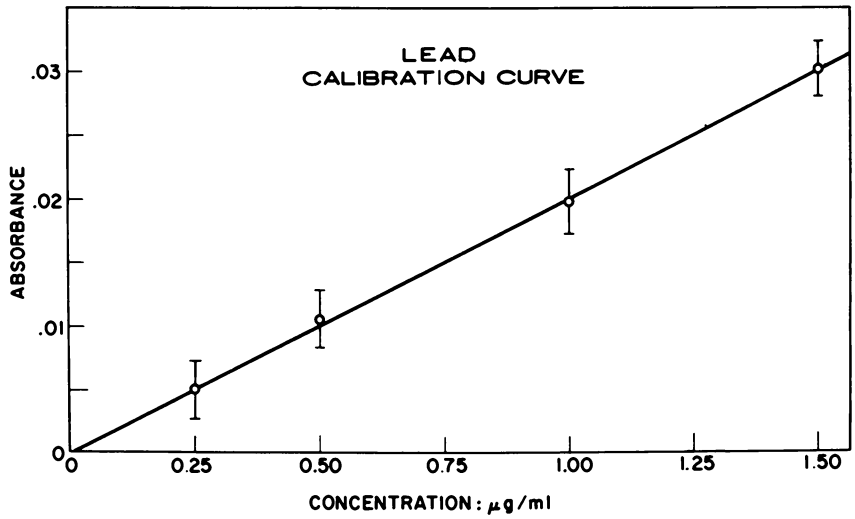

Figure 1. Calibration curve for lead, showing standard deviation of standards

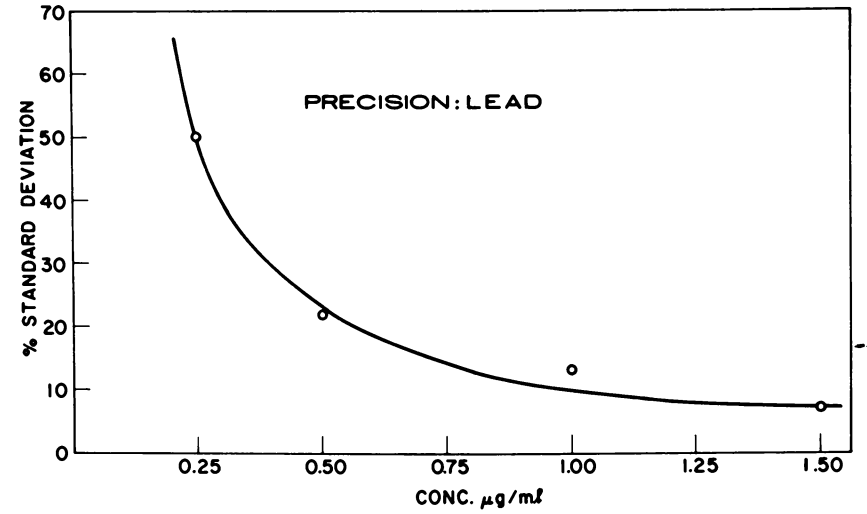

Figure 2. Variation with concentration of the standard deviation of lead

magnesium present without further dilution. By maintaining an optimum fuel-air ratio at this reduced sample consumption condition, no deteriorating effect was noted in the precision values. This figure summarizes work done over a period of six months with a total of thirty determinations. The variance curve shown in Figure 4 indicates results similar to that found with lead with the highest percent standard deviation for the

lowest concentration. The other elements, including those analyzed by flame emission, showed much the same type of characteristic. One can trace the cause of the variations by isolating and examining the different portions of the analytical system. The electronic noise from the detection and amplifier system was found to be very low and its effect on precision or detection limit can be neglected for the elements included in this study. The cathode lamp noise was generally less than 1 or 2% of the signal, but for an analysis at or near the limit of detection, this noise was a factor in both the limit obtained and the precision. By far the greatest contribution to the variations in the analyses was found to be the flame. For example, with the Beckman three burner set, large variations in the data were encountered with iron and so this element was used to evaluate the burner system, using water standards. These variations were apparently caused by large fluctuations in sample consumption, inasmuch as the sample flow rate was varying 20% or more on both a short term (25 minutes) and a day-to-day basis.

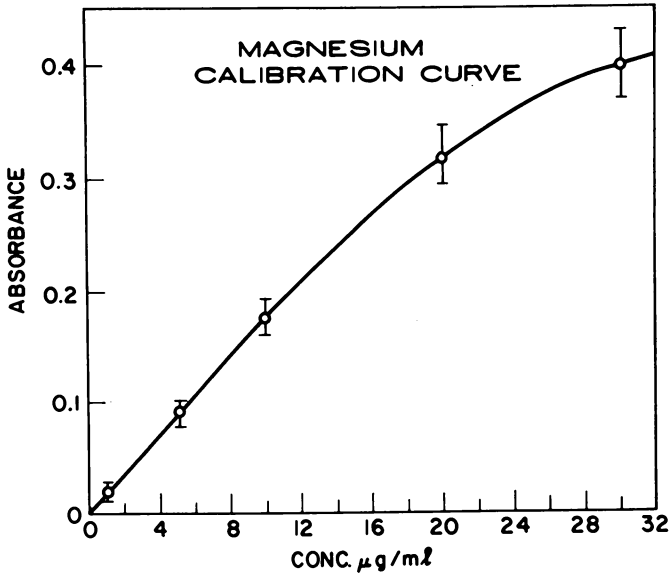

Figure 3. Calibration curve for magnesium, showing standard deviation of standards

At this point it became apparent that: 1) The precision attainable was relatively poor, even in cases well above the limit of detection for several elements. 2) The burners appeared to be the principal factor affecting the precision, inasmuch as the results were about the same in using flame emission as in atomic absorption.

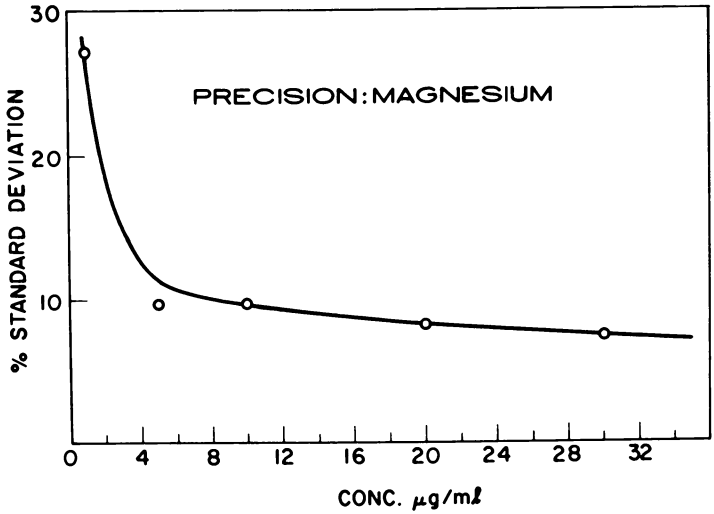

Figure 4. Variation with concentration of the standard deviation of magnesium

To investigate this matter of precision further, as well as the limit of detection, two other types of burners and various hollow cathode lamps were tested under similar conditions. The primary objective was to compare a new single flame total consumption burner, operated on a hydrogen-air fuel mixture, with a premix burner using acetylene and air for fuel. The total consumption burner is the Hetco type, and was used with the Jarrell-Ash spectrophotometer. The premix burner is the Perkin-Elmer type and it was tested as a part of the Perkin-Elmer Model 290 Atomic Absorption Spectrophotometer. Synthetic standards for Ca, Mg, Fe, Pb, and Cu were analyzed in varying concentrations. The data was assessed on both a short-term (daily) basis, where new standard curves were prepared daily, and on a long-term basis, where the shift in the calibration curve was included in the data.

The results obtained in the analysis of lead, comparing the total consumption and premix burners on a short-term basis, is shown in Figure 5. The same hollow cathode lamp was used with both burners. It will be noted that the premix burner exhibits better precision at high concentrations of lead but becomes poorer below 2 p.p.m. At less than 7 p.p.m., the original Beckman three-burner system appears superior to the other two. This was the only element where the three-burner system showed an advantage. Figure 6 shows the precision obtained in analyzing for copper. In this case, the two types of burners perform similarly with the premix burner slightly better when used with the same hollow cathode lamp.

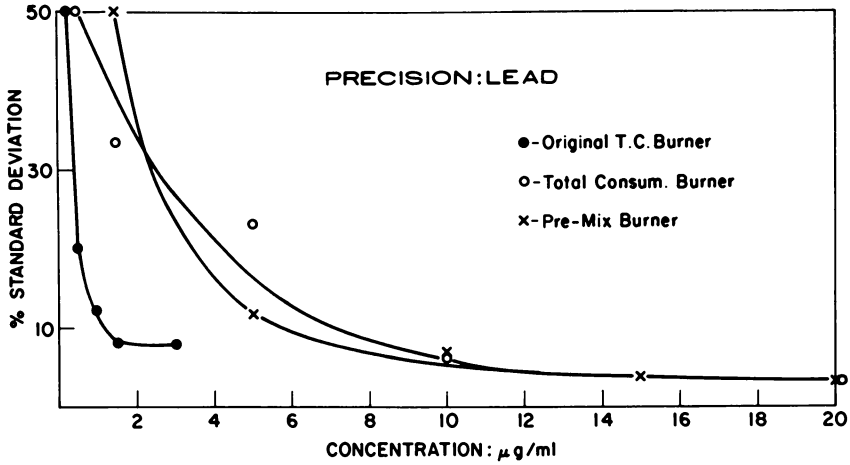

Figure 5. Variation with concentration of the standard deviation of lead for three types of burners

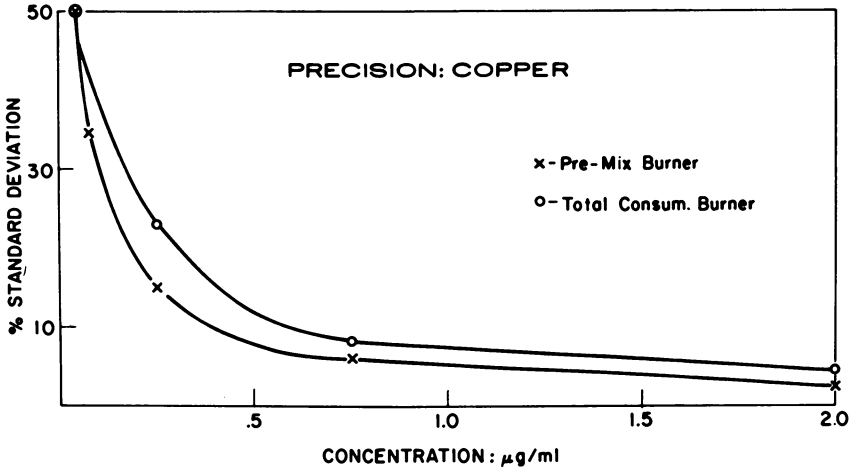

Figure 6. Variation with concentration of the standard deviation of copper for two types of burners

Figure 7 shows the results in the analysis of magnesium in water, where the precision with the premix burner is slightly better. However, a different lamp was used here with each burner so some or all of this difference could be attributable to a difference in the lamps. The older three burner set was rechecked with no improvement in precision. The effect that the hollow cathode lamp can have on precision can be seen in Figure 8, where two different lamps were used with the premix burner

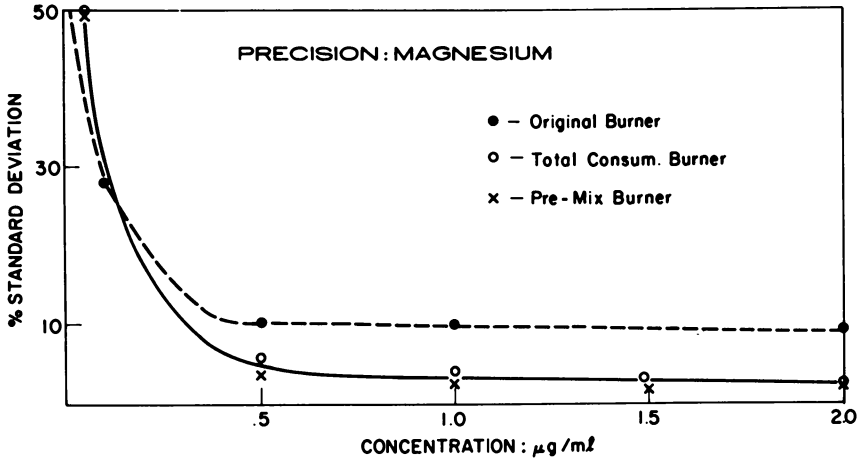

Figure 7. Variation with concentration of the standard deviation of magnesium for three types of burners

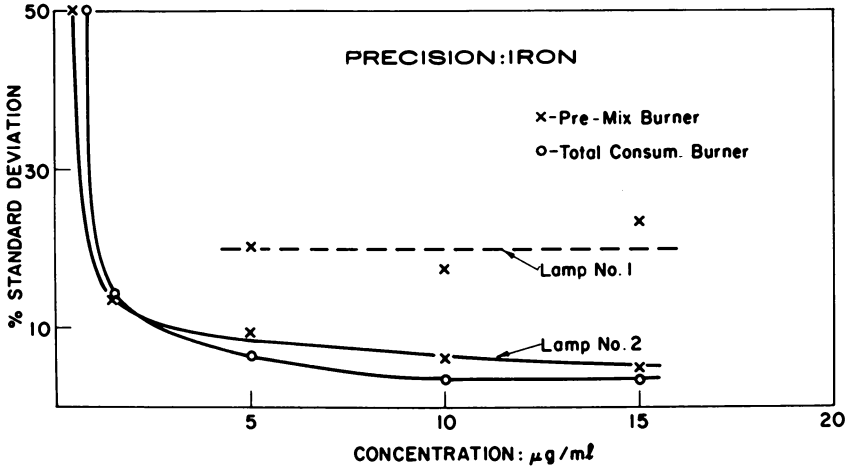

Figure 8. Variation with concentration of the standard deviation of iron for two types of burners and two hollow cathode lamps

in the analysis of iron. Variation in energy output of one lamp affected the precision obtained on the premix burner, such that the values were approximately twice as poor as with a second lamp. The second lamp was used with both flames and the precision data showed the total consumption burner to be about a factor of two better than the premix. The precision obtainable for the two burners in the analysis of calcium is

shown in Figure 9. Here the two burners show about the same performance except for the superiority of the total consumption type at the lower concentrations of calcium.

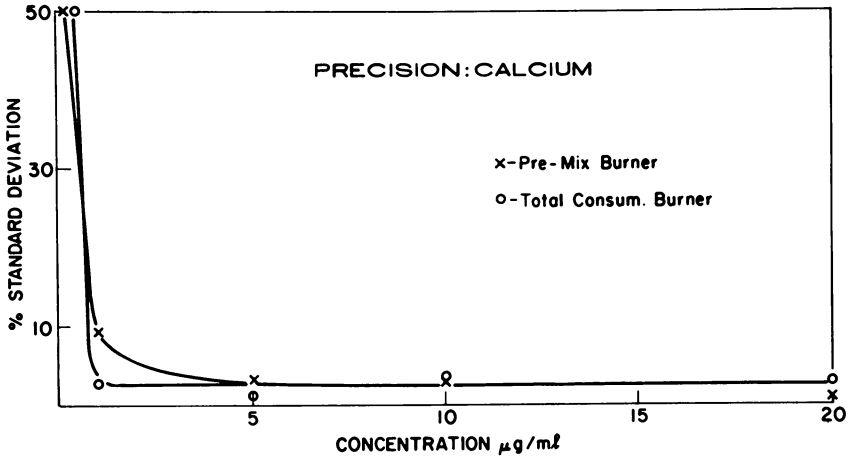

Figure 9. Variation with concentration of the standard deviation of calcium for two types of burners

The data in Figures 5 through 9 were computed on the basis of a single day's run of ten determinations, and then averaged over several days. This then gives the precision obtainable for the case where one checks his calibration curve each day with known standards and then adjusts the curve if any shift is observed. To determine the importance of this procedure, the same absorption data were converted to concentration using a single calibration curve over the period of the tests, with the result that there was generally a decrease in precision. This information is summarized in Table II, where the precisions attainable are given on both the short and long term basis.

Several points are apparent in Table II. First, the precision data on these two burners are considerably better than that shown in Table I for the older three-burner system. This was true both for flame emission and flame absorption. Second, the two burners are about equal on an overall basis for the five elements examined.

The other information summarized here are the detection limits obtainable. It will be noted that these figures are not as low as some cited (*6*) in the literature for a signal-to-noise ratio of two while comparable to others (*5*). For the first three elements, it was neither necessary nor desirable to set up conditions for maximum sensitivity because of the large amount of these elements in water. However, with the last

three elements, instrumental conditions were optimized, except that scale expansion was not used to the maximum. But the most important factor here appears to be the quality of the hollow cathode lamps, in that the limit of detection for any one element will vary from lamp to lamp. Secondly, the sensitivity and stability attainable with a particular lamp will frequently deteriorate with age. An example of this was noted with a particular lamp for lead, where the detection limit dropped from 0.2 p.p.m. to 0.5 p.p.m. within the first few hours of operation. The ability to produce hollow cathode lamps in a uniform and reproducible manner has improved considerably since atomic absorption equipment became available commercially, but the quality control of these lamps is still a problem.

Table II. Limits of Detection and Effects on Overall Precisions for Six Elements When Using Single Calibration Curves and Curves Prepared Daily

	Limit of Detection, p.p.m.		*Precision, % Std. Dev.*	
Element	*Total Cons.*	*Pre-Mix*	*Total Cons. Short Term/ Long Term*	*Pre-Mix Short Term/ Long Term*
Na	0.2		5.0	
Ca	0.5	0.2	2.5/2.5	2.5/4.0
Mg	0.05	0.05	4.0/8.5	2.5/4.0
Fe	0.8	0.5	3.5/3.5	7.0/10.0
Pb	0.5	1.5	5.0/9.0	4.0/4.0
Cu	0.04	0.04	6.0/6.0	5.0/6.0

Conclusions

This study was conducted for the purpose of evaluating atomic absorption and flame emission spectroscopy for the routine quantitative analysis of large numbers of water samples for elements present in quantities ranging from large to trace amounts.

The conclusions reached are as follows:

1. The alkali metals and alkaline earth elements are generally present in sufficient quantities to be analyzed directly without concentration. Flame emission is preferable for the alkalies because of its good sensitivity and few interferences in the analysis of this class of elements in waters and because the technique eliminates the need for hollow cathode lamps. For the alkali earth elements, the flame emission method is still applicable, but with some problems owing to chemical interferences in some waters. Atomic absorption is preferred for this class of elements and although the chemical interference problem still exists, it is not as serious as in flame emission. Those elements present in amounts less than

their limit of detection require concentration by evaporation or extraction before analysis by atomic absorption.

2. The two instrumental components which have the most significant effect on the limit of detection and precision of analysis are the burners and the hollow cathode lamps. For the two instruments used in this study, there was no evidence that other components (monochromator, detector, amplifier, etc.) were limiting factors in the detection limit or precision.

3. Of the two types of burners available (total consumption and pre-mix burners) neither has an over-all advantage for the five elements compared.

4. The state of the art in the production of hollow cathode lamps still leaves much to be desired, both as to uniformity between lamps and changes within single lamps with time.

5. The precision of analysis can be within 3 to 5% standard deviation if care is taken to check calibration curves frequently. Also, frequent maintenance of the burners is necessary to attain this precision consistently.

6. Even with the difficulties cited above, the combination of flame emission and atomic absorption spectroscopy has become in a very short time one of our better methods for the analysis of waters for cations for the following reasons: limited sample preparations necessary, high sensitivity, good analytical precision, low cost, and simplicity of equipment.

Literature Cited

(1) Biechler, D. G., *Anal. Chem.* **37**, 1054 (1965).
(2) Dean, John A., "Flame Photometry," McGraw-Hill Book Co., New York, 1960.
(3) Dickson, Richard E., Johnson, C. M., *Appl. Spectr.* **20**, No. 4, 214 (1966).
(4) Fishman, M. J., Downs, S. C., *U. S. Geol. Surv. Water Supply Papers* **1540C** (1966).
(5) Mavrodineanu, R., "Encyclopedia of Industrial Chemical Analysis," F. D. Snell, C. L. Hilton, eds., p. 160, Interscience, New York, 1966.
(6) Robinson, James W., "Atomic Absorption Spectroscopy," Marcel Dekker, Inc., New York, 1966.
(7) West, T. S., *Nat. Bur. Std. (U. S.) Monograph* **100**, 266 (1967).
(8) Yofe, J., Finkelstein, R., *Anal. Chim. Acta* **19**, 166 (1958).
(9) Youden, W. J., "Statistical Methods for Chemists," John Wiley & Sons, Inc., New York, 1951.

RECEIVED April 24, 1967. This investigation was supported in part by USPHS Research Grant OH-00232, Division of Occupational Health, Bureau of State Services.

Analysis of Industrial Waters by Atomic Absorption

J. A. PLATTE

Calgon Corporation, Hall Laboratories Division, Pittsburgh, Pa.

Simplicity, rapidity, and specificity have caused adoption of atomic absorption as a standard method in water analysis. Often solutions must be concentrated prior to measurement. Freezing, evaporation, ion exchange, and solvent extraction techniques have been reported. This paper describes a method for concentrating ferric iron, copper, zinc, cadmium, and lead using sodium diethyldithiocarbamate and methyl isobutyl ketone. Data shows increase in sensitivity caused by (1) concentrating effect of extraction, and (2) choice of the ketone solvent in preference to water. Recovery data on various industrial waters indicate that the method is reliable, reproducible, and accurate.

In the field of water analysis, an increasing number of laboratories are adopting atomic absorption as a standard method for the determination of many metals. Simplicity, rapidity, and specificity are the predominant factors for its wide acceptance, particularly in areas where the number of water samples analyzed is large (3). However, the concentration of certain metals in many industrial water applications must be maintained and controlled below the practical limit of detectability by atomic absorption. For instance, in modern high pressure boiler operations, the desired limit of iron, copper and zinc in the boiler feedwater cycle is usually less than 5-10 parts per billion (p.p.b.). The concentration of lead in drinking water should be less than 50 p.p.b. Therefore, when the metal or metals of interest are present in the low p.p.b. range, the constituents to be measured in the sample must be concentrated in some manner before analysis by atomic absorption. Concentration by freezing, evaporation, ion exchange, and solvent extraction of metal organic complexes has been reported by others. The solvent extraction

technique was chosen for investigation because of its simplicity and the definite possibility that several metals could be simultaneously extracted in one operation.

Allan (*1*) has shown that when copper or the copper complex of ammonium pyrrolidene dithiocarbamate is dissolved or extracted into methyl isobutyl ketone (MIBK), sensitivity is increased 3.7 to 4.7 times over the same concentration of copper in aqueous solution depending on the type of burner employed. A further increase in sensitivity can be gained by extracting metal ions from a large volume of sample into a much smaller volume of an organic solvent. The total relative gain in sensitivity is equal to the gain caused by the organic solvent times the number of concentrations obtained by organic extraction.

Malissa and Schoffmann (*2*) describe the preparation of ammonium pyrrolidene dithiocarbamate and show it to be advantageous because it is a broad spectrum complexing agent, and that its metal complexes can be extracted over fairly broad pH ranges. However, we found that the commercially available material would not dissolve when prepared according to directions given in the literature.

Sodium diethyldithiocarbamate (*4*) forms complexes with many metals which are more or less soluble in various organic solutions. Preliminary tests showed that at pH 2–3, the carbamate complexes of ferric iron, zinc, cadmium, copper, and lead are extractable from water with methyl isobutyl ketone.

Experimental Work

Comparison tests shown in Table I were run on small amounts of iron, copper, zinc, lead, and cadmium in methyl isobutyl ketone to determine the increase in sensitivity over the same concentration of metals in water solutions. The organic solutions were prepared by adding known volumes of acidified aqueous standards by means of a micro-buret to 5 ml. methyl alcohol and diluting to 100 ml. with methyl isobutyl ketone. The absorbance of each metal was measured by a Perkin-Elmer 303 Atomic Absorption Spectrophotometer using the standard instrumental parameters suggested by the manufacturer for each metal. The absorbance values were taken either at 3X or 10X range expansion using a recorder. When spraying organic solvents into the flame, the volume of acetylene must be reduced until the flame becomes nonluminous. The zero reference solution contained a quantity of reagent grade water equal to that used to prepare the standards and the same volume of methyl alcohol and methyl isobutyl ketone.

The relative increase in sensitivity for lead is quite surprising. The test was repeated several times with higher concentrations of lead and the same values were obtained. The values found for iron and copper agree fairly well with those reported by Allan (*2*). However, the increase for zinc does not agree with that reported in the same article. He found that zinc had the same relative increase as that for copper.

Table I. Absorbance Values of Water vs. Methyl Isobutyl Ketone

Metal	*Wavelength*	*Concentration, p.p.m.*	*Absorbance*		*Relative Increase in Sensitivity*
			Water	*MIBK*	
Fe^{3+}	2483.3	0.25	0.018	0.067	3.7
		0.50	0.037	0.140	3.8
Cu^{2+}	3247.5	0.25	0.036	0.168	4.6
		0.50	0.072	0.331	4.6
Pb^{2+}	2170	0.5	0.009	0.056	6.2
		1.0	0.018	0.114	6.3
Zn^{2+}	2138	0.25	0.035	0.105	3.0
		0.50	0.071	0.201	2.9
Cd^{2+}	2288	0.25	0.022	0.055	2.5
		0.50	0.050	0.130	2.6

Extraction Procedure

Several tests were run to determine the efficiency and precision of extraction of metal complexes with sodium diethyldithiocarbamate and methyl isobutyl ketone by the following procedure. A single liter solution was prepared to contain 0.25 p.p.m. of the following: ferric iron, copper, zinc, cadmium, and lead in 1% hydrochloric acid (V/V). The solution was split into four 250-ml. portions. The concentration of each metal was determined in the normal manner prescribed for aqueous solutions on one portion. The remaining three portions were adjusted to pH 2.5 with an ammonium acetate-acetic acid buffer solution and transferred to 500-ml. separatory funnels. Twenty ml. of a 5% sodium diethyldithiocarbamate solution was added to each sample and shaken. Each solution was then extracted with two 20-ml. portions of methyl isobutyl ketone. The extracts were combined for each sample and diluted to 50 ml. with methyl alcohol. The absorbance of each metal was determined in the three 50-ml. organic solutions.

By this procedure, each metal was theoretically concentrated five times. Using the factors given in Table I, the total theoretical increase in sensitivity of absorbance values over those for aqueous solutions can be calculated as shown in Table II. For instance, the total increase in sensitivity for lead would be 31 (6.2 × 5). By calculation, 31 × 0.25 p.p.m. taken for analysis should be equal to 7.75 p.p.m. lead when the absorbance

Table II. Recovery of Various Metals by Complex Solvent Extraction

Metal	*Concentration Factor*	*p.p.m. Found*		% Recovery
		Theoretical	*Actual*	
Fe^{3+}	19.4	4.85	4.6, 4.8, 4.7	93-97
Cu^{2+}	23	5.75	5.6, 5.6, 5.7	97-99
Zn^{2+}	15	3.75	3.6, 3.5, 3.4	91-96
Pb^{2+}	31	7.75	7.8, 7.8, 7.7	99-101
Cd^{2+}	13	3.25	3.0, 3.0, 3.1	92-95

value for the organic solvent is read from a curve prepared with aqueous standards, providing the metal was completely extracted. Table II compares the theoretical and determined values. The rate of recovery was checked again by comparing the absorbance of the three test solutions against calibration curves prepared by adding known amounts of standards to 5 ml. methyl alcohol and diluting to 50 ml. with methyl isobutyl ketone.

The buffer solution used above was prepared by dissolving 62.5 grams reagent grade ammonium acetate ($NH_4C_2H_3O_2$) in about 200 ml. deionized water. Add exactly 17.5 ml. glacial acetic acid and dilute to 250 ml. Remove possible meal contaminants by adding 20 ml. of a 5% sodium diethyldithiocarbamate solution and extract the buffer solution with two 50-ml. portions of methyl isobutyl ketone.

Analysis of Samples

Recovery tests were run on samples of various industrial waters by the above proposed atomic absorption-solvent extraction procedure. However before extraction, all samples were acidified with 1 ml. concentrated hydrochloric acid per 100 ml. sample and boiled for five minutes to dissolve precipitated metals. The samples were then cooled and filtered to remove any remaining particulate matter which could clog the atomizer. For the determination of iron, 0.1 gram potassium persulfate was added in addition to the acid and then boiled to oxidize ferrous iron to the ferric state. The values shown in Table III are typical of the results that can be expected.

Table III. Recovery Tests on Various Types of Water

Type of Sample	*Metal Determined*	*Amount Present p.p.b.*	*Amount Added p.p.b.*	*Total Recovered p.p.b.*
Condensate	Iron	8	5	12
Saturated Steam	Iron	12	10	24
Boiler Feed	Iron	27	10	35
Condensate	Copper	5	5	8
Saturated Steam	Copper	8	5	12
Condensate	Zinc	5	5	11
Treated Plating Waste	Zinc	22	10	30
River Water	Cadmium	18	15	31
Surface Water	Cadmium	7	5	11
Tap Water	Lead	8	5	13
Lake Water	Lead	12	10	19

Much of the iron present in most condensates exists as finely divided suspended iron oxide particles. Since most operators of high pressure boiler plants are concerned with the total concentration of iron in the various water cycles, solubilizing the suspended iron (usually hematite) is a necessary part of any procedure for this determination. Tetlow and Wilson (5) have shown that the suspended iron oxide is not completely

dissolved when condensates are acidified with hydrochloric acid and boiled. They recommend thioglycolic acid and show it to be much more effective than hydrochloric acid. We prefer ascorbic acid because of the odor problem with thioglycolic acid and the fact that comparative tests made in our laboratory indicate that ascorbic acid is comparable to thioglycolic acid for effectively dissolving iron oxide compounds. However, when either of these reducing acids is used, very low iron values are found by the proposed extraction method. Evidently, either ferrous iron forms no complex with sodium diethyldithiocarbamate or the complex is not extractable with methyl isobutyl ketone. This observation was confirmed from tests made with standard solutions containing ferrous iron and the recovery by the prepared solvent extraction technique was almost nil.

Therefore, we do not recommend solvent-extraction for condensates treated with either thioglycolic acid or ascorbic acid. Perhaps the excess reducing acid could be destroyed and the iron oxidized to the ferric state, but this approach would not be practical for a number of obvious reasons.

Table IV. Comparison of Detection Limits

	Gain in Sensitivity			*Detection Limit, p.p.b.*	
Metal	*Concentration by Extraction*	*Caused by Organic Solvent*	*Overall*	*Aqueous*	*By Proposed Method*
Fe^{3+}	5	3.8	19.4	50	2-3
Cu^{2+}	5	4.6	23	5	0.2
Zn^{2+}	5	3.0	15	5	0.3
Pb^{2+}	5	6.2	31	150	5
Cd^{2+}	5	2.6	13	10	0.7

Detection Limits

Table IV compares the present reported limit of detectability of iron, copper, zinc, lead, and cadmium in aqueous solutions with that obtainable with the proposed solvent extraction procedure. Detectability is defined as that concentration of metal which gives a signal twice the variability of the background. Since the amount of metal recovered as shown in Table II was not 100% for most metals, the limit of detectability by this method should be increased by about 5–10%.

Conclusion

The results of this investigation show that the method described can be effectively used when the concentration of metals in water is too low for analysis by normal atomic absorption procedures provided the metals form solvent extractable complexes with sodium diethyldithiocarbamate. We use this method routinely for the determination of iron, lead,

and copper in high brines and phosphate compounds and for lead and cadmium in most industrial waters. By increasing the ratio of sample to organic solvent, the practical level of detectability should be even less than that shown in Table IV.

Literature Cited

(1) Allan, J. E., *Spectrochim. Acta* 17, 467 (1961).
(2) Malissa, H., Schoffmann, E., *Mikrochim. Acta* 1, 187 (1955).
(3) Platte, J. A., Marcy, V. M., *Proc. Am. Power Conf.* 27, 851 (1967).
(4) Sandell, E. B., "Colorimetric Determination of Traces of Metals," 2nd ed., p. 304, Interscience Publishers, Inc., New York, 1950.
(5) Tetlow, J. A., Wilson, A. L., *Analyst* 89, 447 (1964).

RECEIVED April 24, 1967.

Evaluation of Laboratory Methods for the Analysis of Inorganics in Water

E. F. McFARREN and R. J. LISHKA

Analytical Reference Service, National Center for Urban and Industrial Health, Public Health Service, U. S. Department of Health, Education, and Welfare, Cincinnati, Ohio

Recent studies conducted by Analytical Reference Service and involving the analysis of inorganics in water have been of methods for (1) cadmium, chromium, aluminum, iron, manganese, magnesium, lead, copper, zinc, and silver (Water Metals No. 3, Study 23); (2) arsenic, boron, selenium, beryllium, and vanadium (Water Trace Elements No. 2, Study 26); and (3) ammonia nitrogen, organic nitrogen, nitrate nitrogen, phosphates, and silicates (Water Nutrients No. 1, Study 27). A summation of the major findings of these three studies conducted to determine the precision and accuracy of some of the procedures given in "Standard Methods for the Examination of Water and Wastewater" is the subject of this paper.

Analytical Reference Service (ARS) is a voluntary association of 302 laboratories responsible for the detection, identification, and measurement of contaminants in the environment. These participants include 51 municipal, 88 state, 43 Federal, and 36 foreign agencies; 59 industries; and 25 universities.

The primary purpose of ARS is to evaluate analytical methods by submitting samples of known composition to member laboratories for analysis by a specified method or methods. From the analytical results obtained, the statistical parameters of precision and accuracy are calculated and used as measures of the acceptability or non-acceptability of the method(s). In this effort, ARS cooperates with organizations such as the American Public Health Association, the American Water Works Association, and the Water Pollution Control Federation to determine the suitability of methods for inclusion in "Standard Methods for the Exami-

nation of Water and Wastewater." Inasmuch as the statistical treatment of the data not only determines the precision and accuracy of the methods but also ranks the data and rejects values grossly in error, a coincidental benefit to the individual participant is that the program serves also as a check on their laboratory work.

Since the inception of ARS in 1953, 27 studies involving more than 80 different methods have been completed. Of these studies, 18 have entailed determinations of substances in water, two in food, and four in air; and three had to do with radiochemistry. Eight of the studies have been repeated either to re-evaluate old methods or to determine the value of new ones.

Recent studies involving the analysis of inorganics in water have been of methods for (1) cadmium, chromium, aluminum, iron, manganese, magnesium, lead, copper, zinc, and silver (Water Metals No. 3, Study 23); (2) arsenic, boron, selenium, beryllium, and vanadium (Water Trace Elements No. 2, Study 26); and (3) ammonia nitrogen, organic nitrogen, nitrate nitrogen, phosphates, and silicates (Water Nutrients No. 1, Study 27). A summation of the major findings of these three studies constitutes the subject of this paper.

Design of the Studies

In the Water Metals No. 3 Study, 79 participating laboratories were instructed to dilute 5 ml. of a provided concentrated water sample to 1 liter and analyze for nine specified metals. The water sample was prepared as a concentrated solution to ensure greater stability of the sample and to reduce shipping costs. The solution was shipped in sterile JEB tubes and consisted of sterile, distilled, deionized water which when diluted as instructed contained the concentration of metallic compounds indicated in Table I.

Table I. Composition of Water Metals Sample

Compound	*Metal*	*mg./liter*
$K_2Al_2(SO_4)_4 \cdot 24H_2O$	Al	0.50
Copper metal	Cu	0.47
$Fe(NH_4)_2(SO_4)_2 \cdot 6H_2O$	Fe	0.30
$KMnO_4$	Mn	0.12
Zinc metal	Zn	0.65
$AgNO_3$	Ag	0.15
Cadmium metal	Cd	0.05
$K_2Cr_2O_7$	Cr	0.11
$Pb(NO_3)_2$	Pb	0.07

The solid compounds were dissolved in excess nitric acid in order to reduce the final pH below 1.0. The extreme acidity was necessary to prevent precipitation and adsorption of the metals on the walls of the container. Repeated analysis in the ARS laboratory indicated that there was no change in the sample stored in a boro-silicate glass bottle.

In their analysis for cadmium, lead, silver, and zinc, participants were instructed to use the procedures sent with the sample; these procedures now appear in the 12th edition of "Standard Methods for the Examination of Water and Wastewater." For the remaining metals (aluminum, copper, iron, manganese, and chromium), the participant was permitted to use the method of his choice. The method chosen often turned out to be the Standard Method.

The design of the Water Trace Elements No. 2 Study was similar to that of the Water Metals study in that a concentrate was provided and the participants were asked to dilute it from 5 ml. to a liter.

It consisted of sterile, distilled, deionized water containing the concentrations indicated in Table II when diluted as instructed.

Table II. Composition of Water Trace Elements Sample

Compound	*Metal*	*mg./liter*
SeO_2	Se	0.02
$BeSO_4 \cdot 4H_2O$	Be	0.25
H_3BO_3	B	0.24
As_2O_3	As	0.04
NH_4VO_3	V	0.006

Copies of procedures for the analysis of arsenic, selenium, and beryllium were also provided. Procedures for the other two metals (boron and vanadium) were suggested, and references to their appearance in the literature were provided. Fifty-nine laboratories participated in this study.

In the study of water nutrients, three samples containing various concentrations of silicate, phosphate, ammonia nitrogen, organic nitrogen, and nitrate nitrogen were provided, and each participant was requested to do a single analysis for each element in each of the three samples. The solutions were shipped in sterile, sealed glass ampoules and consisted of sterile, deionized water containing the concentrations indicated in Table III when diluted as instructed.

The chloride was added as an interference in the nitrate determination and the pH was adjusted to 1.5 with sulfuric acid to preserve the samples. In the determination of silica, the participants were to analyze the samples by either the colorimetric molybdosilicate method or the heteropoly blue method. Phosphates were to have been determined by

the aminonaphtholsulfonic acid method or the stannous chloride method (with or without extraction). For nitrogen analysis, participants were given a choice of the phenoldisulfonic acid method, brucine method, or modified brucine method. Ammonia nitrogen was to have been determined either by distillation followed by nesslerization, distillation followed by titration, or direct nesslerization. Finally, organic nitrogen was to be determined by either boiling to remove ammonia followed by kjeldahl digestion and nesslerization, boiling followed by kjeldahl digestion and titration, or total kjeldahl minus ammonia. All of these procedures, except the modified brucine, are Standard Methods, which were to be evaluated in this study.

Table III. Composition of Water Nutrients Samples

		mg./liter		
Compound	*Nutrient*	*Sample 1*	*Sample 2*	*Sample 3*
$Na_2SiO_3 \cdot 9H_2O$	SiO_2	5.00	15.00	30.00
$(NaPO_3)_6$	PO_4	10.00	5.00	0.50
KNO_3	N(nitrate)	1.00	1.00	1.00
NH_4Cl	N(ammonia)	0.20	0.80	1.50
Glutamic acid	N(organic)	1.50	0.80	0.20
NaCl	Cl(interference)	10.00	200.00	400.00

In addition, a few selected laboratories were requested to analyze the samples for nitrate by the chromotropic acid method, and another group was to determine any or all of the nutrients by autoanalyzer.

A total of 110 laboratories participated in the water nutrients study.

Treatment of the Data

Before statistical parameters were developed, the mean of the results reported by each participant in the water metals and water trace elements studies were plotted on normal probability paper to determine the distribution. Values showing a gross deviation from the normal distribution were then rejected as nonrepresentative because of errors in calculation, dilution, or other indeterminate factors and were not used in subsequent calculations. For the water nutrients study, a somewhat more sophisticated, and more objective, computer-programmed technique was used for rejection of outliers. As verified by plotting of the data on probability paper, however, the results were about the same.

The mean and standard deviation as used in this report have their usual meaning. The standard deviation expressed as a percentage of the mean (relative standard deviation) is used as a measure of the precision of the results. To obtain a measure of the accuracy of the results, the mean

error expressed as a percentage (relative error) of the true value is used. The mean error is equal to the difference between the mean of the series of test results and the true value.

Results

As can be seen in Table IV, neither the aluminon (*2*) nor spectrographic (*23*) method gave satisfactory results in the determination of aluminum. In fact, on the basis of this and previous studies, it seems safe to state that no satisfactory procedure exists for aluminum.

Table IV. Summary of Data on Aluminum, Copper, and Iron

Method	*No.*	*Mean*	*Std. Dev.*	*Mean Error*	*Relative Std. Dev.*	*Relative Error*
		Aluminum 0.50 mg./liter				
Aluminon [a]	44	0.400	0.153	0.10	38.2	20.0
Spectrograph	4	0.235	0.091	0.26	38.7	52.0
		Copper 0.47 mg./liter				
Cuprethol [a]	25	0.514	0.090	0.04	17.5	8.5
Sodium diethyl dithiocarbamate	12	0.495	0.058	0.03	11.7	6.0
Bathocuproine [a]	7	0.470	0.021	0.00	4.4	0.0
Neocuproine [a]	6	0.448	0.079	0.02	17.6	4.2
Zinc dibenzyl dithiocarbamate	4	0.460	0.016	0.01	3.4	2.1
Spectrograph	3	0.400	0.056	0.07	14.0	14.9
Atomic absorption	3	0.477	0.011	0.01	2.3	2.1
Polarograph	2	0.557	0.125	0.09	22.5	19.1
		Iron 0.30 mg./liter				
1, 10-Phenanthroline [a]	44	0.337	0.086	0.04	25.5	13.3
Thiocyanate [a]	11	0.352	0.085	0.05	24.2	16.6
Tripyridine	6	0.260	0.162	0.04	62.4	13.3
Spectrograph	5	0.280	0.090	0.02	32.2	6.6
Bathophenanthroline	3	0.327	0.006	0.03	1.8	10.0
Atomic absorption	2	0.295	0.078	0.00	26.4	0.0

[a] Standard Method.

In the determination of copper, the best results were obtained by the bathocuproine (*8*) procedure, although the zinc dibenzyl dithiocarbamate (*28*) and atomic absorption (*1*) procedures produced essentially the same precision and accuracy.

The bathophenanthroline (*25*) and the 1, 10-phenanthroline (*9*) procedures produced the best results in the determination of iron, except that the precision of the 1, 10-phenanthroline procedure was rather poor.

Five different methods for the determination of manganese were studied (Table V). The colorimetric procedure using persulfate (*10*) to oxidize manganous compounds to permanganate gave good accuracy, but the precision was only fair.

Table V. Summary of Data on Manganese, Silver, and Cadmium

Method	*No.*	*Mean*	*Std. Dev.*	*Mean Error*	*Relative Std. Dev.*	*Relative Error*
		Manganese 0.12 mg./liter				
Persulfate[a]	33	0.118	0.031	0.00	26.3	0.0
Periodate[a]	14	0.150	0.054	0.03	36.0	25.0
Spectrograph	4	0.113	0.022	0.01	19.4	8.3
Atomic absorption	3	0.127	0.025	0.01	19.6	8.3
Formaldoxime	3	0.180	0.069	0.06	38.4	50.0
		Silver 0.15 mg./liter				
Dithizone[a]	14	0.049	0.030	0.00	61.0	66.6
Spectrograph	3	0.090	0.066	0.06	73.5	40.0
		Cadmium 0.05 mg./liter				
Dithizone[a]	44	0.053	0.013	0.00	24.5	0.0
Polarograph	4	0.040	0.034	0.01	68.0	20.0

[a] Standard Method.

For the determination of silver, neither the dithizone (*19*) nor the spectrographic (*18*) method was found to be satisfactory. In the determination of cadmium, however, the dithizone (*5*) method gave excellent accuracy, but poor precision.

In the determination of chromium (Table VI), none of the methods studied gave very good results. The accuracy of the permanganate (*6*) and alkaline hypobromite (*7*) procedures were only fair, and the precision of the permanganate method was rather poor.

Atomic absorption (*27*) appeared to be the best method for the determination of lead.

The results obtained on zinc indicated that all methods were reasonably good. Unfortunately, the high acidity of the sample attacked the stopper of the JEB tube and leached zinc from the rubber. Because of the many variables involved, such as the position in which the tube was stored and the length of time that the solution was in contact with the rubber, the amount of contamination was indeterminate. The accuracy and precision of the zinc data were, therefore, questionable and are not reported here.

As indicated in Table VII, only one method for each of the trace elements was studied; namely, the method suggested.

Table VI. Summary of Data on Chromium and Lead

Method	*No.*	*Mean*	*Std. Dev.*	*Mean Error*	*Relative Std. Dev.*	*Relative Error*
			Chromium 0.11 mg./liter			
Permanganate[a]	31	0.092	0.044	0.03	47.8	27.2
Alk. hypobromite[a]	7	0.089	0.023	0.03	25.9	27.2
Hex. chromium[a]	5	0.010	0.012	0.10	120.0	91.0
Spectrograph	4	0.145	0.053	0.04	37.6	36.3
Polarograph	3	0.130	0.020	0.03	18.4	27.2
			Lead 0.07 mg./liter			
Dithizone[a]	43	0.076	0.032	0.006	42.1	8.5
Spectrograph	3	0.093	0.058	0.023	62.4	32.8
Atomic absorption	2	0.085	0.007	0.015	8.2	21.4

[a] Standard Method.

Table VII. Summary of Data on Trace Elements

Method	*No.*	*Mean*	*Std. Dev.*	*Mean Error*	*Relative Std. Dev.*	*Relative Error*
			Selenium 0.020 mg./liter			
3, 3′ diamino-benzidine[a]	35	0.021	0.0044	0.001	21.2	5.0
			Beryllium 0.250 mg./liter			
Aluminon	32	0.247	0.0176	0.003	7.13	12.0
			Boron 0.240 mg./liter			
Curcumin	30	0.240	0.0547	0.000	22.8	0.0
			Arsenic 0.040 mg./liter			
Silver diethyl dithiocarbamate[a]	46	0.040	0.0055	0.000	13.8	0.0
			Vanadium 0.006 mg./liter			
Gallic acid	22	0.006	0.0012	0.000	20.0	0.0

[a] Standard Method.

The aluminon (*24*) procedure for the determination of beryllium produced the best precision and the curcumin (*4*) procedure for boron, the poorest. In general, all of the methods (*3, 15, 20*) were found to be acceptable.

In the determination of silica, only about half of the participants digested the sample with sodium bicarbonate, because the sample appeared to contain no insoluble material. Unfortunately, the conditions present in the sample converted most of the silica in the sample to a molybdate-unreactive state. Although these results are not reported here,

it is interesting to note that the molybdate reactive silica concentration appeared to be about the same in all samples (slightly more than 1 mg./liter), even though the total silica content was quite different. The remaining half who did digest the sample with bicarbonate obtained nearly equivalent results by using either the colorimetric molybdosilicate (*16*) or heteropoly blue (*17*) method except at the lower concentrations (Table VIII), where poor results were obtained by the heteropoly blue method.

Table VIII. Summary of Data on Silica

Method	*No.*	*Mean*	*Std. Dev.*	*Mean Error*	*Relative Std. Dev.*	*Relative Error*
			Sample 1, 5.0 mg./liter			
Molybdosilicate	19	4.6	0.66	0.4	14.3	7.8
Heteropoly blue	11	4.8	1.32	0.2	27.2	3.0
Autoanalyzer [a]	3	1.3	0.21	3.7	16.4	95.3
			Sample 2, 15.0 mg./liter			
Molybdosilicate	19	14.4	1.20	0.6	8.4	4.2
Heteropoly blue	11	15.4	2.78	0.4	18.0	2.9
Autoanalyzer [a]	3	1.5	0.53	13.5	35.2	95.0
			Sample 3, 30.0 mg./liter			
Molybdosilicate	20	27.0	2.09	3.0	7.7	9.8
Heteropoly blue	10	28.5	1.38	1.5	4.9	5.1
Autoanalyzer [a]	3	1.8	0.78	28.2	43.4	94.0

[a] Undigested.

In the determination of phosphate, almost half of the participants neglected to hydrolyze the sample and obtained low results since the samples contained hexametaphosphate. These results are not included in Table IX.

As can be seen in Table IX, the stannous chloride (*14*) method without extraction was the most popular and gave the best results. Good results were also obtained with the aminonaphtholsulfonic acid (*13*) and auto analyzer methods except at the lower concentration, where poor results were obtained.

All three samples contained the same amount of nitrate (1.0 mg./liter) but increasing concentrations of chloride; namely, 10, 200 and 400 mg./liter. The best results were obtained with the modified brucine (*21*) method (Table X), although nearly equal precision and accuracy were obtained by the chromotropic acid (*26*) method. All nitrate methods, however, failed to produce accurate results in the presence of a moderately high chloride concentration.

Table IX. Summary of Data on Phosphate

Method	*No.*	*Mean*	*Std. Dev.*	*Mean Error*	*Relative Std. Dev.*	*Relative Error*
		Sample 1, 10.0 mg./liter				
Stannous chloride	33	9.50	0.816	0.50	8.5	5.0
Aminonaphthol-sulfonic acid	18	9.16	0.374	0.84	4.0	8.4
Stannous chloride with extraction	4	9.19	0.448	0.81	4.8	8.2
Autoanalyzer	5	9.50	0.401	0.50	4.2	5.0
		Sample 2, 5.0 mg./liter				
Stannous chloride	33	4.81	0.515	0.19	10.7	3.8
Aminonaphthol-sulfonic acid	20	4.79	0.635	0.21	13.2	4.2
Stannous chloride with extraction	6	6.07	2.830	1.07	46.6	21.2
Autoanalyzer	5	4.45	0.168	0.55	3.7	11.2
		Sample 3, 0.5 mg./liter				
Stannous chloride	32	0.52	0.099	0.02	19.1	4.0
Aminonaphthol-sulfonic acid	20	0.65	0.314	0.15	48.3	30.0
Stannous chloride with extraction	6	0.76	0.258	0.26	33.9	52.0
Autoanalyzer	5	0.51	0.195	0.01	38.3	2.0

The determination of ammonia by direct nesslerization (*12*) and by autoanalyzer (22) produced good accuracy and precision (Table XI), except at the lower concentration, in samples containing no interference, but distillation (*11*) introduced a substantial error.

Regardless of the method used, the measurement of organic nitrogen was poor (Table XII), and, in fact, at a concentration of 0.20 mg. per liter, all were unacceptable.

Conclusions

On the basis of this and previous studies, no satisfactory procedure exists for determining aluminum. In the determination of copper the best results were obtained by the bathocuproine procedure. Likewise, the bathophenanthroline procedure produced the best results in the determination of iron. Manganese was best determined by persulfate oxidation of manganous compounds to permanganate. The dithizone procedure gave good results in the determination of cadmium, but poor results for silver. In fact, none of the methods studied gave good results for silver,

Table X. Summary of Data on Nitrate

Method	No.	Mean	Std. Dev.	Mean Error	Relative Std. Dev.	Relative Error
Sample 1, 1.0 mg./liter plus 10 mg./liter Cl						
Phenoldisulfonic	46	0.62	0.461	0.38	74.4	38.0
Brucine	23	1.02	0.289	0.02	28.2	2.0
Modified brucine	17	0.94	0.053	0.06	5.5	6.0
Autoanalyzer	8	1.09	0.179	0.09	16.4	9.0
Chromotropic acid	5	0.97	0.080	0.03	8.1	2.6
Sample 2, 1.0 mg./liter plus 200 mg./liter Cl						
Phenoldisulfonic	46	0.69	0.399	0.31	57.9	31.0
Brucine	21	1.01	0.140	0.01	13.8	1.0
Modified brucine	17	1.00	0.080	0.00	7.9	0.0
Autoanalyzer	8	1.12	0.186	0.12	16.6	11.7
Chromotropic acid	4	1.00	0.013	0.00	1.2	0.0
Sample 3, 1.0 mg./liter plus 400 mg./liter Cl						
Phenoldisulfonic	45	0.81	0.436	0.19	53.8	19.0
Brucine	22	1.28	0.217	0.28	16.8	29.0
Modified brucine	17	1.26	0.117	0.26	9.2	26.0
Autoanalyzer	8	1.42	0.227	0.42	15.9	42.0
Chromotropic acid	5	1.38	0.128	0.38	9.2	38.0

Table XI. Summary of Data on Ammonia Nitrogen

Method	No.	Mean	Std. Dev.	Mean Error	Relative Std. Dev.	Relative Error
Sample 1, 0.20 mg./liter						
Distillation with nesslerization	44	0.22	0.100	0.02	46.3	10.0
Distillation with titration	21	0.24	0.167	0.04	69.8	20.0
Direct nesslerization	20	0.20	0.077	0.00	38.1	0.0
Autoanalyzer	7	0.28	0.094	0.08	33.8	40.0
Sample 2, 0.80 mg./liter						
Distillation with nesslerization	42	0.73	0.155	0.07	21.2	8.7
Distillation with titration	20	0.76	0.218	0.04	28.6	5.0
Direct nesslerization	20	0.80	0.090	0.00	11.2	0.0
Autoanalyzer	7	0.79	0.084	0.01	10.6	1.2
Sample 3, 1.50 mg./liter						
Distillation with nesslerization	42	1.44	0.261	0.06	18.0	4.0
Distillation with titration	21	1.46	0.315	0.04	21.6	2.6
Direct nesslerization	21	1.49	0.174	0.01	11.6	0.6
Autoanalyzer	7	1.46	0.148	0.04	10.1	2.6

Table XII. Summary of Data on Organic Nitrogen

Method	*No.*	*Mean*	*Std. Dev.*	*Mean Error*	*Relative Std. Dev.*	*Relative Error*
			Sample 1, 1.5 mg./liter			
Boiled, Kjeldahl, titration	30	1.16	0.633	0.34	54.7	22.6
Boiled, Kjeldahl, nesslerization	26	1.36	0.586	0.14	43.1	9.3
Kjeldahl minus ammonia by nesslerization	16	1.44	0.660	0.06	45.9	4.0
Autoanalyzer	3	1.82	0.766	0.32	42.1	21.3
			Sample 2, 0.8 mg./liter			
Boiled, Kjeldahl, titration	31	0.83	0.373	0.03	44.8	3.7
Boiled, Kjeldahl, nesslerization	26	0.70	0.364	0.10	52.1	12.5
Kjeldahl minus ammonia by nesslerization	16	0.87	0.458	0.07	52.6	8.7
Autoanalyzer	3	0.69	0.101	0.11	14.6	13.7
			Sample 3, 0.2 mg./liter			
Boiled, Kjeldahl, titration	29	0.34	0.360	0.14	104.4	70.0
Boiled, Kjeldahl, nesslerization	26	0.31	0.290	0.11	94.8	55.0
Kjeldahl minus ammonia by nesslerization	15	0.34	0.235	0.14	68.8	70.0
Autoanalyzer	3	0.49	0.406	0.29	82.7	145.0

and only fair results were obtained by the alkaline hypobromite procedure for chromium. The few participants who used atomic absorption spectroscopy achieved excellent results for copper and the best results for lead. In general, poor results were obtained for all the metals by the spectrographic method.

In the determination of the trace elements, selenium, beryllium, boron, arsenic, and vanadium, all of the methods studied were found to be acceptable.

In the study of water nutrients, nearly half of the participants obtained poor results in the analysis of silica because they failed to digest the sample with sodium bicarbonate to convert it all to molybdate-reactive silica. Similarly, in the analysis of phosphates, only about half of the participants hydrolyzed the sample to convert the polyphosphates to ortho phosphate and hence, the remainder obtained low results. In silicate

analysis, the best results were obtained by the colorimetric molybdosilicate method. The aminonaphtholsulfonic acid method produced good results in analysis for phosphates. The best results were obtained for nitrates by the modified brucine method, although nearly equally good results were obtained by the chromotropic acid method. All methods failed to produce accurate results in the presence of moderately high chloride concentrations. The determination of ammonia by direct nesslerization produced the best results. None of the methods studied were satisfactory for the determination of organic nitrogen.

Literature Cited

(1) Allen, J. E., *Spectrochim. Acta* 17, 459 (1961).
(2) American Public Health Association, "Standard Methods for the Examination of Water and Wastewater," 12th ed., p. 53, Am. Public Health Assoc., New York, New York, 1965.
(3) *Ibid.*, p. 56.
(4) *Ibid.*, p. 61.
(5) *Ibid.*, p. 67.
(6) *Ibid.*, p. 124.
(7) *Ibid.*, p. 126.
(8) *Ibid.*, p. 133.
(9) *Ibid.*, p. 156.
(10) *Ibid.*, p. 173.
(11) *Ibid.*, p. 187.
(12) *Ibid.*, p. 193.
(13) *Ibid.*, p. 231.
(14) *Ibid.*, p. 234.
(15) *Ibid.*, p. 251.
(16) *Ibid.*, p. 261.
(17) *Ibid.*, p. 264.
(18) *Ibid.*, p. 267.
(19) *Ibid.*, p. 271.
(20) Fishman, M. J., Skougstad, M. W., *Anal. Chem.* **36**, 1643 (1964).
(21) Jenkins, D., Medsker, L. L., *Anal. Chem.* **36**, 610 (1964).
(22) Kamphake, L. J., Hannah, S. A., Cohen, J. M., *Water Research* 1, 205 (1967).
(23) Kopp, J. F., Kroner, R. C., *J. Appl. Spectroscopy* **19**, No. 5, 155 (1965).
(24) Luke, C. L., Campbell, M. E., *Anal. Chem.* **24**, 1056 (1952).
(25) Smith, F. G., McCurdy, W. H., Diehl, H., *Analyst* **77**, 418 (1952).
(26) West, P., Ramachandran, T. P., *Anal. Chim. Acta* **35**, 317 (1966).
(27) Willis, J. B., *Anal. Chem.* **34**, 614 (1962).
(28) Wilson, A. L., *Analyst* **87**, 884 (1962).

RECEIVED April 24, 1967.

The Differentiation, Analysis, and Preservation of Nitrogen and Phosphorus Forms in Natural Waters

DAVID JENKINS

Sanitary Engineering Research Laboratory, Department of Civil Engineering, Division of Hydraulic and Sanitary Engineering, University of California, Berkeley, Calif.

The paper describes the development and application of analytical techniques for determining the various forms of nitrogen and phosphorus at levels commonly encountered in estuarine waters. A series of techniques have been developed which allow the differentiation of suspended and soluble organic nitrogen, ammonia nitrogen, nitrite nitrogen, nitrate nitrogen, total and soluble phosphate, soluble orthophosphate, and condensed phosphate in waters whose salinity varies from that of fresh surface water to that of the ocean. In addition, the paper describes and recommends short-term and long-term preservation techniques that are satisfactory for the various forms of nitrogen and phosphorus investigated.

One of the more important reasons for determining the concentrations and the forms of nitrogen and phosphorus in natural waters is that these materials are often the nutrients that limit the growth of photosynthetic aquatic macro- and microorganisms.

The interest of the Sanitary Engineering Research Laboratory in the analysis of N and P forms in water originally stemmed from the conduct of a comprehensive investigation of the water quality of San Francisco Bay (*12*) and more recently from two studies of the analysis and preservation of these materials in estuarine waters in conjunction with the Central Pacific Basin Comprehensive Project of the FWPCA (*9, 10*). Because of this association, the separative, analytical and preservative techniques developed were tailored to suit the extremely variable conditions that

exist in an estuarine water such as San Francisco Bay. It is indeed felt that an estuarine water, with a salinity that may fluctuate between that of fresh water and that of ocean water and with a suspended matter content that may reach values of over 100 mg./liter, places a severe test on the applicability of an analytical method.

A result of this might be the fact that while standard texts are available both for the analysis of fresh surface waters (*1*) and the analysis of ocean waters (*20*), no such volume exists for estuarine waters.

Since the fertilizing effect of N and P forms is of prime interest in natural waters, several prominent biologists working in the limnological field were approached to determine their opinion of the desired analytical classification and the sensitivity and detectability of analytical techniques that would be necessary to make N and P analysis meaningful in the determination of the fertilizing potential of a water.

The opinions of the aquatic biologists (*4, 5, 15, 16*) were all qualified by two statements. These were: (1) the required sensitivity of an N or P analysis depends greatly on the biological productivity of the water, and (2) refinements in analytical differentiation of N and P forms should not exceed the present ability of the biologist to make interpretive judgments of the biological effect of the various N and P forms in the aquatic environment. Within the bounds of these qualifications it was universally thought that nitrogen should be differentiated into organic, ammonia, nitrate, and nitrite. It was generally agreed that nitrite analysis may prove to be insignificant, but that this point should be first proven for any particular water. Recommended limits of detectability were 0.1 mg. N/liter for all forms of nitrogen for more productive waters and 3 to 10 μg N/liter for all forms of nitrogen in less productive waters.

While broad agreement existed on the forms and limits of detectability required for the adequate biological interpretation of nitrogen analyses there was less meeting of the biological minds on the required attributes of phosphorus form differentiation. It was pointed out that the present ability to make interpretive judgments from phosphorus data was limited so that differentiation beyond total P, soluble P, and soluble orthophosphate was probably not justifiable. The detectable limits recommended for the analysis of P forms ranged between 3 to 10 μg. P/liter.

While most of these recommendations were met in the methods developed for use in San Francisco Bay, it should be borne in mind that in these waters the concentrations of N and P forms were significantly greater than those that would be encountered in an oligotrophic water. It is therefore imperative to consider the N and P concentration range expected before adopting any specific method for N and P forms. The methods discussed herein have all performed exceptionally in estuarine waters of highly variable salinity and high turbidity.

Nitrogen Forms

The forms of nitrogen determined are summarized in Table I.

Table I. Analytical Differentiation of Nitrogen Forms

Nitrogen Form	
(1) Total Unoxidized N	Kjeldahl on whole sample
(2) Soluble Unoxidized N	Kjeldahl on membrane filtered sample
(3) Ammonia N	Distill and nesslerize whole sample
(4) Soluble Organic N	(2) minus (3)
(5) Suspended Organic N	(1) minus (2)
(6) Nitrite N	Diazotize membrane filtered sample
(7) Nitrate N	Brucine method on membrane filtered sample

Ammonia Nitrogen. An attempt was made to use a direct method for the determination of ammonia nitrogen. The pyrazolone technique of Strickland and Parsons (*20*) which employs standards prepared in sea water of low NH_3–N content to combat the effect of high salinity was adapted to the analysis of estuarine waters by employing a salt-masking technique similar to that used by Jenkins and Medsker (*11*) in their brucine method for nitrate. The absorbance of the pyrazolone ammonia complex was constant for salinities in the range of 20 to 40 grams Cl^-/liter. Thus, NaCl to give 20 grams Cl^-/liter was added to eliminate salinity interference in samples containing 0–20 grams Cl^-/liter. The reproducibility and recovery of NH_3–N obtained by the method was unsatisfactory on estuarine water samples but it performed satisfactorily on distillates from such samples. However, because of the instability of the pyrazolone reagent, distillation and nesslerization were adopted for the determination of NH_3–N.

The "Standard Methods" (*1*) technique for distillation and nesslerization includes the use of a phosphate buffering system to maintain pH at 7.4 during distillation. In the presence of the high concentrations of Ca^{2+} and Mg^{2+} ions which occur in estuarine waters, the phosphate is precipitated and further buffer must be added. This technique is unsatisfactory for low NH_3–N concentrations since the phosphate buffer is a major contributor to the blank. In the method used for estuarine waters the phosphate buffer described in "Standard Methods" (*1*) was replaced by a sodium carbonate solution (20 ml. of 10% Na_2CO_3). No interference resulted with this buffer system and satisfactory blank values were obtained. It may be argued that the use of the Na_2CO_3 buffer would produce a higher pH (~8.3) and during distillation organic nitrogen-containing materials might tend to decompose more readily. While no such decomposition was evident in the waters of San Francisco Bay (which do not

contain high organic nitrogen concentrations) it was only possible to offer circumstantial evidence in favor of the absence of such decomposition.

Unfiltered samples and samples filtered through 0.45 μ membrane filters had identical NH_3–N contents, showing that the suspended matter in San Francisco Bay water (which is in fact mainly inorganic in nature) did not contain any decomposable organic nitrogen. The presence of a considerable amount of membrane filterable (0.45 μ) organic nitrogen was demonstrated. This so-called 'soluble organic nitrogen' did not start to decompose during distillation until the original volume of sample had been reduced from about 350 ml. to 50 ml. and until well after a plateau had been reached in the amount of ammonia recovered by distillation. Thus complete ammonia recovery was attained after the distillation of about 150 ml. from an original volume of about 350 ml. while high and erratic results only occurred after the distillation of about 300 ml. when the increasing salt concentration in the distillation flask markedly raised its boiling point.

In further support of the lack of decomposition of organic nitrogen during distillation it may be noted that the pyrazolone method performed directly on a sample gave results that agreed semi-quantitatively with those obtained by distillation and nesslerization.

Recoveries of NH_3–N from waters varying in salinity from 120 to 14,000 mg. Cl^-/liter were quantitative at the 100 μg./liter NH_3–N level. The precision of the technique fell off for the distillation of a 200 ml. sample below NH_3–N concentrations of 100 μg./liter (Table II). Thus at 110 μg. NH_3–N/liter a coefficient of variation of 1.8% was obtained while at 35 μg. NH_3–N/liter the coefficient of variation was about 13%. It was concluded therefore that to obtain precise results with this technique below NH_3–N levels of about 60 μg./liter samples of greater than 200 ml. volume should be distilled.

Total Unoxidized Nitrogen (Total Kjeldahl Nitrogen). The classical macro-scale digestion first proposed by Kjeldahl (*13*) using a copper catalyst (added as one bag of the commercial product Kelpak) and 20 ml. conc. H_2SO_4/200 ml. sample was used. Although mercury salts are recognized to be more effective catalysts than copper salts, recoveries of Kjeldahl nitrogen from San Francisco Bay waters using copper salts was comparable to when mercury salts were used and since a shorter analytical procedure results, their use was adopted. The ammonia released was determined as previously described.

Recovery of 50 μg. NH_3–N by the total unoxidized nitrogen technique was quantitative from waters of all salinities. It would seem, therefore, that the salt that accumulates from highly saline samples when the volume is reduced during digestion has no deleterious effect on the technique.

Table II. Precision of Techniques for Analysis of Forms of Nitrogen

Nitrogen Form	*Mean Concentration μg./liter*	*Standard Deviation μg./liter*	*Coefficient of Variation (%)*	*Reported Precision of "Standard Method" (1)*
Ammonia	36	4.69	13.2	± 5%
	66	4.53	6.9	
	111	2.04	1.8	
Soluble Unoxidized	340	12	3.6	—
Total	702	97	13.9	
Unoxidized	382	90	2.4	—
	265	48	18.2	
Nitrite	2.2	0.03	1.2	Standard Deviation = 30 μg./liter at 250 μg./liter level
	5.6	0.14	2.6	
	8.0	0.15	1.9	
Nitrate	290	4.8	1.7	Standard Deviation = 490 μg./liter at 1,100 μg./liter level for Standard Method

Replication of the total unoxidized nitrogen technique for unfiltered Bay water samples was generally poor (Table II). Usually, out of ten replicates, there were one or two unusually high values and all efforts to eliminate them failed, including mixing for several minutes in a high-speed Waring blender.

Since the total unoxidized nitrogen technique gave excellent reproducibility for membrane filtered Bay water, it would seem that the poor reproducibility of the technique for unfiltered samples is because of inhomogeneity caused by uneven distribution of suspended matter.

Soluble Unoxidized Nitrogen. This form of nitrogen was determined by a Kjeldahl digestion (then distillation and nesslerization) on a sample filtered through a washed 0.45 μ Millipore membrane filter. Membrane filters used for separations of this type must be thoroughly washed with distilled water since it has been found that they contain soluble organic material that contributes significantly to the N content of the filtrate.

Excellent replication of the technique (coefficient of variation = 3.6%) was obtained at the 340 μg./liter N level (Table II).

A promising recent technique that could possibly be applied to the determination of soluble oxidized nitrogen is the photooxidation of organic matter by ultraviolet radiation (*3*).

Nitrite Nitrogen. The standard diazotization and coupling procedure with sulfanilic acid and α-naphthylamine was used for nitrite determination (*1*). It should be emphasized that the presence of even

small amounts of suspended solids drastically hinders the recovery of NO_2–N. For example the excellent recoveries obtained in 0.45 μ membrane filtered estuarine waters was reduced to a recovery of 86% by the presence of 12 mg./liter suspended solids and to 53% when 20 mg./liter suspended solids were present. Chloride concentrations varying between 150–12,300 mg. Cl^-/liter had no effect on the excellent performance of the method.

Excellent precision was found down to NO_2–N concentrations of 2 μg./liter where the method yielded a coefficient of variation of never greater than 2.6% (Table II).

Nitrate Nitrogen. The brucine method of Jenkins and Medsker (*11*) was used for the estimation of nitrate. This method is designed for the measurement of intermediate to low NO_3–N concentrations, such as those found in relatively unpolluted estuarine or offshore waters. Its limit of detectability is 0.01 mg. NO_3–N using a 10 ml. sample and with this sample volume the range of the technique is from 0.01 to 0.9 mg. NO_3–N/liter, while higher nitrate concentrations can be determined by prior dilution of the sample. The method would therefore not be sensitive enough for application in highly oligotrophic waters or in the open ocean. For these situations the cadmium reduction method of Strickland and Parsons (*20*) is recommended especially since in these situations large fluctuations in salinity are not generally encountered. The recommended brucine technique differs from the brucine method given in "Standard Methods" (*1*) in several important respects.

The sulfuric acid solution used in the "Standard Methods" (*1*) technique (500 ml. conc. H_2SO_4 + 75 ml. water) was found to give erratic results but satisfactory results were obtained when an acid mixture of 500 ml. conc. H_2SO_4 and 125 ml. water was used. Since the brucine-nitrate color development depends greatly on the amount of heat generated during the reaction, the modified method seeks to control the heat by altering the order of reagent addition to: sample, acid, and then brucine solution. This cooled mixture is then heated in a boiling water bath for exactly 20 minutes, following which the mixture is cooled rapidly to room temperature before reading the developed color (Table III).

Contrary to the statement in "Standard Methods" (1), it has been found that high concentrations of chloride ion produce a decrease in brucine-nitrate color in the standard brucine technique. The modified technique only gives a constant response with chloride concentrations between 27 to 50 grams Cl^-/liter. In our modification the effect of variable chloride concentrations is masked out by adding a large amount of sodium chloride to the reaction mixture before color development (Table III).

The recovery of 0.2 mg./liter NO_3–N from waters varying in chlorosity from 10 mg./liter to 16 grams/liter was quantitative using brucine

Table III. Comparison of Brucine Techniques for Nitrate Determination

	"Standard Methods" (1)	*Modified [Jenkins and Medsker* (11)]
Acid Mixture	500 ml. H_2SO_4 } 75 ml. H_2O }	500 ml. H_2SO_4 } 125 ml. H_2O }
Reagent Addition Sequence	Sample Brucine Acid	Sample Acid Brucine
Heat Control	None or water bath	Water bath and order of reagent addition
Chloride Effect	Decrease in response at high Cl^-	Chloride masking used to prevent chloride interference
Standard Curve	Non-linear	Linear between 0.05 mg./liter and 0.9 mg./liter NO_3–N

sulfate reagents purchased from three different manufacturers. At a level of 0.29 mg.NO_3–N/liter the coefficient of variation of the test was about 1.7% (Table II).

Phosphorus Forms

General Scheme of Phosphorus Analysis. In the analysis of natural waters the measurement of all forms of phosphorus (P) can be divided into two parts: (1) a preliminary treatment in which the P form of interest is separated and converted to orthophosphate, and (2) the colorimetric analysis of orthophosphate (usually by the formation of phosphomolybdic acid followed by its reduction with one of a variety of reducing agents to molybdenum blue). The forms of P in natural waters identified in this study are enumerated in Table IV.

Table IV. Analytical Differentiation of Phosphorus Forms

(1) Soluble P	Persulfate oxidation on 0.45 μ membrane filtered sample then colorimetry
(2) Soluble Ortho P	Colorimetry on 0.45 μ membrane filtered sample
(3) Soluble Organic P	(1) minus (2)
(4) Suspended P	Perchloric acid digestion of solids retained by 0.45 μ membrane filter followed by colorimetry
(5) Soluble Condensed P	Acid hydrolysis of 0.45 μ membrane filtered sample followed by colorimetry

A chemical classification into orthophosphate, polyphosphate, and organic P is made as well as the physical separation of these three chemical forms into "soluble" and "insoluble" components by filtration through

an 0.45 μ membrane filter. While this classification of soluble and insoluble forms is somewhat arbitrary, (Rigler (*19*) has shown that the percentage of soluble organic P in three lake waters decreased from 42% to 18% of the total P as the pore size of the filters was reduced from 5 μ to 0.1 μ), the 0.45 μ size was chosen since it provided a good compromise between slow rates of filtration and poor retention of particles. In turbid estuarine or offshore waters it should be noted that when a 200 ml. sample is filtered through a 47 mm. filter a considerable solids pack builds up and after the start of filtration particles much smaller than the nominal pore size of the filter may be removed.

Millipore filters (47 mm. diameter) were found to contain about 1.3 μg.P/filter of which about 1 μg. P could be washed out. It is therefore necessary thoroughly to wash membrane filters prior to their use in separations involved in P analysis.

In the waters of San Francisco Bay condensed phosphates were not found in any significant concentrations and hence the analytical scheme does not include a method for their determination. Should condensed phosphate be present the use of the American Association of Soap and Glycerine Producers (AASGP) method (*2*) is recommended on both a whole and a membrane-filtered sample.

Orthophosphate. The method used on San Francisco Bay water is a modification of the technique suggested by the AASGP (*2*) in which a membrane-filtered sample reacts with ammonium molybdate in acid solution and the resulting phosphomolybdic acid complex is extracted into an isoamyl alcohol/benzene mixture. Stannous chloride is used to reduce the extracted phosphomolybdic acid to molybdenum blue which is measured colorimetrically.

The ascorbic acid reduction method of Murphy and Riley (*18*) can also be used for orthophosphate analyses in estuarine waters since hydrolysis of polyphosphates and salt effects are absent in this technique.

It is extremely important that orthophosphate analyses on natural waters containing large amounts of suspended particulate material be carried out on membrane-filtered or clarified samples. In the investigation of the orthophosphate technique it was impossible to obtain consistent results if samples were not filtered.

The amount of orthophosphate which could be recovered from a sample seemed to depend largely on how long and how vigorously the sample was shaken during the analysis. It appeared that orthophosphate which was either adsorbed on or associated with the sediment was being released into solution. Since it was also found that salinity variations affected color development and that large turbidity corrections that were necessary when samples high in suspended solids were analyzed, it was decided that only a soluble orthophosphate determination was possible.

The solvent used for extraction of the phosphomolybdate complex was changed from the 1:1 benzene/isobutyl alcohol recommended by AASGP (2) to a 1:1 mixture of benzene/isoamyl alcohol. The change in solvent composition produced a slight (10 to 15%) increase in sensitivity but of far greater importance was the fact that isoamyl alcohol is about one-fifth as soluble in water as isobutyl alcohol. It was therefore not necessary to bring up the volume of the organic phase following extraction (as is necessary when isobutyl alcohol is used and large (200 ml.) aqueous samples are analyzed).

The method gave results that were slightly affected by salinity. The depression of absorbance caused by 20 grams Cl^-/liter varied with the amount of orthophosphate present. Thus, 20 grams Cl^-/liter produced depressions of 4.5, 2.8, and 0.5% respectively for sample contents of 5 μg., 20 μg., and 50 μg. orthophosphate–P. These depressions represent approximately the same absolute amount of PO_4–P.

Since 200 ml. samples of sea water contain about 20 μg. orthophosphate–P, depressions of 2 to 3% may be expected in water of a salinity equivalent to about sea water concentration. While a deviation of this magnitude can be tolerated, further studies of the technique showed that depressions were only about 1 to 2% when a solvent mixture of 25 ml. isoamyl alcohol + 30 ml. benzene was used instead of the 1:1 solvent mixture. It is probable that further investigation could yield a solvent mixture that would be completely devoid of a salt effect.

The hydrolysis of condensed phosphates during the orthophosphate analysis was virtually eliminated by minimizing contact time between the acidic reagents and the sample. Negative results were obtained when concentrated solutions of sodium tripolyphosphate were analyzed by this technique, however in the reactive phosphate technique of Strickland and Parsons (*20*)—a widely used oceanographic method—considerable hydrolysis of the polyphosphate took place.

Silica (50 mg. SiO_2/liters) did not interfere, neither did arsenate (500 μg. as arsenic). The absence of arsenate interference may be caused by conditions of molybdate concentration and pH unfavorable for the formation of arsenomolybdate or possibly insolubility of the arsenomolybdate in the organic phase.

Copper and iron which may be released into solution by the digestion of suspended sediment material in the analysis of total insoluble phosphorus, did not interfere in concentrations (200 μg. Cu^{2+} and 3 mg. Fe^{3+}/sample) several times greater than those found in typical San Francisco Bay sediments.

Mercuric chloride (40 mg. Hg^{2+}/liter) and chloroform (5 ml. $CHCl_3$/liter) which are commonly used sample preservatives, did not

significantly interfere with the method although in the presence of $CHCl_3$ a small decrease in orthophosphate recovery was observed.

It was possible to recover quantitatively 5 μg. and 20 μg. PO_4–P added to Bay water containing approximately 19 grams Cl^-/liter. Excellent reproducibility was obtained down to levels of about 50 μg. P/liter (the lowest tested) in waters with salinities varying from fresh water to ocean water. Coefficients of variation never exceeded 1.5% (Table V).

Table V. Precision of Techniques for Analysis of Forms of Phosphorus

Phosphorus Form	*Mean Concentration μg./liter*	*Standard Deviation μg./liter*	*Coefficient of Variation (%)*	*Reported Precision of Standard Method*
Soluble Ortho	48	0.56	1.2	Standard Deviation = 20 μg/liter
	76	0.74	0.97	
	94	1.30	1.4	
Total Soluble	49.6	0.59	1.2	—
	79.6	0.52	0.66	
	99.5	0.79	0.80	
Total Insoluble	113	2.7	2.4	—
	65	0.8	1.2	
	14	0.4	2.9	

Total Soluble Phosphorus. Total soluble phosphorus includes soluble orthophosphate (soluble condensed phosphate if present) and soluble organic phosphorus. A membrane-filtered sample is treated to release phosphorus as orthophosphate from combination with organic matter and condensed phosphates by some form of oxidation (and hydrolysis).

Several oxidants and techniques have been suggested for this pretreatment, *viz.* ignition (*14*), digestion with 30% H_2O_2 (*8*), acid treatment at 30 to 40 psi (*7*), nitric acid/sulfuric acid digestion (*2*), perchloric acid digestion (*6*), digestion with a perchloric acid/nitric acid mixtures (*2*), and digestion with potassium persulfate (*17*).

Each of the above digestion techniques (with the exception of acid hydrolysis at 30 to 40 psi) were studied for their applicability to estuarine waters. With the exception of the persulfate digestion, all methods were unsatisfactory or impractical for the analysis of samples with high dissolved solids contents. Any digestion technique that causes a significant volume reduction (i.e., ignition, perchloric acid digestions, nitric acid/sulfuric acid digestion) causes the precipitation of large quantities of salt. For example 200 ml. of sea water (which is the volume required for the determination of low amounts of total soluble phosphorus) will produce about 7 grams residue when evaporated to dryness.

In perchloric acid and nitric acid/sulfuric acid digestions, salts precipitate out as the digestion reduces the volume of solution. Danger exists

that dry spots may be formed in a heavy crystal mass during perchloric acid digestions and create an explosion hazard. In perchloric acid digestions chloride ion is replaced by perchlorate and the acidity of the solution decreases. Since the subsequent colorimetric orthophosphate technique relies on the presence of a precise amount of acid, it is necessary to adjust the volume of perchloric acid used according to the salinity of the sample. This is a tedious procedure that does not lend itself well to the routine analysis of large numbers of samples.

Digestion by boiling in the presence of 30% hydrogen peroxide (Jackson (*8*)) yielded incomplete recoveries of total soluble phosphorus from all the estuarine water samples tested and from organic media such as Difco tryptone and peptone. Moreover, the method failed to yield quantitative recovery of an orthophosphate standard carried through the test procedure.

The low result for the orthophosphate standard was probably caused by the presence of unreacted peroxide which during the subsequent colorimetric procedure reacted with molybdic acid to form permolybdic acid (Table VI).

Table VI. Comparison of Several Techniques for the Analysis of Total Soluble Phosphorus (Based on Recovery)

		Method of Analysis			
Type of Sample	*Unit of Expression*	H_2SO_4/HNO_3 *Digestion* (2)	*Ignition 800°* (14)	H_2O_2 *Digestion* (8)	*Persulfate Digestion* (17)
Orthophosphate standard 16.3 μg. PO_4–P	μg.	16.3	16.3	14.6	16.3
Orthophosphate standard 16.3 μg. PO_4–P in 20 gram Cl^-/liter	μg.	—	—	—	16.3
Difco Tryptone 3–30 μg.; 0.97% P[a]	%	0.92	0.97	0.66	0.97
Difco Tryptone 3–30 μg.; 0.97% P[a] in 20 gram Cl^-/liter	%	—	—	—	0.97
Difco Peptone 15–100 mg.; 0.22% P	%	—	0.26	0.18	—
Bay Water, Pittsburg	μg. P/liter	47.0	56.1	38.5	51.9
Bay Water, Crockett	μg. P/liter	80.0	90.5	66.0	79.5
Bay Water, Fort Baker	μg. P/liter	97.6	116	72.5	99.3

[a] Values for Peptone and Tryptone supplied by Difco Company.

The persulfate digestion technique carried out by autoclaving the sample in the presence of persulfate at 15 to 20 psi for one hour (*17*)

gave excellent results and had a simplicity in execution that made it especially attractive for routine analysis. Complete recovery of orthophosphate, of soluble organic phosphorus in tryptone (both in the presence and absence of 20 grams Cl^-/liter and in samples from three points in San Francisco Bay were obtained (Table VI).

Menzel and Corwin (*17*) have reported excellent recoveries of organic phosphorus from several resistant organic phosphorus-containing compounds (lecithin, phosphorocholine, and 5-adenylic acid) as well as from zooplankton tissue using the persulfate digestion. During the present study the ability of persulfate to cleave P–C bonds was tested by performing the total soluble phosphorus test on phenylphosphoric acid and phenylphosphorous acid. Quantitative recovery of phosphorus from each of these materials was obtained at the 50 μg. P level.

The precision of the persulfate digestion technique for the determination of total soluble phosphorus was tested on estuarine water samples of widely differing salinity at total soluble phosphorus concentrations varying between 60–100 μg. P/liter. The maximum coefficient of variation of the technique was 1.2% (Table V).

Total Insoluble Phosphorus. A drastic digestion and oxidation technique is necessary to release all phosphorus associated with the particulate material present in estuarine waters such as those of San Francisco Bay. Although most soil analyses for total phosphorus involve the use of perchloric acid digestions (*8*) there is a widespread acceptance that, however drastic the digestion, some P-containing materials will not be released. This conclusion was substantiated for the suspended solids in San Francisco Bay water where it was found that, by using a sodium carbonate fusion technique, P yields of 2 to 5% higher than those from nitric acid/perchloric acid digestions were obtained. Results obtained for total insoluble phosphorus by a perchloric acid digestion method will be slightly lower than the actual total phosphorus content.

The method used for the analysis of total insoluble phosphorus was a nitric acid/perchloric acid digestion performed on the suspended material retained on a washed membrane filter and followed by a colorimetric estimation of the orthophosphate released by digestion. By performing the analysis on the filtered suspended matter it was possible to obtain suspended material from large volumes of water and carry out a direct analysis of suspended P. The method eliminated the previously mentioned difficulties encountered in performing perchloric acid digestions on large volumes of highly saline sample material.

A perchloric acid volume of 21 ml. reagent grade 70 to 72% $HClO_4$ and a digestion time of 10 to 15 minutes following the evolution of the dense white fumes of perchloric acid were found to produce a satisfactory digestion and a final digestion mixture with the correct acidity to proceed

directly to the analysis of orthophosphate by the AASGP technique (2) using 25 ml. of 10% neutral ammonium molybdate in place of the 50 ml. of acidified ammonium molybdate used in the orthophosphate determination. Acid concentrations varied no more than ±10 to 12% after digestion so that of the original 21 ml. perchloric acid introduced at the start of digestion, 19 ml. ±1 ml. remained at the end of the digestion procedure.

Replicate analyses of total insoluble P on the suspended solids from samples of estuarine water gave results with a coefficient of variation of less than 3% in the range of total insoluble P concentration of between 15 μg. P/liter and 110 μg. P/liter (Table V).

Preservation of Nitrogen and Phosphorus Forms

A study was made to determine the length of time that samples could be stored prior to analysis in the presence of various preservatives. Large volumes of bay water were collected and mixed well before splitting them into aliquots for preservative treatment. A separate plastic container was used for each day that the stored samples were analyzed, so that quiescent storage conditions could be maintained.

Preservation of Nitrogen Forms. The preservation methods investigated were (1) Storage at 4°C., (2) Storage at −10°C., (3) Storage at 4°C. with addition of 2 ml./liter 5% H_2SO_4, and (4) Storage at 4°C. with addition (as $HgCl_2$) of 40 mg. Hg^{2+}/liter.

In evaluating the results (Figure 1) it should be remembered that they apply to the relatively unpolluted waters of San Francisco Bay and that somewhat different results might be obtained if the biological activity in the samples was increased by larger amounts of organic materials.

The erratic nature of the soluble and insoluble organic nitrogen concentrations is partly attributed to the difficulty of preparing an homogenous distribution of the initial large sample into aliquots and partly to the variation inherent in the analysis. For all forms of nitrogen the best preservation method seems to be storage at 4°C. in the presence of 40 mg. Hg^{2+}/liter, although even this method does not satisfactorily maintain the initial levels of insoluble organic nitrogen and nitrite nitrogen over long periods (30 days). It is however the only preservation technique of those investigated that satisfactorily maintained the nitrite nitrogen concentration for about one week. Nitrate and ammonia levels were maintained satisfactorily for one month by the 4°C. acid treatment, however the use of a sulfuric acid preservative cannot be recommended if nitrite nitrogen measurements are to be made. The acid treatment produced an immediate and rapid decrease in nitrite nitrogen, as may be predicted from the Van Slyke reaction:

$$H^+ + NO_2^- + R\text{–}NH_2 \rightarrow N_2 \uparrow + ROH + H_2O.$$

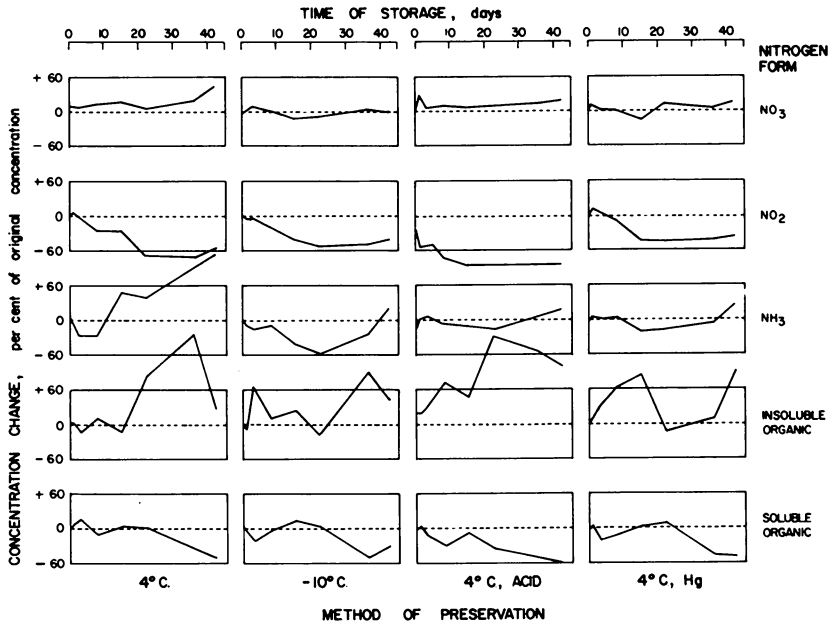

Figure 1. Preservation of nitrogen forms in estuarine water

Preservation of Phosphorus Forms. Because of the good results obtained in the study of the preservation of nitrogen forms, with an Hg^{2+} preservative, it was decided to test the efficacy of mercury preservation for P forms at both 4°C. and −10°C. Acid preservation was not considered because of the extreme lability of condensed phosphates in acid conditions. Since chloroform has been widely used as a preservative for waters to be later analyzed for forms of P, its preservative properties were investigated. Glass containers were used in this preservation study. The preservative treatments were as follows: (1) Storage at 4°C., (2) Storage at 4°C. with 5 ml. $CHCl_3$/liter, (3) Storage at 4°C. with 40 mg. Hg^{2+}/liter, (4) Storage at −10°C., and (5) Storage at −10°C. with 40 mg. Hg^{2+}/liter.

The results of the preservation study (Figure 2) show that for long periods (one month) the best preservation technique was storage at −10°C. with 40 mg. Hg^{2+}/liter. For storage periods of a few days, any of the methods, except storage at 4°C. with $CHCl_3$, were satisfactory. The chloroform treatment produced a dramatic reduction in soluble orthophosphate and an accompanying rise in total insoluble phosphorus.

Summary

A complete set of analytical techniques for the analysis and differentiation of various forms of nitrogen and phosphorus has been presented.

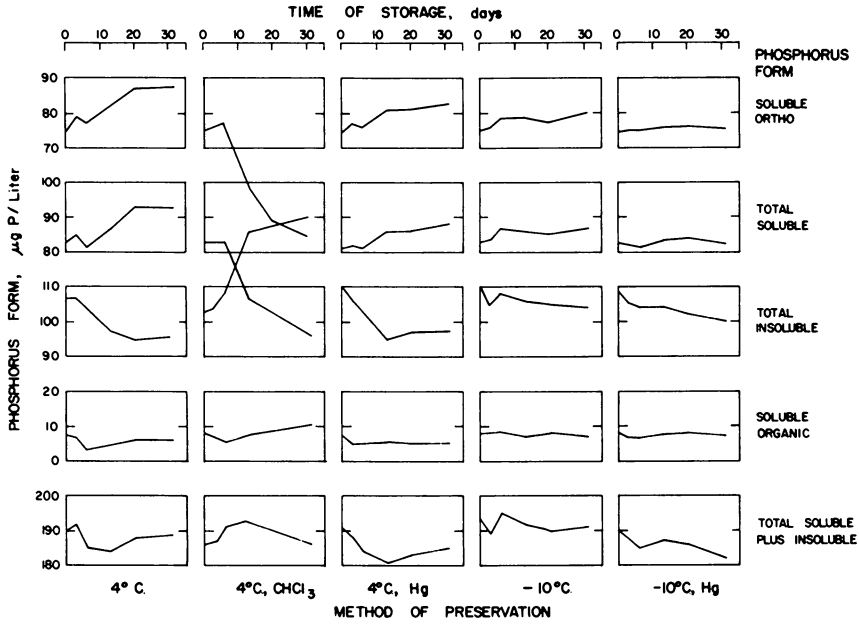

Figure 2. Preservation of phosphorus forms in estuarine water

The techniques are suitable for the analysis of estuarine waters whose high and variable salinity and suspended matter content creates considerable difficulties in analytical techniques designed for use in ocean waters and fresh waters. The precision and accuracy of the developed techniques has been determined under the entire range of conditions encountered in San Francisco Bay. Several methods of sample preservation have been investigated and methods that are reliable in preserving nitrogen and phosphorus forms in San Francisco Bay water are recommended.

Literature Cited

(1) Am. Public Health Assoc., "Standard Methods for the Examination of Water and Wastewater," 12th ed., Am. Public Health Assoc., New York, 1965.
(2) Am. Soap and Glycerine Producers Comm. *J. Am. Water Works Assoc.* **50,** 1563 (1958).
(3) Armstrong, F. A. J., Williams, P. M., Strickland, J. D. H., *Nature* **211,** 481 (1966).
(4) Davis, Ernst, Univ. of Texas (Private Communications).
(5) Goldman, C., Dept. of Zoology, Univ. of Calif. (Davis) (Private Communication).

(6) Hansen, A. L., Robinson, R. J., *J. Marine Res. (Sears Found. Marine Res.)* **12,** 31 (1953).
(7) Harvey, H. W., *J. Marine Biol. Assoc. U. K.,* **27,** 337 (1948).
(8) Jackson, M. L., "Soil Chemical Analysis," Prentice-Hall, Inc., Englewood Cliffs, New Jersey, 1958.
(9) Jenkins, D., *Univ. Calif. (Berkeley) Sanit. Eng. Res. Lab. Rept.* **65,** 13 (1965).
(10) *Ibid.,* **16,** 18 (1965).
(11) Jenkins, D., Medsker, L. L., *Anal. Chem.* **36,** 610 (1964).
(12) Jenkins, D., Selleck, R. E., Pearson, E. A., *Univ. Calif. (Berkeley) Sanit. Eng. Res. Lab. Rept.* **65,** 7 (1965).
(13) Kjeldahl, J., *Zeits. Anal. Chem.* **22,** 366 (1883).
(14) Legg, J. O., Black, C. A., *Soil Sci. Soc. Am. Proc.* **19,** 139 (1955).
(15) Mackenthun, K. M., Federal Water Pollution Control Admin., Cincinnati, Ohio (Private Communication).
(16) Martin, C. V., Calif. State Dept. of Water Resources (Private Communication).
(17) Menzel, D. W., Corwin, N., *Limnol. Oceanog.* **10,** 28 (1965).
(18) Murphy, J., Riley, J. P., *Anal. Chim. Acta* **27,** 31 (1962).
(19) Rigler, F. H., *Limnol. Oceanog.* **9,** 511 (1964).
(20) Strickland, J. D. H., Parsons, T. R., *Bull., Fisheries Res. Board Can.* 125 (1960).

RECEIVED April 24, 1967.

A Thioacetamide-Precipitation Procedure for Determining Trace Elements in Water

EDWARD C. MALLORY, JR.

U. S. Geological Survey, Denver, Colo.

When minor elements in water residues are determined spectrographically, major constituents sometimes interfere by producing unpredictable matrix effects, and by diluting the minor elements below limits of detection. Precipitation of minor elements in waters can be used to remove major elements and to concentrate minor ones before spectrographic analysis. In the procedure described here, thioacetamide is used as the precipitant for both the acid and the ammoniacal sulfide groups. Palladium is added to the samples as an internal standard. Tin is added to the acid sulfide group as a spectrographic buffer and coprecipitant; indium is used for the same purposes with the ammoniacal sulfide group. Quantitative precipitations are obtained for aluminum, antimony, arsenic, beryllium, bismuth, cadmium, chromium, copper, iron, lead, lanthanum, titanium, zinc, and zirconium.

Determining trace elements in natural waters involves a fairly large number of elements whose concentrations rarely exceed 1 milligram per liter, even in highly mineralized waters. Most of these are subgroup elements, although several important elements, such as the rare alkalies, rare alkaline earths, and such elements as boron, aluminum, gallium, antimony, and lead are also of more than occasional interest and should be considered when trace element evaluations are made. Emission spectrographic methods are the most practical means of determining more than a few trace elements. The spectrographic detection limits for most elements are adequate, and as a means of determining the greatest number of elements in a single sample, the emission spectrographic method can scarcely be equalled.

The detection limits for the trace elements can be lowered and the spectrographic analysis simplified if the trace elements are separated from a comparatively large volume of water sample and from the major solutes present in the sample. One means of accomplishing such separations involves precipitation of the trace elements with a reagent or reagents which form very slightly soluble compounds with as many trace elements as possible. Such techniques have been described (*4, 5, 7*). Of particular interest from the standpoint of water analysis are the methods of Heggen and Strock (*8*), Mitchell and Scott (*11*), and Silvey and Brennan (*15*). In these methods, precipitation by organic precipitants at a controlled pH results in the quantitative or near-quantitative recovery of up to 17 minor elements. Although claims have been made that manganese and beryllium are completely precipitated, our experience has shown that the recovery of these two elements is often far from complete. Furthermore, the organic reagents themselves, 8-hydroxyquinoline, thionalide, and tannic acid, contain traces of some of the metals sought and the ultimate detection limit for these metals is limited by the impurities in the reagents. The ideal precipitant, of course, does not contain as impurities any of the metals being sought. Such a reagent must also be capable of precipitating all or most of the important minor elements in water analysis.

Many heavy metals are quite insoluble as sulfides or hydroxides in hydrogen sulfide solutions of properly adjusted pH. However, hydrogen sulfide has several disadvantages, such as being toxic and having an unpleasant odor.

Thioacetamide has been used as a substitute for hydrogen sulfide. It is readily obtainable, and the commercial product tested was free of all heavy-metal sulfides except a trace of silver. Thioacetamide is very soluble in alcohol, benzene, or water. The neutral water solution is stable for long periods of time. A slight cloudiness may form in long-stored water solutions but this may be removed by filtration. A solution of thioacetamide can be added directly to solutions so there is no loss of precipitate in hydrogen sulfide delivery tubes.

Thioacetamide hydrolyzes readily in hot acid or alkaline solutions to give hydrogen sulfide. The equations for the hydrolysis are as follows:

$$\text{In acid: } CH_3CSNH_2 + 2H_2O = CH_3COONH_4 + H_2S$$

$$\text{In base: } CH_3CSNH_2 + 30H^- = CH_3COO^- + NH_3 + S^{2-}$$

The rate of hydrolysis can be controlled by controlling the temperature of the solution so the rate of precipitation can be regulated. The precipitates obtained with thioacetamide are coarsely crystalline, easily filtered, easily washed, and not so likely to contain foreign ions. Since thioacetamide has so many advantages over hydrogen sulfide, an attempt

to evaluate the reagent as a precipitant to recover trace elements from water samples seemed worthwhile.

Considerable basic work has been done concerning the reactions of thioacetamide, particularly with heavy metals, and the conditions which affect these reactions. Flaschka (*6*) discusses optimum conditions and some difficulties of precipitating antimony, arsenic, bismuth, cadmium, copper, lead, mercury, molybdenum, and tin with thioacetamide. Swift and Anson (*16*) discuss the analytical chemistry of thioacetamide. They also give preliminary results (*17*) for the mechanisms of sulfide precipitation by thioacetamide for silver, mercury (III), copper (II), tin (IV), and molybdenum (IV). Bowersox, Smith, and Swift used thioacetamide to precipitate nickel (*2*) and zinc (*3*) and studied reactions concerning these precipitations. Swift and Butler (*18*) have studied the reactions during the precipitation of lead with thioacetamide. Many others have directed their efforts to the separation of one or a few metals. References *1, 9, 12,* and *14* are only a few examples. For the present purpose, conditions must be adjusted so as to ensure essentially complete precipitation of as many elements as possible but still maintain maximum simplicity of the operational procedure. For example, the sulfides of certain metals are quite insoluble in strongly acid solution but soluble in neutral or alkaline solution. For other elements of the sulfide group the reverse is true. With the general insolubility of the sulfides for a guide, the use of thioacetamide as a precipitant for separation of the heavy metals was evaluated. Lundell and Hoffman (*10*) and Waggoner (*20*) are good references for sulfide insolubility.

Admittedly, sulfide precipitations offer no means of separating the important rare alkalies and alkaline earths. Nevertheless, an improved technique for the recovery of a significant number of the heavy metals would certainly be worthwhile. Accordingly, optimum conditions were established for the quantitative precipitation of the greatest number of trace elements.

Initial experiments indicated the necessity for using two separate aliquots for the precipitations. All attempts first to precipitate those metal sulfides insoluble in acid, filter them off, and then neutralize the filtrate to make the ammoniacal precipitation met with failure. Incomplete precipitation of aluminum, beryllium, cobalt, iron, molybdenum, manganese, nickel, and zinc always resulted with this procedure. When one aliquot was used for the acid sulfide precipitate and another aliquot was used for the ammoniacal sulfide precipitate, much better results were obtained for aluminum, beryllium, iron, and zinc. Apparently the additional operations involved in reducing the volume of the sample and washings, and the readjustment of the pH, result in conditions which are far from ideal for the subsequent precipitation. Only by carrying out precipitations on

two separate aliquots could acceptable recovery of a significant number of the elements of interest be achieved. While this defeats one of the goals of the investigation, the success in accomplishing the isolation of a number of trace elements makes the method worthy of consideration as a technique for the analysis of water samples.

Preparation of Stock Solutions

Four separate stock solutions are necessary to provide stable mixtures of all 19 elements investigated. The components of each of these are tabulated in Tables I and II. Compounds used in stock solutions must be of known high purity or be examined to demonstrate the absence of harmful impurities. All dilutions must be made with demineralized water.

Table I. Stock Solutions Nos. 1 and 2 [a]

Stock Sol. No.	*Element*	*Compound Used*	*Weight Required (mg./liter)*	*Solvent*
1	As	As_2O_3	66.02	HCl (warm only) ..... 10 ml.
	Bi	Bi_2O_3	55.74	HCl ..... 10 ml.
	Cd	CdO	57.11	HCl ..... 10 ml.
	Cu	CuO	62.59	HCl ..... 10 ml.
	Pb	PbO	53.86	HCl ..... 15 ml.
	Mo	MoO_3	75.02	HCl ..... 15 ml.
2	Sb	$KSbOC_4H_4O_6 \cdot 1/2H_2O$	137.13	H_2O

[a] 50 mg./liter of each element.

Stock solutions Nos. 1 and 2 contain those elements whose sulfides are precipitated from strongly acid solution. High-purity oxides of all these elements except antimony are readily soluble in hydrochloric acid. Antimony must be prepared as a separate stock solution because of its tendency to hydrolyze and precipitate as a basic chloride in dilute hydrochloric acid solution. This stock solution is stable for at least 30 days.

Stock solutions Nos. 3 and 4 contain those elements whose sulfides or hydroxides are precipitated from neutral or slightly ammoniacal solution. Either the high-purity oxide or sulfate of each element is used, except for chromium, where a dichromate salt is satisfactory, and titanium, where the most convenient compound is ammonium titanyl oxalate. The titanium stock solution is stable for at least 30 days.

Logarithmic standards are made as follows:

I. A. Dilute 100 ml. of stock solution No. 1 to 1 liter with water. This gives a standard containing 5000 μg./liter of each element.

B. Dilute 200 ml. of the 5000 μg./liter standard with 229 ml. of water and 1 ml. of hydrochloric acid. This gives a standard of 2325 μg./liter.

C. Dilute 200 ml. of the 2325 μg./liter standard with 229 ml. of water and 1 ml. of hydrochloric acid to make a standard of 1081 μg./liter.

Table II. Stock Solutions Nos. 3 and 4[a]

Stock Sol. No.	*Element*	*Compound Used*	*Weight Required (mg./liter)*	*Solvent*
3	Al	$Al_2(SO_4)_3$	3.175 ml. of 10% specpure sol.	H_2O
	Be	BeO	138.76	7 ml. H_2SO_4
	Cr	$K_2Cr_2O_7$	141.46	H_2O
	Co	Co_3O_4	68.10	12 ml. H_2SO_4
	Fe	Fe_2O_3	71.48	5 ml. HCl for solvent, then fume in 5 ml. H_2SO_4
	La	La_2O_3	56.84	3 ml. H_2SO_4
	Mn	Mn_3O_4	69.41	5 ml. HCl for solvent, then fume in 5 ml. H_2SO_4
	Ni	NiO	63.63	12 ml. H_2SO_4
	Ag	Ag_2O	53.71	5 ml. H_2SO_4
	Zn	ZnO	62.23	5 ml. H_2SO_4
	Zr	$Zr(SO_4)_2 \cdot 4H_2O$	194.81	5 ml. H_2SO_4
4	Ti	$(NH_4)_2TiO(C_2O_4)_2 \cdot 2H_2O$	306.93	H_2O

[a] 50 mg./liter of each element.

D. Continue the dilutions as above so that standards of 503, 233, 108, 50, 23, 11, 5, 2.3, and 1.1 μg./liter are obtained. Each standard solution contains 46.5% of the elements found in the next higher standard.
II. Standards made from stock solutions Nos. 2 and 4 are diluted the same as I except that 230 ml. of water are used. No acid is necessary.
III. Standards made from stock solution No. 3 are diluted the same as I except that 1 ml. of sulfuric acid is used instead of the 1 ml. of hydrochloric acid.

Reagents

Ammonium chloropalladite (0.1 mg. Pd/ml.). Dissolve 133.6 mg. of ammonium chloropalladite in 450 ml. of demineralized water acidified with 5 ml. of concentrated H_2SO_4. Dilute to 500 ml. Dilute this solution 1:1 before using as an internal standard.

Indium sulfate solution (1 mg. In/ml.). Dissolve 1.209 grams of In_2O_3 in 40 ml. of concentrated H_2SO_4, heating until solution is complete. Dilute to 1 liter with demineralized water.

Stannous chloride solution (1 mg. Sn/ml.). Dissolve 0.3902 grams of $SnCl_2 \cdot 2H_2O$ in 4 ml. of concentrated HCl and dilute to 200 ml. with demineralized water. Prepare fresh before use.

Ammonium hydroxide solution (1*N*). Use ammonia gas and demineralized water to make 4*N* NH_4OH. Dilute 25 ml. of 4*N* NH_4OH to 100 ml.

Hydrochloric acid (12*N*). Distill reagent grade concentrated HCl, collecting only the middle one-third portion of distillate.

Hydrochloric acid (3*N*). Dilute 25 ml. of the redistilled 12*N* HCl to 100 ml. with demineralized water.

Ammonium chloride solution (2%, wt./vol.). Dissolve 2 grams in 100 ml. of demineralized water.

Ammonium sulfite solution (0.2%, wt./vol.). Dissolve 0.5 gram in 250 ml. of demineralized water.

Thioacetamide solution (2%, wt./vol.). Dissolve 2 grams in 100 ml. of demineralized water. Stir or expose the solution mixture to ultrasonic agitation until dissolved. Any small amount of insoluble white residue may be ignored.

Wash solution I (acid precipitation). Dissolve 80 mg. of thioacetamide in 1 liter of demineralized water. Adjust the pH to 0.75 with 3*N* HCl.

Wash solution II (Ammoniacal precipitation). Dissolve 0.5 gram each of ammonium chloride and ammonium sulfite, and 2 grams of thioacetamide in 1 liter of demineralized water. Adjust the pH to 8.0 with 1*N* ammonium hydroxide.

Spectrographic Equipment

A spectrograph with a 3-meter concave grating having 15,000 lines per inch and a reciprocal linear dispersion of 2.7 Angstroms per mm. is used to record the spectra on Eastman III-O spectroscopic plates. A 220-volt d.c. arc of 6 amperes between graphite electrodes (about 5 mm. gap) is used for sample excitation. Each sample charge of 24 mg. is burned to completion in the arc. Plate development is by mechanical agitation in a commercially available plate processor unit at controlled temperature. Spectral line transmissions are measured in the usual way on a scanning, non-recording densitometer.

All calculations are made by the system of Trandafir (*19*) in which transmissions of standards and samples are plotted directly, eliminating the need for plate calibration and calculation of intensity ratios.

Procedure

The sample to be analyzed should first be filtered through a micropore membrane filter of 0.45 micron average pore diameter. This effectively removes suspended matter and insures subsequent determination of only that material considered to be in true solution. The suspended material may then be examined by x-ray analysis. If the thioacetamide method were used to analyze the unfiltered sample, some of the suspended sediment might not dissolve and would remain to contaminate the sulfide precipitate. The amount of sample taken for analysis must provide adequate amounts of the trace elements being determined. A 100-ml. aliquot is a convenient volume in which to make the precipita-

tions. Larger volumes, up to 1 liter or more, of dilute waters can be evaporated to 100 ml. Highly mineralized waters cannot be concentrated to such an extent, hence correspondingly smaller volumes must be taken. For brines, a sample of less than 100 ml. may be necessary and such samples must be diluted to 100 ml. with demineralized water.

The specific conductance of a water can be used as an aid in determining the size of the aliquot needed. A 1-liter aliquot is generally sufficient for waters with a conductivity less than 2,000 micromhos. Samples with a greater conductivity require smaller aliquots. However, if a water is high in some elements and low in others, both a large and a small aliquot may be necessary.

The samples are conveniently evaporated in the 400-ml. beakers in which the subsequent precipitations are made to minimize both the risk of contamination and the possible loss of trace elements from the solution. Aliquots (100 ml.) of the standard solutions are tested by the rest of the procedure.

Acid Precipitation. Evaporate a measured portion of the sample to about 100 ml. or, if less than 100-ml. aliquots are used, adjust the final volume to about 100 ml. Add 3 ml. of the ammonium chloropalladite solution and 30 ml. of stannous chloride solution. Adjust the pH to 0.75 with 3*N* HCl and add 20 ml. of the thioacetamide solution. Cover the beaker with a watch glass, heat the sample to just below the boiling point, and allow it to stand overnight at room temperature.

Filter the solution through a fine filter paper (Whatman No. 42 or equivalent). Wash the precipitate several times, using the acid-thioacetamide wash solution (No. I). Discard the filtrate and washings.

Place the filter paper and precipitate in an uncovered porcelain crucible and ash at 450°C. Thoroughly grind and mix the cool, dry precipitate with an equal weight of spectrographic-grade powdered graphite in an agate mortar. The mixture is then ready for spectrographic analysis. Weigh a 24-mg. portion of the sample-graphite mixture and tamp gently into the cavity of a graphite electrode (Ultra Carbon 1590, Met-Bay 1120, and similar to National Carbon L 3942, except for modification to 0.015-inch wall thickness). Burn to completion in a 220-volt d.c. arc of about 6 amperes.

Ammoniacal Precipitation. Evaporate a measured portion of the sample to about 100 ml. or, if less than 100-ml. aliquots are used, adjust the final volume to about 100 ml.

Add successively 3 ml. of ammonium chloropalladite solution, 30 ml. of indium sulfate solution, and 25 ml. of ammonium chloride solution. Adjust the pH of the solution to 7.2 with 1*N* ammonium hydroxide and add successively 20 ml. of ammonium sulfite solution and 20 ml. of thioacetamide solution. Adjust the pH of the sample to 8.0 with 1*N* ammonium hydroxide and allow the sample to stand overnight at room temperature.

Filter the solution through a fine filter paper (Whatman No. 42 or equivalent) and wash the precipitate with several portions of wash solution II, the ammoniacal thioacetamide solution containing small amounts of ammonium chloride and ammonium sulfite. Ash the precipitate at 450°C., cool, and mix with an equal weight of powdered graphite. Mix the ashed precipitate and powdered graphite thoroughly by grinding

together in an agate mortar. A portion of the precipitate-graphite mixture weighing 24 mg. is analyzed spectrographically the same as the precipitates obtained from the acid precipitations.

Discussion

Palladium has been recommended as an internal standard for spectrographic analysis of precipitated heavy metals such as are involved in this procedure (*15*). Palladium sulfide precipitates readily and completely under both acid and ammoniacal conditions, and, therefore, it seemed satisfactory for the purpose.

The choice of an appropriate spectroscopic buffer and collector for the precipitated trace elements is somewhat more difficult. Adding stannous chloride to the acid precipitation and indium sulfate to the ammoniacal precipitation appeared satisfactory. Although tin is a fairly common element and its determination in water is occasionally of interest, it is of sufficiently infrequent occurrence in water so it can be used with little disadvantage. Indium is only rarely detected in natural water and, since its ammoniacal sulfide is readily precipitated under the conditions of this procedure, it serves adequately as both a collector for the precipitate and as a spectrographic buffer.

According to Lundell and Hoffman (*10*), the optimum conditions for the complete precipitation of the sulfides which are insoluble in strong acid solution require adjustment of the solution to 0.2*N* with hydrochloric acid. Hydrochloric acid is preferable to sulfuric acid primarily because of the difficulty of completely precipitating lead from strong sulfuric acid solution. The pH of the acidified aliquot is therefore adjusted to 0.75 with 3*N* hydrochloric acid.

To determine the optimum pH for the precipitation of the metal sulfides insoluble in ammoniacal solution, several precipitations were made under identical conditions except that pH values of 7.0, 7.5, 8.0, 8.5, and 9.0 were used. The filtrates from each precipitation were examined to measure the completeness of precipitation. Maximum recovery of most elements occurred in the solution adjusted to a pH of 8.0. Zirconium precipitated completely at all pH values.

Adding ammonium chloride decreases the solubility of aluminum hydroxide and prevents the precipitation of magnesium hydroxide. Scott (*13*) states that the precipitation of nickel, cobalt, manganese, and zinc sulfides may be incomplete because of the formation of polysulfides in the presence of air or other oxidizing agents. A small amount of ammonium sulfite is therefore added to promote their precipitation. In spite of this precaution, cobalt, nickel, and manganese were never quantitatively recovered and the procedure is not considered entirely satisfactory for these elements.

The optimum conditions for forming the acid and ammoniacal sulfide precipitates were also studied. Whether a moderate or a large excess of thioacetamide is added appears to have little or no effect on the completeness of precipitation. Precipitation of the acid-insoluble sulfides occurs slowly at room temperature; however, precipitation may be hastened by heating the solution to just below boiling. To ensure complete precipitation and an easily filtered precipitate, the solution should be filtered only after the residue has settled for several hours or overnight. An examination of the filtrate showed complete removal of antimony, arsenic, bismuth, cadmium, copper, and lead; only molybdenum was not completely removed.

On the other hand, the metallic sulfides and hydroxides which precipitate from the ammoniacal solution form readily at a pH of 8.0 and no heating is necessary. The precipitates are allowed to stand overnight before filtering.

Attempts to recover the precipitates on micropore membrane filters were unsuccessful both because of the loss of precipitate between the edges of the filter disc and the filter holder and because of the difficulty

Table III. Elements Completely or Nearly Completely Precipitated Over the Concentration Range Shown

Acid Precipitations

Element	*Analytical Line (A.)*	*Concentration Range, μg./liter*	*Concentration in Filtrate, μg./liter*
Antimony	2598.1	5.00-500	None
Arsenic	2780.2	10.80-500	None
Bismuth	3067.7	0.23-10.8	None
	2989.0	10.80-232	None
Cadmium	3261.1	5.00-232	None
Copper	2824.4	5.00-500	None
Lead	2873.3	5.00-232	None

Ammoniacal Precipitations

Element	*Analytical Line (A.)*	*Concentration Range, μg./liter*	*Concentration in Filtrate, μg./liter*
Beryllium	3131.1	0.23-5.0	None
		10.80	<0.1
Chromium	3021.6	0.50-23	None
Iron	2723.6	0.50-232	<0.5
Titanium	3242.0	1.10-50	<1.1
Zinc	3345.0	2.30-50	None
		108.00	<1.1
		232.00	16
		500.00	12
Zirconium	3392.0	0.23-23	None

of ashing the membrane material. Satisfactory filtration rates and recoveries were obtained when the solutions were filtered, without suction, through a fine paper such as Whatman No. 42.

The precipitates from the two aliquots cannot be combined since traces of acid-insoluble sulfides are inevitably occluded with the ammoniacal precipitate and vice versa.

Recovery Evaluations

Two series of standard solutions were prepared, each containing from 0.1 to 500 μg./liter of each element. In the first series, prepared from stock solutions Nos. 1 and 2, only those elements which were expected to precipitate completely, or nearly completely, from acid solution were included (Table I). Similarly the second series, prepared from stock solutions Nos. 3 and 4, contained only those expected to precipitate completely, or nearly so, from ammoniacal solution (Table II).

The precipitations were carried out on each set of standards according to the foregoing procedure. In each case, however, the filtrate and washings from each standard were saved, evaporated to a volume of 100 ml., and the precipitations repeated. A spectroscopic examination

Table IV. Density Ratios of Analytical Line to Internal Standard

		Acid Precipitations			
Element	*Analytical Line (A.)*	*Std. 1 0.23 μg./liter*	*Std. 2 0.50*	*Std. 3 1.1*	*Std. 4 2.3*
Molybdenum	3208.8		.05	.14	.16
			0	0	.06
		Ammoniacal Precipitations			
Element	*Analytical Line (A.)*	*Std. 1 0.23 μg./liter*	*Std. 2 0.50*	*Std. 3 1.1*	*Std. 4 2.3*
Aluminum	2652.5				
Cobalt	3453.5	.02	.07	.16	.55
		.02	.13	.48	.42
Lanthanum	3337.5			.04	.09
				0	0
Nickel	3414.8		.18	.35	.59
			.56	1.00	.59
Manganese	2949.2				.09
					.12
Silver	3382.9	.94	1.54	2.27	3.18
		1.00	.68	1.39	1.21

[a] The first number of each pair is the ratio of the density of the analysis line to the ard solution). The second number is similarly obtained from the spectrum of the Concentration range is indicated by the columns used.

of the precipitate obtained from the filtrate and washings gave an indication of the completeness of the precipitation, while examination of the precipitates from each original standard solution permitted establishing working curves. A spectrographic examination of the entire filtrate was not possible because the major ions and the salts resulting from the reagents would have prevented detection of the minor elements.

Of the acid group, only molybdenum could be detected in the filtrate and washings, and the method was deemed satisfactory for the separation of antimony, arsenic, bismuth, cadmium, copper, and lead.

Of the elements of the ammoniacal group, beryllium, chromium, and zirconium were not detected in the filtrate, and only traces of iron and titanium were detected. The separation, therefore, was considered acceptable for these elements. In addition, the recovery of lanthanum and zinc was generally satisfactory (Table IV) and these two elements could well be included. Traces of aluminum were always found in the filtrate. The amounts, however, were small and generally not proportional to the concentrations of the standards.

The recoveries of cobalt, manganese, nickel, and silver were far from complete, and a reliable determination of these elements by this method could not be made.

Line in Original Precipitate and Precipitate from Resulting Filtrate[a]

Acid Precipitations

Std. 5	*Std. 6*	*Std. 7*	*Std. 8*	*Std. 9*	*Std. 10*	*Std. 11*
5.0	*10.8*	*23*	*50*	*108*	*232*	*500*
.38	.83	1.62	2.61	3.16		
.18	.40	1.09	1.89	2.32		

Ammoniacal Precipitations

Std. 5	*Std. 6*	*Std. 7*	*Std. 8*	*Std. 9*	*Std. 10*	*Std. 11*
5.0	*10.8*	*23*	*50*	*108*	*232*	*500*
	.17	.31	.84	1.16	1.96	2.80
	.11	.11	.14	.31	.34	.38
.82	2.15	3.04				
.81	1.88	>2.00				
.22	.79	1.45	2.47	3.34		
0	.03	.12	.58	.63		
.54	1.00	1.67	1.88	3.32		
.80	1.30	2.00	>2.00	>2.00		
.22	.64	1.04	1.45			
.30	.70	1.30	2.50			

density of the internal standard line in the spectrum of the first precipitation (stand-
second precipitation (resulting filtrate).

Table V. Micrograms per Liter of Elements Determined

No.	*1*		*2*		*3*		*4*	
Dissolved solute conc. (p.p.m.)	32		58		66		76	
Volume (ml.)	250		250		250		250	
			Acid Precipitations[b]					
	S	*F*	*S*	*F*	*S*	*F*	*S*	*F*
Cadmium	—	—	—	—	—	—	—	—
Copper	—	—	—	—	—	—	—	—
Lead	4	0	4	0	12	0	29	0
Molybdenum	—	—	—	—	—	—	—	—
			Ammoniacal Precipitations					
	S	*F*	*S*	*F*	*S*	F	*S*	*F*
Aluminum	110	0	120	0	1700	0	160	0
Beryllium	—	—	—	—	—	—	3	0
Chromium	—	—	—	—	1	0	—	—
Iron	180	0	580	0	560	0	840	0
Lanthanum	—	—	—	—	—	—	—	—
Titanium	13	0	9	0	76	0	7	0
Zinc	—	—	52	0	—	—	112	0
Zirconium	—	—	3	0	2	0	2	0

[a] *S* = sample; *F* = filtrate.

Table VI. Analytical Results of Thioacetamide Method

		Part a—Elements Precipitated as Acid Sulfides			
Sample	*Method*	*Cd*	*Cu*	*Pb*	*Mo*
Ref. No. 1	Thioacetamide	<2	<5	2	12
	Lab. A	—	2	<2	26
	Lab. B	—	3.5	<10	73.5
	Lab. C	—	3	>3	30
Ref. No. 2	Thioacetamide	<2	<5	3	0.5
	Lab. A	—	1	2	0.6
	Lab. B	<3	2.2	<3	19.8
	Lab. C	2	3	2	50
Ref. No. 3	Thioacetamide	5	11	5	2
	Lab. A	—	2	1	1
	Lab. B	<3	2.6	<7	66
	Lab. C	—	1	<0.6	0.8

Tables III and IV summarize these data. When precipitation is incomplete, a working curve cannot be constructed and concentrations cannot be determined. In such cases, element line-internal standard line

in Natural Waters and Resulting Filtrates[a]

5		6		7		8	
102		352		1,380		3,020	
250		250 (Zn 25)		100 (Zn 25)		100 (Fe,Cu,Zn,Ni-25)	
			Acid Precipitations[b]				
S	*F*	*S*	*F*	*S*	*F*	*S*	*F*
—	—	6	0	130	0	130	0
—	—	190	0	800	0	4400	0
5	0	5	0	77	0	42	0
—	—	—	—	—	—	5	0
			Ammoniacal Precipitations				
S	*F*	*S*	*F*	*S*	*F*	*S*	*F*
100	0	1200	0	>5000	230	>5000	145
—	—	—	—	—	—	—	—
—	—	—	—	45	0	—	—
260	0	680	0	>2300	0	>2300	11
—	—	—	—	500	0	400	0
10	0	6	0	19	0	—	—
60	0	2700	0	>20,000	0	>20,000	2200
—	—	—	—	13	0	55	0

[b] *See* Table VII for recovery of antimony, arsenic, bismuth, and lanthanum.

Compared with Results Obtained by Other Laboratories

Part b—Elements Precipitated as Ammoniacal Sulfides

Al	*Be*	*Cr*	*Fe*	*Ti*	*Zn*	*Zr*
135	<0.2	0.5	17	2	25	<0.2
84	<0.3	<1	5	0.8	<50	<2
77.8	<0.04	<4	12.9	—	30.1	—
—	—	1.5	800	—	9	—
9	<0.2	<0.5	40	3	700	<0.2
10	<0.09	<0.4	20	0.6	<590	<0.6
<6	<0.02	<2	28.3	—	360	—
—	—	1	100	<3	300	1
14	<0.2	8	30	2	460	<0.2
<150	—	1.5	9	<4	400	1
13	<0.02	<2	13	—	244	—
6	<0.2	<0.4	10	<1	270	<0.6

density ratios were compared (Table IV) to indicate the relative amounts of the element in the two precipitates, one obtained from the sample and one from the filtrate and washings.

To test completeness of recovery from natural water samples, a similar experiment was carried out using eight natural waters whose dissolved solute concentrations ranged from 32 to 3020 milligrams per liter. Not all of the elements of interest were detected in all of the eight samples. For those elements which were detected, the data generally supported the findings obtained on the standard solutions (Table V).

Three water samples which had previously been analyzed by several other spectrographic laboratories were analyzed by the thioacetamide precipitation method described here. Although there is a considerable range of reported concentrations, as might be expected for such analyses, the results of the thioacetamide-spectrochemical method generally were comparable with those reported by others (Table VI).

Since arsenic, antimony, bismuth and lanthanum were not detected in the above samples (Table VI), no similar comparison of data could be obtained for these elements. To gain an indication of the reliability of the thioacetamide-precipitation method for arsenic, bismuth, antimony, and lanthanum, known amounts of these elements were added to a sample which had been analyzed and shown to contain no detectable amounts. Analysis of the spiked sample showed a complete recovery of the amounts added (Table VII). The analytical results obtained by another laboratory which analyzed the sample before the four elements were added are also tabulated.

Table VII. Analysis of a Mine Drainage Sample to Which was Added 30 μg. Each of Antimony, Arsenic, Bismuth, and Lanthanum

Method	*Sb*	*As*	*Be*	*Bi*	*Cd*	*Cr*	*Cu*	*La*	*Pb*	*Zn*	*Zr*
Thioacetamide	30	30	<0.2	30	4	<0.5	<5	30	5	200	0.2
Lab. A			<2			<3	<0.8		<3	260	

Conclusions

Trace concentrations of antimony, arsenic, bismuth, cadmium, copper, and lead can be precipitated with thioacetamide from a strongly acid (0.2*N* HCl) solution and determined spectrographically. The precipitation of molybdenum is not complete under the conditions of acid precipitation.

A similar ammoniacal-thioacetamide precipitation permits complete or essentially complete separation of aluminum, beryllium, chromium, iron, lanthanum, titanium, zinc, and zirconium. Cobalt, nickel, and manganese are not completely precipitated from the ammoniacal solution. The determination of silver is uncertain because of its presence as an impurity in the thioacetamide reagent.

This method permits the separation and concentration of at least 14 minor elements from natural water samples and their subsequent spectrographic determination with a high degree of reliability.

Literature Cited

(1) Amin, A. M., *Chemist-Analyst* **44**, 66 (1955).
(2) Bowersox, D. F., Smith, D. M., Swift, E. H., *Talanta* **2**, 142 (1959).
(3) Bowersox, D. F., Smith, D. M., Swift, E. H., *Talanta* **3**, 282 (1960).
(4) Braidech, M. M., Emery, F. H., *Ohio Conf. Water Purification, 13th Ann. Rept.*, **68** (1933).
(5) Eristavi, D. I., Salukvadze, E. K., *Tr. Gruzinsk. Politekhn Inst.* **4**, 11 (1959).
(6) Flaschka, H., *Z. Anal. Chem.* **133**, 103 (1951).
(7) Forster, W., Zeitlin, H., *Anal. Chem.* **38**, 649 (1966).
(8) Heggen, G. E., Strock, L. W., *Anal. Chem.* **25**, 859 (1953).
(9) Lipiec, T., Ramotowski, S., *Farm. Polska* **12**, 3 (1951).
(10) Lundell, G. E. F., Hoffman, J. I., "Outlines of Methods of Chemical Analysis," pp. 49, 59, Wiley, New York, 1948.
(11) Mitchell, R. L., Scott, R. O., *J. Soc. Chem. Ind. (London)* **66**, 330 (1947).
(12) Monte Bovi, A. J., *J. Am. Pharm. Assoc., Sci. Ed.* **45**, 765 (1956).
(13) Scott, W. W., "Standard Methods of Chemical Analysis," Vol. I, 306, 309, D. Van Nostrand, New York, 1952.
(14) Shvaikova, M. D., *Sudebno-Med. Ekspertiza, Min. Zdravookhr. SSSR* **1**, 103 (1934).
(15) Silvey, W. D., Brennan, R., *Anal. Chem.* **34**, 784 (1962).
(16) Swift, E. H., Anson, F. C., *Advan. Anal. Chem. Instr.* **1**, 293 (1960).
(17) Swift, E. H., Anson, F. C., *Talanta* **3**, 296 (1960).
(18) Swift, E. H., Butler, E. A., *Anal. Chem.* **28**, 146 (1956).
(19) Trandafir, N., *Appl. Spectr.* **18**, 175 (1964).
(20) Waggoner, W. H., *J. Chem. Educ.* **35**, 339 (1958).

RECEIVED May 29, 1967. Publication authorized by the Director, U.S. Geological Survey.

18

The Strontium and Barium Content of Sea Water

NEIL R. ANDERSEN

Research and Development Department, Naval Oceanographic Office, Washington, D. C.

DAVID N. HUME

Massachusetts Institute of Technology, Cambridge, Mass.

The strontium and barium analyses of sea water are reported. Concentrations of these elements in sea water were simultaneously determined by a combination of ion exchange concentration and flame photometry to ascertain more precisely strontium/chlorinity and barium/chlorinity ratios and to investigate the magnitude and nature of the strontium/chlorinity ratio variation if it was found. The results of the analyses of several ocean stations presented indicate that there is a small (ca. 3%) *but statistically significant variation in the strontium/chlorinity ratio with respect to depth in sea water. An indication of a possible variation in the absolute amounts of strontium in sea water with the geographical location has also been observed. The barium/chlorinity ratio variation with respect to depth was found to be much larger* (ca. 90%) *than that of strontium.*

There have been several reports on studies of the determinations of the strontium (*2, 4, 5, 6, 8, 10, 12, 14, 17, 19, 20, 23*) and barium (*7, 8, 9, 11, 22*) concentrations of sea water and the resulting calculated strontium/chlorinity and barium/chlorinity ratios. The samples analyzed were from numerous geographical locations and depths, with the pretreatment and methods of analysis of the samples not always being similar. The majority of the reports concerning strontium distributions indicate a constant strontium/chlorinity ratio with respect to depth and geographical location within the limits of experimental error of the methods used. The range of the values for this ratio which have been reported most recently

is from 4.4×10^{-3} (*20*) to 4.8×10^{-3} (*10*) in units of (mg.-at. Sr/kg.) $(Cl\ ‰)^{-1}$ with the absolute amount of strontium varying from 6.2 to 8.6 p.p.m. (*10*). Several other investigators on the other hand, have reported large variations in the strontium/chlorinity ratio of sea water (*4, 5, 17, 19, 20*). The range of the ratio in these reports is from 3.33×10^{-3} (*4, 5*) to 5.8×10^{-3} (*17*) in units of (mg.-at. Sr/kg.) $(Cl\ ‰)^{-1}$ with the absolute amounts of strontium varying from 5.77 (*4, 5*) to 10.0 p.p.m. (*17*).

The results of the studies on the barium concentration of sea water have conversely, clearly demonstrated the existence of a variation in the barium/chlorinity ratio. Prior to 1966 very few analyses of the barium concentration of sea water had been reported. Turekian and Johnson (*22*) have recently reported the results of over 250 determinations of the barium concentration of sea water. The average values reported for the barium content of 24 samples from the Atlantic Ocean, the area which is of concern in the present investigation, range from 9 to 30 p.p.b.

The present authors have recently described (*1, 2*) the development of an accurate and precise analytical method using ion-exchange concentration and flame photometry to measure the strontium and barium concentration of sea water from the same sample. Initial analyses indicated that there is possibly a small, but significant, variation in the strontium/chlorinity ratio with respect to depth (*2, 3*). The results of the analyses for barium indicated that, as expected, the variation in the barium/chlorinity ratio is much larger. This communication reports the results of the analyses of samples from several ocean stations for strontium and barium.

Experimental Methods and Results

Water samples taken at sea by standard techniques were placed in polypropylene bottles containing sufficient distilled hydrochloric acid to make the final pH 3.0. Prior to analysis, the stored samples were filtered through Millipore membrane filters type HA(0.45μ). One liter samples were then passed through a 35 × 13 cm. borosilicate glass column containing 35 grams of Dowex 50 × 12 (200–400 mesh) cation exchange resin in the calcium form. An extensive description of the analytical methods utilized for isolating the strontium and barium fractions and their determinations by flame photometry has been given (*2*) and will not be dealt with in length here.

To measure the precision of the method, six replicates of 1.000 liter sea water samples were analyzed for strontium and barium following the recommended procedure (*2*). The mean strontium value obtained was 6.57 p.p.m. with a standard deviation of 0.03 p.p.m. and that for barium was 11.3 p.p.b. with a standard deviation of 0.5 p.p.b.

The accuracy of the method with respect to strontium was measured by adding 6.50 mgms. of strontium as "Specpure" strontium carbonate

(1 p.p.m. barium) to nine 1.000 liter samples of the same sea water used for replication. The mean recovery of the strontium was 6.51 p.p.m. with a standard deviation of 0.05 p.p.m. The accuracy of the method with respect to barium was measured by adding 46.4μgms. of barium as "Specpure" barium carbonate (1 p.p.m. strontium) to 1.000 liter samples of sea water which showed no detectable levels of barium when analyzed by this method. The mean recovery of the barium was 46.8 p.p.b. with a standard deviation of 0.6 p.p.b. These results correspond to experimental variations in the strontium/chlorinity and barium/chlorinity ratios of ±0.03 and ±0.3 respectively in the units previously noted.

Tables I–VI contain the data obtained from the strontium and barium of two ocean stations from the North Atlantic and four ocean stations from the Atlantic Equatorial region. Table III also has included

Table I. Data Taken 7-IX-64 at 41°33′N;50°03′W, ATLANTIS II; Cruise 13, Station 428

Depth Meters	*Temp. °C.*	*Chlorinity ‰*	*Sr p.p.m.*[a]	*Sr/Cl × 10⁻³ mg.-at./kg. ‰*	*Ba p.p.b.*	*Ba/Cl × 10⁻⁶ mg.-at./kg. ‰*
1	16.1	18.407	6.11	3.79	6.8	2.7
49	5.50	18.504	6.42	3.96	9.4	3.7
96	4.82	18.991	6.70	4.03	15.2	5.8
281	4.39	19.257	6.40	3.79	22.8	8.6
489	4.50	19.333	6.36	3.75	1.8	0.7
786	4.23	19.352	6.35	3.74	8.6	3.2
1006	3.91	19.344	6.47	3.82	5.3	2.0
2098	3.33	19.358	6.37	3.76	16.2	6.1

[a] References *3, 4, 5.*

Table II. Data Taken 20-IX-64 at 41°33′N;29°43′W, ATLANTIS II; Cruise 13; Station 430

Depth Meters	*Temp. °C.*	*Chlorinity ‰*	*Sr p.p.m.*[a]	*Sr/Cl × 10⁻³ mg.-at./kg. ‰*	*Ba p.p.b.*	*Ba/Cl × 10⁻⁶ mg.-at./kg. ‰*
1	20.6	19.912	6.46	3.70	9.7	3.5
53	15.50	19.905	6.41	3.67	3.1	1.2
93	14.38	19.882	6.61	3.79	12.9	4.7
292	12.93	19.778	6.72	3.87	3.3	1.2
487	11.71	19.679	6.61	3.83	4.7	1.7
683	10.66	19.621	6.88	4.00	<0.04	—
994	7.64	19.553	6.48	3.78	<0.04	—
1579	4.66	19.380	6.20	3.65	<0.04	—

[a] References *3, 4, 5.*

the results of a strontium analysis of sea water utilizing the technique of Chow and Thompson (*10*) of direct aspiration of the sample into the flame. In using this method, difficulty was experienced in adjusting the monochromator to the wave-length of maximum emission after each background measurement, and severe corrosion of the burner by the sea water occurred. Nevertheless, by applying the experimental error cited by the authors of $\pm 0.2 \times 10^{-3}$ in units of (mg.-at. Sr/kg.) $(\text{Cl}\ ‰)^{-1}$, a value reproduced in the present study, with the exception of the surface value, all values obtained by the direct aspiration method agreed within the experimental error of that method with the results obtained by the more precise method of Andersen and Hume (*2*).

Discussion

Strontium. The average values for the strontium/chlorinity ratio from the vertical profile of the ocean station located at 05°01'S; 32°34'W (Table III) obtained by direct aspiration of sea water into the flame and the combination ion-exchange concentration and flame photometry are $4.51 \pm 0.25 \times 10^{-3}$ and $4.57 \pm 0.15 \times 10^{-3}$ respectively, in the units indicated previously. The mean value of this ratio obtained recently by Culkin and Cox (*12*) for 58 sea water samples from various locations, using a modification of the method of Chow and Thompson (*10*) is $4.6 \pm 0.2 \times 10^{-3}$; a value justifiably considered constant among the samples analyzed within the experimental error of the method. The mean strontium/chlorinity ratio obtained from the data in Tables III–VI, representing 36 analyses of sea water from the Atlantic Equatorial region is $4.56 \pm 0.19 \times 10^{-3}$. This variation is greater by about six-fold than that of the experimental variation of the method—*i.e.*, $\pm$ 0.03 in the respective ratio units. Based on these considerations, we are forced to conclude that there is a variation of the strontium/chlorinity ratio in sea water with respect to depth of the order of 3% and certainly not 7–20% as reported earlier (*4, 5*). We feel that the results of this comparison of data requires us to consider that the values obtained previously for the North Atlantic stations [Tables I and II and (*2*)], having some of the lowest absolute amounts of strontium in sea water from an open ocean reported to date, are valid for the samples obtained at that time, although the cause of such low values is not clear. These considerations then lead us to believe that there is possibly a variation in the strontium/chlorinity ratio with respect to geographical location as well as depth. Also, this variation appears to be smaller than heretofore reported (*4, 5, 17, 19, 20*) and probably within the experimental variation of the methods used where variations have not been observed, substantiating earlier suggestions by other investigators (*23*). Our data suggest that the average strontium/chlorinity ratio is slightly lower than the presently accepted value of $4.8 \pm 0.2 \times 10^{-3}$.

Table III. Data Taken 1-V-65 at 05°01'S;32°34'W,

Depth Meters	*Temp. °C.*	*Chlorinity ‰*	*Sr p.p.m.* [*Ion exchange-flame photometry* (2)]	$Sr/Cl \times 10^{-3}$ [*mg.-at./kg.* / ‰]
Surf	28.40	19.73	7.72	4.47
23	28.40	19.73	7.93	4.59
45	26.97	19.99	7.97	4.55
93	18.33	19.74	8.00	4.63
108	14.08	19.60	7.94	4.62
156	12.63	19.50	7.90	4.62
178	12.03	19.44	7.88	4.63
270	10.80	19.36	7.05	4.16
487	6.68	19.14	7.93	4.73
718	4.17	19.08	8.06	4.82
983	4.16	19.17	7.73	4.61
1493	4.13	19.34	8.23	4.86
2486	—	19.33	7.85	4.63
4387	0.96	19.23	6.93	4.11
				Avg. 4.57 ± 0.15

We feel that great caution must be exercised when considering the oceanographic aspects of our data. We are of the opinion, based on the sea water analyzed, that our data are sufficient to demonstrate that a strontium/chlorinity ratio variation does exist but that any oceanographic conclusions based on the relatively limited amount of data we have obtained to date would be extremely tentative. The results describe only six stations and of the four equatorial stations reported in this communication, only the station at 05°01'S; 32°34'W has sufficient number of samples from depth to describe a vertical profile. It is also important to remember that our values represent the amount of cation in solution at the time of filtration, less any amount being present as a dissolved complex whose formation constant is larger than that of the ion-resin formation constant, although this is probably negligible at the pH at which the concentration step is carried out.

The collection of water samples obtained from 05°01'S; 32°34'W based on the temperature and salinity data represent sample collections from sub-tropical water, Antarctic intermediate water, North Atlantic deep and bottom water and Antarctic bottom water; all the major types of sub-surface water present at this location (*13*). The lowest strontium/chlorinity ratio value was found at 4387 meters in the Antarctic bottom

Crawford: Cruise 125: Station 1751

Sr p.p.m.	$Sr/Cl \times 10^{-3}$ $\left[\frac{mg.\text{-}at./kg.}{0/00}\right]$	*Ba* p.p.b.	$Ba/Cl \times 10^{-6}$ $\left[\frac{mg.\text{-}at./kg.}{0/00}\right]$
	[*Direct aspiration of sea water* (10)]		
6.99	4.04	2.40	0.89
8.24	4.77	2.70	1.00
8.07	4.61	2.10	0.76
8.37	4.84	1.93	0.71
8.02	4.67	—	—
8.00	4.68	1.22	0.46
7.64	4.49	0.77	0.29
7.12	4.20	6.83	2.57
7.58	4.52	3.59	1.37
7.74	4.63	4.85	1.85
7.90	4.71	3.86	1.47
8.22	4.85	4.06	1.53
8.12	4.79	3.43	1.29
6.72	3.99	2.18	0.83
	Avg. 4.51 ± 0.25		

water (4.11). Other minimum values in the profile found at 983 meters (4.61) in the Antarctic intermediate water and at 270 meters (4.16), are associated with increasing values in the oxygen distribution. The highest values fall generally within the depth range of 500 meters to 1500 meters, a depth range containing mostly Antarctic intermediate water.

The two stations located approximately on the equator also contain the same water masses as the southern station. Unfortunately, the distribution of samples was not sufficient to have a complete collection of representative samples. Only one depth of the Antarctic intermediate water was sampled and the Antarctic bottom water was not sampled at all at these stations and a comparison between Antarctic bottom water at these stations and that at the southern station, unfortunately is not possible. The data that are available, nevertheless, show that at 00°08′N; 32°32′W, the observed variation is much larger than at corresponding depths in the southern station at 05°01′S; 32°34′W and generally indicates a lower value for the ratio in the upper 75 meters. There is no agreement observed between the two profiles at a depth of about 300 meters, a depth where an increasing oxygen concentration with depth occurs. However, the value of the ratio for the northerly flowing Antarctic intermediate water at 450 meters is comparable with that at the southerly

station located at 05°01′S; 32°34′W. The station at 00°02′S; 35°00′W has a maximum value of the strontium/chlorinity ratio for water representing the Antarctic intermediate water, in qualitative agreement with the profiles of the other stations indicated previously. The ratio variation in the surface layers is small and the data possibly suggests that it varies inversely with those at 00°08′N; and 05°01′S. The ratio obtained from a sample from 2969 meters, water representing North Atlantic bottom water is comparable with the value for the strontium/chlorinity ratio observed at a similar depth at 05°01′S; 32°34′W.

The station at 09°00′N; 47°00′W has a maximum strontium/chlorinity ratio at the surface (4.82) with a minimum being observed at 45 meters (4.12), unlike the other equatorial stations. However, the ratio at 2958 meters (4.57), a depth representing North Atlantic bottom water, is in general agreement with the other equatorial stations having samples representing this water mass.

There are several general features which emerge from the data obtained in the present analyses. The averages of the strontium/chlorinity ratio from the respective water masses present within the particular water columns sampled vary. The magnitude of the average of the ratio decreases in the order: Antarctic intermediate water > North Atlantic bottom water > sub-tropical lower water > Antarctic bottom water. The greatest variations appear in the surface layers, with the waters from 0 to 200 meters in depth having the lowest average value for the ratio. If the values for the ratios are represented in a meridonal profile depicting the region of the Western Atlantic basin from 05°S; 32°W; to 09°N;47°W, with strontium/chlorinity contours indicated, although because of the limited amount of data no detailed diagram results, there is a correlation with a similar representation using the more numerous salinity data. This indicates certain water masses may be identified and their origins estimated to some degree by their strontium/chlorinity ratio.

Analyses for strontium were not conducted on the different phases present in the sample at the time of collection, therefore the causes of the strontium/chlorinity variation have yet to be assessed quantitatively. There are reports concerning the biological activity of strontium in the marine environment (*15, 18, 21, 24*) indicating that biological removal may play an important role in causing a variation in the strontium concentration of sea water. On the other hand, if we approximate the wet weight of a standing crop of plankton in the oceans as a whole to be 0.3 mg./liter (*16*), it appears that the biological removal of strontium from the oceans is not the sole controlling factor causing the variations we are observing. In fact, to cause a variation in the strontium/chlorinity ratio of sea water of 3% (*i.e.*, $\sim$ 0.24 mg. Sr/liter) would require an abundance of several grams per liter of organisms, such as *Acantharia,*

which selectively extract strontium from sea water. A similar consideration of the strontium content of the carbonate fraction of marine sediments (*21*), results in requiring approximately 0.1 gm. /liter of material of biological origin to be present in a volume of sea water, to produce a variation of 3% in the strontium/chlorinity ratio. The variations presently being observed, and in particular within the surface layers, are considerably larger than could be expected to be caused by biological alteration alone when considering an average standing crop of plankton. Moreover, there does not appear to be a consistent relationship between the strontium/chlorinity ratio and the oxygen distribution. Although additional alteration of the strontium concentration by adsorption on particulate matter and inclusion in crystal structure can also be expected to occur (*21*) in nonbiological processes, as well as "plankton blooms" increasing the effects from the biosphere, it is still not clear what the basis of the variations we are observing is and more work is needed to elucidate the relative importance of the various possible mechanisms. The data tend to suggest that the cause (or causes) is not an ocean wide process. In addition, it must be further pointed out that the sea water samples of which the strontium concentrations were determined, were stored at pH 3.0 for several months prior to analysis. As a result, although the samples were filtered just before analysis there is a possibility that the "soluble" strontium determined may differ from that of a sample filtered immediately subsequent to collection and prior to pH adjustment. Results of experiments concerning this aspect of sample collection will be reported in a future communication.

Barium. The results of the barium analyses [Tables I–VI and (*3*)] show that the range of the barium content of sea water, analyzed in this work, ranges from 0.8 to 37.0 p.p.b. in the equatorial region and from <0.04 to 22.8 p.p.b. in the North Atlantic, with average values of 6.5 p.p.b. and 7.6 p.p.b., respectively. In the North Atlantic, the station at 41°33′N; 50°03′W has a maximum barium content of 281 meters, minimum values at 489 meters and 1006 meters, and the barium concentration increasing below this depth to the next to highest value in the profile at 2098 meters. This distribution is similar to a North Atlantic profile constructed from the results of the barium analysis of sea water from 21 unfiltered samples collected at various locations, dates and depths reported recently (*22*) and a profile near Bermuda (*9*). There is little correlation with the profile of the barium distribution at the indicated locations with that of a station at 41°33′N; 29°43′W. In the former station a maximum barium concentration was observed at 93 meters with no detectable amounts below 683 meters to 1579 meters.

The barium profile at 05°01′S; 32°34′W has much less variation than the North Atlantic profiles. There is a maximum in the barium

Table IV. Data Taken 28-IV-65 at 00°08′N;32°32′W, Crawford; Cruise 125; Station 1750

Depth Meters	Temp. °C.	Chlorinity ‰	Sr p.p.m.	$Sr/Cl \times 10^{-3}$ [mg.-at./kg. / ‰]	Ba p.p.b.	$Ba/Cl \times 10^{-6}$ [mg.-at./kg. / ‰]
1	27.92	19.64	7.37	4.28	4.77	1.77
35	27.24	19.88	7.62	4.39	3.03	1.11
63	21.82	19.97	6.99	3.99	2.07	0.75
75	18.89	19.94	7.37	4.22	4.86	1.77
104	17.25	19.80	8.20	4.73	6.66	2.45
131	15.30	19.69	7.85	4.55	5.25	1.94
166	13.85	19.58	7.80	4.55	1.00	0.37
200	13.38	19.55	8.04	4.69	5.60	2.09
310	9.52	19.28	8.02	4.75	4.68	1.77
450	7.66	19.20	8.00	4.76	6.73	2.55

Table V. Data Taken 15-IV-66 at 09°00′N;47°00′W, Atlantis II; Cruise 20; Station 969

Depth Meters	Temp. °C.	Chlorinity ‰	Sr p.p.m.	$Sr/Cl \times 10^{-3}$ [mg.-at./kg. / ‰]	Ba p.p.b.	$Ba/Cl \times 10^{-6}$ [mg.-at./kg. / ‰]
1	26.75	19.77	8.35	4.82	10.65	3.92
45	26.75	19.77	7.14	4.12	12.78	4.71
95	26.59	19.86	8.12	4.67	36.96	13.55
296	9.41	19.31	7.59	4.49	10.70	4.03
2958	2.83	19.34	7.75	4.57	19.02	7.16

distribution at 270 meters, a minimum at 178 meters with the value of a sample from 4387 meters approximately equal to that of a sample from the surface. There is no apparent correlation of the data with the different water masses present at this location or the oxygen profile. The station at 00°08′N; 32°32′W has values for the barium content which are comparable to that of the southern station at 05°01′S; 32°34′W. The minimum value occurring at the southern station at 178 meters, also being observed at 00°08′N; 32°32′W. The values of the two stations at approximately 475 meters, however, are in sharp contrast; a minimum value of 1.37 being observed in the 05°01′S profile and a maximum value of 2.55 being observed in the 00°08′N profile.

The stations at 00°02′S; 35°00′W and 09°00′N; 47°00′W generally show higher and more variable barium/chlorinity ratios with the more northern station having the higher values. The profile at 00°02′S has the maximum value for the ratio at the surface, the only location at which

Table VI. Data Taken 26/27-III-66 at 00°02′S;35°00′W, Atlantis II; Cruise 20; Station 956

Depth Meters	*Temp. °C.*	*Chlorinity ‰*	*Sr p.p.m.*	*Sr/Cl × 10⁻³* [*mg.-at./kg.* / *‰*]	*Ba p.p.b.*	*Ba/Cl × 10⁻⁶* [*mg.-at./kg.* / *‰*]
1	27.47	19.88	7.97	4.58	21.62	7.92
30	27.22	19.89	7.75	4.45	18.84	6.90
56	26.89	19.96	8.19	4.68	2.86	1.04
96	17.71	19.86	8.00	4.60	3.86	1.42
297	10.05	19.33	7.89	4.66	18.55	6.99
489	6.94	19.15	8.45	5.04	2.60	0.99
2969	2.66	19.27	7.94	4.70	3.45	1.30

this occurs, and values slightly less for the water at 30 meters and 297 meters. Minimum values are observed at depths of 56 meters and 489 meters. The general pattern is one of greater variation in the surface layers. There is close agreement, however, in the barium content of the water at 2969 meters at this station and that of similar water at 2486 meters at 05°01′S; 32°34′W. The station at 09°00′N; 47°00′W has the highest average barium content of the four equatorial stations. A maximum barium concentration occurs at 95 meters, with a significant increase with depth from 296 meters to 2958 meters apparently being present. Unfortunately, there were no samples representing water at intermediate positions between these two depths.

The values obtained in this report for the barium content of sea water have a range which is consistent with other recently reported determinations of Atlantic Ocean samples. However, the values generally tend to be lower than those previously reported with the percent variations being slightly larger. Aside from the generally low values obtained with these analyses and large variations occurring when they are present, there appears to be little correlation between the vertical distribution of barium at the various locations, indicating geographical variations in the barium content of sea water as well as depth variations.

The alterations of the barium concentration in the surface layers because of biological activity is possible and has been discussed previously (*11*, *22*). However, there is no consistent pattern which emerges from the present data in this regard. Increased concentrations of barium due to the increase in solubility of barium sulfate with depth as discussed earlier for Pacific Ocean waters (*11*) is not apparent from our profiles or those already reported by other investigators (*9*, *22*) for Atlantic Ocean waters. The possibility of high barium values at certain depths being caused by barium rich particles in unfiltered samples

analyzed as has been suggested earlier (23) is considered negligible in the present analyses. As yet, the variation in the barium distribution does not appear to be associated with any single oceanographic parameter.

Acknowledgments

We wish to thank V. T. Bowen of the Woods Hole Oceanographic Institution, Woods Hole, Mass., for his advice and encouragement, Alan Gordon, Brian Schroeder, the officers and crews of the R. V. Atlantis II and R. V. Crawford for collection of the samples and to J. Richard Jadamec for his very capable assistance in the analysis of the samples. The initial work was supported at the Woods Hole Oceanographic Institution, Woods Hole, Mass., under contract AT(30-1)-2174 and AT(30-1)-3145 from the U. S. Atomic Energy Commission and under grant 12178 from the U. S. National Science Foundation and at Massachusetts Institute of Technology, Cambridge, Mass., under contract AT(30-1)-905 from the U. S. Atomic Energy Commission. To each of these agencies, the authors wish to express their thanks.

Literature Cited

(1) Andersen, N. R., Hume, D. N., *Anal. Chim. Acta* **35,** 441 (1966).
(2) *Ibid.*, **40,** 207 (1968).
(3) Andersen, N. R., Ph.D. thesis, Massachusetts Institute of Technology, Cambridge, Mass. (1965).
(4) Andersen, N. R., *Chem. Geol.* **2,** 77 (1967).
(5) Angino, E. E., Billings, B. K., Andersen, N. R., *Chem. Geol.* 1, 145 (1966).
(6) Billings, G. K., Bricker, O. P., Mackenzie, F. T., *A. G. U. Ann. Meeting, 1967, Washington, D. C.*
(7) Bolter, E., Turekian, K. K., Schutz, D. F., *Geochim. Cosmochim. Acta* **28,** 1459 (1964).
(8) Bowen, H. J. M., *J. Marine Bio. Assoc., U. K.* **38,** 451 (1956).
(9) Chow, T. J., Patterson, C. C., *Earth Plan. Sci. Letter* 1, 397 (1966).
(10) Chow, T. J., Thompson, T. G., *Anal. Chem.* **20,** 18 (1955).
(11) Chow, T. J., Goldberg, E. D., *Geochim. Cosmochim. Acta* **20,** 192 (1960).
(12) Culkin, F., Cox, R. A., *Deep-Sea Res.* **13,** 789 (1966).
(13) Defant, A., "Physical Oceanography," Vol. 1, MacMillan Co., New York, 1961.
(14) Fabricand, B. P., Imbimbo, E. S., Brey, M. E., Weston, J. A., *J. Geophys. Res.* **71,** 3917 (1966).
(15) Goldberg, E. D., Arrhenius, G. O. S., *Geochim. Cosmochim. Acta* **13,** 153 (1958).
(16) Hill, M. N. (Ed.), "The Seas," Vol. 2, Interscience Publishers, New York, 1963.
(17) Mackenzie, F. T., *Science* **146,** 517 (1964).
(18) Odum, H. T., *Pub. Inst. Marine Sci.* **4,** 39 (1957).
(19) Sugawara, K., Kawasaki, N., *Records Oceanog. Works Japan* **March 2,** 227 (1958).

(20) Sugawara, K., Terada, K., Kanamori, S., Okabe, S., *J. Earth Sci.* **10,** 34 (1962).
(21) Turekian, K. K., *Geochim. Cosmochim. Acta* **28,** 1479 (1964).
(22) Turekian, K. K., Johnson, D. G., *Geochim. Cosmochim. Acta* **30,** 1153 (1966).
(23) Turekian, K. K., Schutz, D. F., *Proc. Univ. of Rhode Island Symp. Marine Geochem.*, Occasional Publ. 3, 41 (Oct. 1964).
(24) Vinogradov, A. P., "The Elementary Compositions of Marine Organisms," Sears Found. for Marine Res., Mem. II, Yale Univ., New Haven, Conn., 1953.

RECEIVED May 25, 1967.

19

Neutron Activation Analysis of Lanthanide Elements in Sea Water

OVE T. HØGDAHL and SIGURD MELSOM

Central Institute for Industrial Research, Oslo 3, Norway

VAUGHAN T. BOWEN

Woods Hole Oceanographic Institution, Woods Hole, Mass.

Neutron activation analyses of sixteen samples of sea water (eight in duplicate) taken at six widely spaced stations in the Central Atlantic Ocean between 16° N and Equator (depths below 1000 m.) showed that the lanthanide patterns are relatively conservative characteristics of water masses. The differences in lanthanide distribution and total abundance between different water masses are small but significant. The absolute mass abundances of the lanthanides can be illustrated by the following values for North Atlantic Deep Water:

La: 0.0034 μg./liter,	*Ce: 0.0012 μg./liter,*	*Pr: 0.00064 μg./liter*
Nd: 0.0028 μg./liter,	*Sm: 0.00045 μg./liter,*	*Eu: 0.00013 μg./liter*
Gd: 0.00070 μg./liter,	*Tb: 0.00014 μg./liter,*	*Dy: 0.00091 μg./liter*
Ho: 0.00022 μg./liter,	*Er: 0.00087 μg./liter,*	*Tm: 0.00017 μg./liter*
Yb: 0.00082 μg./liter,	*Lu: 0.00015 μg./liter,*	*Y: 0.0133 μg./liter*

Recent development of our knowledge of lanthanide distributions in nature encouraged us to believe that variations in ratios of these elements might well characterize individual water masses: as summarized by Haskin *et al.* (5), considerable lanthanide fractionation has occurred in the formation of the earth's crust; it might be expected that these fractionations would be reflected in the lanthanide patterns of material eroded from different regions and supplied to the oceans. Since, on the other hand, the lanthanide patterns of marine shales and sediments (*5, 6, 11*) do not reflect these regional differences but are essentially uniform on a world-wide basis, sea water should express the differential residues on a

quite conservative basis, and in spite of the rather short residence times calculated by Goldberg *et al.* (*4*) for the lanthanides. Indication that this might be the case was given by the demonstration (*4*) that sea water is enriched in those heavy lanthanides which are not enriched in marine sediments (*6*). In this circumstance the relative and overall concentrations of the lanthanides in a specific mass of water would change mainly by mixing with other water masses having different overall or relative concentrations (or both).

In addition to change of concentration by mixing processes, the relative concentrations of lanthanides may be changed by oxidation-reduction reactions followed by differential mineral uptake (as for manganese nodules (*4, 10*), or phosphorites (*4*)), or by differential solubility or ion-exchange processes affected by variations in ionic radius. The lanthanides are the group of elements for which such processes are known to be least effective: only two, cerium and europium, are expected to exhibit stable ions other than trivalent, and as summarized by Moeller *et al.* (*13*), lanthanide complexes are typically weak, and show within the series, only modest variations in strength.

Experimental

The ultimate goal for any trace element analysis of sea water is to determine the amount and chemical activities of the element associated with the different forms in which it may exist. The development of a procedure for such an analysis requires both a thorough knowledge of the physico-chemical behaviour of the element in question and methods capable of fractionating a sample. Presently, we have not the necessary knowledge of the chemistry of the lanthanides in sea water. In addition, the present state of the art of fractionation of sea water samples prohibits the development of such procedures as mentioned above.

In this work we have determined the amount of lanthanides coprecipitated on iron hydroxide from 10-liter samples of unfiltered sea water previously acidified below pH 2 for some weeks. Experiments with radioactive ^{88}Y tracer had shown no adsorption to the containers below pH 4.

Sampling. Samples have been collected by employing the 140-liter sampler designed by Bodman *et al.* (2). Comparisons of the samples analyzed with simultaneously collected salinity samples and complete hydrographical station data, provided criteria of good sampler performance. Ten-liter samples were drawn from the large sampler directly into acid-washed polyethylene containers. The ten-liter samples were acidified with 50 ml. purified 6*N* hydrochloric acid and stored on board ship. The pH after acidification was 1.5.

Procedure. On arrival at the laboratory, purified iron carrier solution and radioactive ^{88}Y and ^{139}Ce tracers were added, and the acidified solutions were allowed to equilibrate for one to four month periods. The iron was precipitated with ammonia gas (pH of about 8.5-9.0) and separated by settling and subsequent centrifugation. The precipitate was dissolved

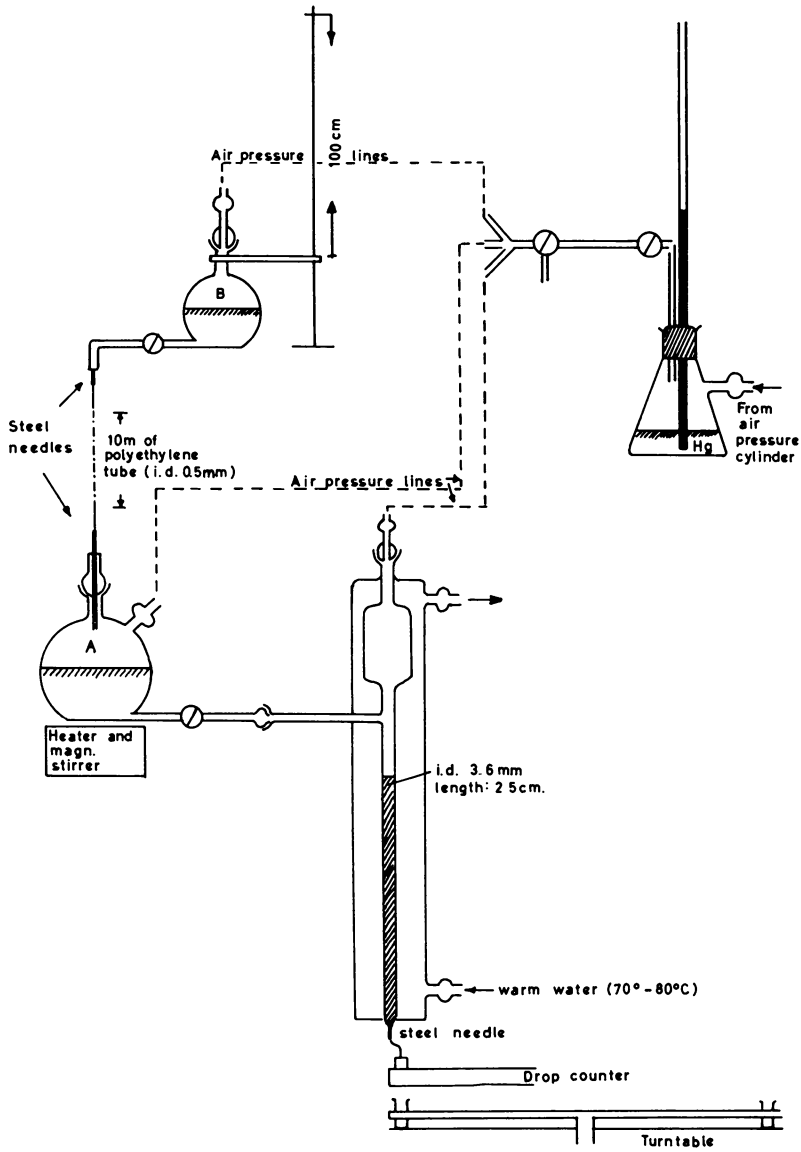

Figure 1. Schematic diagram of apparatus for continuous gradient elution

by saturating with hydrogen chloride gas, and iron together with uranium, which might have been coprecipitated, was removed by an anion exchange step using Dowex 1. About 10 mg. of iron were added to the eluate, precipitated with ammonia gas, centrifuged, dissolved with hydrogen chloride gas, and transferred to a clean 5-ml. polyethylene centrifuge tube.

After reprecipitation with ammonia gas and subsequent centrifugation and drying at 70° C. for 12 hours, the tube was heat-sealed. The overall chemical yields of the pre-irradiation procedure were determined by measuring the added tracers.

Each tube irradiated was provided with three zinc foil flux monitors (10-15 mg., 0.2 mm. thick) to provide normalization for neutron flux. Sample tubes were irradiated for three days, flux about $2.5 \cdot 10^{12}$ neutrons/cm.^{2} sec. Previously, a set of dilute standard solutions of all the lanthanides, in sealed quartz ampoules, had been irradiated under identical conditions. The specific activities of the elements normalized to a constant neutron flux were shown to be constant in nine subsequent irradiations (7). These normalized specific activities were used in the determination of the concentration of the lanthanides in the samples.

Table I. List of Samples Analyzed (Atlantis-II, Cruise No. 20)

Sample No.	*Position, Date*	*Depth m*	*Salinity ‰*	*Temp. °C.*	*Sigma − T*[b]
B.2	St. No. 944	1000	34.788	5.51	27.46
B.3	16° 05′N, 59° 05′W	1991	34.986	3.62	27.83
B.4	Feb. 10-11, 1966	1991	34.986	3.62	27.83
B.5		4720	34.876	2.17	27.88
B.6	St. No. 948	974	34.743	5.14	27.47
B.7	11° 00′N, 29° 45′W	2435	34.940	3.01	27.85
B.8	Feb. 24-25, 1966	2435	34.940	3.01	27.85
B.9	Sonic depth: 5600 m	5696	34.878	2.35	27.86
B.10	St. No. 949	994	34.684	4.71	27.47
B.11	05° 15′N, 23° 30′W	994	34.684	4.71	27.47
B.12	Feb. 27, 1966	2452	34.934	2.92	27.86
B.13	Sonic depth: 4300 m	4302	34.888	2.33	27.87
B.14		4302	34.888	2.33	27.87
B.15	St. No. 951	993	34.660	4.36	27.49
	00° 08′S, 18° 30′W				
B.16	March 8, 1966	993	34.660	4.36	27.49
B.17	Sonic depth: 7739 m	1987	34.966	3.49	27.83
B.18	St. No. 956	991	34.623	4.38	27.47
B.19	00° 02′S, 35° 00′W	991	34.623	4.38	27.47
	March 27, 1966				
B.20		2000	34.960	3.4-3.6	27.82
	Sonic depth: 4540 m				
B.21[a]		4526	34.762	1.002	27.87
B.22[a]		4526	34.762	1.002	27.87
	St. No. 968				
B.24	07° 30′N, 45° 30′W	1974	34.956	3.58	27.82
B.25	April 14, 1966	4339	34.867	2.06	27.88
B.26	Sonic depth: 4387 m	4339	34.867	2.06	27.88

[a] Contained mud.
[b] Sigma − T = [(Density at one atmosphere) − 1]/1000.

Table II. Absolute Abundances of

	B.2	B.3	B.4	B.5	B.6
La	39	32	28	66	10.0
Ce	26	9.0	14	24	6.2
Pr	15.8	5.6	4.7	11.8	4.9
Nd	37	27	23	46	22
Sm	10.0	3.6	4.3	6.9	3.4
Eu	7.9	1.5	1.1	2.2	0.9
Gd	11.5	6.9	6.5	6.9	5.6
Tb	2.0	0.8	2.0	1.3	—
Dy	14.0	9.5	9.5	11.2	5.2
Ho	5.9	1.2	2.1	2.8	1.8
Er	12.4	8.8	8.4	10.9	8.6
Tm	3.7	1.3	1.8	0.9	1.7
Yb	17.2	6.0	6.9	8.9	6.2
Lu	7.5	1.45	1.2	2.0	1.3
Y	129	122	124	155	127
Sc	8	13	14	9	10

Table II. Absolute Abundances of Lanthanides,

	B.14	B.15	B.16	B.17	B.18
La	36	25	29	43	25
Ce	6.0	15	8.2	26	—
Pr	8.9	4.1	4.3	6.8	5.5
Nd	31	15	18	23	18
Sm	5.7	3.2	3.6	4.6	3.7
Eu	1.4	0.9	1.1	1.2	1.0
Gd	7.6	5.2	6.0	7.5	7.6
Tb	3.6	0.6	1.3	(3.2)	0.6
Dy	11.4	6.6	6.8	9.8	5.9
Ho	2.3	2.1	2.2	2.9	2.1
Er	8.9	8.0	7.5	10.5	7.8
Tm	2.5	1.7	—	2.4	1.3
Yb	9.3	8.7	8.6	9.2	9.2
Lu	1.6	1.8	1.7	1.75	1.75
Y	139	126	119	152	153
Sc	18	7	17	7	0.1

After irradiation the sample was dissolved in hydrochloric acid. A known amount of all the lanthanides (0.5-1 mg. each) and 10 mg. of barium were added, the cerium was oxidized and subsequently reduced to ensure complete exchange of carrier and cerium activity, and the lanthanides were separated and purified as a group using a series of fluoride and hydroxide precipitations. The final hydroxide precipitate was dissolved in dilute hydrochloric acid and adsorbed to 80 mg. of Dowex 50. The resin was transferred to the top of an ion exchange column (Dowex 50×12, NH_4^+-form, settling rate 0.5-1.5 cm./min.), and the lanthanides were eluted using α-hydroxy-isobutyric acid and continu-

Lanthanides, Y and Sc (10^{-4} μg./liter)

B.7	*B.8*	*B.9*	*B.10*	*B.11*	*B.12*	*B.13*
27	39	39	26	31	33	52
15	36	25	13	14	6.4	14
5.2	7.2	5.1	5.8	5.2	7.9	8.9
21	39	37	19	30	26	65
3.8	5.5	5.5	4.2	4.0	4.1	6.1
1.2	1.7	1.3	1.85	1.0	1.5	1.6
7.2	7.9	8.3	7.4	5.7	6.3	—
1.6	1.2	1.1	1.0	1.6	1.1	2.8
8.4	10.8	8.0	7.4	7.6	5.9	10.2
2.3	2.3	2.6	2.6	2.2	2.4	2.1
8.5	9.9	9.8	8.5	6.9	7.0	9.3
1.2	1.6	1.4	2.6	2.2	2.3	2.6
8.7	10.0	8.6	9.2	8.3	7.8	9.7
1.5	1.9	1.6	3.2	1.45	1.4	1.8
119	144	130	121	144	126	161
6	12	3	6	—	6	14

Y and Sc (10^{-4} μg./liter) (Continued)

B.19	*B.20*	*B.21*	*B.22*	*B.24*	*B.25*	*B.26*
34	29	22400	25000	26	43	63
—	14	68300	66000	5.7	28	37
5.2	5.9	6890	7900	5.9	10.5	11.1
26	31	25400	33300	13	29	40
4.3	4.6	5980	7350	2.6	6.3	7.6
1.2	1.35	1240	1950	1.0	1.9	2.0
6.4	7.3	5280	6610	—	9.2	11.0
1.8	2.2	780	905	0.7	1.4	2.0
8.9	10.3	3420	6000	7.9	9.6	11.3
2.3	2.5	1030	994	2.2	2.4	3.0
9.1	9.2	2560	2800	6.6	9.1	11.0
1.3	2.1	340	420	1.1	1.7	2.6
9.5	9.1	2200	2150	6.0	9.1	9.8
2.1	1.7	322	366	1.0	2.0	2.25
132	148	21700	28600	112.	150	163
6	11	3190	3200	2	5	16

ous gradient elution (variation of pH and of concentration of eluant). The experimental set-up is shown schematically in Figure 1. To each of the fractions (0.3-1 ml.) were added 2 drops of a saturated solution of 8-hydroxyquinoline in 2*N* ammonium hydroxide. The fractions representing each element, identified by precipitation, were combined, converted to the oxide by heating, to the nitrate by nitric acid, and finally dissolved in about 0.25 ml. of dilute nitric acid. One tenth of a milliliter of each solution was evaporated on aluminum coated mylar film for β-counting, and two 0.050 ml. portions were used for a spectrophotometric determination of the chemical yield using a modification of Rinehart's method (*14*).

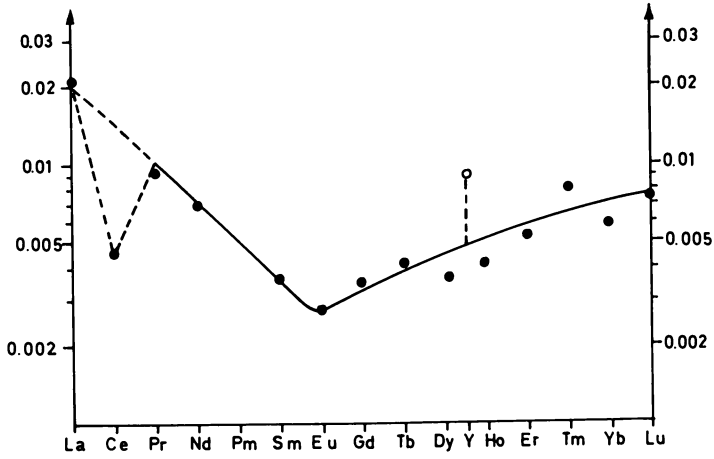

Figure 2. μg./liter lanthanides in sample B.26 relative to p.p.m. lanthanides in twenty chondrites (5)

The activity of the standards and separated elements was measured under identical counting arrangement. All activities were corrected for self-absorption and self-scattering. (A correction of less than 9% (7).)

Interferences from fission of uranium which might not have been removed by the preirradiation procedure were checked by separating barium from the irradiated samples and looking for ^{140}Ba-^{140}La-activities. No interferences have been observed. The barium was separated using a method by Minkkinen (*12*).

Blank determinations were made by adding the same amount of radioactive tracer solutions, iron carrier-solution and purified 6*N* hydrochloric acid as used for the sea water samples to an empty acid-washed 10-liter polyethylene container. After washing the bottle for a few minutes, the acid solution was carried through the same procedure as described above.

Results

The results of the analyses of sixteen sea water samples (eight in duplicate) taken on cruise No. 20 of R.V. ATLANTIS-II, Woods Hole Oceanographic Institution, are presented in this paper. Sampling positions and characterization of samples are given in Table I. The results are summarized in Table II. Although scandium is not a lanthanide, the absolute abundance of this element is also given in the table. However,

Table III. The Average Lanthanide Distribution of Samples

	La	*Ce*	*Pr*	*Nd*	*Sm*	*Eu*	*Gd*
10^{-4} *μg./liter*	34	12	6.4	28	4.5	1.3	7.0

scandium results were not used in the following discussion of the data.

Information concealed in data can often be most rapidly comprehended from graphical displays. Owing to the alternation in abundance between adjacent even-Z and odd-Z elements simple plots of the type "absolute abundance versus atomic number" will often easily obscure small differences in lanthanide distribution patterns. The method often used to remove the even-Z, odd-Z effect is to divide one distribution, element by element, by a known distribution, and plot the resulting ratios on a logarithmic scale against a linear scale of atomic number or ionic radius (5). If the two distributions are identical, all the ratios are the same and a horizontal line appears. Trends of differences in the distributions appear as curves or sloped lines.

As the first step in the analysis of our data, we divided each of the twenty-four distributions, element by element, by the average absolute mass abundance of the lanthanides in twenty chondrites (5) and plotted the ratios on a logarithmic scale against a linear scale of atomic number. A visual inspection of the normalized patterns indicated that at least eleven distributions, apart from differences in total lanthanide abundance, were identical; nearly all the other patterns differed only slightly from the eleven samples mentioned. The normalized pattern for one sample is shown in Figure 2. Obviously, the distributions of lanthanides in sea water are quite different from the pattern in chondrites.

Small differences in the lanthanide patterns of the twenty-four sea water samples will more easily be detected by normalizing against a distribution more similar to that of sea water, for example an average distribution derived from our sets of data. The average distribution of the eleven samples noted above (B.3, B.4, B.7, B.8, B.9, B.12, B.13, B.14, B.17, B.20 and B.24) was used on the hypothesis that they represented a single population; not only do the distributions look identical, but the samples all come from a single water mass (North Atlantic Deep Water).

Because the total lanthanide abundances of these eleven samples are different, the average distribution was found by taking the arithmetic mean of the logarithm of the absolute abundances of each element. The antilogarithms of these results are given in Table III.

The correctness of our assumption (the eleven samples having identical patterns) was tested by normalizing the raw analytical data of the eleven samples by using the calculated average distribution, and fitting

B.3, B.4, B.7, B.8, B.9, B.12, B.13, B.14, B.17, B.20 and B.24

Tb	*Dy*	*Y*	*Ho*	*Er*	*Tm*	*Yb*	*Lu*
1.4	9.1	133	2.2	8.7	1.7	8.2	1.5

Table IV. Relative Weight Factors Used for the Weighted

	La	*Ce*	*Pr*	*Nd*	*Sm*	*Eu*	*Gd*
Weight factor	9	1	4	1	9	4	4

regression lines to the logarithms of the experimental values of the ratios using different weight factors for the various elements. These factors were selected on the basis of the confidence we had in the data based on our experience in the method. The relative weight factors are given in Table IV. If our hypothesis is correct, the eleven regression lines should all have zero slope (with due regard to statistical variations).

The following statistical analysis in which standard statistical methods (3) have been modified to our special problem of fitting regression lines to normalized lanthanide patterns has been performed by Kolboe (9).

For each of the eleven samples under question the estimated regression equation is

$$Y = a + b(x - \bar{x})$$

where Y is the logarithm of the normalized lanthanide abundance, and x is proportional to the atomic number. The value of $\bar{x}$, a and b, and the variance of a and b is given from the following equations (3):

$$x = \frac{\Sigma w_i x_i}{\Sigma w_i}$$

$$a = \frac{\Sigma w_i y_i}{\Sigma w_i}$$

$$b = \frac{\Sigma w_i (x_i - \bar{x}) Y_i}{\Sigma w_i (x_i - \bar{x})^2}$$

$$V[a] = \frac{1}{\Sigma w_i}$$

$$V[b] = \frac{1}{\Sigma w_i (x_i - \bar{x})^2}$$

The weight factors w_i are such that

$$E\left[\frac{\Sigma w_i (y_i - Y_i)^2}{k - 2}\right] = 1 \qquad (1)$$

and such that the relative weight factors are equal to those in Table IV. E means the expectation of the function in the larger brackets. The summation is taken from $i = 1$ to 16 (sixteen elements). The values of x_i are integers for all the lanthanides except for yttrium:

$x_i = i$ for $i = 1$ to 10 (lanthanum through dysprosium)

$x_i = i - 0.5$ for $i = 11$ (yttrium)

$x_i = i - 1$ for $i = 12$ to 16 (holmium through lutetium)

Linear Regression Analyses of the Analytical Data

Tb	*Dy*	*Y*	*Ho*	*Er*	*Tm*	*Yb*	*Lu*
1	4	9	4	4	1	9	3

To obtain the values of y_i the logarithm of the normalized abundance of the i-th element was taken. That is, for a particular sample, the abundance of the i-th element is divided by the abundance of that element in the average lanthanide distribution (Table III), and the logarithm of this ratio is formed to give y_i.

Note that for promethium, $x_5 = 5$, the weight factor, w_5, is equal to zero. The value of $k - 2$ in Equation 1 which is the degrees of freedom, is in our case equal to thirteen. Note also that $\bar{x}$ and the variance of a and b, $V[a]$ and $V[b]$, are the same for all the eleven distributions in question.

Results of the weighted regression analyses of the data for the eleven distributions are summarized in Table V. The normalized lanthanide patterns for the two samples which have the smallest (B.14) and largest

Table V. Results of the Weighted Regression Analyses
$Y = a + b(x - \bar{x})$

	$a \cdot 10^{-2}$	$b \cdot 10^{-3}$
B.3	−6.3	−3.1
B.4	−4.6	1.2
B.7	−3.7	7.3
B.8	7.1	−1.3
B.9	2.6	−3.3
B.12	−2.9	−1.6
B.13	9.7	−9.2
B.14	5.1	0.1
B.17	4.9	−0.3
B.20	1.5	8.5
B.24	−13	1.7
B.2	29	15
B.5	13	−18
B.10	1.4	17
B.11	3.2	3.6
B.18	3.9	13
B.19	0.8	8.1
B.25	9.3	−7.7
B.26	17	−13

Standard deviation in b: $3.5 \cdot 10^{-3}$
$\bar{x}$: 8.67

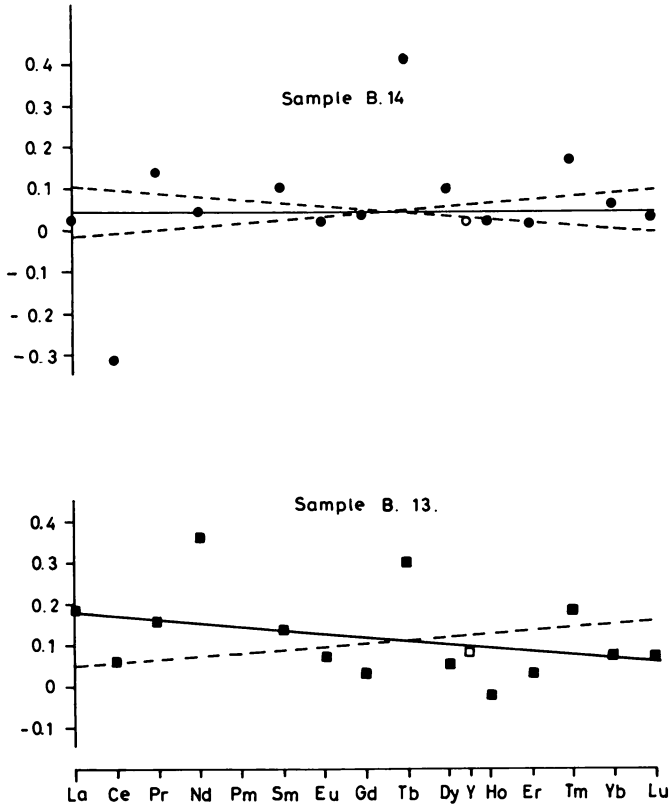

Figure 3. Logarithm of ratio of μg./liter lanthanides in sample to μg./liter lanthanides in eleven sea water samples (Table III). The dashed lines represent the 95% confidence limits for the expected normalized distribution

(B.13) deviation in slope from the expected value of zero are shown in Figure 3.

A test of the zero hypothesis shows that the slope of sample B.13 lies within the 98% confidence limits of the mean. Thus, it is not possible to find any significant difference between the eleven lanthanide patterns, and the average distribution given in Table III has to be accepted as the true average lanthanide pattern for these eleven samples.

The regression lines through a set of normalized data can be looked upon as the lanthanide pattern of that sample relative to the average distribution given in Table III. These patterns will be called the normalized patterns in the following. The normalized pattern of the eleven samples will be described as a type "A" pattern.

The data of the remaining thirteen samples were normalized to the type "A" pattern. A visual fitting showed that five samples, possibly a

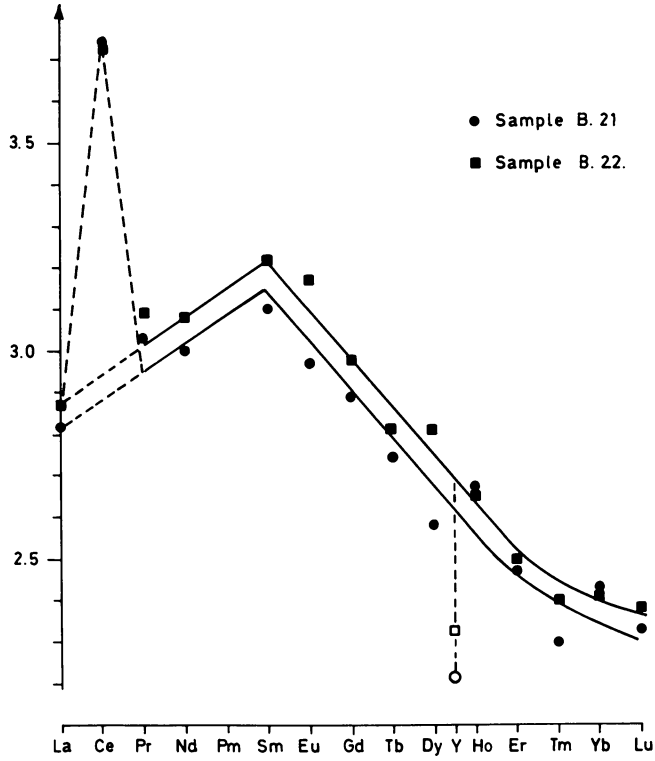

Figure 4. Logarithm of ratio of μg./liter lanthanides in sample to μg./liter lanthanides in eleven sea water samples (Table III)

sixth, have normalized patterns which best can be represented by two straight lines. The normalized pattern of samples B.21 and B.22 is shown in Figure 4. It is difficult to detect any significant difference between this pattern and the average pattern of forty North American shales which is believed to represent the best average pattern of oceanic sediments (5). As mentioned in Table I, these two samples contained mud, and, obviously, reflect the pattern of this contamination.

The normalized patterns of samples B.2, B.6, B.15 and B.16 are shown in Figures 5 and 6. The data for sample B.2 scatter to such an extent that the pattern equally well can be represented by one straight line; the two lines for B.2 are dashed in order to indicate their uncertainty. We have considered the possibility that the normalized patterns for the other three samples also are attributed to statistics. It can be seen from the figures that these special types of patterns depend to a large extent on the lanthanum value. However, the results for the other twenty samples indicate that the lanthanum values are determined with such an accuracy

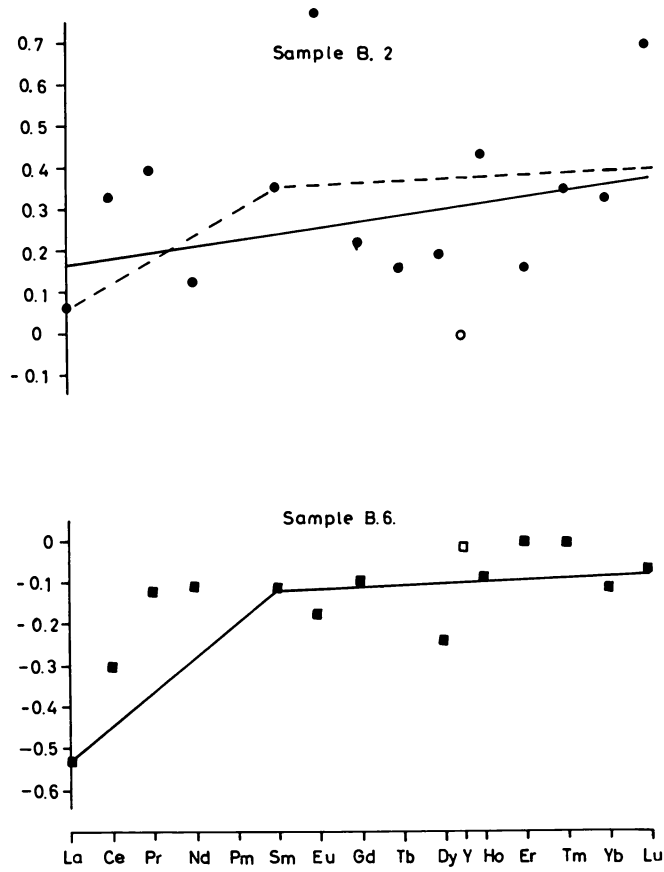

Figure 5. Logarithm of ratio of μg./liter lanthanides in sample to μg./liter lanthanides in eleven sea water samples (Table III)

that it is more probable that the patterns drawn are closer to the true patterns than straight lines. This assumption is supported by the two facts that all three samples are taken at 1000 meters, and that the two samples, B.15 and B.16, which are duplicates, show very similar normalized patterns.

The normalized patterns for another seven samples (B.5, B.10, B.11, B.18, B.19, B.25 and B.26) can best be fitted by single straight lines. The slopes of these lines have been calculated by the weighted regression analysis described previously. Because the pattern of B.2 could be fitted by a straight line too, this sample was included with this set of seven samples. The results of the regression analysis are summarized in Table V. Of these eight samples only samples B.11, B.19 and B.25 do not differ

significantly from the average distribution given in Table III. However, these three samples are parallels to samples B.10, B.18 and B.26, respectively. The mean of the slope of these three sets of duplicate samples is outside the 98.5% confidence limits for the average distribution. Thus, we have concluded that these eight water samples have normalized patterns significantly different from the type "A" previously mentioned. Three samples (B.5, B.25 and B.26) have a pattern of type "B" with negative slope, and five samples (B.2, B.10, B.11, B.18 and B.19) have a pattern of type "C" with positive slope. Both type "B" and type "C" are significantly different from the type "A" pattern.

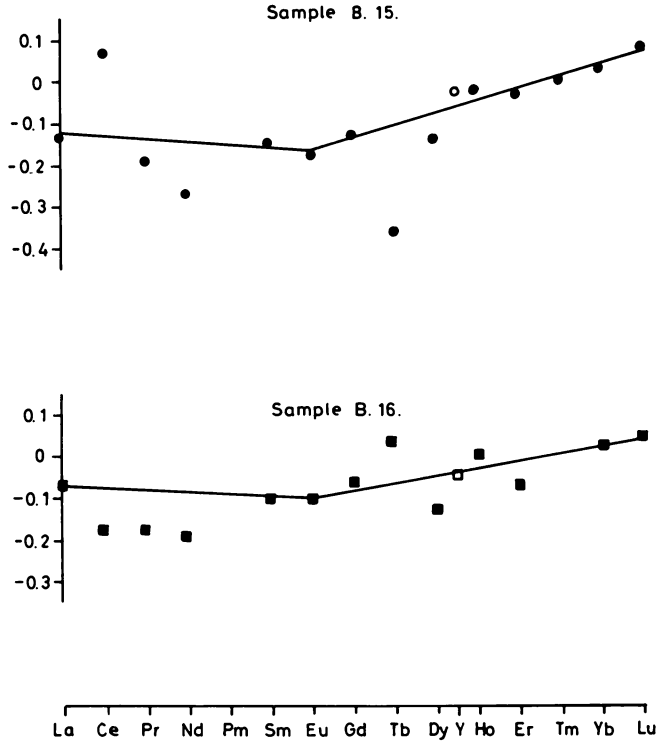

Figure 6. Logarithm of ratio of μg./liter lanthanides in sample to μg./liter lanthanides in eleven sea water samples (Table III)

Of the three samples which have normalized patterns which best can be represented by two lines, one (B.6) has a normalized pattern of type "D", and the pair of duplicates (B.15 and B.16) have a normalized pattern of type "E".

Table VI. Total Mass Abundances of

	La	*Ce*	*Pr*	*Nd*	*Sm*	*Eu*	*Gd*
	30	—	12	44	10	13	—
10^{-4} μg.	38	100	16	99	12	11	9.5

Table VII. Normalized Lanthanide Patterns

		Western
Station No.	*944*	*968*
Position	*16° 05'N* *59° 05'W*	*07° 30'N* *54° 30'W*
Depth		
900-1000 m	B.2 C	
1800-2500 m	B.3; B.4 A A	B.24 A
4000-5000 m	B.5 B	B.25; B.26 B B

[a] Normalized lanthanide patterns are as follows:
(A) Arctic deep water = N. Atlantic deep water
(B) Antarctic bottom water
(C) Antarctic intermediate water

Discussion

The total concentrations of the lanthanides in the Indian Ocean (*1*) are about 100 times greater than in the deep Central Atlantic Ocean, but comparable with that of surface waters of the Pacific Ocean near California (*4*).

Because of the small amount of lanthanides in sea water (approximately 0.003 p.p.b. of lanthanum and 0.0001 p.p.b. of europium) it is necessary, even with the use of the sensitive method of neutron activation, to concentrate the lanthanides from sea water prior to the irradiation. This procedure requires the addition of radioactive tracers for the determination of the chemical yield of the preirradiation procedure; thus abandoning the most outstanding advantage of activation analyses, the elimination of blank corrections.

The results of duplicate determinations of the blank are shown in Table VI. Blanks of several elements (Ce, Nd, Gd, and Tm) are close to the amounts found in samples but are also close to the available detection limits; the final recorded values, after blank subtraction, are good, therefore, only to ±50%. This uncertainty has been taken care of by giving these elements low weight factors (Table IV).

Lanthanides, Y and Sc in Blank (Duplicates)

Tb	*Dy*	*Y*	*Ho*	*Er*	*Tm*	*Yb*	*Lu*	*Sc*
27	44	53	2.5	—	3.0	—	—	33
14	40	54	3.4	5.4	4.6	6.5	2.4	10

in Relation to Water Masses

Basin		*Eastern Basin*	
956	*951*	*949*	*948*
00° 02'S *35° 00'W*	*00° 08'S* *18° 30'W*	*05° 15'N* *23° 30'W*	*11° 00'N* *29° 45'W*
B.18; B.19 C C	B.15; B.16 E E	B.10; B.11 C C	B.6 D
B.20 A	B.17 A	B.12 A	B.7; B.8 A A
B.21; B.22 F F		B.13; B.14 A A	B.9 A

(D) Distinct but unrelated to pattern "C"
(E) Uncertain
(F) Contained mud, lanthanides like marine shales

The main source of the contamination is the added tracers. Although the blanks are relatively high, they are constant because of the constant addition of tracers and other reagents to the samples. Blanks for other series of water samples show similar values.

Since cerium because of its 4-valence state might behave chemically differently from the other lanthanides in sea water, we are adding both ^{139}Ce- and ^{88}Y-tracers to the samples prior to the concentration step. No significant difference between the chemical yields calculated on the basis of ^{139}Ce- and ^{88}Y-tracers was found in 23 of our set of 24 samples. Only sample B.2 showed a significant difference of 24% (chemical yields of ^{139}Ce and ^{88}Y: 47% and 38%, respectively). The chemical yields of all the other samples were approximately 85%. While the iron was precipitated from the 23 samples at a pH of approximately 8.5, the corresponding pH of sample B.2 was only 7-7.5. The higher yield of ^{139}Ce in this case may be explained by assuming that cerium is co-precipitated in its 4-valence state. However, the results of the concentration of the 23 samples show that under conditions which favor a complete precipitation of iron, no fractionation of cerium relative to the other lanthanides occurs.

The accuracy of the determination of the absolute mass abundances given in Table II depends to a large extent in the accuracy of the

determination of the chemical yields of the preirradiation procedure. The main factor controlling this accuracy is the degree of exchange between the added radioactive tracers and the stable lanthanides in the sample. The time of exchange for 16 samples (pH about 1) was 30 days. For the other eight samples (duplicates) the time of exchange was 90 days. The difference in total abundance between duplicates was less than 20%. No correlation between total abundance and time of exchange was found. This we take as a strong indication of complete exchange. An alternative possibility that part of the lanthanides exists in sea water in a form which has a low rate of exchange (half time much larger than 90 days) at pH 1, we believe untenable, especially in view of the relatively weak lanthanide complexes known (*13*).

If one assumes that both cerium and yttrium are normal relative to the other lanthanides in chondrites, the present work shows that for open ocean samples cerium is depleted relative to the lanthanides in sea water by an average factor of approximately 5. On the other hand, yttrium is enriched by an average factor of 2.3.

The accuracy of the determination of the absolute cerium abundance is not very good because of a relatively high blank for this element (Table VI). The amount of cerium contamination is of the same order as that originally in the sample. This is largely from the ^{139}Ce-tracer added to the sea water sample. However, even without subtracting for the blank, the cerium will be depleted. The average depletion of cerium by a factor of approximately 5 is in nice agreement with the value of 4.8, which can be deduced from the data of Goldberg *et al.* (*4*) for the Pacific Ocean water sample.

There exists a strong relationship between lanthanide patterns and sea water masses (*8*). The result of the discussion is shown in Table VII. We want to stress that the waters at 1800-2500 meters at all stations and at 4000-5000 meters at the two stations in the eastern basin are all from the same water mass, the North Atlantic Deep Water. All these samples have the same normalized pattern of type "A". The fact that all these samples have the same pattern (within statistical variation) shows that the reproducibility of the method is good enough to lend confidence in the small variations from this pattern shown by the other samples.

Acknowledgment

The original idea for this project originated from A. C. Pappas, Department of Nuclear Chemistry, University of Oslo, Norway. His active participation in the initial phase of the project is highly appreciated. We also want to express our gratitude for the great help received from

Professor H. Mosby, Department of Oceanography, University of Bergen, Norway, through valuable discussions.

During the work with the ion exchange method we received important suggestions from J. Alstad, Department of Nuclear Chemistry, University of Oslo, and from D. W. Hayes, Department of Oceanography, Texas A & M University, College Station, Texas. Their contribution to the development of the ion exchange method is deeply appreciated.

It is a pleasure to acknowledge the assistance of several people at the Central Institute for Industrial Research. Special thanks go to B. Juel for assistance in analysis of samples, and to S. Kolboe for the statistical treatment of the analytical data.

Literature Cited

(1) Balashov, Yu., Khitrov, L. M., *Geochemistry (USSR) English Trans.* **9**, 877 (1961).
(2) Bodman, R. H., Slabaugh, L. V., Bowen, V. T., *J. Marine Res.* **19**, 141 (1961).
(2) Brownlee, K. A., "Statistical Theory and Methodology in Science and Engineering," Chapt. 11, John Wiley & Sons, Inc., New York, 1960.
(4) Goldberg, E. D., Koide, M., Schmitt, R. A., Smith, R. H., *J. Geophys. Res.* **68**, 4209 (1963).
(5) Haskin, L. A., Frey, F. A., Schmitt, R. A., Smith, R. H., "Physics and Chemistry of the Earth," Vol. 7, L. H. Ahrens, F. Press, S. K. Runcorn, and H. C. Urey, eds., p. 167, Pergamon Press, New York, 1966.
(6) Haskin, L. A., Gehl, M. A., *J. Geophys. Res.* **67**, 2537 (1962).
(7) Høgdahl, O. T., *Central Inst. Ind. Res. (Oslo, Norway), NATO Res. Grant. No. 203, Semi-annual Progress Rept.* **No. 3** (Nov. 1966).
(8) Høgdahl, O. T., Bowen, V. T., Melsom, S. (to be Published).
(9) Kolboe, S., Central Institute for Industrial Research, Oslo, Norway (Private Communication).
(10) Manheim, F. T., *Proc. Symp. Marine Geochemistry, Narragansett Marine Lab., Univ. of Rhode Island, Kingston, R. I.*, **NYO-3450-1**, 217 (1965).
(11) Minami, E., *Nachr. Ges. Wiss. Göettingen, Math.-physik. Kl. IV* 1, 155 (1935).
(12) Minkkinen, C. O., "Collected Radiochemical Procedures," Los Alamos Report **LA-1721** (Jan. 1958).
(13) Moeller, T., Martin, D. F., Thompson, L. C., Ferrus, R., Feistel, G. R., Randall, W. J., *Chem. Rev.* **65**, 1 (1965).
(14) Rinehart, R. W., *Anal. Chem.* **26**, 1820 (1954).

RECEIVED June 2, 1967. The support of this study has been from the NATO Scientific Affairs Division under Research Grant No. 203. Dr. Bowen's participation has been supported by the U. S. Atomic Energy Commission under contract AT(30-1)-2174 with the Woods Hole Oceanographic Institution; the cruise of ATLANTIS II on which our samples were collected was supported by USAEC (contracts AT(30-1)-2174 and AT(30-1)-1918) and by the U. S. National Science Foundation (Grant GP 5319). We are grateful for all this support, and for assistance by the scientists, officers and crew of A II on cruise 20.

This is contribution number 1954 from the Woods Hole Oceanographic Institution.

20

Atomic Fluorescence Flame Spectrometry

DAVID W. ELLIS and DONALD R. DEMERS

University of New Hampshire, Durham, N. H.

Atomic fluorescence flame spectrometry is a new flame method of analysis which is competitive with and often superior to atomic absorption and flame emission methods for the analysis of trace inorganics. Various experimental arrangements with different burners, flames, and excitation sources have been used successfully. Several advantages of atomic fluorescence as compared with the other flame methods are discussed. Using an intense line source, atomic fluorescence is more sensitive for most elements than other flame methods. Using a continuum source, such as the xenon arc, a qualitative and quantitative analysis can be performed simultaneously by scanning the spectrum. Chemical interferences are similar to those found in atomic absorption and can usually be eliminated by use of a suitable suppressing agent, such as strontium chloride.

Atomic fluorescence flame spectrometry has received increasing attention during the last six years, particularly since 1964, (*1, 2, 3, 4, 5, 6, 8, 9, 11, 14, 15, 16, 17, 18, 19, 20, 21, 22*). This is primarily attributed to the interest generated by the work of Winefordner and coworkers (*8, 9, 15, 16, 17, 18, 19, 20, 21, 22*). Winefordner (*16, 20*) has reviewed the early work in the field.) Simply stated, the method is based upon radiational excitation of netural atoms present in a flame and the detection of their fluorescence. Atomic fluorescence differs from flame emission because in the former excitation is produced primarily by electromagnetic radiation while in the latter heat is primarily responsible. Atomic absorption, as the name implies, depends upon absorption and hence is a method dependent upon a difference between two signals, while atomic fluorescence is dependent upon the magnitude of the fluorescence signal which is measured above whatever background may be present.

Winefordner and Vickers (*16*) have described four basic types of atomic fluorescence: resonance fluorescence, direct-line fluorescence, stepwise line fluorescence, and sensitized fluorescence. Resonance fluorescence almost always refers to the line corresponding to the transition between the ground state and the first excited state of the atom; it has received by far most of the attention to date. Direct-line fluorescence refers to the process where an atom is excited to a higher excited state and then emits a photon in undergoing a transition to a lower excited state (not the ground state). Stepwise line fluorescence involves excitation to a higher excited state, radiationless deactivation to a lower excited state, and then emission accompanying the transition from that state to the ground state. Both direct-line and stepwise line fluorescence will occur at longer wavelength than the wavelength of absorption. Though no useful applications for these phenomena have as yet been published, they may have some potential usefulness in specialized applications. Sensitized fluorescence is the phenomenon whereby an excited atom transfers its excitation to another atom which then emits radiation. The probability that this phenomenon will be analytically useful seems slight, because the concentration of donor and acceptor atoms in flames is low, and because excited atoms are primarily deactivated by collisional and radiational means. A study by Goodfellow (*6*) with Cd, In, Tl, and Zn supports this hypothesis.

Winefordner and co-workers (*9, 16, 20, 22*) have developed the theory of atomic fluorescence flame spectrometry most extensively. The integrated intensity of atomic fluorescence, I_f, in w-sec./cm.^{2}-ster. for low concentrations of absorbing atoms is given by the following equation:

$$I_f = \frac{I_o \Omega_A \Phi \epsilon A_t}{4\pi}$$

where I_o is the excitation intensity in w-sec./cm^2-ster. for a continuous source, Ω_A is the solid angle (no units) over which excitation occurs, Φ is the total power or energy efficiency for fluorescence (no units) which is equal to the quantum efficiency ϕ for resonance absorption-fluorescence, ϵ is the sample aspiration efficiency, which is related lineraly to N, the atomic concentration of the absorbing atoms, A_t is the fraction of the incident radiation absorbed by the atoms of interest (the total absorption factor) in sec^{-1} and 4 π is the number of steradians in a sphere. A more detailed discussion of the theoretical and applied considerations has been presented by Winefordner (*9, 21, 22*). At low concentrations, the theory predicts calibration curves with linear slopes; with high concentrations, self-absorption and other effects may cause a decrease in the slope of the calibration curve.

Several advantages of atomic fluorescence, as compared with thermal emission and atomic absorption methods, are apparent.

(1) The intensity of the fluorescence can be increased by increasing I_o, the intensity of the source. Generally, the limit of detection is also decreased as I_o increases, because the signal to noise ratio is increased.

(2) Any change which increases the value of Φ or ϵ (for example changing the character of the flame or the solvent) will result in an increased signal.

(3) For atomic fluorescence, the emission profile of the source can be wider than the absorption profile of the line—even a continuum can be used. A source with a spectral profile narrower than the absorption profile of the line is usually preferred for atomic absorption.

(4) With atomic fluorescence, the fluorescence signal is added to a constant small background signal which permits improvement of the fluorescence signal by electronic amplification until the system becomes noise-limited. This advantage is also inherent to flame emission; however, with atomic absorption a difference measurement is made such that, as the concentration of the ion decreases, the signals of the blank and sample approach each other. A theoretical comparison of the sensitivities of the different flame methods has been presented by Winefordner (9).

While it is not immediately apparent, another advantage of atomic fluorescence is the unusually wide concentration range over which linear calibration curves are obtained, usually of the order of 10^2 to 10^4. This represents a major improvement over atomic absorption with which the practically useful linear region of concentration may be as small as ten and seldom exceeds 100. Naturally the greater the region of linearity of a calibration curve the less time is consumed in necessary sample dilutions. As a disadvantage of atomic fluorescence, there are some cases where scattering by liquid droplets or solid particles in the flame contributes to the background signal. This disadvantage is largely eliminated if a continuum source is used and the spectrum is scanned over the line of interest. Both atomic absorption and atomic fluorescence methods have the advantage over flame emission methods that ultraviolet lines are useful.

The various instruments used for the measurement of atomic fluorescence have been similar to each other in principle and optical design. In most studies, the source of excitation, of whatever type, has been focused on the flame; the fluorescence, usually at a right angle, has been focused on the entrance slit of the monochromator. The detector in all studies has been a photomultiplier tube, the output of which has been amplified and recorded. Figure 1 is a block diagram of the apparatus used successfully in our laboratory (5); it is quite similar to one described by Winefordner

(*15*). An atomic absorption spectrophotometer modified for atomic fluorescence measurements has been used by Dagnall *et al.* (*3, 4*).

A wide variety of excitation sources have been used successfully. They are conveniently separated into two categories: The line sources emitting one or a few lines (such as the resonance lamps, electrodeless and arc discharge lamps, various types of hollow cathode lamps) and continuum sources such as the xenon arc. The obvious advantage of a continuum source is that only one source is needed for all elements, provided the source has sufficient intensity. If one wishes to analyze for more than one element, the xenon source is particularly advantageous. By scanning the spectrum, the region between the lines of interest provides the background signal because of scattering; the fluorescence signal is superimposed on this. However, for those applications where the best possible limit of detection must be obtained, a line source would normally be preferred; this is because there are available line sources for most elements which have much more intense emission at the resonance line than can be obtained practically with a continuum source. Thus, as mentioned above, use of a line source would result in a lower limit of detection, provided that the source is intense over the atomic absorption line.

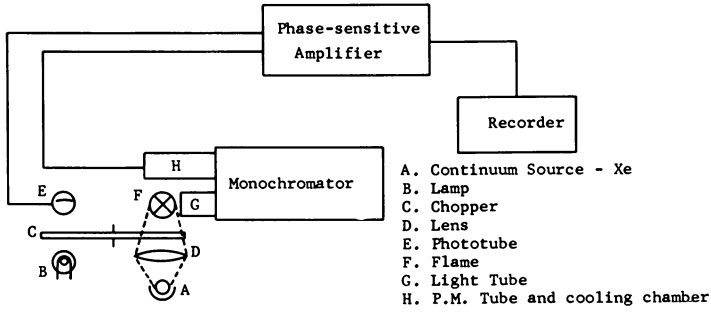

Figure 1. Block diagram of an atomic fluorescence flame spectrometer

Almost all studies have involved aqueous solutions; however, two studies (*3, 18*) have indicated that the use of non-aqueous solvents results in an enhancement of the fluorescence signal for certain systems. The maximum improvement has been of the order of 5 to 8. The background signal caused by scattering is also markedly reduced with organic solvents.

Various different types of burners have been used by different workers. In most of the studies by Winefordner and co-workers (*8, 15, 17, 18*), a total consumption burner was used. Other workers (*2, 5*) have also used total consumption burners with considerable success. Veillon and co-workers (*15*) reported that the background signal caused by scattering

from water droplets and salt particles was less with a heated-chamber aspirator-burner than with a total consumption burner. Dagnall *et al.* (*3, 4*) have also had excellent results with a chamber type aspirator-burner. In a comparison of two different total consumption burners, Ellis and Demers (*5*) observed only minor differences.

Table I. Limits of Detection (in p.p.m.) for Several Elements in Oxyhydrogen and in Hydrogen—Entrained-Air Flames

Element	H_2/O_2	H_2/*Entrained-Air*
Ag	0.003	0.001
Co	3.50	0.18
Cu	0.10	0.018
Fe	25.00	1.8
Mg	0.18	0.004
Mn	35.00	0.04
Ni	5.00	1.0
Tl	0.30	0.07
Zn	0.35	0.01

Two additional variables have been shown to be extremely important: the type of flame used and the height in the flame above the burner at which excitation and emission occur. (Naturally, the height in the flame is also dependent upon the type of burner and the flow rates of the gases.) Both of these variables are important since the population of neutral atoms (N) depends directly on them. Work in this laboratory (*5*) has shown that the use of an hydrogen-entrained-air flame is greatly superior to an oxyhydrogen flame for those elements which tend to form refractory oxides while the improvement was much less for elements that do not tend to form refractory oxides. Table I presents some representative data. Veillon and co-workers (*15*) found similar results using an argon-hydrogen-entrained-air flame. Dagnall and co-workers (*3, 4*) have recommended that air-propane be used in preference to other flames, especially below 3200 A. In most of the studies to date, the use of a reducing flame has been generally preferred. As would be expected the concentration of free neutral atoms varies both horizontally across the flame and vertically within the flame. At some particular height, the concentration reaches a maximum and it is at this height that one wishes to operate. Winefordner and Staab (*17, 18*) have stressed the importance of determining the best height. Dagnall and co-workers (*4*) have investigated the effect caused by the height above the burner at which excitation occurred as well as measuring the effect of changing the fuel gas pressure at a constant burner height. In our studies, we have found that 8.5 cm. is optimum for silver while 5.5 cm. is optimum for calcium.

The different types of detection and readout systems have all included photomultiplier tubes as detectors. The readout systems have been based on a number of different modes of operation. D.C. systems have been used successfully (*6, 8, 17*) though it is then necessary to measure the fluorescence as a signal which is additive to the background emission signal. D.C. systems are most usable if measurements are made above the luminous tip of the flame or below 3000 A. where the background emission owing to thermal emission is much reduced. Mechanical or electrical choppers and various types of a.c. amplifiers have been used extensively as a means of eliminating any background signal caused by d.c. processes, such as thermal emission. Tuned a.c. amplifiers have been used by Armentrout (*2*) and by Goodfellow (*6*) in conjunction with a mechanical chopper. Dagnall and co-workers (*3, 4*) have used an electrically modulated source and a tuned a.c. amplifier. Both Winefordner and co-workers (*15*) and Ellis and Demers (*5*) chopped the excitation mechanically and used phase-sensitive (or lock-in) amplifiers.

Typical calibration curves obtained for several elements are shown in Figures 2 and 3. The lowest concentration indicated is that for which the magnitude of the signal equals the peak-to-peak, or absolute magnitude, of the noise. This represents a point which is easily measured experimentally. The plots shown in Figures 2 and 3 show varying slopes which for some elements deviate appreciably from unity. If the entire flame cell is illuminated by the excitation source and all of the fluorescence radiation is measured, the absorption factors should approach unity (*22*) and the experimental analytical curves should have a slope of unity. At high concentrations of absorbing atoms, the absorption factors can approach zero

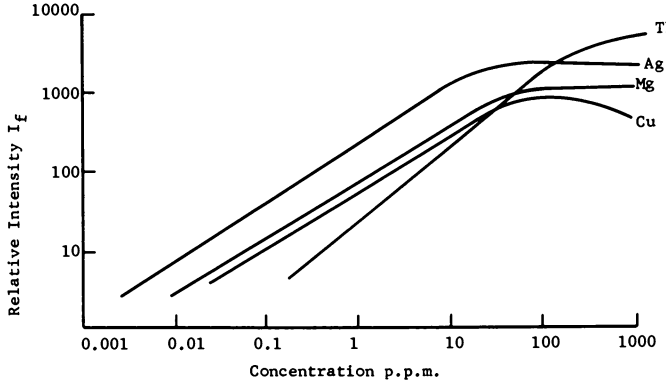

Figure 2. Experimental analytical curves for copper (Cu 3248 A.), magnesium (Mg 2852 A.), silver (Ag 3281 A.), and thallium (Tl 3776 A.)

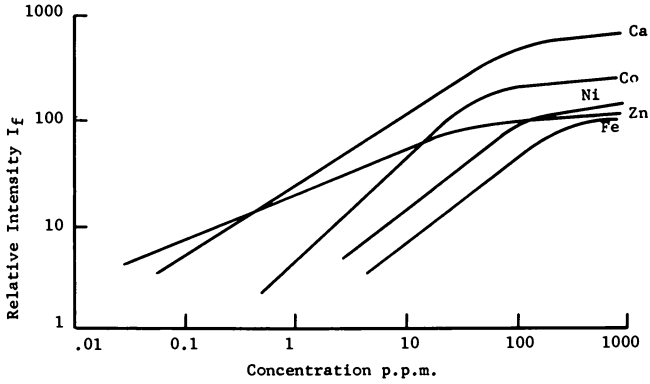

Figure 3. Experimental analytical curves for calcium (Ca 4228 A.), cobalt (Co 2407 A.), iron (Fe 2481 A.), nickel (Ni 2320 A.), and zinc (Zn 2139 A.)

and the curves will level off or they may even bend back toward the abscissa in some cases, for example, with copper.

A fair comparison of atomic fluorescence with atomic absorption and flame emission is difficult because there is little agreement on a standard definition for the term "detection limit." Table II is an attempt to make such a comparison for selected elements. From the data in Table II it can be concluded that for atomic fluorescence the use of a high-intensity line source improves significantly the limits of detection as compared with the use of the 450 watt xenon source. This is attributed to the increased intensity of the exciting radiation at the specific wavelength of interest, as for example with the elements Cd, Hg, Ni, Tl, and Zn. For these same elements, the detection limits using a line source are equal or superior to those obtained using either atomic absorption or flame emission methods. A comparison of the limits of detection for atomic fluorescence using the 450 watt xenon source are better than those of flame emission and are approximately equal to those of atomic absorption, except for Fe and Ni, for which atomic absorption is superior. Although several workers (*4, 15*) have used a 150 watt xenon source, as expected, the limits of detection obtained were poorer than those obtained with the 450 watt source; data obtained with the larger source is therefore listed.

For routine work it is often important to know the minimum concentration that can be reliably and conveniently included as part of a calibration curve, rather than to know the detection limit. For this purpose, the 1% absorption column in Table II under atomic absorption becomes extremely useful. Comparable values for atomic fluorescence can be obtained using that solution concentration which results in a signal whose absolute magnitude is equal to the absolute magnitude of the noise. To

obtain such comparable values, the values listed in Table II should be multiplied by a factor of about three. (The detection limits in Table II are in terms of a signal to rms noise ratio of unity.)

Table II. A Comparison of Detection Limits in p.p.m. for Different Flame Methods

	Atomic Fluorescence		*Atomic Absorption*[b]		*Flame Emission*[c]
	Xe(450 watt)[a]	*Line Source*	*1% Abs.*	*Det. Lim.*	*Det. Limit*
Ag	0.001	—	0.1	0.02	0.04
Ca	0.02	—	0.1	0.01	0.01
Cd	—	0.0002[e]	0.04	0.01	0.05
Co	0.18	—	0.45	0.15	0.25
Cu	0.018	0.04[e]	0.2	0.005	0.1
Fe	1.8	—	0.3	0.05	0.12
Hg	—	0.1[e]	10	0.5	6
Mg	0.004	—	0.01	0.003	0.02
Mn	0.04	—	0.15	0.01	0.01
Ni	1.1	0.1[d,e]	0.2	0.05	0.12
Tl	0.07	0.04[e]	1.0	0.2	0.1
Zn	0.01	0.0001[e]	0.04	0.005	—

[a] Unpublished data by Ellis and Demers, limit of detection taken as signal-to-noise ratio of 1.
[b] See Ref. *12, 13.*
[c] See Ref. *7.*
[d] See Ref. *2.*
[e] See Ref. *8, 18.*

Various types of interferences are found with flame methods in general. Both atomic absorption and atomic fluorescence are not susceptible to excitation interference, which is caused by changes in flame temperature and results primarily in changes in the excited-state population; radiation interference can be largely eliminated using a modulated system. Dagnall *et al.* (*3, 4*) have studied exhaustively the effect of 41 cations, 18 anions and five reagents on the atomic fluorescence of cadmium and zinc; they found no evidence of interference. Interference studies in this laboratory have been concerned with calcium which would be expected to show interferences much more readily than cadmium or zinc. The ions studied were chosen on the basis that they might be present in water. Standard solutions of calcium chloride were used for comparison. The anions studied were present as the sodium or potassium salt, and the cations as the chloride salt.

The results obtained are listed in Table III and several interference curves are shown in Figure 4. The interferences found were similar to those obtained for calcium with atomic absorption (*10*); this agrees with what would be expected on theoretical grounds. The addition of

$SrCl_2 \cdot 6H_2O$ (final concentration 0.1%) eliminated all of the interferences with the exception of the ones attributed to sulfide and silicate anions, for which the interference was decreased.

Table III. Interference Studies with Calcium[a]

No Interference	*Interference—% Signal Depression*			
Ba, Co, Cu, K	Al	65	CO_3^{2-}	75
La, Mn, Na, Sr	Cr	75	F^-	85
Zn	Fe	25	HCO_3^-	75
	Li	70	I^-	80
	Mg	10	NO_3^-	65
	Pb	50	PO_4^{3-}	100
	citrate	70	S^{2-}	80
	oxalate	100	SO_4^{2-}	75

[a] $CaCl_2$ as standard (4.0 p.p.m.). Interfering ion (400 p.p.m.): anions present as Na or K salts, cations as Cl salts.

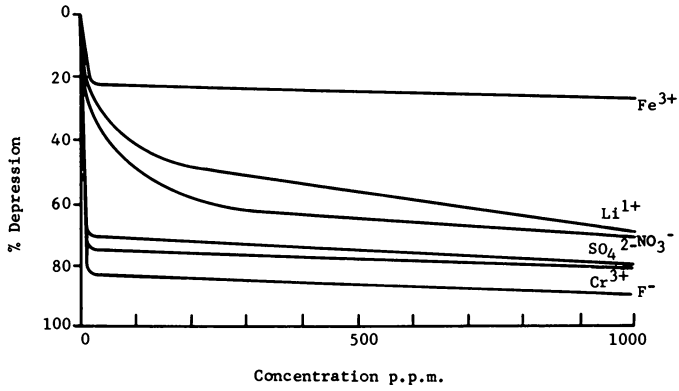

Figure 4. Depression of the atomic fluorescence of calcium by selected ions

As of this time, atomic fluorescence flame spectrometry has not been reported as having been applied to any specific analytical problem. One can readily ascertain that it should be applicable in many areas where atomic absorption is commonly used. In addition, for the analysis of multiple elements in a single sample, for example cations in water, atomic fluorescence flame spectrometry incorporating a xenon arc source should have major advantages.

Experimental

All results listed except where specifically noted were obtained with an apparatus composed of a 450-watt Osram high pressure xenon arc

source; the burner was a Jarrell-Ash Hetco total consumption burner operated at a hydrogen flow rate of 20 liter/min. through the central orifice. Oxygen for combustion was provided by the entrained air (5). Aqueous samples were used; they were injected using a Sage motor-driven syringe at a rate of 7.5 ml./min. (This rate of introduction of sample provided a 60% enhancement of the signal as compared with a sample introduction rate of 2.0 ml./min.). Excitation and fluorescence were at a height of 8.5 cm. above the burner for all elements except calcium, which was measured at a height of 5.5 cm. above the burner. The fluorescence was detected using a Jarrell-Ash 0.5 meter scanning monochromator equipped with an EMI 6255B photomultiplier tube which was thermoelectrically cooled at −15°C. The output of the photomultiplier tube was fed to an E.M.C. phase-sensitive amplifier (Model RJB) with a 3 second time constant and recorded on a Leeds and Northrup strip chart recorder. The limits of detection listed in Table II are optimum values for Ag and Ca; it is anticipated that the other values can be improved by further optimization of the experimental parameters, such as the flow rate of hydrogen, the rate of introduction of sample, height above the burner, slit widths, etc.

Conclusion

Atomic fluorescence flame spectrometry is receiving increased attention as a potential tool for the trace analysis of inorganic ions. Studies to date have indicated that limits of detection comparable or superior to those currently obtainable with atomic absorption or flame emission methods are frequently possible for elements whose emission lines are in the ultraviolet. The use of a continuum source, such as the high-pressure xenon arc, has been successful, although the limits of detection obtainable are not usually as low as those obtained with intense line sources. However, the xenon source can be used for the analysis of several elements either individually or by scanning a portion of the spectrum. Only chemical interferences are of concern; they appear to be qualitatively similar for both atomic absorption and atomic fluorescence. With the current development of better sources and investigations into devices other than flames for sample introduction, further improvements in atomic fluorescence spectroscopy are to be expected.

Acknowledgment

The work upon which this publication is based was supported in part by funds provided by the United States Department of the Interior, Office of Water Resources Research, as authorized under the Water Resources Research Act of 1964. The authors also wish to express their appreciation to Michael Pleva for his assistance in part of the work.

Literature Cited

(1) Alkemade, C. T. J., "Xth Colloquium Spectroscopicum Internationale, Proceedings," E. R. Lippincott and M. Margoshes, Eds. p. 143. Spartan Books, Washington, D. C., 1963.
(2) Armentrout, D. N., *Anal. Chem.* **38**, 1235 (1966).
(3) Dagnall, R. M., West, T. S., Young, P., *Talanta* **13**, 803 (1966).
(4) Dagnall, R. M., Thompson, K. C., West, T. S., *Anal. Chim. Acta* **36**, 269 (1966).
(5) Ellis, D. W., Demers, D. R., *Anal. Chem.* **38**, 1943 (1966).
(6) Goodfellow, G. I., *Anal. Chim. Acta* **36**, 132 (1966).
(7) Herrmann, R., Alkemade, C. T. J., (trans. by P. T. Gilbert, Jr.), "Flame Photometry," Interscience Publishers, John Wiley & Sons, Inc., New York, N. Y., 1963.
(8) Mansfield, J. M., Winefordner, J. D., Veillon, C., *Anal. Chem.* **37**, 1049 (1965).
(9) Parsons, M. L., McCarthy, W. J., Winefordner, J. D., *J. Chem. Ed.* **44**, 214 (1967).
(10) Ramakrishna, T. V., Robinson, J. W., West, P. W., *Anal. Chim. Acta* **36**, 57 (1966).
(11) Robinson, J. W., *Anal. Chim. Acta* **24**, 254 (1961).
(12) Robinson, J. W., "Atomic Absorption Spectroscopy," Chap. 5, Part III, Marcel Dekker, In., New York, N. Y., 1966.
(13) Slavin, W. R., *Bio-Medical Lab. Dir.* 1, 8 (1966).
(14) Sullivan, J. V., Walsh, A., *Spect. Acta* **21**, 727 (1965).
(15) Veillon, C., Mansfield, J. M., Parsons, M. L., Winefordner, J. D., *Anal. Chem.* **38**, 204 (1966).
(16) Winefordner, J. D., Vickers, T. J., *Anal. Chem.* **36**, 161 (1964).
(17) Winefordner, J. D., Staab, R. A., *Anal. Chem.* **36**, 165 (1964).
(18) *Ibid.*, **36**, 1367 (1964).
(19) Winefordner, J. D., Vickers, T. J., *Anal. Chem.* **36**, 1939 (1964).
(20) Winefordner, J. D., "Conference on Trace Characterization, Chemical and Physical," Analytical Chemistry Division, Natl. Bur. of Std., Washington, D. C., Oct. 1966.
(21) Winefordner, J. D., Parsons, M. L., Mansfield, J. M., McCarthy, W. J., *Anal. Chem.* **39**, 436 (1967).
(22) Winefordner, J. D., Parsons, M. L., Mansfield, J. M., McCarthy, W. J., *Spectrochim. Acta* **23B**, 37 (1967).

RECEIVED April 24, 1967.

Controls on Mn, Fe, Co, Ni, Cu, and Zn Concentrations in Soils and Water: the Significant Role of Hydrous Mn and Fe Oxides

E. A. JENNE

U. S. Geological Survey, Denver, Colo.

It is proposed that the hydrous oxides of Mn and Fe, in general, furnish the principal control on the fixation of Co, Ni, Cu, and Zn (heavy metals) in soils and fresh water sediments; hydrous oxides of Mn and Fe are nearly ubiquitous in clays, soils, and sediments. The common occurrence of these oxides as coatings allows the oxides to exert chemical activity far out of proportion to their total concentrations. Sorption or desorption of these heavy metals occurs in response to the following factors: (1) aqueous concentration of the metal in question; (2) aqueous concentration of other heavy metals; (3) pH; and (4) amount and strength of organic chelates and inorganic complex ion formers present in solution. Other suggested controls on the concentration of the heavy metals in soils and fresh waters are: (1) organic matter; (2) clays; (3) carbonates; and (4) precipitation as the discrete oxide or hydroxide. The available information on these controls is reviewed and found to be inadequate to explain the fixation of Co, Ni, Cu, and Zn.

An understanding of the controls on the concentration of metals in natural waters and soil solutions is of great significance to the art of maintaining and improving the fertility of soils, is of rapidly growing importance in understanding the areal incidence of certain diseases of man and animals, and is of considerable significance in facilitating the treatment of water for municipal and industrial use.

Other proposed controls on the concentrations of certain of the first transition series metals in soil solutions and natural waters are reviewed and are found to be inadequate to explain the existing data. The princi-

pal control on the concentrations of these metals in soils and fresh waters is proposed to be the hydrous oxides of manganese and iron. Much of the available experimental data are reviewed and are shown to be highly consistent with the hydrous oxide model.

The geochemistry of certain of the first transition series metals, manganese, cobalt, nickel, copper, and zinc, and to a lesser extent iron, is sufficiently similar so that these metals may be treated as a group for the purposes of this paper. This group of metals is also referred to as "heavy metals," "trace elements," "minor elements," and "micronutrients." The groups, "trace elements," "minor elements," and "micronutrients" commonly include additional elements, particularly molybdenum and boron. The term "heavy metals" normally includes a larger group of metals than those under consideration here. However, for simplicity, iron, manganese, cobalt, nickel, copper, and zinc will be subsequently referred to collectively as heavy metals.

The role of the hydrous oxides of manganese and iron as a control on heavy metal availability can be satisfactorily understood only in terms of the factors which influence the sorption and desorption of the heavy metals by these oxides. The principal factors affecting the availability of hydrous oxide occluded heavy metals are Eh, pH, concentration of the metal of interest, concentration of competing metals, concentration of other ions capable of forming inorganic complexes, and organic chelates. Of these factors, pH and Eh are probably the most significant. The frequently noted influences of pH, organic matter, lime, and phosphate on heavy metal availability in soils are to be understood principally in terms of the influence of these variables on the chemistry of the hydrous oxides of manganese and iron, rather than on the heavy metals themselves. A serious limitation in the development of this picture is the scarcity of reliable data on Eh of the pore water of sediments and soils showing diurnal and seasonal variations, and the effect of treatments such as liming, fertilization, and irrigation. The study of redox potential and its variations in response to different treatments of soils and sediments is potentially one of the most rewarding areas for investigations of soil chemistry and geochemistry.

Other Proposed Controls

The other principal controls on heavy metal availability proposed previously are the layer silicates, organic matter, and carbonates. Where the controls for a given process are not understood, numerous hypotheses are to be expected. The previous explanations of heavy metal sorption by the layer silicates include surface sorption, surface complex ion formation, lattice penetration, and ion exchange. The mechanisms of heavy

metal fixation by organic matter are presumed to be the formation of complexes and chelates, while surface sorption or surface precipitation has been suggested as the retention mechanism of carbonates. Several of the sorption mechanisms were proposed to account for the fixation of heavy metals in the sense that they could not be extracted with salt solutions. However, some investigators have considered only the portion of the metal retained against acid extractions as being fixed. Fixation is herein used in the former sense unless otherwise specified.

Solid state diffusion, known in the soil chemistry literature as "lattice penetration," has historical precedence as a fixation mechanism. It was noted as an accepted mechanism, but not subscribed to, by Hibbard (*101*). Since then it has been accepted as a fixation mechanism (*66, 67, 238*). Tiller and Hodgson (*238*) considered only the cobalt not displaced by copper, nickel, zinc, iron, manganese, or by more cobalt or alternatively not extracted with successive dilute acetic acid treatments as being fixed by lattice penetration. The nonextractable portion was in all cases small compared with the total amount sorbed in the presence of 0.1*N* calcium chloride. A reduction in cation exchange capacity concomitant with the fixation of some of the heavy metals has sometimes been observed. This has lent credulity to solid state diffusion as a mechanism. It seems unlikely that heavy metals will enter a layer silicate structure, except that they may penetrate to a distance of a few atomic planes at the crystal edges and along fractures. For example, temperatures of 200+°C. maintained for several hours are required to obtain an adequate diffusion of Li^+, a small monovalent cation, into the dioctahedral end member (beidellite) of the montmorillonite group to cause irreversible collapse (*89*). Therefore, it seems most unlikely that significant amounts of larger divalent cations would diffuse into the octahedral structure of 2:1 and 1:1 layer silicates in the course of laboratory studies at ambient temperature. It is particularly difficult to conceive of this mechanism as being operative for kaolinite and talc, whose sorptive capacities for cobalt and zinc were not greatly dissimilar to that of montmorillonite (*238*), since neither of these layer silicates possesses significant tetrahedral or octahedral cation deficiencies.

Many investigators have noted the unavailability of both manganese and zinc in alkaline soils, particularly in highly calcareous soils (*185*). Based on this observation, some investigators have postulated that heavy metal deficiencies in calcareous soils are commonly a result of the adsorbent ability of calcium carbonate for these metals (*143*). Jurinak and Bauer (*126*) concluded that zinc is adsorbed on the crystal surfaces of dolomite and magnesite at lattice sites that might normally be occupied by magnesium. However, Canals *et al.* (*46*) found that only 18 to 35% of the copper and 10 to 17% of the zinc from solutions containing 5×10^{-7}

to 50×10^{-7} gram ions of the metal per liter were sorbed by finely divided calcium carbonate (50 mgm. $CaCO_3$/liter). Also, it has been established that the presence of calcium carbonate in a soil does not necessarily indicate that a zinc deficiency hazard exists since Thorne *et al.* (*233*) and Thorne and Wann (*234*) found that the calcareous soils of Utah seldom suffer from zinc deficiency. Brown and Jurinak (*37*) found little or no reduction in plant uptake of either zinc or copper from Yolo fine sandy loam due to calcium carbonate additions beyond 5% (w/w) where either zero or ten lbs./acre of zinc sulfate had been added. Similarly, there was little increase in pH with calcium carbonate additions in excess of 5%. Unless one supposes that calcium carbonate varies widely in its sorption capacity for these metals, it seems apparent that the effect ascribed to sorption of zinc and copper by calcium carbonate is primarily a pH effect and secondarily an effect of carbonate-bicarbonate ions on heavy metal solubility.

Of all the suggested controls, organic matter is by far the most frequently implicated cause of heavy metal fixation (*13, 34, 36, 51, 58, 59, 105, 124, 130, 161, 187, 200, 201, 216, 233*). The role of organic matter has been deduced from four principal lines of reasoning: (1) the known chelating ability of certain organics, such as EDTA, and more recently from studies with fluvic acid; (2) the numerous experiments showing heavy metal extractability, especially of iron, from earth materials by boiled, fermented, or aged extracts of various plant materials such as leaves and pine needles; (3) the positive correlation sometimes found between heavy metal sorption and organic matter content of soils; and (4) the increased extraction of fixed heavy metals, or alternatively the reduction of fixation capacity (at fixed equilibrium times), by treatment with hydrogen peroxide for the purpose of oxidizing organic matter. The data on which the reasoning outlined in (2), (3), and (4) above is based, are reinterpreted in a subsequent section to show that organic matter plays a significant but generally indirect role in the hydrous oxide control of heavy metal availability. As will be discussed in a following section, organic matter does play a direct role as a control in: (1) highly organic soils and sediments and (2) most soils and sediments when Eh and/or pH conditions are such that the hydrous oxides and the occluded heavy metals undergo partial dissolution. Recent studies have shown that the fulvic acid fraction of soil organic matter has relatively high stability constants for metals (*200, 201*). Unfortunately, comparable stability constants are unavailable for the hydrous oxides.

The observed lowering of cation exchange capacity as a result of treatment with heavy metals (*12, 67*) is probably caused by precipitation because no decrease in cation exchange capacity is observed where the pH conditions are such that precipitation would not be expected to occur

(*see* Ref. *114, 172*). Furthermore, when the pH at which precipitation could occur is not exceeded and prolonged equilibration times are avoided, the amount of a heavy metal which is exchangeable is generally equivalent to the cation exchange capacity (*36*). Sorption in excess of cation exchange capacity is, in some cases, because of molecular salt sorption (*67*).

Convincing evidence that the fixation of heavy metals is not related to cation exchange capacity is furnished by the results of Tiller *et al.* (*239*). They found that a plot of cobalt sorption (from $1.1 \times 10^{-3}M$ $CoCl_2$) *vs.* pH for 15 out of 16 soils could be fitted by a single curve, although the soils were of widely divergent mineralogy. This certainly indicates the operation of some control mechanism apart from that of cation exchange. On the basis of the information available, it appears reasonable that adequate amounts of hydrous iron and manganese oxides are present in these soils to account for the cobalt sorption. The sorption curve for the 16th soil may be superimposed on the other 15 by subtracting a set amount of sorbed cobalt from each experimental point. This may indicate that the control on cobalt sorption for this soil is the same as for the remainder of the soils, but that either the sorption capacity or the sorption rate of this particular sample is considerably more than the others. It is striking that the curves of cobalt sorption *vs.* pH for all 16 of these soils are nearly identical in shape to those of manganese sorption by $\delta(?)$–MnO_2 (*167*), although the pH at which the inflection occurs is about one pH unit higher for the soils than for the laboratory-prepared δ–MnO_2.

There appears to be little point in a detailed evaluation of the more ambiguous hypotheses of heavy metal fixation. However, it may be noted that a number of investigators have considered the possibility of either the sorption of complex ions on clay mineral surfaces or reaction of heavy metal cations with clay surfaces in some manner other than simple electrostatic sorption (*31, 66, 67, 156, 157, 217*). However, the solubility products of $Cu(OH)_2$ and $Zn(OH)_2$ in aqueous suspensions of montmorillonite (*19*) have been found to be quite similar to those previously found for solutions in contact with only the pure hydroxides. This would indicate that metal ion–clay mineral surface complex formation is not important; otherwise the apparent solubility would have been greater in the presence of montmorillonite.

One of the factors which has confused mechanism analysis has been the failure to make a distinction between studies involving micro- and macro-concentrations of the heavy metals. Whereas, with micro-concentrations, sorption reactions may predominate, precipitation frequently occurs with macro-concentrations (*68*). Exchange of copper and zinc with hydrogen on clay mineral surfaces was proposed as a cause of zinc and copper fixation in soils by DeMumbrum and Jackson (*59*) who noted

an alteration in the hydroxyl peak in the infrared spectrum of montmorillonite as a result of metal sorption. Precipitation has also been indicated as the dominant reason for the retention of copper chloride and acetate by montmorillonite at pH values above 5.0 and 6.5, respectively, at copper concentrations twice the cation exchange capacity (*19*). The pH of the precipitation shifted 0.5 pH unit to the acid side with a metal ion concentration ten times the cation exchange capacity of the clay minerals utilized. The comparable zinc salts precipitated at 1 pH unit higher than the copper salts (*19*).

Hydrous Oxide Control Model

Hydrous oxides of manganese and iron are nearly ubiquitous in clays (*6*), soils, and sediments, both as partial coatings on other minerals and as discrete oxide particles. It is proposed that these oxides act as a "sink" for the heavy metals. Sorption or desorption of heavy metals occurs in response to: (1) solution concentration of the metal in question; (2) concentration of competing metals; (3) hydrogen ion concentrations; and (4) formation and destruction of organic chelates and inorganic complexes. The presence of only a fraction of a percent to a few weight percent of hydrous oxides of manganese and/or iron may be adequate to control the distribution of the heavy metals between earth materials and the associated aqueous phase. The displacement of sorbed heavy metals from earth materials is rarely stoichiometric and very rarely completely reversible (*106*). This is a result of sorption onto hydrous oxide surface sites which are largely specific for the heavy metals, as well as solid state diffusion into the hydrous oxides. Superimposed on the sorption-desorption phenomenon is the dissolution-precipitation of manganese and iron oxides in response to pH-Eh variations and to leaching of manganese and iron by ground and surface water.

These complications provide an explanation for the lack of agreement obtained from many studies which have been carried out to assess the effect of pH on heavy metal availability, as well as the relative effectiveness of various reagents for the extraction of these metals from clays, soils, and sediments. The extractability or leachability of these metals should be viewed in terms of the Eh and pH of the system, soil plus extractant, as compared with that of the system soil plus pore water, and the solubilities of $Fe(OH)_3(a)$ and $MnO_2(a?)$, especially the latter, in the extractant utilized. [(a) indicates an x-ray amorphous solid as opposed to (c), a crystalline phase.]

The general mode of occurrence of the hydrous oxides in soils and recent sediments as partial coatings on the silicate minerals rather than as discrete, well-crystallized minerals, allows the oxides to exert chemical

activity which is far out of proportion to their concentration. The tendency of these oxides to occur as coatings suggests that most of the sorption of heavy metal by clays and soils could be because of hydrous oxides of manganese and iron present in minor amounts. In the following sections, it is shown that the hydrous oxide model provides the most consistent interpretation of the published literature and recent experimental data.

Hydrous Oxide Colloid Chemistry

Laboratory preparations of the hydrous oxides of manganese and iron are frequently microcrystalline with high surface areas of up to 300 meter^2/gram for δ-MnO_2 (*42*) and 230 to 320 meter^2/gram for α- and γ-FeOOH (*76*). Surface area data are lacking for hydrous oxide coatings on other minerals although it is excepted that the surface areas of the coatings will approach those of the laboratory preparations. The hydrous oxides have high moisture contents, are highly reactive, and are somewhat labile. Part of the iron in soil concretions is even present as an amorphous oxide (*204*). Since it is believed that the amorphous oxides of manganese and iron are much more important than the crystalline oxides, the presence of amorphous oxides in concretions suggests that concretionary manganese and iron also serve as a sink for the other heavy metals, although the rate of sorption by the concretionary oxides would be slower than that of the hydrous oxides which occur as coatings. Concretionary manganese oxides in soils contain large quantities of various metals (*229*). This indicates the ability of these oxides to take up the heavy metals, either by sorption or coprecipitation. Weir and Miller (*249*) concluded from isotope exchange kinetics and the extractability of sorbed radioactive manganese that at least five forms of soil manganese were in equilibrium with the aqueous phase.

It has been found that the Mn^{4+} of δ-MnO_2 can be reduced to Mn^{2+} without a change of phase (*71*). The unit-cell volume was found to increase linearly as the Mn:O ratio varied between 1:1.96 and 1:1.46, suggesting the reaction

$$MnO_2 + n\ e^- + n\ H^+ = MnO_{2-n}(OH)_n$$

whereby a part of Mn^{4+} is reduced to a lower oxidation state and a corresponding number of oxygen atoms are bonded to protons forming hydroxyl groups. The diffusion of hydrogen ions into δ-MnO_2 crystals, forming hydroxyls, may well facilitate the desorption of occluded metals. Buser *et al.* (*43*) found that all of the zinc in a manganese-zinc manganite ($3\ MnO_2 \cdot Zn(OH)_2 \cdot XH_2O$) was exchangeable with divalent manganese ions.

The findings of Kurbatov *et al.* (*137*) are interesting as they have shown clearly that identical amounts of barium and strontium are taken up by a $Fe(OH)_3(a)$ precipitate regardless of whether the iron hydroxide was precipitated in the presence of barium or strontium ions (coprecipitation), or whether the freshly precipitated hydroxide was added to a solution containing one of the two alkaline earth cations (sorption). Although the heavy metals are more effectively scavenged by the hydrous oxides of manganese and iron than are the alkaline earth cations, the availability of the occluded metal in hydrous manganese and iron oxide coatings may be largely independent of whether retention of the heavy metals occurred by coprecipitation or sorption. Morgan and Stumm (*168*) reported pH 8.0 sorption capacities of $Fe(OH)_3(a?)$ and $\delta(?)$-MnO_2 for manganous ions to be 0.3 and 1.0 mole/mole, respectively (equilibration times unspecified). They state that the sorption capacities for nickel, zinc, and cobalt were only slightly less than for manganese.

When $[(Fe^{3+})(OH^-)^3]_{soln}$ is greater than the solubility product, iron precipitates, presumably as $Fe(OH)_3(a)$, as a coating on clay surfaces. Discrete iron hydroxide particles appear to form only after a certain quantity of iron has been precipitated as a coating on the clay surface (*17, 76*). Attempts have been made to relate this phenomenon to the cation exchange capacity of the clay. For example, Fripiat and Gastuche (*76*) found that the amount of iron oxide occurring as coatings on kaolinite was ten times the cation exchange capacity. However, Berg (*17*) demonstrated that the amount of iron precipitated as coatings, before discrete oxide particles appeared, was about one weight % and eight weight % iron for the 2 to 0.2μ and the less than 0.2μ kaolinite size fractions, respectively; hence, the amount precipitated as coatings was related to the surface area of the clay rather than to cation exchange capacity. Fripiat and Gastuche (*76*) observed that hydrogen (aluminum?) saturation of the kaolinite led to a definitely amorphous iron oxide precipitate such that iron oxide continued to precipitate on the surface, whereas alkali or alkaline earth cation saturation of the clay led to a compact, nonporous coating which resulted in the latter portions of the iron precipitate forming discrete particles. In addition to iron precipitation on clay surfaces, colloidal iron hydroxide is readily sorbed onto clay mineral surfaces (*73, 76*).

The data of Robinson (*194*) show that the chemical properties of the manganese oxide associated with the clay fraction are definitely different from those of the manganese oxide in the silt fraction of soils, as the manganese oxide in the clay fraction exhibited very little ability to catalyze the decomposition of hydrogen peroxide. Furthermore, Robinson found that the amount of manganese extracted with 1*N* ammonium acetate was about five times as great from the clay as from the silt fraction,

even though the total amount of manganese in the silt fraction was greater. Thus, the solubility of the oxidic manganese coating must be appreciably greater than that of the concretionary manganese which occurs in the silt fraction. Although both iron (*17, 76, 136*) and manganese oxides (*244*) occur extensively as partial coatings on clay size minerals, the free-iron oxides present in a soil appear to have a greater tendency than the free-manganese oxides in a soil to occur as coatings rather than as discrete particles.

Eh and pH are so intimately related, that a change in one normally results in a change in the other, since $2\ H_2O = 4\ H^+ + O_2 + 4\ e^-$. (However, there is some question as to the degree of reversibility of this couple.) The scarcity of reliable Eh data is partly due to the difficulty of obtaining unambiguous redox values for poorly poised systems (*99, 215, 224*).

Doyle (*64*) reports that colloidal iron oxide sorbed onto the platinum electrode from the aqueous phase of the system whose Eh is being measured enhances the reversibility of the electrode to the Fe^{3+}–Fe^{2+} couple. He notes that the reaction of Fe^{2+} in the aqueous phase with oxygen sorbed on the electrode may also result in the formation of colloidal iron oxide on the platinum electrode.

It must be emphasized that pH and Eh are both intensity, not capacity, parameters. The truth of this is attested to by the numerous efforts in recent years to devise lime requirement tests for crops, especially for legumes, since pH is only partly satisfactory as an indicator of the need for additional calcium and magnesium. Unfortunately, no comparable effort has been made with "redox capacity" determinations, although an approach has been suggested by Lamm (*141*). He circumvented the poorly poised soil-water system by adding potassium ferri- and ferro-cyanide (pH buffered with 1*M* ammonium acetate) in varying ratios at constant total cyanide concentration and then measured the resultant Eh of the suspensions. The ferri-ferro ratio which did not change its solution Eh upon equilibration with the soil was taken to be the Eh of the aqueous suspension. Lamm's use of ammonium acetate as a buffer raises some question as to the accuracy of the results because of solubilization of manganese oxides in ammonium acetate [*see* Organic Matter (and Eh) Effects section]. The effect of manganese oxide dissolution by ammonium acetate on the suspension Eh is unclear. However, since Lamm observed no effect of dilution ($\times$ 10) on the suspension Eh, the use of ammonium acetate may not pose a serious problem. The ferri- to ferro-cyanide ratio required to lower the suspension Eh by 100 mv., for example, might be a useful measure of Eh buffer capacity of an earth material system.

A visualization of Eh and pH effects on the occurrence of iron and manganese minerals under equilibrium conditions can be achieved most

simply in terms of Eh(pE)–pH diagrams (Figures 1 and 2). These diagrams are constructed by deriving equations, which include Eh and pH terms, relating the adjacent phases. The construction of these diagrams is presented in some detail by Pourbaix (*186*), Hem (*93*), and Garrels and Christ (*82*). The free-energy values used for these figures are from Garrels and Christ (*82*) and Pourbaix (*186*). The lines between the various phases represent Eh-pH values at which the two phases are in equilibrium. The boundaries between soluble species imply equiva-

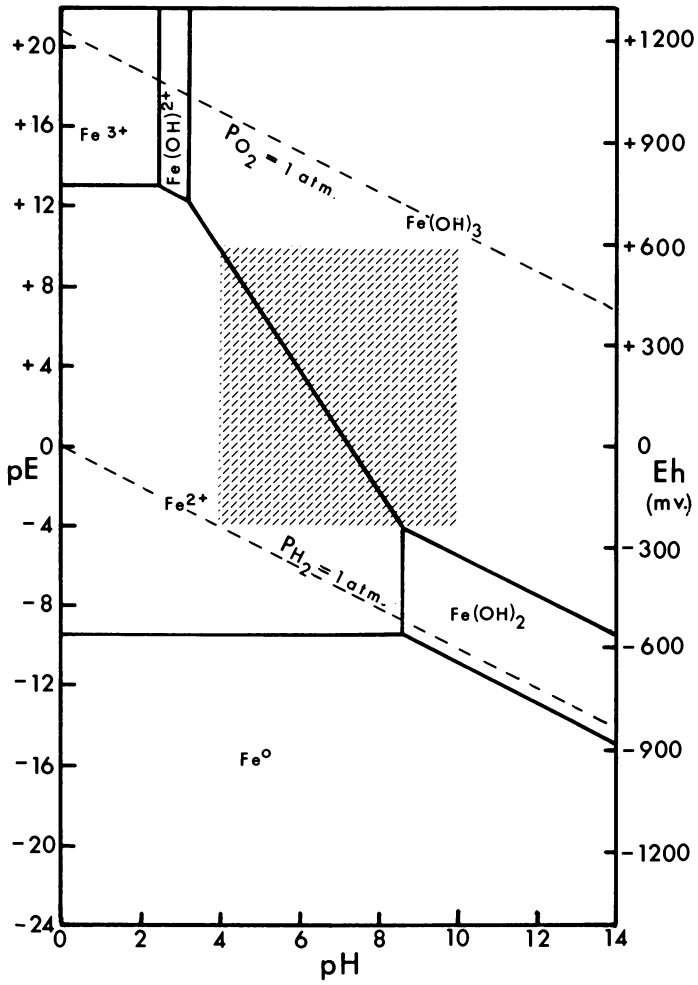

Figure 1a. Eh(pE) vs. pH stability field diagram for iron (a_{Fe} = 10^{-4}M; $P_{CO_2} = 0$; $P_{tot} = 1$ atm.; $T. = 25°C.$)

lent activity. If a lower activity of manganese or iron had been chosen, the phase boundaries would have been shifted to slightly higher pH values (*93*).

The diagrams have been provided with both pE and Eh scales. The use of Eh has historical precedent but pE has recently come into favor. Both are log functions, so log–log plots result regardless of whether pE or Eh is utilized. The pE can be calculated more rapidly than the Eh if stability constants rather than free-energy values are utilized; however,

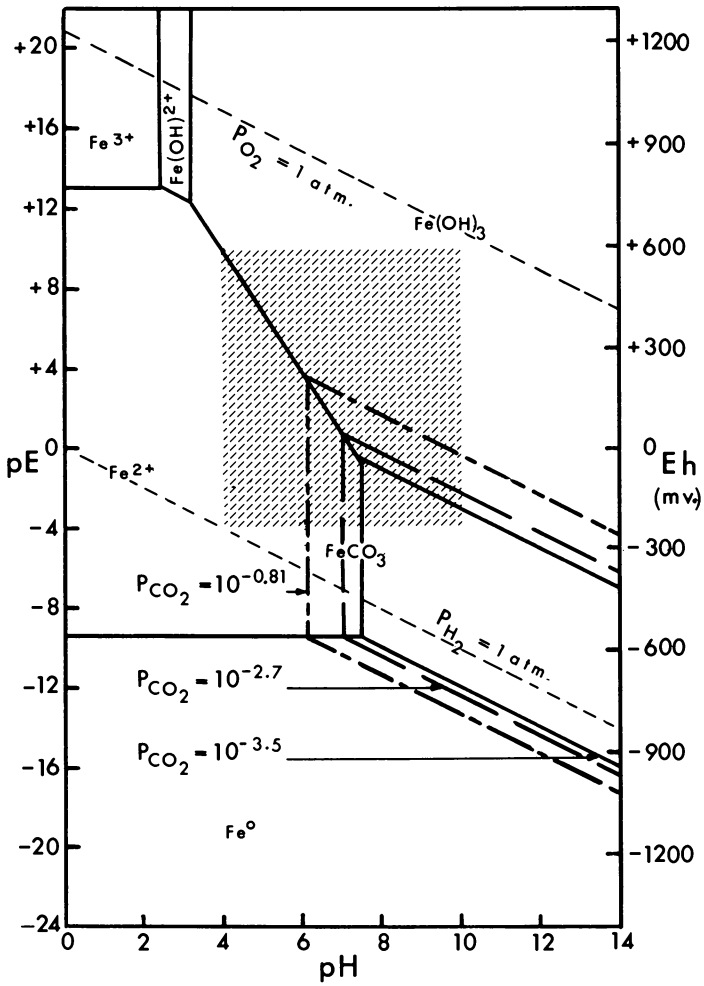

Figure 1b. Eh(pE) vs. pH stability field diagram for iron (a_{Fe} = 10^{-4}M; P_{CO_2} = $10^{-0.81}$, $10^{-2.7}$ and $10^{-3.5}$ atm.; P_{tot} = 1 atm.; T. = 25°C.)

this time difference is hardly significant. Since redox potentials are measured in millivolts, there is an advantage to using Eh rather than pE to facilitate mental reference to Eh–pH diagrams. Sillén (*211*) has suggested that the principal advantage of pE is that it is a theoretical value, and should be kept distinct from measured Eh values, which he suspects are largely erroneous. While there are many possible sources of error in Eh measurements, their self-consistency indicates a degree of accuracy adequate to make them usable, particularly for soil solutions and interstitial solutions in sediments which are generally fairly well poised. However, because of transient biotic effects and slow dissolution and reprecipitation rates, the minerals present are not necessarily in equilibrium with the existing Eh.

Stability field diagrams are widely utilized to depict the possible mineral assemblage resulting from a given set of conditions or, alternatively, to deduce the Eh–pH environment under which a given mineral suite was formed. Several assumptions are inherent in the construction of stability field diagrams. One atmosphere total pressure, a temperature of 25°C., and an activity of the gaseous phases equal to their partial pressure, are assumptions which do not introduce obvious complications. Equilibrium is an unavoidable assumption, since little is known of the rates of the reactions involved, yet, with the hydrous oxides it appears to be the general case that the oxides which first precipitate are not the thermodynamically stable phases. It is also assumed that the activity of each of the solid phase compounds is one. This is almost certainly inaccurate in many cases for naturally occurring minerals since they are not pure compounds but are mixtures; thus, the activity coefficients of their components cannot be accurately calculated. As pointed out by Hem (*92*), it would be desirable to use the mole fractions of manganese and of iron in mixed oxides for the activity of these two metals. However, as the available information is contradictory, we do not know the extent to which manganese and iron occur in soils and sediments as the mixed oxides. Furthermore, it appears rather difficult actually to determine the amount of manganese or of iron present as a mixed oxide rather than as a separate phase.

A relatively modest portion of Figures 1 and 2 represents the range of conditions to which soils and surficial sediments are exposed. As will be noted later, the Eh values of soils and sediments range from +800 to −250 mv., but +600 to 0 mv. is the more general range. A pH range of 4 to 10 brackets all but the most extreme surficial environments. This area is hash marked in Figures 1 and 2.

Commonly, the manganese and iron oxide plus carbonate diagrams are constructed at a fixed total activity of the combined carbonate species. This is a boundary condition requiring a closed system which is not a

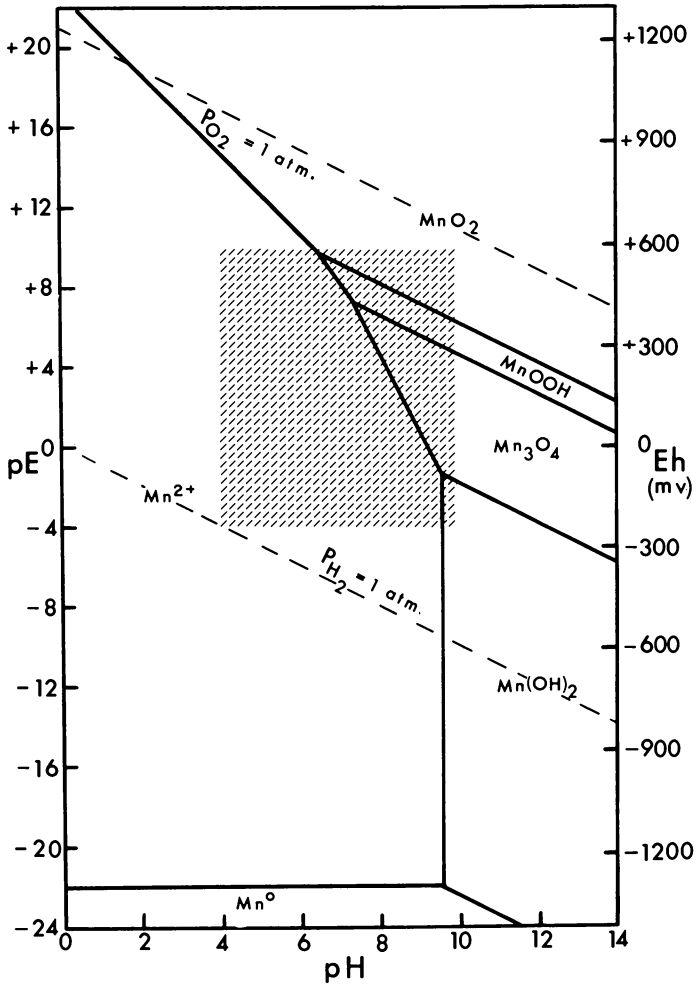

Figure 2a. Eh(pE) vs. pH stability field diagram for manganese ($a_{Mn} = 10^{-4}$M; $P_{CO_2} = 0$; $P_{tot} = 1$ atm.; $T. = 25°C.$)

desirable assumption for surficial materials such as soils and streams. Instead, fixed partial pressures of carbon dioxide have been used in Figures 1b and 2b to indicate the likelihood of manganese and iron carbonate precipitation in soils and sediments. Baver (*14*) cites a value of 0.20% ($P_{CO_2} = 1 \times 10^{-2.7}$ atm.) for the average carbon dioxide content of soil air. He notes that carbon dioxide contents as high as 15.5% ($P_{CO_2} = 1 \times 10^{-0.81}$ atm.) have been reported. In addition, the minimum carbon dioxide content of surficial waters was taken as that of the atmosphere—*i.e.*, 0.03% ($P_{CO_2} = 1 \times 10^{-3.5}$). The case of $P_{CO_2} = 0$, shown in Figures 1a and 2a completes the picture. The area between $P_{CO_2} = 1 \times 10^{-3.5}$

and $P_{CO_2} = 1 \times 10^{-2.7}$ probably represents the situation for most fresh waters and soil solutions although many soil solutions will fall in the area between $P_{CO_2} = 1 \times 10^{-2.7}$ and $1 \times 10^{-0.81}$. A comparison of Figures 1a *vs.* 1b and 2a *vs.* 2b indicates that at any finite P_{CO_2}, it is the carbonate, not the hydroxide, which is the stable divalent metal compound. Stability fields for both manganous carbonate and manganous hydroxide result if one assumes a constant total activity of the carbonate species, rather than a constant partial pressure of carbon dioxide (*93*). However, it is believed that the constant partial pressure of carbon dioxide is the better assumption. It should be noted that for the case of constant P_{CO_2}, that the total carbonate, and particularly the bicarbonate, activity becomes quite high at the higher pH values (Figures 3a and 3b). (The area of the manganese carbonate stability field would have been different if the free-energy value (*82*) of precipitated manganese carbonates rather than of natural rhodochrosite had been used; however, the free-energy value for the natural mineral is believed to provide the more realistic case.) That divalent metal carbonates are rare in soils and fresh water sediments is further evidence for the generally well oxidized nature of surficial deposits.

Within the area of interest in the stability diagrams, ferric hydroxide precipitation is possible at lower oxidation potentials than manganic manganese oxides at any given pH. Similarly, at a fixed Eh ferric hydrox-

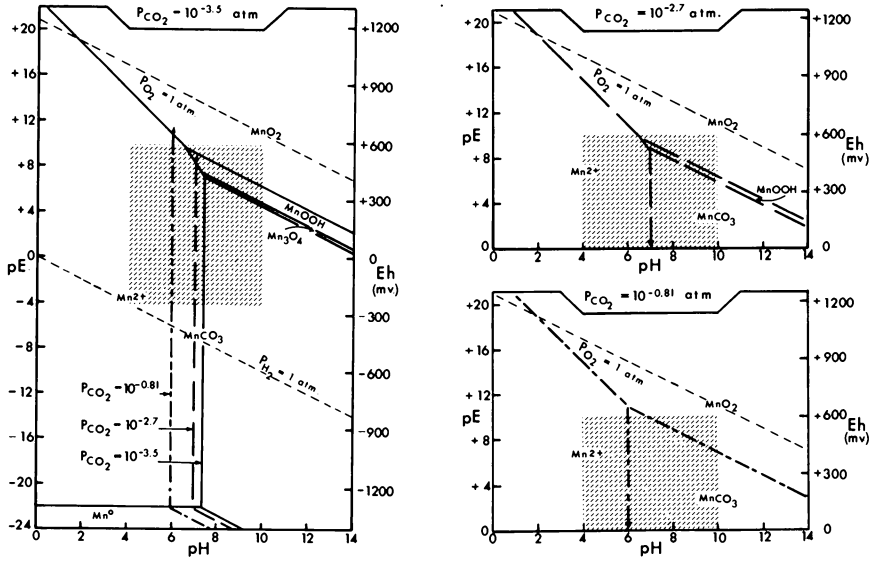

Figure 2b. Eh(pE) vs. pH stability field diagrams for manganese (a_{Mn} = 10^{-4}M; $P_{CO_2} = 10^{-0.81}$, $10^{-2.7}$ and $10^{-3.5}$ atm.; $P_{tot} = 1$ atm.; T. = 25°C.)

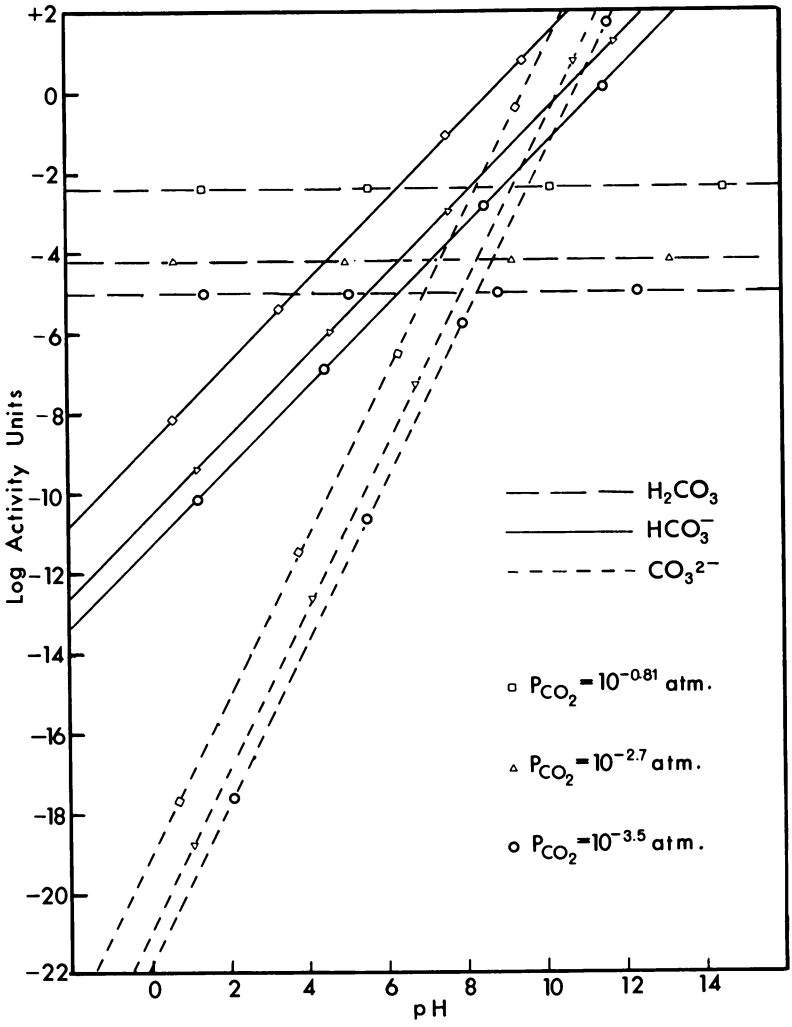

Figure 3a. Variation of activity of the individual carbonate species in solution with pH at fixed values of P_{CO_2}

ide precipitation is possible at a lower pH than manganese oxides. In case environmental conditions are such that carbonates can be deposited, both metals will tend to precipitate together because the solubility of manganese and iron carbonates are similar, although manganous carbonate is less soluble than ferrous carbonate.

Figures 3a and 3b relate the activity of the various carbonate species and the summation of their activity, respectively, to pH at the fixed P_{CO_2} values. It may be noted that the total carbonate species activity decreases markedly with pH.

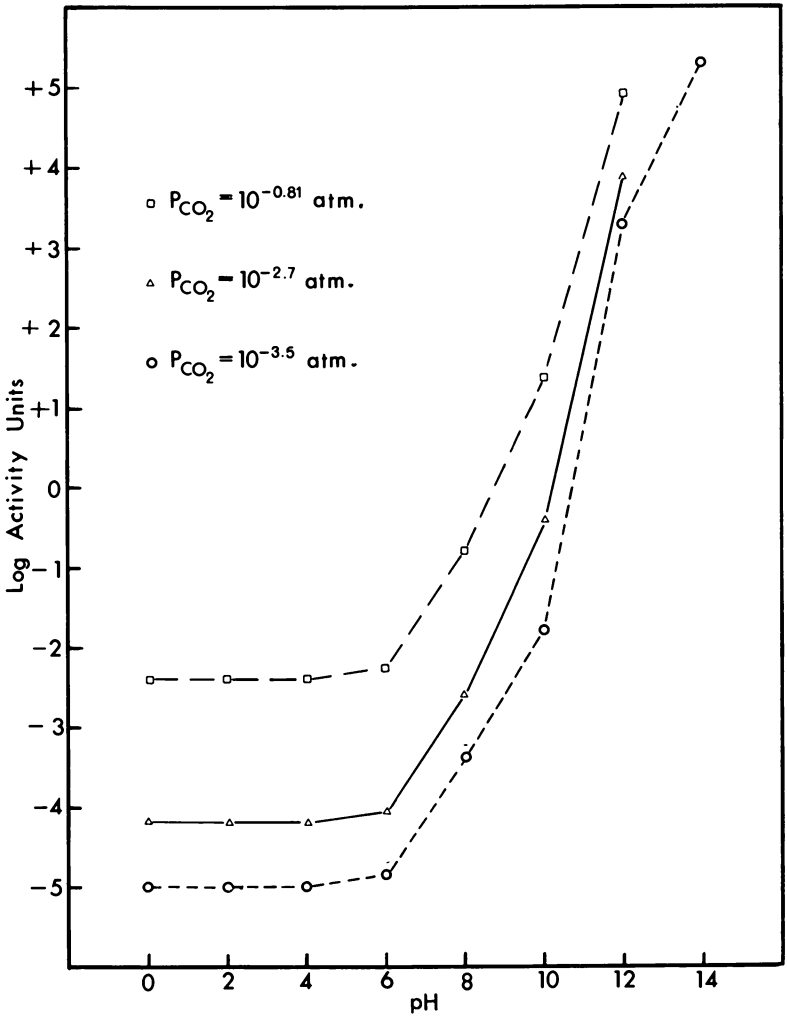

Figure 3b. Variation of total activity of the carbonate species with pH at fixed values of P_{CO_2}

The dashed lines superimposed upon Figures 1 and 2 bound the area within which oxygen and hydrogen gases are in equilibrium with water. These lines identify the Eh–pH values at which water decomposes to yield oxygen and hydrogen at high and low Eh values, respectively. The Equations for the upper line are

$$2\ H_2O\ (1) = 2\ H^+ + 2\ OH^- \quad (1)$$

$$2\ OH^- = O_2\ (g) + 2\ H^+_{(aq)} + 2\ e^-, \quad (2)$$

and for the lower line is

$$2\ H^+ = H_2 - 2\ e^-. \tag{3}$$

If Equation 2 is substituted into Equation 1, then

$$Eh = E^\circ + \frac{0.0591}{4} \log \frac{P_{O_2}\ [H^+]^4}{[H_2O]^2}. \tag{4}$$

Where $P_{O_2} = 1$,

$$Eh = E^\circ + \frac{0.0591}{4} \log\ [H^+]^4 \tag{5}$$

or

$$Eh = 1.23 - 0.0591\ pH. \tag{6}$$

The lines are drawn at P_{O_2} and P_{H_2} values of one atmosphere for the upper and lower line, respectively. At Eh–pH values above the $P_{O_2} = 1$ line, water is oxidized according to Equation 2 and below the P_{H_2} line, water is reduced according to Equation 3. (The intercept is, of course, the value of E°). The position of these lines is shifted almost imperceptibly by assuming P_{O_2} and P_{H_2} values of 0.1 rather than 1 atmosphere. Thus, the upper boundary line of the water stability field at a partial pressure of oxygen equivalent to the average content of the atmosphere is almost identical with that of pure oxygen at one atmosphere. Overvoltages of about 500 mv. are commonly required in the laboratory to obtain observable decomposition rates of water (*82*). However, hydrogen gas evolution from sediment under anaerobic conditions (*134*) occurs without appreciable overvoltages.

There are several important aspects about which Figures 1 and 2 tell little or nothing: (1) the reversibility of the reactions; (2) the probability of metastable, rather than the stable (free energy-wise), mineral species formation; (3) the rate at which the mineral transformations will occur in response to pH–Eh changes; (4) the effect of solid solution (both anions and cations); and (5) the effect of complex ion formation. All of these aspects are important for a quantitative description of the solution concentration of heavy metals in dynamic systems. The particle size of the hydrous oxides affects several of the above items, particularly (2) and (3). Microbiological activity is undoubtedly important with regard to the occurrence of metastable oxide species.

The application of mineral solubility data (Figure 4) to soils and sediments is at best semi-quantitative because of unknown effects of complex ion formation, solid solution, and armoring. The apparent solubility of $Fe(OH)_3(a)$ has been reported to be essentially constant at about $10^{-7}M$ between a pH of 6 and 11, presumably because of undissociated $Fe(OH)_3$ (*70*). Armoring by iron and aluminum oxides was believed to be responsible for the reduced solubilization rate of rounded quartz

as compared to freshly fractured quartz (*69*). In the extraction of free-iron oxides with dithionite–citrate from a sample of the Chinle Formation from the Colorado Plateau, it has been found that the extraction rate—*i.e.*, mg. Fe/minute/gram sample—was initially first order with a relatively high specific reaction rate constant. The dissolution rate then decreased abruptly, although still following first order kinetics (*119*). It seems apparent that formation water was reacting with the outer armoring iron oxide, not the protected inner iron oxide. One of the two oxides must be metastable with regard to formation waters. Hem (*93*) observed in laboratory experiments that the dissolution of manganese sulfide was apparently controlled by the solubility of manganese

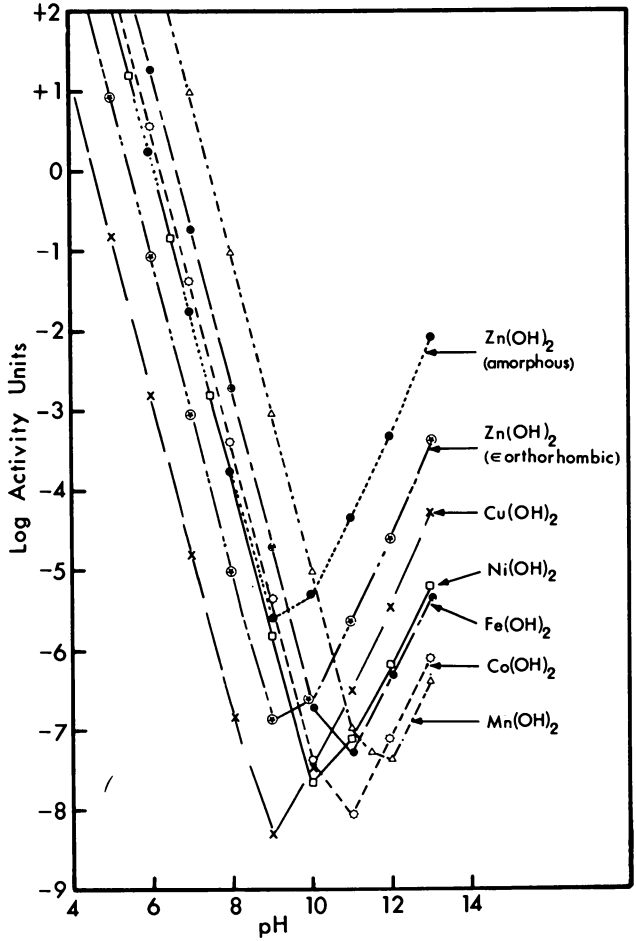

Figure 4. Maximum activity of heavy metals, in equilibrium with their hydroxide, vs. pH

carbonate because of the formation of a protective coating of manganese carbonate in bicarbonate-containing solutions. Schollenberger (*203*) found a black precipitate containing manganese on the surface of calcium carbonate particles picked out of greenhouse pots that had been recently limed.

In the pH range of natural waters, soluble bivalent iron and manganese exist predominantly as Fe^{2+}, Mn^{2+}, $FeOH^{+}$ (*168*). Figures 1 and 2 were constructed utilizing an activity of the soluble ions of 1×10^{-4} which is an upper limit to the concentration of manganese and iron found in extracts of soils. At this manganese concentration $MnOH^{+}$ does not occur in significant amounts. However, as the activity of manganese becomes less than 1×10^{-6}, which is the case for stream waters, $MnOH^{+}$ becomes of increasing significance. In carbonate-bearing waters, within the common pH range (6 to 9), the solubility of both elements in their bivalent oxidation state is generally governed by the solubility product of their carbonates and not by the solubility of the hydroxides (*168*). The concentration of trivalent iron in noncarbonate waters is reported to be governed by solubility of $Fe(OH)_3(a)$ (*97*). Recently, iron concentrations in Maryland ground waters from three aquifers have been found to be bounded by the solubility of $Fe(OH)_3(a)$ and hematite (*11*). The formation of undissociated $Fe(OH)_3(a) \cdot X\,H_2O$ species in neutral or alkaline solutions (*85*) may partly explain the occurrence of $Fe(OH)_3(a)$ in soils and sediments (*28*).

An important property of the hydrous oxide surfaces is that of catalyzing oxidation reactions. There is some indication that oxides of iron catalyze the oxidation of Fe^{2+} to Fe^{3+}. Gasser and Bloomfield (*83*) found that ferrous iron chelated by natural organics was readily oxidized at ferric oxide surfaces in the presence of oxygen. Sludge recycling in a coagulation treatment was found to definitely improve the extent of ferrous ion removal by oxygenation (*170*), from which it was concluded that the ferric ion species had a catalytic action on the oxygenation of the ferrous ion. However, the catalytic effect may have been the result of colloidal iron oxides formed in the sludge.

The oxides of manganese also catalyze the oxidation of Mn^{2+} to Mn^{4+}. Zapffe (*256*) found that the oxidation of manganese in a water treatment plant was speeded up, following aeration, by the catalytic influence of pyrolusite (β-MnO_2) and also by *in situ* precipitated manganese oxide. Hem (*94*) noted a catalytic effect of feldspar on the Mn^{2+} to Mn^{4+} reaction rate. It seems likely that this was caused by minute amounts of manganese oxide impurities on the feldspar surfaces.

The rate of Mn^{2+} oxidation can be quite rapid and increases markedly with pH (*93, 95*), although the presence of bicarbonate decreases the oxidation rate (*95*). Bricker (*33*) noted that chemical analysis of freshly

precipitated $Mn(OH)_2$ could not be made owing to the difficulty in preventing oxidation during handling. This is in agreement with the findings of Morgan (*166*) who observed that rather high pH values (> pH 8) were required to initiate precipitation of manganese from Mn^{2+} solutions, but as soon as some $Mn(OH)_2$ was precipitated the Mn^{2+} to Mn^{4+} reaction went rapidly. Kindle (*132*) noted that in a shallow area of a protected inlet, concretionary manganese coatings on pebbles showed vigorous renewal of growth after breakage of the coating, while alongside them were pebbles which showed little deposition of manganese. Manheim (*150*) concluded that as soon as manganese oxides precipitate, the catalytic effect of the oxide on sorbed Mn^{2+} is such that the nodules can continue to grow even though the waters bathing the nodules are undersaturated with respect to nodular manganese minerals.

Mehlich (*155*) found that the oxidation of Mn^{2+} to Mn^{4+} occurred at pH 5.8 in the presence of fresh aluminum or ferric hydroxides, otherwise it occurred at pH 8.5. The presence of an aged aluminum gel did not lower the pH of the oxidation-precipitation of divalent manganese.

No data have been found which would clearly establish the ability of manganese oxides to catalyze the Fe^{2+} to Fe^{3+} oxidation, although it has been suggested that this situation occurs in the formation of oceanic manganese nodules. Johnson (*123*) found that both growth and iron uptake by pineapple was much reduced on black Hawaiian soils high in manganese oxides. The unavailability of the iron was presumed to result from the large amounts of manganese in these soils. Hem (*96*) calculated an equilibrium constant of $10^{-5.67}$ for the reaction

$$2\ Fe(OH)_3(c) + Mn^{2+} + 2\ H^+ = MnO_2(c) + 4\ H_2O + 2\ Fe^{2+}. \quad (7)$$

The appropriate mass action expression is

$$\frac{[Fe^{2+}]^2}{[Mn^{2+}][H^+]^2} = 10^{-5.67}. \quad (8)$$

Thus, Fe^{2+} is a strong reducing agent with regard to MnO_2. Zapffe (*256*) noted that when water containing manganous and ferrous ions was passed through a pyrolusite bed, iron as well as manganese was precipitated on the manganese dioxide surfaces. Taylor *et al.* (*229*) noted that the outer surfaces of many soil manganese concretions, composed predominantly of birnessite, were coated with "ferruginous material" while lithiophorite concretions were often coated with goethite and/or hematite.

Jacks and Scherbatoff (*115*) suggested that copper acts as an oxidizing catalyst in soils. It has been noted that the application of copper sulfate to soils produced iron deficiency (*253*) and manganese deficiency (*221*). Iron deficiency occurred despite the fact that the copper sulfate was applied in a thin layer at mid-depth in the pots (*253*). In fact,

Mehlich (*155*) observed that ferrous sulfate solutions were able to solubilize freshly precipitated manganese oxide. The addition of copper sulfate increased the Eh value of unlimed Dunbar fine sandy loam from about +460 mv. to about +530 mv., whereas, when lime was added, copper sulfate increased the Eh from +310 to +380 mv. (*253*). These data also show a decrease of 0.1 pH unit upon the addition of copper sulfate for both the limed and unlimed samples. Dhar and Kishore (*60*) observed that several metal cations increased the oxidation rate of $Mn(OH)_2$. Also, Futral and Ingols (*80*) found that 0.5 p.p.m. copper sulfate speeds up the oxidation of manganese during water treatment and metallic copper parts often have manganese oxide coatings. In the case of iron, Stumm and Lee (*226*) have found a marked catalytic effect of copper ions on the ferrous to ferric oxidation rate.

It is well to note that biota play a significant role in the oxidation and reduction of metals in aqueous earth material systems (*212*). The information presented above is intended to show that these reactions may also be catalyzed by hydrous manganese and iron oxides.

Manganese and Iron Oxide Content of Clays, Soils, Sediments, and Waters

The oxides of iron and manganese are nearly ubiquitous in earth materials, even in reference clays (*6*). Possible exceptions are relatively unweathered volcanic ash and pumice, the bleached A_2 horizon of podzols, and certain sediments having very low redox potentials. In the case of volcanic ash soils, weathering has sometimes been insufficient to release adequate amounts of heavy metals for plant growth (*131*), whereas, in podzol soils the oxides have often been removed by highly acidic organic leachates. In the case of low Eh sediments, the oxides may have been largely dissolved. In acidic sandy soils developed under moderate to heavy rainfall, the oxides of manganese and iron and their occluded heavy metals may have been largely leached out of the soil profile resulting in a deficiency of zinc, cobalt, or other heavy metals owing to the minute amount present rather than to fixation in an unavailable form (*3, 104, 131, 154*). Bloomfield (*22*) noted that two gleyed soils contained insufficient total manganese to be determined by a colorimetric means.

Although there are only about a half dozen oxides of iron, some 33 to 36 oxidic manganese minerals are known (*33, 100*). Taylor *et al.* (*229*) report that lithiophorite, birnessite, and hollandite are the dominant concretionary manganese minerals occurring in soils. Todorokite, birnessite (δ-MnO_2), psilomelane, and ramsdellite have been reported in marine manganese nodules (*151*). Determination of the amounts of the individual hydrous oxides of manganese and iron oxides present in minor amounts in earth materials is largely beyond current technology

because of : (1) their widespread occurrence as partial coatings, (2) their microcrystalline nature, and (3) their occlusion of highly variable amounts of other metals. The latter is particularly true in the case of the manganese oxides (*229*). Some investigators consider the interpretation that microcrystalline iron and manganese oxides occur as coatings is simply a result of inadequate technology. However, reference clays and stream sediments bleach noticeably with the first few extractions while localized dark colors bleach slowly with additional extractions. These observations, in addition to those of Fripiat and Gastuche (*76*) and Berg (*17*) discussed earlier indicate the probable occurrence of iron and manganese oxides as partial coatings on other minerals.

The amounts of free-iron oxides in soils vary widely. On the average, the clay fraction of several Appalachian soils derived from limestone was reported to contain 11.2% iron as Fe_2O_3, while the clay fraction of soils from various parts of the United States was found on the average to contain 10.3% iron as Fe_2O_3 (*48*). In contrast, the Fe_2O_3 content of U. S. soils commonly ranges between 1 and 6%. Excluding concretionary iron horizons, the iron oxide content of mature tropical soils is 10 to 12.5% as Fe_2O_3 (*62*). This amount corresponds to the saturation of the external clay surface as indicated by precipitation of synthetic iron oxides on kaolinite. Little information is available on the free-iron oxide content of fluvial sediments but their oxide content would be expected to be somewhat less than the average of the surficial lands from which the stream sediment was eroded due to partial dissolution in the stream bed environment. The free-iron oxide content of Whiteoak Creek (near Oak Ridge, Tenn.) was recently found to be 2.6 and 6.0% iron as Fe_2O_3 for the $<$ 60-mesh and 9- to 60-mesh fractions, respectively (*119*). The higher concentration of iron oxide in the coarse fraction is caused by an appreciable amount of discrete oxides in this fraction.

Although data on water soluble, "exchangeable" (most commonly determined with 1*N* ammonium acetate), and "reducible" (most commonly determined with 0.2% hydroquinone in 1*N* ammonium acetate) manganese are numerous, these forms of manganese are defined only with regard to the method of their extraction rather than any fundamental property of the system. Information on these forms of manganese has little application to the problem at hand except that additional evidence for the ubiquitous presence of manganese oxides in soils and sediments is provided. These forms of manganese represent a highly variable and generally unknown portion of the total oxidic manganese, although Biswas and Gawande (*20*) found the hydroquinone reducible manganese to range from 11 to 34% of the free-manganese oxide in several soils of the Chhatishgarh Basin of India, and Baars (*9*) found the pH 4.8 acetate-soluble manganese to vary from 45 to 1.5% and from 76 to 15% of the

total manganese in going from the 2.5 to 22.5 cm. depth in two Indonesian rice-field soils. There is no evidence that "reducible" manganese represents the bulk of the oxidic manganese which participates in the redox cycle of a soil or sediment. It has been shown that the amount of "reducible" manganese in a particular soil is a function of the moisture regime, organic matter content, and pH (*88*). Sherman *et al.* (*208*) found that the "reducible" manganese content of Kentucky soils varies between 0.8 and 960 p.p.m. of Mn (0.0001 and 0.15% MnO_2). Baars (*9*) obtained "reducible" manganese values ranging from 0.11 to 1.0% MnO (0.14 to 1.2% MnO_2) for samples from two rice-field soils. Sherman *et al.* (*208*) found that manganese was likely to be deficient for plant growth where the "reducible" manganese was less than 25 p.p.m. Mn (0.0039% MnO_2) in neutral to alkaline soils and that strongly acid soils with a "reducible" manganese content of less than 25 p.p.m. Mn were likely to exhibit manganese deficiency following liming.

Only two papers have been found which give the free-manganese oxide content of soils and no data have been found for recent sediments. Daniels *et al.* (*54*) determined the distribution of free-manganese oxide in the profiles of several soils of Iowa representing a number of great soil groups. They found a range from about 0.01 to 0.25% Mn (0.02 to 0.41% MnO_2) in the various soil profiles. Their data show that the iron oxide content followed the profile distribution of clay more closely than did the manganese oxide content. Biswas and Gawande (*20*) found the free-manganese oxide content of six soil profiles of the Chhatishgarh Basin of India to vary from 328 to 2403 p.p.m. of MnO (0.040 to 0.30% MnO_2) with a mean of 1103 p.p.m. MnO (0.14% MnO_2). Free-manganese oxide contents of 0.076 and 0.24% as MnO_2 have been found for the $<$ 60 and 9 to 60 mesh fractions of Whiteoak Creek, Tenn. (*119*).

Total manganese values are generally of no use here, as the proportion in the silicate *vs.* the free oxide is unknown. However, John Cady of the USDA Soil Conservation Service has pointed out that an exception occurs in the case of laterites, as essentially all of the original silicate minerals have been weathered to secondary minerals. Thus, chiefly all of the manganese present in laterites would be oxidic manganese.

There are very little data available on the colloidal iron or manganese oxide contents of fresh waters, although considerable information is available for marine waters. Goldberg and Arrhenius (*86*) noted that less than 10% of the manganese present in Pacific Ocean waters was retained by 0.5 μ filters. The actual amount ranged from 0.06 to 0.22 μg./liter with a mean of 0.088 μg./liter. Laevastu and Thompson (*139*) found that the iron content of particulate matter in the waters off the coast of Washington collected on type HA Millipore filters varied from 51 to 163 μg./liter of iron with a mean of 114 μg./liter, whereas Joyner

(*125*) found particulate iron to range from 0.05 to 1.50 μg. atom Fe/liter for Pacific Northwest coastal waters. It has been noted that the greatest amount of iron in Maryland ground water occurred where the pH was between 5.0 and 6.3 and the Eh was less than +200 mv. Although some water samples were obtained with pH values near or below pH 4, these samples contained less dissolved (colloidal?) iron than those between pH 5.0 and 6.3 at similar Eh values (*11*). Tanaka (*228*) found that the amount of particulate iron in Lake Kizaki-ko (Japan) varied from about 25 mg./liter to a maximum of 1000 mg./liter. Particulate manganese was also observed.

Direct Evidence for Hydrous Oxide Control

Tiller and Hodgson (*238*) found that hematite (2 to 20 μ) sorbed quantities of cobalt similar to that sorbed by clay minerals. This may mean that the manganese and iron oxide surface area available in the clays was similar to that of the crushed hematite. The uptake by hematite was not solely by "surface sorption," but occurred in the interior of the oxide particles as well. This is indicated by the fact that dissolution of 21% of the hematite by hydrochloric acid only removed 78% of the "non-exchangeable" cobalt—*i.e.*, cobalt not dissolved in two 3-day 2.5% acetic acid extractions. Nontronite, the iron-analogue of montmorillonite, which would be expected to have considerable nonstructural iron oxide associated with it, was shown to fix ten times as much cobalt as the other clays tested against two 3-day acetic acid extractions (*238*). However, Hodgson (*112*) has found that a mild iron oxide removal treatment did not affect the amount of cobalt sorbed by nontronite. It has recently been found that an Fe_3O_4 precipitate continued to sorb additional cobalt for a period of three months or longer (*119*).

The zinc content of soil limonite was found to be always greater than that of the soil matrix in Tennessee subsurface soil samples (*251*). Burns and Fuerstenau (*40*) determined the occluded heavy metal concentrations in oceanic manganese nodules *via* an electron probe. They found that nickel and copper occurred in the high manganese bands while cobalt occurred predominantly in the iron rich areas.

Canney and Nowlan (*47*) have shown that the amount of dithizone-extractable heavy metals removed from stream sediments with ammonium citrate-hydroxylamine hydrochloride was linearly related to the amount of manganese dissolved. This indicates that the cobalt is present in the manganese oxides. In accordance with this data, it has been found that the slope of plots of the extraction rate *vs.* time (with dithionite-citrate) for cobalt from < 60 mesh fraction of Whiteoak Creek sediment was closer to that of manganese than that of iron, indicating that more of the

cobalt had been sorbed by manganese than by iron oxides (*121*). Recently the free-manganese oxides and associated metals have been extracted with 10% hydrogen peroxide in 0.001*N* nitric acid for 3 days (*230*). With few exceptions, manganese, cobalt, nickel and zinc were much more concentrated in the extracts than in the bulk sample. A good correlation ($r = 0.87$) was found between % cobalt removed and % manganese removed.

The heavy metals are scavenged by naturally occurring manganese and iron oxides as well as by laboratory precipitates. Krauskopf (*135*) found that cobalt, nickel, copper, and zinc were removed from solution by both hydrous manganese and iron oxide precipitates. Hem and Skougstad (*98*) found that from 10 to 60% of the copper present in solution (0.6 p.p.m.) was scavenged by iron hydroxide precipitates (originally 3 p.p.m. of Fe^{2+}). The higher the pH of precipitation, the greater the amount of copper removed from solution. Morgan and Stumm (*168*) found that the sorption capacities of $\delta(?)$-MnO_2 and $Fe(OH)_3$(a?) precipitates for nickel, cobalt, zinc, and manganese were significantly higher than for calcium or magnesium. Fukai *et al.* (*79*) found that adding as little as 10 mg. of manganese dioxide per liter of sea water resulted in the recovery of about 80% of the cobalt present in solution. Boyle *et al.* (*32*) report that in the New Brunswick (Canada) area, stream sediments enriched in manganese are likewise enriched in zinc, copper, nickel, and cobalt. Fleischer and Richmond (*72*) have shown that cobalt commonly occurs in at least four manganese minerals: lithiophorite (a hydrous lithium-manganese aluminate), psilomelane (which contains essential barium), cryptomelane (which contains essential potassium), and hollandite (which contains essential barium). In the last three, the cobalt ranged from 0 to 2%. All the samples of lithiophorite examined contained appreciable quantities of cobalt, the maximum percentage being 4.84. Taylor *et al.* (*229*) separated manganese concretions from numerous soil samples and determined, among other components, the cobalt and nickel content. Some of their results are shown in Table I.

Information on the heavy metal content of marine manganese nodules has been summarized by Mero (*158*) and Manheim (*151*).

Indirect Evidence for Hydrous Oxide Control

Organic Matter (and Eh) Effects. Evidence for organic matter control, by complex formation, of heavy metal availability to plants has previously been deduced from a positive correlation of the organic matter and the heavy metal contents of soils (*2, 13, 102, 103, 122, 130, 216, 233*), and from the release of heavy metals upon treatment of soils with hydrogen peroxide (*13, 53, 248*). On the contrary, it is proposed that the gen-

eral role of organic matter is to produce a periodic reducing environment (following rainfall or irrigation) necessary to maintain manganese and iron oxides in a hydrous microcrystalline condition (a secondary effect). It is further proposed that hydrogen peroxide treatments release heavy metals already present in hydrous manganese oxides, or greatly decrease sorption of the subsequently added heavy metal by dissolution of the manganese oxides present in minor amounts and by reduction of the surface area of the iron oxides (artifacts of the treatment). The marked decrease in extractable zinc and copper below the surface soil horizon which is sometimes observed (*102, 103, 129, 233*) is interpretable in these terms: (1) under vegetative cover, heavy metals tend to be concentrated in the surface horizon as a result of extraction from the profile by plant roots and deposition on the surface by plant litter; and (2) the greater portion of these metals, released from decaying vegetation, will be retained in the upper few inches of the soil by the hydrous oxides except where the hydrous oxides themselves have largely been leached to lower horizons. The data of Sokoloff (*214*) argue against organic matter as a principal sorber of heavy metals in Mississippi soils as heating to 300°–400°C. did not effect the capacity of the soils to sorb zinc and cobalt, since complete oxidation of metal-fluvic acid complexes was found to occur at temperatures varying from 340° to 570°C. (*199*). Of course there could have been a compensating effect of the heat treatment upon inorganic sorbers although this appears unlikely from the available data.

The role of organic matter described above is believed to represent the general case. However, organic matter plays a direct role in at least three instances: (1) during periods of low Eh (and pH) the organic complexes serve to reduce the amount of these metals removed by water passing through the soil or sediment; (2) in case of overliming, the effect may be mitigated due to a portion of these metals being complexed by the organic matter; and (3) in highly organic soils and sediments the sheer quantity of organic matter dominates the availability of heavy

Table I. Cobalt and Nickel Content of Some Concretionary Manganese Minerals Separated from Soils[a]

		Percent								
	Number of	*CoO*			*NiO*			Mn_3O_4		
Mineral	*Samples*	*Minimum*	*Maximum*	*Mean*	*Minimum*	*Maximum*	*Mean*	*Minimum*	*Maximum*	*Mean*
Lithiophorite	9	0.05	4.7	1.53	0.05	0.41	0.13	37	83	73
Birnessite	8	.19	2.3	.57	.04	1.4	.43	62	90	84
Hollandite	3	.45	2.9	1.37	.06	.40	.21	52	84	65

[a] Ref. 229.

metals. In accordance with the above, Nielsen (*174*) found most of the cobalt and zinc of a McNary Reservoir (Columbia River) sediment sample to be in an organic fraction (carbon tetrachloride extractable). Reid (*191*) found that when Mn^{2+} was added to soil as the EDTA chelate, the decrease in plant uptake of manganese from the soil was not as rapid upon liming, and more manganese remained in the water-soluble form at the same pH level than when a manganese salt was added. It is also known that organic soils require much higher fertilizer applications of cobalt (*65*) to cure plant deficiencies than other types of soils, and that deficiencies of copper (*216, 221*) and manganese (*142*) are most common on organic soils. Mulder and Gerretsen (*169*) note that manganese deficiencies occur in the northern part of the Netherlands, particularly on reclaimed peaty soils which have become neutral or slightly alkaline through the use of lime or certain other fertilizers.

A further complication is that water and particularly dilute acid extractants remove organic matter which contain complexed heavy metals. The recent finding that 98 to 99% of the water soluble copper and up to 75% of the water soluble zinc is complexed by soluble organics (*109*) is a case in point. However, since the hydrous oxide model presented here is concerned with fixation of heavy metals by the solid phase, there is no apparent conflict with the findings of Hodgson *et al.* (*109*). Dilute acids were found to remove from 30 to 90% of the total organic carbon present in the Bh horizons of podzol soils (*202*). The organic matter thus extracted was not flocculated by >53,000 mg. of magnesium or calcium per gram of organic matter (*255*). Presumably, similar amounts of other divalent metals would be required to flocculate Bh horizon organic matter. Gupta and MacKay (*90*) found up to 60% more copper (by a colorimetric method) in 2% citric acid extracts after treatment to destroy organic matter in the extracts.

SECONDARY EFFECT. Various lines of evidence indicate that organic matter reactions in soils and sediments are instrumental in maintaining iron and manganese oxides in a hydrous high-surface-area state: (1) direct reduction of ferric and manganic oxides by organic matter; (2) indirect reduction of the oxides *via* a lowering of pH and Eh of the system because of other organic matter reactions; and (3) direct biological reduction of the oxides.

Morgan and Stumm (*168*) found that a variety of organic substances, especially those containing hydroxy and/or carboxylic functional groups (phenols, polyphenols, gallic acid, tannic acid, etc.) can reduce both ferric and manganic oxides reasonably fast (minutes to hours) in synthetic solutions. Bloomfield (*26*) found that when a ferric solution was added to a water extract of fermented grass, ferrous iron was immediately detectable. Bloomfield, in studies of gleying, has found that aqueous

extracts of anaerobically fermenting organic matter, such as leaves and bark (*24, 27*) or sterile extracts of pine needles (*23*) reacted with ferric iron to form organic complexes of ferrous iron. Bloomfield (*25*) concluded that the effectiveness of aspen leaves in dissolving ferric oxides was not one of acid effect *per se* as the process was still effective at a pH of 7. The complexes were sufficiently stable to be transported by percolating water, but if brought into contact with ferric oxides, they were sorbed and the ferrous iron was then readily reoxidized upon the admittance of air (*83*). That at least a portion of the dissolution is a direct effect of the organic matter and is nonbiological is indicated by the solution of ferric oxides in the presence of toluene or chloroform (*23*). Page (*179*) suggested that the considerable increase in extractable manganese as a result of sterilization of greenhouse soils is a result of the breakdown of organic manganese complexes. However, in view of the information presented above, it is also possible that moisture and temperature conditions during sterilization are such that reduction of manganese oxides by organics is accelerated.

Apparently some of the organic chelates are occluded in ferric oxides, as Blümel (*28*) found that iron concretions in gley and pseudogley soils contained appreciable organic matter. Baas Becking and Moore (*10*) concluded that most of the iron in marine sediments exists chiefly in organic matter complexes. These authors noted a tendency for organic matter and iron to occur in a ratio of approximately 3:1 (w/w, iron as FeOOH) in marine sediments. Jenne (*120*) found that it was necessary to alternate free-iron oxide removal and organic matter oxidation treatments (acidified hydrogen peroxide) to obtain the desired free-iron oxide removal of coastal Oregon soils, as the iron oxides and organic matter provide mutually protected coatings. Appreciable amounts of organic matter are frequently found in the ironpans in podzolic soils. Manheim (*151*) notes the presence of appreciable organic carbon in marine manganese nodules.

Indirectly, organic matter causes the reduction of iron and manganese oxides due to the hydrogen ions and electrons made available during anaerobic respiration. Soil and sediment suspension may develop pH values as low as 3 under anaerobic conditions (*5*) and Eh values as low as −250 mv. (*118*). Camp (*44*) may have been the first to anticipate this effect of organic matter when he noted that "In addition to carrying zinc, these organic materials [manure] probably form pockets or particles of acid material in the alkaline soils and so retain zinc in an available form." Sherman and Harmer (*207*) found that manganese deficiency symptoms of oats could be eliminated in an alkaline organic soil by adding: (1) manganese sulfate; (2) free sulfur; and (3) other reducing agents (sodium bisulfate, stannous chloride, creatinine, and hemoglobin).

Yields of oats were higher as a result of creatinine and stannous chloride treatments as compared with the manganese sulfate treatment. Soluble manganese determinations established that the beneficial effect of the free sulfur and the reducing chemicals was to solubilize the manganese oxides of the soil.

In laboratory studies of anaerobic reduction of the hydrous oxides only one or two of the significant variables, namely, pH, Eh, and manganese and iron concentrations in solution have been generally measured. Carroll (*48*) determined pH and Eh of aliquots taken periodically during anaerobic bacterial reduction of iron oxides from clays. Initial Eh values were generally between +450 and +470 mv. Visible bleaching occurred at Eh values between +200 and +280 mv. (the pH values being between 4.2 and 5.8). Likewise the data of Bloomfield (*21*) indicate that iron dissolved more rapidly after the pH dropped below 5 (Eh data not given). Carroll stated that the Eh at which visible bleaching occurred was related to the dominance of hematite *vs.* goethite in the samples, hematite being reduced at higher Eh values than goethite. Jeffery (*118*) added organic matter (5 grams grass roots and 250 ml. of water) to 30 grams of an oxidized soil, excluded air, and observed four reaction stages: (1) a fall in Eh from about +550 to −250 mv. in 1–1/4 days; (2) a constant low value for 1–1/4 days; (3) a rapid increase in Eh to ≈+260 mv. in one day; and (4) a slow decline for several days, leveling off at an Eh between +100 and +150 mv. In contrast, the soil without added organic matter decreased to an Eh of only ≈+120 mv. The final Eh values of the systems with and without added organic matter were similar.

Baars (9) added glucose to samples of five rice-field soils (Indonesia) in closed containers and found that the pH decreased from 6.55 ± 0.05 to 5.35 ± 0.5 and the manganese increased to a maximum of 240 mg. of MnO/liter (295 p.p.m. MnO_2/liter). The manganese concentration appeared to increase until the glucose was used up. Jeffery (*118*) found that manganese came into solution during the initial stage (two days) when the Eh was rapidly decreasing. The slow decrease in Eh during stage three was ascribed to iron oxide reduction. Ng and Bloomfield (*173*) found that manganese dioxide was more readily dissolved by ground-up plant material under anaerobic conditions than were iron oxides.

Probably the most striking data available are those of Takai and Kamura (*227*) and Koyama (*134*) for a paddy soil. These results show that under anaerobic conditions an appreciable amount of manganese comes into solution at an Eh value of +300 mv. (Figure 5). Most of the reducible manganese was dissolved by the time the Eh had decreased to +100 mv. Figure 2a shows that the existing Eh–pH conditions are far to the left of the Mn^{2+}-$Mn(OH)_2$ or Mn^{2+}-Mn_3O_4 boundaries, hence, the

rate of manganese oxide dissolution should be quite rapid. (The pH would be expected to be in the range of 4.5 to 6.0.) Significantly, Takai and Kamura found very little iron dissolved until nearly all of the available manganese was reduced (four days). The Eh–pH decrease was apparently sufficient to change the stability field of iron from $Fe(OH)_3$ to Fe^{2+}. Iron dissolved at a more or less constant rate with time from the fourth through the thirtieth day when the experiment was terminated. Furthermore, Koyama (*134*) found in subsequent experiments that the concentration of both NO_3^- and NO_2^- was reduced to zero (fourth day) at the point at which iron began to dissolve (Figure 6). He found that hydrogen gas was evolved after the Eh was reduced to about −200 mv.

In a field study, De Gee (*56*) found the surface of an irrigated rice field to have Eh values ranging from +400 to +600 mv. which dropped to a minimum of 0 to +75 mv. at depths of from 2 to 17 cm. Of particular interest is his observation that in the horizon of manganese oxide accumulation the Eh values had risen to +300 to +500 mv. Also noteworthy is his laboratory data wherein he measured Eh values of +502 mv. in ammonium acetate suspensions of $Mn(OH)_2$ and MnO_2. It is puzzling that similar Eh values were obtained for suspensions of both the oxidized and reduced forms of manganese and that the values were so high. It appears most likely that the Eh value of one or both of the suspensions is in error.

The foregoing data showed rapid dissolution of manganese oxides under low Eh-pH conditions explain the observations of Leeper (*142*) who found that waterlogging a calcareous sandy loam soil for a period of four weeks eliminated manganese deficiency in oats (the agronomic plant most sensitive to manganese deficiency). Adams and Honeysett (*1*) found that waterlogging for nine days increased the copper, nickel, iron, zinc, and cobalt content of subterranean clover by 2, 7, 10, 22, 66 and 91%, respectively. However, it was noted in a study of submerged soils that samples low in organic matter showed no appreciable solubility of manganese upon submergence (*195*). Likewise, Piper (*185*) found that moisture levels from 45 to 90% of the water-holding capacity of a sandy calcareous (70% $CaCO_3$) soil had little effect on the availability of soil copper. Thus, the increased availability of heavy metals as a result of waterlogging is clearly dependent upon the presence of adequate organic matter. This is in accordance with the observations of Låg and Dev (*140*) that the highest ammonium acetate extractable manganese values coincided with minimum pH and maximum organic matter content of some Norwegian podzol soils. Middelburg (*160*) working with a volcanic ash soil observed that waterlogging had little effect on the amount of extractable manganese. However, adding sugar prior to water-

logging markedly increased the amount of extractable manganese. Thus, the necessity for organic matter to be present during waterlogging is indicated.

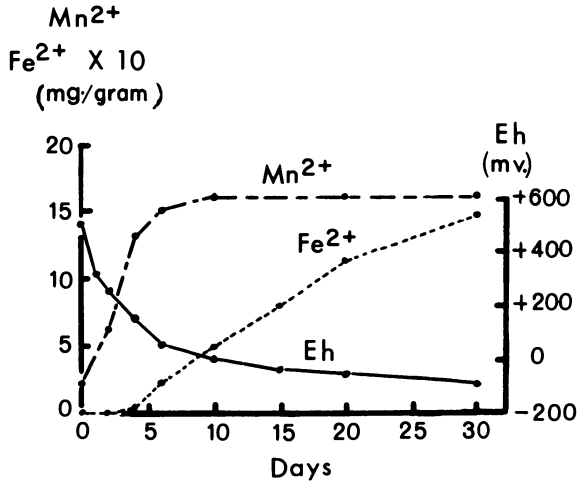

Figure 5. Anaerobic dissolution of manganese and iron oxides (134, 227)

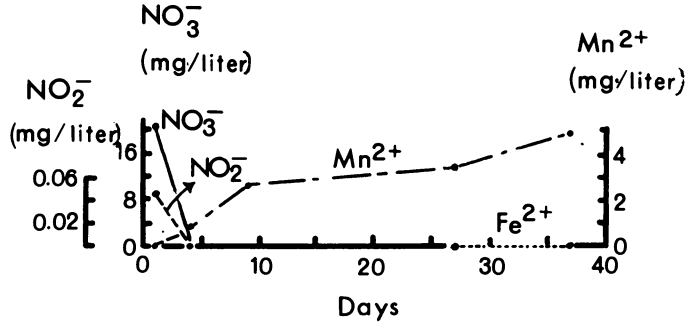

Figure 6. Changes in aqueous concentration of NO_3^-, NO_2^-, Mn^{2+}, and Fe^{2+} during anaerobic incubation (134)

Rogers *et al.* (*196*) found that copper was higher in soils with poor drainage and only the soils having poor drainage gave a residual effect from copper fertilization. Hill *et al.* (*104*) and Mitchell *et al.* (*165*) reported that poorly drained soils produced plants higher in cobalt than did well drained soils. Mitchell (*164*) observed that the ratios of total to acetic acid-extractable cobalt and nickel were much higher in freely drained soil profiles (1:20 and 1:200, respectively), than in poorly drained soil profiles (1:2 and 1:20, respectively), indicating that a larger portion

of these metals resides in the acid soluble hydrous oxides in the poorly drained than in the well drained soils (it would be most informative to know the amount of manganese and iron dissolved by the acid treatment from the well and poorly drained soils).

The presence of adequate organic matter is also believed to reduce the rate of the conversion of manganous fertilizers to unavailable forms. The addition of organic matter to mineral soils was found to increase the exchangeable manganese (*52, 198*) and electrodialyzable manganese (*188*).

Considerable seasonal variation has been noted in the heavy metal content of forage. Askew and Maunsell (*8*) found that whereas the cobalt content of forages was high in the spring, the cobalt content decreased as the summer advanced. Wain *et al.* (*245*) noted that each of four species of pasture grass contained the highest manganese content in the month of December. DeLong *et al.* (*57*) found that 0.2*N* acetic acid-extractable manganese increased after spring and summer rains. Kosegarten (*133*) observed that, whereas exchangeable manganese increased following rainy periods, easily reducible manganese decreased correspondingly. Winter and spring rain and snow result in soils being frequently wetted to field capacity with a resultant decrease in Eh and pH. As the soils become progressively drier the iron and manganese oxides become more highly oxidized as well as less hydrous. This decreases the availability of the occluded heavy metals, as solid state diffusion is considerably restricted with increased crystallinity and dehydration of these oxides. Additional pertinent literature on seasonal variation of heavy metal availability is cited by Beeson (*15*).

The appearance of a zinc deficiency as a result of extensive surface erosion or of loss of the A horizon by land leveling operations (*29, 30, 127*) may partly be ascribed to higher pH values below the surface horizon but principally to a loss of the principal soil reservoir of zinc as well as to a loss of the organic matter, the latter being necessary for the periodic reduction of the hydrous oxides to make the occluded heavy metals available. That the deficiency on these lands is not simply a loss of zinc is shown by the frequent failure of a single zinc fertilization to prevent zinc deficiency on land which has had the surface soil removed by leveling (*29, 30, 127*) or erosion (*129*).

The organic matter–Eh–pH effects are believed to provide the best explanation of the above data. The main function of high soil moisture levels is to exclude atmospheric oxygen and to reduce the loss of carbon dioxide. The former favors a lowering of the Eh and the latter favors an increase in hydrogen ion concentration; together they periodically facilitate valence reductions in the oxides of iron and manganese. Thus, it is frequently observed that water-soluble or "exchangeable" manganese in-

creases with increasing clay content of soils because of increased moisture retention and to decreased aeration because of a lesser permeability. Passioura and Leeper (*181*) found that compaction of two manganese deficient Australian soils [bulk density increases of 0.85 to 1.0 and 1.2 to 1.5 gram/cc. (?)] greatly increased the yield response of oats to applied manganese even though the compaction did not result in an increase in EDTA (pH 8.1) extractable manganese. They interpreted this effect as an increase in contact between soil grains and plant roots as a result of the increase in soil density. However, EDTA is probably most effective in extracting organic forms of manganese and may not provide a reliable test for reduced, but not dissolved, manganese.

The Eh–pH effects on heavy metal availability may also be illustrated with the data of Shukla (*210*). Significant pH, and presumably Eh, decreases occurred in soil samples following sucrose addition and incubation. The striking aspect is that only when the incubation resulted in a pH decrease was there an increase in water-extractable zinc. In fact, in the absence of any pH decrease (and presumably little or no Eh decrease) less zinc was water extractable after incubation than before. A somewhat similar situation occurred in a study by Zende (*257*). He noted that the increase in exchangeable manganese as a result of moist storage was not well correlated with the organic matter content of the soil. However, if his samples are grouped by pH, then it is found that the amount of extractable manganese generally increased with organic matter content.

While several investigators have utilized bacterial action for the removal of iron oxides from soils (*5, 21, 35, 48, 175*), the extent to which the reduction process is organic rather than inorganic has not been unequivocally established. Closely related to the "biological" oxide reduction approach is the one of evaluating the availability of heavy metals to crops *via* bioassay procedures. The success of biological methods of determining heavy metal availability appears to rest on a combination of: (1) lowering the Eh and the pH [Martens *et al.* (*153*), used a pH 1.8 buffer], resulting initially in manganese oxide and subsequently in iron oxide dissolution; (2) increasing the activity of hydrogen which then displaces the sorbed heavy metal; and (3) reducing the higher valence oxides *via* biological catalysis.

ARTIFACT EFFECTS. Best (*18*) has postulated the following reactions of hydrogen peroxide with manganese dioxide in neutral or alkaline suspensions:

$$MnO_2 + H_2O_2 = Mn(OH)_2 + O_2 \quad (9)$$

$$Mn(OH)_2 + H_2O_2 = MnO_2 + 2\,H_2O \quad (10)$$

while in acidic media (pH < 5)

$$MnO_2 + H_2O_2 + 2\,H^+ = Mn^{2+} + 2\,H_2O + O_2. \quad (11)$$

Jackson (*116*) utilized hydrogen peroxide in a pH 5 sodium acetate buffer to remove manganese oxides which serve as cementing agents as well as particulate manganese oxides. Taylor *et al.* (*229*) have utilized the solubility of manganese oxides in acidified (pH 3) hydrogen peroxide (3%) to extract quantitatively the manganese from soil manganese concretions.

Jenne and Wahlberg (*121*) found that much of the cobalt-60, as well as manganese, in Whiteoak Creek surficial bed sediment below the Oak Ridge National Laboratory, was removed by acidified hydrogen peroxide treatments. Hodgson (*107*) reported that certain subsoils released rather large amounts of copper and cobalt to a 30% hydrogen peroxide-0.25*N* calcium chloride extractant, although the subsoils were essentially devoid of organic matter, suggesting that these two metals were being released by dissolution of manganese oxides. Hodgson (*112*) suggests that exfoliation of vermiculitic minerals may account for the release of copper and cobalt during hydrogen peroxide treatment found by Hodgson (*107*). Further indication that the hydrogen peroxide treatment effect is caused by manganese oxide dissolution, rather than organic matter oxidation, is the finding that neither potassium permanganate nor free bromine, in alkaline solution, removed naturally occurring zinc, whereas hydrogen peroxide did (*101*). When the removal of manganese oxides in the course of hydrogen peroxide treatments is not taken into account, the results of heavy metal sorption studies may be almost uninterpretable (*162*).

Another problem arises in that after hydrogen peroxide is added to sediment samples for organic matter oxidation, the suspension is frequently evaporated to a paste. This step may cause reprecipitation of much of the manganese dissolved by the hydrogen peroxide. Sample treatment with hydrogen peroxide under these conditions could well have the effect of increasing the manganese oxide sorptive capacity for heavy metals, as these precipitation conditions can be expected to yield a poorly crystalline type of manganese oxide with a high surface area. This situation is exemplified by the data of Zende (*257*). He found that the M/2 calcium nitrate-extractable manganese increased from 18 to 107 p.p.m. and 16 to 43 p.p.m. (oven-dry basis) for soils "B" and "D" following hydrogen peroxide treatment for organic matter oxidation. (Soil B = a subsoil sample from a "red friable clay with free drainage," D = "typical Australian podzol of grey sandy loam . . .") In view of the effect of hydrogen peroxide in dissolving manganese oxides, it might appear surprising that Tiller (*236*) found hydrogen peroxide pretreatments to have

little effect on cobalt sorption by reference clays. However, it should be borne in mind that manganese dioxide decomposes hydrogen peroxide catalytically at neutral and alkaline pH values; thus, hydrogen peroxide may have little effect on the manganese oxide content of the samples treated unless the system is acidic. In early studies of the oxidation of organic matter with hydrogen peroxide, it was noted that even a fraction of one percent of manganese oxide inhibited the destruction of organic matter (*4, 193*). Hosking (*113*) was able to obtain essentially complete organic matter oxidation with hydrogen peroxide at pH 5.8 or lower, but in the black soils of Australia (perhaps high in free-manganese oxides) pH values of < 3 yielded superior results.

Although for the most part, Tiller *et al.* (*239*) found little effect of hydrogen peroxide pretreatment on the sorption of cobalt by soil clays, two notable exceptions occurred. In the case of the Pachappa soil (California) cobalt sorption was reduced by about half by the hydrogen peroxide treatment. Current studies in this laboratory show that the Pachappa soil is quite high in free-manganese oxides which may account for its unusual cobalt sorption ability. In the case of the Nipe soil (Puerto Rico), which contains a considerable amount of iron oxides and a lesser amount of manganese oxides, cobalt sorption was significantly increased by the hydrogen peroxide treatment. No explanation is currently available for this effect, although it may be related to the observation of Davidtz (*55*) that hydrogen peroxide reduces the surface area of amorphous iron oxide. Chemical changes in amorphous iron oxides concomitant with the reduction in surface area may increase the rate of, or capacity for, heavy metal sorption. Insufficient procedural data is given by Tiller *et al.* (*239*) to evaluate the possibility that manganese oxides might have been removed by the hydrogen peroxide treatments from the one soil but reprecipitated in the other.

pH Effects. Most of the available information on the effect of pH on heavy metal fixation and availability can be interpreted in terms of competitive exchange of hydrogen with the heavy metals occluded by the hydrous oxides as well as dissolution-precipitation and oxidation of the hydrous manganese and iron oxides. It would appear to be more than coincidence that all great soil groups of Australia which show cobalt, zinc, molybdenum, or boron deficiency also show either a manganese or iron deficiency for one or more crops (*222, 231*). This suggests that where pH–Eh conditions are such that manganese or iron concentrations in the soil solution are inadequate for plant growth, solution-reprecipitation reactions are inadequate to maintain iron and manganese oxide in the hydrous microcrystalline state necessary for the occluded heavy metals to be available. In Western Australia, manganese deficiency is of common occurrence over a wide area of the cereal belt although only limited

patches, a few square yards or acres in size, are actually affected. Teakle and Wild (*232*) state that these sites are rich in ferruginous gravel, especially in the subsurface layers, and the surface sandy layer has a loose, ashy, or powdery, structure. Passioura and Leeper (*181*) suggest that these patches have lower bulk densities than the surrounding areas. Thus, the available information suggests that these patches have higher Eh values (more oxidizing) than the surrounding area, partly caused by greater permeability, so that the oxides of manganese and iron rarely experience dissolution and reprecipitation.

The pH effect has been investigated from many directions. Numerous investigators have noted that: (1) less metal is sorbed by soil samples in more acid systems (*12, 182, 185*); (2) at least a portion of the sorbed nonexchangeable heavy metal is acid extractable (*12, 53, 106, 110, 172, 238*); (3) more of the sorbed metal is removed as the pH of the extractant is decreased (*12, 36, 63, 101, 124, 172, 219*); or (4) more manganese is extracted from the more acid soils (*246, 252*). Conversely, several studies show that the liming of soils: (1) decreases plant uptake of manganese (*163, 207*), of cobalt (*7, 8, 65, 104, 163, 183*), of zinc (*45, 81, 124, 148, 192, 197, 206, 247, 254*), and nickel (*163, 180*); (2) decreases ammonium acetate-extractable nickel (53) and "exchangeable" manganese (*52, 75, 178, 188*); (3) decreases the amount of water-soluble iron (*152*) and manganese (*178*); and (4) increases the amount of copper sorbed by soils (*162*). Of course, various nutrient interactions occur which modify the simple effect of availability of an element upon its uptake by plants.

Satisfactory correlations between extractable heavy metals and pH for a variety of soils are notoriously poor. Thorne *et al.* (*233*) found no consistent correlations for Utah soils between pH 3.2 acetic acid plus 0.05*N* potassium chloride extractable or total zinc with pH (or organic matter content). They concluded that total zinc differentiated zinc-deficient soils as well as the extraction procedure used. Brown *et al.* (*38*) observed no correlation between soil pH and either response to zinc application or ammonium acetate-dithizone extractable zinc. Kanehiro (*129*) did not find a satisfactory relation between soil pH and acid-extractable zinc; however, if his samples which were more acid than pH 5.5 are ignored then there is a tendency for acid-extractable zinc to decrease with soil pH. Furthermore, if surface and subsurface samples are segregated the relationship is improved. This may be because of the presence of greater amounts of organic matter in the surface horizon samples; hence, the hydrous oxides and their occluded metals were more soluble.

Peech (*182*) noted that a pH of 3 was required to prevent zinc fixation by Norfolk fine sand (initial pH of 5.0), whereas at pH 8 the fixation was nearly 100% complete in 48 hours, against 1*N* sodium chloride ex-

tractant. With copper, fixation accounted for 95 to 98% of added metal at pH 6 to 8 and was 60% at pH 3. Some cobalt fixation on clays, which is interpreted in the context of this review as being manganese and iron oxide coatings, occurred at least as low as pH 4 (*238*). Of interest here are the findings of D. W. Fuerstenau and colleagues (*77*) that the sorption of cobalt, nickel, and copper by δ-MnO_2 became less as the pH of the solution was decreased to the isoelectric point of the oxide, and fell off markedly below the isoelectric point. This may also be seen in the data of Morgan and Stumm (*167*) where ratios of $[Mn^{2+}]_{sorbed}/[Mn^{2+}]_{soln}$ decreased markedly as the pH approached the isoelectric point (about pH 2.8).

It is known that little or no zinc is removed from soils by alkaline extractants (*102*) unless a chelating organic or some reducing agent is used. Increasing pH tends to decrease the availability of these metals to salt extractants but copper is less susceptible to changes of pH than zinc (*182*) and is very much less susceptible than manganese (*242*). As a result of liming from a pH of 5.8 to 6.3, the "available" manganese of certain podzolic sands of Australia fell from 20 to as little as 2 p.p.m. (*222*). Christensen *et al.* (*52*) found that liming a soil from pH 4.6 to 6.5 decreased the exchangeable manganese 20 to 50 times. Mitchell (*163*) found that the cobalt uptake by red clover from a granitic soil decreased from 0.26 to 0.16 p.p.m. as the pH was increased from 5.4 to 6.4. Increasing the pH from 5.2 to 6.1 reduced the uptake of cobalt, added to the soil *via* solution, by timothy while further pH increases to 7.0 had little effect on cobalt uptake (*53*). The critical nature of pH 6.0 to 6.5 may be due to a catalytic action of manganese (or iron) oxides on the oxidation of Mn^{2+} to Mn^{4+}. Graven (*88*) noted that in the case of soils over pH 5.8 the amount of manganese extractable with 1*N* magnesium nitrate decreased markedly in a few days, when the samples were held at field moisture capacity following waterlogging. Those soils having pH values of 5.3 or less showed little decrease in extractable manganese within a month when held at field moisture capacity. These data are best interpreted in terms of the hydrous oxides as the principal control.

There is no evidence that a pH value of about 6 is critical in the formation of organic matter–heavy metal complexes. The apparent significance of pH 6 would also discount the possibility that the heavy metals, other than manganese and iron, generally occur as the hydroxides. It appears that sorption by hydrous manganese and iron oxides plus complex formation by organics keeps the activity of the other heavy metals so low that hydroxide precipitation is unlikely.

The significance of pH as a variable, affecting both rate and capacity of heavy metal sorption, has tended to be overlooked in comparisons of the effect of cation saturation on heavy metal sorption. Kanehiro (*129*)

compared the effect of calcium and hydrogen "saturation" on zinc sorption by the Wahiwa soil (a low humic latasol) after leaching with 0.05*M* calcium chloride or 0.05*M* hydrochloric acid (leaching rate and duration not specified). The lower zinc sorption (in 24 hours) following the hydrochloric acid treatment, 3.25 meq. *vs.* 6.7 meq. for calcium chloride leached samples, may well be caused by both acid dissolution of the hydrous oxides and the residual pH difference. The magnitude of reduction in zinc sorption found by Kanehiro as a result of hydrogen saturation is similar to that found by Hodgson (*106*) for hydrochloric acid-treated montmorillonite, which again is consistent with the proposed significance of the hydrous oxides as opposed to organic matter. (pH variation also confounds the cation saturation (H^+ *vs.* Ca^{2+}) effects examined by Banerjee *et al.* (*12*), and Nelson and Melsted (*172*).)

A soil pH of 6 is almost a magic number for manganese, zinc, copper, and sometimes nickel deficiency. Zinc deficiencies occur at 6 or higher in Utah (*235*), at 6 for both tung oil and citrus trees on sandy Florida soils (*44, 182*) and at 6.2 to 8 for apple trees in California (*50*), while manganese toxicity to dwarf beans occurs at pH value of 6 and below in Australia and manganese deficiency occurs at 5.8 in Florida (*154*). The availability of manganese is high in many Australian soils which are characterized by pH values below 6.5 (*242*). Zinc toxicity caused by overfertilization was found to be inhibited at pH 6 and above (*148, 218, 219*). Zinc availability was found to reach a minimum in soils at pH 7.5 (*242*). In Australia, on deep podzolic sands formed on Pliocene sediments with a natural pH of 5.0 to 5.8, vegetables show a yield loss caused by manganese deficiency when the pH is increased to only 6.3 by liming (*222*). The pH of the soil has a marked effect on the amount of iron extracted with pH 4.8 ammonium acetate (*176*). If two straight lines are drawn through Olson's data, their intersection is between pH 5.5 and 6.0. Thus, it appears that some more soluble form of iron predominates in soils below pH 6.0. This is particularly interesting in view of the critical nature of pH 6 on the availability to plants of other heavy metals.

There are several causes of the generally poor correlation between the "extractable" quantity of a heavy metal and soil pH or availability to plants. Varying amounts of carbonates, organic matter, hydrous oxides of manganese and iron, as well as soil Eh values all affect the amounts of these metals which are "extractable." Much better correlations than those obtained would be expected if the heavy metals were located on clay mineral exchange sites or were complexed by organic matter.

Carbonates are probably the major cause of the poor relationships found between amounts of acid-extractable heavy metals and their availability to plants. Hibbard (*101*) noted that the greater the solid to solution ratio, the greater the difference between soils in the amount of zinc

extracted. This implies that the buffer capacity of the extractant was inadequate. The most significant paper since those of Hibbard (*101, 102, 103*) is probably the infrequently referenced paper of Nelson *et al.* (*171*). These authors clearly show that progressively more hydrochloric acid is required to extract the acid-soluble zinc from soils as the soil carbonate content increases. They note that "little or no zinc was extracted until all the lime had reacted and enough acid had been added to bring the pH down to 5.0 or slightly lower."

A further reason for the range in pH values at which a deficiency of a given heavy metal occurs in soils is the variation in Eh values which may exist in different soils at a common pH. Since coarse-textured soils may be expected to have better aeration and higher Eh values than finer textured soils at comparable moisture tensions, lower pH values are probably required to maintain the same degree of heavy metal availability in the coarser textured soils. pH itself is inadequate to explain the variations in heavy metal availability (*178*). However, in the case of a single soil, Tisdale and Bertramson (*240*) found a good relationship between ammonium acetate soluble manganese and pH. Thus, it is suggested that when other variables are held constant, pH controls the desorption of manganese from the hydrous oxides as well as other soil chemical reactions.

A further complication is that of the differential effect of liming on the availability of the naturally occurring *vs.* the fertilizer applied metal. Beeson *et al.* (*16*) found that applying calcium carbonate to test pots of Norfolk fine sand did not affect the sorption of naturally occurring cobalt by soybeans but greatly decreased the intake of added cobalt. The added cobalt was presumably largely precipitated as either the carbonate or hydroxide. At a P_{CO_2} of $10^{-3.5}$ atmosphere, cobalt carbonate is three orders of magnitude less soluble than cobalt hydroxide between pH 4 and 9. At higher P_{CO_2} values, the cobalt carbonate would be even less soluble than cobalt hydroxide. Thus, it appears likely that the added cobalt may have been largely rendered unavailable to plants by precipitation as the carbonate. The radically different time frame within which the plant and the chemical extractants are operative renders a correlation difficult. The "pH effect" on the availability of these metals to plants must be found in the combined effect of the activity of hydrogen on: (1) the direct precipitation of the metal as the oxide (Mn) or hydroxide (Fe, Co, Ni, Cu, Zn); (2) the concentration of carbonate, phosphate, and possibly silicate ions in the associated aqueous phase; (3) the precipitation-dissolution of manganese and iron oxides; and (4) the rate of sorption and desorption of heavy metals by the hydrous oxides. Figure 4 shows the solubility of the metals under consideration as a function of pH, as calculated from free-energy data (*82*). Within the accuracy of the free

energy data, the values given in Figure 4 represent the maximum activity of the metal that occurs in soil solutions or fresh waters. However, it is doubtful if these concentrations are ever reached, because of ubiquitous presence of carbonate and phosphate, as well as the hydrous oxides.

Relation to Oxide Content of Soils. The zinc concentration of limonite was always higher than in the soil matrix, and in many cases the percent zinc correlated with percent iron in the subsurface soil samples studied by White (*251*). Fujimoto and Sherman (*78*) noted that cobalt was concentrated in the well-developed or incipient ferruginous layers of Hawaiian soils. Likewise, Hill *et al.* (*104*) noted that the cobalt content of podzol soils was generally higher in the B horizon than in the A horizon. Painter *et al.* (*180*) also found the nickel content of New Jersey soils to be greater in the B than A horizon. Kubota [as quoted by Hodgson (*107*)] found that the ratio of cobalt to iron in some soil concretions approached a ratio of one to one. It is probable that the concretionary iron is predominantly ferric. Although information on the limit of solid solution of cobalt in ferric hydroxide is not at hand, Trautmann (*241*) has shown that $Fe(OH)_2(c)$ can take up to 50% cobalt in solid solution, the unit cell dimensions increasing linearly with increasing cobalt substitution. Kanehiro (*129*) found that the 0.1*N* hydrochloric acid extractable zinc decreased with depth in lateritic soils, while D'Hoore (*61*) found that ammonium thiocyanate extractable iron similarly decreased with depth in lateritic soils. This is in accordance with the generally observed decrease in organic matter with depth; hence, a lesser portion of the oxides are in the microcrystalline state with increasing depth.

There appears to be a general relationship between cobalt and iron concentrations in soils (*41, 87, 136, 189, 190, 213*). Because of the tendency for the amount of free-iron oxides to be related to the surface area of the soil minerals, a positive correlation may also be found between total cobalt content and clay content (*136, 189, 190*). A poor correlation between total cobalt and manganese, which was improved by taking into account the clay content, was found by Gonzalez Garcia and Garcia Gomez (*87*) for several Spanish soils.

The possibility exists that some of the apparent correlations between cobalt and iron-oxide concentrations in reality reflect a correlation between cobalt and manganese oxide concentrations since the amount of free manganese oxides have only rarely been determined in soils and sediments.

Sorption, Desorption, and Fixation Rates. A further indication that the basic immobilization mechanism for heavy metals is one of sorption and fixation by the hydrous oxides, is indicated by the slowness with which the heavy metals often become deficient after fertilization. In

contrast, ion exchange reactions involving alkali and alkaline earth metals are of the order of seconds to minutes (*39*). Askew and Dixon (*7*) found that the cobalt content of New Zealand pastures dropped markedly in a period of one month subsequent to cobalt fertilization. Chandler (*49*) reported that with California soils of lowest zinc fixing power 1,000 pounds of zinc sulfate per acre, spread uniformly over the soil surface, controlled nearly all the zinc deficiency symptoms of trees for up to three years. Leeper (*142*) found that in coarse-textured soils both manganese sulfate and manganese dioxide precipitates, when intimately mixed with a calcareous sandy loam soil, prevented manganese deficiency symptoms from reoccurring for a period of eight to ten years although in some cases the benefits of manganese sulfate fertilization only lasted one to four years. (The slow oxidation of Mn^{2+} from the manganous sulfate in the soil may have resulted in manganic oxides of greater crystallinity than that of the laboratory precipitate.) Waterlogging the unfertilized soil for a period of four weeks eliminated manganese deficiency symptoms in oats for about 11 years (*142*). It may be that a number of years were required to convert the high surface area δ-MnO_2, resulting from the precipitation of manganese following the waterlogging, to more crystalline oxides. Increased zinc sorption, as a result of grinding the Aiken soil, which was attributed to a probable increase in cation exchange capacity (*36*), may well have been the result of an increased sorption rate of the hydrous oxides owing to a greater surface area.

The extent and rate of the reversibility of heavy metal sorption by the hydrous oxides, as well as the exact nature of the pH effects on the reversibility, is not entirely clear. The available data indicate that heavy metal sorption by the hydrous oxides is at least partially competitive with and reversible to exchange with other heavy metals. On synthetic hydrous oxides, sorption of manganese is competitive with hydrogen (*167*) whereas ammonium competes only weakly with cobalt (*138*). On reference clays nearly all of which contain appreciable amounts of free-manganese and free-iron oxides (*6*), heavy metal sorption is competitive with other cations; hydrogen competes strongly with cobalt (*106, 238*), whereas calcium does not (*108*); magnesium competes effectively with cobalt sorption (*108*) but is ineffective in causing cobalt desorption (*106*). Brown (*36*) notes only a minor decrease in zinc sorption because of competition with magnesium as compared with calcium, namely, 6.98 *vs.* 7.56 meq./100 grams. Studies by Steenbjerg (*220*), quoted by Leeper (*142*), indicate that 0.5*M* magnesium nitrate was a more effective extracting agent for manganese than ammonium nitrate or sodium nitrate, while calcium nitrate was intermediate. Tiller and Hodgson (*238*) observed a pH drop after adding cobalt to the clay minerals of greater sorption capacity and noted that isotherm experiments with higher amounts of

cobalt were limited because of the concomitant pH decrease. Stewart and Leonard (*223*) observed a pH drop upon sorption of zinc by a soil as did Merrill *et al.* (*159*) following manganous sulfate applications. Unpublished data of the author show that of 24 meq./grams of cobalt sorbed by δ-MnO_2 in 48 hours, only 1.4% of the 24 meq. was desorbed by calcium chloride (0.1*M*, pH 5.5) in a similar length of time. The data currently available indicate that the initial rate of heavy metal sorption is more rapid by microcrystalline MnO_2 than $Fe(OH)_3(a)$ (*135*).

Immobilization rates of the order of years for the heavy metals in soils are in marked contrast to solution oxidation rates of Mn^{2+} and Fe^{2+}. The time required for 50% oxidation of Fe^{2+} to Fe^{3+} in solution ranged from a few hours at pH 5 to a few minutes at pH 7 (*225*). At pH 8 the rate appeared to be controlled by O_2 solution diffusion rates. However, according to these authors, the oxidation rate is decreased by complexing anions, especially phosphate and organic matter.

The immobilization rates in soils are also in marked contrast to heavy metal sorption rates obtained in the laboratory. The data of Hodgson (*106*) on the sorption of cobalt by montmorillonite yield sorption rates similar to those obtained with freshly precipitated Fe^{3+}-Fe^{2+} oxide (*119*).

Industrial waste to the Saale River (Germany) resulted in zinc concentrations at Rubolstadt of several thousand milligrams per liter which decreased by a factor of 10 within 6 to 8 miles downstream. Surficial sediment in front of a dam 7.4 miles downstream had a zinc content of 0.86%, whereas similar sediment 21.8 miles further downstream had only 0.36% zinc (*91*). Since the hydrous oxides of iron and manganese are ubiquitous in surficial stream sediments, it is suggested that the zinc decontamination of the Saale River in this case may have been caused by the scavenging ability of the hydrous oxides.

Needed Research

Many points remain disturbingly vague. Several areas of inadequate knowledge regarding the controls on the concentration of heavy metals in the aqueous phase associated with earth materials are noted and briefly discussed below.

(1) The relative affinity of soil and stream sediment organic matter *vs.* iron and manganese oxides for the heavy metals.

(2) The relative importance of manganese *vs.* iron oxides as controls. In several instances, quite good correlations have been found between total cobalt and total iron. However, in other cases the cobalt is clearly associated with the manganese oxides. Pierce (*184*) notes the absence of cobalt in iron oxides even where the iron oxides occur in association with manganese oxides containing cobalt in the southern Appalachians. Gonzalez Garcia and Garcia Gomez (*87*) found a close relation between the

cobalt and iron contents of some Spanish soils ($r = 0.96$). They found that the amount of cobalt present was poorly related to the amount of manganese present ($r = 0.51$). In ocean floor nodules, Burns and Fuerstenau (*40*) found that nickel and copper were concentrated in the high manganese areas, while cobalt was concentrated in the high iron areas. However, Ng and Bloomfield (*173*) concluded from precipitation experiments that while copper and zinc were concentrated by ferric oxide, the tendency was very slight for cobalt, nickel, and manganese to coprecipitate with the ferric oxide. The partition of the various heavy metals between manganese and iron oxides should be investigated, particularly in view of the greater ease with which manganese oxides are reduced (*134, 227*).

(3) The extent to which concretionary iron and manganese oxides participate in the control of the solution concentration of heavy metals. If the concretionary oxides are not significant, relative to the oxidic coatings, then sorption-desorption studies could largely be confined to the clay fraction of soils and sediments. Thus, Kubota (*136*) found a much closer relationship between total cobalt and clay content than between total iron and clay content, indicating a preferential sorption by the iron occurring as coatings as compared to concretionary iron oxides.

(4) The chemical, physical, and mineralogical nature of the hydrous oxides. Several lines of evidence indicate that the oxidic coatings of manganese and iron are largely amorphous, however, this is difficult to reconcile with the conclusion of Fripiat and Gastuche (*76*) that the discrete iron particles were dissolved prior to the iron coatings on kaolinite with oxalic acid plus aluminum or with dithionite. The role of other metals present at the time of precipitation should be investigated since Vinayak *et al.* (*243*) found "exchangeable" manganese to be higher in soils high in soluble sodium and it is known that the salt content at the time of precipitation and the degree of salt removal by dialysis affect the structure of aluminum trihydrates (*84*). Follett *et al.* (*74*) have concluded that the iron oxides in soils they studied were complexed with alumina and silica. Schwertmann (*205*) found that the presence of soluble phosphorus, silica, and organics slowed down considerably the formation of goethite and hematite from amorphous ferric hydroxide. The reason why some B horizons which are enriched in iron are not concomitantly enriched in the other heavy metals (*147*) should be investigated.

(5) The possible role of amorphous aluminum and silicon oxides as controls. These merit further investigation since Elgabaly (*66*) found increased zinc fixation by kaolinite after nine days of grinding even though Tiller *et al.* (*239*) found little effect of sodium hydroxide extractions on cobalt sorption by soil clays. Tiller (*237*) has recently found that zinc sorption by montmorillonite is enhanced by the addition of soluble silicon.

(6) The factors affecting the rates of sorption and desorption of the heavy metals by the hydrous oxides.

(7) pH relations. (a.) Variation of the amount of extractable metal with pH. Tisdale and Bertramson (*240*) found a linear relation between

ammonium acetate extractable manganese and soil pH, whereas the plotting of some other data generally indicates a linear log-log relationship. (b.) The critical nature of pH 6. This merits further study inasmuch as the extractability of these metals decreases above 4–5 (*44, 53, 182*). It is reasonably well established that when acid soils are limed above a pH of about 6, zinc, copper, and manganese are quite likely to become deficient. However, it appears that deficiencies of these elements do not occur with great frequency on naturally alkaline soils except when the soils are old and highly weathered or when sandy soils occur under moderate to high rainfall conditions. (c.) The appreciable availability of heavy metals at pH values well above neutrality. This may indicate that a significant portion of the heavy metals is held in these soils by organic matter, as Staker and Cummings (*219*) found it necessary to lime some peat soils to pH 7 to reduce the toxic effect of naturally occurring zinc. On the other hand, Jurinak and Thorne (*128*) noted a minimum in plots of zinc concentration in solution *vs.* pH in the range of 5.5 to 7 where the zinc-Utah bentonite system was titrated with either sodium or potassium hydroxide. However, when this system was titrated with calcium hydroxide, a minimum in the zinc concentration in solution occurred at about 7.6 and remained relatively constant at higher pH values. Thus, the availability of these metals may be related to the soluble sodium:calcium ratio. The more rapid reoxidization of manganese which occurs at higher pH values and results in a more disordered manganese dioxide structure may also be a significant factor. (d.) pH *vs.* the preferential sorption by manganese and iron oxides. Shipman (*209*) obtained greater selectivity by *in situ* precipitated manganese oxide for strontium than for cobalt or cerium at pH 12. One wonders if the pH of the aqueous phase would affect the distribution of these metals between iron and manganese oxides. (e.) The extent to which the success of various extractants utilized, for estimating the amount of "available" heavy metal, is dependent on their solubilization of the hydrous oxides or to their ability to extract "soluble" organic matter. The Eh, as well as the pH, of the various chemical extractants needs to be evaluated.

(8) The relative dissolution rates of manganese and iron oxides as affected by Eh, pH, and amount and kind of organic matter. Takai and Kamura (*227*) and Koyama (*134*) found almost no iron coming into solution until nearly all the manganese was dissolved from a lake bed sediment under anaerobic conditions. However, Mandal (*149*) found that the iron coming into solution in a waterlogged rice soil was in excess of the manganese when green foliage was added, but little iron and sizable amounts of manganese dissolved when organic matter was not added (soil contained 0.77% organic carbon). Thus, it is necessary to study the dissolution rates in terms of Eh and pH. A modest decrease in Eh–pH is enough to shift from the MnO_2 stability field to the Mn^{2+} stability field but a larger Eh–pH decrease is required to shift from $Fe(OH)_3(c)$ to the Fe^{2+} stability field (Figures 1a and 2a).

(9) The reactions involved in causing the increased availability of the heavy metals caused by adding chloride salts. The availability of zinc (*223*) and manganese (*117, 144, 145, 146, 223, 250*) increased by the addition of large amounts of calcium or potassium chloride to soils.

Acknowledgments

It is a pleasure to acknowledge Elisabeth F. Snyder's capable bibliographic, editorial, and figure drafting assistance, Eunice Speiser's extensive efforts to locate and borrow reference materials, Carol J. Lind's preparation of the Eh–pH and solubility diagrams, and Richard L. Snyder's free oxide extraction work.

Literature Cited

(1) Adams, S. N., Honeysett, J. L., *Australian J. Agr. Res.* **15,** 357 (1964).
(2) Agerberg, L. S., *Kgl. Skogs. Lantbruksakad. Tidskr.* **98,** 343 (1959).
(3) Alben, A. O., Boggs, H. M., *Soil Sci.* **41,** 329 (1936).
(4) Alexander, L. T., Byers, H. G., *U. S. Dept. Agr. Tech. Bull.* **317,** 25 (1932).
(5) Allison, L. E., Scarseth, G. D., *Am. Soc. Agron. J.* **34,** 616 (1942).
(6) Anderson, B. J., Jenne, E. A. (unpublished data).
(7) Askew, H. O., Dixon, J. K., *New Zealand J. Sci. Tech.* **18,** 688 (1937).
(8) Askew, H. O., Maunsell, P. W., *New Zealand J. Sci. Tech.* **19,** 337 (1937).
(9) Baars, J. K., *Trans. Intern. Congr. Soil Sci., 4th, Amsterdam* **1,** 192 (1950).
(10) Baas Becking, L. G. M., Moore, D., *J. Sediment. Petrol.* **29,** 454 (1959).
(11) Back, William, Barnes, Ivan, *U. S. Geol. Surv. Profess. Papers* **498-C,** 16 (1965).
(12) Banerjee, D. K., Bray, R. H., Melsted, S. W., *Soil Sci.* **75,** 421 (1953).
(13) Baughman, N. M., Ph.D. thesis, Purdue University, p. 87 (1956).
(14) Baver, L. D., "Soil Physics," 3rd ed., p. 489, John Wiley & Sons, New York, 1956.
(15) Beeson, K. C., *U. S. Dept. Agr., Agr. Infor. Bull.* **7,** 44 (1950).
(16) Beeson, K. C., Gray, L., Hamner, K. C., *Am. Soc. Agron. J.* **40,** 553 (1948).
(17) Berg, W. A., Ph.D. thesis, North Carolina State College, p. 79 (1960).
(18) Best, R. J., *J. Agr. Sci.* 21, 337 (1931).
(19) Bingham, F. T., Page, A. L., Sims, J. R., *Soil Sci. Soc. Am. Proc.* **28,** 351 (1964).
(20) Biswas, T. D., Gawande, S. P., *Indian Soc. Soil Sci. J.* **12,** 262 (1964).
(21) Bloomfield, C., *J. Soil Sci.* **1,** 205 (1950).
(22) *Ibid.*, **3,** 167 (1952).
(23) *Ibid.*, **4,** 5 (1953a).
(24) *Ibid.*, **4,** 17 (1953b).
(25) *Ibid.*, **5,** 50 (1954).
(26) Bloomfield, C., *J. Sci. Food Agr.* **6,** 641 (1955).
(27) Bloomfield, C., *Chem. Ind.* **9,** 259 (1958).
(28) Blümel, F., *Z. Pflanzenernaehr. Dueng. Bodenk.* **98,** 258 (1962).
(29) Boawn, L. C., Leggett, G. E., *Soil Sci.* **95,** 137 (1963).
(30) Boawn, L. C., Viets, F. G., Jr., *Agron. J.* **44,** 276 (1952).
(31) Bower, C. A., Truog, E., *Soil Sci. Soc. Am. Proc.* **5,** 86 (1940).
(32) Boyle, R. W., Tupper, W. M., Lynch, J., Friedrich, G., Ziauddin, M., Shafiqullah, M., Carter, M., Bygrave, K., *Can. Geol. Surv. Paper* **65-42,** 50 (1966).
(33) Bricker, Owen, *Am. Mineralogist* **50,** 1296 (1965).
(34) Broadbent, F. E., Bradford, G. R., *Soil Sci.* **74,** 447 (1952).
(35) Bromfield, S. M., *J. Soil Sci.* **5,** 129 (1954).

(36) Brown, A. L., *Soil Sci.* **69,** 349 (1950).
(37) Brown, A. L., Jurinak, J. J., *Soil Sci.* **98,** 170 (1964).
(38) Brown, A. L., Krantz, B. A., Martin, P. E., *Soil Sci. Soc. Am. Proc.* **26,** 167 (1962).
(39) Brown, T. E., *U. S. Geol. Surv. Profess. Papers* **501-C,** C96 (1964).
(40) Burns, R. G., Fuerstenau, D. W., *Am. Mineralogist* **51,** 895 (1966).
(41) Burriel, F., Gallego, R., *Anales Edafol. Fisiol. Vegetal.* **11,** 569 (1952).
(42) Buser, W., Graf, P., *Helv. Chim. Acta* **38,** 830 (1955).
(43) Buser, W., Graf, P., Feitknecht, W., *Helv. Chim. Acta* **37,** 2322 (1954).
(44) Camp, A. F., *Soil Sci.* **60,** 157 (1945).
(45) Camp, A. F., Reuther, W., *Florida Agr. Expt. Sta. Ann. Rept.* p. 132 (1937).
(46) Canals, E., Marignan, R., Cordier, S., *Ann. Pharm. Franc.* **8,** 368 (1950).
(47) Canney, F. C., Nowlan, G. A., *Econ. Geol.* **59,** 721 (1964).
(48) Carroll, Dorothy, *Geochim. Cosmochim. Acta* **14,** 1 (1958).
(49) Chandler, W. H., *Botan. Gaz.* **98,** 625 (1937).
(50) Chandler, W. H., Hoagland, D. R., Hibbard, P. L., *Am. Soc. Hort. Sci. Proc.* **28,** 556 (1931).
(51) *Ibid.*, **29,** 255 (1932).
(52) Christensen, P. D., Toth, S. J., Bear, F. E., *Soil Sci. Soc. Am. Proc.* **15,** 279 (1950).
(53) Crooke, W. M., *Soil Sci.* **81,** 269 (1956).
(54) Daniels, R. B., Brasfield, J. F., Riecken, F. F., *Soil Sci. Soc. Am. Proc.* **26,** 75 (1962).
(55) Davidtz, J. C., M.S. thesis, Natal University, Pietermaritzburg, p. 99 (1963).
(56) De Gee, J. C., *Trans. Intern. Congr. Soil Sci., 4th, Amsterdam* **1,** 300 (1950).
(57) DeLong, W. A., Sutherland, A. J., Salisbury, H. F., *Sci. Agr.* **21,** 89 (1940).
(58) DeMumbrum, L. E., Jackson, M. L., *Soil Sci.* **81,** 353 (1956a).
(59) DeMumbrum, L. E., Jackson, M. L., *Soil Sci. Soc. Am. Proc.* **20,** 334 (1956b).
(60) Dhar, N. R., Kishore, N., *India Natl. Acad. Sci. Proc.* **19A,** 89 (1950).
(61) D'Hoore, J. L., *Bull. Agr. Congo Belge* **40,** 66 (1949).
(62) D'Hoore, J. L., Fripiat, J. J., Gastuche, M. C., *Inter-African Soils Conf. 2d. Proc.* **1,** 257 (1954).
(63) Dion, H. G., Mann, P. J. G., Heintze, S. G., *J. Agr. Sci.* **37,** 17 (1947).
(64) Doyle, Roger W., Ph.D. thesis, Yale University, p. 100 (1967).
(65) Ekman, P., Karlsson, N., Svanberg, O., *Acta Agr. Scand.* **2,** 103 (1952).
(66) Elgabaly, N. M., *Soil Sci.* **69,** 167 (1950).
(67) Elgabaly, N. M., Jenny, H., *J. Phys. Chem.* **47,** 399 (1943).
(68) Epstein, E., Stout, P. R., *Soil Sci.* **72,** 47 (1951).
(69) Evans, W. David, *Proc. 11th E. Sch. Agr. Sci.* 14, "Experimental Pedology," Nottingham University, 1964 (Pub. 1965).
(70) Feitknecht, W., *Z. Elektrochem.* **63,** 34 (1959).
(71) Feitknecht, W., Oswald, H. R., Feitknecht-Steinmann, U., *Helv. Chim. Acta* **43,** 1947 (1960).
(72) Fleischer, Michael, Richmond, W. E., *Econ. Geol.* **38,** 269 (1943).
(73) Follett, E. A. C., *J. Soil Sci.* **16,** 334 (1965).
(74) Follett, E. A. C., McHardy, W. J., Mitchell, B. D., Smith, B. F. L., *Clay Minerals Bull.* **6,** 35 (1965).
(75) Fox, R. L., Plucknett, D. L., *Hawaii Farm Sci.* **13,** 9 (1964).
(76) Fripiat, J. J., Gastuche, M. C., *Publ. Inst. Natl. Etudes Agron. Congo Belge, Sér. Sci.* **no. 54,** 7 (1952).
(77) Fuerstenau, D. W., personal communication (1965).

(78) Fujimoto, Giichi, Sherman, G. D., *Agron. J.* **42**, 577 (1950).
(79) Fukai, R., Huynh-Ngoc, L., Vas, D., *Nature* **211**, 726 (1966).
(80) Futral, F. L., Ingols, R. S., *J. Am. Water Works Assoc.* **45**, 804 (1953).
(81) Gall, O. E., Barnette, R. M., *Am. Soc. Agron. J.* **32**, 23 (1940).
(82) Garrels, R. M., Christ, C. L., "Solutions, Minerals, and Equilibria," p. 450, Harper and Row, New York, 1965.
(83) Gasser, J. K. R., Bloomfield, C., *J. Soil Sci.* **6**, 219 (1955).
(84) Gastuche, Marie-Claire, Herbillon, Adrien, *Bull. Soc. Chim. France* **1962**, 1404 (1962).
(85) Gayer, K. H., Woontner, Leo, *J. Phys. Chem.* **60**, 1569 (1956).
(86) Goldberg, E. D., Arrhenius, G. O. S., *Geochim. Cosmochim. Acta* **13**, 153 (1958).
(87) Gonzalez Garcia, F., Garcia Gomez, A. M., *Analis. Edafol. Agrobiol. (Madrid)* **23**, 563 (1964).
(88) Graven, E. H., Ph.D. thesis, Wisconsin University, p. 72 (1965).
(89) Greene-Kelly, R., *J. Soil Sci.* **4**, 233 (1953).
(90) Gupta, Umesh, MacKay, D. C., *Soil Sci.* **101**, 93 (1966).
(91) Heide, F., Singer, E., *Naturwiss* **41**, 498 (1954).
(92) Hem, J. D., *U. S. Geol. Surv. Water-Supply Papers* **1459-B**, 33 (1960).
(93) *Ibid.*, **1667-A**, 64 (1963a).
(94) Hem, J. D., *U. S. Geol. Surv. Profess. Papers* **475-C**, C216 (1963b).
(95) Hem, J. D., Abstracts of Papers, 145th Meeting ACS, Sept. 1963, p. 1W.
(96) Hem, J. D., *U. S. Geol. Surv. Water-Supply Papers* **1667-B**, 42 (1964).
(97) Hem, J. D., Cropper, W. H., *U. S. Geol. Surv. Water-Supply Papers* **1459-A**, 31 (1959).
(98) Hem, J. D., Skougstad, M. W., *U. S. Geol. Surv. Water-Supply Papers* **1459-E**, 95 (1960).
(99) Hem, J. D., *J. Am. Water Works Assoc.* **53**, 211 (1961).
(100) Hewett, D. F., Fleischer, Michael, *Econ. Geol.* **55**, 1 (1960).
(101) Hibbard, P. L., *Hilgardia* **13**, 1 (1940a).
(102) Hibbard, P. L., *Soil Sci.* **49**, 63 (1940b).
(103) *Ibid.*, **50**, 53 (1940c).
(104) Hill, A. C., Toth, S. J., Bear, F. E., *Soil Sci.* **76**, 273 (1953).
(105) Himes, F. L., Barber, S. A., *Soil Sci. Soc. Am. Proc.* **21**, 368 (1957).
(106) Hodgson, J. F., *Soil Sci. Soc. Am. Proc.* **24**, 165 (1960).
(107) Hodgson, J. F., *Advan. Agron.* **15**, 119 (1963).
(108) Hodgson, J. F., Geering, H. R., Fellows, Martha, *Soil Sci. Soc. Am. Proc.* **28**, 39 (1964).
(109) Hodgson, J. F., Lindsay, W. L., Trierweiler, J. F., *Soil Sci. Soc. Am. Proc.* **30**, 723 (1966).
(110) Hodgson, J. F., Tiller, K. G., "Proceeding, 9th National Conference Clays and Clay Minerals," p. 404, Pergamon Press, New York, 1962.
(111) Hodgson, J. F., Tiller, K. G., Fellows, Martha, *Soil Sci. Soc. Am. Proc.* **28**, 42 (1964).
(112) Hodgson, J. F., personal communication (1967).
(113) Hosking, J. S., *J. Agr. Sci.* **22**, 92 (1932).
(114) Hüser, R., *Z. Pflanzenernaehr. Dueng. Bodenk.* **80**, 56 (1958).
(115) Jacks, G. V., Scherbatoff, H., *Imp. Bur. Soil Sci. (Harpenden, England) Tech. Commun.* **no. 31**, 46 (1934).
(116) Jackson, M. L., "Soil Chemical Analysis—Advanced Course," p. 991, (Pub. by author), Wisconsin University, Madison, 1956.
(117) Jackson, T. L., Westermann, D. T., Moore, D. P., *Soil Sci. Soc. Am. Proc.* **30**, 70 (1966).
(118) Jeffery, J. W. O., *J. Soil Sci.* **11**, 140 (1960).
(119) Jenne, E. A. (unpublished data).
(120) Jenne, E. A., Ph.D. thesis, Oregon State University, p. 121 (1961).

(121) Jenne, E. A., Wahlberg, J. S., *Am. Geophys. Union Trans.* **46,** 170 (1965).
(122) Jensen, H. L., Lamm, C. G., *Acta Agr. Scand.* 11, 63 (1961).
(123) Johnson, M. O., *J. Indus. Eng. Chem.* 9, 47 (1917).
(124) Jones, H. W., Gall, O. E., Barnette, R. M., *Florida Univ. Agr. Expt. Sta. (Gainesville) Bull.* **298,** 43 (1936).
(125) Joyner, Timothy, *J. Marine Res.* **22,** 259 (1964).
(126) Jurinak, J. J., Bauer, N., *Soil Sci. Soc. Am. Proc.* **20,** 466 (1956).
(127) Jurinak, J. J., Inouye, T. S., *Soil Sci. Soc. Am. Proc.* **26,** 144 (1962).
(128) Jurinak, J. J., Thorne, D. W., *Soil Sci. Soc. Am. Proc.* **19,** 446 (1955).
(129) Kanehiro, Yoshinori, Ph.D. thesis, Hawaii University, p. 113 (1964).
(130) Kanwar, J. S., *Indian Soc. Soil Sci. J.* **2,** 73 (1954).
(131) Kidson, E. B., *New Zealand J. Sci. Tech.* **18,** 694 (1937).
(132) Kindle, E., *Am. J. Sci. Ser. 5,* **24,** no. 144, 496 (1932).
(133) Kosegarten, E., *Z. Pflanzenernaehr. Dueng. Bodenk.* **73,** 25 (1956).
(134) Koyama, Tadashiro, "Recent Researches in the Fields of Hydrosphere, Atmosphere, and Nuclear Geochemistry," p. 143, Y. Miyake, T. Koyama, eds., Maruzen Co., Ltd., Tokyo, 1964.
(135) Krauskopf, K. B., *Geochim. Cosmochim. Acta* **9,** 1 (1956).
(136) Kubota, Joe, *Soil Sci.* 85, 130 (1958).
(137) Kurbatov, J. D., Kulp, J. L., Mack, Edward, Jr., *J. Am. Chem. Soc.* **67,** 1923 (1945).
(138) Kurbatov, M. H., Wood, Gwendolyn B., Kurbatov, J. D., *J. Phys. Colloidal Chem.* **55,** Part 2, 1170 (1951).
(139) Laevastu, Taivo, Thompson, Thomas, *J. Marine Res.* **16,** 192 (1958).
(140) Låg, J., Dev, G., *Indian Soc. Soil Sci. J.* **12,** 215 (1964).
(141) Lamm, C. G., *Nature* **177,** 620 (1956).
(142) Leeper, G. W., *Soil Sci.* **63,** 79 (1947).
(143) Leeper, G. W., *Ann. Rev. Plant Physiol.* **3,** 1 (1952).
(144) Leonard, C. D., Stewart, Ivan, *Proc. Florida State Hort. Soc.* **72,** 38 (1959).
(145) Leonard, C. D., Stewart, Ivan, Edwards, George, *Proc. Florida State Hort. Soc.* **69,** 72 (1956).
(146) *Ibid.,* **71,** 99 (1958).
(147) Le Riche, H. H., Weir, A. H., *J. Soil Sci.,* **14,** 225 (1963).
(148) Lott, W. L., *Soil Sci. Soc. Am. Proc.* **3,** 115 (1938).
(149) Mandal, L. N., *Soil Sci.* **91,** 121 (1961).
(150) Manheim, F. T., *Geochim. Cosmochim. Acta* **25,** 52 (1961).
(151) Manheim, F. T., *Proc. Symp. Marine Geochem. Univ. Rhode Island, Oct. 29-30, 1964.* Occasional Pub. **No. 3-1965,** 217 (1965).
(152) Mann, H. B., *Soil Sci.* **30,** 117 (1930).
(153) Martens, D. C., Chesters, G., Peterson, L. A., *Soil Sci. Soc. Am. Proc.* **30,** 67 (1966).
(154) McCool, M. M., *Boyce Thompson Inst. Contrib.* **6,** 147 (1934).
(155) Mehlich, A., *Soil Sci. Soc. Am. Proc.* **21,** 625 (1957).
(156) Menzel, R. G., Jackson, M. L., *Trans. Intern. Congr. Soil Sci., 4th, Amsterdam* 1, 125 (1950a).
(157) Menzel, R. G., Jackson, M. L., *Soil Sci. Soc. Am. Proc.* **15,** 122 (1950b).
(158) Mero, John L., "Mineral Resources From The Sea," p. 312, Elsevier, New York, 1964.
(159) Merrill, Samuel, Jr., Potter, G. F., Brown, R. T., *Proc. Am. Soc. Hort. Sci.* **62,** 94 (1953).
(160) Middelburg, H. A., *Trans. Intern. Congr. Soil Sci., 4th, Amsterdam* **2,** 136 (1950).
(161) Miller, M. H., Ohlrogge, A. J., *Soil Sci. Soc. Am. Proc.* **22,** 225 (1958).
(162) Misra, S. G., Tiwari, R. C., *Plant Soil* **24,** 54 (1966).

(163) Mitchell, R. L., *Proc. Intern. Congr. Pure Appl. Chem., 11th, London, 1947*, **3**, 157 (1951).
(164) Mitchell, R. L., "Chemistry of the Soil," p. 320, F. E. Bear, ed., Reinhold, New York, ACS Monograph **160** (2nd ed.), 1964.
(165) Mitchell, R. L., Reith, J. W. S., Johnston, I. M., "Plant Analysis and Fertilizer Problems," p. 249, I. R. H. O., Paris, 1957.
(166) Morgan, J. J., *Proc. Rudolfs Res. Conf., 4th, Rutgers Univ., 1965*, p. 561 (Pub. 1967).
(167) Morgan, J. J., Stumm, Werner, *J. Colloid Sci.* **19**, 347 (1964).
(168) Morgan, J. J., Stumm, Werner, *Intern. Water Pollution Res. Conf. Proc., 2nd, Tokyo, 1964*, p. 103 (Pub. 1965).
(169) Mulder, E. G., Gerretsen, F. C., *Advan. Agron.* **4**, 221 (1952).
(170) Nagayama, Masaichi, Goto, Katsumi, Yotsuyanagi, Takao, *Intern. Water Pollution Res. Conf. Proc., 2nd, Tokyo, 1964*, p. 126 (Pub. 1965).
(171) Nelson, J. L., Boawn, L. C., Viets, F. C., Jr., *Soil Sci.* **88**, 275 (1959).
(172) Nelson, J. L., Melsted, S. W., *Soil Sci. Soc. Am. Proc.* **19**, 439 (1955).
(173) Ng, Siew Kee, Bloomfield, C., *Geochim. Cosmochim. Acta* 24, 206 (1961).
(174) Nielsen, J. M., "Behavior of radionuclides in the Columbia River," p. 91, **TID-7664**, 1963.
(175) Oborn, E. T., Hem, J. D., *U. S. Geol. Surv. Water-Supply Papers* **1459-H**, 213 (1961).
(176) Olson, R. V., *Soil Sci. Soc. Am. Proc.* **12**, 153 (1947).
(177) Ormsby, W. C., Shartsis, J. M., *J. Am. Ceramic Soc.* **43**, 335 (1960).
(178) Page, E. R., *Plant Soil* **16**, 247 (1962).
(179) Page, E. R., *J. Soil Sci.* **15**, 93 (1964).
(180) Painter, L. I., Toth, S. J., Bear, F. E., *Soil Sci.* **76**, 421 (1953).
(181) Passioura, J. B., Leeper, G. W., *Nature* **200**, 29 (1963).
(182) Peech, Michael, *Soil Sci.* **51**, 473 (1941).
(183) Percival, Gordon P., Josselyn, Dorothy, Beeson, Kenneth C., *Tech. Bull. New Hampshire Agr. Expt. Sta.* **93**, 3 (1955).
(184) Pierce, W. G., *U. S. Geol. Surv. Bull.* **940-J**, 265 (1944).
(185) Piper, C. S., *J. Agr. Sci.* **32**, 143 (1942).
(186) Pourbaix, Marcel, "Atlas d'équilibres électrochimiques," p. 644, Gauthier-Villars, Paris, 1963.
(187) Powers, W. L., Pang, T. S., *Soil Sci.* **64**, 29 (1947).
(188) Prince, A. L., Toth, S. J., *Soil Sci.* **46**, 83 (1938).
(189) Reddy, K. G., Mehta, B. V., *Soil Sci.* **92**, 274 (1961).
(190) Reddy, K. G., Mehta, B. V., *Indian Soc. Soil Sci. J.* **10**, 167 (1962).
(191) Reid, W. S., Ph.D. thesis, Mississippi State University, p. 157 (1965).
(192) Reith, J. W. S., Mitchell, R. L., *Plant Anal. Fertilizer Probl.* **4**, 241 (1964).
(193) Robinson, W. O., *J. Agr. Res.* **34**, 339 (1927).
(194) Robinson, W. O., *Soil Sci.* **27**, 335 (1929).
(195) *Ibid.*, **30**, 197 (1930).
(196) Rogers, L. H., Gall, O. E., Gaddum, L. W., Barnette, R. M., *Florida Agr. Expt. Sta. Tech. Bull.* **341** (1939).
(197) Rogers, L. H., Wu, Chih-Hwa, *Am. Soc. Agron. J.* **40**, 563 (1948).
(198) Sanchez, C., Kamprath, E. J., *Soil Sci. Soc. Am. Proc.* **23**, 302 (1959).
(199) Schnitzer, M., Hoffman, I., *Geochim. Cosmochim. Acta* **31**, 7 (1967).
(200) Schnitzer, M., Skinner, S. I. M., *Soil Sci.* **102**, 361 (1966).
(201) *Ibid.*, **103**, 247 (1967).
(202) Schnitzer, M., Wright, J. R., *Can. J. Soil Sci.* **37**, 89 (1957).
(203) Schollenberger, C. J., *Soil Sci.* **29**, 261 (1930).
(204) Schwertmann, U., *Neues Jahrb. Mineral. Abhandl.* **93**, 67 (1960).
(205) Schwertmann, U., *Intern. Clay Conf. Proc., Jerusalem* **1**, 159 (1966).
(206) Seatz, L. F., *Trans. Intern. Congr. Soil Sci., 7th, Madison* **2**, 271 (1960).

(207) Sherman, G. D., Harmer, P. M., *Am. Soc. Agron. J.* **33**, 1080 (1941).
(208) Sherman, G. D., McHargue, J. S., Hodgkiss, W. S., *Soil Sci.* **54**, 253 (1942).
(209) Shipman, W. H., *Anal. Chem.* **38**, 1175 (1966).
(210) Shukla, U. C., Ph.D. thesis, Georgia University, p. 122 (1965).
(211) Sillén, L. G., *Arkiv Kemi* **24**, 431 (1966).
(212) Silverman, Melvin P., Ehrlich, Henry L., *Advan. Appl. Microbiol.* **6**, 153 (1964).
(213) Slater, C. S., Holmes, R. S., Byers, H. G., *U. S. Dept. Agr. Tech. Bull.* **552**, 23 (1937).
(214) Sokoloff, V. P., *Science* **118**, 296 (1953).
(215) Solomin, G. A., "Methods of determining Eh and pH in sedimentary rocks," p. 56, Consultants Bur., New York, 1965.
(216) Sommer, A. L., *Soil Sci.* **60**, 71 (1945).
(217) Spencer, W. F., Gieseking, J. E., *Soil Sci.* **78**, 267 (1954).
(218) Staker, E. V., *Soil Sci. Soc. Am. Proc.* **7**, 387 (1942).
(219) Staker, E. V., Cummings, R. W., *Soil Sci. Soc. Am. Proc.* **6**, 207 (1941).
(220) Steenbjerg, F., *Tidsskr. Planteavl* **39**, 401 (1933).
(221) Steenbjerg, F., Boken, E., *Plant Soil* **2**, 195 (1950).
(222) Stephens, C. G., Donald, C. M., *Advan. Agron.* **10**, 167 (1958).
(223) Stewart, Ivan, Leonard, C. D., *Soil Sci.* **95**, 149 (1963).
(224) Stumm, Werner, *Intern. Conf. Water Pollution Res., 3rd, Munich, Sept.* 5-9, p. 16 (1966).
(225) Stumm, Werner, Lee, G. F., *Schweiz. Z. Hydrol.* **22**, 295 (1960).
(226) Stumm, Werner, Lee, G. F., *Ind. Eng. Chem.* **53**, 143 (1961).
(227) Takai, Y., Kamura, T., *Kagaku (Tokyo)* **31**, 618 (1961).
(228) Tanaka, Motoharu, "Recent Researches in the Fields of Hydrosphere, Atmosphere, and Nuclear Chemistry," p. 285, Y. Miyake, T. Koyama, eds., Maruzen Co. Ltd., Tokyo, 1964.
(229) Taylor, R. M., McKenzie, R. M., Norrish, K., *Australian J. Soil Res.* **2**, 235 (1964).
(230) Taylor, R. M., McKenzie, R. M., *Australian J. Soil Res.* **4**, 29 (1966).
(231) Teakle, L. J. H., Morgan, E. T., Turton, A. G., *J. Dept. Agr. Western Australia* **18**, 96 (1941).
(232) Teakle, L. J. H., Wild, A. S., *J. Dept. Agr. Western Australia* **17**, 223 (1940).
(233) Thorne, D. W., Laws, W. D., Wallace, Arthur, *Soil Sci.* **54**, 463 (1942).
(234) Thorne, D. W., Wann, F. B., *Utah Agr. Expt. Sta. Bull.* **338**, 29 (1950).
(235) Thorne, Wynne, *Advan. Agron.* **9**, 31 (1957).
(236) Tiller, K. G., Ph.D. thesis, Cornell University, p. 209 (1961).
(237) Tiller, K. G., *Nature* **214**, 852 (1967).
(238) Tiller, K. G., Hodgson, J. F., "Proceedings, 9th National Conference Clays and Clay Minerals," p. 393, Pergamon Press, New York, 1962.
(239) Tiller, K. G., Hodgson, J. F., Peech, M., *Soil Sci.* **95**, 392 (1963).
(240) Tisdale, S. L., Bertramson, B. R., *Soil Sci. Soc. Am. Proc.* **14**, 131 (1949).
(241) Trautmann, Jean-Marie, *Compt. Rend.* **259**, 3270 (1964).
(242) Trumble, H. C., "A Symposium on Copper Metabolism," p. 336, W. D. McElroy, Bentley Glass, eds., Johns Hopkins Press, Baltimore, Md., 1950.
(243) Vinayak, C. P., Talati, N. R., Mathur, C. M., *Indian Soc. Soil Sci. J.* **12**, 275 (1964).
(244) Wahhab, A., Bhatti, H. M., *Soil Sci.* **86**, 319 (1958).
(245) Wain, R. L., Hunt, I. V., Marsh, G. C., *J. Southeastern Agr. Coll., Wye, Kent,* **no. 44**, 114 (1939).
(246) Walker, J. M., Barber, S. A., *Soil Sci. Soc. Am. Proc.* **24**, 485 (1960).
(247) Wear, J. I., *Soil Sci.* **81**, 311 (1956).

(248) Wei, Lun-Shin, Ph.D. thesis, Illinois University, p. 71 (1958).
(249) Weir, C. C., Miller, M. H., *Can. J. Soil Sci.* **42**, 105 (1962).
(250) Westermann, D. T., M.S. thesis, Oregon State University, p. 56 (1965).
(251) White, M. L., *Econ. Geol.* **52**, 645 (1957).
(252) Williams, C. H., Moore, C. W. E., *Australian J. Agr. Res.* **3**, 343 (1952).
(253) Willis, L. G., Piland, J. R., *J. Agr. Res.* **52**, 467 (1936).
(254) Woltz, S., Toth, S. J., Bear, F. E., *Soil Sci.* **76**, 115 (1953).
(255) Wright, J. R., Schnitzer, M., *Soil Sci. Soc. Am. Proc.* **27**, 171 (1963).
(256) Zapffe, Carl, *Econ. Geol.* **26**, 799 (1931).
(257) Zende, G. K., *Indian Soc. Soil Sci. J.* **2**, 55 (1954).

RECEIVED August 21, 1967.

INDEX

D

E

F

M

N

O

P